AD NUMBER

AD857062

NEW LIMITATION CHANGE

TO

Approved for public release, distribution unlimited

FROM

Distribution authorized to U.S. Gov't. agencies and their contractors; Operational and administrative use; Jul 1969. Other requests shall be referred to AFRPL [RPOR/STINFO], Edwards AFB, CA, 93523.

AUTHORITY

AFRPL ltr, 29 Sep 1971

AFRPL-TR-69-97

DEVELOPMENT OF AFRPL FLANGED CONNECTORS FOR ROCKET FLUID SYSTEMS

T. M. Trainer, J. V. Baum, J. R. Thompson,
and N. D. Ghadiali

Battelle Memorial Institute
Columbus Laboratories

TECHNICAL DOCUMENTARY REPORT NO. AFRPL-TR-69-97

July 1969

Air Force Rocket Propulsion Laboratory
Air Force Systems Command
Edwards, California

NOTICES

When U. S. Government drawings, specifications, or other data are used for any purpose other than a definitely related government procurement operation, the Government thereby incurs no responsibility nor any obligation whatsoever; and the fact that the Government may have formulated, furnished, or in any way supplied the said drawings, specifications, or other data is not to be regarded by implication or otherwise, as in any manner licensing the holder or any other person or corporation, or conveying any rights or provisions to manufacture, use, or sell any patent invention that may in any way be related thereto.

Qualified requestors may obtain copies from the Defense Documentation Center. Orders will be expedited if placed through the librarian or other person designated to request documents from the Defense Documentation Center.

Defense Documentation Center release to the Office of Technical Services is not authorized.

If this copy is not needed, return to AFRPL (RPRPD), Edwards, California, 93523.

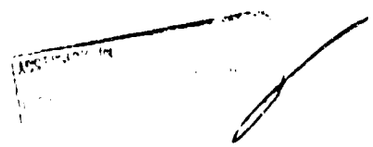

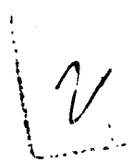

DEVELOPMENT OF AFRPL FLANGED CONNECTORS FOR ROCKET FLUID SYSTEMS

by

T. M. Trainer, J. V. Baum, J. R. Thompson,
and N. D. Ghadiali

FOREWORD

This report summarizes research conducted under Phases II and III of USAF Contract AF 04(611)-11204 from January, 1966 to March, 1969. The research was performed by the Columbus Laboratories of Battelle Memorial Institute under the auspices of the Air Force Rocket Propulsion Laboratory, Edwards Air Force Base, with Capt. John L. Feldman and Capt. F. M. Cassidy serving as project monitors. The principal investigators were N. D. Ghadiali, D. E. Netter, J. G. St. Clair, J. R. Thompson, Research Engineers; J. V. Baum and B. Goobich, Associate Fellows; E. C. Rodabaugh, Senior Engineer; and T. M. Trainer, Project Manager.

This technical documentary report has been reviewed and is approved.

John L. Feldman
Captain, USAF
Project Engineer

ABSTRACT

A 3-year program was conducted to develop a family of flight-weight flanged tube connectors which utilize the "Bobbin" seal concept for both 6061-T6 aluminum and Type 347 stainless steel tubing systems. In addition, engineering support was furnished during the evaluation of AFRPL stainless steel threaded connectors by selected organizations. The activities in relation to the first objective consisted of: (1) the selection of bolted, flanged connectors as the best means of joining tubing from 1 to 16 inches in diameter, (2) the development of stainless steel and aluminum Bobbin seals for typical flanged connector sizes, (3) the preparation of a detailed computer program for the optimum design of flanged connectors incorporating Bobbin seals, (4) the design, fabrication, and qualification testing of representative flanged connectors, and (5) the preparation of designs for a family of stainless steel and aluminum flanged connectors. The activities directed toward the second objective consisted of: (1) the investigation of seal-removal tools, (2) the design and evaluation of connector modifications to achieve seal retention and misalignment limitation, (3) the investigation of increased radial seal loading techniques, and (4) the investigation of stress relaxation in threaded connectors. In addition to a summary of the technical activities, the report contains the computer design program for flanged connectors, and designs for aluminum and stainless steel flanged connectors for pressures up to 1500 psi and for tube sizes through 16 inches. It is recommended that MS standards and specifications be prepared for cryogenic stainless steel and aluminum flanged connectors for tubing through 3 inches in diameter. Additional developmental work is recommended in regard to larger flanged connectors, and in regard to certain aspects of the stainless steel threaded connectors.

TABLE OF CONTENTS

TABLE OF CONTENTS
(Continued)

TABLE OF CONTENTS
(Continued)

LIST OF TABLES

LIST OF TABLES
(Continued)

LIST OF TABLES
(Continued)

LIST OF TABLES
(Continued)

LIST OF ILLUSTRATIONS

LIST OF ILLUSTRATIONS
(Continued)

LIST OF ILLUSTRATIONS
(Continued)

LIST OF ILLUSTRATIONS
(Continued)

LIST OF ILLUSTRATIONS
(Continued)

LIST OF ILLUSTRATIONS
(Continued)

ABBREVIATIONS AND SYMBOLS APPEARING IN REPORT BODY*

F_S	Radial sealing force per inch of seal disk circumference, lb/in.
F_T	Radial force per inch of seal tang outside circumference at the root of each seal disk, lb/in.
S_y	Material yield stress, psi
D_o	Seal disk outside diameter, in.
D_e	Seal tang outside diameter, in.
D_i	Seal tang inside diameter, in.
L	Seal tang length, in.
t	Seal tang thickness, in.
P_T	Pressure on outside seal tang circumference, psi
K	Dimensionless factor for relating seal tang length to seal tang inside diameter and seal tang thickness
S_a	Allowable stress at most severe operating condition, psi
P	Operating pressure, proof pressure, or burst pressure, psi
D	Tube outside diameter, in.
TAL	Connector design axial load, lb
PL	Pressure end load, lb
TBM	Tube bending moment, lb-in.
Z	Tube section modulus, $in.^3$
S_A	Minimum stress for calculating tube bending moment, psi
AL_B	Equivalent axial load, lb
S_B	Bending stress, psi
T	Tube-wall thickness, in.
MSL	Minimum residual seal load, lb
BL	Maximum allowable bolt load, lb

*Individual listings of abbreviations and symbols have been prepared for each Appendix, where applicable.

FS	Factor of safety
A_s	Bolt tensile stress area, $in.^2$
D_b	Basic bolt diameter, in.
S	Axial stress in bolt, in.
n	Number of threads per inch
T_o	Torque, lb-in.
R	Factor relating bolt torque, stress, and diameter
LT	Seal disk thickness, in.
DSA	Axial deflection rate of seal tang, in./lb
SEE	Modulus of elasticity of seal material, psi
σ_θ	Circumferential stress, psi
a	Inner seal tang radius, in.
b	Outer seal tang radius, in.
P_i	Internal pressure, psi
P_o	External pressure, psi
r	Location of stress, in.
ΔF_S	Radial seal load increment contributed by seal disk, lb/in.

DEVELOPMENT OF AFRPL FLANGED CONNECTORS FOR ROCKET FLUID SYSTEMS

by

T. M. Trainer, J. V. Baum, J. R. Thompson,
and N. D. Ghadiali

I

INTRODUCTION

In April, 1962, the Air Force Rocket Propulsion Laboratory initiated a program at Battelle's Columbus Laboratories to develop a family of separable fluid connectors capable of meeting the stringent requirements of present and future rocket propulsion systems. The primary objective of this program, Contract AF 04(611)-8176, was to design and evaluate lightweight mechanical connectors that could successfully seal helium to 2×10^{-7} atm cc/sec in missile-system environments. As a result of this program, connector design criteria were established, a unique Bobbin seal was conceived, and a threaded connector incorporating the Bobbin seal, for tubing sizes up to 1 inch, was designed and its feasibility demonstrated. This work is described in Technical Documentary Report No. RTD-TDR-63-1115, dated December 1963 (AD 426290).

A subsequent program, Contract AF 04(611)-9578, was initiated in December 1963, to design families of threaded-type tube connectors and to demonstrate their ability to meet the extreme requirements of missile fluid systems. Elbows, tees, crosses, and unions made from Type 347 stainless steel, René 41, and 6061-T6 aluminum were designed for standard tubing sizes ranging from 1/8 to 1 inch, and limited qualification tests were performed with selected connector configurations for 3/8- and 3/4-inch tubing systems. Preliminary MS standards and specifications were prepared for selected sizes of 4000-psi stainless steel connectors and 1000- and 750-psi aluminum connectors. This effort is described in Technical Documentary Report No. AFRPL-TR-65-162, dated November 1965 (AD 474789).

Two concurrent efforts were then initiated. In one effort, the Air Force Rocket Propulsion Laboratory reviewed the preliminary standards and specifications, purchased a number of 4000-psi stainless steel connectors, conducted qualification tests with many of the connectors, provided connectors to various facilities for evaluation, published MS standards and specifications,[1]* and conducted tests directed toward improving the sealing reliability of 3/4- and 1-inch stainless steel connectors. Concurrently, a three-phase program was conducted by Battelle-Columbus under Contract AF 04(611)-11204. Under Phase I, a number of procedures were investigated for achieving a softer sealing surface on 6061-T6 aluminum seals, and an overaging process was selected as being ideal for aluminum seals of all sizes. The Battelle work is described in Technical Documentary Report No. AFRPL-TR-67-191, dated July 1967 (AD 817843).

*MS Standards and Specifications and references are given on page 194.

Phase II, the major effort of Contract AF 04(611)-11204, was directed toward the development of flight-weight stainless steel and aluminum flanged-type separable connectors utilizing the Bobbin seal for tubing diameters from 1 through 16 inches. The activities included the investigation of promising types of flanged connectors; the design, fabrication, and qualification testing of selected connectors; and the preparation of specifications for families of stainless steel and aluminum connectors. Phase III included support for the work at the Rocket Propulsion Laboratory on threaded connectors, and the development of a modified threaded-connector configuration to provide seal retention and a limitation to the degree of misalignment that can be imparted to the connector during assembly. This report describes the work on Phases II and III under the following major headings:

FLANGED-CONNECTOR DESIGN

FLANGED-CONNECTOR EVALUATION

FLANGED-CONNECTOR SPECIFICATIONS

THREADED-CONNECTOR SUPPORT

II

FLANGED-CONNECTOR DESIGN

The flanged-connector-design work consisted of four major efforts: (1) the development of Bobbin seals for tubing sizes from 1 through 16 inches, (2) the investigation of flanged-connector-design criteria, (3) the development of a flanged-connector-design procedure, and (4) the design of representative connectors.

Design Requirements

As defined by the work statement, flanged connectors were to be designed for the following service ranges:

Size, inches	Pressure, psi	Temperature, F
1 to 3	0 to 6000	-423 to 200
1 to 3	0 to 4000	-423 to 600
1 to 16	0 to 1500	-423 to 200
1 to 16	0 to 1500	0 to 1200

The flanged connectors were to be designed for a 5-year storage requirement and for service with the following fluids:

Oxidizers	Fuels	Gases
N_2O_4	N_2H_4	Helium
H_2O_2	UDMH	Nitrogen
ClF_3	UDMH/NH (50/50)	Hot gas from bi-
F_2	MAF	propellant-, mono-
RFNA	MHF	propellant-, and
Compound "A"	MMH	solid-propellant
	H_2	gas generator

On the basis of the work with threaded connectors and the consideration of the tubing systems generally used in rocket propulsion systems, it was mutually agreed and specified in the contract work statement that the tubing materials of primary interest to the program were 6061-T6 aluminum and Type 347 stainless steel.

Development of Bobbin Seals for Large-Diameter Tubing

At the beginning of the program, a study was made to determine the best plating for stainless steel seals. Tentative dimensions for stainless steel and aluminum Bobbin seals were then established for typical large tubing sizes, on the basis of the design criteria developed previously for threaded connector seals. Seals of these dimensions were fabricated and tested, and seal-design formulas were developed for inclusion in the flange-connector-design computer program. The formulas were subsequently modified as a consequence of the qualification testing.

Sealing Principles of the Bobbin Seal

Figure 1 shows the configuration of a typical Bobbin seal and the four major stages of seal installation. First, the seal is positioned in the flange seal cavity. As the flange members are moved closer together, contact between the seal and the flanges is established at the edges of the seal disks. An increase in the axial force on the flanges causes the Belleville-type disks to rotate at the disk root radii and to take up the diametral clearance. Further deflection of the disks causes an interference fit at the sealing surfaces on the circumference of the seal disks, and as the deflection increases, the contact force on the sealing surfaces exceeds the compressive yield strength of the seal material and the ID of the seal becomes smaller. When the seal is fully assembled, the flanges bear against the seal tang, and continued application of the axial force needed for preloading is transmitted through the short cylindrical tang.

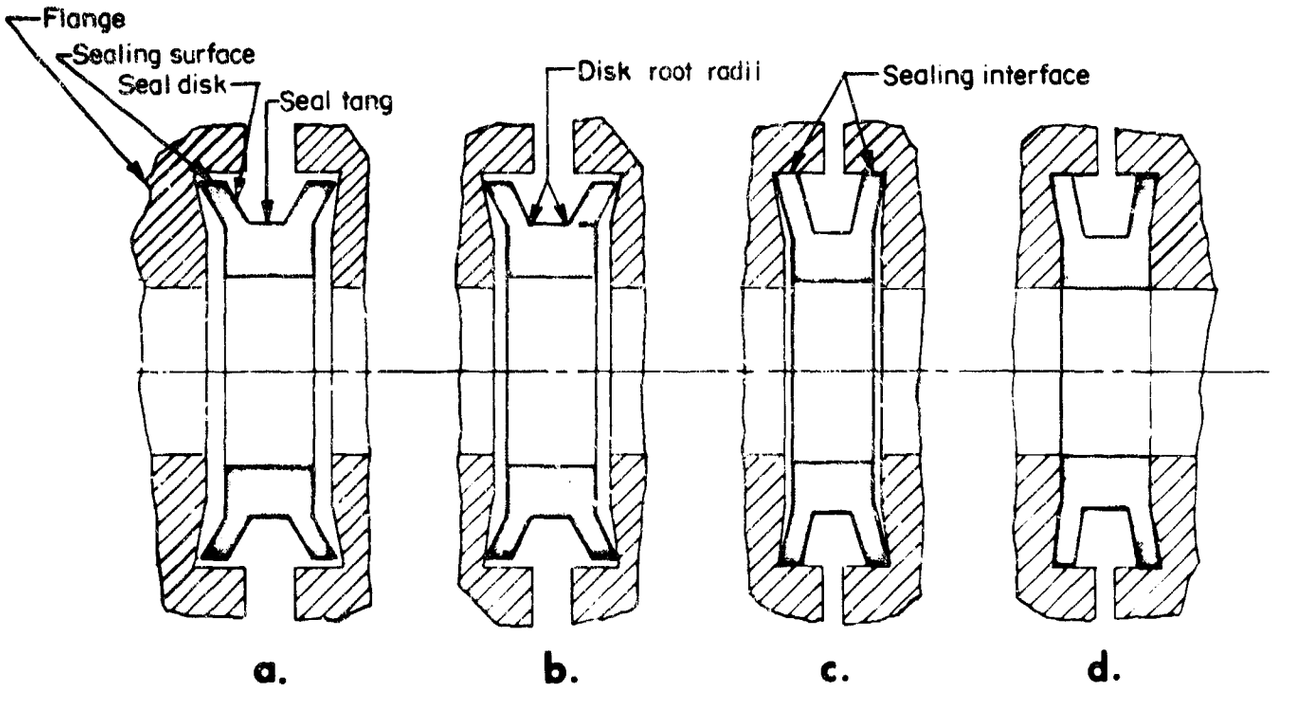

FIGURE 1. FOUR STAGES OF BOBBIN SEAL ASSEMBLY

Low helium leakage can be achieved reliably in a metal-to-metal seal only if plastic deformation is attained at the sealing interface. The disks of the Bobbin seal provide mechanical-force magnification to create a sufficient sealing stress to achieve plastic deformation at the interface while keeping the axial seal seating force to a minimum. Consequently a minimum-weight connector or housing can be obtained. The seal tang serves four important functions: (1) it resists the radial sealing force until the proper contact stress is established at the radial sealing interface; (2) it yields owing to the radial sealing force after the proper contact stress is reached, and, by yielding, maintains a relatively constant sealing contact stress as the flanges are brought into contact with the tang; (3) it facilitates the independent deflection and yielding of each seal disk, which may not occur simultaneously owing to variations in diametral clearance; and (4) it provides a loading path so that the connector is preloaded independently of the radial sealing force, and the force on the sealing surfaces is unaffected by changes in the external loads on the connector.

Corrosion Compatibility of Seal Plating Materials

The yield strength of the surface of the circumference of the seal disks determines the radial sealing force that must be developed. If possible, the basic seal material should be softer than the flange material, thus circumventing the cost and quality control problems associated with plating. This was accomplished for 6061-T6 aluminum connectors by the use of overaged 6061-T6 aluminum for the Bobbin seals. However, when both the seal and the flange materials are soft, as is the case with Type 347 stainless steel, or when a high-strength seal material is required, plating should be used on the seal.

Although soft nickel has been used almost exclusively as the plating material for stainless steel during the development of the AFRPL threaded and flanged connectors, nickel is not compatible with all missile fluids. Therefore, as a part of this program, a study was made to determine the optimum plating materials for stainless steel Bobbin seals for all typical missile fluid systems, and to consider the corrosion problems of the two structural materials of interest – 6061-T6 aluminum, and Type 347 stainless steel.

Table 1 is a list of candidate plating materials. In the first group are common materials for which considerable propellant-compatibility data exist. The second group comprises the precious metals for which some compatibility data exist. The third group consists of exotic metals for which little or no compatibility data exist.

TABLE 1. CANDIDATE METALS FOR PLATING STAINLESS STEEL BOBBIN SEALS

Metal	Hardness	Melting Point, F
	Group 1	
Nickel, ann.	64(a)	2635
Copper, ann.	40(a)	1980
Lead	4(a)	620
Tin, ann.	7(a)	450
	Group 2	
Gold, ann.	25(a)	1945
Silver, ann.	25-35(a)	1760
Platinum, ann.	38-52(a)	3225
Tantalum, ann.	150(b)	5425
	Group 3	
Palladium, ann.	40(b)	2825
Rhodium, ann.	122(b)	3560
Cerium	31(b)	1480
Lanthanum	51(b)	1690
Praseodymium	45(b)	1685

(a) Brinell Hardness Number.
(b) Vickers Hardness Number.

Preliminary Plating Selection. The following conclusions were reached during the initial stages of plating evaluation and selection:

(1) Tin appeared to be the only metal that might exhibit reasonable compatibility with all candidate propellants. However, its resistance to N_2O_4, H_2O_2, and F_2 is questionable, and it has a low melting point.

(2) Tantalum appeared to have excellent compatibility with all fuels and oxidizers except fluorine-containing oxidizers, but plating experience with tantalum is very limited.

(3) Copper, nickel, lead, and silver show poor compatibility with some of the candidate propellants. Only copper and nickel have outstanding compatibility in some propellants, and nickel is preferred over copper.

(4) Gold and platinum have good resistance to several fluids.

(5) The plating materials selected on the basis of the preliminary studies were: gold, platinum, and nickel.

Corrosion Resistance of Candidate Materials to Fluids. The corrosion ratings for the tentatively selected plating materials and for the materials of construction are given in Table 2. The fluids are separated in groups: oxidizers, propellants, and products of combustion. Specific compatibility data were not available for all metals exposed to all of the media in each temperature range. In some instances, the ratings in Table 2 are based on the performance of similar alloys, or the performance of the alloy in similar media. A combination of metal and environment is listed as questionable when insufficient data are available from which to make a good estimate or when there are discrepancies in the available data.

Nickel is suitable for chlorine and fluorine-containing media in the medium and upper temperature ranges, and for two of the hydrazine propellants. Nickel is not compatible with H_2O_2 or RFNA, and it is not compatible with the nitric acid formed in water-contaminated N_2O_4. Gold is compatible with RFNA and N_2O_4. However, no candidate plating material is compatible with H_2O_2, and all plating materials are questionable for N_2H_4, MMH, MAF, and MHF.

Aluminum (6061-T6) is compatible with all the fluids except HCl and possibly HF which are products of combustion. Use of aluminum is limited to 200 F systems. The compatibility of Type 347 stainless steel with most of the environments being considered is excellent. In the temperature range up to 200 F there exists a susceptibility to stress-corrosion cracking in environments containing chlorides. In the temperature range up to 600 F, stainless steel can handle the fluorine-containing fuels, but at higher temperatures these fluids are expected to cause rapid attack. However, since the connectors will be subjected to the medium and higher temperatures for only limited periods, the use of stainless steel should be satisfactory even at 1200 F.

Galvanic Attack. The problem of galvanic attack is particularly important because of the 5-year storage requirement. Various combinations of coatings and materials of construction were considered. In general, the use of aluminum seals in a stainless steel connector or of nonaluminum seals in an aluminum connector should be avoided because the galvanic couple will accelerate the corrosion of the aluminum. Of course, this is true only with those fluids that will serve as an electrolyte.

The galvanic couple created by Type 347 stainless steel in contact with nickel is not considered to be a significant factor affecting the 5-year-storage requirement. There is some doubt about the gold-stainless steel combination, although this combination should also be acceptable with fluids that do not act as electrolytes.

Conclusions. On the basis of the work conducted, it was concluded that nickel should be used if possible. Gold should be used when nickel is questionable and gold is acceptable. For those applications where neither plating is satisfactory, it will be necessary to use unplated stainless steel seals; this will result in some reduction in sealing reliability.

Preliminary Design of Large-Diameter Seals

The design of large-diameter Bobbin seals began with the consideration of Bobbin seal parameters based on work with threaded-connector seals. These parameters

TABLE 2. COMPATIBILITY OF TENTATIVELY SELECTED PLATING MATERIALS AND MATERIALS OF CONSTRUCTION WITH VARIOUS FLUID MEDIA

Temperature Range and Alloys	Oxidizers						Propellants							Gases and Products of Combustion							
	N_2O_4	H_2O_2	RFNA	F_2	ClF_3	ClF_5	N_2H_4	UDMH	50/50	MMH	MAF	MHF	H_2	H_2O	CO_2	CO	Cl_2	N_2	He	HF	HCl
-423 to 200 F																					
Nickel	C[a]	NC	NC	C	C	C	Q	C	C	Q	Q	Q	C	C	C	C	C	C	C	C	C
Gold	C	NC	C	C	C	C	Q	Q	C	Q	Q	Q	C	C	C	C	C	C	C	C	C
Platinum	C	NC	C	C	C	C	Q	Q	Q	Q	Q	Q	C	C	C	C	C	C	C	Q	NC
6061-T6 aluminum	C	C	C	C	C	C	C	C	C	C	C	C	C	C	C	C	C	C	C	C	NC
347 stainless steel	C	C	C	C	C	C	C	C	C	C	C	C	C	C	C	C	C	C	C	C	NC
-423 to 600 F																					
Nickel	Q[a]	a	a	C	C	C	a	a	a	a	a	a	C	C	C	C	C	C	C	Q	C
Gold	Q	a	a	NC	Q	Q	a	a	a	a	a	a	C	C	C	C	C	C	C	Q	C
Platinum	Q	a	a	NC	Q	Q	a	a	a	a	a	a	C	C	C	C	C	C	C	Q	C
347 stainless steel	Q	a	a	C	C	C	a	a	a	a	a	a	C	C	C	C	C	C	C	Q	NC
600 to 1200 F																					
Nickel	NC	a	a	C	C	C	a	a	a	a	a	a	C	C	C	C	C	C	C	Q	C
Gold	Q	a	a	NC	NC	NC	a	a	a	a	a	a	C	C	C	C	NC	C	C	Q	C
Platinum	Q	a	a	NC	NC	NC	a	a	a	a	a	a	C	C	C	C	NC	C	C	Q	C
347 stainless steel	NC	a	a	NC	NC	NC	a	a	a	a	a	a	C	C	C	C	NC	C	C	NC	NC

C = compatible
NC = not compatible
Q = questionable
a = media decomposes owing to temperature.
(a) The nitric acid formed by water contamination of N_2O_4 is corrosive to nickel.

included (see Figure 1) the disk root radii, the sealing interface, the disk proportions, the initial and final angles of the seal disks, and the seal tang dimensions.

Disk Root Radii. During the previous two contracts, two types of problems were encountered at the roots of the seal disks. For certain combinations of disk thickness and tang strength, the compressive load on the seal disks was sufficient to cause a slight bulging of material at the root of the seal disks as the disks were rotated during seal assembly. This bulging, which was noticed primarily with aluminum seals, prevented proper mating of the flanges with the seal tang for preloading. As summarized in Technical Documentary Report No. AFRPL-TR-67-191, this problem was solved for small-diameter aluminum seals by offsetting the seal disks slightly inward from the edges of the tang. This is illustrated in Figure 2. It was decided that this feature would be used in large aluminum and stainless steel seals. As shown in Figure 2, this offset required a second radius at the root of each seal disk.

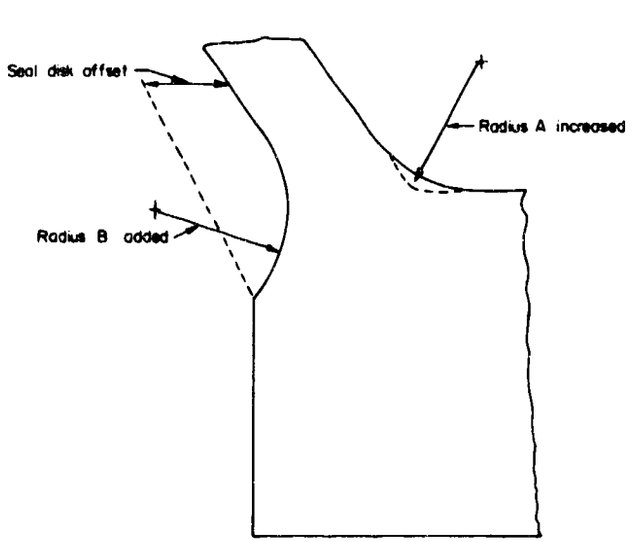

FIGURE 2. SELECTED MODIFICATIONS FOR SEAL DISK ROOTS

Another problem noted in the earlier work was the cracking of material at the inside corners of the seal disk roots. This seemed to be associated with the sharpness of the inside root radii, and the problem was overcome in small-diameter seals by making these radii larger, as shown in Figure 2. This approach was also selected for inclusion in the large-diameter seals.

Sealing Interface. As indicated in Figure 3, the initial contact at the seal interface occurs at the edge of the seal disk along a relatively narrow surface. Moreover, because of the rotation of the sealing disk, Angle B diverges, thus tending to reduce the contact surface even further. In the small-diameter seals, the potential problem of a narrow sealing surface is overcome because the interacting stresses and plastic-deformation mechanism in these seal sizes causes the edge of the seal disk to deform in such a way that the seal surface width is increased. Figure 4 shows a typical seal interface for small-diameter seals. The deformation mechanism is the same for plated and unplated seals.

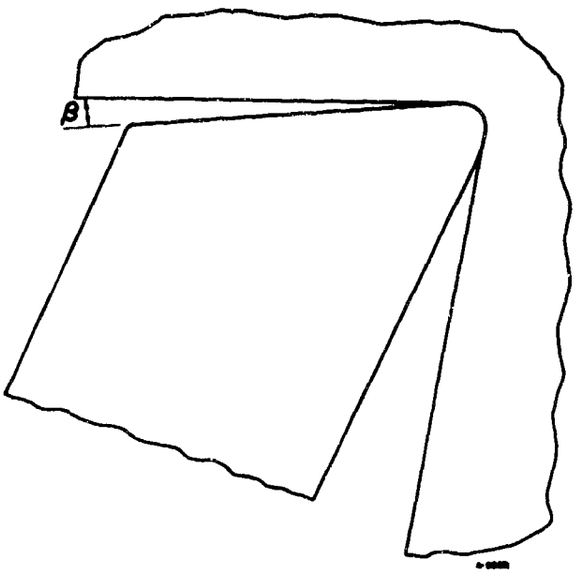

FIGURE 3. SEAL INTERFACE AT MOMENT OF CONTACT

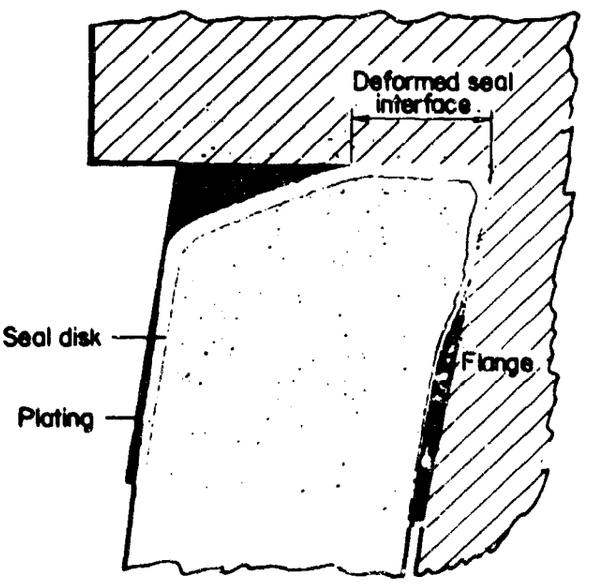

FIGURE 4. TYPICAL SEAL INTERFACE FOR SMALL-DIAMETER SEALS

Because it was expected that the disks of large-diameter seals would be designed to provide the same radial force per inch of seal circumference as the small seals, the cross sections of the disks were expected to be similar, and it was believed that the large seal disks would deform in a manner similar to that of the disks of the small-diameter seals. However, during the preparation of the proposal for this contract, it was found that the disks of tentative 6-inch seals did not deform at the edges, and a very narrow sealing surface resulted. This action was confirmed during Phase II of this program by the fabrication and assembly of tentative 3-inch stainless steel seals. Although the reason for this change in seal disk deformation was not known, it was assumed to be characteristic of large-diameter seals and was believed to be associated with the radius of curvature of the seal disks.

Two means were considered for achieving an increase in seal width for large-diameter seals. The first, an increase in radial force per inch of seal circumference, produced no significant change in seal disk deformation. The second is illustrated in Figure 5. Geometric analysis showed that the seal disk rotated approximately 6 degrees while the diametral clearance was being overcome. It was hypothesized that if the eventual sealing surface on each seal disk were machined with a reverse angle of 8 to 10 degrees as shown in Figure 5a, the flange and seal disk sealing surfaces at the moment of initial contact would be similar to that shown in Figure 5b. As assembly of the seal was continued, it was believed that the angle between the sealing surfaces would decrease to approximately 0 degrees, and that the high radial sealing force during the final stages of assembly would be sufficient to maintain seal contact across the entire disk sealing surface.

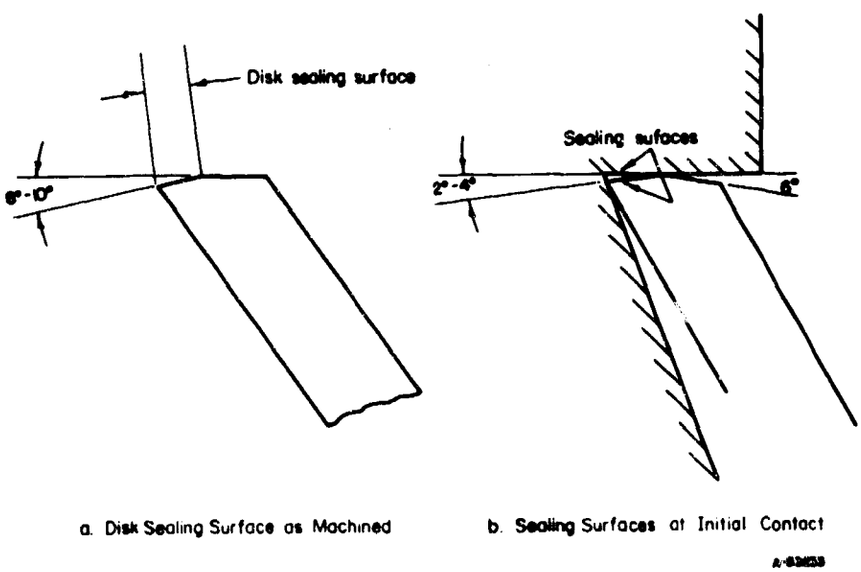

a. Disk Sealing Surface as Machined b. Sealing Surfaces at Initial Contact

FIGURE 5. MODIFICATION OF DISK SEALING SURFACE

(See Figure 3 for initial configuration.)

Stainless steel seals were fabricated according to the preliminary 3-inch design shown in Figure 6. Examinations of cross sections of assembled seals (Figure 7) showed that the seal interface was approximately 0.017 inch and that no cracking

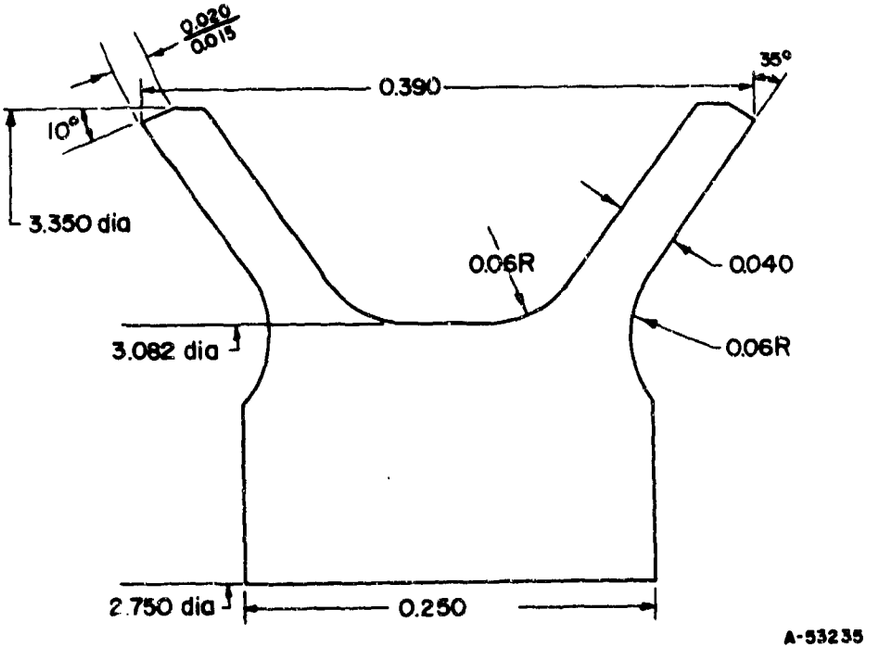

FIGURE 6. PRELIMINARY DESIGN OF 3-INCH SEAL

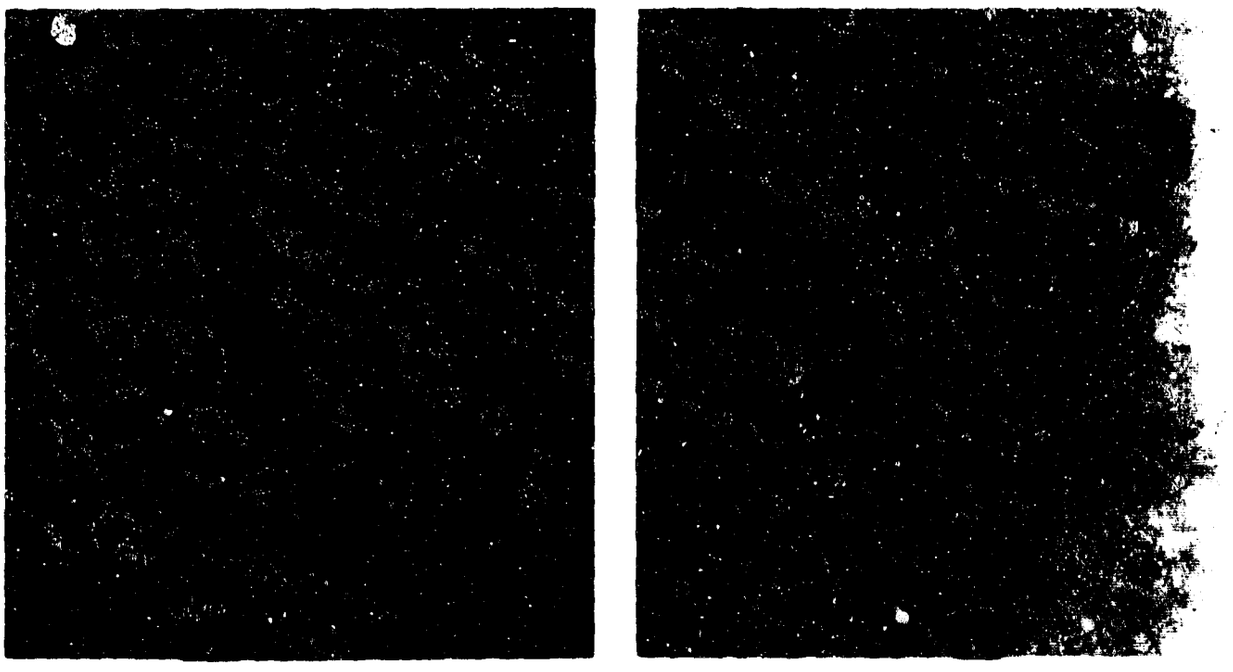

100X 2A867 100X 2A866

a. Sealing Surface 1 b. Sealing Surface 2

FIGURE 7. PHOTOMICROGRAPHS OF SEALING INTERFACE OF PRELIMINARY 3-INCH SEAL

occurred at the inner disk root radii. The results were sufficiently conclusive to warrant incorporation of the reverse-angle feature for large-diameter seals.

As described in Technical Documentary Report No. AFRPL-TR-67-191, the reverse-angle feature was investigated as a means of possible improvement of the sealing action of small-diameter aluminum seals. Since no change in seal interface or sealing action could be observed, it was decided to omit this extra machining operation for seals for threaded connectors. However, the reverse-angle feature proved to be effective in helping to achieve satisfactory assembly of misaligned flanged connectors. Thus, if the misalignment-limitation feature developed during Phase III of this program and described in this report is not sufficient to prevent misalignment problems, the reverse-angle feature might still be desirable for seals for threaded connectors.

Disk Proportions and Initial and Final Disk Angles. The selection of the proportions and of the initial and final angles for the seal disks is determined by a number of factors; the most important are the available axial force, the manufacturing tolerances to be accommodated, and the deformation characteristics of the metal. For the larger threaded connector seals, it was found that desirable values for the disk dimensions were: (1) initial disk angle, 30 degrees, (2) final disk angle, 10 degrees, (3) seal disk thickness, 0.027 inch, and (4) seal disk length, 0.090 inch. Although no change in radial force per inch of seal circumference was anticipated for the large-diameter seals, it was realized that the larger machining tolerances associated with the larger diameters required additional consideration of the disk proportions and angles.

Consideration of the initial disk angle led to the conclusion that an increase from 30 to 35 degrees would be desirable for the large-diameter seals. The 35 degrees was not believed to be too steep to prevent proper toggling action of the seal disks during assembly, and a 20-degree rotation from 35 degrees would provide a 33 percent greater diametral change than would a 20-degree rotation from 30 degrees. While this change in initial seal disk angle would increase the axial force required to seat the seal, the seal seating force needed in large-diameter connectors was estimated to be much less than the preload force needed to resist pressure and structural loading. (In contrast, for the smaller threaded connectors, the seal seating force was a significant percent of the required preload.) Satisfactory assembly was achieved with the 35-degree initial angle on the 3-inch seal design shown in Figure 6.

Although the best length of seal disk was difficult to estimate, it was apparent that the 0.027-inch thickness used on the small-diameter seals would be difficult to machine in large diameters. Consequently, the disk thickness was increased to 0.040 inch. On the basis of general disk proportions and machining tolerances, the following approximate disk lengths were selected: (1) 0.165 inch for tubing through 9 inches in diameter, (2) 0.230 inch for tubing through 12 inches in diameter, and (3) 0.305 inch for tubing through 16 inches in diameter. As described later, these dimensions were subsequently revised as a result of the qualification tests.

Seal Tang Dimensions. As described in Technical Documentary Report No. AFRPL-TR-65-162, the deformation mechanism of the Bobbin seal is a complex combination of elastic and plastic strains in the axial as well as the radial direction. Because the development of an accurate theoretical strain analysis would have been very costly, the design of threaded connector seals was based on a combination of theoretical and experimental information. It was decided that the same method would be used to establish tang dimensions for the large-diameter seals.

The design approach used for the threaded- and flanged-connector seal tangs began with the following steps:

(1) The radial sealing force per inch of seal disk circumference, F_S, was selected as 600 lb/in. (a discussion of this value is given on page 165).

(2) The radial force per inch of outside seal tang circumference, F_T, at the root of each seal disk due to F_S varies as a ratio of seal disk outside diameter, D_o, to seal tang outside diameter, D_e, viz.,

$$F_T = F_S D_o/D_e . \tag{1}$$

(3) The radial force per inch of seal tang outside circumference from the two seal disks, $2F_T$, can be equated to a pressure, P_T, on the outside circumference of the seal tang (this assumes that the effect of the two disk forces is distributed evenly across the short seal tang length)

$$P_T = 2F_T/L , \tag{2}$$

where L = seal tang length.

(4) The pressure needed to produce a totally plastic state in the seal tang[2] is

$$P_T = \frac{2}{\sqrt{3}} S_y C \ln (D_e/D_i) = 2F_T/L , \tag{3}$$

where

S_y = seal material yield stress, psi

C = 0.72 [from calculations by Beliaev and Sinitskii[3]]

D_i = seal tang inside diameter, in.

D_e = seal tang outside diameter, in.

Thus, for a given inside or outside tang diameter and a given seal material yield strength, Equation (3) can be used to establish a number of seal tang dimensions that will produce the desired radial force per inch on the outside circumference of the seal tang.

The tang of the 3-inch seal shown in Figure 6 was established by using Equation (3) and by selecting the tang inside diameter to be approximately the same as the inside diameter for heavy wall tubing. Examination of the microsections, shown in Figure 7, showed that the nickel plating was less deformed than expected. However, it was decided that this basis of calculation should be used until more experimental data could be obtained.

Because it was not clear whether the optimum seal width of 0.020 inch (see page 165) could be achieved in the large-diameter seals, tentative tang dimensions were calculated for two widths of sealing surfaces, 0.015 and 0.020 inch. Also, in

anticipation that a higher strength material might be required to keep the large-diameter seals sufficiently small in cross section, tang dimensions were calculated for three typical yield-stress levels of candidate seal materials. The results of these calculations for three typical seal sizes are shown in Table 3.

TABLE 3. TENTATIVE TANG DIMENSIONS FOR THREE TYPICAL SEAL SIZES

Yield Strength of Seal Material, S_y, psi	Width of Sealing Surface, in.	Tang Inside Diameter, D_i, in.	Tang Outside Diameter, D_e, in.	Seal Disk Outside Diameter, D_o, in.	Tang Length, L, in.
30,000	0.020	1.800	2.230	2.500	0.120
		3.585	4.430	4.700	0.410
		7.450	8.730	9.000	0.690
	0.015	1.900	2.230	2.500	0.165
		3.800	4.430	4.700	0.305
		7.745	8.730	9.000	0.525
60,000	0.020	2.000	2.230	2.500	0.110
		4.000	4.430	4.700	0.215
		8.070	8.730	9.000	0.330
	0.015	2.060	2.230	2.500	0.085
		4.100	4.430	4.700	0.165
		8.230	8.730	9.000	0.255
90,000	0.020	2.065	2.230	2.500	0.083
		4.140	4.430	4.700	0.145
		8.275	8.730	9.000	0.228
	0.015	2.115	2.230	2.500	0.058
		4.200	4.430	4.700	0.115
		8.395	8.730	9.000	0.168

In addition, the graphs shown in Figures 8 and 9 were prepared using the above mathematical analysis. From Figure 8 it can be seen that for a small tang length, the use of a material with a yield strength of 60,000 to 90,000 psi will greatly reduce the size and weight of the larger seals and the size and weight of the larger connectors. It can be seen from Figure 9 that an increase in seal tang length results in a reduction in the outside diameter of the seal, thus reducing the diameter and weight of the connector. However, the weight of the seal remains high if a material yield strength of 30,000 psi is used. Further, if the L/t ratio for the tang is too great, the assumption that the radial disk forces can be equated to a uniform external pressure on the tang is no longer valid. A judgmental compromise between a reduction in tang thickness and a limitation on tang length was approximated by the expression:

$$L = K\,(tD_i)^{1/2}, \qquad (4)$$

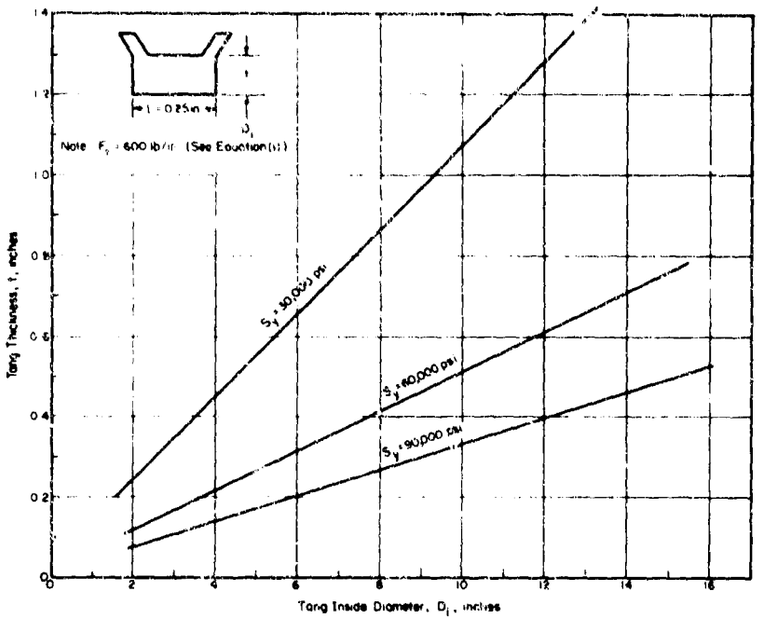

FIGURE 8. TANG THICKNESS VERSUS TANG INSIDE DIAMETER FOR A SMALL TANG LENGTH AND THREE SEAL-MATERIAL YIELD STRENGTHS

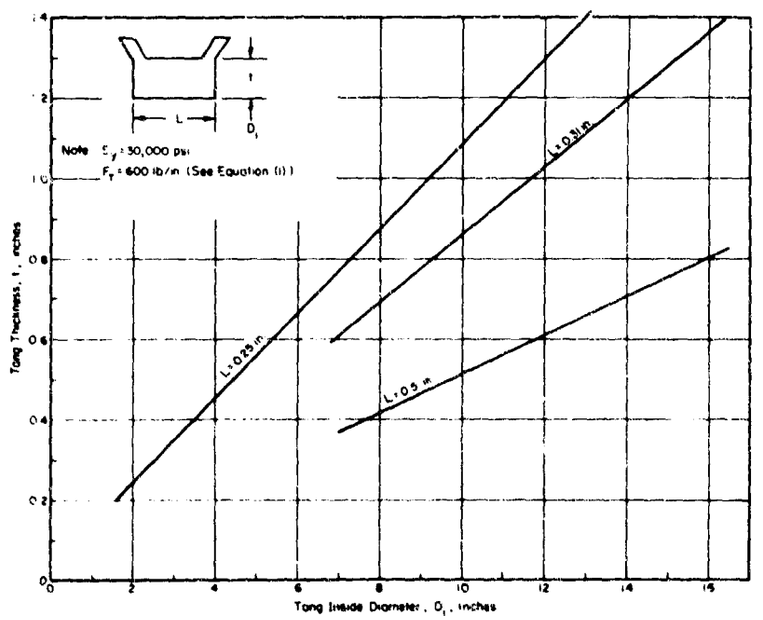

FIGURE 9. TANG THICKNESS VERSUS TANG INSIDE DIAMETER FOR THREE TANG LENGTHS

where

L = tang length, in.

K = 0.250

t = tang thickness, in.

D_i = inside tang diameter, in.

Equations (3) and (4) form a set of simultaneous equations which can be solved through iteration on a digital computer. The tang calculations for typical yield-strength values are shown in Table 4.

As the program developed, it became increasingly obvious that the seal tang would often have to be as long as possible to achieve the lightest connector. The reduction in tang thickness as a function of an increase in tang length was computed by increasing K in Equation 4. These data are shown in Table 5. To investigate the practical limits of seal tang length, seals were fabricated from overaged aluminum and from Type 304 stainless steel for the 2- and 4-inch sizes with various L/t ratios. Assembly data for these seals are given in Table 6.

Examination of the microsections of the stainless steel seals showed that bowing of the tang was negligible at an L/t ratio of less than 2.5 for 2-inch seals and 3.5 for 4-inch seals. Typical cross sections are shown in Figures 10, 11, and 12. The bowing in the 2-inch seal even at an L/t ratio of 3.80 was not too great. Although the aluminum seals did not deform uniformly because of faulty material, it was apparent that an L/t ratio of 3.50 would be satisfactory.

On the basis of the L/t tests, it was concluded that the tang could be designed with a maximum L/t ratio of 3.50 for seal sizes at least as large as 4 inches, and probably larger. However, it was decided that a tang thickness equal to the tube wall thickness would be specified, except for thin-wall tubing (low pressure systems) and for L/t ratios greater than 3.50.

Evaluation of Preliminary Large-Diameter Seals

Preliminary, representative large-diameter seals were evaluated by deformation and leakage tests using techniques formulated during the development of threaded-connector seals.

Deformation Evaluation of 2- and 4-Inch-Diameter Seals. During work with seals for threaded connectors, it was found that the sealing capabilities of the seals could be reasonably estimated by means of the maximum axial loads needed to assemble the seals, and by examinations of cross sections of the seal interface (for example, see Figure 7). Similar studies were made with 2- and 4-inch nickel-plated austenitic stainless steel seals with dimensions approximately those shown for a material yield stress of 30,000 psi in Table 3. The actual tang dimensions, the peak axial loads required to assemble each seal, and the calculated minimum force per inch of seal circumference are shown in Table 7.

TABLE 4. COMPUTED DIMENSIONS OF SEAL TANGS FOR K = 0.25
FOR DIFFERENT SEAL-MATERIAL YIELD STRENGTHS

D_i, in.	S_y, psi	D_e, in.	L, in.
1.0000	30000.0000	1.4457	0.1305
1.0000	40000.0000	1.3646	0.1161
1.0000	50000.0000	1.3122	0.1062
1.0000	60000.0000	1.2752	0.0989
1.0000	70000.0000	1.2475	0.0932
1.0000	80000.0000	1.2258	0.0886
1.0000	90000.0000	1.2082	0.0848
1.0000	100000.0000	1.1937	0.0815
2.0000	30000.0000	2.5505	0.1978
2.0000	40000.0000	2.4515	0.1772
2.0000	50000.0000	2.3874	0.1630
2.0000	60000.0000	2.3420	0.1523
2.0000	70000.0000	2.3079	0.1440
2.0000	80000.0000	2.2811	0.1371
2.0000	90000.0000	2.2595	0.1314
2.0000	100000.0000	2.2416	0.1265
3.0000	30000.0000	3.6247	0.2543
3.0000	40000.0000	3.5131	0.2285
3.0000	50000.0000	3.4406	0.2106
3.0000	60000.0000	3.3893	0.1971
3.0000	70000.0000	3.3506	0.1865
3.0000	80000.0000	3.3202	0.1778
3.0000	90000.0000	3.2957	0.1706
3.0000	100000.0000	3.2754	0.1643
4.0000	30000.0000	4.6841	0.3047
4.0000	40000.0000	4.5623	0.2743
4.0000	50000.0000	4.4832	0.2531
4.0000	60000.0000	4.4270	0.2371
4.0000	70000.0000	4.3847	0.2245
4.0000	80000.0000	4.3515	0.2142
4.0000	90000.0000	4.3246	0.2055
4.0000	100000.0000	4.3023	0.1980
5.0000	30000.0000	5.7344	0.3510
5.0000	40000.0000	5.6040	0.3163
5.0000	50000.0000	5.5192	0.2921
5.0000	60000.0000	5.4589	0.2739
5.0000	70000.0000	5.4135	0.2594
5.0000	80000.0000	5.3779	0.2475
5.0000	90000.0000	5.3491	0.2376
5.0000	100000.0000	5.3251	0.2290
6.0000	30000.0000	6.7785	0.3943
6.0000	40000.0000	6.6405	0.3557
6.0000	50000.0000	6.5567	0.3286
6.0000	60000.0000	6.4969	0.3082
6.0000	70000.0000	6.4508	0.2920
6.0000	80000.0000	6.4011	0.2788
6.0000	90000.0000	6.3705	0.2676
6.0000	100000.0000	6.3461	0.2580
7.0000	30000.0000	7.8180	0.4352
7.0000	40000.0000	7.6732	0.3929
7.0000	50000.0000	7.5790	0.3632
7.0000	60000.0000	7.5120	0.3407
7.0000	70000.0000	7.4614	0.3229
7.0000	80000.0000	7.4218	0.3083
7.0000	90000.0000	7.3896	0.2960
7.0000	100000.0000	7.3630	0.2854
8.0000	30000.0000	8.8540	0.4742
8.0000	40000.0000	8.7030	0.4283
8.0000	50000.0000	8.6047	0.3961
8.0000	60000.0000	8.5347	0.3717
8.0000	70000.0000	8.4820	0.3523
8.0000	80000.0000	8.4406	0.3364
8.0000	90000.0000	8.4071	0.3230
8.0000	100000.0000	8.3792	0.3115
9.0000	30000.0000	9.8871	0.5117
9.0000	40000.0000	9.7304	0.4623
9.0000	50000.0000	9.6283	0.4276
9.0000	60000.0000	9.5557	0.4014
9.0000	70000.0000	9.5010	0.3805
9.0000	80000.0000	9.4579	0.3634
9.0000	90000.0000	9.4231	0.3490
9.0000	100000.0000	9.3942	0.3366
10.0000	30000.0000	10.9179	0.5477
10.0000	40000.0000	10.7558	0.4951
10.0000	50000.0000	10.6503	0.4581
10.0000	60000.0000	10.5752	0.4300
10.0000	70000.0000	10.5186	0.4077
10.0000	80000.0000	10.4741	0.3894
10.0000	90000.0000	10.4380	0.3740
10.0000	100000.0000	10.4081	0.3607
11.0000	30000.0000	11.9467	0.5826
11.0000	40000.0000	11.7767	0.5268
11.0000	50000.0000	11.6709	0.4875
11.0000	60000.0000	11.5934	0.4577
11.0000	70000.0000	11.5350	0.4340
11.0000	80000.0000	11.4891	0.4146
11.0000	90000.0000	11.4520	0.3982
11.0000	100000.0000	11.4211	0.3841
12.0000	30000.0000	12.9738	0.6164
12.0000	40000.0000	12.8021	0.5575
12.0000	50000.0000	12.6902	0.5160
12.0000	60000.0000	12.6106	0.4846
12.0000	70000.0000	12.5505	0.4595
12.0000	80000.0000	12.5033	0.4390
12.0000	90000.0000	12.4651	0.4216
12.0000	100000.0000	12.4334	0.4067
13.0000	30000.0000	13.9995	0.6493
13.0000	40000.0000	13.8233	0.5874
13.0000	50000.0000	13.7086	0.5438
13.0000	60000.0000	13.6268	0.5107
13.0000	70000.0000	13.5652	0.4844
13.0000	80000.0000	13.5168	0.4627
13.0000	90000.0000	13.4775	0.4445
13.0000	100000.0000	13.4449	0.4288
14.0000	30000.0000	15.0239	0.6814
14.0000	40000.0000	14.8435	0.6166
14.0000	50000.0000	14.7260	0.5708
14.0000	60000.0000	14.6423	0.5361
14.0000	70000.0000	14.5791	0.5085
14.0000	80000.0000	14.5295	0.4858
14.0000	90000.0000	14.4893	0.4667
14.0000	100000.0000	14.4559	0.4502
15.0000	30000.0000	16.0472	0.7127
15.0000	40000.0000	15.8628	0.6456
15.0000	50000.0000	15.7426	0.5973
15.0000	60000.0000	15.6570	0.5610
15.0000	70000.0000	15.5924	0.5322
15.0000	80000.0000	15.5417	0.5084
15.0000	90000.0000	15.5006	0.4884
15.0000	100000.0000	15.4664	0.4712
16.0000	30000.0000	17.0695	0.7434
16.0000	40000.0000	16.8812	0.6729
16.0000	50000.0000	16.7585	0.6231
16.0000	60000.0000	16.6711	0.5853
16.0000	70000.0000	16.6052	0.5553
16.0000	80000.0000	16.5533	0.5305
16.0000	90000.0000	16.5113	0.5097
16.0000	100000.0000	16.4765	0.4917

TABLE 5. COMPUTED DIMENSIONS OF SEAL TANGS FOR D_i = 1 THROUGH 8 INCHES USING DIFFERENT VALUES OF K (S_y = 30,000 PSI)

D_i, in.	D_e, in.	L, in.	K
1	1.4460	0.1306	0.2500
2	2.5509	0.1979	0.2500
3	3.6251	0.2544	0.2500
4	4.6846	0.3048	0.2500
5	5.7349	0.3511	0.2500
6	6.7791	0.3944	0.2500
7	7.8186	0.4354	0.2500
8	8.8546	0.4744	0.2500
1	1.3837	0.1482	0.3100
2	2.4750	0.2260	0.3100
3	3.5395	0.2911	0.3100
4	4.5912	0.3493	0.3100
5	5.6349	0.4028	0.3100
6	6.6732	0.4528	0.3100
7	7.7074	0.5000	0.3100
8	8.7388	0.5451	0.3100
1	1.3331	0.1675	0.3800
2	2.4130	0.2565	0.3800
3	3.4695	0.3311	0.3800
4	4.5147	0.3978	0.3800
5	5.5530	0.4590	0.3800
6	6.5865	0.5162	0.3800
7	7.6164	0.5704	0.3800
8	8.6439	0.6220	0.3800
1	1.3009	0.1830	0.4400
2	2.3735	0.2812	0.4400
3	3.4249	0.3635	0.4400
4	4.4660	0.4370	0.4400
5	5.5007	0.5045	0.4400
6	6.5312	0.5676	0.4400
7	7.5584	0.6273	0.4400
8	8.5833	0.6842	0.4400
1	1.2754	0.1979	0.5000
2	2.3423	0.3048	0.5000
3	3.3895	0.3944	0.5000
4	4.4273	0.4744	0.5000
5	5.4593	0.5479	0.5000
6	6.4872	0.6167	0.5000
7	7.5123	0.6817	0.5000
8	8.5351	0.7436	0.5000

D_i, in.	D_e, in.	L, in.	K
1	1.2547	0.2122	0.5600
2	2.3168	0.3274	0.5600
3	3.3607	0.4241	0.5600
4	4.3957	0.5104	0.5600
5	5.4254	0.5897	0.5600
6	6.4514	0.6638	0.5600
7	7.4744	0.7339	0.5600
8	8.4958	0.8007	0.5600
1	1.2375	0.2260	0.6200
2	2.2956	0.3493	0.6200
3	3.3366	0.4528	0.6200
4	4.3694	0.5451	0.6200
5	5.3972	0.6299	0.6200
6	6.4214	0.7093	0.6200
7	7.4432	0.7843	0.6200
8	8.4630	0.8558	0.6200
1	1.2206	0.2415	0.6900
2	2.2748	0.3734	0.6900
3	3.3131	0.4850	0.6900
4	4.3434	0.5842	0.6900
5	5.3695	0.6753	0.6900
6	6.3921	0.7605	0.6900
7	7.4124	0.8411	0.6900
8	8.4308	0.9179	0.6900
1	1.2084	0.2544	0.7500
2	2.2597	0.3944	0.7500
3	3.2959	0.5118	0.7500
4	4.3248	0.6167	0.7500
5	5.3493	0.7130	0.7500
6	6.3707	0.8031	0.7500
7	7.3899	0.8883	0.7500
8	8.4074	0.9695	0.7500

TABLE 6. ASSEMBLY DATA FOR STAINLESS STEEL AND ALUMINUM SEALS WITH DIFFERENT L/t RATIOS

Seal Size and Material	Specimen	Tang Thickness, t, in.	Tang Length, L, in.	L/t Ratio	Axial Force, lb		Axial Seating Force (Peak 1) per Inch of Seal Circumference, lb/in.
					Peak 1	Peak 2	
2-in. aluminum	1	0.229	0.215	0.939	5,676	6,000	708
	2	0.199	0.239	1.201	5,496	5,880	688
	3	0.179	0.270	1.508	5,760	5,784	720
	4	0.154	0.296	1.922	5,460	5,520	682
	5	0.130	0.322	2.477	5,124	5,488	642
	6	0.102	0.352	3.451	4,584	4,872	572
4-in. aluminum	7	0.306	0.332	1.084	9,960	10,200	702
	12	0.123	0.538	4.374	7,560	8,400	532
2-in. stainless	13	0.235	0.213	0.906	7,560	-	932
	14	0.200	0.246	1.230	7,120	7.200	880
	15	0.180	0.269	1.494	7,475	7,800	922
	16	0.153	0.294	1.922	7,080	7,200	872
	17	0.128	0.318	2.484	6,730	6,820	830
	18	0.098	0.378	3.857	6,240	6,480	770
4-in. stainless	19	0.268	0.330	1.231	11,000	11,500	775
	20	0.230	0.380	1.652	11,400	11,750	803
	21	0.205	0.414	2.020	10,750	10,650	758
	22	0.173	0.454	2.624	10,250	11,600	723
	23	0.138	0.494	3.580	10,000	10,450	704
	24	0.101	0.541	5.350	9,000	9,200	633

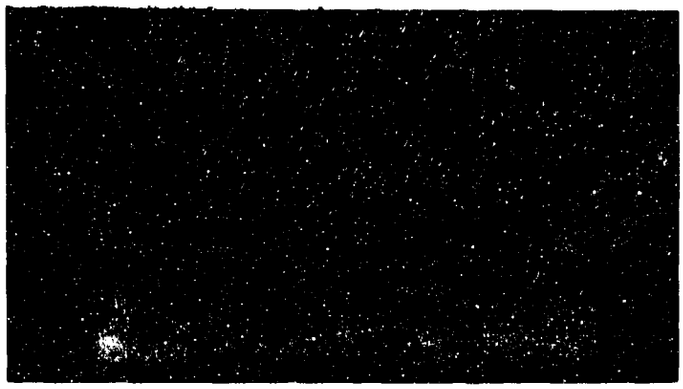

9A681

FIGURE 10. 2-INCH STAINLESS STEEL SEAL

L/t = 3.857

9A684

FIGURE 11. 4-INCH STAINLESS STEEL SEAL

L/t = 3.580

9A685

FIGURE 12. 4-INCH STAINLESS STEEL SEAL

L/t = 5.35

TABLE 7. DIMENSIONS AND MAXIMUM AXIAL ASSEMBLY FORCES FOR NICKEL-PLATED STAINLESS STEEL SEALS

Specimen	Seal Outside, Diam., D_o, in.	Tang Inside Diam., D_i, in.	Tang Thickness, t, in.	Axial Force, lb		Axial Seating Force (Peak 1) per Inch of Seal Circumference, lb/in.
				Peak 1	Peak 2	
1	2.505	1.920	0.155	5,225	5,775	734
2	2.508	1.820	0.205	6,975	7,725	980
3	4.709	4.020	0.205	8,250	10,350	700
4	4.709	3.820	0.305	7,950	10,000	676
5	4.700	3.622	0.405	10,800	13,250	897

The maximum axial forces per inch of seal circumference corresponded well with the forces required on threaded-connector seals to seal helium to 10^{-7} atm cc/sec. Examination of the seal interfaces for the different specimens led to the following conclusions:

(1) Except for Specimen 1, all seals had a seal interface width close to 0.020 inch (all specimens had a sealing surface machined on a 10-degree reverse angle on each seal disk).

(2) A higher force per inch of seal circumference resulted in Specimen 2 having a better seal interface than Specimen 1.

(3) A higher force per inch of seal circumference resulted in Specimen 5 having a better seal interface than Specimens 3 and 4.

Leakage Evaluation of 2-, 4-, 8-, 12-, and 16-Inch-Diameter Seals. Because of the promising results of the deformation tests with the 2- and 4-inch-diameter seals, the decision was made to conduct leakage tests with representative seals. Overaged aluminum was selected as the seal material for major use because it is easily machined, it requires no plating, and its sealing action is believed to be similar to that of nickel-plated stainless steel. The dimensions for 4-, 8-, 12-, and 16-inch-diameter seals and the seal seating forces are given in Table 8.

The peak seal seating forces per inch of seal circumference were almost 50 percent greater than the average 450 lb/in. of seal circumference achieved for aluminum seals for threaded connectors. Unfortunately, the construction of the leakage test fixture did not provide for adequate restraint of the deflection of the fixture because of pressure end loads. However, on the basis of the adequate sealing of the seals up to the different pressures (2000 psi maximum) at which deflection caused leakage, it was concluded that the seals were satisfactory. It was also decided that the higher axial force per inch of seal circumference (750 lb/in.) would be retained for the aluminum seals for flanged connectors.

TABLE 8. DIMENSIONS OF ALUMINUM SEALS FOR LEAKAGE TESTS

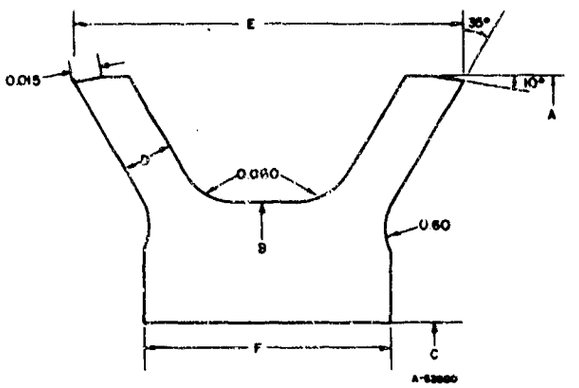

Tube Diameter	A +.000 -.002	B +.000 -.002	C +.002 -.000	D ± .002	E	F ± .002	Peak Axial Force, lb	Axial Force per Inch of Seal Circumference, lb/in.
4	4.708	4.440	3.760	0.040	0.480	0.290	9,050	612
8	9.008	8.740	7.900	0.040	0.660	0.470	14,750	522
12	11.998	11.625	10.685	0.060	0.830	0.570	29,300	778
16	15.998	15.500	14.325	0.060	0.958	0.608	35,600	708

Note: All dimensions in inches.

Because soft nickel plating has approximately one-third the yield strength of aluminum, and because nickel-plated stainless steel seals were apparently performing satisfactorily in threaded connectors with a design axial seal seating force of 600 lb/in. of seal circumference, a design value of 750 lb/in. of seal circumference was also selected for stainless steel seals for flanged connectors. A 2-inch nickel-plated stainless steel seal with a measured peak axial seal seating force of 768 lb/in. of seal circumference gave a leak rate of 6.6×10^{-9} atm cc/sec with a helium pressure of 2000 psi.

Determination of Minimum Seal Load. The design of the Bobbin seal substantially separates the axial preload from the radial sealing load. However, some residual axial load is required and tests were conducted with aluminum seals to determine the reduction in axial seal load that could be tolerated without excessive seal leakage. Representative overaged 6061 aluminum seals were assembled and pressurized with helium at 2000 psi. An initial preload equal to the pressure end load plus one-half the seal seating load was applied. Once a leakage rate (Column 4 in Table 9) was established, the applied external load was decreased in increments until the leakage rate exceeded the allowable limit. The difference between the threshold load (Column 5) and the pressure end load was the minimum axial seal load.

For the 2-inch seal, the minimum axial seal load was 31 percent of the seal seating load, whereas for the 6- and 8-inch seals, the minimum loads were 45 and 41 percent, respectively. In the case of the 4-inch seal, the external load was actually less than the pressure end load before an increase in leakage rate could be detected. As a general

rule for designing the connector, it was decided that the residual axial load should not be less than 50 percent of the axial seal seating load.

TABLE 9. MINIMUM AXIAL SEAL SEATING LOADS FOR ALUMINUM SEALS

Nominal Seal Size, in.	Axial Seal Seating Load, lb.	Total Initial Axial Load, lb	Initial Leakage Rate at 2000 Psi, atm cc/sec/in. of seal circumference	Load at Allowable Leakage Rate, lb	Pressure End Load, lb.	Minimum Axial Seal Load, lb
2	5,500	11,650	9.3×10^{-10}	10,600	8,900	1700
4	9,500	36,250	4.6×10^{-10}	28,500	31,200	-2700(a)
6	13,500	73,000	3.2×10^{-8}	70,000	64,000	6000
8	16,000	134,000	2.2×10^{-10}	119,000	112,400	6600

(a) This value indicates that the final external force was less than the pressure end force.

Development of Computerized Seal-Design Procedure

Seal-Design Procedure for Qualification Tests. On the basis of the results from the seal-development work, the following step-by-step procedure was derived to design the seals for the connectors used in the qualification tests. The tube inside diameter was calculated in the tube-design section of the computerized connector-design program. In the seal-design section of the program, the seal inside diameter was made equal to the tube inside diameter plus 0.04 inch (to allow for seal contraction) for tube sizes through 8 inches in diameter, or to the tube inside diameter plus 0.06 inch for tube sizes greater than 8 inches. As shown by Curve 1 of Figure 13, the seal disk height was calculated as a step function of tube size. The seal disk thickness was made 0.04 inch for all tube sizes.

The seal tang thickness was first made equal to the tube wall thickness, and Equation (3) was used with the appropriate material yield stress and the required radial force to calculate a tang length. The ratio of seal tang length to seal tang height was checked to determine that it was not greater than: (1) 3.5 for tube sizes up to and including 3 inches, (2) 2.5 for tube sizes up to and including 8 inches, and (3) 2.0 for tube sizes greater than 8 inches. If the calculated ratio was greater than allowable, the tang thickness was increased by steps of 0.005 inch and the calculation of seal tang length was repeated until a satisfactory ratio was obtained. The previously established seal disk dimensions were then used with the selected tang to determine the final seal design.

Revised Seal-Design Procedure. As discussed on pages 144 through 146, the qualification tests showed that the seal design procedure had to be revised for three reasons. First, the selected disk thickness of 0.040 inch had to be increased because of the pressure-impulse requirements of the high-pressure aluminum connectors. Second, the disk height of the larger, high-pressure stainless steel seals had to be increased to provide more elastic recovery for thermal-gradient requirements. Third, the radial force per inch of seal circumference for all stainless steel seals, and in particular for the high-pressure seals, had to be increased to provide better sealing

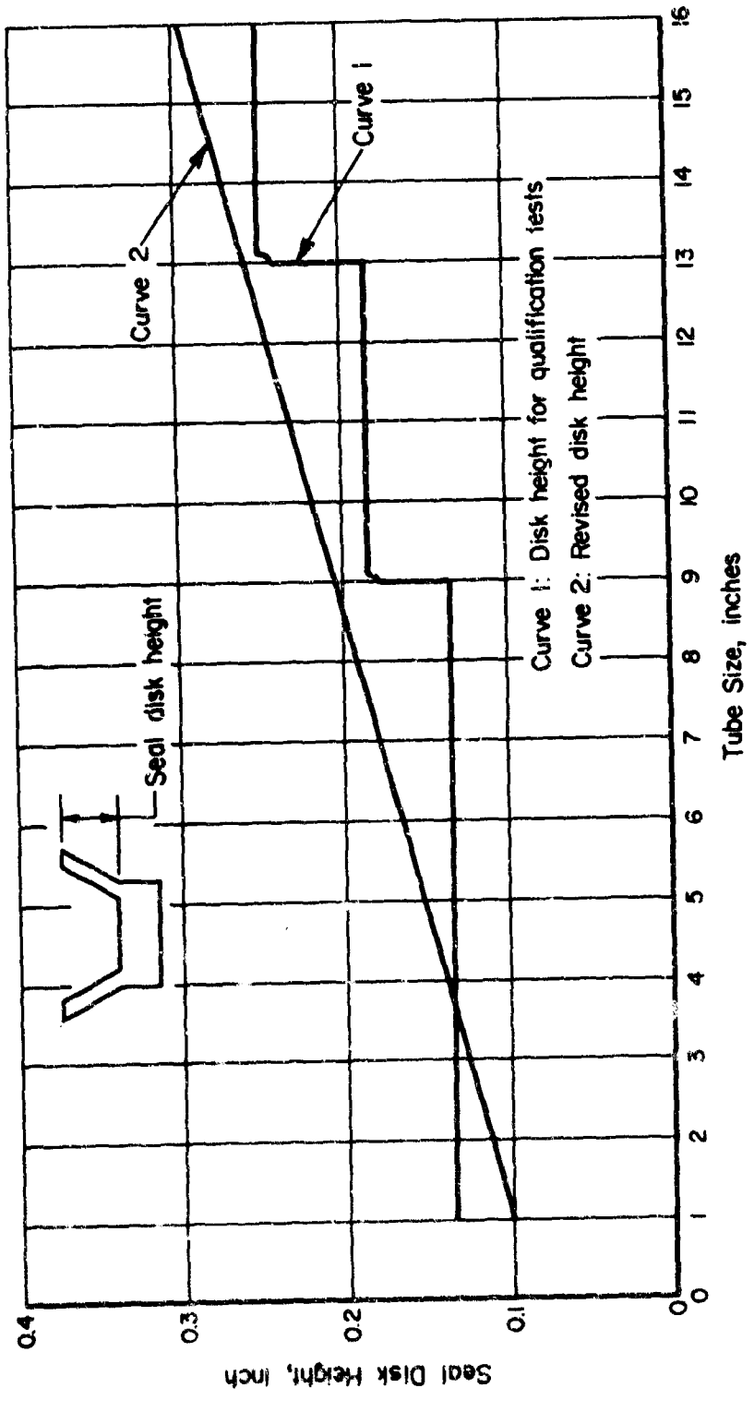

FIGURE 13. SEAL DISK HEIGHT VERSUS TUBE SIZE

contact to overcome imperfections and manufacturing variations in the nickel surface of the seals. During consideration of these requirements, it also became apparent that shorter disk heights were needed for the seals for tubing less than 3 inches in diameter.

The design procedure was revised to begin with the calculation of seal disk height as a linear function of tube size. As shown by Curve 2 in Figure 13, the linear variation was made to approximate the disk height of the 3-inch qualification-test seals because of the satisfactory thermal-gradient performance of the 3-inch stainless steel connectors. The seal disk height for the 1-inch size was based on engineering judgment and on seals used under Contract AF 04(611)-8176 for threaded connectors. For the larger seals, the seal disk height was made as great as possible without increasing the basic connector structure as determined by the operating conditions and the material properties. Following the seal-disk-height calculation, the inside diameter of the seal was made equal to the tube inside diameter plus an allowance for seal contraction proportional to the seal disk height.

The seal tang thickness was initially made equal to 0.9 times the tube wall thickness, and a tang length was calculated using Equation (5a):

$$L = 2F_T \Big/ [S_y \ln (D_e/D_i)], \tag{5a}$$

where

L = tang length, in.

F_T = radial force per inch of outside seal tang circumference at root of each seal disk, lb/in. [F_T was made equal to 750 lb/in. for all aluminum seals, 1200 lb/in. for low-pressure stainless steel seals, and 2500 lb/in. for high-pressure stainless steel seals.]

S_y = seal material compressive yield stress, psi

D_e = tang outside diameter, in.

D_i = tang inside diameter, in.

On the basis of additional consideration of allowable bowing in the seal tang, the maximum allowable ratio of seal tang length to seal tang thickness was set at 4 for all tube sizes, and an iterative check (see page 23) was performed on the calculated ratio until a satisfactory ratio was obtained. Equations (5b) and (5c) below show the calculations derived for seal disk thickness. The maximum of the two values obtained was the designed disk thickness. These equations were based on the successful performance of a seal disk thickness of 0.060 inch in the pressure-impulse test of the 8-inch aluminum connector, and on the judgmental application of beam-strength considerations to other disk sizes.

$$LT = F_T D_o / D_e S_y \ , \tag{5b}$$

and

$$LT = 0.04 + 0.001\, D \sqrt{P/12} \ , \tag{5c}$$

where

LT = seal disk thickness, in.

D_o = seal disk outside diameter, in.

D = tube outside diameter in.

P = operating pressure, psi.

Investigation of Connector-Design Criteria

Several criteria must be considered in the design of separable connectors for large tubing systems. An investigation was made of these criteria prior to the development of a computerized, connector-design program. In addition to the seal development work described previously, this work included: (1) design approximations for conventional flanged connectors; (2) investigation of nonconventional connector configurations; (3) comparison of conventional and nonconventional connectors; (4) investigation of connector thermal gradients; (5) investigation of bolt parameters; and (6) investigation of stress relaxation considerations.

Design Approximations for Conventional Flanged Connectors

Conventional connectors include either integral or loose-ring flanges fastened together by bolts. These configurations are illustrated in Figure 14. The important factors that determine the physical dimensions and weight of conventional connectors

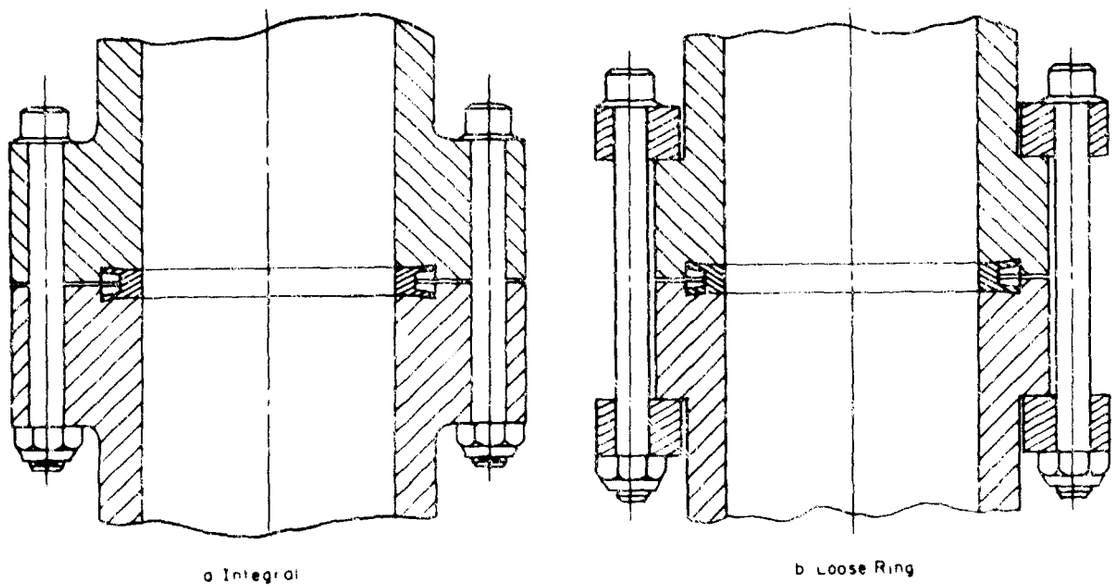

FIGURE 14. CONVENTIONAL FLANGE CONNECTORS

include the (1) design conditions, (2) seal dimensions, (3) material properties, (4) tube-wall thickness, (5) connector loads, (6) bolt strength, and (7) wrench clearance. Each of these factors is discussed briefly, and approximate comparative weights are given for conventional integral and loose-ring connectors.

Design Conditions. On the basis of the requirements of missile systems as defined by the work statement, five combinations of temperature, pressure, material, and tube size were selected for design approximations. These are listed in Table 10. Some design penalties were imposed for the low-pressure system because the computed tube-wall thickness for pressure retention (for smaller tube sizes especially) was not great enough for normal handling or fabrication of the tubing system, and heavier tube-wall thicknesses required a heavier connector to withstand the higher bending moment loads.

TABLE 10. CONDITIONS FOR DESIGN APPROXIMATIONS

Tube Diameter, in.	System Pressure, psi	Maximum Temp, F	Material
1 to 16	100	200	Type 347 SS
1 to 16	1500	200	Type 347 SS
1 to 16	1500	200	6061-T6 Al
1 to 3	4000	600	Type 347 SS
1 to 3	6000	200	Type 347 SS

For the design approximations, no consideration of thermal gradients was included in the load and/or stress analyses. However, on the basis of concurrent laboratory measurements of thermal gradients (see page 56), it was decided not to use steel bolts with aluminum flanges.

Seal Dimensions. As shown in Figure 15a, if the seal OD is relatively large, the bolt-circle diameter will be larger than that required to accommodate wrench clearance at the bolt head. If the seal OD is small and the seal length is excessive (Figure 15b), then the length of the bolt may be longer than necessary. It is desirable, therefore, to select an "optimum" seal configuration (Figure 15c) which will not penalize the flange design. For comparison purposes, the seal dimensions selected were based on a seal tang thickness equal to the tube-wall thickness. The other dimensions of the seal were then selected to satisfy seal-performance parameters as discussed previously.

Material Properties. To provide a common basis for stress and weight calculations, values were selected for the minimum strength properties of the connector materials. Some of these values are listed in Table 11. For 6061-T6 aluminum connectors, the bolt material selected was 2024-T3 aluminum, while for stainless steel connectors, the bolt material selected was heat-treated, high-strength A286. Also, for analysis purposes, factors of safety of 1.5 for aluminum materials and 1.25 for steel materials were selected.

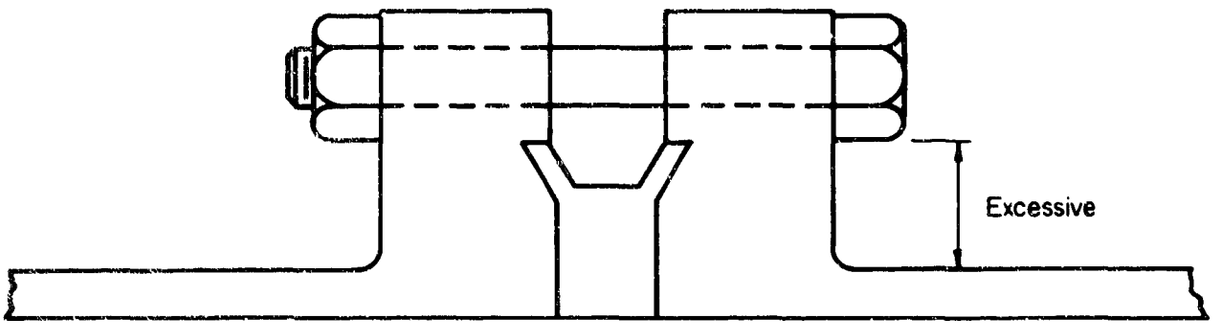

a. Tang too Thick

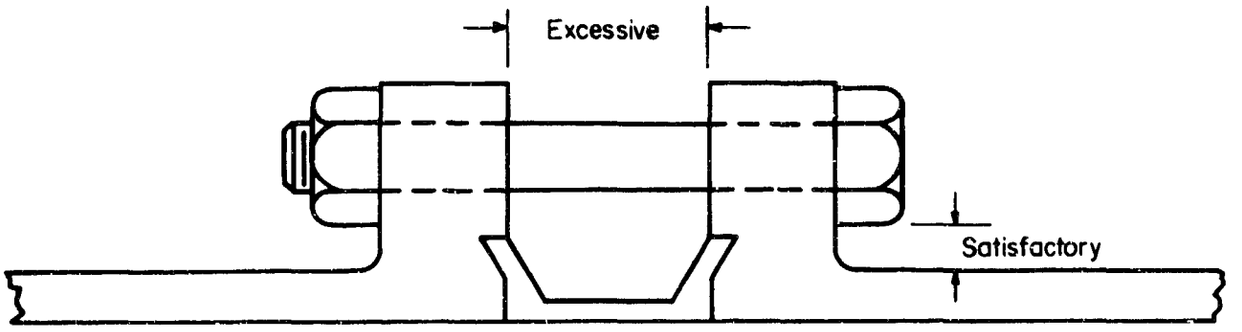

b. Tang too Long

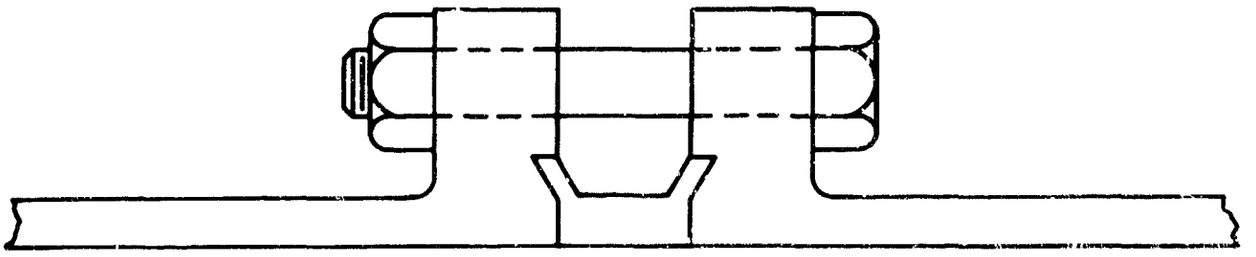

c. Tang Thickness=Tube-Wall Thickness

FIGURE 15. EFFECT OF SEAL TANG ON CONNECTOR DESIGN

TABLE 11. MATERIAL MINIMUM-STRENGTH PROPERTIES SELECTED FOR CONNECTOR COMPARISONS[a]

	6061-T6 Aluminum	2024-T3 Aluminum	Type 347 SS	High-Strength A286
Modulus of Elasticity, 10^6 psi	9.9	9.9	28.0	29.0
Density, lb/in.^{3}	0.098	0.098	0.288	0.286
Room Temperature (70 F)				
Tensile Yield Strength, psi	35,000	50,000	35,000	131,000
Ultimate Tensile Strength, psi	42,000	62,000	90,000	200,000
200 F				
Tensile Yield Strength, psi	32,200	47,000	30,000	128,000
Ultimate Tensile Strength, psi	38,100	59,000	76,500	196,000
600 F				
Tensile Yield Strength, psi	–	–	25,000	120,000
Ultimate Tensile Strength, psi	–	–	68,000	180,000

(a) Some of these properties were revised in later designs.

Tube-Wall Thickness. The tube-wall thicknesses selected for this study were calculated by the following formula from Section I of the ASA Code for Pressure Piping:

$$\text{Tube-Wall Thickness} = \frac{1.1\,PD}{2S_a + 0.8P}, \qquad (6)$$

where

S_a = allowable stress of tube material at most severe operation condition, psi

P = operating pressure, proof pressure, and/or burst pressure, psi

D = tube outside diameter, in.

1.1 = factor applied for fabrication tolerance.

The most severe operating conditions that determined minimum tube-wall thickness were (1) proof pressure (one-and-one-half times maximum working pressure) for Type 347 stainless steel, and (2) burst pressure (two times maximum working pressure) for 6061-T6 aluminum. For the 100-psi conditions, a minimum wall thickness was selected on the basis of weldability and ease of handling. Table 12 shows the calculated tube-wall thicknesses.

TABLE 12. TUBE-WALL THICKNESS CALCULATED FOR CONNECTOR COMPARISONS

Tube Diameter, D, in.	Tube-Wall Thickness, inches				
	6061-T6 Aluminum, 1500 Psi, 200 F	Type 347 Stainless Steel			
		100 Psi, 200 F	1500 Psi, 200 F	4000 Psi, 600 F	6000 Psi, 200 F
1	0.042	0.022	0.040	0.120	0.147
2	0.084	0.028	0.080	0.240	0.294
3	0.126	0.035	0.120	0.360	0.441
4	0.168	0.035	0.160		
5	0.210	0.050	0.200		
6	0.252	0.050	0.240		
7	0.294	0.050	0.280		
8	0.336	0.050	0.320		
9	0.378	0.050	0.360		
10	0.420	0.050	0.400		
11	0.460	0.050	0.440		
12	0.504	0.063	0.480		
13	0.546	0.063	0.520		
14	0.588	0.063	0.560		
15	0.630	0.063	0.600		
16	0.672	0.063	0.640		

Connector Loads. Three types of loads (pressure end load, tube bending load, and minimum residual seal load) combine in different ways to determine the operating conditions. The connector design axial load (TAL) was determined on the worst-case basis of:

(1) Axial load due to proof pressure plus minimum seal load

(2) Axial load due to operating pressure plus equivalent bending load plus minimum seal load.

The design axial loads (TAL) for each tube OD and combination of temperature, pressure, and material are shown in Table 13.

TABLE 13. DESIGN AXIAL LOADS CALCULATED FOR CONNECTOR COMPARISONS

Tube Diameter, D, in.	Design Axial Load (TAL), lb			
	6061-T6 Aluminum,	Type 347 Stainless Steel		
	1500 Psi, 200 F	1500 Psi, 200 F	4000 Psi, 600 F	6000 Psi, 200 F
1	3,951	3,472	8,296	12,082
2	13,414	12,754	32,942	45,083
3	30,592	30,958	59,502	83,480
4	47,868	46,367		
5	64,348	62,525		
6	84,770	81,686		
7	107,356	103,814		
8	135,187	128,758		
9	165,122	159,032		
10	204,083	194,326		
11	248,840	241,760		
12	292,546	284,865		
13	334,785	331,507		
14	397,426	381,681		
15	452,201	434,853		
16	510,487	492,636		

The pressure end loads at operating and proof pressure conditions were calculated:

$$PL = \frac{\pi P(D_o)^2}{4}, \tag{7}$$

where

PL = pressure end load, lb

P = operating pressure or proof pressure, psi

D_o = seal outside diameter, in.

The tube bending moment was calculated on the basis of Equations (8) and (9) and the lower value was selected. The static bending moment due to misalignment at assembly was defined as half of the tube bending moment.

$$TBM1 = Z S_A, \tag{8}$$

$$TBM2 = 60 (D + 3)^3, \tag{9}$$

where

TBM1 and TMB2 = tube bending moment, lb-in.

Z = tube section modulus, $in.^3$

S_A = minimum of 2/3 yield strength, 0.8 stress to rupture in 2 years, or 0.5 fatigue strength, psi

D = tube outside diameter, in.

The equivalent axial load due to tube bending was calculated:

$$AL_B = S_B \pi T (D-T) \quad , \tag{10}$$

where

AL_B = equivalent axial load, lb

S_B = bending stress, psi

T = tube-wall thickness, in.

D = tube outside diameter, in.

The minimum residual seal load, MSL, was calculated to be 10 percent of the assembly-seal sealing load, i.e., about 75 lb/in. of seal circumference:

$$MSL = 75 \pi (D_o) \quad , \tag{11}$$

where

MSL = minimum seal load, lb

D_o = seal outside diameter, in.

Bolt Strength. For design approximation, high-strength A286 bolts and 2024-T3 aluminum bolts were selected for the stainless steel and aluminum connectors, respectively. The room-temperature strength properties of these bolt materials are shown in Figures 16 and 17. The maximum allowable bolt loads at maximum operating temperature for various bolt sizes are shown in Table 14. The allowable bolt loads were computed as follows:

$$BL = \frac{S_y}{FS} A_s \quad , \tag{12}$$

where

BL = maximum allowable bolt load, lb

S_y = tensile yield strength of bolt material at maximum operating temperature, psi

FS = factor of safety; for 2024-T3, FS = 1.5, for A286, FS = 1.25

A_s = tensile stress area = $\frac{\pi}{4}\left(D - \frac{0.9743}{n}\right)^2$

and D = basic major bolt diameter, in.,

n = number of threads per inch.

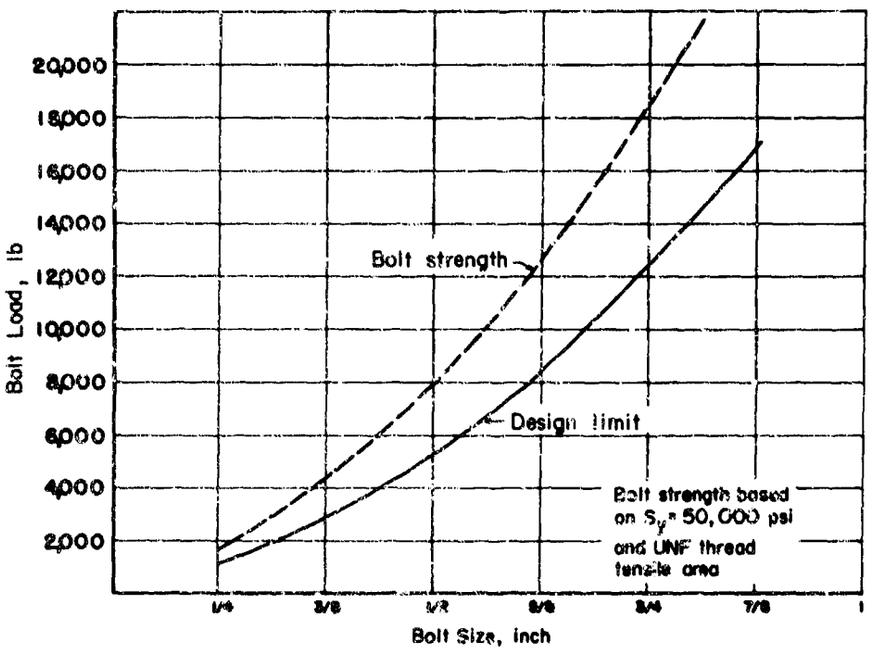

FIGURE 16, STRENGTH OF 2024-T3 ALUMINUM BOLTS

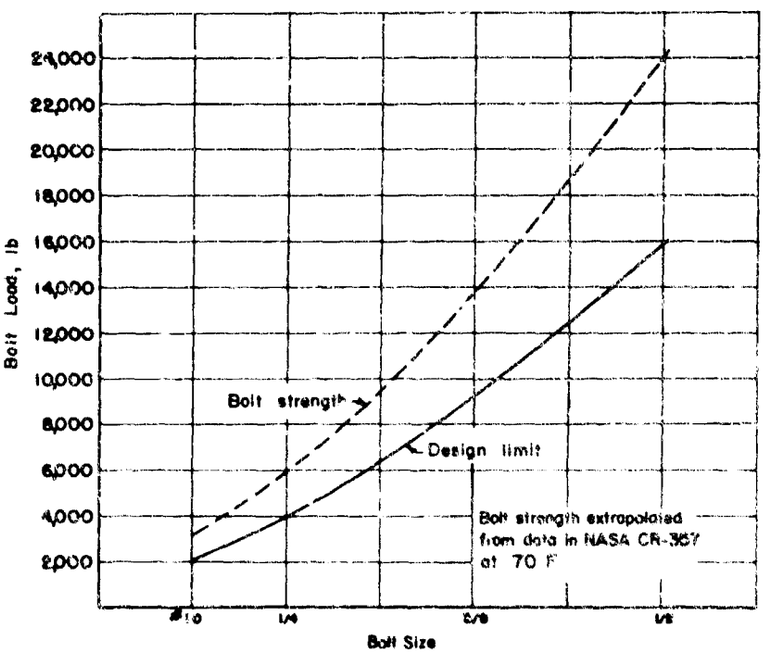

FIGURE 17, STRENGTH OF A286 BOLTS BASED ON JOHNSON'S APPROXIMATION

TABLE 14. MAXIMUM ALLOWABLE BOLT LOADS, POUNDS

Bolt Size, in. – TPI	2024-T3 Aluminum, 200 F	A286	
		200 F	600 F
10-32	--	2,050	1,925
1/4-28	1,139	3,734	3,505
5/16-24	1,818	5,960	5,595
3/8-24	2,751	9,015	8,463
7/16-20	3,719	12,186	11,440
1/2-20	5,011	16,418	15,413
9/16-18	6,360	20,835	19,560
5/8-18	8,010	26,273	24,665
3/4-16	11,686	38,284	35,940
7/8-14	15,963	52,297	49,095
1-12	20,774	68,061	63,894

Wrench Clearance. One of the bolt characteristics that influences the dimensions of the connector is the bolt-head size and its corresponding wrench-clearance requirement. One minimum limit on the bolt-circle diameter is established by the tube outside diameter plus the wrench-clearance diameter. A limit on the maximum number of bolts that can be used in a flange is the space between the bolts required for wrench clearance. Table 15 lists the across-flats dimensions and the wrench-clearance diameters that were used in this comparison study.

TABLE 15. BOLT-WRENCH CLEARANCE

Bolt Size, in.	Hexagon Head Size Across Flats, in.	Wrench-Clearance Diameter, in.
1/4	7/16	0.88
5/16	1/2	0.94
3/8	9/16	1.00
7/16	11/16	1.08
1/2	3/4	1.34
9/16	7/8	1.51
5/8	15/16	1.59
3/4	1-1/16	1.73
7/8	1-1/4	1.94
1	1-7/16	2.16

Integral-Flange Connector. The total-axial-load data in Table 13 were used to determine the number and size of bolts required for integral flange connectors for each representative tube size and pressure condition. A computer program was established for designing integral flanges in accordance with the formulas and methods set forth in

the ASME Code for Unfired Pressure Vessels - Section VIII. Bolt-circle inputs were determined from the minimum of two conditions: (1) connector hub OD + 2 x (nut radius + wrench clearance between nut and hub) or (2) seal-cavity-clearance diameter + 2 x bolt radius. Flange OD inputs were found by adding two times the bolt diameter to the calculated bolt circle.

Loose-Ring Flange Connector. The number and size of bolts required for the loose-ring configuration were identical to those required for the integral-flange connectors. Loose-ring-thickness calculations were made using the bolt-circle and ring OD dimensions established for the integral-type flanges. The stub flanges were designed by a computer program set up for the loose-ring design. The OD of the stub flanges was the minimum that would contain the seal cavity while providing adequate bearing area between the flange face and the loose ring.

Weight Comparison. Comparative weights for the integral and the loose-ring connectors were computed and are shown in graphical form in Figures 18 through 21.

Investigation of Nonconventional Connector Configurations

The investigation of nonconventional connectors was initiated by a search for basic configurations. Three major sources were searched: (1) patents, (2) commercially available connectors, and (3) connector concepts available from the literature and from past Battelle projects. Approximately 60 patents were obtained, studied, and classified according to the basic design approaches. Letters were sent to approximately 316 companies requesting design information on available or promising connector configurations. A search was made of the extensive literature on connectors collected under Contract AF 04(611)-8176, and of the connector concepts conceived during that project and during other Battelle projects on connectors. From this work, five connector configurations were selected as containing design features worthy of detailed study.

To permit a comparison of nonconventional and conventional configurations, a preliminary design of each nonconventional connector was developed for the design conditions given in Table 10. Type 347 stainless steel was chosen as the material for all nonconventional connector designs. This selection permitted a more general comparison of the different configurations and simplified the comparison procedure. The tube-wall thickness and the total axial load were common to all conventional and nonconventional connector configurations. The residual seal-seating-load requirement was also common to all connectors.

X-Connector. The X-connector designed by the Parker Aircraft Company is shown in Figure 22. The outer portion or fastener of this connector serves the same function as the bolts in a conventional connector. The fastener is fabricated with end diameters large enough to pass over the stub flanges during assembly. A special tool is used to swage or deform the end portions of the fastener inwardly and around the stub flanges. The fastener is contained and deformed in such a way that it seats the seal and provides joint preload.

A 1/2-inch X-connector and a 3/4-inch X-connector have been developed through funding from General Electric and NASA, and tests have been conducted satisfactorily with helium at 4000 psi. Development of the X-connector with the Bobbin seal in the larger tube sizes would be somewhat questionable because of the large axial seal-seating motion and high joint preloads which are required. Furthermore, the connector is a

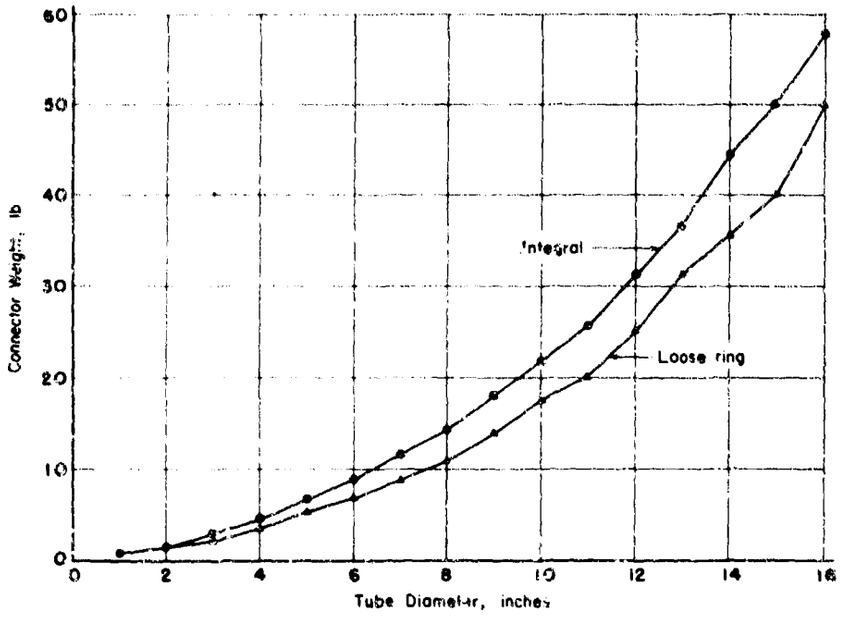

FIGURE 18. WEIGHT OF TYPE 347 STAINLESS STEEL LOOSE-RING AND INTEGRAL-FLANGE CONNECTORS FOR 100-PSI, 200 F SYSTEMS

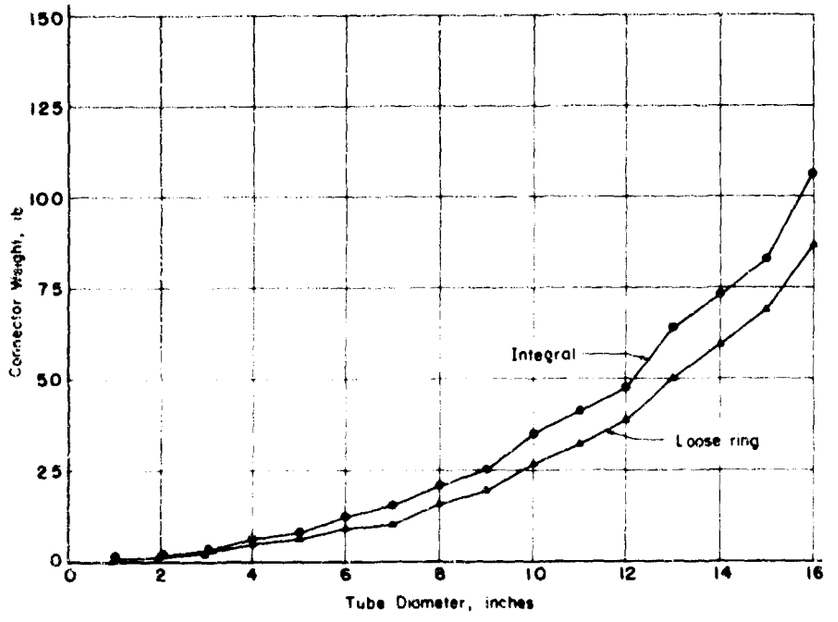

FIGURE 19. WEIGHT OF 6061-T6 ALUMINUM LOOSE-RING AND INTEGRAL-FLANGE CONNECTORS FOR 1500-PSI, 200 F SYSTEMS

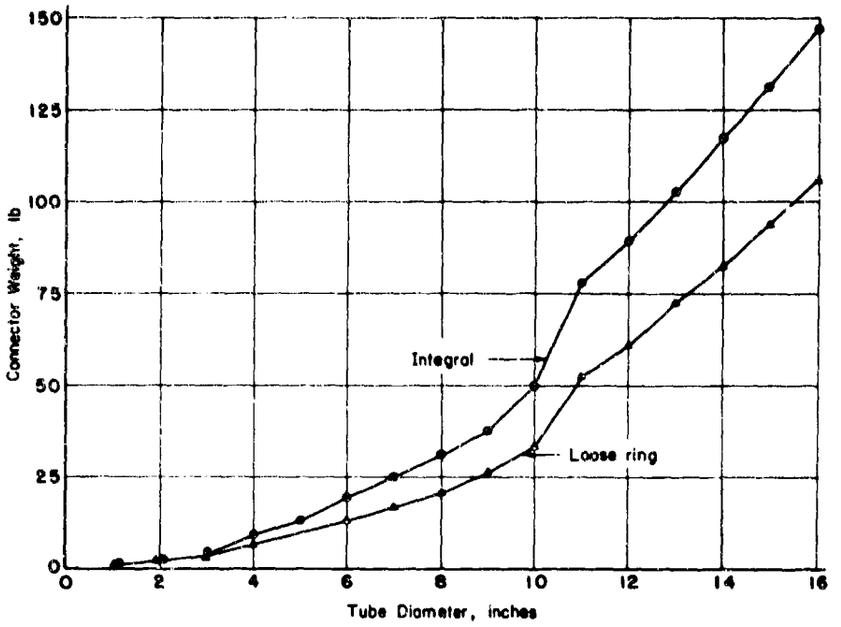

FIGURE 20. WEIGHT OF TYPE 347 STAINLESS STEEL LOOSE-RING AND INTEGRAL-FLANGE CONNECTORS FOR 1500-PSI, 200 F SYSTEMS

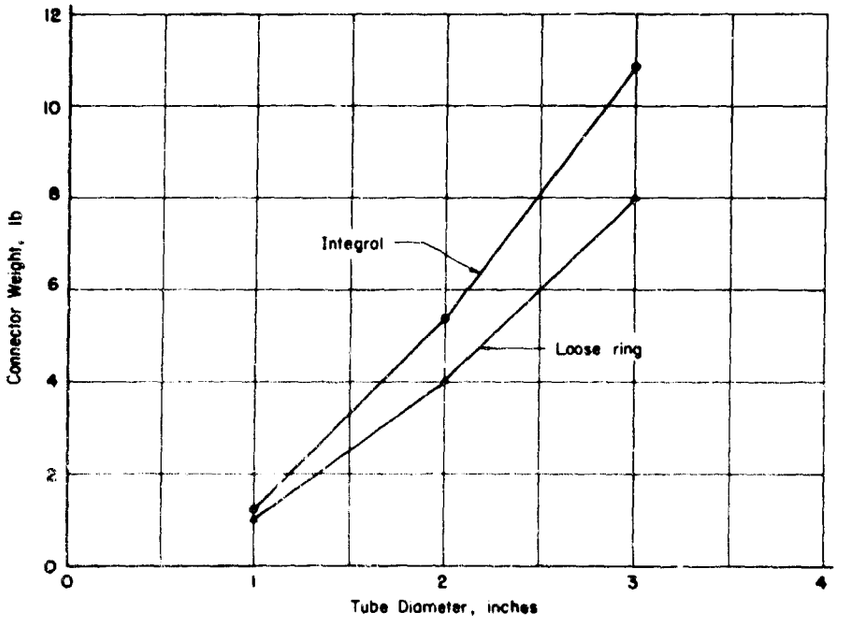

FIGURE 21. WEIGHT OF TYPE 347 STAINLESS STEEL LOOSE-RING AND INTEGRAL-FLANGE CONNECTORS FOR 6000-PSI, 200 F SYSTEMS

semipermanent rather than a separable connector. However, not only does the connector have unique features, but it appears to have been investigated more thoroughly than any other nonconventional connector in the past few years.

A design similar to the X-connector, shown in Figure 23, was established for the estimate of connector weight. The weight of the connector fastener was calculated using the computer program established for the nut of the threaded-flange connector. The weights of the stub flanges were made identical to those of the stub flanges of the conventional loose-ring connector.

V-Band Connector. The V-band connector is an acceptable tube fastener for many industrial and aerospace applications. Several design variations are possible in the V-band structure, but limitations must be imposed owing to tube size, system pressure, and permissible leakage. A three-segment band interconnected by the stud and nut arrangement shown in Figure 24 was chosen as the best configuration for liquid rocket propulsion systems. This design is more suitable for large tube diameters and for the high axial seal-seating motion required by the Bobbin seal. Also, a more accurate preload can be realized with this configuration than with a single-fastener, single-strap configuration, since less relative motion exists between the band and flange pressure faces during assembly.

The flange-face pressure angle and the thickness of the flange beyond the tube OD were chosen to provide the axial motion required for seal-seating and joint preload. The included angle on the V-band was not allowed to exceed 35 degrees. The distance between the pressure faces of the V-band was determined from the summation of dimensions of the contained flanges and seal. These parameters, together with the total-axial-load data and an assumed friction angle, provided the inputs to a computer program established to calculate the weight of the V-band. The flange weights were calculated by the stub-flange computer program.

Compression-Collar Connector. The load-carrying member of this connector is a two-segment collar similar to a two-segment V-band with parallel faces on the inwardly projecting flanges. The design as presented by Allied Research Associated is shown in Figure 25. One of the inwardly projecting flanges of this connector is tapped for socket-head screws which bear against a hardened steel ring on one of the flange faces. These screws, when tightened against the hardened steel ring, produce axial motion which forces the flanges against the seal to provide joint preload.

The fastener for the redesigned compression collar is in the form of a continuous thin-walled nut as shown in Figure 26. The two end rings of the nut member are designed to contain the bending loads, and this permits the thin-wall construction of the interconnecting cylinder. This design was chosen because it represents a lighter weight than can be realized with the thick-walled two-segment design, where bending loads must be carried through the entire length of the connector. Computations of the weight for the nut, the nut ring, and the flanges were accomplished by computer programs. The weights of these elements plus the socket-head screws and hardened steel ring make up the total connector weight.

Breech-Type Connector. The breech-type connector uses a nut member to carry the total axial load over and around the seal area. The design as it is manufactured by Thornhill-Craver Company, Inc., is shown in Figure 27. One of the flanges, called the lug hub member, contains outwardly projecting tapered shelves. The nut member contains inwardly projecting tapered shelves which contact the tapered surfaces of the

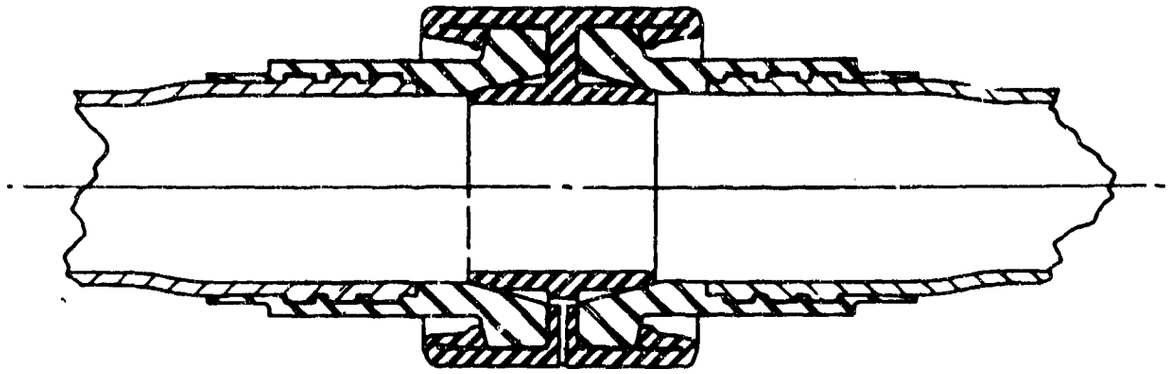

FIGURE 22. X-CONNECTOR

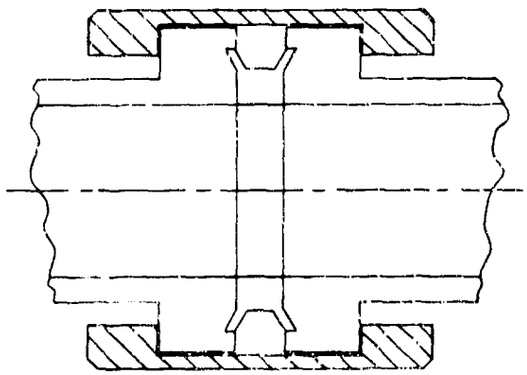

FIGURE 23. X-CONNECTOR APPROXIMATION USED FOR WEIGHT ANALYSIS

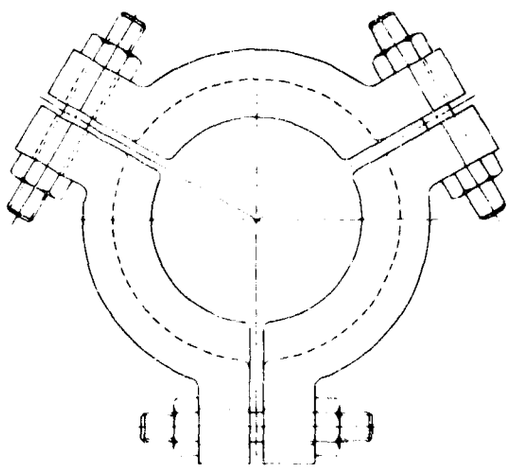

FIGURE 24. THREE-SEGMENT V-BAND CONNECTOR

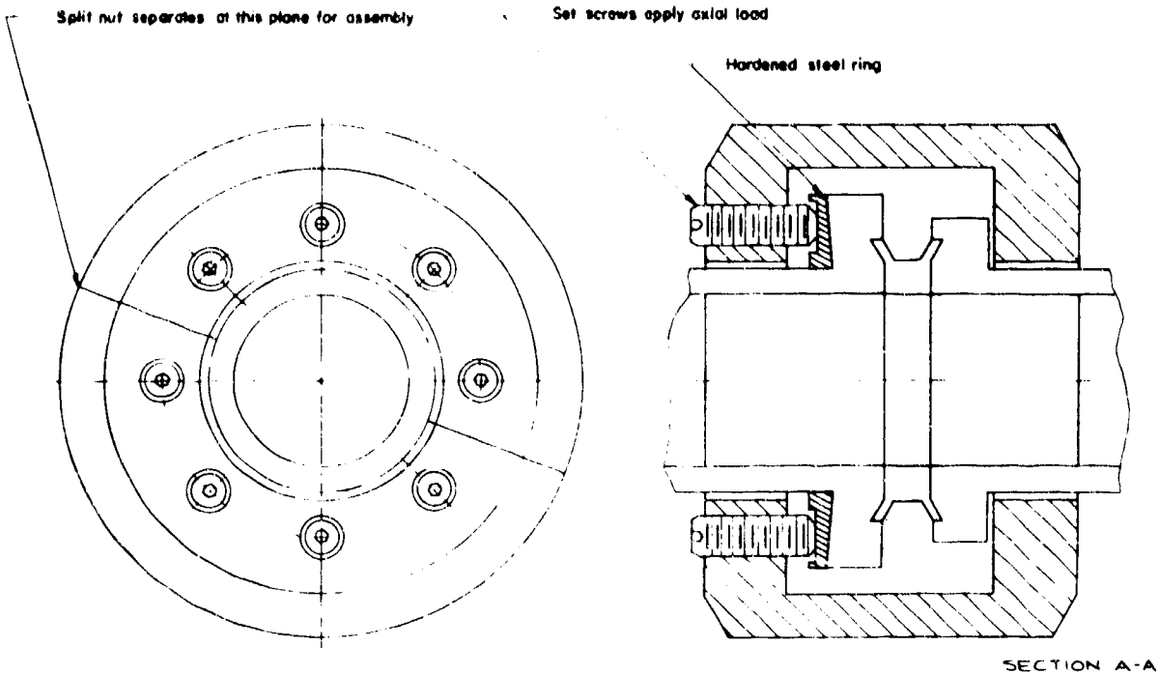

FIGURE 25. COMPRESSION-COLLAR CONNECTOR DESIGNED BY ALLIED RESEARCH ASSOCIATES

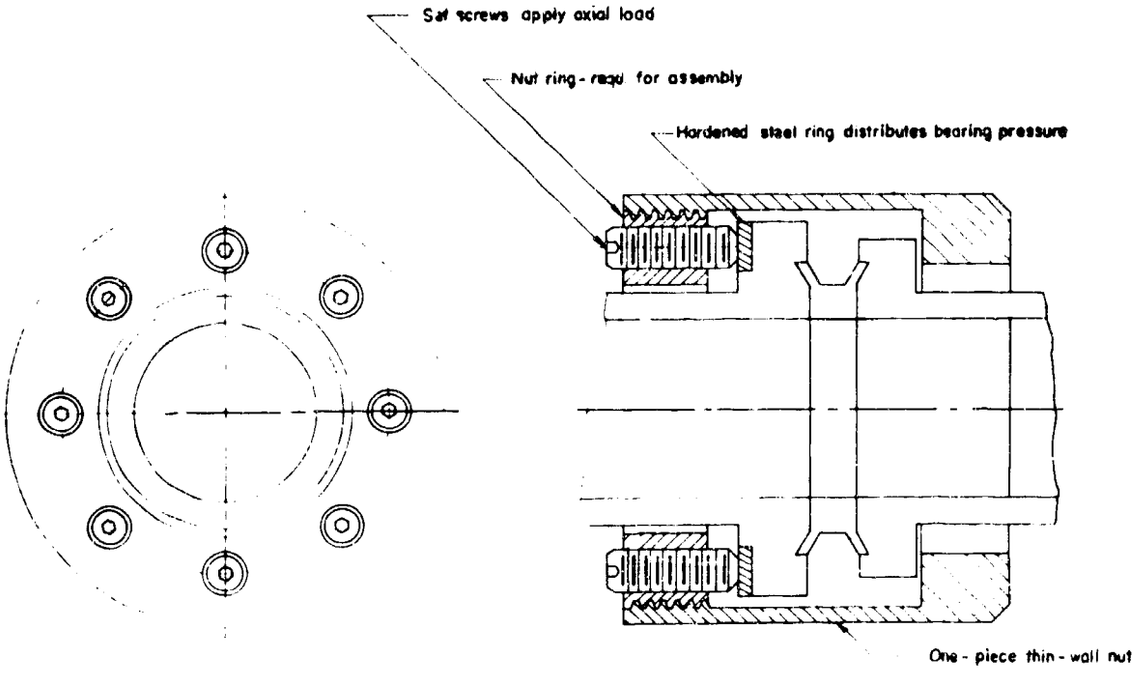

FIGURE 26. REDESIGNED COMPRESSION-COLLAR CONNECTOR

hub-member shelves. Relative rotating motion between the lug hub and nut member produces an axial motion and compressive force on the flanges and seal. Only a few degrees of nut member rotation are required for connector preload. The torque is applied by the arm and bolt device shown in Figure 27.

The redesigned breech-type connector is shown in Figure 28. To save weight, the arm and bolt arrangement for applying axial preload was removed. Splines were designed on the nut and hub to provide the contact surfaces through which a special tool can transmit joint assembly torques. Cammed surfaces on the joint loading tabs were designed with a 9-degree lead angle, and tab-face areas were sized to provide a bearing stress less than the allowable for Type 347 stainless steel. The nut-wall thickness was calculated to withstand the total axial load in tension, together with the bending loads imposed by the tabs. These data were used in the nut and flange computer programs to complete the required calculations. The total connector weight consists of the stub- and tab-flange weights and the tab, spline, and nut weights.

Threaded-Flange Connector. A gear-powered union designed by Resistoflex Corporation contains a worm and worm-gear arrangement to reduce the wrench torque required to assemble the connector (see Figure 29). This type of torquing device increases connector weight for two reasons: (1) the gear reduction assembly is an integral part of the connector and (2) the diameter of the load path is considerably greater than the flange OD and this produces increased bending moments, requiring thicker nut-wall construction. A redesign of this connector produced the more familiar threaded-flanged connector, shown in Figure 30. Weight data for the threaded flange and nut were provided by separate computer programs set up for the threaded-flange connector, while the plain-hub data came from the stub-flange computer program. The high nut torques required for preloading this design must be provided by a special tool attached to the connector through the hub and nut splines.

One design of a special tool which could be used with this connector is shown in Figure 31. A chain similar to a timing chain would be wrapped around the hub spline of the connector and tightened to anchor the tool and to sustain the countertorque imposed by the tool. A second chain would be wrapped around the tool drive gear and nut-spline area of the connector, and the ends would be connected to form an endless chain drive. This drive chain would be tightened by an idler wheel to complete the attachment of the special tool. Torque could be applied to the connector nut through either of two wrench positions on the special tool. The low-torque position would be used to attain greater speed in seating the seal, and the high-torque position would be used to apply the preload.

Comparison of Conventional and Nonconventional Connectors

Weight is believed to be the most important parameter in the comparison of conventional and nonconventional connectors. The information pertaining to weight, and to comparisons of a more general nature are discussed in the following sections.

Weight Comparison. The connector weights for the representative systems are summarized in parametric-curve form in Figures 32 through 35. The weights shown represent the flange and fastener portion of the connector external to the tube outside diameters. The weight of the seal is not included. The V-band connector is the heaviest for the four conditions investigated. The high weight exhibited by this configuration

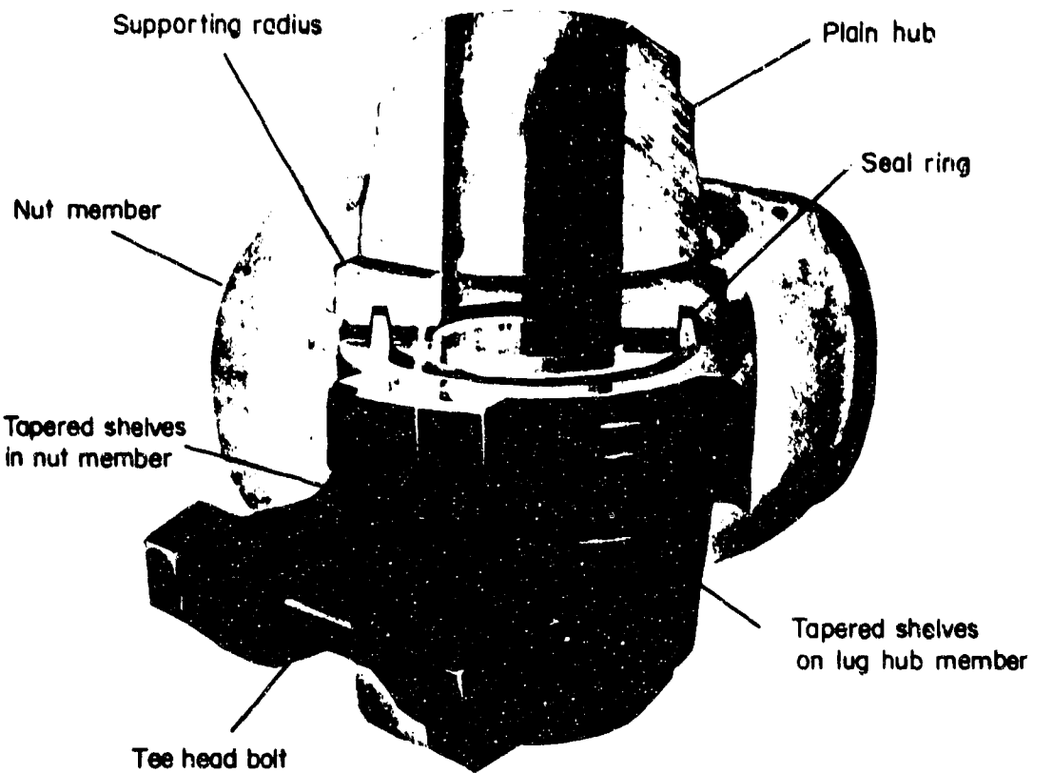

FIGURE 27. THORNHILL-CRAVER CO., INC.
BREECH-TYPE CONNECTOR

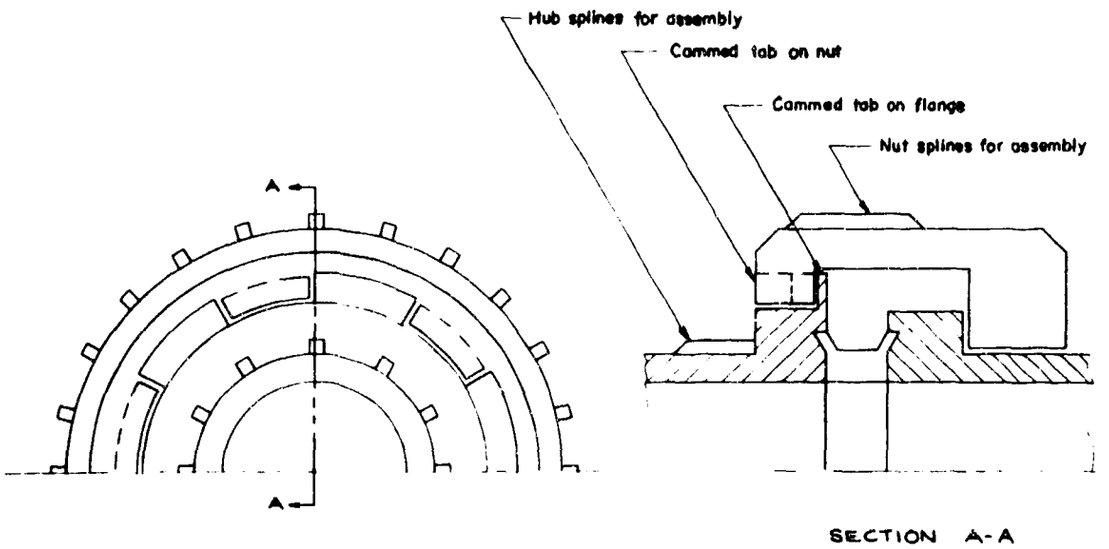

FIGURE 28. REDESIGNED BREECH-TYPE CONNECTOR

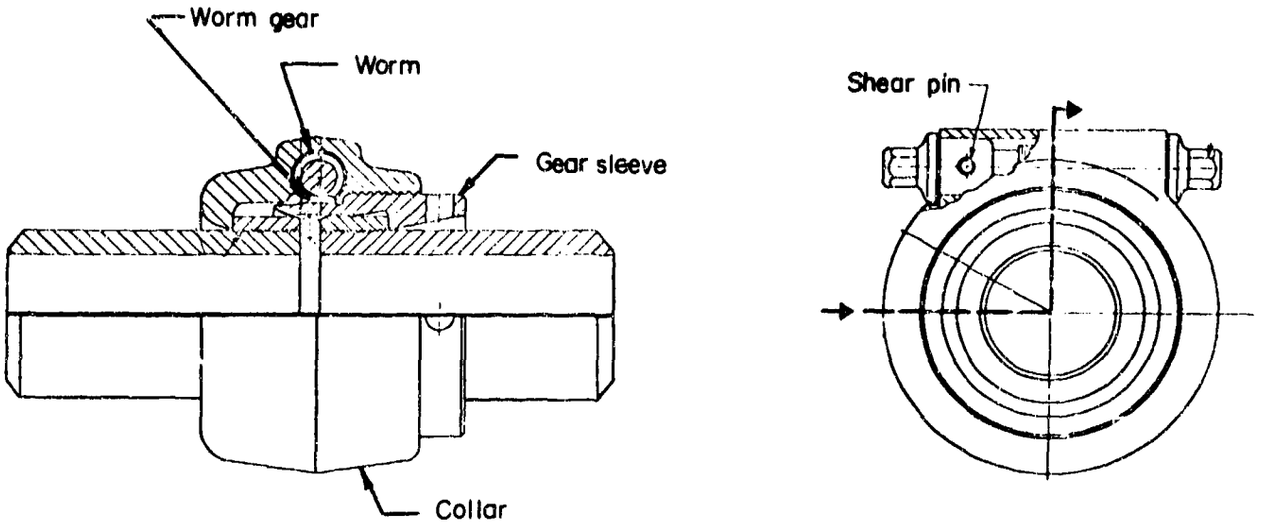

FIGURE 29. RESISTOFLEX GEAR-POWERED UNION

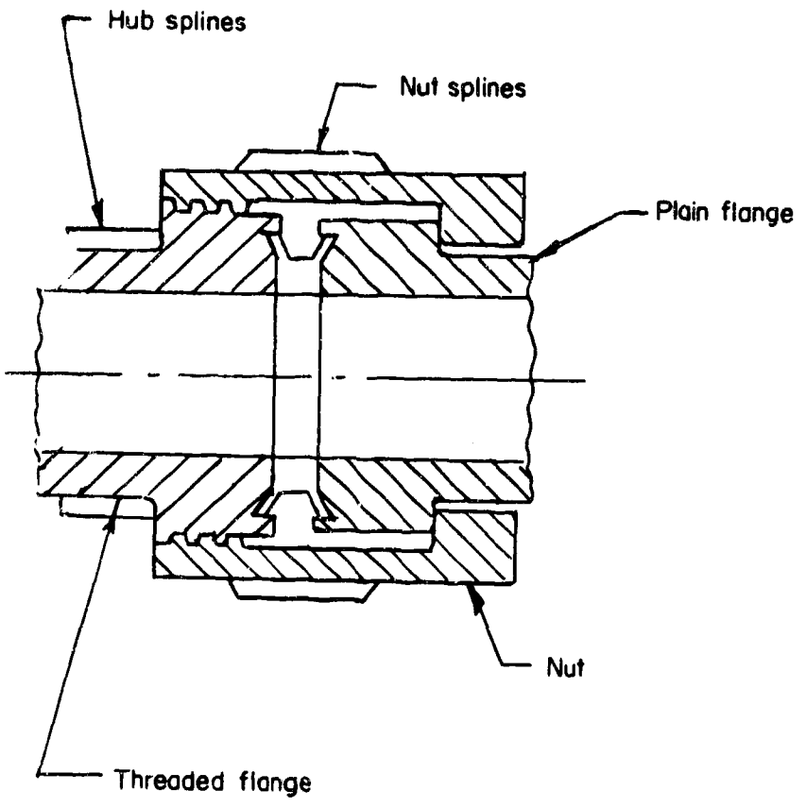

FIGURE 30. RESISTOFLEX GEAR-POWERED UNION REDESIGNED FOR MINIMUM WEIGHT

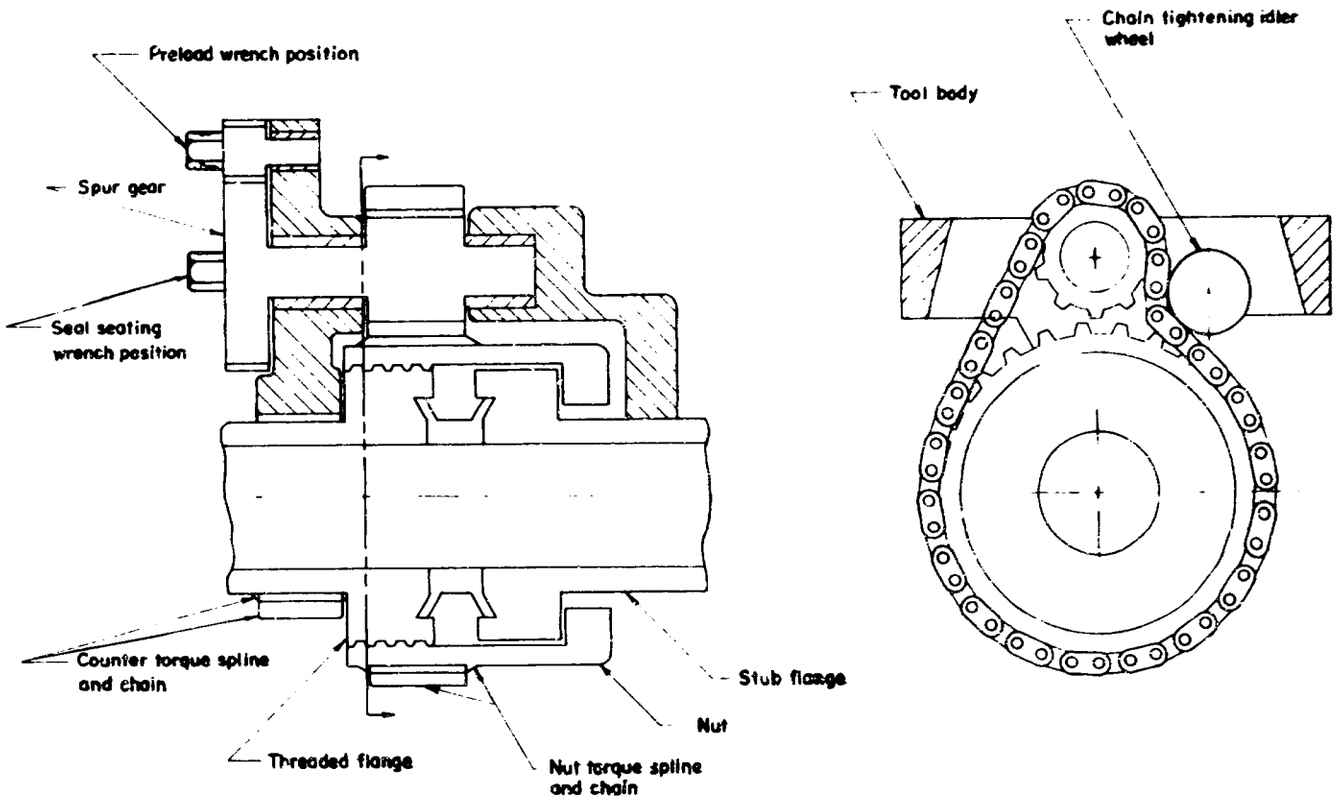

FIGURE 31. SPECIAL TOOL FOR REDESIGNED THREADED-FLANGE CONNECTOR

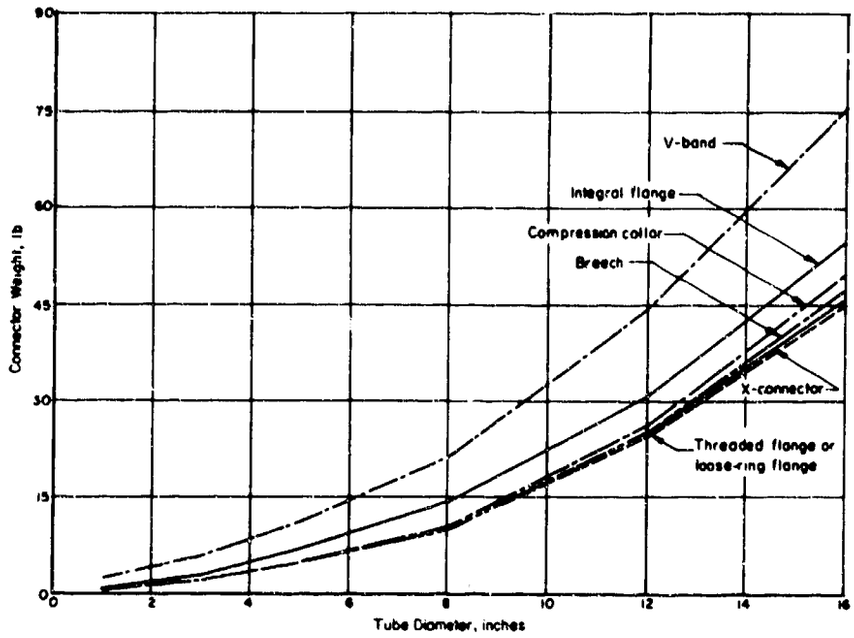

FIGURE 32. CONNECTOR WEIGHTS FOR A 100-PSI, 200 F SYSTEM

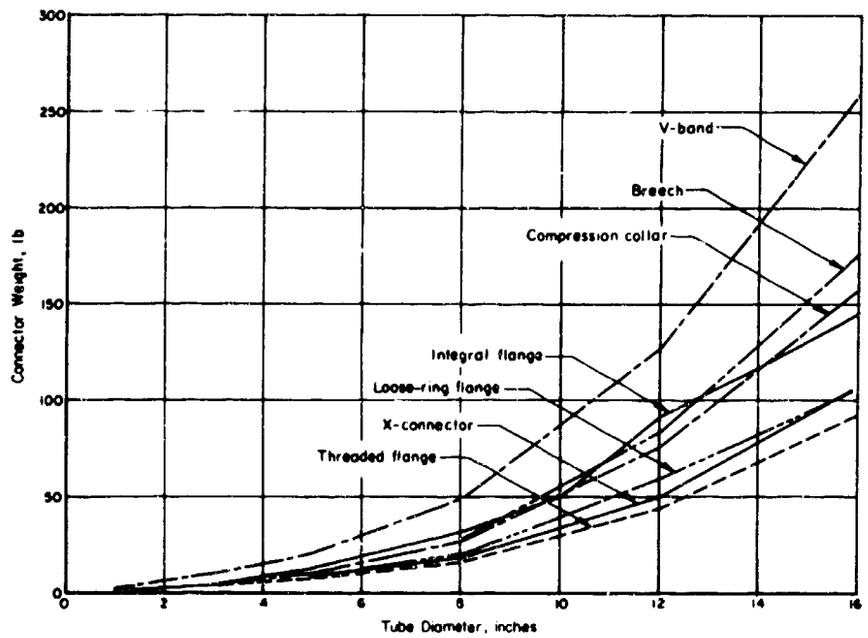

FIGURE 33. CONNECTOR WEIGHTS FOR A 1500-PSI, 200 F SYSTEM

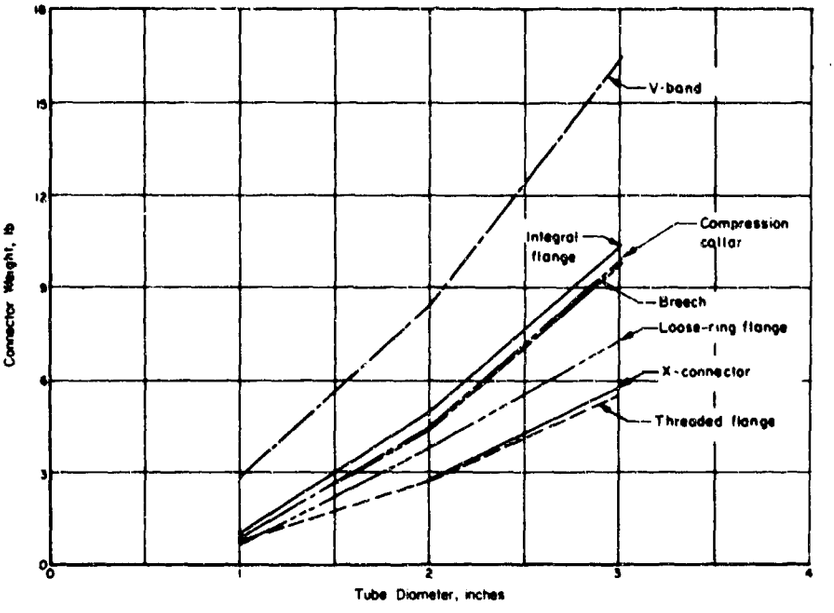

FIGURE 34. CONNECTOR WEIGHTS FOR A 4000-PSI, 600 F SYSTEM

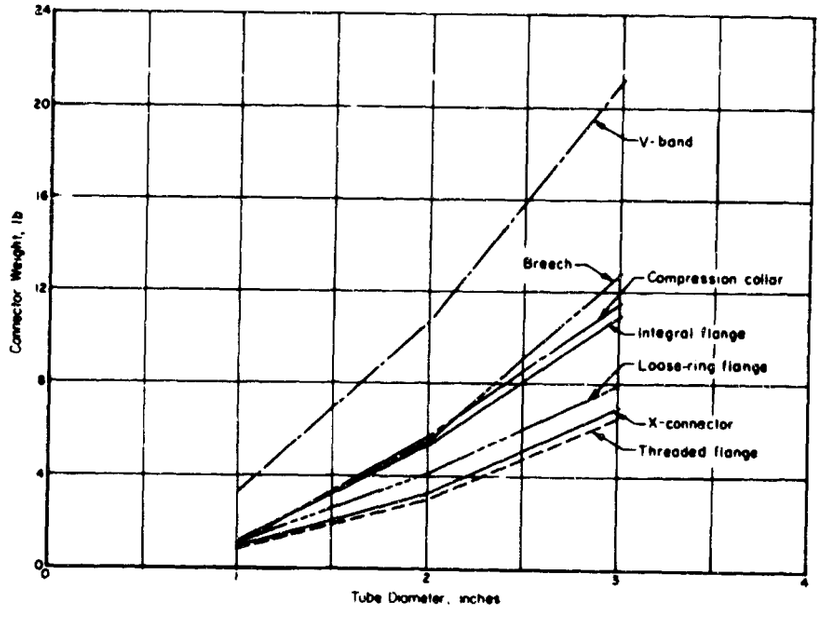

FIGURE 35. CONNECTOR WEIGHTS FOR A 6000-PSI, 200 F SYSTEM

is due primarily to the noncontinuous fastener element. The fastener does not have the structural-strength advantage that can be realized with a composite ring-and-cylindrical-fastener arrangement, and the imposed bending moments must be sustained in a structure similar to a simple beam. The fastener must also carry the tensile load due to total axial load. The fastener thickness required to carry the combined tensile and connector-imposed bending loads is in excess of four times the thickness required for the pure tensile load.

According to the curves representing the compression-collar and breech-type connectors for each of the four conditions, there is no weight advantage of these connectors as compared with the conventional integral-flange connector. The curves denoting the loose-ring flange, the threaded flange, and the X-connector show that these connectors are the lightest in weight of those investigated during the analysis. However, the feasibility of the X-connector is low when examined in relation to the program requirements for zero leakage, reassembly, and use with the Bobbin seal.

The threaded-flange connector represents the lowest weight design of all the connectors investigated. A more detailed weight comparison for the loose-ring and threaded-flange connectors is shown in Table 16. Weight savings in excess of 25 percent are possible in several instances, as shown by this comparison. The low weight of the threaded-flange connector is due to the fact that the axial load path is contained within a minimum envelope around the seal cavity.

TABLE 16. WEIGHT COMPARISON FOR LOOSE-RING AND THREADED-FLANGE CONNECTORS

System Pressure and Temperature	Tube Diameter, in.	Stainless Steel Connector Weights, lb		
		Loose-Ring Flange	Threaded Flange	Percent Lighter
100 psi 200 F	1	0.40	0.26	35.0
	3	2.00	1.66	17.0
	5	5.13	4.20	18.1
	8	10.76	9.86	8.4
	12	24.77	24.15	--
	16	45.06	45.26	--
1500 psi 200 F	1	0.56	0.49	12.5
	3	3.82	3.21	16.0
	5	9.68	7.31	24.5
	8	20.51	16.37	20.2
	12	60.87	43.60	28.4
	16	105.73	89.54	15.3
4000 psi 600 F	1	0.95	0.71	25.2
	2	3.77	2.71	28.1
	3	7.26	5.44	25.1
6000 psi 200 F	1	1.06	0.82	22.6
	2	4.09	3.09	24.4
	3	7.95	6.47	18.6

Miscellaneous Comparisons. A second area of connector comparison was concerned with some general features of each design. The features evaluated are shown in Table 17. The conventional integral-flange and loose-ring-flange connectors are combined under the single heading "Bolted Flange" in Table 17 since the designs are identical for the features being considered. The best overall rating for these general design features was shown by the bolted-flange and compression-collar connectors.

TABLE 17. COMPARISON OF GENERAL DESIGN FEATURES

Condition	Bolted Flange	Compression Collar	Threaded Flange	Breech Type	Segmented V-Band	X-Connector
Special tools	Good	Good	Undesirable	Undesirable	Good	Undesirable
Required clearance - beyond connector envelope	Acceptable	Acceptable	Good	Good	Acceptable	Undesirable
Preload accuracy	Good	Good	Acceptable	Acceptable	Acceptable	Acceptable
Required machining tolerance	Good	Good	Acceptable	Undesirable	Acceptable	Acceptable
Flange load distribution with axial misalignment	Good	Good	Undesirable	Undesirable	Acceptable	Acceptable

A third area of comparison was the estimated assembly time required for each connector type. The calculations were based on "Assembly Time Units". One (1) Assembly Time Unit (ATU) was defined as the time required to insert one bolt (for the smaller connectors) through the holes of a conventional connector, to start the nut, and to run the nut to a hand-tight condition (1ATU = 15 to 30 seconds). The ATU values for basic assembly functions are shown in Table 18.

TABLE 18. SINGLE-BOLT ASSEMBLY-TIME-UNIT REQUIREMENTS

Connector Assembly Function	Tube Diameter	
	1 Through 4 In.	5 Through 16 In.
Hand Assembly	1	2 to 3
Seal seating	1/2 per nut turn	3/4 per nut turn
Preload torque	1	1 to 2

Table 19 gives the breakdown and summarization of ATU's for the individual assembly functions of bolted-flange connectors. Table 18 was prepared for conventional connectors in particular, but slight alterations made the data applicable to compression-collar and V-band connectors. Tables 20 and 21 present the estimates for these two configurations. Although time estimates for breech-type and threaded-flange connectors were less accurate, since their assembly functions could not be directly associated with the assembly functions of a simple bolt, Tables 22 and 23 present the estimated assembly times for these two connectors. The final column in each of the five assembly-time tables represents the range of estimated real time. The summary of assembly-time estimates, as listed in Table 24, represents the average of this real-time range.

TABLE 19. BOLTED-FLANGE-CONNECTOR ASSEMBLY-TIME ESTIMATES

Pressure, psi	Tube Diameter, in.	Bolts		Turns to Seat Seal	Single-Bolt ATU				Total ATU	Time Range, min
		No.	Size		Hand Assembly	Seal Seating	Preload Torque	Total		
100	1	6	# 10	3-3/4	1	2	1	4	24	6 to 12
	8	20	1/4	3-1/2	2	3	1	6	120	30 to 60
	16	36	1/4	6	3	4	1	8	288	72 to 144
1500	1	6	# 10	3-3/4	1	2	1	4	24	6 to 12
	8	16	3/8	2-3/4	2	3	2	7	112	28 to 56
	16	30	1/2	4-1/4	3	4-1/2	2	9-1/2	285	71 to 142
6000	1	6	# 10	3-3/4	1	2	1	4	24	6 to 12
	3	10	3/8	2-3/4	1	1-1/2	2	4-1/2	45	11 to 22

TABLE 20. COMPRESSION-COLLAR-CONNECTOR ASSEMBLY-TIME ESTIMATES

Pressure, psi	Tube Diameter, in.	Bolts		Turns to Seat Seal	Joint Hand Assembly	Single-Bolt ATU				Total ATU	Time Range, min
		No.	Size			Insert Bolt	Seal Seating	Preload Torque	Total		
100	1	6	# 10	3-3/4	3	1	2	1	4	27	7 to 14
	8	20	1/4	3-1/2	5	1	3	1	5	105	26 to 52
	16	34	1/4	6	8	1	4	1	6	212	53 to 100
1500	1	6	# 10	3-3/4	3	1	2	1	4	27	7 to 14
	8	20	5/16	3	5	1	2-1/2	1-1/2	5	105	26 to 52
	16	34	7/16	4-1/4	8	1	3-1/2	2	6-1/2	229	57 to 114
6000	1	6	# 10	3-3/4	3	1	2	1	4	27	7 to 14
	3	12	5/16	3	4	1	1-1/2	1-1/2	4	52	13 to 26

TABLE 21. V-BAND-CONNECTOR ASSEMBLY-TIME ESTIMATES

Pressure, psi	Tube Diameter, in.	Nuts		Nut Turns to Seat Seal	Single Nut ATU				Total ATU	Time Range, min
		No.	Size		Hand Assembly	Seal Seating	Preload Torque	Total		
100	1	6	# 10	7	1/2	5	1/2	6	36	9 to 18
	8	6	5/16	5	1	4	1	6	36	9 to 18
	16	6	7/16	8	1-1/2	6	1-1/2	9	54	14 to 28
1500	1	6	# 10	7	1/2	5	1/2	6	36	9 to 18
	8	6	3/4	3-1/2	1	6	1	8	48	12 to 24
	16	6	1-1/4	5	1-1/2	9	1-1/2	12	72	18 to 36
6000	1	6	1/4	6-1/2	1/2	5	1/2	6	36	9 to 18
	3	6	5/8	4	1	5	1-1/2	7-1/2	45	12 to 24

TABLE 22. BREECH-TYPE-CONNECTOR ASSEMBLY-TIME ESTIMATES

Pressure, psi	Tube Diameter, in.	Joint Hand Assembly	Attach Special Tool	Seat Seal	Preload Joint	Lock Joint	Remove Tool	Total ATU	Time Range, min
100	1	2	Not reqd.	2	2	2	--	8	2 to 4
	8	2	16	14	2	6	6	46	12 to 24
	16	4	24	40	4	10	10	92	23 to 46
1500	1	2	Not reqd.	2	2	2	--	8	2 to 4
	8	2	16	14	8	6	6	52	13 to 26
	16	4	24	40	16	10	10	104	26 to 52
6000	1	2	8	2	2	2	4	20	5 to 10
	3	3	8	4	2	3	4	24	6 to 12

TABLE 23. THREADED-FLANGE-CONNECTOR ASSEMBLY-TIME ESTIMATES

Pressure, psi	Tube Diameter, in.	Joint Hand Assembly	Attach Special Tool	Seat Seal	Preload Joint	Remove Tool	Total ATU	Time Range, min
100	1	2	No. reqd.	2	2	--	6	1-1/2 to 3
	8	4	16	14	2	6	42	11 to 22
	16	8	24	40	4	10	86	21 to 42
1500	1	2	Not reqd.	2	2	--	6	1-1/2 to 3
	8	4	16	14	8	6	48	12 to 24
	16	8	24	40	16	10	98	25 to 50
6000	1	2	8	2	2	4	18	4-1/2 to 9
	3	3	8	4	2	4	21	5 to 10

TABLE 24. SUMMARY OF ASSEMBLY-TIME ESTIMATES

Pressure, psi	Tube Diameter, in.	Bolted Flange	Compression Collar	Threaded Flange	Breech Type	Segmented V-Band
100	1	9 min	10 min	2 min	3 min	14 min
	8	45 min	39 min	16 min	18 min	14 min
	16	1 hr 45 min	1 hr 20 min	31 min	35 min	21 min
1500	1	9 min	10 min	2 min	3 min	14 min
	8	42 min	39 min	18 min	19 min	18 min
	16	1 hr 45 min	1 hr 25 min	38 min	39 min	27 min
6000	1	9 min	10 min	7 min	8 min	14 min
	3	18 min	19 min	8 min	9 min	18 min

The threaded-flange connector shows the lowest time requirement for the largest range of system parameters. The V-band connector requires slightly lower assembly times in tube diameters from 8 to 16 inches at system pressures of 1500 psi and below.

Conclusions and Recommendations. On the basis of the investigations described above, the following conclusions were reached:

(1) Optimized conventional integral- and loose-ring-flange connectors will be lighter in weight than most flanged connectors that might be developed from nonconventional configurations.

(2) Nonconventional threaded-flange connectors offer the promise of a weight savings of up to 25 percent as compared with conventional flanged connectors.

(3) The successful development of large, threaded-flange connectors depends on the development of easily used assembly tools.

The following recommendations were made concerning the development of flanged connectors during the remainder of the program:

(1) Conventional integral- and loose-ring-flange connectors should be developed for all sizes and service conditions.

(2) With funds in addition to those allocated, a parallel program should be undertaken to develop large threaded-flange connectors and appropriate assembly tooling. This development could be undertaken in the following major steps: (a) the design of representative connectors and associated assembly tools and (b) the fabrication and field evaluation of selected connectors and assembly tools.

Investigation of Connector Thermal Gradients

As described in Technical Documentary Report No. AFRPL-TR-65-162, a separable connector can achieve very low helium leakage rates over a wide temperature range only if the connector design can accommodate the effects of thermal gradients. This degree of design sophistication is not usually required for connectors containing liquids, and as a result, most separable-connector designs do not include a detailed thermal-gradient analysis. The development of such an analysis technique for the AFRPL threaded connectors is believed to be a major reason for the success of the connector in maintaining low gas leakage over large temperature ranges. Consequently, the decision was made to incorporate a thermal-gradient analysis in the design procedure for flanged connectors.

The effects of thermal gradients on a connector are strongly dependent on the configuration and operating principles of the connector. As discussed previously, the Bobbin seal specifically incorporates a feature to minimize the effect of changes in axial load on the effectiveness of the seal. Because of the complex configuration of flanged connectors, a theoretical analysis of heat transfer in a connector is not only very costly, but is also subject to significant inaccuracies. Thus, the decision was made to estimate the connector thermal gradients by making temperature measurements on connector parts similar to those expected for the final connectors.

Experiments With Flange Segments. The initial thermal-gradient tests were conducted with bolted flange segments. The use of segments that were sized to simulate a typical portion of a connector flange greatly reduced not only the cost of the parts but also the cost of the tests. It was believed that the results of these tests would facilitate the selection of optimum connector proportions. The details of the segments are shown in Figures 36 and 37. Two segments of each size were bolted together, and thermocouples were attached to the bolt and to the segment as shown in Figure 38. The sides of the segments were insulated, and the surface simulating the inside surface of the connector and the tube wall was subjected to hot and cold fluid temperatures according to the required connector temperature limits.

Figure 39 shows the thermocouple readings when the inner surface of a simulated high-pressure, stainless steel connector was placed in contact with liquid nitrogen. The sudden drop in temperature near TC-6 after 11 minutes was attributed to increased heat transfer between the nitrogen and the connector as local boiling of the nitrogen subsided. The decision was made to mount the simulated connector in a vertical position to permit the bubbles to escape more readily and more closely simulate a flowing liquid.

Figures 40, 41, and 42 show typical results for vertically mounted specimens. The average flange temperatures were obtained from the arithmetic average of four thermocouples in the flange segments. One thermocouple located in the center of the bolt was

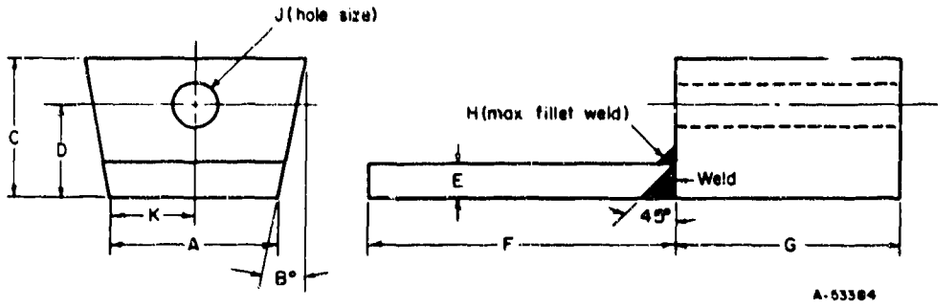

Tube Diam, in.	Pressure, psi	A	B'	C	D	E	F	G	H	J	K	No. of Sim. Bolts	Deg. of Sim. Flange
1	6000	0.38	27-1/2	0.68	0.49	0.149	3.87	0.63	0.12	0.201	0.19	6	60
3	6000	0.67	17-1/2	1.32	0.94	0.44	2.95	1.55	0.15	0.397	0.34	10	36
1	4000	0.40	27-1/2	0.65	0.46	0.1196	4.00	0.50	0.12	0.201	0.20	6	60
3	4000	0.72	17-1/2	1.15	0.85	0.375	3.22	1.28	0.15	0.332	0.36	10	36
1	1500	0.48	27-1/2	0.57	0.38	0.0418	4.17	0.33	0.12	0.201	0.24	6	60
3	1500	1.08	21-1/2	0.81	0.56	0.1196	3.54	0.96	0.15	0.266	0.54	8	45
5	1500	1.45	19-1/2	0.88	0.67	0.20	3.11	1.39	0.15	0.332	0.73	10	36
8	1500	1.45	11	1.20	0.82	0.320	2.61	1.89	0.15	0.397	0.73	16	22.5
12	1500	1.45	8	1.65	1.15	0.48	1.78	2.72	0.19	0.531	0.73	24	15
16	1500	1.45	5-1/2	1.81	1.31	0.64	1.00	3.50	0.19	0.531	0.73	32	11.25

Note: All dimensions in inches unless otherwise noted.

FIGURE 36. DETAILS OF SEGMENTS FOR THERMAL-GRADIENT TESTS FOR SIMULATED TYPE 347 STAINLESS STEEL BOLTED FLANGES

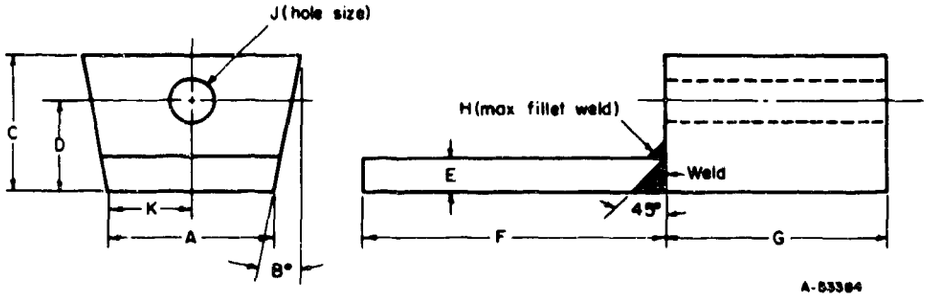

Tube Diam, in.	A	B	C	D	E	F	G	H	J	K	No. of Sim. Bolts	Deg. of Sim. Flange
1	0.48	27-1/2	0.73	0.48	0.042	4.23	0.27	0.15	0.266	0.24	6	60
3	1.08	21-1/2	1.06	0.69	0.126	3.75	0.75	0.15	0.397	0.54	8	45
5	1.20	14-1/2	1.27	0.84	0.210	3.27	1.23	0.15	0.531	0.60	12	30
8	1.28	10	1.71	1.09	0.336	2.82	1.68	0.15	0.656	0.64	18	20
12	1.44	7-1/2	2.38	1.38	0.504	2.09	2.41	0.18	0.813	0.72	24	15
16	1.53	6	2.55	1.67	0.672	1.50	3.00	0.15	0.938	0.76	32	11.25

Note: All dimensions in inches unless otherwise noted.

FIGURE 37. DETAILS OF SEGMENTS FOR THERMAL-GRADIENT TESTS FOR SIMULATED 1500-PSI 6061 ALUMINUM BOLTED FLANGES

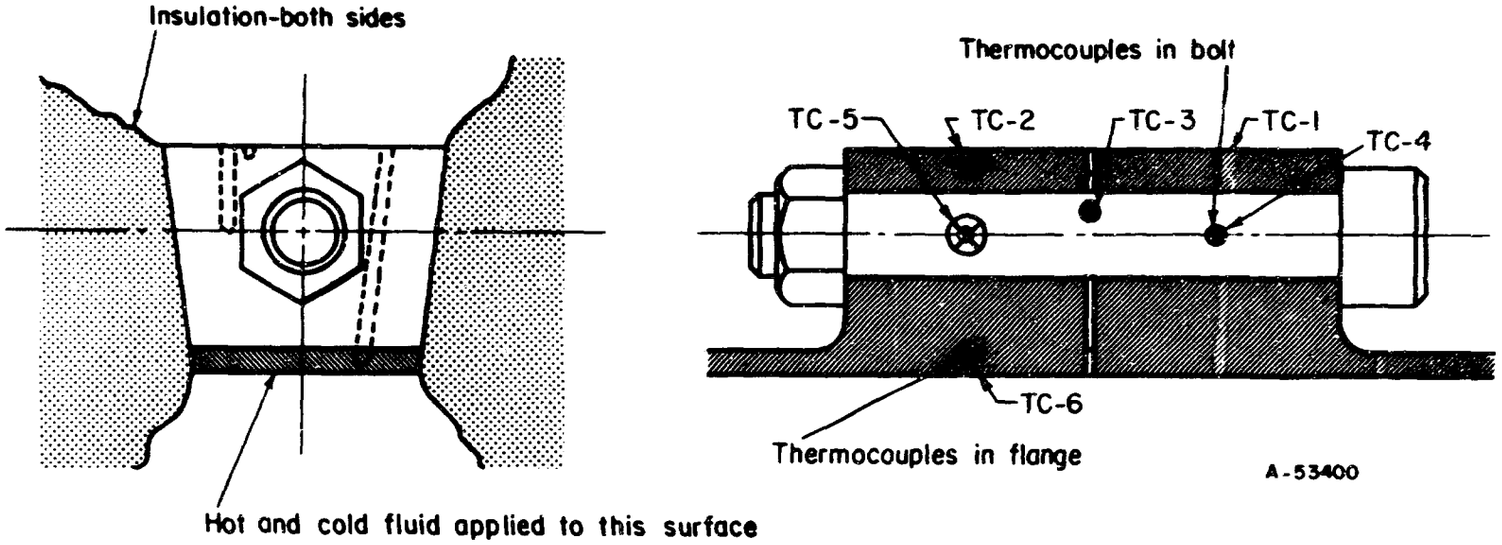

FIGURE 38. LOCATION OF THERMOCOUPLES FOR THERMAL-GRADIENT TESTS WITH BOLTED FLANGED SEGMENTS

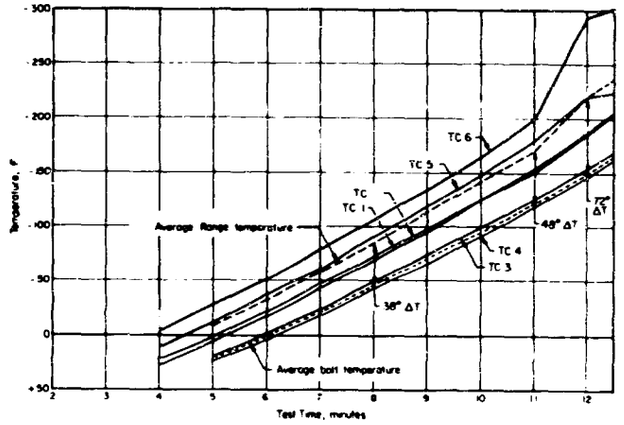

FIGURE 39. RESULTS OF THERMAL-GRADIENT TESTS WITH FLANGE SEGMENTS SIMULATING A 3-INCH, 6000-PSI, TYPE 347 STAINLESS STEEL CONNECTOR
(Test Run No. 5

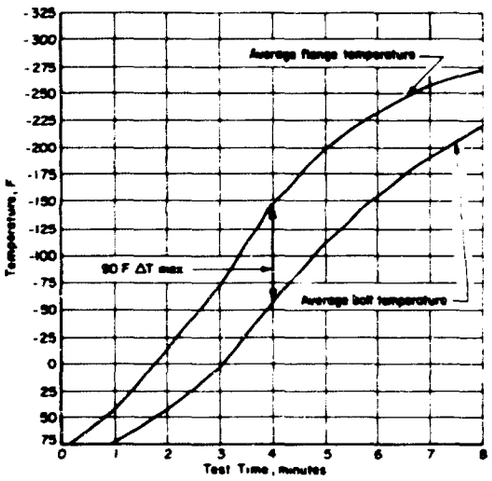

FIGURE 40. RESULTS OF THERMAL-GRADIENT TESTS WITH FLANGE SEGMENTS SIMULATING A 3-INCH, 4000-PSI STAINLESS STEEL CONNECTOR WITH STAINLESS STEEL BOLTS AND NUTS

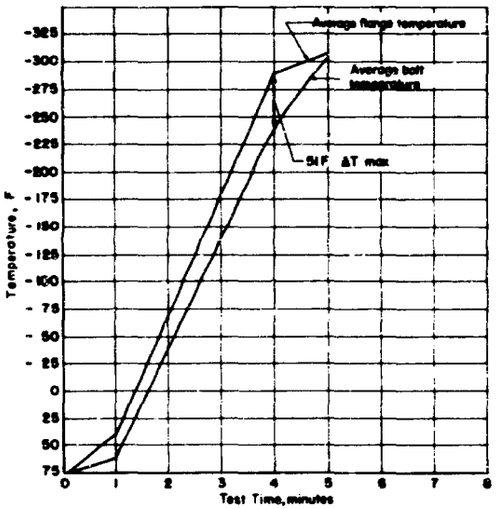

FIGURE 41. RESULTS OF THERMAL-GRADIENT TESTS WITH FLANGE SEGMENTS SIMULATING A 5-INCH, 1500-PSI ALUMINUM CONNECTOR WITH ALUMINUM BOLTS AND NUTS

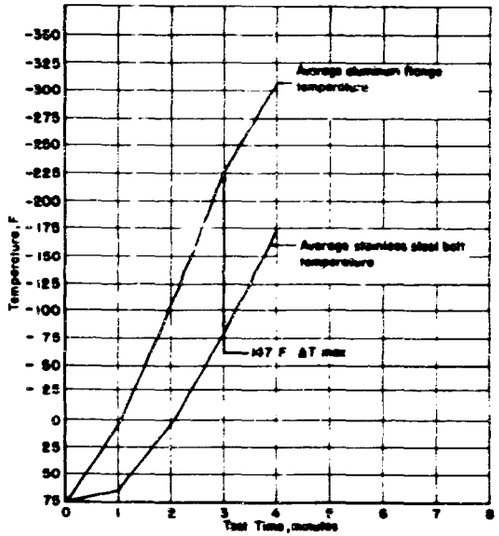

FIGURE 42. RESULTS OF THERMAL-GRADIENT TESTS WITH FLANGE SEGMENTS SIMULATING A 5-INCH, 1500-PSI ALUMINUM CONNECTOR WITH STAINLESS STEEL NUTS AND BOLTS

used to measure the bolt temperature. The results showed that a significantly greater thermal-gradient problem exists with stainless steel connectors than with aluminum connectors. The tests also showed that it would be undesirable to use steel bolts with aluminum connectors despite their higher strength and greater resistance to damage due to handling. Figure 43 shows the maximum temperature difference measured for different sizes of aluminum and stainless steel connector flange segments when in contact with liquid nitrogen and boiling water.

Experiments With Connectors. Thermal-gradient measurements were made with 2- and 3-inch connector assemblies made of Type 347 stainless steel and 6061-T6 aluminum in both integral and loose-ring configurations. For the integral-flange assembly, measurements were made of the temperatures at the Bobbin seal tang, the integral flange at the bolt circle, and the bolt shank between the flanges. For the loose-ring assembly, temperatures were measured at the Bobbin seal tang, the outside diameter of the stub flange, the loose ring at the bolt circle, and the bolt shank midway between the flanges. Table 25 shows the results of the tests. A comparison of the integral-flange-to-bolt temperature differences for the 3-inch aluminum and stainless steel connectors in Table 25 (35 F and 55 F, respectively) shows good correlation with the values measured for the 3-inch-connector flange segments shown in Figure 43b and d (25 F and 62 F, respectively).

TABLE 25. RESULTS OF THERMAL-GRADIENT MEASUREMENTS FOR CONNECTOR ASSEMBLIES AT ROOM TEMPERATURE EXPOSED TO LIQUID NITROGEN

Tube Diameter, in.	Flange Type	Material	Temperature Difference, F: Seal to Integral Flange	Integral Flange to Bolt	Seal to Stub Flange	Stub Flange to Loose Ring	Loose Ring to Bolt
3	Integral	Type 347 SS	70	55			
2	Integral	Type 347 SS	30	49			
3	Integral	6061-T6 Al	60	35			
2	Integral	6061-T6 Al	30	50			
3	Loose Ring	Type 347 SS			65	65	75
2	Loose Ring	Type 347 SS			35	60	60
3	Loose Ring	6061-T6 Al			30	30	48
2	Loose Ring	6061-T6 Al			40	32	34

Deflection Measurements. Measurements were made of the deflections in the flanges of the 2- and 3-inch aluminum and stainless steel connectors subjected to liquid nitrogen temperatures. The connectors were assembled and the bolts were stressed to selected preload levels. When the connectors were filled with liquid nitrogen, the deflections of the flange elements were measured to determine the effects of the thermal gradients. The results of these measurements are shown in Figures 44 through 47.

As shown in Figure 44, when the 3-inch, Type 347 stainless steel, integral flanged connector was cooled, the thermal gradients caused the flange elements to rotate

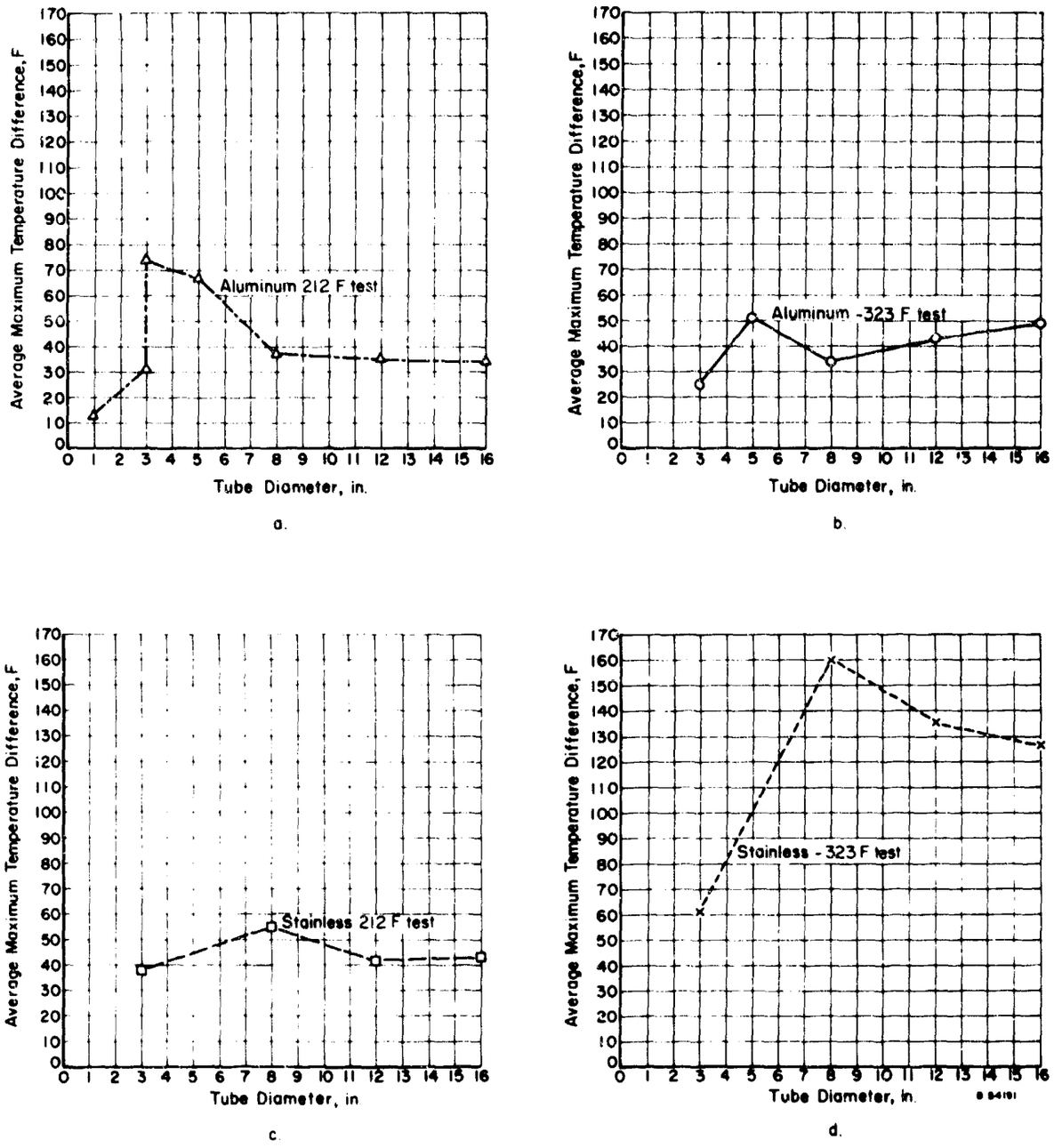

FIGURE 43. 212 F AND -323 F THERMAL-GRADIENT TEST RESULTS FOR 1500-PSI ALUMINUM AND STAINLESS STEEL CONNECTOR FLANGE SEGMENTS

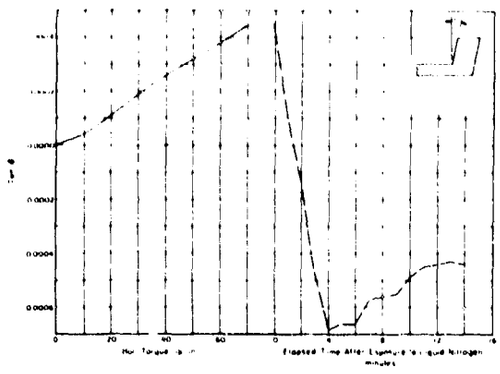

FIGURE 44. FLANGE DEFLECTION FOR 3-INCH, 1500-PSI, STAINLESS STEEL INTEGRAL-FLANGE CONNECTOR

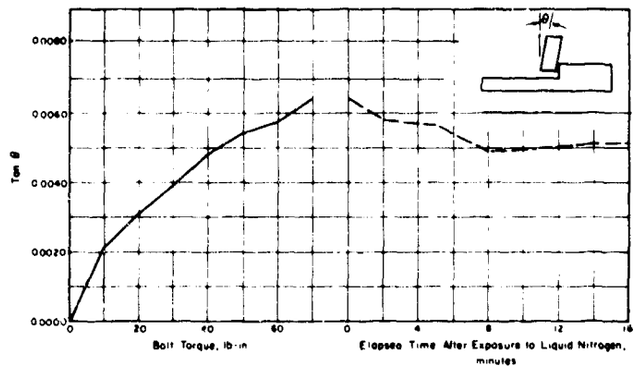

FIGURE 45. FLANGE DEFLECTION FOR 3-INCH, 1500-PSI STAINLESS STEEL LOOSE-RING-FLANGE CONNECTOR

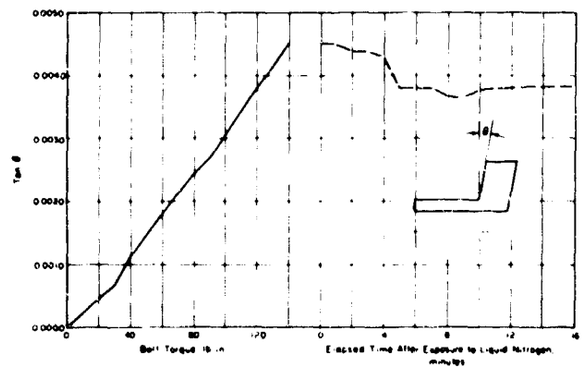

FIGURE 46. FLANGE DEFLECTION FOR 3-INCH, 1500-PSI ALUMINUM INTEGRAL-FLANGE CONNECTOR

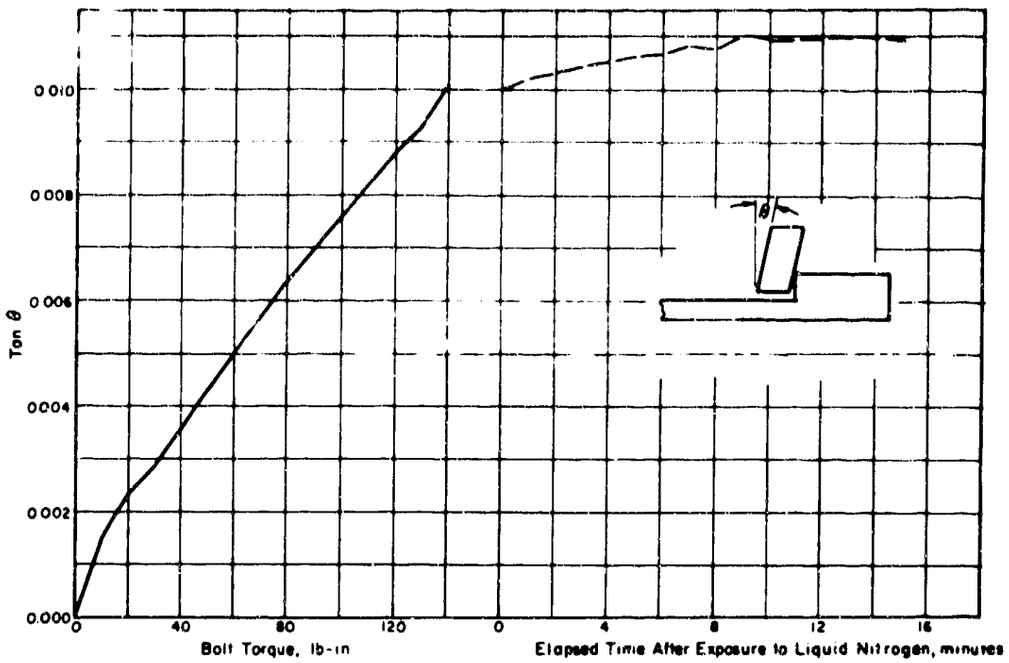

FIGURE 47. FLANGE DEFLECTION FOR 3-INCH, 1500-PSI ALUMINUM LOOSE-RING-FLANGE CONNECTOR

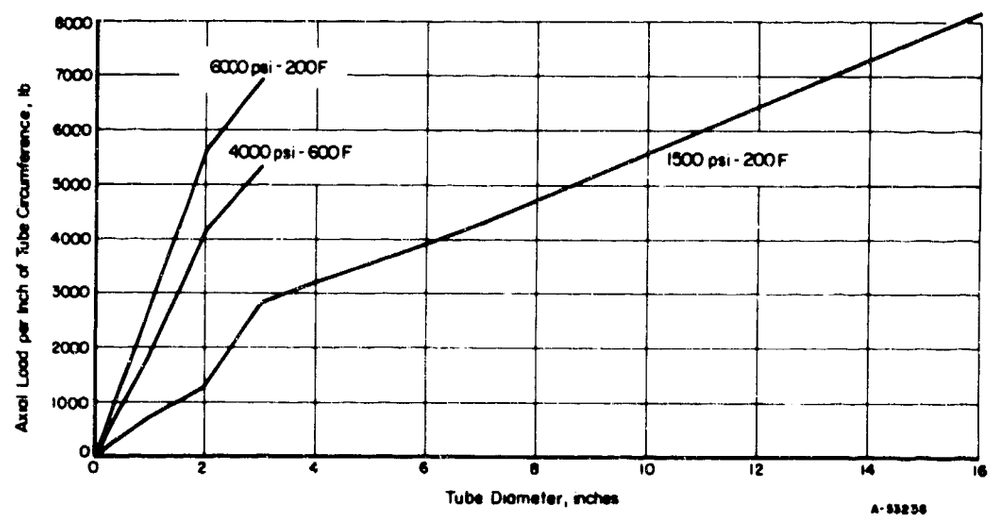

FIGURE 48. PRESSURE PLUS BENDING LOADS (AXIAL) FOR TYPE 347 STAINLESS STEEL TUBE CONNECTORS

conversely to the direction of rotation during bolt-up. This resulted from axial shrinkage of the seal and the flange plus radial shrinkage of the tube adjacent to the flange. Thus, in the flange-design program, it appeared necessary to account for the effects of thermal gradients in the radial direction as well as in the axial direction.

Investigation of Bolt Parameters

A survey was made of the technical literature available at Battelle-Columbus on bolted fasteners. Approximately 120 references were selected and cataloged. Also, about 25 reports on material properties were surveyed and cataloged. Catalogs and technical literature on other types of fasteners were included in the information survey. Although several interesting types of fasteners were identified, it was decided that no fastener configuration seriously challenged nut and bolt fasteners for the conventional integral- and loose-ring-flange connectors that were selected for development.

Preliminary Investigation of Fasteners for Stainless Steel Connectors. Preliminary calculations for estimating fastener loads per inch of connector circumference were made on the basis of the system requirements given in Table 10. Tentative values of the axial loads due to pressure and bending that must be sustained by the fasteners for Type 347 stainless steel tubing systems are given in Figure 48.

The strengths of bolt-nut fasteners were obtained from catalog data for commercially available socket-head-type bolts with an ultimate tensile strength of the order of 190,000 psi. Figure 49 shows the strength/weight ratios for these fasteners using three different bolt spans or grips. It can be seen that the smaller bolt sizes give a somewhat better strength/weight ratio. Figure 50 shows the tensile load that can be sustained by bolt-nut fasteners made from A286, on the basis of data published in NASA CR-357[4]. Preliminary selections of A286 bolt sizes for the three high-pressure service ranges are listed in Table 26.

Preliminary Investigation of Fasteners for Aluminum Connectors. A search was made for suppliers of high-strength aircraft-quality aluminum bolts, and for information on bolt yield strength at 200 F and -400 F. Fastener supply companies and fastener manufacturers were contacted. Several companies could supply 6061-T6 aluminum bolts, and a few could supply 2024-T4 aluminum bolts from stock, but none could supply higher strength aluminum bolts from stock. None of the companies contacted could supply information on bolt yield strength for any of the alloys at the desired temperatures or at room temperature.

A preliminary estimate was made of the axial loads that must be sustained by the fasteners for the 6061-T6 aluminum connectors. An estimate was made of the tensile-load capability of 2024-T4 aluminum bolts in sizes from 1/4 to 7/8 inch, as illustrated in Figure 51. Table 27 shows the preliminary selection made of the bolt size and number required for bolted flanged connectors for 1500-psi aluminum connectors.

Two quotations were obtained for 7075 aluminum bolts, as shown in Table 28. It appeared possible to obtain bolts of the diameter and length required for the connectors in AN 300 series 7075-T73 aluminum with a NAS 624-type 12-point head. Commercial-quality-aluminum bolts in alloy 7075-T6 manufactured in compliance with American Standard B18.2-1955 also appeared to be available as required. However, it was concluded that the use of 7075 aluminum bolts for the connectors would impose a substantial cost disadvantage.

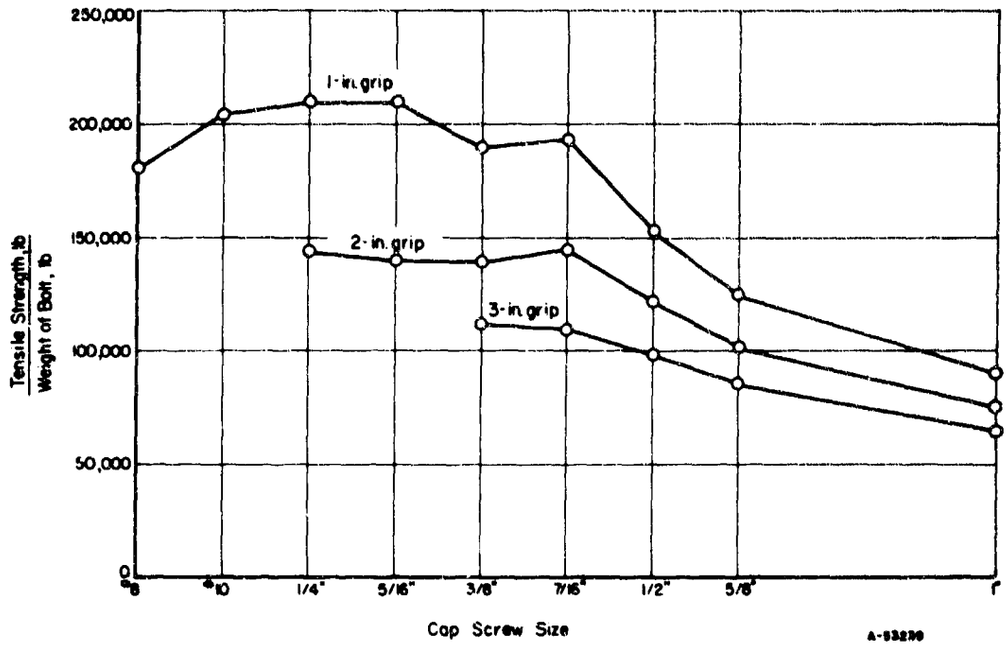

FIGURE 49. STRENGTH/WEIGHT RATIOS FOR UNF SOCKET-HEAD CAP SCREWS WITH LIGHT HEX FULL-HEIGHT LOCK NUT AND WASHER

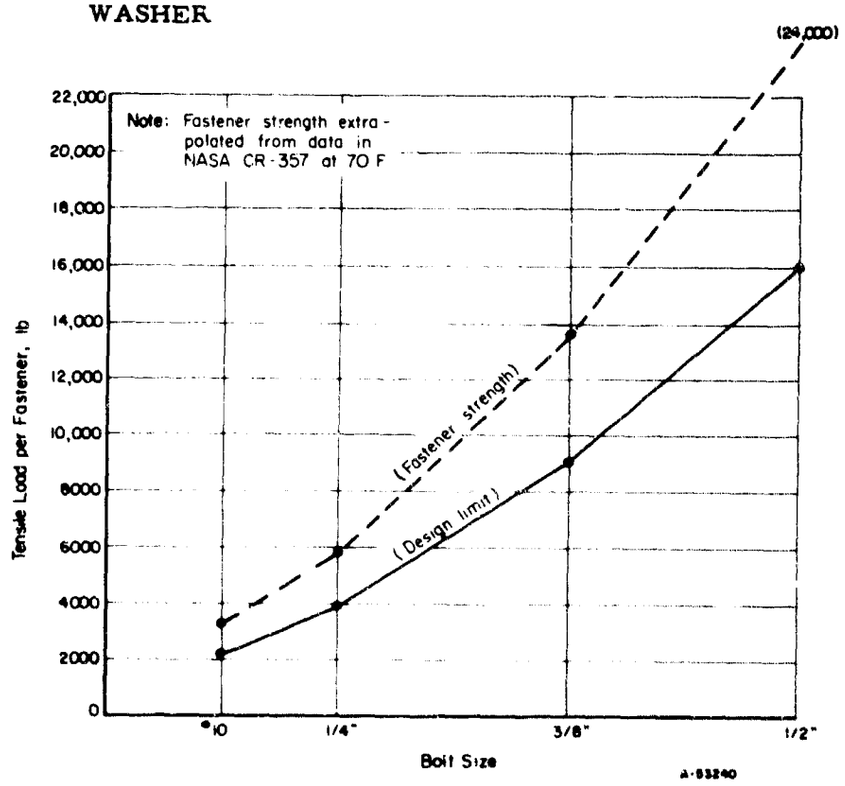

FIGURE 50. FASTENER LOAD CAPACITY (A286 BOLT AND NUT)

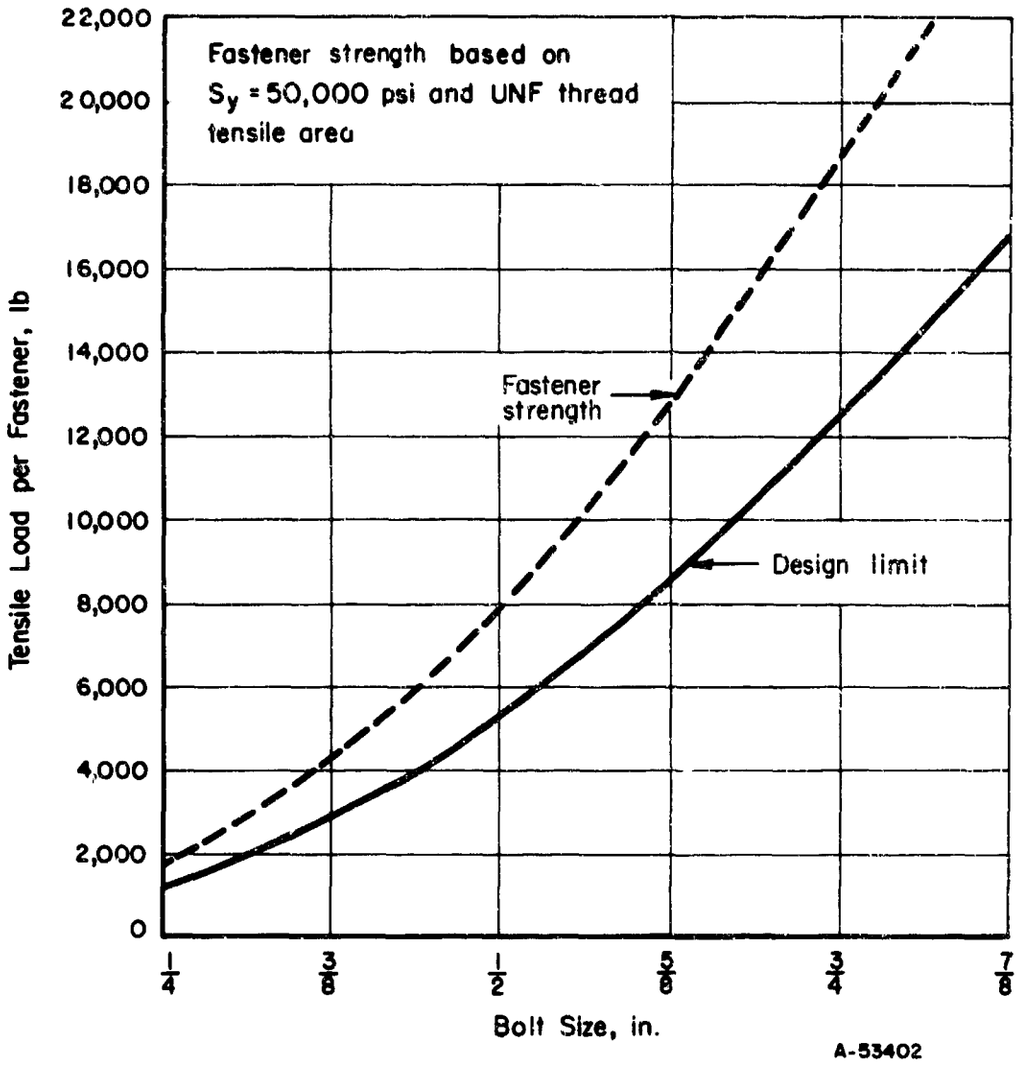

FIGURE 51. FASTENER LOAD CAPACITY (2024-T4 ALUMINUM)

TABLE 26. PRELIMINARY SELECTION OF A286 BOLT SIZES FOR STAINLESS STEEL CONNECTORS

Tube Diameter, in.	6000-Psi, 200 F System		4000-Psi, 600 F System		1500-Psi, 200 F System	
	Bolt Size	No. of Bolts	Bolt Size	No. of Bolts	Bolt Size	No. of Bolts
1	No. 10	6	No. 10	6	No. 10	6
2	5/16"	8	1/4"	8	No. 10	6
3	3/8"	10	5/16"	10	1/4"	8
4					5/16"	8
5					5/16"	10
6					3/8"	12
7					3/8"	14
8					3/8"	16
9					3/8"	20
10					3/8"	24
11					1/2"	20
12					1/2"	22
13					1/2"	24
14					1/2"	26
15					1/2"	30
16					1/2"	32

TABLE 27. PRELIMINARY SELECTION OF 2024-T4 ALUMINUM BOLT SIZES FOR 1500-PSI, 200 F, 6061-T6 ALUMINUM CONNECTORS

Tube Diameter, in.	No. of Bolts	Size of Bolts
1	6	1/4-28
2	6	5/16-24
3	8	3/8-24
4	10	1/2-20
5	12	1/2-20
6	14	9/16-18
7	16	9/16-18
8	18	5/8-18
9	20	5/8-18
10	22	5/8-18
11	20	3/4-16
12	24	3/4-16
13	26	3/4-16
14	24	7/8-14
15	26	7/8-14
16	30	7/8-14

TABLE 28. QUOTED COST OF 7075 ALUMINUM BOLTS

7075-T73 AN3DD Series		7075-T6 American Standard B18.2-1955	
Size	Cost per 100 Lb, $	Size	Cost per 100 Lb, $
BM9138-4-7	439.00	1/4-28 x 3/4	49.70
BM9138-6-20	524.40	3/8-24 x 2	46.00
BM9138-8-30	593.00	1/2-20 x 3	53.35
BM9138-10-40	844.20	5/8-18 x 4	83.50
BM9138-12-54	1067.10	3/4-16 x 6	140.00
BM9138-14-67	1863.00	7/8-14 x 7	168.00

Preliminary Consideration of Threaded-Fastener Parameters. A study was made of published information on such factors as preload, fatigue failure, vibration resistance, corrosion resistance, surface finish, hardness, lubrication, fastener stiffness, and the effect of successive tightenings.

Three methods of predicting bolt preload or tension are commonly used: (1) measuring the applied torque, (2) measuring the fastener's extension, and (3) estimating the amount of nut rotation. Patented configurations have begun to appear recently, which are based on the yielding of a part of the bolt-nut assembly. Measurement of the applied torque is the method most often used, although some of the new designs show considerable promise. Price and Trask[5] investigated the following factors and their effect on bolt tension:

(1) Structure material
(2) Bolt grip length
(3) Lubricant
(4) End of fastener turned
(5) Number of successive tightenings.

Variations in the structural materials showed little difference in the bolt torque for lubricated parts. However, steel bolts mated with a titanium structure showed higher torques than steel bolts mated with an aluminum or steel structure for nonlubricated, as-received parts. The maximum bolt load on aluminum structures and other low compressive yield materials is limited by local deformations of the structure at the area of contact with the bolt head and nut. The grip length and the end of the fastener to which tightening torque is applied had little effect on the torque-preload relationship.

Lubrication of the mating parts, however, had a significant effect on the torque required to produce a specified bolt load. The torque required to stress a nonlubricated (specimens as-received) 3/4-inch bolt to 100,000 psi was 5140 lb-in. This torque was 2590 lb-in. when the specimen was lubricated. Price and Trask noted similar results at other stress levels for 3/4-inch and 1/4-inch fasteners.

A computational method for relating bolt torque, stress, and diameter was suggested by these investigations. The ratio R as determined by Equation (13) was used:

$$R = \frac{1000\ T_o}{D_b\ S}, \qquad (13)$$

where

T_o = torque, lb-in.

D_b = bolt diameter, in.

S = axial stress in bolt, psi.

A factor of 1000 was used for convenience in locating the decimal point. Values of R were calculated by Price and Trask for 1/4-inch and 3/4-inch steel bolts for lubricated and as-received conditions for three stress levels. These values are shown in Table 29.

TABLE 29. RATIO R FOR 1/4-INCH AND 3/4-INCH STEEL BOLTS

Bolt Stress, psi	R (Lubricated)		R (As Received)	
	1/4 In.	3/4 In.	1/4 In.	3/4 In.
100,000	3.52	3.48	8.24	6.00
120,000	3.57	3.59	8.29	5.98
140,000	3.60	3.66	8.51	5.92

For lubricated fasteners the value of R was nearly the same for 1/4-inch bolts as it was for 3/4-inch bolts when the bolts were stressed to the same axial stress level. The change in R with changes in stress level was also small. When the formula was applied to bolts in the nonlubricated or as-received condition, however, the ratio was not constant for different bolt sizes.

Repeated installation of threaded fasteners was found to have a significant effect on the torque-tension ratio. Repeated installation for as-received fasteners, in general, required higher torque for a given tension than was required on the first installation. The installation torque for lubricated fasteners was reported to be essentially constant after the second assembly. This effect is shown in Table 30. All torques are for an axial stress of 100,000 psi in the bolt. The lock-nut torque shown is the torque required to turn the lock nut with no axial load on the bolt.

From the report by Price and Trask, it can be concluded that the use of lubricated fasteners permits relatively accurate prediction of bolt tension and reliable reuse of bolt and nut.

Other investigations, however, have shown that lubrication tends to reduce the vibration resistance of threaded fasteners to a marked degree. One comparison[6] of the effect of vibration for lubricated versus nonlubricated fasteners shows that lubricated fasteners lost all preload after 1000 to 2000 cycles, while nonlubricated fasteners held for the duration of the test extending to 125,000 cycles. The nuts used were plain nuts. In other tests, various lock nuts were evaluated for vibration resistance. These included nonmetallic insert, beam type, distorted thread, castellated, and plain. Of these, the nonmetallic-insert type performed best, with the beam type performing next best. Castellated types and those with a distorted thread were less effective in resisting the effects of

TABLE 30. EFFECT OF REPEATED ASSEMBLY ON TIGHTENING TORQUE FOR STEEL BOLTS[a]

Total Tightening Torque and Torque to Turn Lock Nut Alone, lb-in.							
First Installation		Second Installation		Third Installation		Fourth Installation	
Total Torque	Lock-Nut Torque	Total Torque	Lock-Nut Torque	Total Torque	Lock-Nut Torque	Total Torque	Lock-Nut Torque
1/4-Inch Fastener Lubricated							
88	24	68	6	71	6	63	6
95	12	65	5	62	4	65	3
88	8	60	3	54	-	57	-
82	19	68	5	64	5	66	3
89	11	62	4	68	4	60	4
183	18	286	24	357	24	-	-
244	28	360	27	-	-	-	-
253	35	378	35	-	-	-	-
237	27	350	24	-	-	-	-
179	6	295	-	377	-	408	-
3/4-Inch Fastener Lubricated							
2590	-	2550	-	2450	-	2400	-
2530	-	2220	-	2030	-	2040	-
2590	-	2320	-	2370	-	2240	-
2800	-	2350	-	2240	-	2180	-
2550	-	2240	-	2140	-	1990	-
3/4-Inch Fastener As Received							
5140	180	5780	130	6090	100	6250	80
4960	180	6450	100	6720	80	6940	50
4500	230	5960	130	7020	100	6610	80
3700	180	3830	100	4220	100	4500	80
4290	180	4010	80	4370	-	4550	-

(a) From National Bureau of Standards Report 7308, "The Relation Between Torque and Tension for High Strength Threaded Fasteners", J. I. Price and D. K. Trask.

vibration. In general, high installation torque for a given bolt stress level will give the highest resistance to vibration. The results of another investigation[7] indicated that if a fastener system meets room-temperature vibration requirements, it should present no problems at cryogenic temperatures.

The fatigue of bolted fasteners has received much attention[8-12] in recent years. The most important factor is the preload of the bolt. Increasing the bolt preload has the effect of reducing the minimum-to-maximum stress ratio. Although increasing the bolt preload increases the mean stress, the fatigue strength of the bolt is improved.

One study of the fatigue life of threaded fasteners as affected by the ratio of minimum to maximum working load showed that the fatigue life exceeded 2 million cycles for

a ratio of 0.5, dropped to 200,000 cycles at a ratio of 0.4, and dropped further to 100,000 cycles for ratios below 0.3. The angularity of the bearing surface also had a marked effect on fatigue life. An angular deviation of 1 degree reduced the fatigue life by 38 percent and an angular deviation of 2 degrees caused a 91 percent reduction in fatigue life.

Unengaged threads on the bolt and reuse of the nut each have been shown to cause a marked effect on the fastener fatigue life. If two or more threads are unengaged on the bolt, the fastener fatigue life is about three times as great as that in an installation where the nut is close to thread run-out. Reuse of stressed nuts has been shown to decrease the fastener fatigue life about 32 percent on the first reuse. The life then decreases to about 50 percent on the second reuse and remains at this level for repeated reuse.

The relative stiffness of the bolt and bolted assembly were major factors affecting the fatigue life of bolted assemblies. Fatigue life was improved for bolts with relatively low stiffness by designing the surrounding structure assembly, including the washer, with a relative high stiffness. Increasing the thread root radius generally improved the fatigue life. Special nuts, designed to distribute the preload along the nut, are apparently of questionable value from the standpoint of fatigue life. Data on fatigue life for these nuts show much scatter, but generally the fatigue life is somewhat improved by the use of special nuts.

Nuts having a nonmetallic collar insert for vibration resistance show reduced fatigue life. This is probably due to a reduced number of threads to accommodate the collar insert. Higher nut height generally improves fatigue life. The use of a lubricant also improves fatigue life but reduces vibration resistance.

The effect of higher temperatures on fastener fatigue life is both good and bad. One effect of higher temperature is to increase creep rate; thus the higher stressed portions of the nut relax, giving a more even distribution of stress along the nut and, thereby, increased fatigue life. The increased creep rate at higher temperatures, however, has the effect of reducing bolt preload, decreasing the minimum-to-maximum-stress cycle ratio, and reducing the fatigue life. Additional information on the fatigue life of bolts at higher temperatures is needed. There is no dependable way to evaluate the fatigue properties at higher temperatures from room-temperature data.

Chemical methods of locking threaded fasteners appear to be of questionable value. Properly applied chemical locking methods may outperform prevailing torque lock nuts. However, for chemical locking compounds to perform reliably, the compound must be applied to a grease and oil-free surface. Since manufacturing, shipping, and assembly techniques usually require the use of oils, it becomes necessary to clean the bolts and nuts before using chemical locking compounds.

The following design guidelines are suggested for reliable bolted joints:

(1) Use bolts and nuts of as high a strength as practical

(2) Beam-type prevailing-torque lock nuts are preferred

(3) Use a predetermined lubricant and lubricating procedure when installing the fastener

(4) Install the fastener according to predetermined torque-preload data

(5) Install the fastener with the highest preload consistent with the material's strength and application

(6) Use Class 3 threads

(7) Use bolts and nuts with generous thread-root radius

(8) Use hardened washers or hardened faces on the structure to eliminate the use of a washer

(9) Bolts may be reused but do not reuse a nut

(10) Maintain at least two full threads on the bolt under the nut

(11) Periodically retighten all fasteners in a joint

(12) Use a bolt with a coefficient of expansion similar to the joint in which the bolt is used.

Investigation of Stress-Relaxation Considerations

Two major types of system conditions appeared likely to bring about the leakage of a connector because of stress relaxation. One was the system with a maximum operating temperature of 1200 F. Austenitic stainless steel exhibits a noticeable creep rate at this temperature and it was obvious that connectors designed to operate at this temperature would have to sustain considerable creep without failure. Furthermore, the operating time of each connector at temperature would have to be carefully recorded. A method for predicting the operational life of such connectors was developed by E. C. Rodabaugh and M. Cassidy (see Appendix A) on a NASA program.

Another system requirement that could cause stress-relaxation problems was a storage life of 5 years without a significant increase in leakage. This condition anticipates the standby requirement of missiles with occasional evaluation of the various missile systems. Although the normal maximum temperature conditions of this requirement are only 200 F (with occasional excursions to 600 F for the periodical evaluation of stainless steel systems), the compact nature of flanged connectors does not provide for large amounts of preload energy storage. Thus, a small amount of creep or stress relaxation in the connector can cause large changes in the preload conditions. In essence, the decision was made to design the connectors with sufficiently low stresses that creep and relaxation would be negligible.

Only a small amount of long-term creep and stress-relaxation data were available for the materials and temperatures of interest. Therefore, an experimental program was established to determine allowable design stress levels. In the following paragraphs the nature of creep and relaxation is reviewed briefly, the experimental program and its results are described, and the resulting design guidelines are defined for a 5-year-life requirement.

Creep and Relaxation. Although closely related, creep and relaxation are distinctly different effects. Creep is the tendency for material to exhibit time-dependent strains at a constant stress level; i.e., with a constant force on a bolt, creep will be evidenced by a gradual increase in bolt length. Relaxation is the reduction of stress in time under a constant strain; i.e., for a bolt tightened between two rigid flanges, stress relaxation will result in a gradual reduction in bolt load without a change in the assembled bolt length. Both of these characteristics are typical of metals at elevated temperatures.

The four primary parameters in each phenomenon are time, temperature, stress, and rate of creep or relaxation.

Current creep and relaxation theories are of little use in design problems except as they may be used to guide the organization and use of test data. With current theories, data can be interpolated with a fair degree of confidence. Some data can be extrapolated to longer time periods with confidence. However, the extrapolation of data must usually be done with caution, and tests simulating the actual operating conditions should be conducted if possible.

Most creep and relaxation tests have been conducted at elevated temperatures. The materials and temperatures of interest for the connectors are not usually thought of as conditions in which creep is a problem. Recently, for some requirements, such as the long flying time of supersonic transports (36,000 hours), the need for long-term, low-level creep data has been identified, and special machines are being designed and fabricated to obtain such data. However, the measurement of small amounts of creep and relaxation with most present equipment is difficult and the results are subject to a degree of inaccuracy. A significant assist in this problem is that most materials are relatively stable at low temperatures and low stress levels, and a straight-line relationship can be extrapolated with considerable confidence. At elevated temperatures, in the range of stresses customarily used in design, it has been found that plotting the stress versus the second-stage or minimum creep rate produced gives an approximate straight line on a log-log plot.

The physical mechanisms causing relaxation in a material are believed to be very nearly the same as, if not identical to, those causing creep. For this reason it might seem that creep data could be used to predict relaxation data accurately. Unfortunately, stress level and creep rate are significant factors affecting creep behavior, and since stress and relaxation rate are constantly changing in a component experiencing relaxation, a large amount of creep data are needed to make accurate relaxation estimates. On the other hand, it is much more difficult to conduct a relaxation test than a creep test because of the relaxation loading and measuring requirements. For this reason methods have been developed for estimating relaxation from creep data.

Summary of Available Creep and Relaxation Data. Searches were made for creep and relaxation data: (1) on 6061-T6 aluminum at room temperature and at 200 F, (2) on Type 347 stainless steel at 200 F and 600 F, and (3) on A286 at 200 F and 600 F. Table 31 lists data supplied by one manufacturer for 6061-T6 at 75 F and 212 F. These data are compatible with data from two other sources. No information was obtained on the relaxation of 6061-T6 aluminum. Although considerable creep data are available for Type 347 stainless steel and A286 at temperatures between 1000 F and 1400 F, no creep data were obtained at room temperature and 600 F. Likewise, no relaxation data were obtained for these materials at those temperatures.

On the basis of the available theories and the nature of Type 347 stainless steel, the higher temperature creep information cannot be used to predict the creep behavior at room temperature and 600 F. The creep data on 6061-T6 can be used to extrapolate the effects at the given stress levels for the required design life of 40,000 hours. However, the extrapolation of this information to lower stress levels was not believed to be possible. Since the maximum design stress level in the connector was expected to be below the yield strength, it was not possible to predict the creep behavior of the aluminum at most of the anticipated design-stress levels.

TABLE 31. STRESS RUPTURE AND CREEP PROPERTIES FOR 6061-T6 ALUMINUM

Temperature, F	Time Under Stress, hr	Stress, ksi, for Rupture and Creep in Time Indicated				
		Rupture	1.0% Creep	0.5% Creep	0.2% Creep	0.1% Creep
75	0.1	45	45	44	43	42
	1	45	45	43	42	42
	10	45	44	43	42	42
	100	45	44	42	42	41
	1000	45	43	42	41	41
212	0.1	41	41	40	40	40
	1	40	40	40	39	38
	10	39	39	39	37	36
	100	38	37	37	35	34
	1000	37	36	35	33	32

Experimental Determination of Creep Data. From a consideration of the probable modes of missile operation, it was decided that the connectors would remain at room temperature except for those brief periods when the missile was statically operated. On this basis, 10 hours was selected as the longest time that a connector would experience a maximum temperature. Because it was difficult to determine when, during the 5-year storage period, a connector would experience the maximum temperature, the most stringent operational requirement was selected as consisting of a period of 10 hours at maximum temperature, followed by a room-temperature environment for 5 years.

Since the expected period of high-temperature operation was well within normal creep-testing periods, it was decided that specimen tests should be conducted for 100 hours. The additional test time would make the estimate of behavior during the first 10 hours more reliable. For the aluminum, six stress levels were selected: 35, 33, 30, 25, 20, and 15 ksi. These stress levels not only bracketed the expected design stress levels, but also correlated with some of the stress levels of the available data. For the stainless steel, eight stress levels were selected: 50, 45, 40, 35, 30, 25, 20, and 15 ksi. These were chosen to bracket the expected design levels and to insure measurable creep at the higher values. To provide some indication of material stability, three heats were tested. Although the maximum test time possible was 10,000 hours, it was believed that data obtained over this period could be used to extrapolate behavior to 40,000 hours.

Tables 32 and 33 show the data for the specimens prepared for the room-temperature tests. Foil strain gages were attached to the room-temperature specimens, reference gage-length measurements were made for each specimen, and the specimens were stressed in a multiple-lever-arm system. The desired stress on each specimen was obtained by varying the cross sectional area of the specimens. Thus, different stresses could be obtained, although one lever arm was used to load several specimens in series. The elevated-temperature tests were conducted in standard creep-test machines.

TABLE 32. 10,000-HOUR CREEP TESTS, THREE HEATS FOR EACH MATERIAL, TWO SPECIMENS FOR EACH HEAT

Material	Stress, ksi	Specimen Diameter, in.	String	Number of Specimens
347 SS	50	0.2500	1	6
347 SS	45	0.2635	1	6
347 SS	40	0.2798	1	6
347 SS	35	0.2500	2	6
6061-T6 Al	35	0.2500	2	6
6061-T6 Al	33	0.2580	2	6
347 SS	30	0.2500	3	6
347 SS	25	0.2740	3	6
6061-T6 Al	30	0.2500	3	6
347 SS	20	0.2500	4	6
347 SS	15	0.2890	4	6
6061-T6 Al	15	0.2890	4	6
6061-T6 Al	25	0.2500	5	6
6061-T6 Al	20	0.2798	5	6

TABLE 33. 100-HOUR CREEP TESTS, THREE HEATS FOR EACH MATERIAL, ONE SPECIMEN FOR EACH HEAT, 0.2500-DIAMETER GAGE SECTION

Material	Test Temperature, F	Stress, ksi	Number of Specimens
6061-T6	200	15	3
6061-T6	200	20	3
6061-T6	200	25	3
6061-T6	200	30	3
6061-T6	200	33	3
6061-T6	200	35	3
347 SS	600	15	3
347 SS	600	20	3
347 SS	600	25	3
347 SS	600	30	3
347 SS	600	35	3
347 SS	600	40	3
347 SS	600	45	3
347 SS	600	50	3

100-Hour Creep Data for 6061-T6 Aluminum at 200 F. Figures 52 through 58 show the results of the 100-hour creep tests for 6061-T6 aluminum at 200 F. Total strain includes the elastic strain, the initial plastic strain, and the creep strain. The initial point on each curve is the first strain reading taken after application of the load, and represents the total elastic and initial plastic strain. Continued increase in strain with increasing time represents creep strain.

It was concluded from these data that operational stress levels should be kept below 30 ksi. The variation between the three materials was not unusual, and the data were averaged to obtain a design basis.

100-Hour Creep Data for Type 347 Stainless Steel at 600 F. Figures 59 through 65 show the results of the 100-hour creep tests for Type 347 stainless steel at 600 F. The data are reported in the same manner as for 6061-T6 aluminum. As indicated, no creep strain occurred at a stress level of 35 ksi for any of the specimens. Since the design stress levels for the connector were not expected to exceed 35 ksi, it was concluded that creep and relaxation would not be a problem for the expected 10-hour elevated-temperature conditions for Type 347 stainless steel connectors.

10,000-Hour Creep Data for 6061-T6 Aluminum at 70 F. Table 34 shows the creep strain estimated for the 6061-T6 aluminum specimens. Although every attempt was made to set up and conduct the tests carefully, the long duration of the tests and the small amounts of creep involved prevented accurate measurements with the available equipment. However, by making the assumption that no creep occurred at the lowest stress level, it was possible to develop the approximations shown in Table 34. The usefulness of these data is substantiated in part by another Battelle program that showed a creep strain of 10 microinches in 1400 hours for 6061-T6 at a stress of 24,600 psi. These data extrapolated to 10,000 hours would indicate a strain of 35 microinches. These tests showed that a maximum design stress for aluminum of 30 ksi would be satisfactory.

TABLE 34. 10,000-HOUR CREEP STRAIN FOR 6061-T6 ALUMINUM AT 70 F

Tensile Stress, ksi	Creep Strain, μin./in.			
	A	K	R	Average
35	-5	240	210	148
33	-35	55	180	67
30	0	75	110	62
25	-10	110	100	67
20	+5	35	35	27
15	Assumed to be zero			

Note: The negative strain values were believed to be caused by temperature effects on the equipment used to measure the strain.

10,000-Hour Creep Data for Type 347 Stainless Steel at 70 F. The same problems encountered with the aluminum specimens were also encountered with the stainless steel creep specimens. By making the same assumption (zero creep at 15 ksi stress) the values shown in Table 35 were developed. As with the aluminum values, it is assumed that these strains are useful approximations for the stress levels of interest to the program. It was apparent from the tests that a maximum design stress of 35 ksi would be satisfactory for Type 347 stainless steel.

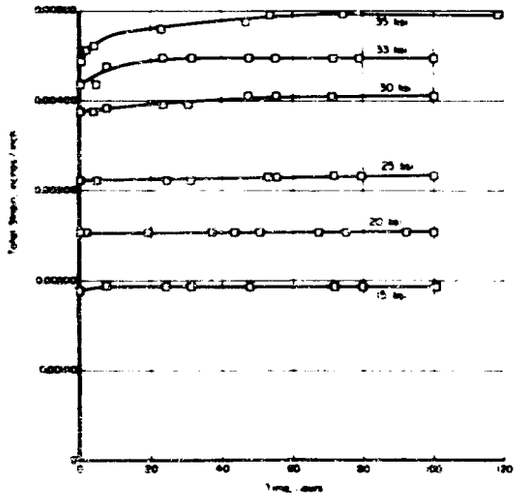

FIGURE 52. CREEP CURVES FOR 6061-T6 ALUMINUM BAR (A-MATERIAL) AT 200 F

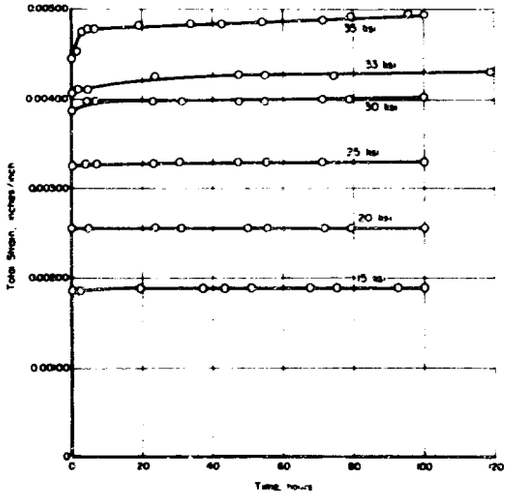

FIGURE 53 CREEP CURVES FOR 6061-T6 ALUMINUM BAR (K-MATERIAL) AT 200 F

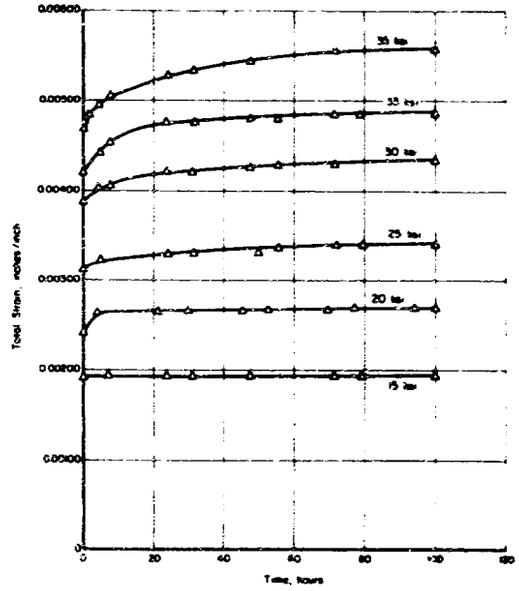

FIGURE 54. CREEP CURVES FOR 6061-T6 ALUMINUM BAR (R-MATERIAL) AT 200 F

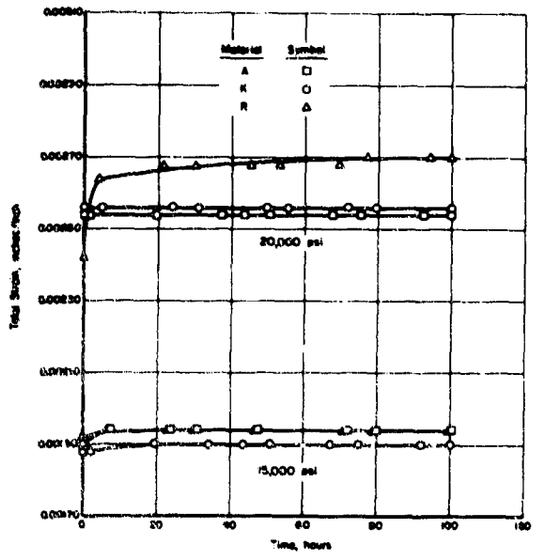

FIGURE 55. CREEP CURVES FOR 6061-T6 ALUMINUM BAR AT 200 F AND 15,000 AND 20,000 PSI

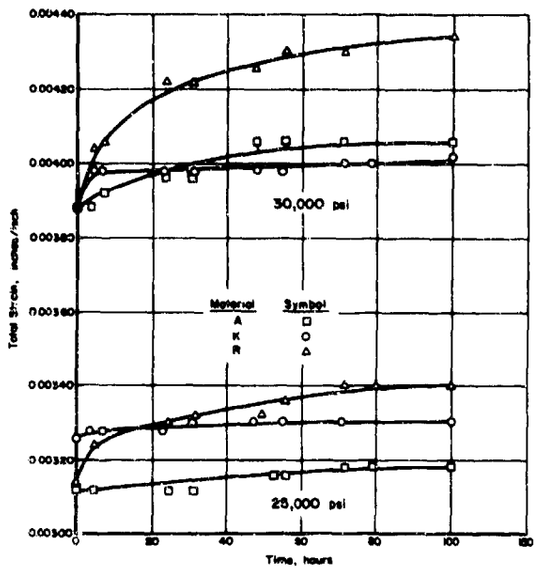

FIGURE 56. CREEP CURVES FOR 6061-T6 ALUMINUM BAR AT 200 F AND 25,000 AND 30,000 PSI

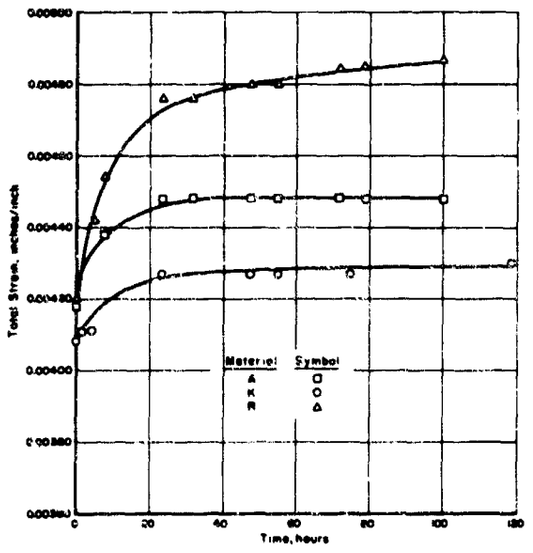

FIGURE 57. CREEP CURVES FOR 6061-T6 ALUMINUM BAR AT 200 F AND 33,000 PSI

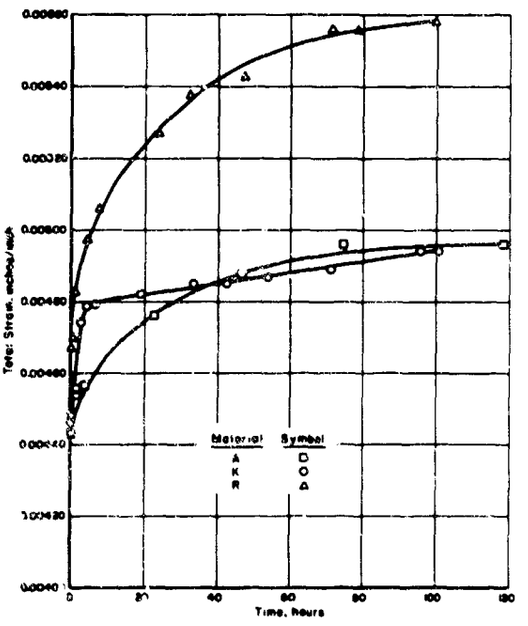

FIGURE 58. CREEP CURVES FOR 6061-T6 ALUMINUM BAR AT 200 F AND 35,000 PSI

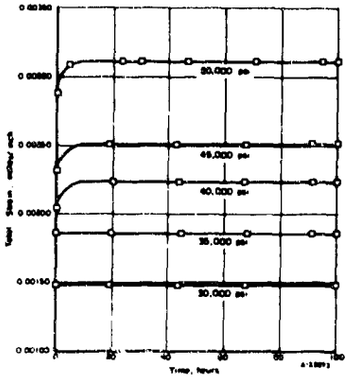

FIGURE 59. CREEP CURVES FOR TYPE 347 STAINLESS STEEL BAR (C-MATERIAL) AT 600 F

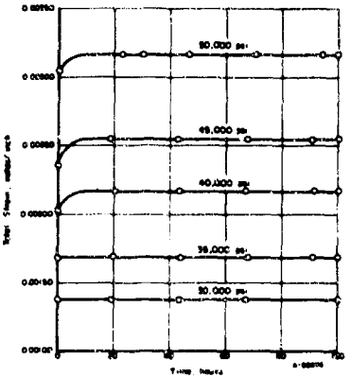

FIGURE 60. CREEP CURVES FOR TYPE 347 STAINLESS STEEL BAR (I-MATERIAL) AT 600 F

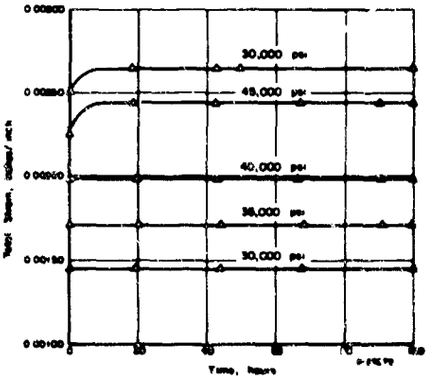

FIGURE 61. CREEP CURVES FOR TYPE 347 STAINLESS STEEL BAR (W-MATERIAL) AT 600 F

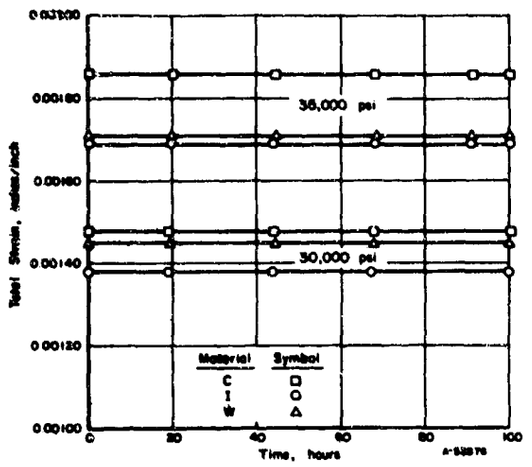

FIGURE 62. CREEP CURVES FOR TYPE 347 STAINLESS STEEL BAR AT 600 F AND 30,000 AND 35,000 PSI

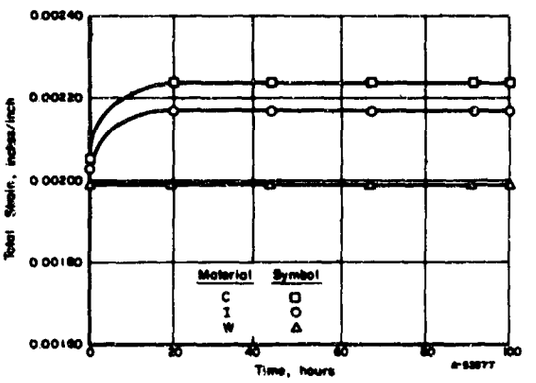

FIGURE 63. CREEP CURVES FOR TYPE 347 STAINLESS STEEL BAR AT 600 F AND 40,000 PSI

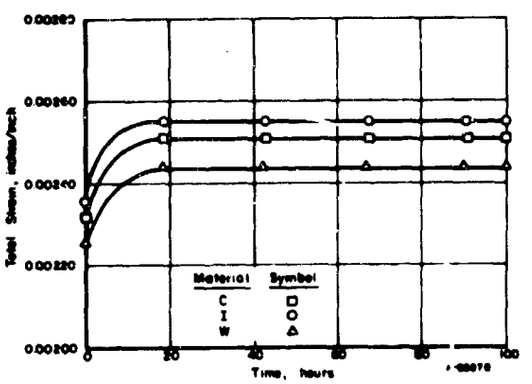

FIGURE 64. CREEP CURVES FOR TYPE 347 STAINLESS STEEL BAR AT 600 F AND 45,000 PSI

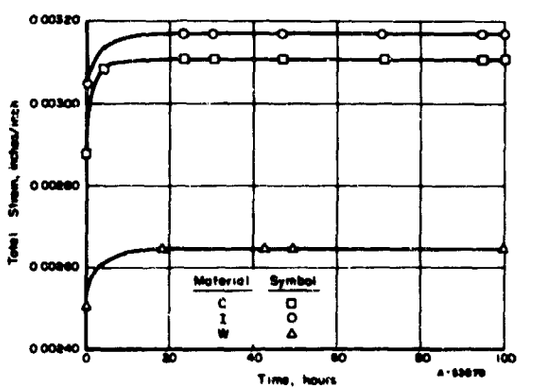

FIGURE 65. CREEP CURVES FOR TYPE 347 STAINLESS STEEL BAR AT 600 F AND 50,000 PSI

TABLE 35. 10,000-HOUR CREEP STRAIN FOR TYPE 347 STAINLESS STEEL AT 70 F

Tensile Stress, ksi	Creep Strain, μin./in.			
	C	I	U	Average
50	103	204	102	136
45	64	91	73	76
40	37	25	34	32
35	38	54	23	38
30	25	46	44	38
25	1	17	18	12
20	19	12	0	10
15	Assumed to be zero			

10,000-Hour Creep Data for 2024-T351 and A286 Bolts. Long-term, room-temperature creep tests were conducted with 2024-T351 aluminum and A286 steel bolts. The program involved conducting duplicate tests on two bolt sizes at two stress levels for each alloy. The aluminum bolts were 1/4 and 1/2 inch in diameter and 3 inches long. Each bolt size was stressed at 33,000 and 42,000 psi. The steel bolts were 1/4 and 3/8 inch in diameter and were also 3 inches long. The steel bolts were stressed at 80,000 and 100,000 psi. The 3/8-inch rather than 1/2-inch steel bolts were used because of the load limitations of Battelle's creep machines.

Two foil strain gages were attached near the center and on opposite sides of each bolt. These two strain gages, along with two dummy gages, formed a 4-arm bridge. The output of each set of two gages was read on a Baldwin SR-4 strain indicator. This output was averaged and the deformation in microinches calculated for each specimen. The grips holding the specimens were designed so that a change in the length of the bolts could be measured with micrometers.

The test results summarized in Tables 36 and 37 include size, stress, total strain achieved in each bolt after 10,000 hours, creep strain, and total residual strain after removal of stress.

It is evident from Table 36 that very little creep occurred in the 2024-T351 alloy in 10,000 hours of exposure. The creep strain recorded at the stress of 33,000 psi was 6.4 μin./in. and at 42,000 psi it was 15.5 μin./in. In the case of the A286 steel, a relatively large amount of deformation occurred in 10,000 hours in the specimens stressed at 100,000 psi. The average residual strain was about 1518 μin./in. or about 0.15 percent. Only 474 (average) microinches or about 30 percent of this total was actual creep strain. The balance was initial plastic strain obtained on loading because the stress exceeded the proportional limit of the material. The lower stress of 80,000 psi produced an average total strain of 141 μin./in. Of this total, 24 microinches represented creep strain, and the balance represented the instantaneous plastic strain obtained on loading.

TABLE 36. SUMMARY OF CREEP DATA FOR 2024-T351 ALUMINUM BOLTS AT ROOM TEMPERATURE (80 F)

Specimen	Bolt Diameter, inch	Stress, ksi	Total Strain at 10,000 Hours, μin./in.	Creep Strain, μin./in.	Total Residual Strain, μin./in.
			Strain-Gage Measurement		
3	1/4	33	3.07×10^3	20.5	20.5
5	1/4	33	3.08×10^3	5.5	2.5
7	1/2	33	3.14×10^3	-3	5
8	1/2	33	3.14×10^3	2.5	1
				6.4 avg	7.2 avg
2	1/4	42	3.91×10^3	13.5	11
4	1/4	42	3.96×10^3	24.5	14.5
9	1/2	42	4.01×10^3	4.5	-6
10	1/2	42	4.03×10^3	19.5	+3.5
				15.5 avg	5.8 avg

TABLE 37. SUMMARY OF CREEP DATA FOR A286 STEEL BOLTS AT ROOM TEMPERATURE (80 F)

Specimen	Bolt Diameter, inch	Stress, ksi	Total Strain at 10,000 Hours, μin./in.	Creep Strain, μin./in.	Total Residual Strain, μin./in.
			Strain-Gage Measurement		
2	1/4	80	3.05×10^3	[e]	172
5	1/4	80	3.04×10^3	19	177
8	3/8	80	2.89×10^3	47	125
10	3/8	80	2.85×10^3	20	91
				24 avg	141 avg
4	1/4	100	5.16×10^3	480	1491
6	1/4	100	5.12×10^3	422	1497
7	3/8	100	5.09×10^3	465	1409
11	3/8	100	5.35×10^3	530	1675
				474 avg	1518 avg

Development of a Computerized Flange-Connector Design Procedure

This effort was started with an extensive survey of the literature. Of approximately 1000 references that were identified, over 250 were obtained and studied, including several different flange design procedures. The following general steps were common to these design procedures:

(1) Assembly of information on design parameters such as pressure, temperature, imposed loads, material properties, and material compatibility

(2) Generation of a preliminary design

(3) Analysis of the preliminary design on the basis of stress, deflection, etc.

(4) Adjustment and reanalysis of the preliminary design

(5) Selection and definition of a final design.

The flange design procedure that was developed for the requirements of this program was incorporated into two digital computer programs entitled IRFDP (Integral Flange Design Procedure) and LRFDP (Loose-Ring Flange Design Procedure). A listing of both programs, together with a brief discussion of the use of the programs, is presented in Appendix B. The major features of the design procedure are discussed below. In evaluating the operation and output of the procedure, it should be remembered that flange connectors incorporating the Bobbin seal have been developed specifically to achieve very low gas leakage for a wide range of operating temperatures and pressures. In other flange design procedures, the capability of designing for specific thermal-gradient temperatures and weight optimization is not usually included.

Procedure for Designing Flanged Connectors

The procedure starts with a trial design and, by stepwise modification, ends with a design that satisfies selected performance requirements and predetermined connector parameters. Then, by selected modification of some connector dimensions, alternative designs are obtained which satisfy the performance requirements. From these alternative designs, the minimum-weight connector design is selected. A schematic diagram of the overall approach is shown in Figure 66.

Predetermined Parameters. The predetermined parameters are derived from the operational and functional objectives for the connectors. For example, the general design configurations (see Figure 67) are significant predetermined parameters. The materials of construction and their properties are other predetermined parameters. Others more directly relatable to the application are the minimum radial and axial seal loads per inch of seal circumference, the length-to-thickness ratio for the seal tang, the dimensions of the seal disks, the bolt-wrench clearance dimensions, the minimum and maximum bolt spacing, the minimum dimensions for the distance from the bolt circle to the flange outside diameter, and the bolt-hole clearance.

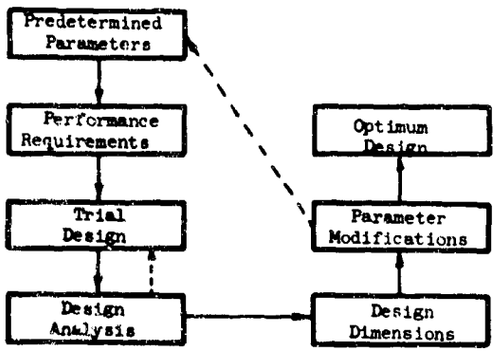

FIGURE 66. GENERAL FLANGE DESIGN PROCEDURE

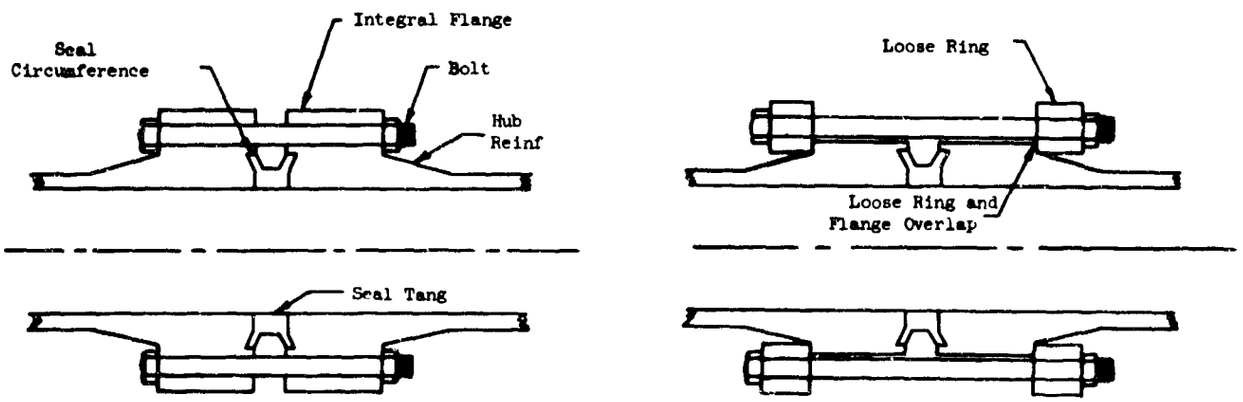

a. Bolted Integral Flange Connector

b. Bolted Loose-Ring Connector

FIGURE 67. CONNECTOR CONFIGURATIONS

Type 347 stainless steel (annealed condition) and 6061-T6 aluminum are the two basic connector materials. For stainless steel connectors, the bolt material selected is A286, and the seal material is an austenitic stainless steel with soft nickel plating. For the aluminum connectors, the bolt material is 2024-T356, and the seal material is overaged 6061 aluminum alloy.

The predetermined seal loads and dimensional parameters were the result of the seal-design studies and of the qualification tests. The bolt-wrench clearances were established from the dimensions of commercially available wrenches. Bolt-hole spacing requirements were established on the basis of design experience and the ASME Unfired Pressure Vessel Code.[13]

Performance Requirements. An important part in the development of a design procedure is the establishment of performance requirements in sufficient detail that the requirements become integrated into the procedure. Seven computer sections were used to define the design performance requirements:

(1) Bolt-up

(2) Operating

(3) Proof pressure

(4) Burst pressure

(5) Pressure impulse

(6) Thermal shock

(7) Misalignment.

The design procedure section for bolt-up imposes the conditions of initial assembly of the connector with no operating loads applied. This section is used as a base-line condition in the computer program. One of the conditions of initial assembly is that the axial bolt loading during bolt-up must be sufficient to seat the seal.

The section for operating conditions includes the requirements that the connector sustain operating pressure at maximum temperature, a specified value of stress-reversal-bending load, and a minimum axial seal load which will assure that the leakage rate of the connector does not exceed the specified minimum.

The proof-pressure section requires satisfactory connector operation with an applied pressure of 1.5 times the maximum operating pressure at maximum temperature, while the burst-pressure section specifies an applied pressure of 2.0 times the maximum operating pressure at ambient temperature. The pressure-impulse section includes a fatigue stress selected to permit 200,000 pressure cycles from 0 psi to approximately 1.5 times the maximum operating pressure at ambient temperature.

The thermal-shock section includes the requirement that the connector perform satisfactorily when temperature differentials exist between the connector components. Numerical values for the temperature differentials are supplied as inputs to the design program. The design program for this condition includes load calculations relating

the flexibility of the connector components to dimensional changes due to temperature differentials under normal connector operating-load conditions.

The misalignment section specifies a maximum bending load as a function of tubing size and tubing-material yield strength.

Trial Design. The selection of a trial design is an important part of an iterative-type design program. Trial dimensions are selected which describe, in full, the connector to be designed. Also, if the trial dimensions are close to the dimensions of a satisfactory design, the number of iterations is reduced. In the connector design procedure, minimum dimensions are selected for the trial design. For example, the trial bolt size is the minimum size, No. 10 (0.190-in. diameter), provided in the bolt-size input data. The trial flange thickness is three times the tube wall thickness. This is a minimum value chosen arbitrarily on the basis of experience. The trial bolt-circle diameter is calculated on the basis of the wrench clearance needed for the trial bolt size. This provides a minimum bolt-circle diameter for the trial design. Other dimensions include the reinforcement at the flange and tube junction.

Design Analysis. For most mechanical parts, there are at least two analyses that should be carried out: (1) load analysis and (2) stress analysis. Many other analyses may also be required, such as thermal analysis, fluid-flow analysis, and vibration analysis. For the tube connectors, only load and stress analyses are conducted. Consideration of thermal characteristics and vibration characteristics is included as part of the load analysis. The consideration of fluid leakage past the seals is explicitly included in the limits established for the minimum seal loads.

As shown in Figure 66, the design analysis provides feedback to the trial design. Changes are made in the trial design to compensate for any unsatisfactory load or stress conditions discovered in the analysis. For example, if the axial seal load is too low, the trial-design bolt load is increased and the analysis is repeated. Also, if the calculated bolt stress is too high with the maximum possible number of bolts, the trial design is changed to include the next larger size bolt. Similarly, if one of the flange stresses is too high, the trial flange thickness is increased and the analysis is repeated.

Design Dimensions. After changes are made in the trial design and the analysis results satisfy all the load and stress requirements, the trial design becomes a satisfactory design.

Parameter Modifications and Optimum Design. Selected parameters can then be systematically varied and the results examined to determine an optimum design. The parameter variations must not obviate the design objectives, however.

For the integral connector, the parameters which are varied are the maximum height of the reinforcing hub at the juncture of the flange and tube, the bolt-circle diameter, and the flange outside diameter. For the loose-ring configuration, these parameters are varied, as is the amount of contact area between the loose ring and the flange. The optimum design is selected on the basis of (1) minimum weight, (2) dimensional compatibility of integral and loose-ring-flange designs, and (3) manufacturability.

Computer Program for Designing Flanged Connectors

The computer program is the mechanism for accomplishing design synthesis and optimization. The form of the computer program is important only because the designer uses the computer program as a tool in the design procedure. Secondary attention must be given to modifying the computer program for efficiency in computer utilization.

In the flange design program, a "building block" or sectional approach is taken to provide flexibility during preparation of the program. This approach also allows relatively easy program modifications to adapt to any future changes in program objectives. Some aspects of the computer program for tube connectors are discussed to further illustrate the design synthesis and optimization procedure. A simplified schematic of the tube connector program is shown in Figure 68. Inputs not only include such things as material properties and system requirements, but provision is also made for the variation of dimensional parameters that influence design optimization.

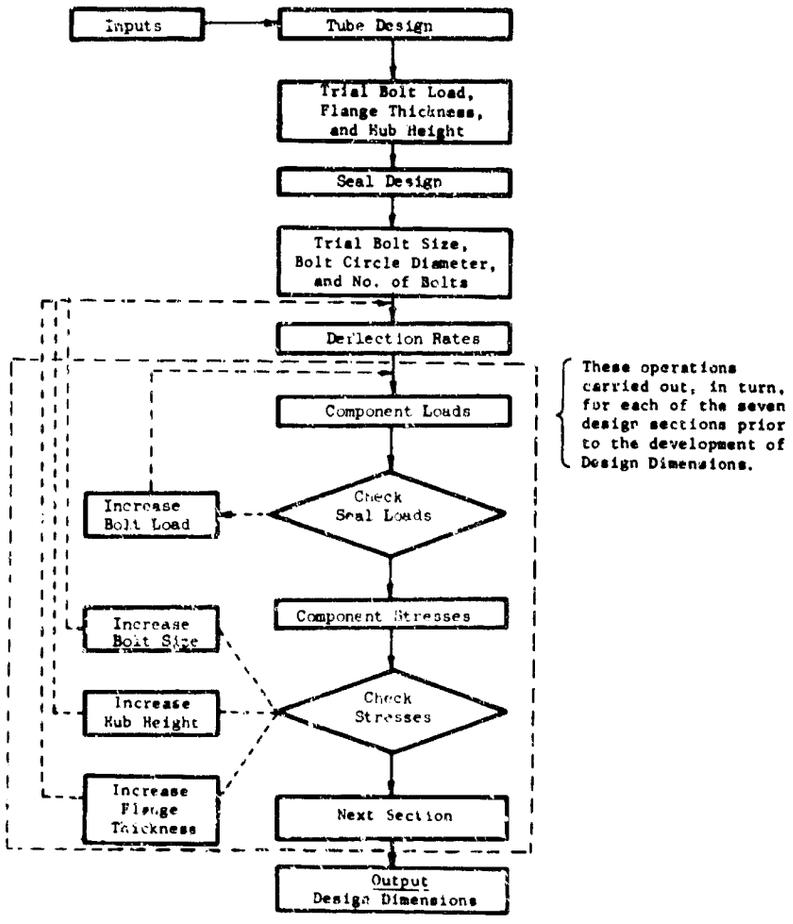

FIGURE 68 SCHEMATIC OF FLANGED-CONNECTOR COMPUTER PROGRAM

Critical Design Parameters. Critical design parameters are selected on the basis of their importance to connector performance. Some of these critical parameters are briefly discussed.

1. Seal Loads

The maintenance of intimate physical contact between the seal and the mating flanges under all required loading conditions is one of the primary design aspects of the tube-connector program. Parameters which describe this aspect are the seal loads in the radial and axial directions. Seal loads, in turn, are dependent on the pressure and structural loads applied to the connector, the dimensional stability of the seal and flanges, and the relative flexure of the seal and flanges under loads.

2. Bolt Load

During bolt-up, the bolt load is applied directly to the seal through the flanges. Then, as other loads are applied, the bolt load must be adequate to provide a margin for maintaining minimum loads on the seal. A somewhat less evident function of the bolt load is to minimize the effects of cyclic loading on the connector. The possibility of fatigue failure is reduced in some cases by the maintenance of unidirectional loads. Also, the chance of loosening of threaded joints is reduced by the maintenance of steady-state loads.

3. Tube Bending Moment

The tube bending moment is considered as an external load applied to the connector; however, the magnitude of the tube bending moment is dependent on the tube properties and on deflections in the tube system. In the connector design program, tube bending moments are calculated on the basis of tube material properties and cyclic loading of the tube. The influence of the tube bending moment applied to the connector design is usually substantial.

4. Internal Pressure

For most pressure vessels, the hoop stress resulting from internal pressure is the most important design parameter. However, for bolted flanged connectors, the structure for transferring axial loads provides increased wall thickness and therefore the hoop stress is not a critical parameter. However, the internal pressure is an important design parameter, particularly because the pressure loading in the axial direction tends to reduce the seal loads. The proof pressure is 1.5 times the maximum operating pressure, while the burst pressure is 2.0 times the maximum operating pressure.

5. Thermal Gradients

Calculations are made for the effects of thermal gradients on connector flange and seal loads. The program does not include an analysis procedure to determine values for thermal gradients.

However, it does include calculations to determine the relative changes in loads and deflections of connector elements in response to thermal gradients. Worst-case emperature differences between bolts, flanges, and seals are provided as inputs to the program. The thermal model used in the program is illustrated in Figure 69. Average worst-case temperature differences are taken to exist between the bolt and the flange and between the flange and the tube. The seal-element temperature is the same as the tube temperature. Relative changes in physical dimensions occur from the temperature differences. For example, when a connector is suddenly exposed to the flow of cryogenic fluid, the tube shrinks radially, the seal shrinks axially and radially, and the bolt shrinks axially. The relative significance of these dimensional changes depends on the flexibility of the connector elements and the load changes that follow.

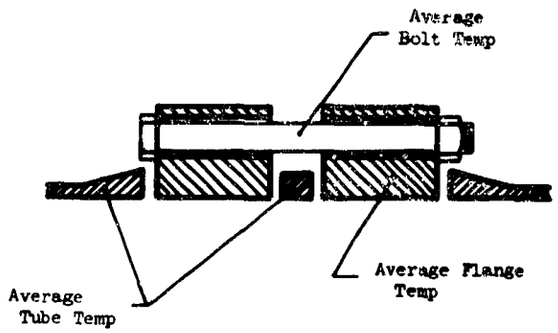

FIGURE 69. FLANGE-CONNECTOR THERMAL MODEL

6. Impulse Pressure

The peak value of the pressure cycle is specified as 1.57 times the operating pressure and the minimum value is atmospheric pressure. For this type of pressure cycling, fluctuating stress levels are experienced at the flange-to-tube joint. The resistance of the flange-to-tube joint to fatigue loads is improved by a reinforcing hub.

An investigation was made of the first design approach used in determination of hub dimensions as a result of the failure of the 3-inch, 1500-psi aluminum connector during the vibration test (see page 111). A stress-concentration factor of 2.0 had been selected to account for stress amplification at the juncture of the hub and the flange. Also, the calculations of maximum and minimum stress levels at the critical regions for assessment of fatigue resistance were based on combined stress levels. On review of this approach, it was found that the stress-concentration factor could, in some cases be greater than 2.0, depending on the size of fillet radius selected and the relative

dimensions of the hub, flange, and tube. Also, the combined stress-level formulation did not adequately account for changes in direction of the maximum and minimum values of the calculated combined stress.

The computer program was extended to select stress-concentration factors based on connector dimensions (flange OD, hub OD, and fillet radius) and published values of calculated stress-concentration factors.[14] Also, initial choices for the fillet radii were made a part of the design procedure according to the tube size. The initial radii are 1/8, 3/16, 1/4, and 5/16 for tube sizes through 4, 8, 12, and 16 inches, respectively. The program includes the option of fixing the fillet radius according to a specified input value.

Fatigue-stress calculations were modified to consider the maximum and minimum stresses at critical sections in the axial direction. Then the assessment of resistance to fatigue failure is made according to the idealized stress-versus-strain-history procedure as outlined in Section III of the ASME Boiler and Pressure Vessel Code for Nuclear Vessels.[15] The computer program includes a fatigue safety factor of 2.0 which is consistent with the method of establishing the value of the applied bending moment based on 0.5 times the fatigue strength of the tube material, and with the appropriate stress-concentration factor applied to the maximum and minimum calculated axial stress values. Calculations for maximum and minimum values of the combined stresses, based on the octahedral shear stress theory, are also made and compared with the allowable yield strength of the connector material.

In addition to the above described improvements in the method of calculation of fatigue stress resistance, an arbitrary minimum value of hub-reinforcement thickness at the hub-flange juncture was established at 1.5 times tube-wall thickness for aluminum connectors and 1.25 times tube-wall thickness for stainless steel connectors. These minimum values are intended to compensate for observed relative sensitivities of the materials to fatigue damage and for possible inaccuracies in machining.

Load Calculations. After a trial connector design is generated, the design-analysis procedure starts with the determination of loads on the connector components. For convenience, preliminary calculations are made to establish the deflection rates of the connector components. For example, the axial deflection rate of the seal is given by:

$$DSA = \frac{L}{2 \times SEE \times 3.14 \times D_e \times t} \qquad (14)$$

where

DSA = Axial deflection rate of seal tang, in./lb

L = Seal tang length, in.

SEE = Modulus of elasticity of seal material, psi

D_e = Seal tang outside diameter, in.

t = Seal tang thickness, in.

Figure 70 illustrates in somewhat more detail the computer-program section used in the design analysis which includes load and stress calculations. These calculations are made in sequence for each of seven design conditions. The component loads for each

condition are dependent upon initial bolt-up loads, pressure-bending moments, and thermal gradients. Some sample calculations are presented for bolt-up loads and operating-pressure loads. Dimensional notations are shown in Figures 71 and 72.

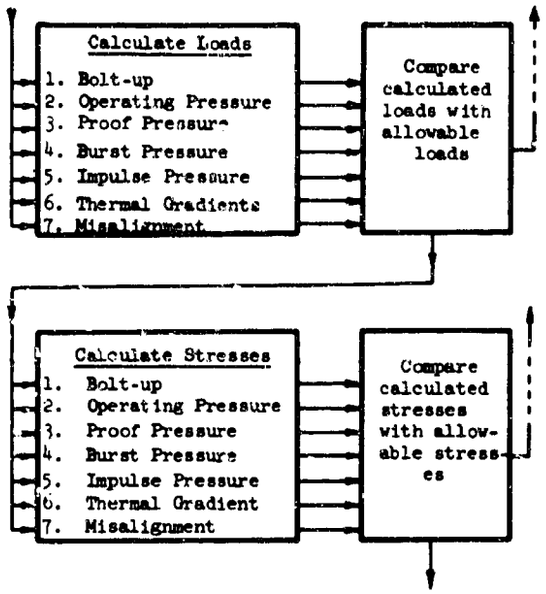

FIGURE 70. SCHEMATIC OF DESIGN ANALYSIS

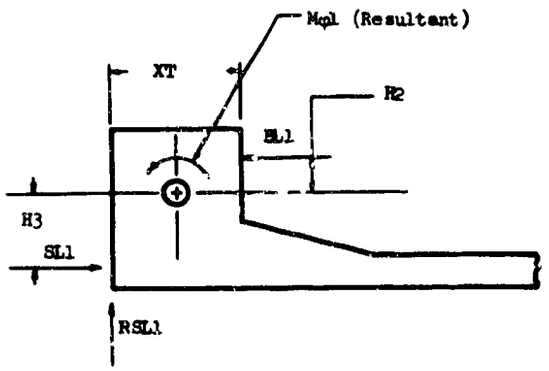

FIGURE 71. DIMENSIONAL NOTATIONS FOR BOLT-UP LOADS

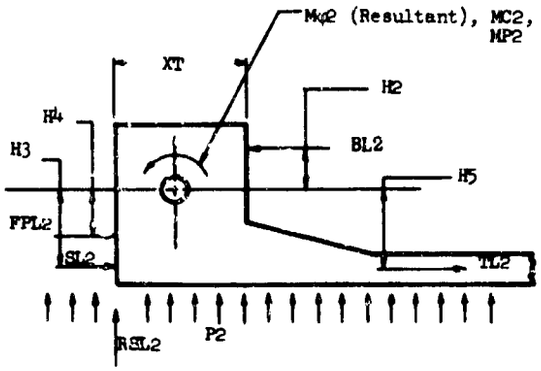

FIGURE 72. DIMENSIONAL NOTATIONS FOR OPERATING-PRESSURE LOADS

Sample Calculations†

For bolt-up loads the horizontal forces are related by:

$$SL1 = BL1. \tag{15}$$

† In the calculations the asterisk symbol indicates multiplication. See Appendix B for further discussion of computer computation.

The flange moment is represented by:

$$M\varphi 1 = RSL1 * XT/2 + BL1 * H2 + SL1 * H3. \quad (16)$$

Similar equations are prepared for the operating-pressure loads:

$$BL2 = FPL2 + SL2 + TL2 , \quad (17)$$

$$M\varphi 2 = - RSL2 * XT/2 + BL2 * H2 + SL2 * H3 + FPL2 * H4 + TL2 * H5 + MP2 \pm MC2 - (P2 * \pi * B * SX) * XT/2 . \quad (18)$$

Then the changes from the bolt-up condition to the operating-pressure condition are obtained:

$$(BL1 - BL2) + \Delta BL = \Delta SL - TL2 - FPL2 ; \quad (19)$$

$$\Delta M\varphi = -\Delta RSL * XT/2 + \Delta BL * H2 + \Delta SL * H3 - FPL2 * H4 - TL2 * H5 + (P2 * \pi * B * SX) * XT/2 - MP2 - MC2 . \quad (20)$$

Two more equations are then obtained from consideration of the relative changes in axial and radial dimensions:

$$\Delta BL * DBA = \Delta SL * DSA + \left(\frac{\Delta M\varphi}{H2 + H3}\right) * DFA + BCR * (XT + SX) + FCR * XT ; \quad (21)$$

$$\Delta RSL * DSR - (P2 * B * SMD)/(4 * TA * SE) = - \Delta M\varphi + DFR * XT/2 - (P2 * B * \left(\frac{A + B}{2}\right)/(4 * \left(\frac{A - B}{2}\right) * FE) . \quad (22)$$

Equations (19) through (22) can now be solved simultaneously to obtain values for ΔBL, ΔSL, ΔRSL, and $\Delta M\varphi$. Then, starting with known bolt-up loads, the connector loads can be calculated for the operating pressure.

A similar method is used for calculating the connector loads for each design condition. For thermal gradients, for example, when the effects of relative thermal expansion are included in the analysis, the calculations include the simultaneous solution of six equations.

Load Checks. After the loads are calculated for each design condition, a check is made to determine whether the loads are satisfactory. If the axial seal load for the operating pressure, say, is calculated to be less than the required minimum, the bolt-up load is increased and the analysis is repeated. This iteration loop is illustrated in the partial computer-logic diagram shown in Figure 73.

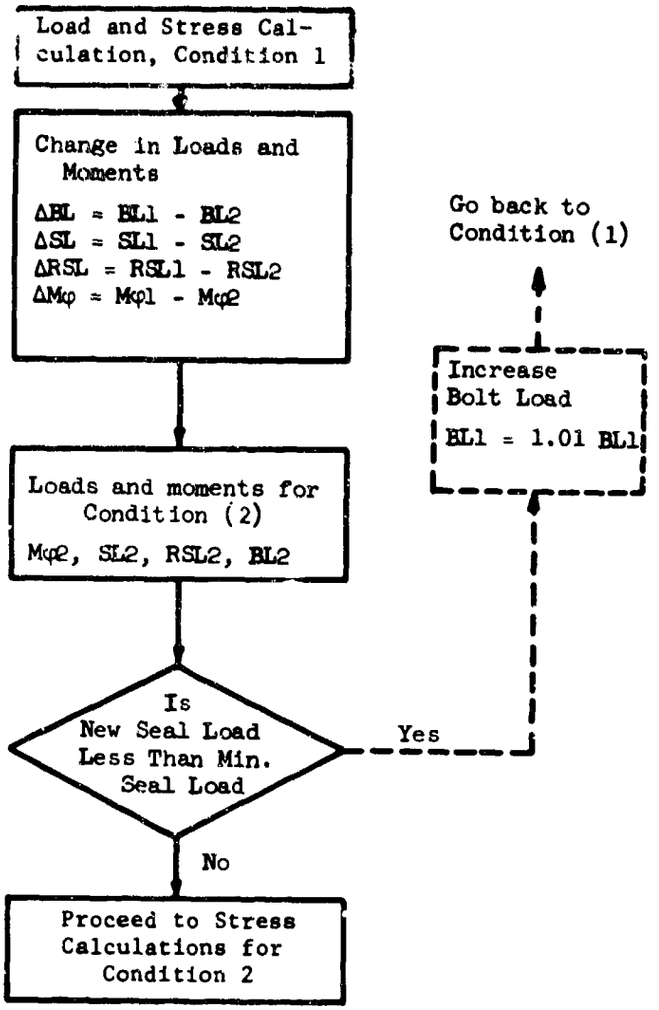

FIGURE 73. PARTIAL LOGIC DIAGRAM SHOWING LOAD CHECKS

Stress Calculations. With emphasis on minimum weight and strength-to-weight ratios in aerospace applications, it becomes necessary that stress calculations be performed for all suspected possible failure modes. For flanged connectors, the criterion of failure generally involves deformation rather than rupture; thus, the material yield strength is an important stress limit. The modulus of elasticity and the coefficient of thermal expansion are important material parameters in connector designs where thermal gradients are significant.

To determine the dimensions of connector designs which are judged to be satisfactory, it is necessary to establish allowable stresses for the materials of construction. Allowable stresses, in relationship to material properties, involve a complex interaction between the accuracy of the stress calculation methods, the accuracy with which loads are known, and the objective functions of the components. For example, the allowable stress for bolts is set relatively lower than the allowable stress for the flanges for several reasons: (1) bolts are loaded in tension, and in case of overload, there is no

ability to transfer loads to any other part of the structure; (2) the only bolt stress calculated is due to axial loading, while in reality the bolts have bending stresses due to flange rotation; (3) the tightening of bolts with a wrench introduces shear stresses and a reduction in axial yield strength; and (4) the threads on the bolts form notches with accompanying stress concentrations.

When a bending-moment load is imposed on the connector through the tubing, a maximum tensile stress will exist at one point on the circumference of the tube section. A diametrically opposed maximum compressive stress will arise simultaneously. However, compressive failure is not likely since the pressure end load reduces the compressive stress. While the maximum tensile stress exists at only one point on the circumference, it can be conservatively assumed that the connector may be designed as if the maximum bending stress existed all around the tube circumference.

Consideration should also be given to fatigue damage due to cyclic bending of the tube-connector assembly. In addition to bending stresses, the connector internal pressure creates axial, radial, and circumferential stresses. A simplified stress-time relationship of the combined stresses in the axial direction is represented graphically in Figure 74.

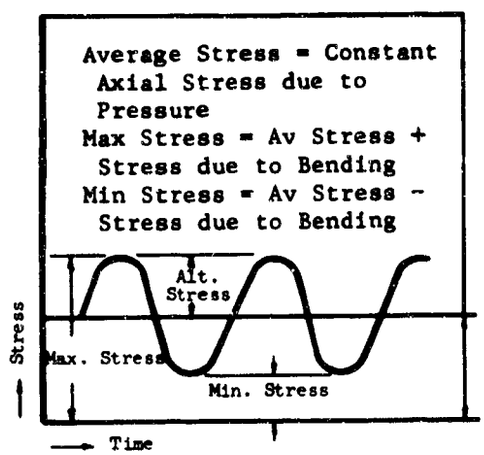

FIGURE 74. STRESS-TIME REPRESENTATION

The allowable fatigue stress when variable and steady stresses are present can be determined with the aid of a modified Goodman diagram. A more complex fatigue problem is created by impulse-pressure variation from 0 to 1.57 times operating pressure. This results in fluctuating stresses in the axial, radial, and circumferential directions. The problem of impulse-pressure fatigue is simplified if fluctuating stresses in the axial direction only are considered. This is the approach taken in the computer program.

The general methods used for stress analysis in the connector design program are based on the same stress theories used in the formulation of the ASME Unfired Pressure Vessel Code.(13) The computer-program logic diagrams applying to parts of the stress calculations for operating pressure are shown in Figures 75 and 76. Also shown on these diagrams are some of the iteration loops corresponding to stress checks. For example, when the calculated bolt stress exceeds the design allowable stress for the bolts, the trial design is changed by increasing the bolt size. Then the design analysis is repeated (load and stress analysis) for the "new" dimensions of the trial design with the "new" bolt size.

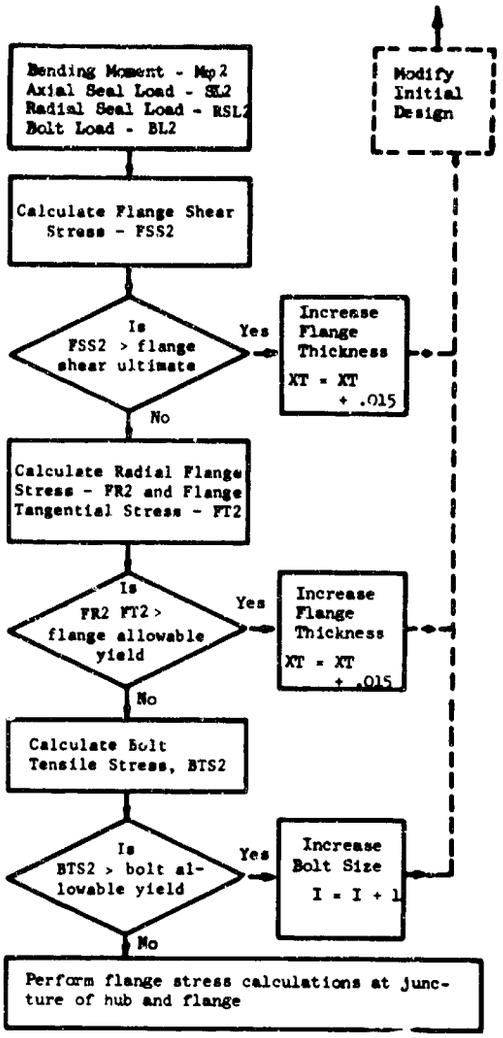

FIGURE 75. PARTIAL LOGIC DIAGRAM FOR STRESS CHECKS ON FLANGE AND BOLT, CONDITION 2

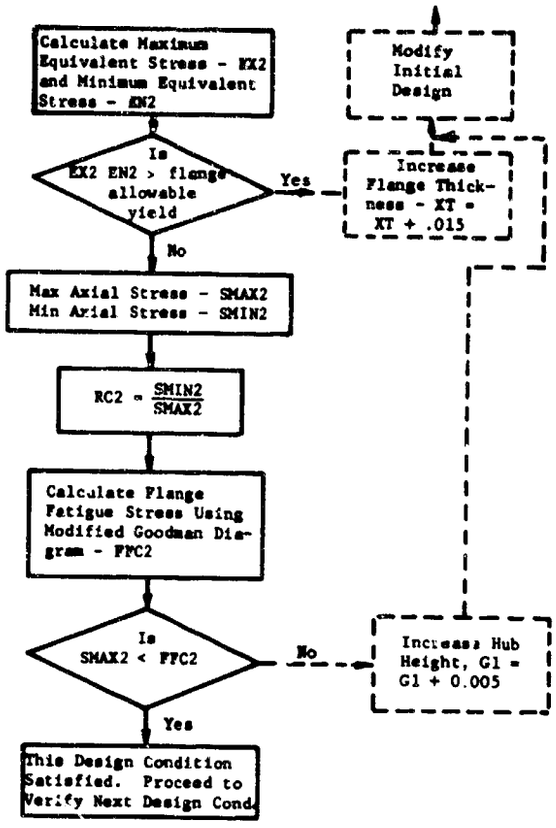

FIGURE 76. PARTIAL LOGIC DIAGRAM FOR STRESS CHECKS ON JUNCTION OF HUB AND FLANGE, CONDITION 2

Design Optimization

An optimum design is one selected from among alternative designs which exhibits maximum (or minimum) values for selected characteristics. For tube connectors for aerospace applications, the optimum design is selected to minimize weight. In the connector-design program, some other characteristics are also considered in the selection of optimum designs. These include matching the bolt-circle diameters for integral-flanged and loose-ring connectors. Also, for ease of manufacturing, the bolt-circle diameters are selected in increments of 1/16 inch.

Parameter Modifications. Alternative designs from which the least-weight designs were selected for the designs given in Appendix C were obtained by systematic variations of input parameters of the computer design program. The input parameters that were varied were: (1) the relative height of the hub reinforcement, (2) the bolt-circle diameter,

(3) the bolt size, (4) the flange outside diameter, and (5) the relative amount of overlap of the loose ring and its corresponding integral flange.

Design Selection. If only one design characteristic is selected to be minimized or maximized, the selection of the optimum design is simplified. When two or more characteristics are used, they must be ordered and weighted with respect to importance. In the selection of optimum connector designs, the criteria used were: (1) minimum weight, (2) dimensional compatibility of integral- and loose-ring-flange designs, and (3) selected dimensional limits for some items to improve manufacturability and handling of the connectors.

Design of High-Temperature Flange Connectors

In 1964, under Contract NAS-8-11523, Battelle developed an analysis procedure for estimating the relaxation time to leakage for separable tube connectors. The procedure was based upon the steady-state creep law, revised to account for the effects of primary creep.

At the beginning of the program described by this report, the possibility of including this procedure in the flange-design computer program was considered. However, as the work developed, it was mutually agreed that the needs of the Air Force were not sufficient to warrant the expense of this effort. For those instances where a high-temperature flange design is required, it is believed that the optimum design for a flange with a Bobbin seal can be most easily determined by use of the computer design program in conjunction with the "hand" calculation defined by the relaxation procedure. Accordingly, the entire final report on Contract NAS-8-11523, Subcontract No. 63-30, has been included in this report as Appendix A. The information contains not only information on the relaxation analysis procedure and its use, but also summary information on high-temperature materials.

Design of Representative Connectors

It was originally intended that, prior to the experimental program, the computerized flange-design procedure would be used to design a number of representative connectors for different tube diameters and system requirements. However, several factors resulted in a modification of this objective. First, because of the existence of three basic connector configurations (integral/integral, loose-ring/loose-ring, and integral/loose-ring), a large number of designs would be required. Second, results from the experimental program might necessitate significant dimensional changes in the designs. Third, very few state-of-the-art large connector configurations were available for comparison with the representative Bobbin seal connectors. Fourth, if a specific flange design were needed at any time in the program, it could be obtained quickly. Finally, since considerable effort was expended in developing an experimental program that would determine the capability of the design procedure to produce a satisfactory flange-connector design for the specified system requirements, the decision was made to consider the test connectors as representative of the requirements. Illustrative aspects of these designs are discussed, and dimensions are given for all of the connectors considered for the experimental program. Subsequently, some of these connectors were eliminated from the test program.

Connectors for Type 6061-T6 Aluminum Systems

Tables 38 through 41 summarize the major system input conditions and present the dimensions developed for integral/integral and loose-ring/loose-ring flange connectors for 3-, 8-, and 16-inch tubing for 100 and 1500-psi aluminum systems. The tables also give the dimensions for compatible integral and loose-ring flanges which are needed to form an integral/loose-ring assembly. A comparison of the connector part weights gives an indication of the weight penalty that is required for this dimensional compatibility. For these designs, the seals are overaged 6061 aluminum, the flanges are 6061-T6 aluminum, and the bolts and loose rings are 2024-T351 aluminum.

Connectors for Type 347 Stainless Steel Systems

Tables 42 through 45 summarize the major system input conditions and present the dimensions developed for integral/integral and loose-ring/loose-ring flange connectors for 3-, 8-, and 16-inch tubing for 100 and 1500-psi stainless steel systems. The tables also give the dimensions for compatible integral and loose-ring flanges which are needed to form an integral/loose-ring assembly. The weight penalty for using compatible flanges can be seen in the tables.

Tables 46 and 47 give three system input conditions and the associated flange dimensions for 4000-psi connectors for stainless steel systems. The original intention was to fabricate and test a connector for the full temperature range from -423 to 600 F. However, the weight penalty caused by the thermal gradients was very high. When a reexamination of the possible future conditions showed that a system would be either for hot gas or cryogenic fluid, the decision was made to test two connectors. Further design analysis showed that connector fabrication costs could be saved if the hot-gas connector was fabricated and tested first, and the cryogenic connector was fabricated by remachining the hot-gas connector. This approach necessitated a small weight sacrifice between the optimum cryogenic connector and the reduced hot-gas connector because the bolt circle and size could not be changed, but the resulting connector was believed to be an acceptable test of the design procedure.

Conclusions From Design Optimization

As a result of the design optimization of the experimental connector configurations, it was concluded that the bolt-circle diameter is the most important variable in achieving a lightweight connector. Every effort should be made to keep this to a practical minimum. As illustrated by the 4000-psi connector, it is also important to select an accurate thermal gradient because of the small amount of deflection in the smallest connector parts. It was also concluded that little weight penalty is paid for making the integral and loose-ring flanges compatible.

TABLE 38. INPUT DATA, DIMENSIONS, AND ESTIMATED WEIGHTS FOR EXPERIMENTAL, ALUMINUM 100-PSI INTEGRAL-FLANGE CONNECTORS

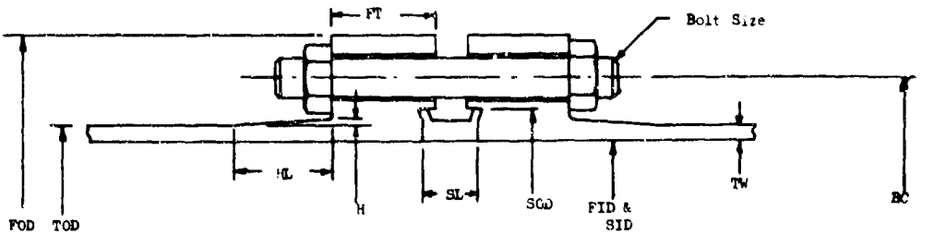

Input Data

Operating pressure, psi	100
Operating temperature range, F	-423/200
Bolt-to-flange cold thermal gradient, F	10
Bolt-to-flange hot thermal gradient, F	4
Flange-to-seal cold thermal gradient, F	20
Flange-to-seal hot thermal gradient, F	8
Flange ultimate strength, psi	42,000
Flange yield strength, psi	32,200
Bolt ultimate strength, psi	62,000
Bolt yield strength, psi	47,000

Size, in.	TOD	TW	FOD	FID	FT	BC	H	HL	SOD	SID	SL	Bolt Size	No. of Bolts	Weight, lb
						Dimensions, in.								
Not Compatible With Loose-Ring Flanges														
3	3.000	0.028	4.300	2.944	0.399	3.898	0.096	0.431	3.54	2.984	0.49	3/16	12	0.7
8	8.000	0.035	9.805	7.930	0.645	9.275	0.161	0.790	8.79	7.970	0.672	1/4	24	3.84
16	16.000	0.065	18.420	15.870	1.140	17.892	0.299	1.524	17.29	15.930	0.855	1/4	78	18.04
Compatible With Loose-Ring Flanges														
3	3.000	0.028	4.300	2.944	0.399	3.898	0.096	0.431	3.54	2.984	0.40	3/16	14	0.7
8	8.000	0.035	9.805	7.930	0.645	9.275	0.161	0.790	8.79	7.970	0.672	1/4	24	3.84
16	16.000	0.065	18.420	15.870	1.140	17.892	0.299	1.524	17.29	15.930	0.855	1/4	78	18.04

TABLE 39. INPUT DATA, DIMENSIONS, AND ESTIMATED WEIGHTS FOR EXPERIMENTAL, ALUMINUM 100-PSI LOOSE-RING CONNECTORS

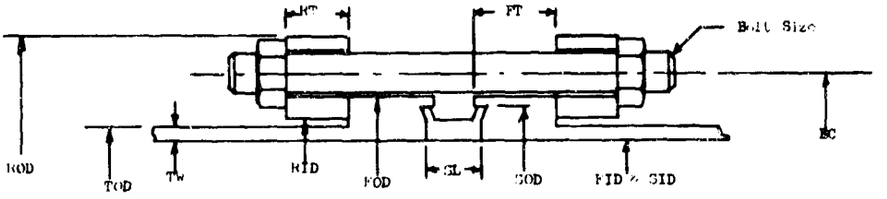

Input Data

Operating pressure, psi	100	Flange-to-seal hot thermal gradient, F	4
Operating temperature range, F	-423/200	Flange ultimate strength, psi	42,000
Bolt-to-ring cold thermal gradient, F	10	Flange yield strength, psi	32,200
Bolt-to-ring hot thermal gradient, F	6	Ring ultimate strength, psi	62,000
Ring-to-flange cold thermal gradient, F	10	Ring yield strength, psi	47,000
Ring-to-flange hot thermal gradient, F	4	Bolt ultimate strength, psi	62,000
Flange-to-seal cold thermal gradient, F	10	Bolt yield strength, psi	47,000

Size, in.	TOD	TW	ROD	RID	RT	FOD	FID	FT	BC	SOD	SID	SL	Bolt Size	No. of Bolts	Weight, lb
							Dimensions, in.								
Not Compatible with Integral Flanges															
3	3.000	0.028	4.300	3.165	0.296	3.697	2.944	0.279	3.898	3.54	2.984	0.490	3/16	14	0.745
8	8.000	0.035	9.742	8.287	0.508	8.947	7.930	0.450	9.212	8.79	7.970	0.672	1/4	24	3.94
16	16.000	0.065	18.240	16.550	0.850	17.444	15.870	0.840	17.709	17.29	15.930	0.855	1/4	76	18.19
Compatible with Integral Flanges															
3	3.000	0.028	4.300	3.165	0.296	3.697	2.944	0.279	3.898	3.54	2.984	0.490	3/16	14	0.745
8	8.000	0.035	9.805	8.287	0.820	8.947	7.930	0.450	9.275	8.79	7.970	0.672	1/4	24	4.1
16	16.000	0.065	18.420	16.550	0.925	17.444	15.870	0.840	17.892	17.29	15.930	0.855	1/4	78	19.89

TABLE 40. INPUT DATA, DIMENSIONS, AND ESTIMATED WEIGHTS FOR EXPERIMENTAL, ALUMINUM 1500-PSI INTEGRAL-FLANGE CONNECTORS

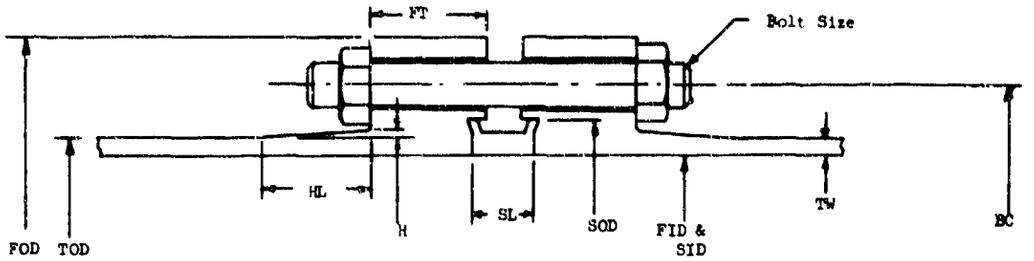

Input Data

Operating pressure, psi	1,500
Operating temperature range, F	-423/200
Bolt-to-flange cold thermal gradient, F	35
Bolt-to-flange hot thermal gradient, F	11
Flange-to-seal cold thermal gradient, F	60
Flange-to-seal hot thermal gradient, F	20
Flange ultimate strength, psi	42,000
Flange yield strength, psi	32,200
Bolt ultimate strength, psi	62,000
Bolt yield strength, psi	47,000

Size, in.	Dimensions, in. TOD	TW	FOD	FID	FT	BC	H	HL	SOD	SID	SL	Bolt Size	No. of Bolts	Weight, lb
Not Compatible With Loose-Ring Flanges														
3	3.000	0.114	4.848	2.771	0.824	4.192	0.221	0.845	3.360	2.811	0.473	5/16	16	2.30
8	8.000	0.306	10.645	7.389	1.952	9.583	0.230	2.253	8.310	7.429	0.567	1/2	28	18.38
16	16.000	0.611	20.791	14.780	4.093	18.917	0.458	4.510	16.438	14.838	0.627	7/8	28	132.5
Compatible With Loose-Ring Flanges														
3	3.000	0.114	4.848	2.771	0.824	4.192	0.221	0.845	3.360	2.811	0.473	5/16	16	2.38
8	8.000	0.306	10.673	7.389	1.967	9.611	0.229	2.253	8.310	7.429	0.567	1/2	28	18.68
16	16.000	0.611	20.895	14.780	4.143	19.021	0.458	4.510	16.438	14.838	0.627	7/8	28	138.6

TABLE 41. INPUT DATA, DIMENSIONS, AND ESTIMATED WEIGHTS FOR EXPERIMENTAL, ALUMINUM 1500-PSI LOOSE-RING CONNECTORS

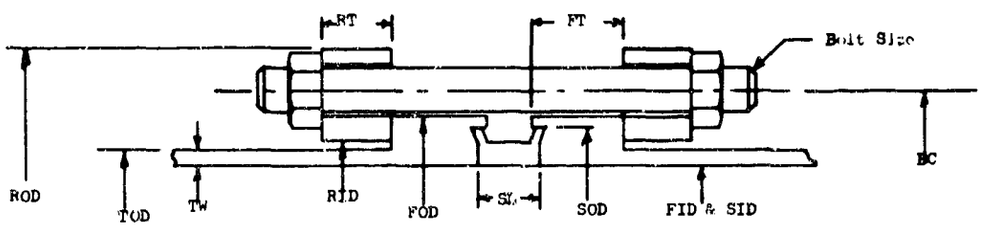

Input Data

Operating pressure, psi	1,500	Flange-to-seal hot thermal gradient, F	16
Operating temperature range, F	-423/200	Flange ultimate strength, psi	42,000
Bolt-to-ring cold thermal gradient, F	60	Flange yield strength, psi	32,200
Bolt-to-ring hot thermal gradient, F	10	Ring ultimate strength, psi	62,000
Ring-to-flange cold thermal gradient, F	30	Ring yield strength, psi	47,000
Ring-to-flange hot thermal gradient, F	10	Bolt ultimate strength, psi	62,000
Flange-to-seal cold thermal gradient, F	48	Bolt yield strength, psi	47,000

Size, in.	Dimensions, in. TOD	TW	ROD	RID	RT	FOD	FID	FT	BC	SOD	SID	SL	Bolt Size	No. of Bolts	Weight, lb
Not Compatible With Integral Flanges															
3	3.000	0.114	4.546	3.202	0.544	3.562	2.771	0.659	3.889	3.360	2.811	0.473	5/16	16	1.86
8	8.000	0.306	10.673	8.424	1.120	9.080	7.389	1.640	9.611	8.310	7.429	0.567	1/2	28	17.48
16	16.000	0.611	20.895	16.860	2.150	18.084	14.780	3.450	19.021	16.438	14.838	0.627	7/8	28	121.70
Compatible With Integral Flanges															
3	3.000	0.114	4.848	3.193	0.649	3.847	2.771	0.614	4.192	3.360	2.811	0.473	5/16	16	2.27
8	8.000	0.306	10.673	8.424	1.120	9.080	7.389	1.640	9.611	8.310	7.429	0.567	1/2	28	17.48
16	16.000	0.611	20.895	16.860	2.150	18.084	14.780	3.450	19.021	16.438	14.838	0.627	7/8	28	121.70

TABLE 42. INPUT DATA, DIMENSIONS, AND ESTIMATED WEIGHTS FOR EXPERIMENTAL, STAINLESS STEEL 100-PSI INTEGRAL-FLANGE CONNECTORS

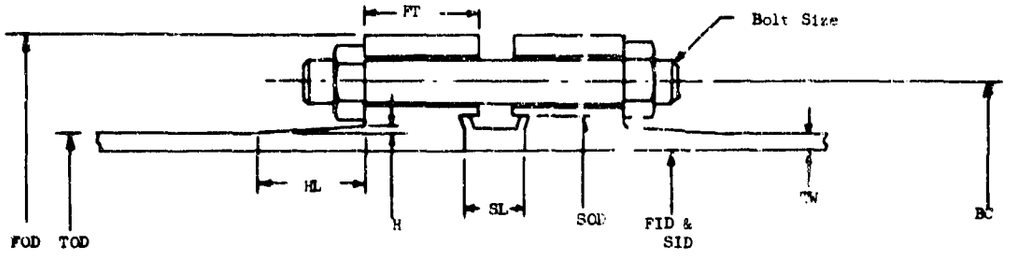

Input Data

Operating pressure, psi	100
Operating temperature range, F	-423/200
Bolt-to-flange cold thermal gradient, F	18
Bolt-to-flange hot thermal gradient, F	0
Flange-to-seal cold thermal gradient, F	25
Flange-to-seal hot thermal gradient, F	8
Flange ultimate strength at RT, psi	90,000
Flange yield strength at 200 F, psi	30,000
Bolt ultimate strength at RT, psi	130,000
Bolt yield strength at 200 F, psi	85,000

Size, in.	TOD	TW	FOD	FID	FT	BC	H	HL	SOD	SID	SL	Bolt Size	No. of Bolts	Weight, lb
						Dimensions, in.								
Not Compatible With Loose-Ring Flanges														
3	3.000	0.028	4.316	2.944	0.534	3.914	0.026	0.431	3.550	2.984	0.509	3/16	10	2.48
8	8.000	0.035	9.825	7.930	0.900	9.295	0.046	0.790	8.810	7.970	0.697	1/4	18	14.03
16	16.000	0.065	18.462	15.870	1.740	17.932	0.084	1.524	17.327	15.930	0.878	1/4	56	70.00
Compatible With Loose-Ring Flanges														
3	3.00	0.028	4.316	2.944	0.534	3.914	0.026	0.431	3.550	2.984	0.509	3/16	10	2.48
8	8.00	0.035	9.825	7.930	0.900	9.295	0.046	0.790	8.810	7.970	0.697	1/4	18	14.03
16	16.00	0.065	18.462	15.870	1.740	17.932	0.084	1.524	17.327	15.930	0.878	1/4	56	70.00

TABLE 43. INPUT DATA, DIMENSIONS, AND ESTIMATED WEIGHTS FOR EXPERIMENTAL, STAINLESS STEEL 100-PSI LOOSE-RING CONNECTORS

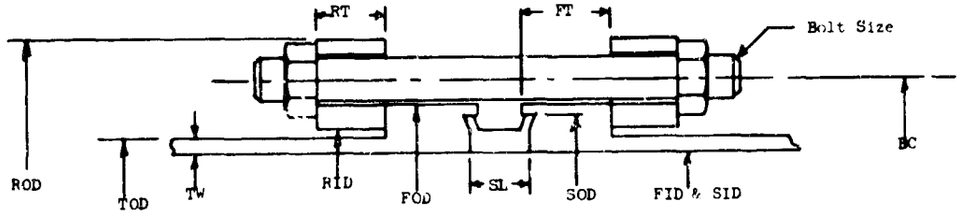

Input Data

Operating pressure, psi	100	Flange-to-seal hot thermal gradient, F	0
Operating temperature range, F	-423/200	Flange ultimate strength at RT, psi	90,000
Bolt-to-ring cold thermal gradient, F	23	Flange yield strength at 200 F, psi	30,000
Bolt-to-ring hot thermal gradient, F	7	Ring ultimate strength at 200 RT, psi	130,000
Ring-to-flange cold thermal gradient, F	18	Ring yield strength at 200 F, psi	85,000
Ring-to-flange hot thermal gradient, F	0	Bolt ultimate strength at RT, psi	130,000
Flange-to-seal cold thermal gradient, F	18	Bolt yield strength at 200 F, psi	85,000

Size, in.	TOD	TW	ROD	RID	RT	FOD	FID	FT	BC	SOD	SID	SL	Bolt Size	No. of Bolts	Weight, lb
						Dimensions, in.									
Not Compatible With Integral Flanges															
3	3.000	0.028	4.316	3.061	0.236	3.713	2.944	0.324	3.914	3.550	2.984	0.509	3/16	12	1.98
8	8.000	0.035	9.768	8.177	0.400	8.973	7.930	0.495	8.238	8.810	7.970	0.697	1/4	20	10.40
16	16.000	0.065	18.285	16.352	0.685	17.490	15.870	0.960	17.754	17.327	15.930	0.878	1/4	48	49.76
Compatible With Integral Flanges															
3	3.000	0.028	4.316	3.061	0.236	3.713	2.944	0.324	3.914	3.550	2.984	0.509	3/16	12	1.976
8	8.000	0.035	9.825	8.177	0.400	8.973	7.930	0.495	8.295	8.810	7.970	0.697	1/4	20	10.650
16	16.000	0.065	18.462	16.340	0.710	17.490	15.870	0.960	17.932	17.327	15.930	0.878	1/4	56	51.800

TABLE 44. INPUT DATA, DIMENSIONS, AND ESTIMATED WEIGHTS FOR EXPERIMENTAL, STAINLESS STEEL 1500-PSI INTEGRAL-FLANGE CONNECTORS

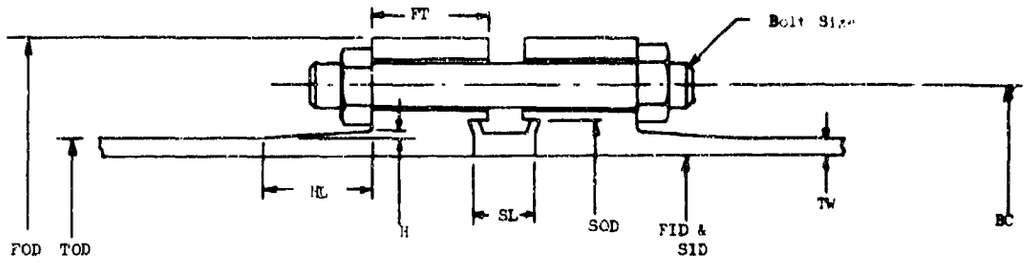

Input Data

Operating pressure, psi	1,500
Operating temperature range, F	-423/200
Bolt-to-flange cold thermal gradient, F	55
Bolt-to-flange hot thermal gradient, F	18
Flange-to-seal cold thermal gradient, F	70
Flange-to-seal hot thermal gradient, F	23
Flange ultimate strength, psi	90,000
Flange yield strength, psi	35,000
Bolt ultimate strength, psi	130,000
Bolt yield strength, psi	85,000

Size, in.	Dimensions, in. TOD	TW	FOD	FID	FT	BC	H	HL	SOD	SID	SL	Bolt Size	No. of Bolts	Weight, lb
Not Compatible With Loose-Ring Flanges														
3	3.000	0.120	4.408	2.760	1.000	3.878	0.095	0.864	3.360	2.799	0.488	1/4	16	5.5
8	8.000	0.320	9.892	7.359	2.100	9.098	0.080	2.303	8.310	7.399	0.579	3/8	34	36.5
16	16.000	0.641	19.006	14.718	3.947	17.520	0.160	4.607	16.432	14.778	0.640	9/16	44	211.0
Compatible With Loose-Ring Flanges														
3	3.000	0.120	4.408	2.760	1.0	3.873	0.095	0.864	3.360	2.799	0.488	1/4	16	5.5
8	8.000	0.320	9.892	7.359	2.1	9.098	0.080	2.303	8.310	7.399	0.579	3/8	34	36.5
16	16.000	0.641	18.787	14.718	3.9	17.725	0.160	4.607	16.432	14.778	0.640	1/2	52	191.0

TABLE 45. INPUT DATA, DIMENSIONS, AND ESTIMATED WEIGHTS FOR EXPERIMENTAL, STAINLESS STEEL 1500-PSI LOOSE-RING CONNECTORS

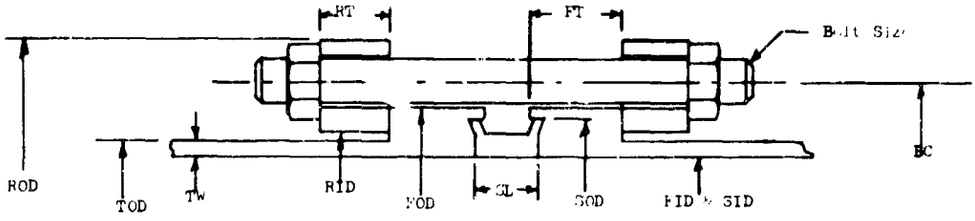

Input Data

Operating pressure, psi	1,500	Flange-to-seal hot thermal gradient, F	14
Operating temperature range, F	-423/200	Flange ultimate strength, psi	90,000
Bolt-to-ring cold thermal gradient, F	79	Flange yield strength, psi	35,000
Bolt-to-ring hot thermal gradient, F	23	Ring ultimate strength, psi	130,000
Ring-to-flange cold thermal gradient, F	55	Ring yield strength, psi	85,000
Ring-to-flange hot thermal gradient, F	14	Bolt ultimate strength, psi	130,000
Flange-to-seal cold thermal gradient, F	55	Bolt yield strength, psi	85,000

Size, in.	Dimensions, in. TOD	TW	ROD	RID	RT	FOD	FID	FT	BC	SOD	SID	SL	Bolt Size	No. of Bolts	Weight, lb
Not Compatible With Integral Flanges															
3	3.000	0.120	4.408	3.157	0.455	3.523	2.760	0.765	3.788	3.360	2.799	0.488	1/4	16	4.09
8	8.000	0.320	9.892	8.148	0.881	8.668	7.359	1.606	9.065	8.310	7.399	0.579	3/8	32	28.10
16	16.000	0.641	18.787	16.299	1.612	17.148	14.718	3.960	17.725	16.432	14.778	0.640	1/2	52	161.00
Compatible With Integral Flanges															
3	3.000	0.120	4.408	3.149	0.430	3.523	2.760	0.756	3.878	3.360	2.799	0.488	1/4	16	4.35
8	8.000	0.320	9.892	8.148	0.896	8.653	7.359	1.575	9.098	8.310	7.399	0.579	3/8	34	29.60
16	16.000	0.641	18.787	16.299	1.612	17.194	14.718	3.906	17.725	16.432	14.778	0.640	1/2	52	161.00

TABLE 46. INPUT DATA, DIMENSIONS, AND ESTIMATED WEIGHTS FOR EXPERIMENTAL, STAINLESS STEEL 4000-PSI INTEGRAL-FLANGE CONNECTORS

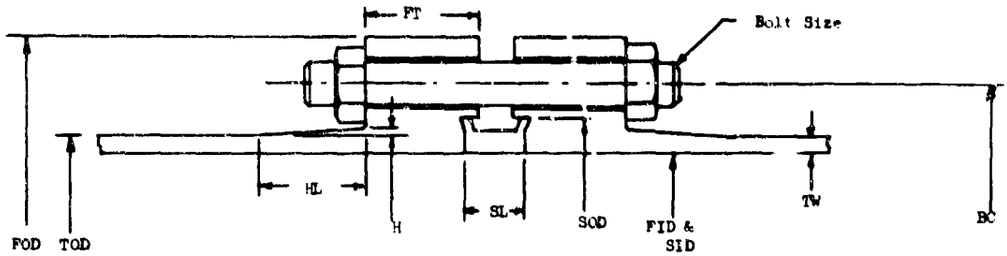

Input Data	-423/600 F System	70/600 F System	-423/200 F System
Operating pressure, psi	4,000	4,000	4000
Operating temperature range, F	-423/600	70/600	-423/200
Bolt-to-flange cold thermal gradient, F	55	1	55
Bolt-to-flange hot thermal gradient, F	55	55	18
Flange-to-seal cold thermal gradient, F	70	1	70
Flange-to-seal hot thermal gradient, F	70	70	23
Flange ultimate strength at RT, psi	90,000	90,000	90,000
Flange yield strength at 600 F, psi	25,000	25,000	30,000
Bolt ultimate strength at RT, psi	130,000	130,000	130,000
Bolt yield strength at 600 F, psi	75,000	75,000	85,000

Size, in.	Dimensions, in. TOD	TW	FOD	FID	FT	BC	H	HL	SOD	SID	SL	Bolt Size	No. of Bolts	Weight, lb
						-423/600 F System								
3	3.00	0.361	5.419	2.280	2.437	4.625	0.155	1.360	3.166	2.317	0.216	3/8	18	24.53
						70/600 F System								
3	3.00	0.361	4.982	2.277	1.853	4.1875	0.185	1.361	3.086	2.317	0.247	3/8	16	15.27
						-423/200 F System								
3	3.00	0.306	4.982	2.389	1.738	4.1875	0.185	1.282	3.197	2.429	0.258	3/8	16	14.42

TABLE 47. INPUT DATA, DIMENSIONS, AND ESTIMATED WEIGHTS FOR EXPERIMENTAL, STAINLESS STEEL 4000-PSI LOOSE-RING CONNECTORS

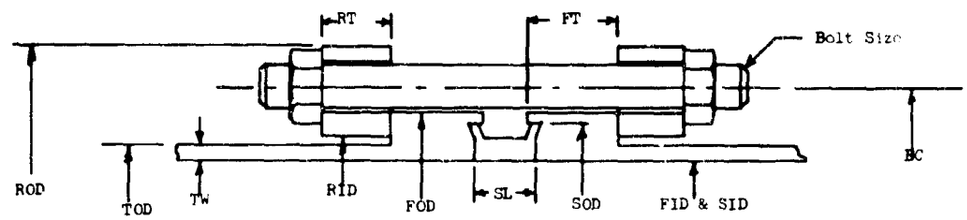

Input Data	-423/600 F System	70/600 F System	-423/200 F System
Operating pressure, psi	4,000	4,000	4,000
Operating temperature range, F	-423/600	70/600	-423/200
Bolt-to-ring cold thermal gradient, F	70	1	70
Bolt-to-ring hot thermal gradient, F	70	70	23
Ring-to-flange cold thermal gradient, F	55	1	55
Ring-to-flange hot thermal gradient, F	55	55	18
Flange-to-seal cold thermal gradient, F	55	1	55
Flange-to-seal hot thermal gradient, F	55	55	18
Flange ultimate strength at RT, psi	90,000	90,000	90,000
Flange yield strength at 600 F, psi	25,000	25,000	30,000
Ring ultimate strength at RT, psi	130,000	130,000	130,000
Ring yield strength at 600 F, psi	75,000	75,000	85,000
Bolt ultimate strength at RT, psi	130,000	130,000	130,000
Bolt yield strength at 600 F, psi	75,000	75,000	85,000

Size, in.	Dimensions, in. TOD	TW	ROD	RID	RT	FOD	FID	FT	BC	SOD	SID	SL	Bolt Size	No. of Bolts	Weight, lb
							-423/600 F System								
3	3.0	0.361	5.419	3.382	0.658	4.128	2.280	2.377	4.625	3.166	2.317	0.216	3/8	18	21.52
							70/600 System								
3	3.0	0.361	5.232	3.382	0.723	4.041	2.277	1.837	4.438	3.086	2.317	0.247	3/8	16	15.32
							-423/200 F System								
3	3.0	0.306	5.232	3.382	0.656	4.041	2.389	1.678	4.9375	3.197	2.429	0.258	3/8	16	14.42

III

FLANGED-CONNECTOR EVALUATION

The laboratory evaluation of representative flanged connectors is described in seven parts: (1) qualification test objectives, (2) qualification testing of small aluminum connectors, (3) qualification testing of small stainless steel connectors, (4) qualification testing of small, high-pressure stainless steel connectors, (5) qualification testing of large aluminum connectors, (6) qualification testing of large, stainless steel connectors, and (7) summary and conclusions.

Qualification Test Objectives

A test plan was prepared and approved prior to the qualification testing. The plan was formulated to demonstrate through tests of representative connectors under worst-case, performance conditions, that the design procedure is applicable to the following:

(1) Flanged connectors made of aluminum or stainless steel

(2) Aluminum flanged connectors for operation from -423 to 200 F

(3) Stainless steel flanged connectors for operation over three temperature ranges: (a) -423 to 200 F, (b) -423 to 600 F, and (c) ambient to 1200 F

(4) Aluminum flanged connectors for operation from 0 to 1500 psi, and stainless steel flanged connectors for operation from 0 to 6000 psi.

Selected Tests

The following general tests were selected as representative of worst-case performance conditions. The procedures followed for each connector are summarized as a part of the discussion of the test results.

1. Proof Pressure. The connector was to be subjected to one-and-one-half times the maximum operating pressure at the maximum design temperature. The maximum acceptable leakage was to be 2×10^{-7} atm cc/sec of helium per inch of seal circumference, and the connector was to show no permanent distortion or damage.

2. Thermal Gradient. The leakage was to be measured at the minimum and maximum design temperature and during the thermal transients. Maximum acceptable leakage with maximum operating pressure was to be 2×10^{-7} atm cc/sec of helium per inch of seal circumference.

3. Stress-Reversal Bending. The connector was to be cantilever mounted and subjected to 200,000 cycles, or the life of the tubing, of stress-reversal bendin , with maximum operating pressure at the maximum design temperature. Maximum acceptable

leakage was to be 2×10^{-7} atm cc/sec of helium per inch of seal circumference. The rate of application was not to exceed 1800 cpm, and the moment applied to the fitting during these tests was to be $M = ZS_b$, but not more than $60 (D + 3)^3$, where

M = moment applied to the connector, in-lb

Z = section modulus of the tubing used with the connector, $in.^3$

S_b = lower of (a) 0.667 x short time yield strength
(b) 0.800 x stress to rupture in 2 years
(c) 0.5 x 200,000 cycle fatigue strength

a, b, and c are evaluated at maximum connector design temperature

D = tubing diameter, in.

4. Pressure Impulse. The connector was to be given a proof-pressure test prior to the pressure-impulse test. All impulse testing was to be conducted at ambient temperature at the rate of 35 ± 5 cycles per minute. Each impulse cycle was to constitute a rise from approximately 0 psi to a peak surge pressure and drop to approximately 0 psi. The peak surge pressure was to be within 1.43 to 1.57 times the working pressure, as shown by an oscillograph or other electronic measuring device. The connector was to complete 200,000 impulse cycles, after which it was again to be given a proof-pressure test.

5. Vibration. The connector was to be vibrated for 200,000 cycles at an approximate resonant frequency of 160 cps, at the maximum design temperature with the maximum operating pressure. The moment at the fitting was to be the same as for the stress-reversal-bending test.

6. Repeated Assembly. A limited number of connectors were to be assembled and disassembled 25 times and subjected to operating pressure. No leakage greater than 2×10^{-7} atm cc/sec of helium per inch of seal circumference was to be acceptable.

7. Misalignment. The connector was to be assembled with angular misalignment of such magnitude that the bending load would equal one-half the bending load used in the stress-reversal-bending test.

8. Tightening Allowance. The connector was to be assembled to the design fastening load plus 10 percent. If no damage occurred, the fastening load was to be increased in increments of 10 percent until damage was detected.

Connectors Selected for Test

The representative connectors selected for test are shown in Table 48. The selection of these connectors is discussed below.

TABLE 48. SELECTED REPRESENTATIVE CONNECTORS

Tube OD, in.	Aluminum, 0 to 1500 Psi, -423 to 200 F		Stainless Steel, 0 to 1500 Psi, -423 to 200 F		Stainless Steel, 0 to 4000 Psi, -423 to 600 F		Stainless Steel, Ambient to 1200 F	
	100 Psi	1500 Psi	100 Psi	1500 Psi	100 Psi	4000 Psi	100 Psi	Max Pressure to be Determined
3	X	X		X	X	X	X	X
8		X	X	X				
16	X	X	X	X				

The materials that can be selected for the four service ranges listed on page 3 of this report are stainless steel for all ranges, and aluminum for the low-pressure range from -423 to 200 F. The representative connectors were selected from four of the five possible service range – material combinations. The fifth combination, stainless steel for 0-6000 psi at -423 to 200 F, was not selected because the applicability of the design procedure to such connectors was expected to be demonstrated by tests with the other selected connectors, particularly the 4000-psi connectors.

The design steps required for low- and high-pressure flange connectors are not necessarily the same. Consequently, high- and low-pressure connectors were included in each service range. Two low-pressure connectors were omitted because the other connectors were expected to demonstrate the applicability of the computerized procedure to these connectors.

The high pressure for the 1200 F service range was to be established on the following basis. The connector used for the test was to be dimensionally the same as the connector designed for the high-pressure test of the 0 to 4000-psi service range. A period of time (approximately 3 hours) at 1200 F was to be selected so as to be representative of high-temperature systems and also to be compatible with the test operations. The pressure was then to be selected as the maximum pressure at which the connector could operate satisfactorily for the time period selected. (As the testing effort encountered unexpected difficulties, tests with 1200 F connectors were deleted from the program.)

If there were no limitations in the facility test capabilities, it would have been necessary only to test connectors of the smallest and largest sizes to demonstrate the applicability of the design procedure over the complete size range. However, an 8-inch connector was the largest connector that could be subjected to the stress-reversal bending test at Battelle. Consequently, 8- and 16-inch connectors were selected to represent the largest connectors, depending on the tests required.

Three-inch connectors were selected to represent the smallest connectors because: (a) the design procedure for smaller sizes included allowances for fabrication limitations, (b) the 3-inch size represented the largest size in two service ranges, and

(c) use of a 3-inch size in all service ranges permitted considerable standardization of test equipment and procedures and consequent cost savings in the test program.

Tests Selected for Each Connector

It was not possible to subject each connector assembly to every test. One reason was that three of the tests (stress-reversal bending, vibration, and pressure impulse) were fatigue tests. Another reason was that the assembly required for a thermal-gradient test could not readily be used for a vibration test. It was decided that two connector assemblies of each design would be used for a complete series of tests. It was also decided that it was not necessary to conduct a complete series of tests for every connector design if the tests for one connector design demonstrated to an acceptable degree the applicability of the design procedure to other connector designs.

As shown in Table 49, a complete series of tests was planned for two connector designs: (1) the 3-inch, 1500-psi aluminum connector, and (2) the 3-inch, 1500-psi stainless steel connector. (The test numbers coincide with those given previously.) These tests were expected to demonstrate the applicability of the design procedure to small connectors for all performance aspects except: (1) low pressure, (2) pressure in excess of 1500 psi, and (3) operation at 600 F.

The low-pressure operation of small connectors was to be demonstrated by Tests 1-3 and 8 on an aluminum connector, and by Tests 1, 2, and 4 on a stainless steel connector at 600 F. Test 5 was not planned for low pressure because the stress-reversal bending at low pressure, combined with the vibration test at 1500 psi, was expected to demonstrate the ability of the connector to sustain vibration at low pressure. Tests 6 and 7 were not planned for low pressure because the connector features related to repeated assembly and misalignment were not significantly affected by the low-pressure design considerations.

The applicability of the design procedure for pressures higher than 1500 psi was to be demonstrated by Tests 1-4 and 8 with a 4000-psi stainless steel connector assembly at 600 F. The overall performance capability of connectors at 600 F was to be demonstrated by the same tests and by Tests 1, 2, and 4 at 600 F on a low-pressure stainless steel connector. Tests 5-7 were not to be conducted for the same reasons described above in relation to the low-pressure demonstrations.

As shown in Table 49, tests with the 8-inch connectors were to demonstrate the performance of large connectors under all conditions except pressure impulse (Test 4), vibration (Test 5), and tightening allowance (Test 8). Tests 6 and 7 were planned for only one assembly each because the design considerations for repeated assembly and misalignment were not expected to be significantly affected by either pressure or material.

The performance of large connectors during Tests 4 and 8 was to be demonstrated with 16-inch connectors. Because of the importance of Tests 1 and 2, Test 1 was to be conducted with every 16-inch connector, and Test 2 was to be conducted with two of the 16-inch connectors. Test 5, the vibration test, was not planned for any large connectors because the test was difficult to conduct with large sizes, and because the resistance to vibration was to be demonstrated by vibration tests with the 3-inch connectors, by stress-reversal-bending tests with the 8-inch connectors, and by pressure-impulse tests with the 16-inch connectors.

TABLE 49. QUALIFICATION TESTS SELECTED FOR REPRESENTATIVE CONNECTOR ASSEMBLIES

Tube OD, inches		Aluminum, -423 to 200 F		Stainless Steel, -423 to 200 F	
		100 Psi	1500 Psi	100 Psi	1500 Psi
3	Tests:	1-3, 8	1-4, 5-8		1-4, 5-8
	Assembly:(a)	L-L	I-L, I-I		L-L, L-L
8	Tests:		1-3, 6	1-3, 7	1-3
	Assembly:		I-L	I-L	I-L
16	Tests:	1, 2, 4, 8	1, 4, 8	1, 2, 4, 8	1, 4, 8
	Assembly:	I-L	I-L	I-L	I-L

		Stainless Steel, -423 to 600 F	
		100 Psi	4000 Psi
3	Tests:	1, 2, 4	I-4, 8
	Assembly:	I-L	I-I

(a) I-I = integral/integral flange assembly
I-L = integral/loose-ring flange assembly
L-L = loose-ring/loose-ring flange assembly.

Qualification Testing of Small Aluminum Flanged Connectors

The test schedule shown in Table 49 was followed, although the type of assembly was altered for some of the tests. Details of the test procedures and the test results are discussed for each of the eight types of tests.

Test 1. Proof Pressure

Test Procedures. Test 1 was conducted with a 100-psi integral/loose-ring connector and a 1500-psi integral/loose-ring connector. Each connector was machined as part of a "thermal-gradient" assembly similar to that shown in Figure 77. First, each connector was assembled with a primary and secondary seal. A torque of 24 in-lb was applied to the fourteen No. 10-32 aluminum studs of the 100-psi connector, and a torque of 175 in-lb was applied to the fourteen 3/8-inch aluminum studs of the 1500-psi connector. A 50/50 mixture of Lubriseal and MoS_2 was used to lubricate the stud threads and the nut collars of both connectors. Following this assembly, thermocouples, strain gages, and heaters were applied to the outside of each connector. One heater was located on the tubular portion of the stub flange, while the other was located on the tubular portion of the integral flange.

Next, an assembled connector and the seal pressurizing line were attached to the base-plate assembly. A Bobbin seal was placed between the transition flange and the base plate. Finally, the vacuum chamber was placed around the connector and the pressurizing, electrical, and vacuum leads were connected.

Each test was started by pressurizing the volume enclosed by the primary connector seal and the secondary seal with helium and by pressurizing the remaining internal connector volume with nitrogen. Both volumes were pressurized simultaneously to the proof-pressure level (150 psi for the 100-psi connector, and 2250 psi for the 1500-psi connector). After 5 minutes, the pressure in both volumes was reduced to zero and the connector temperature was increased to 200 F, at which time the internal pressure in both volumes was again raised to the proof-pressure level. After 15 minutes at maximum temperature and pressure, the connector was cooled to room temperature while the proof pressure was maintained in the secondary seal volume and the connector volume. After 5 minutes at room temperature the test was concluded. The helium mass spectrometer was used to monitor leakage during the entire test.

Test Results. The maximum leakage rate measured during the test of the 100-psi connector was 1.3×10^{-9} atm cc/sec per inch of seal circumference, while the maximum leakage rate measured for the 1500-psi connector was 3.1×10^{-9} atm cc/sec per inch of seal circumference.

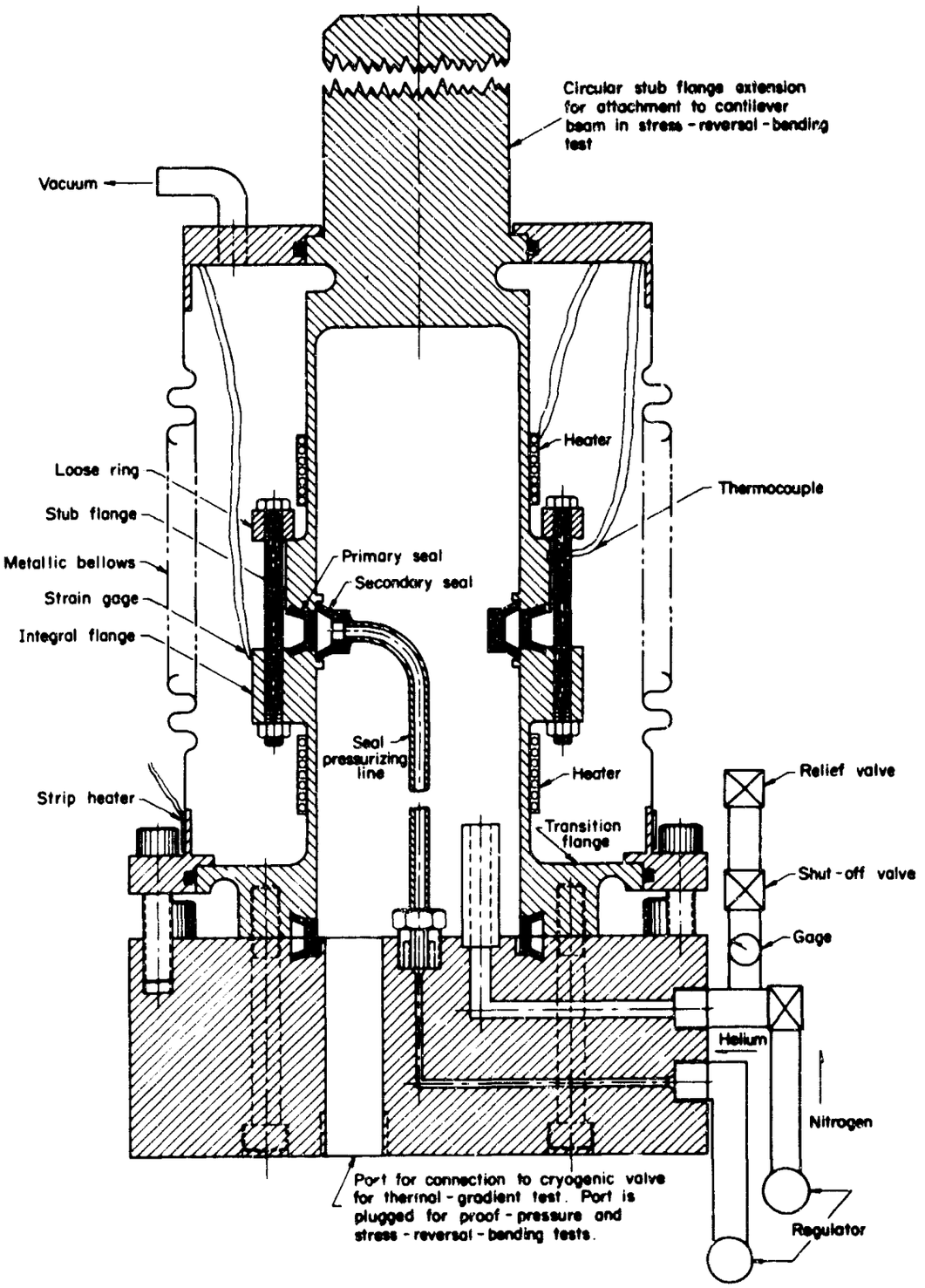

FIGURE 77. THERMAL-GRADIENT ASSEMBLY

Test 2. Thermal Gradient

Test Procedures. The thermal-gradient test was conducted with the 100-psi and 1500-psi assemblies used for the proof-pressure tests. Figure 78 is a schematic drawing of the major components of the thermal-gradient test system that was tried initially. (The connector assembly was rotated 180° from the position shown in Figure 77.) At the start of the test, the LN_2 tank was filled with LN_2 and pressurized to 50 psi. The cryogenic valve was used to valve the LN_2 into the connector. When the boiling of the LN_2 had raised the pressure in the entire system to 1500 psi and the vent valve was venting gaseous nitrogen, the pressure in the LN_2 tank was increased until an equilibrium condition had been reached for the in-flow of LN_2 and the outflow of gaseous nitrogen.

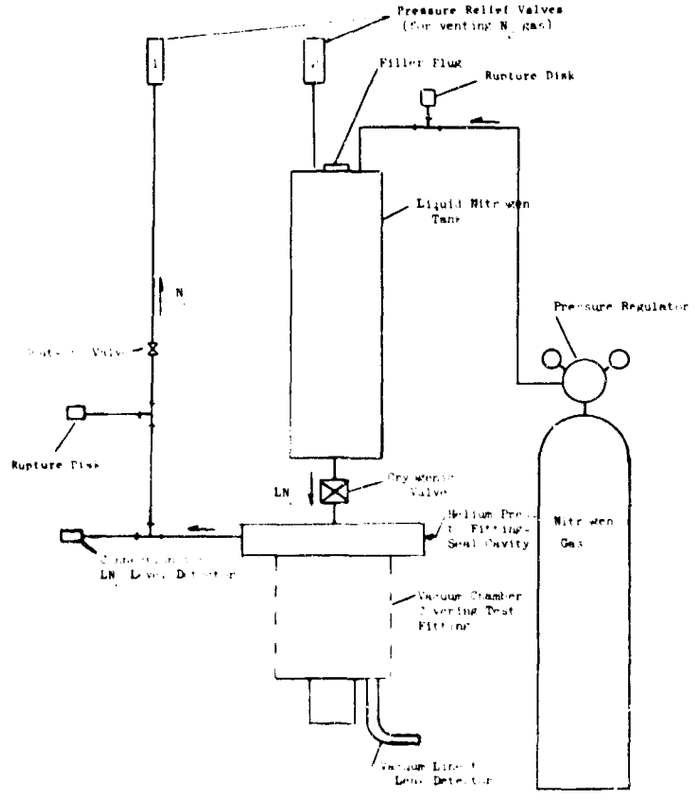

FIGURE 78. THERMAL-GRADIENT-TEST SYSTEM

Operation of this system was unsatisfactory because the large heat sink of the base plate prevented rapid cooling of the connector. It was found that sufficiently rapid cooling could be obtained if the base plate was precooled with dry ice and if the stub flange extension of the thermal-gradient assembly was cooled independently during the cooling cycle. A second type of vacuum chamber was made which completely enclosed the stub flange extension, thus eliminating the elastic seal at that point which would not seal in the presence of liquid nitrogen. Metal-to-metal contact was maintained between the stub flange extension and the vacuum chamber so the extension could be cooled by immersion of the lower part of the vacuum chamber in LN_2.

The temperature of the heaters was controlled by a Variac. Three thermocouples were used to determine the thermal gradients. They were located on the stub flange,

on the middle of one of the studs, and on the loose ring midway between two bolt holes. The thermocouples were also found to provide a good indication of the presence of liquid nitrogen in the connector.

At the start of the thermal-gradient test, the steel base plate was precooled with dry ice, and the extension of the stub flange was precooled with liquid nitrogen. The connector was then heated to 200 F. (The leakage of each connector at this temperature had been checked during the proof-pressure test.) The heaters were then turned off and the volume enclosed by the primary connector seal and the secondary seal was pressurized with helium to the maximum working pressure (100 psi and 1500 psi), while the remaining connector volume and the LN_2 standpipe were pressurized simultaneously, and LN_2 was forced into the connector. When thermal equilibrium had been reached, the in-flow of LN_2 was stopped, and the heaters on the connector were used to raise the connector temperature to 200 F. The test was designed to cool the connector as rapidly as possible to simulate the sudden flow of LN_2 through a connector that had been exposed to the hot sun. The heating cycle was conducted relatively slowly to simulate heating from atmospheric conditions.

Test Results. The thermal gradients, equilibrium temperatures, and maximum leakage rates for the 100-psi and 1500-psi connectors are shown in Table 50. The difference between the average thermal gradients obtained during the qualification tests and those obtained for the simulated assemblies (see Table 26) were caused by differences in the location of the thermocouples. It was believed that the test procedure had produced representative maximum thermal-gradient conditions. It can be seen that all of the measured leak rates were well below the required value of 2×10^{-7} atm cc/sec per inch of seal circumference.

TABLE 50. THERMAL GRADIENTS, EQUILIBRIUM TEMPERATURES, AND MAXIMUM LEAKAGE RATES FOR 3-INCH, ALUMINUM FLANGED CONNECTORS

Maximum Operating Pressure, psi	Cycle	Thermal Gradient, F: Stub Flange to Loose Ring	Thermal Gradient, F: Loose Ring to Stud	Equilibrium Temp, F	Maximum Leakage Rate[a], atm cc/sec
100	1	60	12	-292	1.8×10^{-9}
	2	56	13	-242	0.8×10^{-9}
	3	50	12	-293	0.8×10^{-9}
	4	48	16	-297	0.8×10^{-9}
	5	67	9	-297	1.2×10^{-9}
	Average	65	12	-294	1.1×10^{-9}
1500	1	34	15	-225	1.2×10^{-8}
	2	37	12	-217	0.9×10^{-8}
	3	67	18	-228	0.4×10^{-8}
	4	77	(b)	-210	0.6×10^{-8}
	5	54	(b)	-292	0.6×10^{-8}
	6	64	(b)	-212	0.6×10^{-8}
	Average	58	15	-231	0.7×10^{-8}

(a) Helium leakage rate per inch of seal circumference.

(b) Thermocouple failed after three cycles.

Test 3. Stress-Reversal Bending

Test Procedures. This test was conducted with the thermal-gradient assemblies that were used for Tests 1 and 2 for the 100-psi and 1500-psi connectors. Each assembly was mounted as the base of a rotating cantilever beam in the test equipment shown in Figure 79. The cantilever beam was designed to provide mechanical resonance at the operating speed of the machine (1800 rpm). The cantilever beam was clamped to the stub flange extension provided on the thermal-gradient assemblies, and a fine-tuning weight was used to provide adjustment for mechanical resonance of the different assemblies. Strain gages were attached to the cantilever beam to determine the moment being applied to the connector.

FIGURE 79. 4-INCH-DIAMETER PIPE SPECIMEN BEING INSTALLED IN STRESS-REVERSAL-BENDING MACHINE

The first 1500-psi aluminum connector was fabricated with flanges that were too thick. This connector was used to calibrate the equipment for the proof-pressure test, the thermal-gradient test, and the stress-reversal-bending test. As the speed of the stress-reversal-bending calibrations for this connector was increased to 1800 rpm, the strain gages or the cantilever beam recorded a reduction in strain. This could not be changed by any adjustment of the tuning weight. An examination of the equipment showed that the cantilever beam was not stiff enough to maintain the configuration of a simple cantilever at speeds above 500 rpm, and a reverse bend was being introduced dynamically. Not only did this make the strain-gage readings worthless, but an excessive moment was being applied to the connector. This problem was corrected by selecting a low test speed. However, it was decided that strain gages would be applied to each connector as a check on the strain gages on the cantilever beam.

Each thermal-gradient assembly was mounted in the test equipment and heated to 200 F. The volume between the primary-secondary seals was pressurized with helium at the maximum working pressure (100 psi and 1500 psi), and the connector volume was simultaneously pressurized with nitrogen to the same pressure. A bending moment of 2521 in-lb was applied to the 100-psi connector, and a bending moment of 9500 in-lb was applied to the 1500-psi connector. A speed of 392 cpm was selected for each test.

Test Results. The 100-psi connector was subjected to 218,250 cycles of stress-reversal bending before failure occurred. The failure was a group of three or four very small holes located 3 inches from the bottom of the mounting flange on the tubular portion of the stub flange. It was believed that the failure was caused by localized stresses resulting from an indentation in the 0.028-inch tube wall approximately 1/4 inch from the point of failure. The maximum helium leakage rate measured during the test was 1.5×10^{-9} atm cc/sec/inch of seal circumference.

The 1500-psi connector was subjected to 241,500 cycles of stress-reversal bending before failure occurred. The failure was a fine circumferential crack, approximately 1/2 inch long, located 1-1/2 inches from the O-ring groove, on the tubular portion of the stub flange. The maximum helium leakage rate measured during the test was 0.35×10^{-9} atm cc/sec per inch of seal circumference.

Because neither failure in the aluminum connector assemblies occurred in the connector material, and because each test achieved the required 200,000 cycles of stress-reversal bending, the test results were judged to be satisfactory.

Test 4. Pressure Impulse

Test Procedures. This test was conducted with a 3-inch, 1500-psi "vibration assembly" instead of a "thermal gradient" assembly. The vibration assembly consisted of a connector without a secondary seal, with tube extensions, and with a pressurizing port, similar to the connector shown in Figure 80.

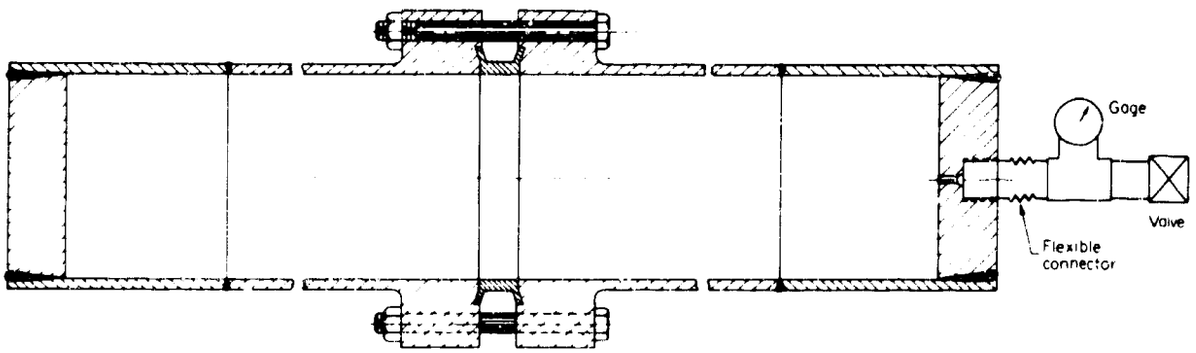

FIGURE 80. VIBRATION ASSEMBLY

Figure 81 shows schematically the arrangement of the pressure-impulse equipment. Hydraulic pressure was adjusted for 2250 psi at the output of the power unit, and a solenoid-actuated directional-control valve was used to control the flow to the test fitting. A Bell-O-Fram type diaphragm was used to separate the hydraulic oil from the alcohol in the test fitting. A switch and motor-driven gear-cam arrangement was designed to operate the solenoid valve to produce the desired cycling rate. Needle valves were installed in the inlet and return lines of the directional-control valve to provide adjustable restriction on the flow of oil and thereby control the rate of pressure rise.

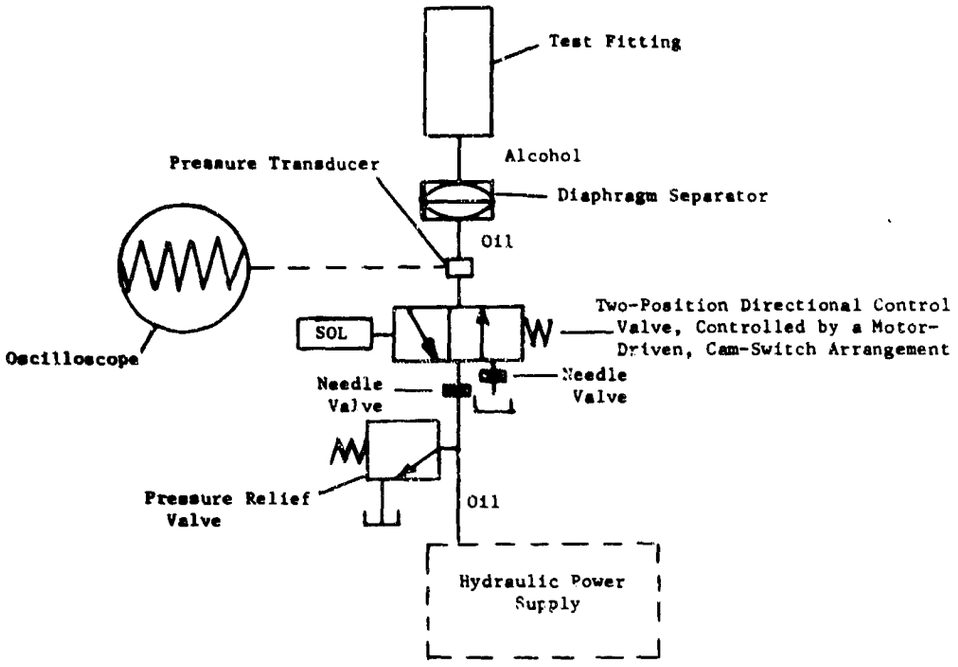

FIGURE 81. SCHEMATIC DIAGRAM OF PRESSURE-IMPULSE EQUIPMENT

The connector was first assembled for a helium leak check. Because of a previous failure in the vibration test (see page 111) a modified 3-inch, 1500-psi aluminum connector was used which contained a stronger hub and sixteen 5/16-inch studs. The nuts were torqued to 110 in-lb, using a 50/50 mixture of Lubriseal and MoS_2 to lubricate the stub threads and nut collars. A leakage check at room temperature showed no detectable leakage at 2250 psi of helium. Pressure traces recorded at various times throughout the test showed that sharp impulses were being obtained at a rate of 40 cycles per minute, and that dwell times of approximately 3/5 second existed at both the maximum and minimum pressure levels. A typical trace is shown in Figure 82.

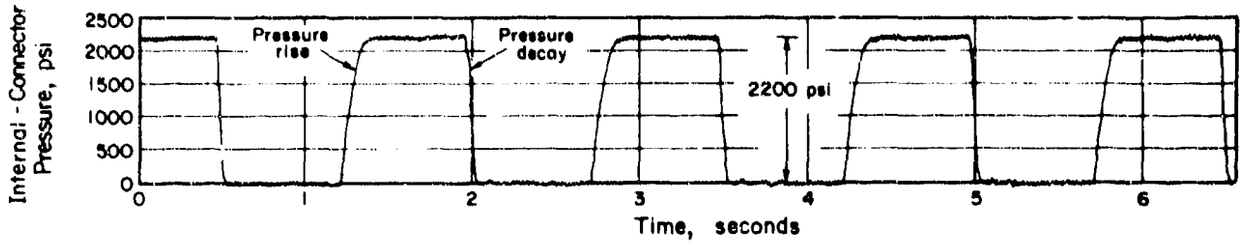

FIGURE 82. PRESSURE CYCLES MEASURED FOR 3-INCH, 1500-PSI ALUMINUM CONNECTOR

Test Results. The testing was terminated after 200,000 impulse cycles with no evidence of liquid leakage. The connector was drained and heat was applied to assist in removal of the alcohol. A leak check showed no detectable leakage at a helium pressure of 2250 psi.

Subsequently, when the seal in the 8-inch, 1500-psi aluminum connector failed after approximately 14,700 cycles of pressure-impulse testing, the seal from the 3-inch connector was given a Zyglow examination. Fatigue cracks were found at the base of both seal disks, which indicated possible failure at about 300,000 cycles. This showed a need for an increase in the thickness of the seal disks for the 3-inch, 1500-psi connector.

Test 5. Vibration

Test Procedures. The vibration test was conducted with a 1500-psi vibration assembly similar to that shown in Figure 80. The assembly was mounted as a simply supported beam. The connector was supported at two nodes, and a yoke-shaped device was fabricated to transmit the input from the Calidyne shaker to the connector at the nodes. A dummy connector was used to check out the test equipment and procedures.

Despite the tests with the dummy connector, considerable difficulty was encountered with the first assembly. The instrumentation used to monitor the test consisted of a vibration meter for monitoring acceleration, velocity, and displacement; an Ellis meter for strain readout for statically calibrated strain gages placed on a tubing extension; and an oscilloscope for strain-level monitoring. Many attempts were made to adjust the tuning weights and connector support locations, but it was impossible to maintain the required frequency of vibration, and the strain never rose above about 50 percent of the required strain. When the connector failed prematurely, it was decided that the connector design had to be modified for a second test and that an improved test procedure had to be developed.

The next vibration test was conducted with a vibration assembly which contained strengthened hubs. The connector was supported at two locations by small steel cables and the center of the connector assembly was fastened horizontally to the Calidyne machine. This arrangement was found to provide good frequency and amplitude control for the assembly. The flexible cables did not adversely affect the vibration of the connector. The connector was pressurized with water at 1500 psi and an enclosure with

radiant heaters was used to heat the assembly to 200 F. The instrumentation of the second test was the same as for the first test, with the addition of a pressure gage and a thermocouple. A test with a third vibration assembly was conducted identically to the test with the second assembly.

Test Results. A pretest room-temperature leak check of the first 1500-psi vibration assembly showed a leakage rate of 6.5×10^{-8} atm cc/sec per inch of seal circumference. During the vibration test, the first assembly broke at the base of the integral flange after only about 50,000 cycles at an average stress of 7000 psi (compared with a design stress of 14,000 psi with a bending moment of 9500 in-lb). This premature failure occurred despite the fact that the connector was neither pressurized nor heated. Examination of the stub flange showed an extensive crack at the flange-to-hub location, indicating incipient failure of that flange also.

A second vibration assembly was fabricated similar to the first but with strengthened hub sections (see page 86). The connector assembly was pressurized to 1500 psi with water, heated to 200 F, and vibrated at the design stress level at a frequency of 160 cps. Failure occurred after 28,200 cycles at the bulkhead in the simulated tubing, about 6 inches from the connector. This premature failure was a surprise because the calculated and measured strain at this location was approximately one-half the strain at the transition joint, the point of expected failure. Although a flaw in the bar stock could have caused the failure, the bulkhead was believed to have caused an unexpected stress raiser.

In the third vibration assembly, the bulkheads were moved to the ends of the assembly, about 18 inches from the connector. With a frequency of approximately 179 cps and the design bending moment, the connector failed at the tube-to-hub transition section after 53,000 cycles. This was the expected location of failure because of the change in section, and the test was considered to be an acceptable test of the connector because the connector was shown to be stronger than the tubing or the tube-to-hub transition. However, the failure of the tube-to-hub transition at such a low stress level was believed to represent a critical problem for the system designer, because substantial evidence was believed to have been developed that an unknown stress raiser was being encountered in the 3-inch tubing system in the vibration mode. (The further investigation of this problem is included in a follow-on effort, Contract No. F04611-69-C-0028).

Test 6. Repeated Assembly

Test Procedures. The repeated assembly test for a 3-inch, 1500-psi aluminum connector was conducted with flanges from the first, failed vibration assembly. The test utilized the seal cavities and the undamaged inside diameter of the flanges. O-ring-sealed supporting base plates were made so an axial load could be applied to the flanges in a Universal testing machine. Pressurized helium was introduced to the inside of the seal area through one base plate, while a cylindrical extension of the other base plate met with an O-ring seal on the outside diameter of the first base plate to form a vacuum chamber for the helium mass spectrometer. All of the assembled seals were checked with 1500-psi helium pressure.

Test Results. Table 51 shows the maximum leakage rate measured for each assembled seal. After the test, an examination of the connector sealing cavities with a 20-power lens showed no sign of wear or deformation at the surfaces where sealing occurred.

TABLE 51. REPEATED-ASSEMBLY-TEST LEAKAGE DATA FOR 3-INCH 1500-PSI ALUMINUM CONNECTOR

Seal	Leakage Rate[a], atm cc/sec	Seal	Leakage Rate[a], atm cc/sec
1	x[b]	14	x
2	x	15	0.14×10^{-9}
3	x	16	x
4	x	17	x
5	x	18	x
6	x	19	0.27×10^{-9}
7	x	20	x
8	x	21	x
9	x	22	x
10	x	23	x
11	x	24	x
12	0.81×10^{-9}	25	x
13	0.97×10^{-9}		

(a) Helium leakage rate per inch of seal circumference.
(b) Denotes no detectable leakage.

Test 7. Misalignment

Test Procedures. The misalignment test was conducted with the 3-inch, 1500-psi "vibration assembly" that had been used for the pressure impulse test. The cavities of this connector were machined to a depth of 0.080 inch instead of the standard 0.020 inch to produce a greater length of seal contact area for conditions of extreme misalignment.

When a tubing system is assembled in practice, it is expected that axial misalignment will exist between component parts of the system. Physical displacement of interconnecting tube ends is required to compensate for axial misalignment, and tube-end displacement results in angular misalignment at the connectors. The assembly of angularly misaligned connector halves produces a bending moment which is distributed among the system components and tubing. The bending moment will increase during connector bolt-up until the angular misalignment between connector halves has been reduced to zero. This action produces more axial motion on one side of the connector than the other, with a resultant relative motion between the sealing disks and connector cavities. The seal must be able to withstand this sliding action while maintaining its ultimate requirement for sealing.

A test fixture was fabricated to simulate a misaligned tubing condition. One half of the connector was clamped to a rigid base with its tube axis at an angle of 2 degrees to the base. The other connector half was positioned but not clamped by a support close to the connector. Shims were used under this support to provide angular changes in the

connector axis which would add to or subtract from the 2-degree angle established by the clamped connector half. Initial test misalignments of 1, 2, and 3 degrees were established by this method.

A tube extension providing a moment arm was added to the unclamped connector half. A bending moment equal to 1/2 the moment established for stress-reversal bending was required for this test, and the moment was provided by placing a weight on the tube extension. During the test it was found that the moment-producing weight caused a high transverse load on the seal due to leverage about the connector inner support block which acted as a fulcrum. A force of this magnitude would not be encountered in the assembly of an actual tubing system, and its effect was therefore removed from the test setup through the use of an outer tube support.

The seal was assembled into the connector at the desired angle of misalignment and the nuts were snugged down fingertight on the connector bolts. The weight was placed on the connector tube extension which was supported by the inner and outer tube supports. The connector bolts were then tightened with progressively increasing torque in a bolt-to-bolt sequence. As the bolt load was increased, the unrestrained connector half raised from the supports and a moment was applied to the entire connector. The bolt torque was increased in a continued bolt-to-bolt sequence until the required bolt preload was attained on all bolts. This assembly procedure satisfied the test requirement of initial angular misalignment of the connector halves while providing the bending moment and transverse loads that are expected during the process of bolt-up. In fact, the application of the full moment during practically the entire bolt-up procedure was significantly more stringent than will be encountered in practice, when the moment will normally increase with bolt tightening.

Test Results. Leakage checks were made with 1500-psi helium on each of the assemblies resulting from initial misalignment angles of 1, 2, and 3 degrees. No measurable leakage was found on any of the assemblies. Because some hand guidance was required during the early portion of the bolt-up of the 3 degrees of misalignment, it was apparent that a greater seal cavity depth will be required if a misalignment capability of 3 degrees is to be provided in the 3-inch connector.

Test 8. Tightening Allowance

Test Procedures. Each of the fourteen No. 10-32 studs of the 100-psi connector was initially tightened with a torque of 24 in-lb, using a 50/50 mixture of Lubriseal and MoS_2 applied to the nut faces and stud threads. Each of the fourteen 3/8-in. studs of the 1500-psi connector was initially tightened with a torque of 175 in-lb with the same lubrication procedure used for the 100-psi connector. Measurements were then made of the dimensions believed to be most useful in determining the occurrence of yielding in the connector (see Figure 83). Each connector was then tightened with additional torque increments of 10 percent, with measurements being made after each torque increment.

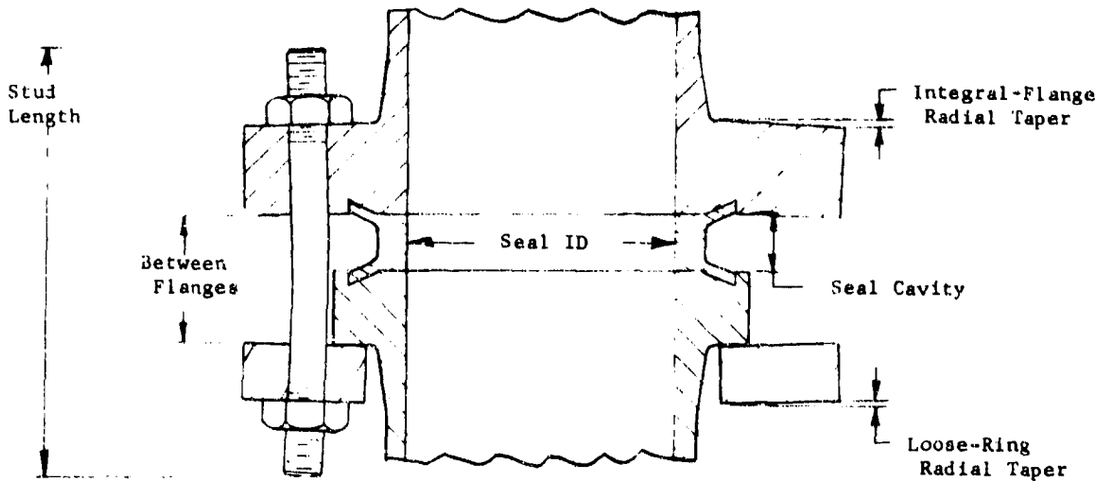

FIGURE 83. TIGHTENING-ALLOWANCE TEST MEASUREMENTS ON 3-INCH ALUMINUM CONNECTORS

Measurements were made at four equally spaced locations.

Test Results. The measurements showed that the greatest portion of the total change in the selected dimensions occurred during the first 10 percent increment of stud overtorque. Because a considerable amount of radial taper in the loose rings occurred as the result of the connector preloads, it is believed that the continued increase in radial taper of the rings caused a shift in the center of pressure between the nut face and loose ring. This shift in pressure toward one side of the stud resulted in an increase in the friction moment arm, which required a larger torque to overcome friction. The portion of the applied torque remaining for conversion to axial stud load was lessened, with a resultant decrease in connector dimensional changes. The radial taper of the loose rings essentially stopped when the stud shanks prevented further increase in the taper.

In the 100-psi connector, increased elongation of the studs was noted with the application of 50 percent overtorque. This was judged to be evidence of yielding of the studs. Although stud yielding was not encountered on the 1500-psi connector with 50 percent overtorque, initial yielding was indicated for the next 10 percent increment. In either case, the sealing capability of the connector was unchanged by the application of 150 percent of the recommended torque.

Qualification Testing of Small, Stainless Steel Connectors

The test schedule shown in Table 51 was followed. Details of the test procedures and test results are discussed for each of the eight types of tests.

Test 1. Proof Pressure

Test Procedures. The proof-pressure test procedures described previously for the 1500-psi 3-inch aluminum flanged connector were used for the 3-inch stainless steel flanged connector. The connector contained two loose-ring flanges machined as part of a thermal-gradient assembly similar to that shown in Figure 77. A torque of 95 in-lb was applied to the sixteen 1/4-inch A286 studs, using the same lubrication procedures as for the aluminum fasteners.

Test Results. The maximum leakage rate measured during the proof pressure test was 1.52×10^{-8} atm cc/sec of helium per inch of seal circumference.

Test 2. Thermal Gradient

Test Procedures. The test procedures developed for the 3-inch aluminum connectors were used for the 1500-psi stainless steel connector.

Test Results. The thermal gradients, equilibrium temperatures, and maximum leakage rates for the 1500-psi stainless steel connector are shown in Table 52. Some difficulty was encountered in controlling the flow of the liquid nitrogen in the first five cycles and this resulted in variation and high readings for the equilibrium temperatures for these cycles. However, for the sixth cycle, the liquid nitrogen was introduced without pressure in the connector so that a very low equilibrium temperature was reached as fast as possible (boiling gas could be vented immediately). The connector was then pressurized for a leak check. Because the thermal gradients in the sixth test were comparable to those in the other tests, and because the thermal gradients were believed to be the most severe condition of this test, the test was judged to be realistically severe. The measured rate of helium leakage remained at very low values for all the test cycles.

TABLE 52. THERMAL GRADIENTS, EQUILIBRIUM TEMPERATURES, AND MAXIMUM LEAKAGE RATES FOR 1500-PSI, 3-INCH STAINLESS STEEL CONNECTOR

Cycle	Thermal Gradients, F		Equilibrium Temperature, F	Maximum Leakage Rate, atm cc/sec[a]
	Stub Flange to Loose Ring	Loose Ring to Stud		
1	100	146	-130	3.1×10^{-9}
2	88	152	-150	2.6×10^{-9}
3	86	142	-160	2.6×10^{-9}
4	107	113	-100	3.7×10^{-9}
5	86	142	-165	1.0×10^{-9}
6	87	134	-300	1.0×10^{-9}
Average[b]	93	139	-141	2.6×10^{-9}

(a) Helium leakage rate per inch of seal circumference
(b) Average shown for first 5 cycles only.

Test 3. Stress-Reversal Bending

Test Procedures. This test was conducted with the 1500-psi thermal-gradient assembly used for the proof pressure and thermal gradient tests. The procedures were identical to those used for the 1500-psi aluminum connector. A bending moment of 11,288 in-lb was applied to the stainless steel connector.

Test Results. The stainless steel connector was subjected to 352,860 cycles of stress reversal-bending without failure. The maximum helium leakage rate measured during the test was 1.42×10^{-9} atm cc/sec per inch of seal circumference.

Test 4. Pressure Impulse

Test Procedures. A 3-inch, 1500-psi stainless steel "vibration assembly" (similar to that shown in Figure 80) was subjected to a pressure impulse test using the same procedures described for the 3-inch, 1500-psi aluminum connector. The stainless steel connector, which had no secondary seal, consisted of an integral/loose-ring configuration. An assembly torque of 110 in-lb was applied to the sixteen 1/4-inch A286 bolts.

A room-temperature leak check of the assembled connector showed no detectable leakage of helium at a pressure of 2250 psi. Operation of the test equipment produced a temperature-stabilized condition with a maximum pressure of 2180 psi (which was greater than the mimimum specified pressure).

Test Results. The test was terminated after 200,005 pressure-impulse cycles with no indication of liquid leakage. A leak check with 2250-psi helium after removal of the alcohol showed no detectable helium leakage.

Test 5. Vibration

Test Procedures. The connector used for the 3-inch, 1500-psi stainless steel vibration test was the integral/loose-ring vibration assembly that had been used previously for the pressure impulse test. On the basis of the failures encountered in the vibration tests of the aluminum connectors it was decided that the flange-to-hub radii should be increased. Consideration was given to machining a new assembly with increased hub thicknesses, but it was decided that the stainless steel would probably be less susceptible to the effects of the stress raiser than the aluminum, and the thinner hub would probably be satisfactory.

Strain gages were attached to the assembled connector at the flange-to-hub radius, at the tube-to-hub transition, and on the tube. The strain gages were calibrated statically for the required bending moment, and the leakage rate was monitored for 30 minutes with the connector pressurized with 1500-psi helium. No leakage could be detected.

A room-temperature vibration check with no internal pressure produced a tube strain of 464 μin./in. at a resonant frequency of 186 cps. Strains of 458 and 710 μin./in. were measured at the tube-to-hub transition and the hub-to-flange radius, respectively.

The assembly was pressurized, heated, and tested in the same manner as was the 1500-psi aluminum connector. Although the power to the Calidyne machine had to be slightly increased periodically, the test was completed without incident.

Test Results. No indication of liquid leakage was detectable after 475,000 cycles. The water was removed from the connector and the connector was heated to remove residual moisture. A leak check with 1500-psi helium showed no detectable leakage.

Although the connector showed no leakage, the diameter of the simulated tubing between the connector and the bulkheads had enlarged 1/16 inch. Because the calculated

and measured stresses in the tubing before and during vibration did not exceed the yield stress of the stainless steel, and in fact were about one-half the yield stress, it was hypothesized that the same, unknown, stress raiser existed in the 3-inch stainless steel connector as in the 3-inch aluminum connector.

Test 6. Repeated Assembly

Test Procedures. The 3-inch, 1500-psi stainless steel thermal-gradient assembly was adapted for use in the repeated assembly test. Seal loading was accomplished in a Universal testing machine. An axial load was applied to the connector through a tube whose mean diameter was equivalent to the connector bolt-circle diameter. The load was transmitted through the tube and connector loose ring to the stub flange. The load path from this point was through the seal tang to the integral flange, and then through the connector to the base plate with its pressurizing fittings. A vacuum chamber, consisting of a tube closed at one end, was placed over the assembly. The testing machine pressed against the closed end of the vacuum chamber, which rested on the loading tube described above. The open end of the vacuum chamber moved down over an O-ring seal located in the outside circumference of the base plate. This arrangement not only provided an accurate means of measuring the seal seating forces, but also saved the time normally required to tighten the studs.

An axial load of 25,000 pounds was applied as a preload to each of the 25 seals tested, and all of the seals were leak checked with 1500-psi helium pressure.

Test Results. Table 53 shows the maximum leakage rates measured for the 25 stainless steel assemblies. At the time, it appeared that the existence of four seals with excessive leakage rates was caused by poor quality control of the nickel plating. However, growing evidence from the use of stainless steel seals in threaded connectors, as well as from subsequent tests with the 8-inch flanged connectors, indicated that a significant increase was required in the radial sealing load of stainless steels to obtain reliable performance. Examination of the seal cavities of the connector flanges with a 5-power microscope showed no wear or deformation at the surfaces where sealing occurred.

Test 7. Misalignment

Test Procedures. The misalignment test was conducted with the 3-inch, 1500-psi stainless steel "vibration assembly" that was used for the vibration test. The enlargement of the tubing extension that occurred in the vibration test had no influence on the misalignment test. The test procedures described previously for the 3-inch, 1500-psi aluminum connector were used for the stainless steel connector. The required bending moment of 5640 in-lb was achieved by placing a 141-pound weight 40 inches from the connector on the extension beam.

Test Results. Tests were conducted with initial misalignment angles of 1, 2, and 3 degrees. A sliding action was noted between the seal and its cavity during each test, and greater motion was evident as the misalignment angle was increased. Some plating was scraped from the seal as a result of this motion, but the material came from areas which did not affect the ultimate sealing surfaces which were on a 10-degree reverse angle. No leakage could be detected with 1500-psi helium on any of the three assemblies resulting from initial misalignments of 1, 2, and 3 degrees.

TABLE 53. LEAKAGE DATA FOR REPEATED-ASSEMBLY TEST WITH 3-INCH, 1500-PSI STAINLESS STEEL CONNECTOR

Seal	Measured Leakage[a], atm cc/sec	Remarks
1	x[b]	
2	x	
3	x	
4	7.2×10^{-10}	Leakage within specified limit
5	1.11×10^{-8}	Leakage within specified limit
6	x	
7	x	
8	x	
9	x	
10	x	
11	Greater than 2.26×10^{-6}	Large flakes in plating on sealing surface
12	x	
13	x	
14	Greater than 2.7×10^{-6}	Pits in plating across sealing surface
15	x	
16	Greater than 4.5×10^{-6}	One large flake in plating on sealing surface
17	x	
18	x	
19	x	
20	x	
21	x	
22	1.76×10^{-8}	Leakage within specified limit
23	x	
24	5.7×10^{-7}	Pits in plating across sealing surface
25	x	

(a) Helium leakage rate per inch of seal circumference.
(b) Denotes no detectable leakage

Test 8. Tightening Allowance

Test Procedures. The 3-inch, 1500-psi stainless steel thermal-gradient-assembly connector containing two loose rings was used for this test. The connector was assembled by applying the maximum torque of 110 in-lb to each of the sixteen 1/4-inch A286 studs. The same lubrication technique was used as for the aluminum connector, and the same measurement and overtorquing procedure was used. In addition, a leak check was made with 1500-psi helium after the initial assembly and after the application of 50 percent torque.

Test Results. The greatest dimensional change after the application of 150 percent of recommended bolt torque occurred in the tilting of the loose rings. However, this was not considered to be excessive. The incremental changes in stud length were consistent and did not suggest a condition of yielding. Neither the pretest nor the posttest leakage check on the connector with 1500-psi helium produced detectable leakage. Calculations of stud capacity showed that failure of the studs could be expected starting at about 170 percent of recommended torque.

Qualification Testing of Small, High-Pressure Stainless Steel Connectors

The applicability of the design procedure for designing connectors for pressures higher than 1500 psi was to be demonstrated by Tests 1 through 4 and 8 conducted on a 3-inch, 4000-psi, -423 to 600 F, stainless steel, integral-integral flange connector assembly. The overall performance capability of connectors at 600 F was to be demonstrated by these tests combined with tests on a low-pressure, 3-inch connector at 600 F.

A reexamination of the primary objectives of the laboratory program resulted in the decision to minimize the high-temperature activities. As a result of this decision, the 1200 F tests were eliminated completely, and the low-pressure 600 F tests were eliminated. It was believed that any significant problem at 600 F would be revealed by the test of the 3-inch, 4000-psi connector at 600 F.

When a 4000-psi connector was designed for the full temperature range of -423 to 600 F, the connector was very heavy (see Tables 46 and 47). Since this temperature range was not expected in a single system, 4000-psi connector designs were optimized for a cryogenic system (-423 to 200 F) and a hot-gas system (ambient to 600 F). The dimensions of these connectors showed that by accepting a slightly heavier than optimum cryogenic connector, it was possible to use dimensions for the cryogenic connector that could be obtained by remachining the hot-gas connector. This choice was selected, and the hot-gas connector was fabricated and tested first. The connector was then disassembled, the flanges were modified, and the cryogenic connector was assembled and tested.

Because two 4000-psi connector designs were tested in this revised approach, the test schedule was reexamined. It was decided that Tests 1 through 3 would be conducted on the hot-gas connector, and Tests 1, 2, and 8 would be conducted on the cryogenic connector. When a question of seal disk strength arose later in the program, a pressure impulse test (Test 4) was also conducted with the cryogenic connector.

Tests for a 3-Inch, 4000-Psi Hot-Gas Connector

Proof-Pressure Test Procedures. The proof-pressure test was conducted with a thermal-gradient assembly similar to that shown in Figure 77. Because of the high temperature, disks were machined on the tubular portions of the connector, and the vacuum chamber was welded to the disks after the connector was assembled. Lubrication was applied to the nut-bearing surfaces and threads of the 3/8-inch, A286 connector bolts, and a preload torque of 296 in-lb was applied to each of the 16 bolts. External heaters were mounted on the outside diameter of each of the integral flanges. Wiring was routed through the vacuum chamber electrical feed-through, and after the connections were checked, the vacuum chamber was welded in place.

Difficulty was encountered with the heating of the connector because the heaters (which had a higher capacity and a higher voltage than the heaters used for the 200 F tests) shorted out in the vacuum required for leakage measurements. A 5500-watt heater had been purchased and modified to fit inside the connector during the

thermal-gradient test. It was decided that this heater would be used for the proof-pressure test. Although the heater filled most of the connector cavity, the remainder of the cavity was filled with water to optimize the flow of heat from the heater to the connector. The water did not boil because of the high pressure.

Although an ambient test at 6000 psi showed a leakage of only 1.16×10^{-9} atm cc/sec of helium per inch of seal circumference, an increase in connector temperature to 600 F resulted in an excessive leak which flooded the mass spectrometer. An examination of the seal showed an imperfection in the nickel plating at the point of leakage. However, it was estimated that this problem may have been aggravated by load interaction between the sealing disks caused by a very short seal tang. Seals with twice the tang length were then fabricated. Load ring tests showed that the redesigned seals had a radial load of about 2550 pounds per inch of seal circumference as compared with a load of about 1300 pounds per inch for the original seal design. Although the lower value was believed to have been sufficient, it was estimated that the higher value would pose no problems for the high-pressure connector.

Proof-Pressure Test Results. Seven proof-pressure test cycles were conducted to "wring out" the new seal design. To simplify installation, a secondary seal was not used during these tests. Although leakage from the connector was not monitored continuously, a constant 6000-psi helium pressure was maintained inside the connector. Leakage was measured at ambient temperatures (considered the condition most likely to leak) and no leakage was detected after any cycle. This series of tests was considered to be ample for the proof-pressure test requirements.

Thermal-Gradient Test Procedures. The connector was then disassembled and reassembled with an unused primary seal, and with a secondary seal. Six cycles of high-temperature thermal-gradient testing were conducted from ambient to 600 F with heat being supplied by the internal heater. The seal leakage was monitored continuously while the pressure inside the connector was maintained at 4000 psi and the helium pressure between the primary and secondary seals was maintained at 4000 psi. Temperatures were monitored throughout each test cycle with thermocouples on the OD of the seal tang, the OD of a flange, and on the midpoint of a bolt. The maximum temperature differential occurred between the seal tang and the bolt during the heating portion of each cycle.

Thermal-Gradient Test Results. The indicated leakages and maximum temperature differentials are shown in Table 54. The rate of heat input was increased each cycle but no significant increase in seal leakage could be associated with the increasing temperature differentials.

Stress-Reversal-Bending Test Procedures. The stress-reversal-bending test was conducted in a manner similar to that used for the 3-inch aluminum and stainless steel connectors. The base plate of the thermal-gradient assembly was rigidly attached to the test machine, and the required bending moment (12,960 in-lb) was applied to the connector through an extension beam. Temperature-compensated strain gages were attached to the tubular section between the connector and the base plate. The gages were first statically calibrated at room temperature with the assembly in a horizontal position and with weights on the extension beam, and these values were compared with those calculated

for the tubular section using the dimensions and the required moment. This comparison was then used to calculate the amount of strain that should be indicated at 600 F with a reduced modulus of elasticity. Finally, the beam deflection required in the machine to produce the required strain was measured by dial-indicator gages and shown to be in close agreement with the calculated deflection requirement.

TABLE 54. THERMAL-GRADIENT-TEST DATA FOR 600 F, 3-INCH, 4000-PSI STAINLESS STEEL CONNECTOR

Test Cycle	Max Leakage Rate[a], atm cc/sec	Max Temp Differential Between Seal Tang and Bolt, F
1	4.6×10^{-9}	132
2	5.4×10^{-9}	198
3	4.1×10^{-9}	195
4	3.7×10^{-8}	201
5	4.8×10^{-9}	223
6	6.7×10^{-9}	242

(a) Helium leakage rate per inch of seal circumference.

The temperature of the connector was stabilized at 600 F by the Variac-controlled internal heater, the internal pressure of the connector and the helium pressure between the seals were raised to 4000 psi, and the cycling was begun. Pressure, temperature, and helium leakage were monitored continuously throughout the test, while the strain-gage readings were checked at half-hour intervals. The cycle rate was 378 cycles per minute.

Stress-Reversal-Bending Test Results. The test was terminated after 202,230 cycles of stress-reversal bending, during which time no leakage could be detected from the connector.

Tests for a 3-Inch, 4000-Psi Cryogenic Connector

Proof-Pressure Test Procedures. As described previously, the cryogenic 4000-psi connector was very similar to the hot-gas 4000-psi connector. The connector was assembled with a primary and secondary seal, and the 3/8-inch A286 bolts were tightened with a torque of 296 in-lb. Because the heating cycle was less critical for the cryogenic connector than for the hot-gas connector, heating was accomplished by passing steam through a copper tube which was coiled about the welded vacuum chamber and the exposed connector tubular sections.

The proof-pressure test of the 3-inch, 4000-psi cryogenic connector was initiated by pressurizing the connector to 6000 psi at ambient temperature for approximately 1 hour. The pressure was then reduced to 1000 psi and the connector was heated to 200 F. Next, the pressure was raised to 6000 psi for approximately 30 minutes, and the connector was then cooled to ambient temperature with a constant internal pressure of 6000 psi.

Proof-Pressure Test Results. No leakage could be detected during two such proof-pressure tests.

Thermal-Gradient Test Procedures. Because of the high pressure of the 4000-psi connector, it was not possible to use the same thermal-gradient-test techniques that were used for the 3-inch, 1500-psi aluminum and stainless steel connectors. The modified procedure consisted of using the liquid-nitrogen test stand to cool the connector as quickly as possible by allowing liquid nitrogen to flow rapidly into the connector at ambient pressure. To hasten the cooling process, the lower part of the connector was immersed in liquid nitrogen during the cooling cycle. The volume between the secondary and primary seals was continuously pressurized to 180 psi, and the mass spectrometer was used to monitor connector leakage continuously. When an equilibrium temperature had been reached, the liquid-nitrogen supply was stopped, and the connector and the secondary-primary seal volume were pressurized to 4000 psi.

Thermal-Gradient Test Results. Four cycles were conducted between temperature extremes of -300 and +195 F. Because the cooling was accomplished in approximately 1 hour, and because the thick flanges of the high-pressure connector represented large masses as compared to the seal, it was believed that the thermal-gradient design parameters were given a severe test. The largest leakage measured during the four cycles was 3.3×10^{-8} atm cc/sec of helium per inch of seal circumference.

Pressure-Impulse Test Procedures. Because a stress-reversal-bending fatigue test had already been conducted on the hot-gas 4000-psi connector, a second fatigue test was not originally scheduled for the cryogenic 4000-psi connector. However, as described later, pressure impulse tests produced seal disk failure in the 8-inch, 1500-psi aluminum connector and extensive seal disk cracking in the 3-inch, 1500-psi aluminum connector. The seal disks in the 3-inch, 4000-psi stainless steel connector had the same thickness as the seal disks in the 3- and 8-inch, 1500-psi aluminum connectors. Although stainless steel was known to be much tougher than the aluminum, it still appeared likely that a pressure-impulse test at 6000 psi might fail the stainless steel disks of the 4000-psi connector. Thus, a pressure-impulse test of the 4000-psi connector was initiated primarily to test the seal disks and secondarily to conduct another fatigue test of the connector structure.

Much of the equipment used to conduct pressure-impulse tests on the 3-inch, 1500-psi connectors was used to test the 4000-psi connector. A modification consisted of substituting an intensifier for the oil/alcohol separation unit so the 2250-psi output pressure of the original equipment could be used to produce 6000-psi pressure impulses. In this arrangement, it was necessary to use a light oil in the connector instead of alcohol, but this was believed to be acceptable since the mode of possible failure was expected to leak oil. The secondary seal was machined away in the assembled connector prior to the test so the pressure impulses could reach the primary seal.

Pressure-Impulse Test Results. For the most part the test was conducted without incident. At one time the intensifier galled and had to be reworked slightly, but by using

a heavy oil at the intensifier seals it was possible to continue. In all, 1,072,422 pressure-impulse cycles were completed without leakage at the primary seal. Upon disassembly of the connector, a Zyglow examination of the seal showed no cracking of the seal material.

Tightening-Allowance Test Procedures. The 3-inch, 4000-psi cryogenic stainless steel connector was assembled by applying the recommended torque of 296 in-lb to each of the 3/8-inch, A286 bolts. The same lubrication and measurement was used as had been used for the 3-inch, 1500-psi aluminum and stainless steel connectors. The torque was then increased in increments of 10 percent.

Tightening-Allowance Test Results. An overtorque of 90 percent was applied without indication of yielding of the bolts. However, at this torque the nut corners had become badly rounded and application of additional torque was not possible.

Qualification Testing of Large Aluminum Connectors

The applicability of the computerized procedure for designing large aluminum flanged connectors was to be demonstrated by the fabrication and test of connectors for 8- and 16-inch tubing systems. As the test program proceeded, the test schedule was reexamined. It was decided that the number of high-pressure, large tubing systems would be low and that the test of a 16-inch, 1500-psi connector would have relatively little applicability. On the other hand, it was also decided that there would be many low-pressure systems, and the absence of an 8-inch, 100-psi connector was undesirable in view of the large size difference between the 3-inch and the 16-inch, 100-psi connectors. Therefore, the decision was made to replace the 16-inch high-pressure connector with an 8-inch low-pressure connector. At the same time, the schedule of tests was revised slightly and the test schedule shown in Table 55 was undertaken.

TABLE 55. REVISED TEST SCHEDULE FOR LARGE ALUMINUM CONNECTORS

Tube OD, in.	Max Operating Pressure, psi	Tests	Assembly Type
8	1500	1, 2, 5-8	Integral/Loose-Ring
8	100	1, 2, 5, 8	Integral/Loose-Ring
16	100	1, 2, 4, 8	Integral/Loose-Ring

Following the successful completion of over 1,000,000 vibration cycles on the 8-inch, 100-psi connector, the decision was made to substitute a pressure-impulse test for the vibration test of the 8-inch, 1500-psi connector. A seal design problem revealed by this pressure-impulse test demonstrated the wisdom of this decision.

Test Assemblies

As described in some detail in previous sections, the tests of the 3-inch connectors were conducted on two types of assemblies: (1) a thermal-gradient assembly or (2) a vibration assembly. Because of the large size of the 8- and 16-inch connectors and because of the more limited test program planned for the large connectors, a different type of test assembly was developed.

Figures 84 and 85 show pictures of the 8-inch, 100- and 1500-psi test assemblies. Figure 86 shows a picture of the 16-inch, 100-psi assembly, while Figure 87 shows a cross section of this assembly. All the large test assemblies had essentially the same configuration. Each assembly contained one loose-ring flange and one integral flange. The internal flange, a short tube section, a tube end closure, and a mounting flange were designed to be machined from one piece of aluminum plate. The mounting flange contained holes for bolt attachment to a rigid mounting pad during the dynamic tests.

The loose-ring stub flange was fabricated from a cylindrical forging approximately 12 inches long. The stub flange design contained a tubular section which extended approximately one tube diameter beyond the tapered hub portion of the flange. Beyond the tube section, the wall thickness was increased to provide material for an O-ring groove and for threaded bolt holes for the attachment of an end closure.

For each assembly, a vacuum chamber was made with a closed end so the entire test assembly could be lowered into the vacuum chamber. An O-ring seal then was used to seal the opening of the vacuum chamber with the edge of a disk machined on the end closure of the stub flange tube extension.

Test 1. Proof Pressure

Test Procedures. Proof-pressure tests were conducted with both 8-inch assemblies and with the 16-inch assembly. During assembly, a torque of 60 in-lb was applied to the twenty-four 1/4-inch studs of the 8-inch, 100-psi assembly, and to the seventy-eight 1/4-inch studs of the 16-inch, 100-psi assembly. A torque of 500 in-lb was applied to the twenty-eight 1/2-inch studs of the 8-inch, 1500-psi assembly. A 50/50 mixture of Lubriseal and MoS_2 was used to lubricate the stud threads and the nut collars.

For the 8-inch assemblies, two-piece ring heaters were clamped to the tubular portion of the connectors. The use of electrical heaters would have been difficult for the 16-inch connector because of the number of heaters required for the large area, and because of the large thermal gradients that would have been caused by the rapid loss of heat from the highly conductive aluminum. The procedure used for heating the 16-inch assembly consisted of submerging the entire vacuum-chamber-enclosed-connector assembly in a tank of water kept at 200 F. The assembly was cooled by raising it out of the tank and allowing it to air cool.

In each proof-pressure test, the connector was pressurized with helium initially to 1-1/2 times the maximum operating pressure at ambient temperature for 30 minutes. The pressure was then decreased to about 10 psi and the temperature of the connector was raised to 200 F. The pressure was then raised again to 1-1/2 times the maximum operating pressure and both temperature and pressure were maintained for 30 minutes.

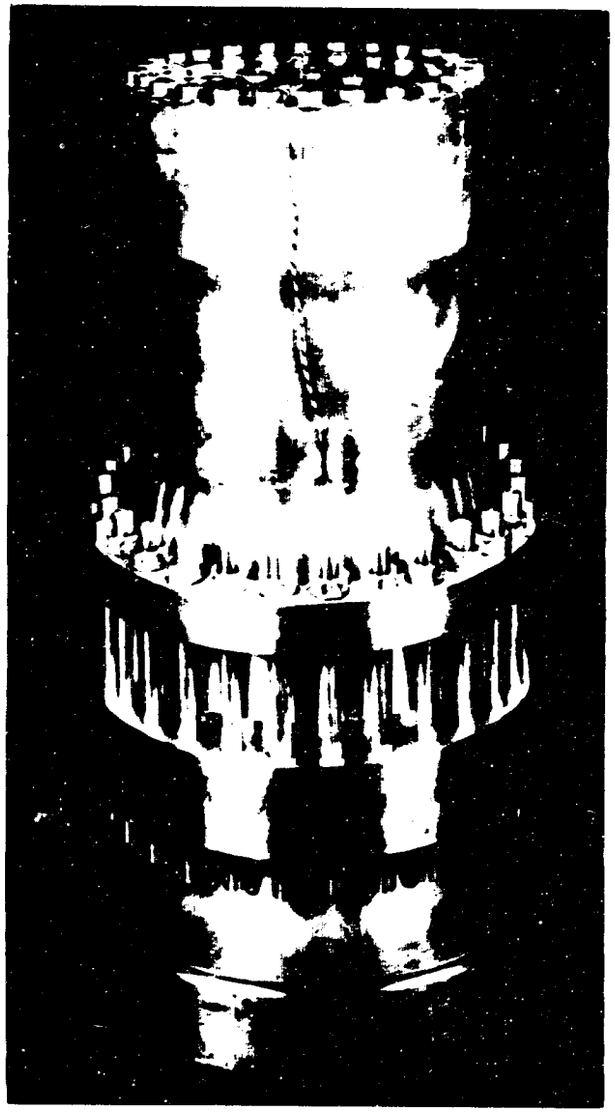

46523

FIGURE 84. 8-INCH, 15,000-PSI ALUMINUM TEST ASSEMBLY

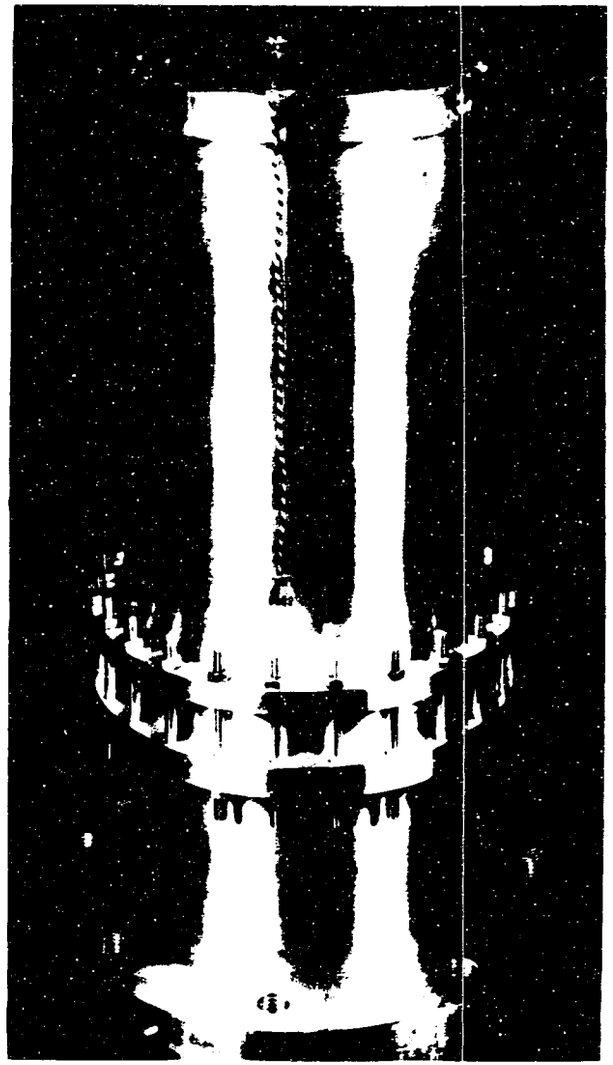

46524

FIGURE 85. 8-INCH, 100-PSI ALUMINUM TEST ASSEMBLY

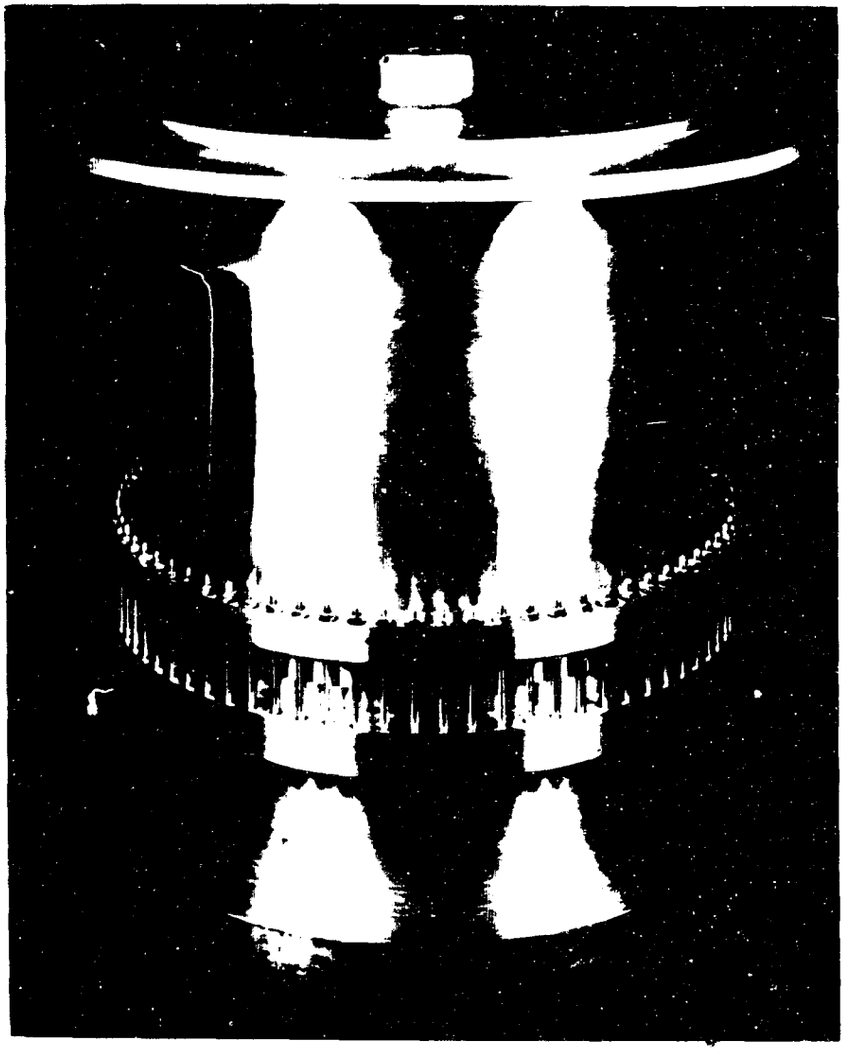

46522

FIGURE 86. 16-INCH, 100-PSI ALUMINUM TEST ASSEMBLY

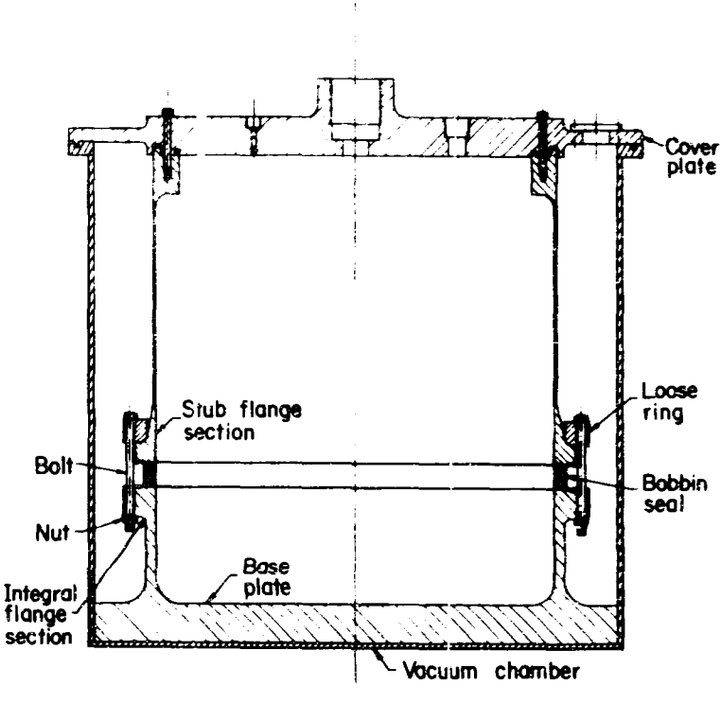

FIGURE 87. CROSS SECTION OF 16-INCH, 100-PSI, ALUMINUM TEST ASSEMBLY

The pressure was then reduced to approximately 10 psi, the connector was cooled to room temperature, and the pressure was raised again to the proof pressure for 15 minutes. The leakage of the connectors was monitored continuously by a helium mass spectrometer.

Test Results. No helium leakage could be detected during the proof pressure test of either the 8-inch, 100-psi connector, or the 8-inch, 1500-psi connector.

The measurement of an accurate leak rate was not possible for the 16-inch connector because considerable helium entered the vacuum chamber through the 16-inch and 22-inch elastomeric O-rings that were used to seal the tube closure. Approximately 2 hours were required to heat the connector assembly. Although two O-rings were used in series to separate the helium in the connector from the vacuum chamber, the helium permeation rate of O-rings increases rapidly with temperature and time (for the first 4 hours). (For instance, the measured permeation rate of helium through a 15-inch O-ring after 2 hours at 176 F was 3×10^{-6} atm cc/sec.) The second O-ring reduced the flow of helium into the connector considerably, but the second O-ring tended to saturate with helium and act as an accumulator. This provided a flow of helium into the vacuum chamber that was fairly high and out of phase with the heating and cooling cycle.

Consideration was given to welding the closure in place. However, the welded closure would have greatly increased the costs of the subsequent tests. Therefore, the decision was made to determine the proof-pressure leakage characteristics of the connector by two measurements: (1) a room-temperature measurement with 150-psi internal pressure, and (2) an estimate of the amount of helium entering the vacuum chamber in addition to the leakage measured from the O-ring.

No leakage could be detected at room temperature with 150-psi internal pressure. During eight heating and cooling cycles conducted over a 6-day period, no leakage could be detected as resulting from the Bobbin seal. During these heating and cooling cycles, variations in helium pressure and variations in time were used in an attempt to produce a helium reading that could be differentiated from the slowly fluctuating flow of helium from the O-ring. These variations provided a good measure of the response of the O-ring installation so that good confidence was achieved that no measurable helium was being supplied to the vacuum chamber of the Bobbin seal.

Test 2. Thermal Gradient

Test Procedures. With the 3-inch connectors it was possible to maintain maximum working pressure in the connectors and maximum helium pressure on the primary seal while the connectors were cycled between the temperature extremes. The large size of the 8- and 16-inch connectors prevented this method of operation because the pressurized liquid-nitrogen reservoir could not supply sufficient liquid nitrogen. Therefore, the test procedure was modified for the large connectors.

The procedure for the 8-inch connectors consisted of filling the internal volume of each connector as rapidly as possible with liquid nitrogen at atmospheric pressure. When an equilibrium temperature had been reached, the liquid-nitrogen supply was cut off and the connector was pressurized with helium to the maximum working pressure.

Although the gas inside the connector was not pure helium, it was believed that the percentage was sufficiently high that the test results would be acceptable. The pressure was held for 30 minutes and the temperatures were recorded. The temperature of the connector was then raised to 200 F for 30 minutes while the pressure was maintained at the maximum working pressure. The connector was then cooled to room temperature and after 15 minutes the connector pressure was reduced to ambient, and another cooling cycle was started.

The procedure used for the 16-inch connector was similar, but the connector was not heated to 200 F because of the O-ring permeation problem described under Test 1. Instead, the connector was allowed to return to room temperature overnight.

Test Results. Four thermal-gradient cycles were conducted for each 8-inch connector. No helium leakage could be detected during any of the cycles for either connector. Table 56 shows the temperatures measured for the major components of the 8-inch, 1500-psi connector. The tube did not reach a low temperature because the level of liquid nitrogen was raised only enough to cover the connector area. On the 8-inch, 100-psi connector, only the integral flange and tube thermocouples were operating and these read -270 F and -10 F, respectively, for each run. The test of the 8-inch, 100-psi connector was judged to be valid, however, because it was known that the thermal gradients were smaller in the 100-psi connector than in the heavier, 1500-psi connector.

TABLE 56. TEMPERATURES OF MAJOR COMPONENTS OF 8-INCH, 1500-PSI ALUMINUM CONNECTOR

	Temperature, F			
Test	Loose Ring	Integral Flange	Stud	Tube
1	-121	-252	-25	-10
2	-125	-260	-30	-12
3	-112	-252	-13	0
4	-112	-267	-15	-05

Three thermal-gradient cycles were completed on the 16-inch connector. In each cycle the connector was cooled from room temperature to -265 F in approximately 4 hours, and the connector was pressurized with helium for 45 minutes. No helium leakage could be detected during any of the three cycles. This test was judged to be valid because the eight heating cycles conducted under Test 1 were believed to have amply demonstrated the sealing capability of the connector at 200 F.

Test 4. Pressure Impulse

Test Procedures. As mentioned previously, the successful vibration test of the 8-inch, 100-psi connector (see page 124) resulted in the decision to subject the 8-inch 1500-psi connector to a pressure-impulse fatigue test instead of a vibration fatigue test. Thus, pressure impulse tests were conducted on the 8-inch, 1500-psi assembly and on the 16-inch, 100-psi assembly.

The test procedures were similar to those used for the 3-inch connectors. Because of the large volume of the connectors it was not possible to use the oil/alcohol separator and oil was pumped directly into the connectors. The equipment shown schematically in Figure 81 was used to create approximately 40 pressure cycles per minute. Figures 88 and 89 show the traces for the 8-inch and the 16-inch connectors. Although it was not possible to obtain pressure dwell in the 16-inch connector, it was believed that the effect of the pressure peaks was satisfactory. During the testing, each connector was placed in a container and a fluid-level switch was arranged to shut off the equipment upon a leakage of approximately 1 pint of oil.

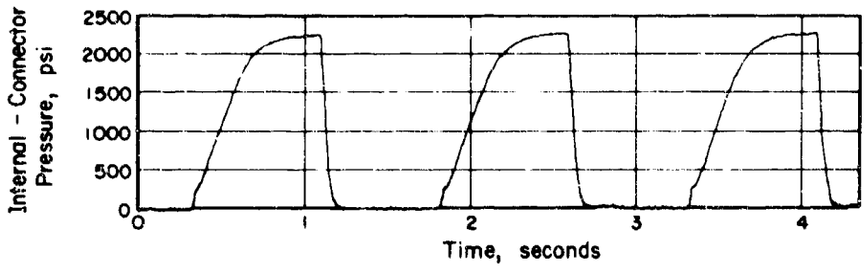

FIGURE 88. PRESSURE CYCLES MEASURED FOR 8-INCH, 1500-PSI CONNECTOR

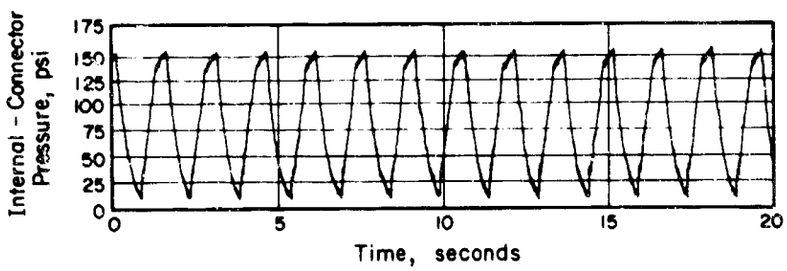

FIGURE 89. PRESSURE CYCLES MEASURED FOR 16-INCH, 100-PSI CONNECTOR

Test Results. Although the pressure-impulse test of the 8-inch, 1500-psi connector was eventually completed successfully, considerable difficulty was encountered with failure in different parts of the assembly. Each of these is discussed briefly.

Following initiation of the pressure-impulse test, the test was automatically terminated after 14,694 cycles when one of the seal disks sheared at the juncture with the tang over a length of about 1/2 inch. This failure came as a surprise because the seal disks for the 3-inch, 1500-psi connector had essentially the same cross section and yet the 3-inch connector did not fail during 200,000 pressure-impulse cycles. A Zyglow examination of the 8-inch seal showed extensive cracking along much of the base of both seal disks, showing conclusively that the seal was under strength. A Zyglow examination of the 3-inch seal also showed two significant cracks about 3 inches long in the same area, indicating that the 3-inch seal disk was also under strength. On the basis of beam-strength approximations, new seals for the 8-inch, 1500-psi connector were machined with seal disk widths of 0.060 inch rather than the initial 0.040 inch.

During the replacement of the Bobbin seal, it was also found that the tongue-in-groove seal housing for the O-ring seal on the end closure had developed fatigue cracks because of the flexing of the flat end closure. The tongue was machined off and the groove was modified to form a simple face seal.

The connector was reassembled with a modified seal and given a successful proof-pressure test. The next failure occurred after an additional 16,890 cycles when two of the high-strength socket-head cap screws on the end closure failed and the O-ring extruded through the gap which was created at the face seal. It was apparent that the flexure of the end closure had to be reduced to reduce the bending loads on the end-closure bolts. This was accomplished by placing an O-ring sealed piston on the inside of the connector against the end closure. A raised ring near the OD of the piston was used to prevent high forces from being applied at the center of the end closure.

The next failure occurred after an additional 20,964 cycles (52,548 total cycles) when the base component cracked. The base had been designed to simulate a flanged opening in a component, such as a pump, and the cylindrical wall and the bottom of the base had been made extra strong because the base was expected to be used for other tests. Despite this precaution, however, the high-pressure end load (approximately 120,000 pounds) caused excessive flexure of the flat bottom of the base, and a fatigue crack developed at the juncture of the base bottom and the cylindrical wall. There was no indication that the failure was associated with the part of the base representing the integral flange. A new base was fabricated with increased thickness and radii at the tube-to-base juncture.

The connector was reassembled with the new base component and with a modified seal, and a proof-pressure test was conducted successfully. After 38,704 cycles, 14 end-closure bolts failed in fatigue (59,668 cycles on these bolts). Although minor damage was done to the piston, it was possible to reassemble the end closure with a special grade of high-strength cap screws and the test was continued.

After an additional 40,400 cycles, the tubular portion of the stub flange developed an axial crack about 6 inches from the stub flange. At this point, a total of 131,652 pressure-impulse cycles had been imposed on the connector. The acceptable conditions stated for this test did not include failure of the tube. However, the stress-reversal bending test does include the concept that the test is successful if the connector is demonstrated to be stronger than the adjacent tubing. Because both of these tests are fatigue tests, it was judged that the pressure-impulse test of the 8-inch, 1500-psi aluminum connector was successful in that the connector was shown to be stronger in fatigue than the adjacent tubing.

For the pressure-impulse test of the 16-inch, 100-psi connector, two precautions were taken to prevent nonconnector failures similar to those described for the 8-inch, 1500-psi assembly. First, the base was clamped at the periphery to a laboratory mounting pad to prevent excessive deflection of the large flat area of the base. Second, two pistons were machined with raised rings near the outside diameters, and the pistons were placed in the connector one behind the other, against the tube end closure to prevent excessive deflection of the flat end closure. The test was stopped after 1,223,500 cycles. No failures had occurred in any of the parts of the connector-simulation assembly, and no evidence of leakage or material yielding could be detected.

The calculated stress in the tubing wall of the 8-inch, 1500-psi connector was 27,500 psi. The calculated stress for the tube wall of the 16-inch, 100-psi connector was 18,000 psi. The difference in the stresses for the two connectors resulted from the need to increase the calculated minimum wall thickness of the 16-inch connector for machining purposes. Since most of the connectors would be designed to the higher stress value, it was obvious that the allowable stress in the tubing would have to be lowered to assure a minimum fatigue life of 200,000 pressure-impulse cycles.

Test 5. Vibration

Because of the premature failure experienced at the tube-to-transition during the vibration testing of the 3-inch aluminum connectors, it was believed that a similar failure would probably be experienced in the 8-inch connectors. In fact, a follow-on program (Contract No. FO4611-69-C-0028) was initiated to include the vibration testing of additional 8-inch connectors. When exceptionally long fatigue life was obtained during the vibration testing of the 8-inch, 100-psi connector, the planned vibration test of the 8-inch 1500-psi connector was replaced with a pressure-impulse test.

Test Procedures. The 8-inch, 100-psi assembly was bolted in an upright position to the laboratory mounting pad used for the Calidyne machine. Strain gages had been mounted on the stub flange. One pair of gages was located at the tube-to-hub transition, while another pair of gages was located 1/2 inch from the transition on the tubular portion of the stub flange. (The strain gages were calibrated before the test with the assembly mounted in a horizontal position. The strain at the transition was approximately twice the strain in the tubular portion.)

Calculations indicated that a pipe extension would have to be fastened to the end closure of the stub flange to reduce the natural frequency of the assembly to 160 cps. A 9-1/2-inch length of 6-inch steel pipe with a 3/16-inch wall was equipped with a flange which was then fastened to the end closure. The extension was then struck a sharp blow and a recording of the strain reaction at the strain gages showed a natural frequency of the assembly of 136 cps. This was judged to be acceptable, and the Calidyne machine was attached to the flange of the pipe extension by a horizontal bolt. The instrumentation used to monitor the test was the same as that used for the 3-inch connectors.

Test Results. It was decided to vibrate the 8-inch connector initially at a low stress level, at room temperature, and unpressurized. A bending moment of 13,400 in-lb was imposed for 603,740 cycles. This produced a measured strain corresponding to a stress of 11,000 psi at the tube-to-hub transition. When no damage at this stress level could be detected, the design bending moment of 18,000 in-lb was imposed for approximately 2.8×10^6 cycles. This produced a stress of 14,800 psi at the tube-to-hub transition. Following this test, the connector was pressurized with 100-psi helium for 1 hour and no helium leakage could be detected by the mass spectrometer.

Consideration of the unexpected success of the 8-inch vibration test resulted in the thought that the following test conditions might have contributed to the test results: (1) the 8-inch connector was tested at room temperature, while the 3-inch connector was tested at 200 F, and (2) the 8-inch connector was unpressurized, while the 3-inch

connector was pressurized with water. To determine whether these different test conditions were responsible for the different test results, the 8-inch connector was vibrated again, but the connector was heated to 200 F and pressurized with water to 100 psi.

The second test was conducted at the design bending moment for 3 hours, during which time the connector was subjected to approximately 1 million cycles. When no failure occurred during this test either, despite the previous fatigue cycles, it was concluded that a size effect existed between the 3- and 8-inch connector, and the stress raiser which existed in the 3-inch connector did not exist in the 8-inch connector.

Test 6. Repeated Assembly

Test Procedures. The repeated-assembly test on the 3-inch connector consisted of 25 assemblies. No appreciable wear or damage could be noted in either flange cavity. Because the radial seal loading was designed to be the same for the 8-inch seals as for the 3-inch seals, it was decided that six assemblies of the 8-inch, 1500-psi connector would be sufficient provided no leakage was encountered, and no damage was caused to the flange cavities. Because of the large size of the seals, and the test time and helium required for each test, this change in procedure was expected to reduce test costs appreciably.

In each test, twenty-eight 1/2-inch studs were torqued to 500 in-lb and the connector was pressurized to 1500-psi with helium for 1 hour, while the leak rate was monitored by the mass spectrometer.

Test Results. No helium leakage could be detected during any of the six repeated-assembly tests. After the tests, no damage could be detected on either flange sealing surface.

Test 7. Misalignment

Test Procedures. The purpose of this misalignment test was to determine the sealing capability of the connector when it is subjected to a combination of axial and angular misalignment which results in a specific bending moment at the seal. It was decided that the test of the 8-inch, 1500-psi connector would be the most stringent for the large connectors. The bending moment required for this connector was one-half the tube bending moment of 79,860 in-lb required for the stress-reversal-bending test.

A test fixture was fabricated to allow horizontal mounting of the test assembly to withstand the bending moment. A 15.5-ft-long 6-inch steel pipe with a 3/16-inch wall was then bolted to the stub flange closure. Supports were fabricated to allow angular positioning of the stub flange against the integral flange so a Bobbin seal would just be contained inside the seal cavities of both flanges. The resulting angular misalignment between the faces of both flanges was approximately 1 degree. Supports were placed at the stub flange and at the end of the pipe extension. The bending moment at the Bobbin

seal supplied by the pipe alone was 20,200 in-lb. A 102-pound weight was placed 197 inches from the Bobbin seal to produce another 20,200 in-lb, making a total bending moment of 40,400 in-lb.

The seal was assembled into the connector and the nuts were snugged down finger-tight. The nuts were then tightened with progressively increasing torque in a stud-to-stud sequence until each nut had been tightened with a 500 in-lb torque. During the torquing procedure the pipe was raised from its supports due to the flange faces becoming parallel. Thus, for the better part of the torquing procedure, the full moment was applied to the connector, simulating the most stringent misalignment condition. When the full torque was achieved, the flange faces were parallel.

A second seal was assembled at the same angle of misalignment. In this case, however, a 235-lb weight was used at a distance of 11 feet from the seal. The pipe length was modified to give a lower moment, and the total moment applied to the connector was 40,200 in-lb. All other procedural steps were the same as those used during the assembly of the first seal. The second test was conducted to give a higher shear loading at the seal.

Test Results. Each of the misalignment tests was concluded by pressurizing the connector with 1500-psi helium while maintaining the full bending moment on the connector. For each assembly, no leakage rate could be detected by the helium mass spectrometer.

Test 8. Tightening Allowance

Test Procedures. The test procedures used for this test were essentially the same as those used for the 3-inch connectors. After the nut faces and stud threads were lubricated with a 50/50 mixture of Lubriseal and MoS_2, the connectors were assembled with the recommended torque – 60 in-lb for the 8- and 16-inch, 100-psi connectors (each connector utilized 1/4-inch studs), and 500 in-lb for the 8-inch, 1500-psi connector. The measurements shown in Figure 83 were then made. Each connector was then tightened with the additional torque increments of 10 percent and additional measurements were made until some form of material yielding was detected.

Test Results. As with the 3-inch connectors, the limitation in overtorque was established by failure of the studs. This is believed to be the most desirable form of limitation because the studs can be replaced if excessive torque is applied. The 1/4-inch studs of the 16-inch connector began to fail between 30 and 40 percent overtorque, while the 1/4-inch studs of the 8-inch, 100-psi connector began to fail between 60 and 70 percent overtorque. This appeared to be caused by the fact that the loose ring of the 8-inch connector angled more than the loose ring of the 16-inch connector and bound against the studs, delaying stud failure. A somewhat similar action had been encountered in the 3-inch connectors. The 8-inch, 1500-psi connector exhibited bolt failure in the overtorque increment above 20 percent.

The degree of overtorque provided by the large aluminum connectors was not as great as had been expected. However, the provision of increased bolt strength would result in a significant increase in connector weight unless a higher strength bolt material were used. It was decided that the specifications would include the allowable torque limits to prevent overtorque of the bolts during connector assembly.

Extra Test – Burst

A burst test was not scheduled for any connector under Contract AF 04(611)-11204 because the other tests, in particular the pressure-impulse test, were believed to demonstrate the required strength of the connectors. However, with the successful completion of the 16-inch pressure-impulse test, it was decided that a burst test of this connector would be desirable. Aluminum connectors are more likely to fail in burst than stainless steel connectors because the yield strength of aluminum is much closer to its ultimate strength than is the case for stainless steel, and aluminum does not strain harden during yielding as does stainless steel. Further, as mentioned above, the wall thickness of the 16-inch connector was greater in relation to the maximum pressure requirements than is the case for higher pressure aluminum connectors. Thus, a burst test of this connector-simulation assembly was expected to be a stringent test of the connector design.

The 16-inch, 100-psi connector burst with an internal pressure of 490 psi. The rupture occurred in the middle of the machined tubing section (see Figure 86) – the area of highest stress. Despite an internal pressure of about 5 times the maximum operating pressure of the connector, no yielding of the connector parts could be detected, and no leakage of the oil was apparent. This test was believed to be an impressive demonstration of the aluminum-connector-design parameters relating to strength.

Qualification Testing of Large, Stainless Steel Connectors

The applicability of the computerized procedure for designing large stainless steel flanged connectors was to be demonstrated by the fabrication and test of connectors for 8- and 16-inch tubing systems. At the same time that the schedule of tests was revised for the large aluminum connectors the schedule of tests for the large stainless steel connectors was also revised. However, in addition to substituting an 8-inch, 100-psi connector for a 16-inch, 1500-psi connector, it was also decided that a 16-inch, 100-psi stainless steel connector need not be fabricated and tested. This decision was based on the belief that the 16-inch, 100-psi aluminum connector would demonstrate the suitability of the design procedure for large, low-pressure connectors. The revised test schedule for the large stainless steel connectors is shown in Table 57.

TABLE 57. REVISED TEST SCHEDULE FOR LARGE STAINLESS STEEL CONNECTORS

Tube OD, in.	Max Operating Pressure, psi	Tests	Assembly Type
8	1500	1, 2, 5, 7, 8	Integral/Loose ring
8	100	1, 2, 5, 8	Integral/Loose ring

It will be noted that neither the original test schedule nor the revised test schedule included a repeated-assembly test. This decision was based on the belief that early, successful tests with the stainless steel seals in the threaded connectors indicated few, if any, problems with stainless steel seals. Thus it was expected that the tests with the 3-inch stainless steel seals would be a sufficient check on the design principles for stainless steel seals for flanged connectors. This was an unfortunate decision. Not only were some problems encountered with the 3-inch seals, as described previously, but the increased use of the stainless steel threaded connectors revealed a sealing reliability problem with 3/4- and 1-inch seals. In addition, extensive problems were encountered with the sealing of the 8-inch, 1500-psi stainless steel flanged connector in the final months of the program. As a result, it was necessary to recommend an overrun effort to investigate the performance of the stainless steel seals in more detail. The uncompleted tests (No. 8 for the 100-psi connector and Nos. 5, 7, and 8 for the 8-inch, 1500-psi connector) would be included in an overrun effort and the test results reported in a supplemental report to this document.

Test 1. Proof Pressure

Test Procedures. The 100- and 1500-psi stainless steel test assemblies had the same configuration as the 8-inch, 1500-psi aluminum test assembly shown in Figure 84. One difference was that the stub-flange tubing extension component consisted of a piece of tubing welded to the steel flange. This design made large stainless steel forgings unnecessary.

The proof-pressure test procedures described previously for the 8-inch aluminum assemblies were used to conduct Test 1 for both 8-inch stainless steel assemblies. A torque of 100 in-lb was applied to the twenty 1/4-in. A286 studs of the 100-psi connector, while a torque of 372 in-lb was applied to the thirty-four 3/8-inch A286 bolts of the 1500-psi connector. The lubrication procedure was the same as described for previous assemblies.

Test Results. No leakage could be detected during the proof-pressure test of the 8-inch, 100-psi connector. The proof-pressure test of the 8-inch, 1500-psi connector proved to be a significant obstacle in the test program. In addition to equipment problems, a design problem was revealed for the Bobbin seal. The primary aspects of these problems are summarized.

Attempts to proof-pressure the 8-inch, 1500-psi connector were unsuccessful with two different seals. An examination of the coined nickel surface of the seals at first seemed to indicate insufficient radial sealing force. However, a hardness check of the nickel plating showed that the nickel plating had not been annealed. This had happened twice during the development of the stainless steel seals for threaded connectors, and its reoccurrence emphasized the need for careful control of the fabrication steps of the stainless steel Bobbin seals. Unfortunately, annealed nickel plating looks the same as unannealed plating.

The proof-pressure test with the first annealed seal showed a minor increase in leakage as the connector was heated to 200 F. When the connector was cooled to ambient, the helium leakage increased to about 3×10^{-7} atm cc/sec per inch of seal circumference.

Because this leakage was beyond the allowable amount, the test was terminated. An examination of the nickel on the seal showed a smaller than normal coined surface, indicating too low a radial sealing force. In addition, a closer inspection of the general condition of the plating indicated a poorer quality of plating than that obtained on the 3-inch stainless steel seals.

To obtain a better idea of the effect of the reduced quality of the nickel plating, three annealed seals that were slightly oversized were given a light machining cut to produce a smooth nickel surface that fitted snugly in the connector flanges. Three proof-pressure cycles were conducted with one of these seals. During the first cycle, no leakage could be detected. During the second cycle, the helium leakage at 200 F was approximately 5×10^{-8} atm cc/sec per inch of seal circumference, and at ambient temperature the leakage increased to about 2×10^{-7} atm cc/sec. The test was terminated when the leakage at 200 F during the thermal cycle was 1.5×10^{-7} atm cc/sec of helium per inch of seal circumference. Although the leakage values obtained were still within the allowable amount, the increasing nature of the leakage, despite the special machining, indicated that the seal was not satisfactory.

Because sealing problems resulting from insufficient sealing load had developed with the stainless steel threaded connectors, and because a relatively small surface was coined on the 8-inch seal, it was decided that an increased radial sealing force was required. This was obtained for the 8-inch, 1500-psi connector by doubling the length of the seal tang. Calculations indicated that this would increase the radial sealing face from about 750 lb/in. of seal circumference to about 1300 lb/in. While new seals were being fabricated, a reinforcing ring was made to fit inside the tang of an original seal to increase the radial sealing load of that configuration to about 1300 lb/in. This technique made possible an interim test of the higher sealing load. Tests with this seal were somewhat uncertain because of problems that developed with the O-ring seal on the vacuum chamber. However, after several proof-pressure cycles similar to those conducted for the 16-inch aluminum connector, no significant leakage could be detected from the Bobbin seal.

Test 2. Thermal Gradient

Test Procedures. Two series of thermal-gradient tests were conducted with the 8-inch, 100-psi connector. The first series was conducted with the same procedures described previously for the 8-inch aluminum connectors. The second series was conducted in a similar manner except that the connector was not placed in a vacuum chamber. Instead, a small probe was used with the helium mass spectrometer to "sniff" for helium leakage along the circumference of each disk of the Bobbin seal. While this procedure cannot be used to measure the rate of a helium leak, it is a good "go-no-go" indication of the presence of a helium leak. The latter procedure was used also for all of the tests with the 8-inch, 1500-psi stainless steel connector.

Test Results. During the first series of tests, three thermal-gradient cycles were conducted with the 8-inch, 100-psi connector. The maximum measured helium leakage during these cycles was 1.2×10^{-9} atm cc/sec per inch of seal circumference. When the thermal-gradient tests with the 8-inch, 1500-psi connector encountered considerable difficulty, the 8-inch, 100-psi connector was reassembled with another seal,

and six thermal-gradient cycles were conducted in a second series of tests. No evidence of leakage could be detected by the helium probe during these tests. A thermocouple attached to the integral flange of the connector showed that the stabilized cold temperature reached during both series of tests was between -315 and -300 F.

Because of the problems encountered with the vacuum chamber during the successful proof-pressure test with the reinforced seal for the 8-inch, 1500-psi connector, it was decided that the first thermal-gradient test would be conducted without the vacuum chamber. The helium probe showed that this seal leaked excessively on the first cold cycle. On the assumption that this leakage was caused by improper action of the reinforced seal, the connector was disassembled and reassembled with one of the modified seals that had then been fabricated.

Although no leakage could be detected during the hot portion of the thermal-gradient cycle, some leakage was evident during the first cold cycle. This leakage increased noticeably during the second cold cycle, and during the third cold cycle it was obvious that the leakage was excessive. When the connector was disassembled, an examination of the Bobbin seal and the lower connector flange showed that several small pieces of copper had gotten into the flange cavity and prevented proper seating of the seal. The connector was then reassembled with a second modified seal.

No leakage could be detected during the first cold cycle with the second modified seal. However, definite leakage could be detected during the second cycle, and two locations of excessive leakage were identified during the third cold cycle. When the connector was disassembled and the seal was examined, two flaws could be seen at the sources of leakage. One appeared to be caused by material left in the flange cavity, while the other appeared to be a crack in the nickel plating.

At this point a careful inspection was made with a 10-power glass of the sealing surfaces of all of the used and unused seals. It was apparent that several of the unused, modified seals had flaws which made sealing questionable. It was also apparent that the 1300 lb/in. sealing force of the modified seals was still not enough to create a consistently shiny coined sealing surface. The lack of consistency seemed to be associated with the effect of the reverse taper of the seal on the sealing action as well as with variations in the nickel plating. With the decision that the sealing force was not sufficient to overcome the fabrication variations in the large seal, a reinforcing ring was made to fit inside the seal tang and to increase the radial sealing load by approximately 100 percent. A load ring was made for the seal, and an assembly with a reinforced, modified seal showed a radial load of 2800 lb/in. of seal circumference.

The modified seal with the best nickel plating was then equipped with a reinforcing ring and the connector was assembled with the expectation that a satisfactory thermal-gradient test would be achieved. Although the first cycle was conducted with no indication of leakage, leakage was again indicated during the second cycle, and by the fourth cycle excessive leakage was indicated over almost 180 degrees of the Bobbin seal.

With the failure of this test, it was apparent that the leakage was being caused by a factor other than an insufficient radial sealing load. During one of the earlier tests, the temperature of the seal tang and the integral flange was measured to determine whether differential radial expansion was causing the leakage. Calculations based on these measurements indicated that there was sufficient elasticity in the seal to maintain an adequate sealing load for the thermal gradients. However, a comparison of the

8-inch seal with the 3-inch seal and the 1-inch threaded seal showed that the 8-inch seal had less than half the compressive strain of the 3-inch seal, and less than one-fourth the compressive strain of the 1-inch seal. Even though some of the compressive strain in all the seals is in the plastic region, the austenitic stainless steel used in the seals is a strain-hardening material so that an increase in strain indicates some increase in elastic-recovery capability. Because the effective thermal-gradients in the connector structure can only be approximated, it was decided that one of the reinforced modified seals would be machined to produce longer sealing disks and provide more compressive strain in the seal. It was possible to make the disks twice as long in this approach, which made the compressive strain similar to that in the 3-inch seal.

A load test was first made with one of the modified seals machined with longer disks. Although the same size reinforcing ring was used as had been used on the previous modified seals, the material removed from the tang to produce the longer disks resulted in a measured radial load of 2200 lb/in. of seal circumference. This was judged to be adequate. A modified seal with good nickel plating was then machined with longer disks, a reinforcing ring was added, and the connector was reassembled with this seal. During seven thermal-gradient cycles, no leakage could be detected from the Bobbin seal; this indicated fairly conclusively that differential thermal expansion was the basic cause of leakage in the thermal-gradient test rather than insufficient radial load.

As described subsequently in this report, it also became apparent during this period of time that a radial sealing load of 1500 lb/in. of seal circumference was desirable for the 3/4- and 1-inch threaded-connector stainless steel seals. Because of the increased variations that are normally encountered in fabricating larger parts, and because of significantly increased chances of accidental damage to the sealing surfaces, an increase in radial sealing load for the 8-inch seals was desirable, in any case, even though insufficient radial load was probably not the cause of leakage in the experimental assembly. However, the increased mass required to achieve high radial sealing loads in the larger seals represented a design problem requiring further consideration.

Test 5. Vibration

Test Procedures. The procedures used to test the 8-inch, 100-psi aluminum connector in its final series were also used to test the 8-inch, 100-psi stainless steel connector. The design bending moment produced a stress at the tube-to-hub transition of 16,800 psi.

Test Results. Failure occurred in 372,000 cycles at the welded juncture of the stub flange and the extension piece of tubing. The welded joint was located approximately 4 inches from the stub flange and since it was in a lower stress zone than the connector, failure of the carefully made weld was not expected. Some thought was given to remaking the weld and continuing the test. However, the vibration tests of the 3-inch connectors showed that the stainless steel parts were much less susceptible to failure in vibration than the aluminum parts, and since the 8-inch, 100-psi aluminum connector had successfully withstood 1.0×10^6 vibration cycles, there seemed to be no need to obtain additional vibration cycles for the stainless steel connector.

Test 8. Tightening Allowance

Test Procedures. Because of the possible conduct of additional tests with the 8-inch, 100-psi and 8-inch, 1500-psi stainless steel connectors in an overrun effort, it was not possible to conduct a complete tightening-allowance test. The overtorque increments at each connector were stopped at 30 percent to prevent failure of the expensive A286 studs. However, the procedures up to this point were identical to those described for previous connectors. An initial torque of 100 in-lb was applied to the twenty 1/4-inch A286 studs of the 100-psi connector, while an initial torque of 372 in-lb was applied to the twenty-four 3/8-inch A286 bolts of the 1500-psi connector.

Test Results. No indication of yielding was obtained within the 30 percent overtorque limitation. As with previous connectors, failure was expected to occur first in the studs and bolts. Tests with the 3-inch stainless steel connector indicated that the 1/4-inch studs would fail with about 70 percent overtorque. Tests with individual bolts showed that the 3/8-inch bolts would fail with about 40 percent overtorque.

Test Summary

Aluminum Flanged Connectors

Test 1. Proof Pressure. The primary purpose of this test was to check the initial sealing capability and the strength of the connectors. Proof-pressure tests were conducted with the following connectors: 3-inch, 100-psi; 3-inch, 1500-psi; 8-inch, 100-psi; 8-inch, 1500-psi; and 16-inch, 100-psi. In the tests with the 3-inch connectors, the maximum helium leakage rate measured was 3.1×10^{-9} atm cc/sec per inch of seal circumference. No helium leakage could be measured during the tests with the large connectors. No yielding of any connector structure could be detected.

Test 2. Thermal Gradient. This test was conducted to determine the effect of maximum thermal gradients on connector sealing. Several thermal-gradient cycles were conducted with each of the assemblies used for the proof-pressure tests (see above). The maximum helium leakage rates measured for the 100- and 1500-psi, 3-inch connectors were, respectively, 1.8×10^{-9} and 1.2×10^{-8} atm cc/sec per inch of seal circumference. No helium leakage could be measured for any of the large connectors.

Test 3. Stress-Reversal Bending. This test was one of three fatigue tests used during the course of the program. Stress-reversal-bending tests were conducted with the 100- and 1500-psi, 3-inch connectors. Although both assemblies lasted the required 200,000 cycles, failures occurred in the tubing portions of both assemblies before 250,000 cycles had been completed. The maximum helium leakage measured during these tests was 1.5×10^{-9} atm cc/sec per inch of seal circumference.

Test 4. Pressure Impulse. Pressure-impulse tests, another type of fatigue test, were conducted with a 3-inch, 1500-psi assembly, an 8-inch, 1500-psi assembly, and a 16-inch, 100-psi assembly. The 3-inch assembly used for this test was not the same assembly as was used for the stress-reversal bending test. Although the 3-inch assembly withstood the required 200,000 cycles satisfactorily, substantial cracking was subsequently found at the base of the seal disks. The 8-inch seal failed at the base of a seal disk after approximately 14,700 cycles. Modified seals were machined with the width of the seal disks increased 50 percent. This type of seal showed no cracking after approximately 80,000 cycles. After several miscellaneous equipment failures, the tubular portion of the 8-inch stub flange component failed after approximately 130,000 cycles. The connector was judged to be satisfactory. No failures occurred in the 16-inch assembly after 1.2×10^6 cycles.

Test 5. Vibration. Vibration tests, the third type of fatigue test, were conducted with three 3-inch, 1500-psi assemblies, and an 8-inch, 100-psi assembly. The first 3-inch assembly failed at the base of the integral flange after only about 50,000 cycles with approximately one-half the required bending moment. The second 3-inch assembly, with strengthened connector hubs, failed at a bulkhead in the tubing portion of the assembly after about 28,000 cycles under the required test conditions. The third assembly, with modified tubing sections, failed after 53,000 cycles at the tube-to-transition section under the required test conditions. In the second and third assemblies, failures occurred in a far shorter time than was indicated by the strain measured by carefully calibrated strain gages placed on the connectors. In contrast, the 8-inch connector withstood 1.0×10^6 vibration cycles under the required test conditions without failure.

Test 6. Repeated Assembly. Because of the high sealing forces needed to seal helium, repeated-assembly tests were conducted to determine whether repeated connector assembly caused damage to the connector flanges. Twenty-five reassemblies were conducted with a 3-inch, 1500-psi connector, and six reassemblies were conducted with an 8-inch, 1500-psi assembly. The maximum helium leakage measured for the 3-inch tests was 0.97×10^9 atm cc/sec per inch of seal circumference, while no leakage could be measured during the 8-inch tests. No damage could be detected on any connector flange after the tests.

Test 7. Misalignment. A misalignment test was established to demonstrate that a connector could be assembled satisfactorily under a certain amount of misalignment. The test was conducted with a 3-inch, 1500-psi assembly, and an 8-inch, 1500-psi assembly. The 3-inch connector was assembled satisfactorily at angles of 1, 2, and 3 degrees and no helium leakage could be measured after these assemblies. The 8-inch connector was assembled satisfactorily twice with a 1-degree angle of misalignment, and no helium leakage could be measured after either assembly. It was estimated that these angles represented realistic conditions for the two connector sizes.

Test 8. Tightening Allowance. The final test of each connector assembly consisted of tightening the studs in increments of 10 percent over the maximum torque until yielding was detected. For the 100-psi and 1500-psi, 3-inch connectors, an overtorque of 40 and 50 percent, respectively, was accomplished satisfactorily. The studs then

began to yield in the next increment of overtorque. For the 100-psi, 8- and 16-inch connectors and for the 8-inch, 1500-psi connector, the overtorque capability was 60, 30, and 20 percent, respectively. Differences in overtorque capability result from the step function by which the computerized design program selects the connector bolt sizes.

Extra Test – Burst. No burst test was scheduled for the contract. However, the unfailed 16-inch, 100-psi connector provided a good opportunity to evaluate the burst safety margin provided by the computerized design procedure. The tubing portion of the assembly burst at a pressure of 490 psi. No deformation could be detected in the connector after the test.

Stainless Steel Flanged Connectors

The purpose of each of the eight standard tests is summarized briefly in the above summary of the aluminum connector tests.

Test 1. Proof Pressure. Proof-pressure tests were conducted with a 3-inch, 1500-psi assembly, two 3-inch, 4000-psi assemblies, an 8-inch, 100-psi assembly, and an 8-inch, 1500-psi assembly. The maximum helium leakage measured for the 3-inch, 1500-psi assembly was 1.5×10^{-8} atm cc/sec per inch of seal circumference. The first test with a 3-inch, 4000-psi, 600 F assembly resulted in excessive leakage at 600 F. A new seal was machined with an increase in the radial sealing load and no leakage could be detected during seven proof-pressure cycles. No helium leakage could be detected for the 3-inch, 4000-psi cryogenic assembly or for the 8-inch, 100-psi assembly. However, the proof-pressure test for two assemblies of the 8-inch, 1500-psi connector resulted in an excessive leakage. When a seal was modified to provide an increased sealing load, no leakage could be measured during the proof-pressure test. No yielding could be detected on any of the connectors as a result of the proof-pressure tests.

Test 2. Thermal Gradient. This test was conducted with each of the assemblies used for the proof-pressure test. The maximum helium leakage measured during six thermal-gradient cycles of the 3-inch, 1500-psi connector was 3.7×10^{-9} atm cc/sec per inch of seal circumference. The maximum leakage measured during six cycles of the 3-inch, 4000-psi, 600 F assembly was 6.7×10^{-9} atm cc/sec per inch of seal circumference, while the maximum leakage measured for the 3-inch, 4000-psi cryogenic connector was 3.3×10^{-8} atm cc/sec. A total of 10 thermal-gradient cycles were conducted on the 8-inch, 100-psi assembly with no detectable leakage. Considerable difficulty was encountered in the testing of the 8-inch, 1500-psi assembly. It was not until the length of the seal disks and the radial sealing load were increased that seven thermal-gradient cycles were conducted without an indication of helium leakage.

Test 3. Stress-Reversal Bending. Stress-reversal-bending tests were conducted with a 3-inch, 1500-psi assembly and a 3-inch, 4000-psi, 600 F assembly. The 3-inch, 1500-psi assembly withstood approximately 350,000 cycles without failure, and the 3-inch, 4000-psi assembly withstood approximately 200,000 cycles without failure. The

maximum helium leakage measured for the 3-inch, 1500-psi assembly was 1.4×10^{-9} atm cc/sec per inch of seal circumference. No leakage could be measured during the test of the 3-inch, 4000-psi assembly.

Test 4. Pressure Impulse. Pressure-impulse tests were conducted with a 3-inch, 1500-psi assembly (different from the one used for the stress-reversal bending test) and a 3-inch, 4000-psi cryogenic assembly. The 1500-psi assembly withstood 200,000 cycles without failure and with no detectable leakage. The 4000-psi assembly withstood approximately 1.0×10^6 cycles without failure and without detectable leakage.

Test 5. Vibration. Vibration tests were conducted with a 3-inch, 1500-psi assembly, and an 8-inch, 100-psi assembly. The 3-inch assembly (which had been used for the pressure-impulse test) withstood 475,000 cycles without failure and without leakage. The 8-inch assembly failed after 372,000 cycles at the weld joint between the stub flange hub and the tube extension. No leakage could be detected during the test and the connector was judged to be satisfactory.

Test 6. Repeated Assembly. Twenty-five reassembly tests were conducted with a 3-inch, 1500-psi assembly. Four assemblies showed excessive leakage. At the time it was judged that the excessive leakage was caused by poor plating. However, on the basis of tests with other stainless steel seals, it subsequently appeared that these seals indicated insufficient radial sealing load.

Test 7. Misalignment. A misalignment test was conducted with a 3-inch, 1500-psi assembly. Assemblies were made at initial misalignment angles of 1, 2, and 3 degrees. No leakage could be detected after any assembly.

Test 8. Tightening Allowance. Tightening-allowance tests were conducted with the same assemblies as were used for the proof-pressure tests. The 3-inch, 1500-psi connector withstood 50 percent overtorque without yielding, while the 3-inch, 4000-psi assembly withstood 90 percent overtorque without yielding. The 8-inch, 100-psi assembly and the 8-inch, 1500-psi assembly were subjected to only a 30 percent overtorque because the assemblies and the fasterners were needed for work under another contract. Tests with individual fasterners showed that the 100-psi assembly would have withstood about 70 percent overtorque, while the 1500-psi assembly would have begun yielding with 40 percent overtorque.

Discussion of Critical Design Parameters

For the most part, the qualification tests verified the applicability of the computerized program for designing lightweight flanged connectors for aluminum and stainless steel tubing systems. As would be expected, the many design parameters and test conditions combined to produce several critical areas. Both the satisfactory and unsatisfactory critical areas are discussed briefly in relation to the major components of the aluminum and stainless steel connectors.

Aluminum Flanged Connectors

Bobbin Seal. The radial sealing load (750 lb/in. of seal circumference) selected for the aluminum Bobbin seal produced excellent initial sealing. The residual axial load (50 percent of the axial seating load) maintained excellent sealing during the performance tests. The use of overaged 6061-T6 aluminum as the seal material was entirely satisfactory.

Two problems were revealed for the Bobbin seal. First, the seal disks were too thin to pass the pressure-impulse test for 1500-psi systems. Second, calculations showed that the length of the seal disks was marginal for some connector sizes (particularly 8 and 16 inch) for providing sufficient elastic recovery for cryogenic thermal-gradients. (This condition was found to exist despite the successful thermal-gradient tests of the 8-inch connectors.)

For the specifications shown in Appendix C, the design of the seal disks was revised to overcome these difficulties. There is little doubt that the thermal-gradient problem has been corrected by a lengthening of the disks of selected seal sizes. However, the calculations for the seal disk thickness are approximations, and tests are needed to verify the pressure-impulse capability of the new length/thickness dimensions of the disks for 1500-psi seals for 8- and 16-inch systems. The revised seal design did not significantly change the low-pressure seals and only marginally changed the high-pressure 3-inch seals. Consequently these successful designs need not be retested.

Integral and Loose-Ring Flanges. The design of the flanges incorporates many stress calculations and assumptions. Although the performance of both types of flanges was excellent in most regards, one minor and two major problems were revealed in the test program. The minor problem was caused by the stress calculation for the thickness of the seal cavity lip for the stub flange providing insufficient material for machining tolerances for the large connectors. This has been corrected in the specifications.

A major problem resulted when the initial design program did not provide sufficient strength at the hub-to-flange joints. This problem was corrected early in the laboratory program and the revised design was shown to be satisfactory in the subsequent tests. The revised design has been included in the specifications. In the second major problem, the tubing wall selected for the high-pressure connectors was not sufficiently strong to provide a minimum of 200,000 pressure-impulse cycles. The calculation for the tubing wall thickness was revised, on the basis of considerable design data, and the specifications incorporate the revised calculation. Because of the importance of failure of the tubing, the adequacy of the calculation should be checked by additional pressure-impulse tests.

In addition to the stress-calculation revisions, consideration of the flange configurations during the laboratory program led to the decision to design the flanges with a slight tube extension so the tubing weld would not occur at the change in section provided by the tapered flange hub. This configuration has also been incorporated in the specifications.

Loose Ring. The loose ring represents a difficult design problem. While the loose ring tilted more for some test connectors than for others, the studs limited the degree of tilt to an acceptable value. Because of the relatively close fit of the studs in the holes of the loose ring, a considerable increase in the weight of the loose ring would be required to prevent any binding against the studs. The tilting of the loose ring did not adversely affect the assembly of any connectors within the required torque values, and the design basis for the loose ring was believed to be satisfactory.

Bolts, Studs, and Nuts. The performance of the aluminum studs and nuts was excellent in all cases. The adequacy of the design basis was particularly well demonstrated with the 8-inch, 1500-psi assembly in which high-strength steel socket-head screws and cap screws kept failing during the pressure-impulse test of the connector. There is little doubt that the use of aluminum studs and nuts poses problems. The threads are easily damaged in handling and the bearing surfaces have to be lubricated carefully to prevent galling. Further, the proximity of the yield strength of aluminum to its tensile strength seriously limits the overtorque capability of aluminum fasteners, requiring extra care to achieve the proper torque. However, calculations show that aluminum fasteners must be used if a lightweight aluminum connector is to maintain good sealing for cryogenic thermal gradients. By selecting 2024-T4 material, and by using standard machining practices, it is believed that practical aluminum fasteners have been designed.

General Comments. In reviewing the tests of aluminum connectors, there was evidence that each increase in connector size introduced unexpected problems. The 3-inch connector introduced vibration problems that had not been encountered with aluminum threaded connectors, and the 8-inch, 1500-psi connector introduced fatigue problems that had not been encountered with the 3-inch, 1500-psi connector. These problems seemed to result primarily from the unanticipated effects of high pressure on large surface areas, and on the tendency of aluminum to crack with overstressing rather than to yield and redistribute the stresses as stainless steel does. Because of these problems, it was concluded that the satisfactory performance of large (over 8 inch), 1000- and 1500-psi connectors remains in some question until they are built and tested. The dimensions for such connectors were included in the specifications, and it was believed that the chances are good that they would function satisfactorily. However, the connectors were not viewed with the same confidence as those that were within the limits of the connectors that were built and tested.

Stainless Steel Flanged Connectors

At the start of the program, the stainless steel connectors were expected to produce fewer problems than the aluminum connectors. This resulted primarily from the greater toughness of stainless steel than aluminum (as discussed above). Because of this expectation, the aluminum connectors in each size were scheduled to be tested before the stainless steel connectors. Unfortunately, in the latter stages of the laboratory program, major problems developed with the stainless steel seal for the 8-inch, 1500-psi connector. Although considerable progress was made toward the solution of these problems, it was not possible to demonstrate the adequacy of the solution for the large connector sizes. At the end of the program, a letter was forwarded,

recommending the investigation of adequate solutions to the large-diameter stainless steel seal problem and the conduct of the necessary tests to demonstrate these solutions.

Bobbin Seal. The dimensions selected for the stainless steel Bobbin seals were satisfactory in several respects. The disk thickness was satisfactory for the radial loading and for the pressure-impulse tests. (For instance, the 0.040-inch thick disk for the 3-inch, 4000-psi connector withstood 1,000,000 pressure-impulse cycles without any sign of fatigue damage.) Also, the residual axial seating loads were satisfactory for the various performance conditions.

The major seal problems that developed related to the radial sealing load or to the inability of the seal to accommodate the radial thermal gradients in the large, high-pressure connectors. The radial-sealing-load problem was found to exist in the 3/4- and 1-inch threaded connectors as well as in the flanged connectors. On the basis of work in both types of connectors, the design radial sealing load was increased from 750 lb/in. of seal circumference for all seals to 1200 lb/in. for 100, 200, and 500-psi connectors, and to 2500 lb/in. for pressures of 1000 psi and higher. These revised values were included in the specifications.

In conjunction with the radial sealing load problem, it was also found that the 8-inch seal did not provide sufficient elasticity for the thermal gradients caused by the heavy flanges for the 1500-psi connectors. Although a 16-inch, 1500-psi connector was not tested, the problem was shown by calculation to be even worse for this connector, and other large, high-pressure connectors were believed to have the same limitation. It was shown by the successful test of the 8-inch, 1500-psi connector that this problem could be corrected by increasing the length of the seal disks. Increased seal disk lengths were then selected for all large connectors and the thickness of the disks was increased to sustain the higher radial loading (2500 lb/in.). These revised dimensions were included in the specifications.

On basis of the qualification tests and on selected calculations, it was believed that the specification dimensions could be viewed with confidence for all connectors through 3 inches, and for 100-, 200-, and 500-psi connectors through 8 inches. However, for the 8-inch, 1500-psi connector, and for all connectors larger than 8 inches, selective tests were desirable to substantiate the revised seal design parameters. It was possible that the disk length in some of the larger, high-pressure connectors would have to be increased still further. If this became necessary, it was believed that a modified seal design should be used in which the disks were machined farther down into the seal tang, leaving some material between the disk sides.

Integral and Loose-Ring Flanges. The design basis for these connector components was found to be satisfactory in almost every respect. On the basis of the problems revealed by the aluminum flanges, the hub-to-flange joint was strengthened, the stub-flange seal cavity lip was increased for the larger sizes, and a tube extension was added to the tapered hub to remove the weld joint from the change in section at the tapered hub.

Loose Ring. The tilting of the loose ring that was encountered in the aluminum loose rings was even more pronounced in some of the stainless steel connectors. However, as with the aluminum connectors, the tilting did not seem to interfere with the normal assembly of the connectors, and the decision was made to leave the design unchanged.

Bolts, Studs, and Nuts. The performance of the A286 studs and nuts was excellent. No problems were encountered in the assembly of the fasteners or in the performance of the connectors, and ample overtorquing capability was demonstrated. The high cost of A286 fasteners and the long lead time often required to get the parts will undoubtedly be a problem for some time. However, the A286 fasteners have so many technical advantages that it is believed that no other fastener will offer serious competition within the foreseeable future.

IV

FLANGED-CONNECTOR MILITARY STANDARDS AND SPECIFICATIONS

The flanged connector military standards and specifications developed under Contract AF 04(611)-11204 are discussed in three sections: (1) background, (2) general standards and specifications characteristics, and (3) recommendations for flanged-connector military standards and specifications.

Background

Under Contract No. AF 04(611)-9578, military standards and specifications were prepared in draft form for AFRPL threaded connectors for 4000-psi stainless steel tubing systems and 1000- and 750-psi aluminum tubing systems. Specifically, the items prepared consisted of: (1) military standards containing assembly instructions and part drawings for typical connector configurations for six tubing sizes: 1/8, 1/4, 3/8, 1/2, 3/4, and 1 inch, (2) a military specification for the plating of soft nickel on stainless steel Bobbin seals, and (3) a military specification for the qualification of AFRPL fittings by prospective manufacturers. Although the preparation of these items required considerable effort, ample guidance was obtained from previous military documents concerning the appropriate format and necessary information.

At the beginning of Contract AF 04(611)-11204, it was mutually agreed that there was little precedence for determining the best form for military standards and specifications for flanged connectors. Flanged connectors for the aerospace industry are usually designed specifically for each system to insure minimum weight. On this basis, it appeared desirable to develop a computerized design procedure that could be used by aerospace designers to determine the dimensions of AFRPL flanged connectors for each aerospace system application.

While this general concept was attractive, further mutual consideration led to the conclusion that it was not practical as an Air Force procurement procedure. As the computer program was developed it became clear that a certain amount of engineering judgment would be required for the selection of input data and for the selection of optimum connector dimensions. If flanged connectors were obtained by the Air Force through use of the design procedure, no control could be exercised over these judgment points. Further, mistakes in the use of the computer program might not be revealed until late in the procurement cycle.

Attention was then directed toward the preparation of a large "steam table" of dimensions that would be sufficiently comprehensive that all foreseeable system requirements could be met closely by selection of the proper connector parts, either by the Air Force or by the contractor. While this approach had considerable merit, the large number of connector sizes and types made it very difficult to specify tolerances for dimensions and assembly torques. Also, there seemed to be a distinct possibility that the large number of connectors might include some combination of parts that would not perform properly under certain application requirements.

Late in Contract AF 04(611)-11204 it was decided that the best procurement procedure would be a combination of the two basic approaches. Military standards and specifications were to be prepared for the sizes and pressures mutually believed to be the most commonly used in the foreseeable future. By including the computer program for the design procedure in this report, it would also be possible for connector dimensions to be developed for special applications. Arrangements could be made between the Air Force and each contractor concerning the necessary steps for qualifying the design of each special connector.

General Characteristics of Flanged-Connector Military Standards and Specifications

It is anticipated that the military standards and specifications eventually prepared by the Air Force for flanged connectors will consist of three documents: (1) an assembly of military standards, (2) a military specification for soft nickel plating, and (3) a military specification for the requirements of fluid connectors. Each of these is discussed briefly.

Military Standards

Military Standards for AFRPL threaded connectors were issued as part of Procurement Specifications MIL-F-27417 (USAF). Five sheets (MS 27850) were prepared describing the proper assembly of the fitting. One sheet (MS 27851) showed the Military Standard numbers for each stainless steel connector assembly, while MS 27856 showed the numbers for each aluminum connector assembly. One sheet was then prepared for each connector part (MS 27852 through MS 27855, and MS 27857 through MS 27868), showing the necessary manufacturing information for producing each part for each of six tubing sizes. (Figure 90 shows MS 27855, which was prepared for stainless steel seals).

Similar military standards are expected to be issued for AFRPL flanged connectors. One set of assembly instructions will probably be satisfactory for all the flanged connectors. However, one drawing of an assembled connector will probably be required for each material, system pressure, and service condition so the necessary part numbers can be given. For each assembly drawing, one military standard sheet will probably be required for each component, i.e., integral flange, loose-ring flange, loose ring, seal, bolt, stud, and nut. If military standards are prepared on this basis for the system conditions included in Appendix C, approximately 70 military standards will be required. Because of the large number of tubing sizes and connector dimensions to be included on each military standard, it may be desirable to issue the flanged-connector military standards in groups, with the most common system conditions being given first priority.

Nickel-Plating Specifications

A military specification, MIL-P-27418 (USAF), has been issued for plating soft nickel on stainless steel Bobbin seals. Except for minor changes that might be needed to update the document, the specification is believed to be satisfactory for the Bobbin seals of the flanged connectors.

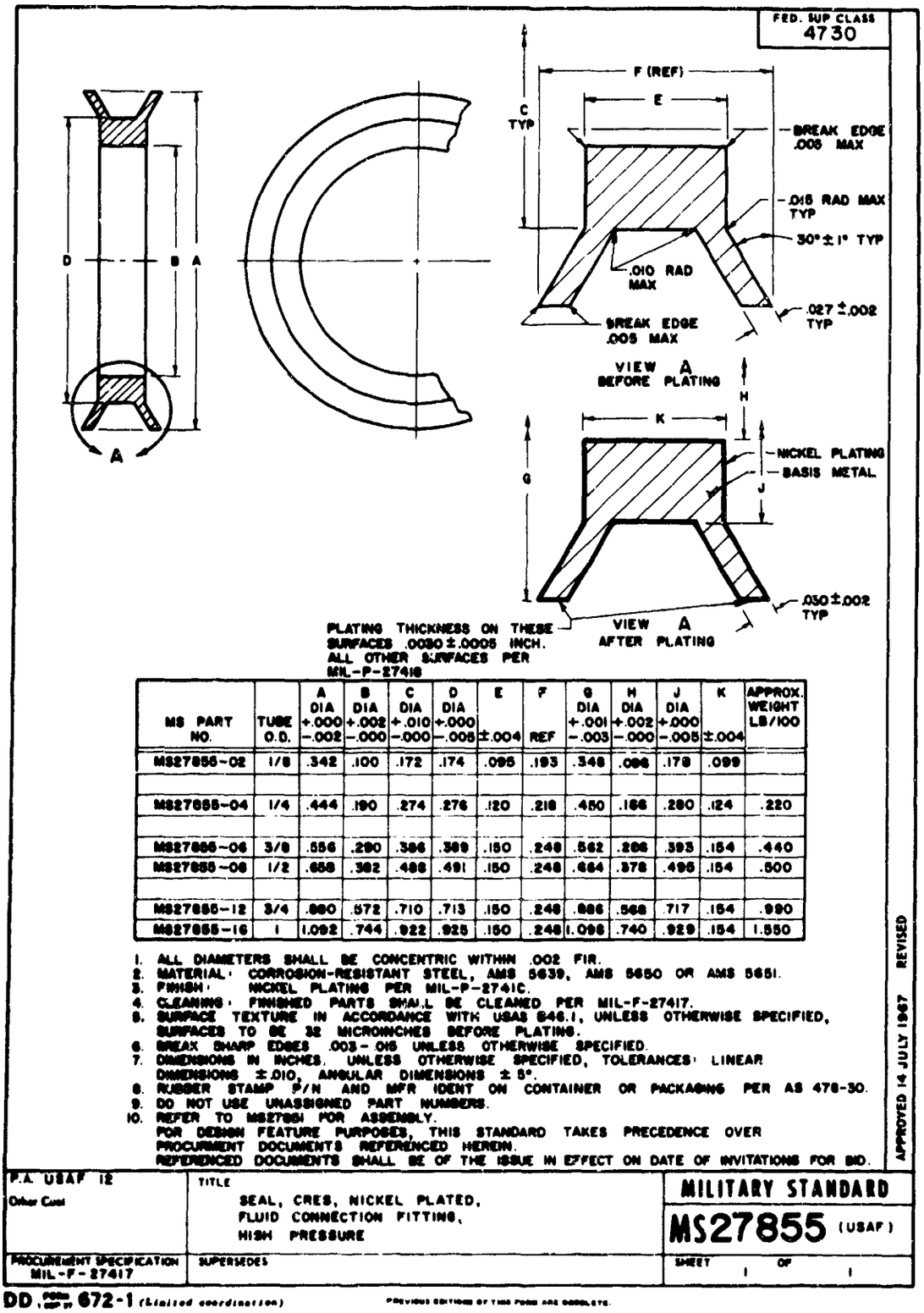

MS PART NO.	TUBE O.D.	A DIA +.000 −.002	B DIA +.002 −.000	C DIA +.010 −.000	D DIA +.000 −.005	E ±.004	F REF	G DIA +.001 −.003	H DIA +.002 −.000	J DIA +.000 −.005	K ±.004	APPROX. WEIGHT LB/100
MS27855-02	1/8	.342	.100	.172	.174	.095	.193	.348	.096	.178	.099	
MS27855-04	1/4	.444	.190	.274	.276	.120	.218	.450	.166	.280	.124	.220
MS27855-06	3/8	.556	.290	.386	.389	.150	.248	.562	.286	.393	.154	.440
MS27855-08	1/2	.658	.382	.488	.491	.150	.248	.664	.378	.496	.154	.500
MS27855-12	3/4	.880	.572	.710	.713	.150	.248	.886	.568	.717	.154	.990
MS27855-16	1	1.092	.744	.922	.925	.150	.248	1.098	.740	.929	.154	1.550

1. ALL DIAMETERS SHALL BE CONCENTRIC WITHIN .002 FIR.
2. MATERIAL: CORROSION-RESISTANT STEEL, AMS 5639, AMS 5650 OR AMS 5651.
3. FINISH: NICKEL PLATING PER MIL-P-27418.
4. CLEANING: FINISHED PARTS SHALL BE CLEANED PER MIL-F-27417.
5. SURFACE TEXTURE IN ACCORDANCE WITH USAS B46.1, UNLESS OTHERWISE SPECIFIED, SURFACES TO BE 32 MICROINCHES BEFORE PLATING.
6. BREAK SHARP EDGES .003 - 015 UNLESS OTHERWISE SPECIFIED.
7. DIMENSIONS IN INCHES. UNLESS OTHERWISE SPECIFIED, TOLERANCES: LINEAR DIMENSIONS ± .010, ANGULAR DIMENSIONS ± 5°.
8. RUBBER STAMP P/N AND MFR IDENT ON CONTAINER OR PACKAGING PER AS 478-30.
9. DO NOT USE UNASSIGNED PART NUMBERS.
10. REFER TO MS27851 FOR ASSEMBLY.

FOR DESIGN FEATURE PURPOSES, THIS STANDARD TAKES PRECEDENCE OVER PROCURMENT DOCUMENTS REFERENCED HEREIN.
REFERENCED DOCUMENTS SHALL BE OF THE ISSUE IN EFFECT ON DATE OF INVITATIONS FOR BID.

Review activities: 11, 14, 19, 69, 85, 8 MAS

APPROVED 14 JULY 1967 REVISED

P.A. USAF 12
Other Cust

TITLE
SEAL, CRES, NICKEL PLATED,
FLUID CONNECTION FITTING,
HIGH PRESSURE

MILITARY STANDARD
MS27855 (USAF)

PROCUREMENT SPECIFICATION
MIL-F-27417

SUPERSEDES

SHEET 1 OF 1

DD FORM 672-1 (Limited coordination)

PREVIOUS EDITIONS OF THIS FORM ARE OBSOLETE.

FIGURE 90. SAMPLE MILITARY STANDARD (MS 27855) FOR THREADED CONNECTORS

Flanged-Connector Requirements Specification

A military specification, MIL-F-27417 (USAF), has been issued to establish the requirements of AFRPL threaded fittings for use in rocket-engine fluid systems. By defining different manufacturing and performance criteria to be met by AFRPL connectors, a means was expected to be provided by which sample connectors from any manufacturer could be evaluated for quality. By means of this procedure, it was expected that interested manufacturers would be placed on a qualified products list.

It is expected that a similar military specification will be issued for AFRPL flanged connectors. Because of the larger sizes and much greater variety of flanged-connector types, it is believed that the performance evaluation of connectors should be minimized and that greater detail should be included concerning inspection and handling of the manufactured parts.

Recommendations for Flanged-Connector Military Standards and Specifications

The uncertainty concerning the final form of the flanged-connector military standards and specifications led to the mutual decision to limit the expenditures under Contract AF 04(611)-11204 to the preparation of typical drawings, nominal component dimensions, and recommendations concerning selected types of information. As Air Force decisions were eventually made concerning the military standards and specifications that should be issued, it was expected that the Rocket Propulsion Laboratory, using information in this report as a basis, could prepare the necessary documents. The recommendations prepared by Battelle-Columbus are discussed in three categories: (1) military standards, (2) nickel-plating specifications, and (3) connector performance specifications.

Military Standards

Appendix C contains the drawings and nominal dimensions prepared by Battelle-Columbus for the flanged-connector military standards. First, suggested assembly instructions have been prepared. Next, an assembly drawing is shown which is believed to be suitable for all of the assembly military standards. Finally, nominal part dimensions have been prepared for Connectors 1 through 10 of the following flanged connectors. Dimensions for Connectors 11 through 27 are to be generated after testing during an overrun effort.

1. 100-psi, aluminum, cryogenic, 1 through 16 inches
2. 200-psi, aluminum, cryogenic, 1 through 16 inches
3. 500-psi, aluminum, cryogenic, 1 through 16 inches
4. 1000-psi, aluminum, cryogenic, 1 through 16 inches
5. 1500-psi, aluminum, cryogenic, 1 through 16 inches
6. 100-psi, stainless steel, cryogenic, 1 through 16 inches
7. 200-psi, stainless steel, cryogenic, 1 through 16 inches

8. 500-psi, stainless steel, cryogenic, 1 through 16 inches
9. 1000-psi, stainless steel, cryogenic, 1 through 16 inches
10. 1500-psi, stainless steel, cryogenic, 1 through 16 inches
11. 2000-psi, stainless steel, cryogenic, 1 through 3 inches
12. 2500-psi, stainless steel, cryogenic, 1 through 3 inches
13. 3000-psi, stainless steel, cryogenic, 1 through 3 inches
14. 4000-psi, stainless steel, cryogenic, 1 through 3 inches
15. 5000-psi, stainless steel, cryogenic, 1 through 3 inches
16. 6000-psi, stainless steel, cryogenic, 1 through 3 inches
17. 100-psi, stainless steel, hot gas, 1 through 3 inches
18. 200-psi, stainless steel, hot gas, 1 through 3 inches
19. 500-psi, stainless steel, hot gas, 1 through 3 inches
20. 1000-psi, stainless steel, hot gas, 1 through 3 inches
21. 1500-psi, stainless steel, hot gas, 1 through 3 inches
22. 2000-psi, stainless steel, hot gas, 1 through 3 inches
23. 2500-psi, stainless steel, hot gas, 1 through 3 inches
24. 3000-psi, stainless steel, hot gas, 1 through 3 inches
25. 4000-psi, stainless steel, hot gas, 1 through 3 inches
26. 5000-psi, stainless steel, hot gas, 1 through 3 inches
27. 6000-psi, stainless steel, hot gas, 1 through 3 inches

It is obvious from an examination of the nominal dimensions of the connector parts that a number of tolerances must be established for the final military standards. It is recommended that normal machining practices be followed for the most part. As an exception, the thickness of the seal disks must be controlled relatively closely, as must the dimensions and the surface finish of the outside diameter of the seal disks, and of the inside diameter of the lips of the flange seal cavities. The outer seal disk edges and the corners of the flange seal cavities must also be closely controlled.

Nickel-Plating Specification

The following comments are made in accordance with the respective paragraphs of MIL-P-27418 (USAF). The paragraphs not discussed are believed to be applicable to the plating of seals for flanged connectors.

3.2 Workmanship. On the basis of work with seals for threaded connectors, it is believed that a third paragraph (3.2.3 Sealing Surfaces) should be added to Paragraph 3.2. A suggested wording for this paragraph is: "The examination of the circumference

of each seal disk for conformance with 3.2.1 and 3.2.2 shall be conducted with a 5-power glass."

4.2 Separate Specimens. It is suggested that the following sentence be added to the paragraph for 4.2: "The examination of the separate specimens shall be conducted with a 5-power glass".

4.3.2.1 Visual Inspection. It is suggested that the following sentence be inserted between the two existing sentences: "The examination of the circumference of each seal disk shall be conducted with a 5-power glass".

5. PREPARATION FOR DELIVERY. The handling damage that has occurred with the seals manufactured by Scientific Advances Inc. has amply demonstrated the need for the inclusion of packaging instructions. Such damage will be greatly amplified for the larger, heavier, flanged connector seals. The proper wording for this section of the specification can probably best be devised by the Rocket Propulsion Laboratory, using existing terminology. The major requirements to be included are: (1) that each seal be individually packaged and (2) that the packaging include some means for protecting the circumference of the seal disks until installation of the seal in the connector.

Flanged-Connector Requirements Specification

The following comments are made in accordance with the respective paragraphs of MIL-F-27417 (USAF). Although there are many similarities between threaded and flanged connectors, the number of differences are believed to be great enough to warrant the preparation of a separate specification for flanged connectors.

1. SCOPE. The existing wording should be adequate with the substitution of "flanged connector" for "fittings".

2. APPLICABLE DOCUMENTS. The Rocket Propulsion Laboratory can best identify the applicable government documents.

3. REQUIREMENTS. This is a large section of the specification and considerable work must be done to make it applicable to flanged connectors. The paragraph on materials (3.2) must be revised to include the material for the aluminum hardware and the stainless steel hardware. The paragraph on design and dimensions (3.3) must be revised to exclude information applicable to threaded fittings (such as 3.3.1) and to include information on flanged connectors such as information on studs, bolts, and nuts. Paragraphs 3.4 and 3.5 appear to be generally applicable.

Paragraph 3.6 on performance needs major revision. In fact, it is believed that serious consideration should be given to the complete elimination of performance testing. The manufacturing variations that are critical to successful performance have been identified, for the most part. Thus, it is believed that pertinent manufacturing capability can best be evaluated by the careful inspection of selected critical components, such as different size seals.

Paragraphs 3.7 and 3.8 appear to be generally applicable to flanged connectors.

4. QUALITY ASSURANCE PROVISIONS. Paragraphs 4.1 and 4.2 appear to be generally applicable to flanged connectors. Paragraphs 4.3 through 4.7 are performance requirements which should be reexamined and either reduced or eliminated in accordance with the comments above. Instead, Paragraph 4.8 on examinations should be greatly expanded to require the manufacture and inspection of selected, critical, and typical components.

Paragraph 4.9 on test methods should be largely eliminated and replaced with a description of applicable examination methods. Paragraphs concerning inspection, such as 4.9.6 through 4.9.11, should probably be retained.

5. PREPARATION FOR DELIVERY. The Rocket Propulsion Laboratory is best able to evaluate the applicability of this material.

6. NOTES. The material in this paragraph appears to be generally applicable to flanged connectors.

V

THREADED-CONNECTOR SUPPORT

Contract AF 04(611)-11204 established Phase III to provide engineering support during the introduction of AFRPL threaded connectors (see Figure 91) to industrial firms and government agencies. Although it was anticipated that support might be required in regard to assembly tools and inspection techniques, the exact nature of the support was to be determined during the course of the contract.

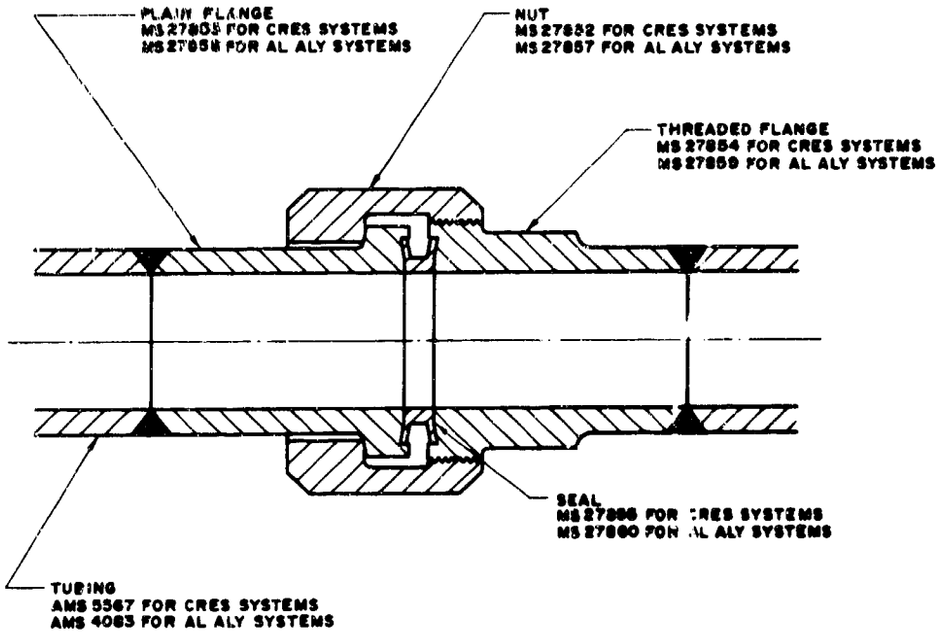

FIGURE 91. AFRPL THREADED CONNECTOR

Work was conducted on four aspects of AFRPL stainless steel threaded connectors: (1) seal removal, (2) seal retention and misalignment limitation, (3) increased radial seal loading, and (4) stress relaxation.

Seal Removal

Although axial loads of up to 3000 pounds are required to assemble Bobbin seals in threaded connectors, the forces required to remove the seated seals are much lower. When the nut of a threaded fitting has been removed, the fitting halves can be separated by hand by a cantilever force applied to one of the connector flanges. A moment of about 150 in-lb is sufficient for the 1-inch connector, with lower moments being required for the smaller connectors.

When the connector halves are separated, the Bobbin seal remains in one of the connector flanges. The most straightforward way of removing the seal is to place the blade of a medium-sized screwdriver at the root of the exposed seal disk and to strike

the handle of the screwdriver a sharp blow. Two or three such blows are almost always adequate to force the Bobbin seal from the connector flange.

Although a screwdriver can be used effectively, such a tool is not desirable if the skill of the technician is limited. There is a strong tendency to use the blade of the screwdriver to pry the seal from the flange, using the flange lip as a fulcrum. Although prying is successful if done by the proper tool, such action with a screwdriver is undesirable because it tends to nick the edge of the relatively soft stainless steel of the flange. Such a nick can cause material to protrude into the seal cavity, and the protrusion damages seals during subsequent assembly.

A prying action is satisfactory for removing the Bobbin seal from a connector flange if the forces are applied properly. Figure 92 shows a simple tool based on this precept that was designed and tested satisfactorily during the program. By dimensioning the yoke to fit snugly between the end of the flange and the exposed seal disk, it is possible to exert a high axial force without a sharp corner of the tool digging into the lip of the flange. The tool can also be used to separate the flanges, as shown in Step 1. After the seal is broken loose, it can be removed easily from the flange. It is believed that this principle could be incorporated into an inexpensive tool with different size yokes for each connector size.

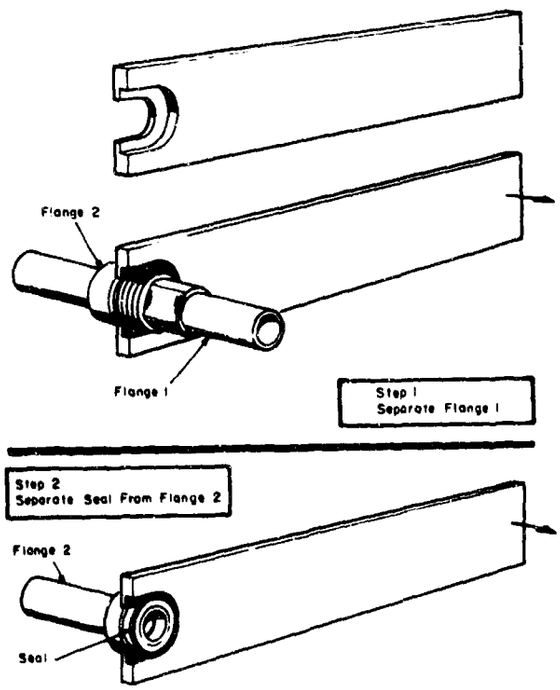

FIGURE 92. SEAL-REMOVAL TOOL

Seal Retention and Misalignment Limitation

During the early part of the program, it became apparent that two improvements would be desirable for the threaded connectors: (1) a method of retaining the seal in a flange cavity during assembly of the connector, and (2) a method of limiting the degree of misalignment at which the connector could be assembled. These problems were first considered separately and their parameters are discussed separately. However, the most desirable solution included features applicable to both improvements, and this configuration is described on pages 161-164.

Seal Retention

Most of the laboratory assemblies of the threaded connectors had been made with the connectors in a horizontal position, and with one flange of the connector relatively unattached. In this assembly mode it was comparatively easy to secure the loose Bobbin seal in one connector flange with one hand while the unattached connector half was brought in contact with the seal by the other hand. It was then relatively easy to snug the nut fingertight while the connector halves were kept pressed together. Hundreds of such assemblies were made at Battelle-Columbus and at the Rocket Propulsion Laboratory without difficulty.

As the AFRPL threaded connector was described to various representatives of industry and government, an increasing number of comments were received concerning the fact that many field assemblies would be more difficult to complete than the laboratory assemblies. Not only would space around the connector often be limited, but in many cases the connector flanges would be attached to rigid or heavy components that would be difficult to move. In such installations, it would usually not be possible to hold the seal in one flange while the other flange was brought into place. With both hands being used to move or support the flanges, it would be easy to jar the flange containing the seal sufficiently to dislocate the seal from the seal cavity. Not only would this be a nuisance, but, more importantly, the sealing surface would probably be damaged. Thus, practical experience indicated a need for snapping the seal in place in one flange prior to assembly of the connector.

Consideration of the configuration of the AFRPL connector led to the early conclusion that a logical means of retaining the seal was to extend one of the flanges to enclose most of the Bobbin seal. The space between the seal disks could then be used for an appropriate element to bear against the inside diameter of the flange extension. Figure 93 is a simplified drawing of this basic approach.

Available Space. One of the basic parameters was the space available for the retention action. In the existing specifications, the length of the seal disk and the length of the seal tang were the same for the 3/8-, 1/2-, 3/4-, and 1-inch seals. Thus, if a retention configuration could be found to work within these dimensions, the same configuration could be used for four of the six specified seals, and few changes would be required in the specifications.

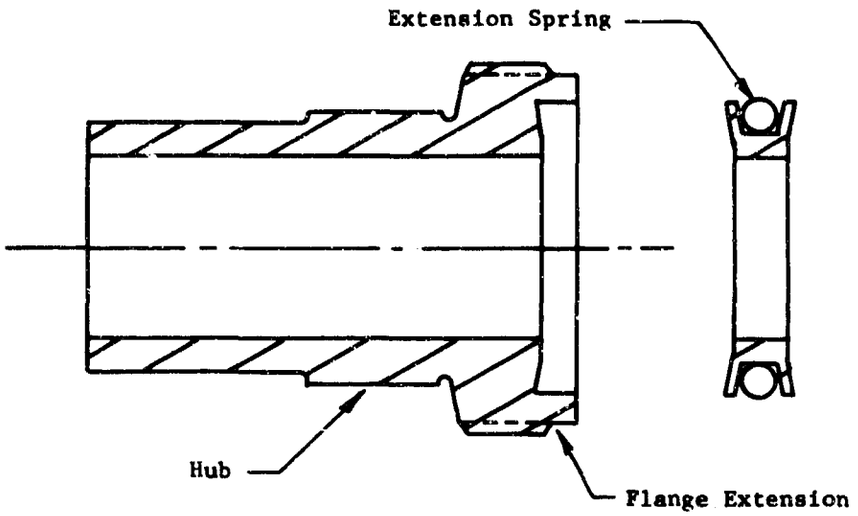

FIGURE 93. MODIFIED FLANGE AND SEAL WITH SPRING

After working with this envelope, it became apparent that sufficient radial space was available, but that the axial space was very limited. The axial limitation stemmed primarily from the relatively large movement needed to seat the seal. When this distance, with its tolerances, was added to a 0.015-inch clearance needed between the seated flanges, the flange extension was very short, and the end of the flange extension was located approximately at the middle of the unseated seal. This meant that simple circular retention shapes such as that shown in Figure 93 were unacceptable and that any retention device located on the seal had to extend to both sides of the midpoint between the seal disks.

Friction Retention. In one approach, seal spring clips were designed to be pushed down by the flange extension as the seal was pushed into the flange cavity. By exerting a radial force against the ID of the extension, the spring clip would hold the seal in the cavity. In these configurations, the extension was not undercut (see Figure 93).

With the proper force and the proper surface conditions on the lip and the spring clip, the seal could be held satisfactorily by this design. The major limitation to this concept was the possible variation in friction between the flange extension and the clip. A small film of lubricant on the clip reduced the friction to the point where the seal could be easily jarred out. It was believed that control of the surface conditions of the lip and clip would be difficult. A second problem with this design was the absence of an axial force tending to hold the seal back in the seal cavity. Thus it would be expected that seals would be only partially inserted on a certain percentage of connectors and this could lead to improper assembly of the connectors.

Snap-Action Retention. As improved seal-retention methods were sought, the following features were identified as being desirable:

(1) The clip should be easily placed on a completed Bobbin seal

(2) The seal (with clip attached) should be easily inserted in the connector

(3) The clip should hold the seal snugly in the connector

(4) The seal and clip should be removable by hand prior to assembly (this may be desired to inspect the seal and the seal cavity)

(5) The clip should not interfere with proper assembly of the connector

(6) The seated seal and clip should be easily removed from the connector upon disassembly of the connector.

The snap-action requirements emphasized the short axial dimensions available. One requirement was that the flange extension had to be undercut to provide an indentation for the retention device. Second, the retention device had to have a cam rise on the leading edge to force the protrusions down. Finally, the retention device had to have a reverse cam on the opposite side of the protrusion so the seal could be removed from the seal cavity by hand.

By using all of the distance between the inside of a seal disk and the midpoint of the seal (approximately 0.090 inch), it was possible to accomplish these actions. However, the taper of the seal disk was found to limit the amount of radial deflection available for inward deflection during insertion of the seal. Thus, in the final design, as shown in Figure 94, the flange extension was given a fairly sharp lip, and the protrusions of the retention device were made to extend at an angle from the main support ring, which clamped around the seal tang.

Misalignment Limitation

During July 1967, approximately twenty 3/4-inch stainless steel AFRPL unions were installed in a 4000-psi liquid-hydrogen piping system at the Rocket Propulsion Laboratory. Despite careful assembly of the connectors, a pressure test showed that five of the connectors leaked badly. It was noted that the leaking connectors were noticeably misaligned prior to the final tightening. Since misalignment conditions can be expected in most tubing and piping systems, sample parts were sent to Battelle-Columbus to determine whether misalignment was the problem and whether modification of the connector configuration could assure satisfactory assembly despite initial misalignment.

After an extensive examination of the parts, it was concluded that leakage had occurred because of two basic factors: (1) large, initial misalignment angles, and (2) insufficient radial sealing forces in the seals. The radial sealing forces are discussed in more detail in a subsequent section. The large misalignment angles seemed to have caused leakage for one of three reasons: (1) the seal, which was not fully enclosed by both flange cavities, was forced initially against the edge of a connector flange, damaging the seal and preventing sealing when the connector was loosened and assembled properly, (2) the large angles and high moments prevented proper seating of the seal disks, and (3) a sealing surface of the seal was damaged as the seal slid in the flange cavity during straightening of the misaligned flanges.

Although it was mutually agreed with the Project Monitors that some misalignment had to be tolerated in a threaded connector, it was also agreed that the large angles (up to 7 degrees) made possible by the dimensions of the connector were too great for the reliable sealing of high-pressure helium. Therefore, an effort was undertaken to modify the connector to limit the amount of possible misalignment.

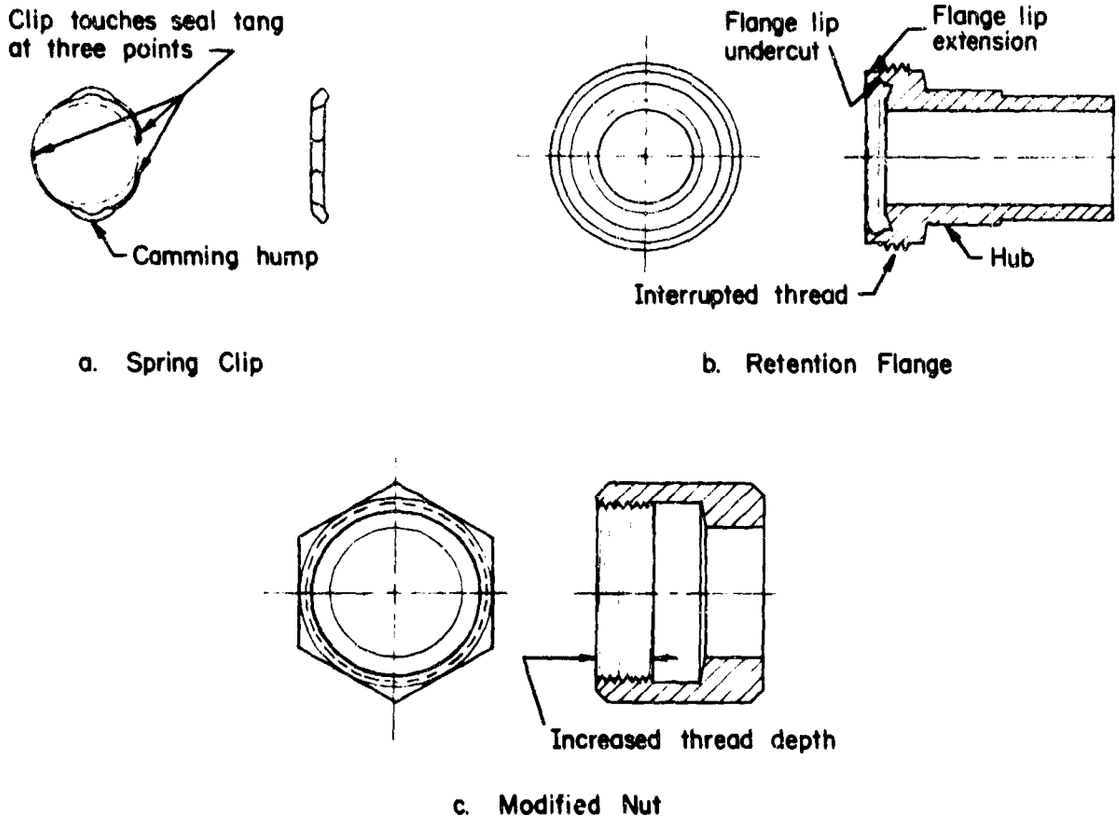

FIGURE 94. PARTS TO ACCOMPLISH SEAL RETENTION AND MISALIGNMENT LIMITATION

Consideration of the misalignment problem led to the basic decision that only minor changes in the connector configuration would be acceptable. This decision was based on the conviction that the existing fitting was simple and that this simplicity was strongly conducive to proper use of the fitting. On the other hand, the introduction of more complicated connectors in the past by industry had demonstrated that an increase in the number of connector parts or an increase in the complexity of assembly could override the advantages that the added features were designed to accomplish. Thus it was decided that changes designed to limit misalignment would be limited to changes in the existing parts.

It was apparent that improper assembly due to misalignment was possible in the connector because the nut could be engaged with the threaded flange even though the plain flange was turned at a large angle to the nut. This assembly angle was possible because of two dimensional relationships: (1) the clearance between the ID of the nut flange and the shoulder of the plain flange and (2) the clearance between the OD of the plain flange and the ID of the nut barrel. Thus, the general method selected to limit the misalignment angle of the threaded connector was to reduce the clearances for these dimensional relationships.

Although this concept was effective in reducing the angle of misalignment at which the connector could be assembled, it was still possible for the seal cavities in the two flanges to become sufficiently misaligned that the seal would not always be guided into the opposing seal cavity. Consideration of this problem produced the concept of using the threads on the nut to position the plain flange. In this way, engagement of the nut with the threaded flange would automatically align the plain flange with the threaded flange.

This guidance was believed to be most easily accomplished by locating the flange extension for seal retention on the plain flange. Then, by extending the threads deeper into the nut (to enclose the Bobbin seal in the assembled connector) the nut threads could be used to enclose the OD of the plain flange extension. This configuration is described more fully below.

Selected Design for Seal Retention and Misalignment Limitation

Figure 94 shows the configuration of the spring clip, the modified plain flange, and the modified nut selected to accomplish seal retention and misalignment limitation. Figure 95 shows the four major stages of assembly of the connector. The modification of the parts, the assembly steps, and the evaluation of the configuration are discussed below.

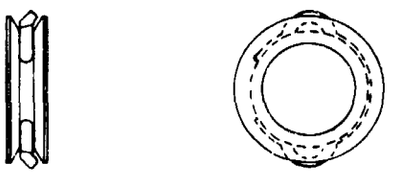

Step 1. Spring Clip Placed on Bobbin Seal

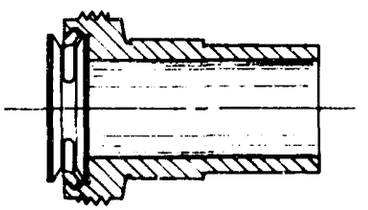

Step 2. Seal-Clip Assembly Snapped into Retention Flange

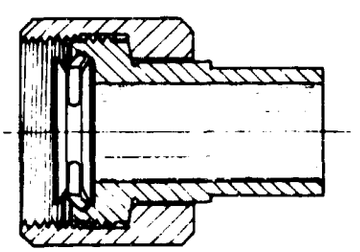

Step 3. Nut Threaded Past Interrupted Thread

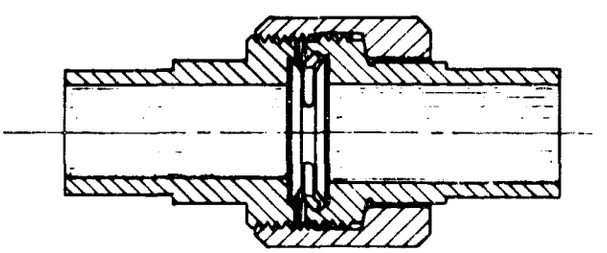

Step 4. Nut Threaded onto Other Flange, Tightened with Proper Torque

FIGURE 95. ASSEMBLY STEPS OF MODIFIED CONNECTOR

Spring Clip. As shown in Figure 94, the spring clip consisted of a C-shaped spring made from flat spring stock that was snapped over the seal tang. Two humps were formed, one near each end of the "C". These humps protruded outward beyond the seal disk diameter. The humps were offset from the rest of the material so the major part of the clip was in line with the tang, but the humps were displaced slightly in the axial direction. This allowed the humps to snap under the flange extension lip. The radii of the humps provided the entrance camming action and the exit camming action. By having the clip touch the tang circumference only at the ends of the "C" and at the middle of the "C", the clip could deflect radially, thus providing a radial spring force. By making the width of the material touching the tang the exact width of the tang, the clip provided good axial rigidity for the seal. The major limitation of the design was the fact that the clip would snap in place in the flange extension only if the humps were slanted toward the flange cavity. However, when the seal was reversed there was no snapping action, and the looseness of the seal was believed to be sufficient evidence that the seal was not properly installed.

Considerable time was required to develop a procedure for fabricating the spring clips. The final process consisted of the following steps:

(1) Layout and cut 1/8-inch strips of spring steel

(2) Layout dimples

(3) Form dimples on first die

(4) Finish-form dimples on second die

(5) Grind off stack to make offset dimple and reduce ring width on bench grinder

(6) Form ring around mandrel

(7) Secure clips to heat-treating mandrel

(8) Heat-treat and draw

(9) Finish fit to seal.

Plain Flange. Most of the connector modifications were limited to the plain flange. Because the plain flange was also equipped with threads, the modified flange was entitled the retention flange. The modifications to the plain flange and their purpose are discussed briefly below.

(1) The plain flange lip was extended, and an undercut was provided on the ID of the extension for the spring clip.

(2) A hub was added to the tube portion of the plain flange to provide a closer fit with the ID of the nut flange.

(3) An external thread, identical to the thread on the threaded flange, was added to the OD of the plain flange, excluding the flange extension. By threading the nut over and past this interrupted

thread, the nut provided protection for the exposed disk of the retained seal prior to assembly of the connector.

Nut. The nut remained unchanged except that the threads were extended deeper into the nut to provide guidance for the OD of the plain flange extension.

Connector Assembly. The major assembly steps of the modified connector are as follows:

(1) Snap the seal into the retention flange

(2) Thread the nut completely over the interrupted threads on the retention flange

(3) Engage the nut with the threaded flange, using the fingers to thread the nut as far as possible

(4) Tighten the nut slowly to the required torque.

Note. When the nut is loosened, it first encounters the interrupted thread on the retention flange. It is necessary to turn the nut slowly while the retention flange is pushed away from the threaded flange. When the nut threads engage the interrupted threads, the nut can then be removed quickly.

Modified Connector Evaluation. Five 3/4-inch retention flanges and modified nuts were fabricated and a number of spring clips were made. Three connectors were forwarded to the Rocket Propulsion Laboratory for evaluation, and two connectors were retained for evaluation at Battelle-Columbus. The results of these evaluations are discussed briefly.

One of the major questions about the configuration was the ability of the nut thread to exert a thrust against the interrupted thread as the fitting was disassembled. Although the primary purpose of threads is to exert high axial loads, the specific function required in the design was believed to be unusual, if not unique. As a preliminary evaluation of this action, a threaded flange was clamped vertically in a vise. A nut was threaded past the interrupted threads on a retention flange and the nut was then threaded on the threaded flange, with the tubular portion of the retention flange extending upward. Weights up to 100 pounds were placed on top of the tube of the retention flange, and the nut was used to raise the weights by creating thrust against the leading threads of the retention flange. The ease with which the weights were raised indicated that the necessary axial force could be supplied to separate the flanges of an assembled fitting to the point that the nut would engage the threads of the retention flange.

The evaluation of the spring clips was not as promising. Although some of the clips worked satisfactorily, it was apparent that the camming action was influenced substantially by small changes in the dimensions of the clips and of the inside disk root radii and tang length. It would be expected that properly made dies would alleviate much of the dimensional variation in the spring clips. However, it appeared that the production costs required to control the related dimensions of the spring clips and of the seal could increase the cost of the seal/spring-clip assembly as much as 50 percent over the cost of the basic seal.

Even more problems were encountered in the evaluation of the misalignment limitation features. The interrupted threads on the modified flange were subject to seizure because of galling, contamination, and peening from the nut. An almost insurmountable problem developed because of the relatively close fit between the outside circumference of the seal disks and the inside surface of the lip of each flange seal cavity. Thus, even with the initial misalignment limited to 1 degree by the tolerance between the nut and the modified flange, the edge of the seal disk extending from the retention flange was not automatically piloted into the seal cavity of the threaded flange by the tightening of the nut. Under these conditions, it would be expected that a number of seal disks would be damaged through contact with the edge of the flange cavity lip, preventing proper sealing action.

Conclusions and Recommendations. It was concluded that neither the spring clip nor the modifications to limit misalignment during assembly were practical. Two courses of future action are recommended. First, work should be done on a tool to preset the seal in either the plain flange or the threaded flange as a means of retaining the seal. Some thought has been given to this approach during the preparation of the report and it appears promising. Second, it is recommended that the assembly procedure for AFRPL connectors require that all parts be sufficiently loose initially that the preseated seal can be placed by hand into the opposing seal cavity and the nut made finger-tight. The proper preload would then be applied. The degree of misalignment possible in this procedure would be limited by the depth of the seal cavity.

Increased Radial Seal Loading

Starting in 1967, a growing amount of evidence was obtained that the radial sealing loads in the 3/4- and 1-inch, 4000-psi stainless steel seals and in certain flanged connector seals were not sufficiently high to insure reliable sealing on assembly. The work in this area increased as the extent of the problem became better known, until, in the last months of the program, the increase in radial sealing loads for selected threaded and flanged connectors was defined as a major area requiring additional theoretical and laboratory effort.

Although the answer to this problem cannot be presented in this report, it is believed advisable to record a relatively systematic description of the problem with the threaded connectors, of the work conducted so far, and of the most promising avenues for solution. It is hoped that this record will serve as a helpful reference during any future work. The pertinent information for flanged connector seals has been included in earlier report sections.

The record is presented in the following major sections: (1) theoretical background, (2) developmental background, (3) qualification tests at Battelle-Columbus, (4) qualification tests at the Rocket Propulsion Laboratory, (5) test installation at the Rocket Propulsion Laboratory, (6) seal investigations at the Rocket Propulsion Laboratory, (7) seal investigations at Battelle-Columbus, (8) candidate materials and configurations, and (9) recommended future activities.

Theoretical Background

The theoretical background to the problem is discussed in four categories: (1) forces required to seal helium, (2) the Bobbin seal configuration, (3) seal material selection, and (4) seal design.

Forces Required to Seal Helium. Extensive work has been done by the IIT Research Institute[16, 17] and by the General Electric Advanced Technology Laboratories[18] on the forces required between two metal surfaces to seal helium to approximately 2×10^{-7} atm cc/sec per linear inch of seal (the maximum leakage specified for the Air Force separable connectors). Although the relationships developed for the different parameters are somewhat complex, in general it was shown by both facilities that the force between two metals with fairly smooth surfaces ($\approx$16 rms) must be from 2 to 3 times the yield strength of the softer material to achieve low helium leakage. The step-by-step application of the IITRI analysis procedure to a separable connector is described on pages 143-148 of a final report on threaded connectors[19].

Although the work by IITRI and General Electric showed that random surface conditions had a significant effect on the actual leakage exhibited by two metal surfaces, neither facility developed design guidelines to overcome these occurrences. On the basis of previous work with many kinds of static seals, and keeping in mind the high forces needed to yield metallic surfaces, project personnel at Battelle-Columbus selected an 0.020-inch-wide sealing surface as being optimum for the AFRPL threaded and flanged connectors. Extensive experience at many facilities has shown that metal sealing surfaces approximately 0.005 inch wide (a width commonly found in high-performance aerospace valves) encounters many leakage problems because of damage and contamination. On the other hand, the 0.060-inch-wide sealing surfaces found in relatively dependable O-ring installations would require excessive force in a metal-to-metal seal. Thus, the 0.020-inch-wide surface (which is found in many installations using small O-rings) was a judgmental selection between two extremes. As an example, for a soft nickel plating with a yield strength of about 10,000 psi, the force on an 0.020-inch-wide sealing surface would be 600 lb/in. to obtain a pressure equal to 3 times the yield strength of the nickel.

Bobbin Seal Configuration. The development of the Bobbin seal configuration has been described in detail in two reports[19, 20], and the principles of the sealing action are summarized on pages 4 and 5 of this report. Two features of the seal are of particular interest to this discussion: (1) the toggle action of the seal disks and (2) the yielding of the seal material during assembly.

The toggle action of the seal disks was developed as a means of amplifying the axial force to attain a higher radial sealing force. As noted above, it was realized that high sealing forces would be required. By keeping the axial force to a minimum, the size and weight of the threaded fittings would be kept to a minimum. In practice, the toggle action of the seal disks produced a radial sealing force approximately twice the axial seal seating force. Although this was very desirable, the mechanical advantage of the toggle action, and the sensitivity of toggle angle to initial diametral tolerances between the seal and the seal cavity made it difficult to determine the radial sealing force accurately from a measured axial seating force.

The yielding of the seal structure was included in the seal design as a means of limiting the sealing forces that could be developed by dimensional variations in production parts. While this objective was accomplished to a certain degree, the actual effect

on the radial sealing forces of differences in the seal dimensions and differences in the material yield strength were much greater than had been anticipated.

Seal Material Selection. Although considerable thought was given to the selection of material for the structure of the threaded fittings[19, 20], the selection of austenitic stainless steel for the connector flanges resulted in the rather automatic selection of annealed austenitic stainless steel for the seal. An appreciable amount of effort was spent in selecting the best plating for the seal, and this work was amplified for the flanged connector seals (see pages 5-7). Nickel and gold plating were selected initially, and this selection was verified in the later effort.

When no apparent problems developed with the austenitic stainless steel seals during the development work, the specifications were based on this material. Thus, when the need arose for an increase in radial sealing force, two problems existed: (1) the problem of achieving increased strength within the specification dimensions, and (2) a lack of information concerning candidate seal materials other than annealed austenitic stainless steel. The work on these problems is described in detail subsequently.

Seal Design. At one time an attempt was made to develop an exact procedure for designing Bobbin seals. This was not successful because of the complex combination of elastic and plastic strains that were developed in the seal. An approximate design procedure was then developed, and seal design nomographs were developed for threaded seals using this procedure and experimental data.[19] Essentially, this calculation procedure was based on the concept that the seal tang developed compressive, plastic strains and that the radial sealing force was developed by the force needed to compress the seal tang.

As work was continued on Contract AF 04(611)-11204, it became increasingly apparent that this design procedure was not sufficiently accurate for small seals. It appeared that the basic reason for inaccuracy was that the material in the seal disks made a significant contribution to the radial sealing force in the small seals.

A new design procedure was then developed which included the material in the seal disks as well as the material in the seal tang. Although the calculation was still an approximation, the results of the revised procedure agreed much more closely with the experimental results for threaded seals, and it was judged to be acceptable for large as well as small seals. The revised seal-design procedure is described below.

For simplicity, the assembled seal disk was assumed to be a completely flattened cone with forces and dimensions according to Figure 96.

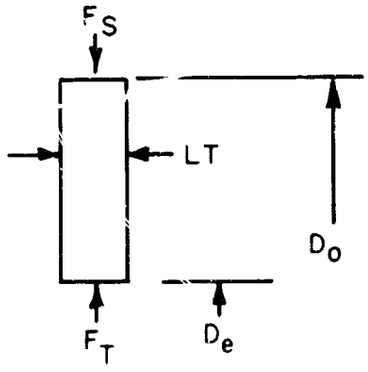

FIGURE 96. SEAL DISK STRESS MODEL

F_S = radial seal force per inch of seal disk circumference, lb/in.

F_T = radial force per inch of seal tang outside diameter at the root of each seal disk, lb/in.

D_o = seal disk outside diameter, in.

D_e = seal tang outside diameter, in.

LT = seal disk thickness, in.

The forces and dimensions for the seal tang model are shown in Figure 97.

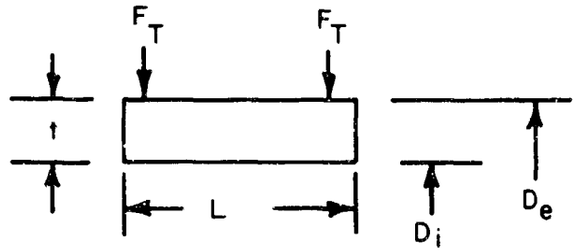

FIGURE 97. SEAL TANG STRESS MODEL

D_i = seal tang inside diameter, in.

L = tang length, in.

t = tang thickness, in.

On the basis of the elastic stress/strain theory for thick-walled cylinders[21], circumferential stress is related to pressure as follows:

$$\sigma_\theta = - \frac{a^2 b^2 (p_o - p_i)}{(b^2 - a^2)} \cdot \frac{1}{r^2} + \frac{p_i a^2 - p_o b^2}{b^2 - a^2} \quad , \tag{23}$$

where

σ_θ = circumferential stress, psi

a = inner cylinder radius, in.

b = outer cylinder radius, in.

p_i = internal pressure, psi

p_o = external pressure, psi

r = radial location of stress, in.

Considering the seal disk first, if the circumferential stress at D_e equals the yield strength of the material, the radial seal force increment contributed by the seal disk is:

$$\Delta F_S = S_y \frac{(D_o^2 - D_e^2) \times LT}{2D_o^2} \tag{24}$$

where

$P_i = o$

$r = a = D_e/2$

S_y = yield strength of seal material, psi

$\sigma_\theta = S_y$

ΔF_S = radial seal force increment contributed by the seal disk, lb/in.

$b = D_o/2$.

Similarly, the radial seal force increment contributed to each seal disk by the tang was calculated:

$$\Delta F_T = S_y \frac{(D_e^2 - D_i^2) \times \frac{L}{2}}{2D_e^2} \tag{25}$$

where

ΔF_T = radial seal force increment contributed to each seal disk by the tang, lb/in.

$r = a = D_i/2$

$b = D_e/2$.

It was assumed that the radial force at the inside diameter of the seal disk was distributed radially to the sealing surface. Thus:

$$F_S = \Delta F_S + \Delta F_T \times \frac{D_e}{D_o} \quad . \tag{26}$$

The foregoing calculations were based on limits from idealized elastic seal elements. Examinations of the dimensions of typical seals showed that sufficient radial compression existed to create plastic deformation at the inside diameter of the seal disks and in the seal tang. Using plastic theory[2] for the seal tang, the seal tang radial force contribution was calculated;

$$\Delta F_T P = \frac{L}{2} \times S_y \ln \frac{D_e}{D_i} \quad , \tag{27}$$

and then

$$F_S = \Delta F_S + \Delta F_T P \times \frac{D_e}{D_o} \quad . \tag{28}$$

Developmental Background

The development of low-leakage threaded connectors began in early 1962. The major steps of each contractual effort are summarized on pages 1 and 2 of this report. Of primary importance to this discussion is the fact that little difficulty was experienced with the performance of nickel-plated, stainless steel Bobbin seals during the two major contracts on the development of threaded fittings. Thus, instead of exploring the performance characteristics of the Bobbin seal in detail, the majority of the work was concerned with designing, fabricating, and testing different types of connectors for aluminum as well as stainless tubing systems.

In fact, the performance of aluminum Bobbin seals was in need of significant work in 1966, at the start of Contract No. AF 04(611)-11204, and Phase I of this contract was established to complete that development. An excellent solution was found to this problem by the use of overaged 6061-T6[22].

The work under Contract No. AF 04(611)-9578[19] to develop specifications for stainless steel Bobbin seals consisted of testing several 3/8- and 3/4-inch seals made to dimensions based on the original calculations (see page 14). In the first series of seals tested, five 3/8-inch and five 3/4-inch seals were made of Type 309 CRES. Although leak tests with these seals were very good, the disks did not deform properly. In a second series of tests, four 3/8-inch seals and four 3/4-inch seals were made with variations in selected dimensions. These tests were used to determine satisfactory tang thicknesses and disk thickness. In a third series of tests, four 3/8-inch seals were made to the selected dimensions and leak tested. Although the widths of the coined sealing surfaces were less than the optimum 0.020 inch, the sealing results were very good, and the radial loads, as estimated from the measured axial loads, were twice as high as required. As described in detail in the final report[19], the design equations then were modified on the basis of the experimental data, and a seal design nomograph was developed incorporating these changes. (A nomograph was also developed for aluminum threaded connector seals.) Seals were then designed for six tubing sizes. Table 58 shows the dimensions of these seals and the maximum axial loads required to seat sample seals made to these dimensions from Type 310 stainless steel.

It should be noted that radial sealing loads had not been measured for some time because the technique used was expensive. Instead, on the basis of early seal load tests, it was assumed that the radial sealing load was twice the axial seal seating load. It can be seen from Table 58 that the final stainless steel seals were thought to provide radial sealing loads from about 1150 lb/in. to about 1350 lb/in.

TABLE 58. MEASURED DIMENSIONS, COMPUTED AND EXPERIMENTAL VALUES FOR AXIAL FORCE FOR TYPE 310 CRES BOBBIN SEALS

Tube Size, in.	Inside Tang Radius, r_i	Tang Thickness, t	Outside Tang Radius, r_e	Outside Disk Radius, r_o	Tang Length, L	Seal Disk Thickness, LT	Minimum Axial Seal Seating Load, P_A, lb	P_A per In. of Seal Circumference, lb/in.
1/8	0.050	0.036	0.086	0.171	0.095	0.027	665	620
1/4	0.095	0.043	0.138	0.222	0.120	0.030	950	680
3/8	0.145	0.049	0.194	0.278	0.150	0.026	1215	683
1/2	0.191	0.053	0.244	0.329	0.150	0.026	1388	662
3/4	0.286	0.069	0.355	0.440	0.150	0.026	1595	572
1	0.372	0.089	0.461	0.546	0.150	0.026	2030	586

For a sealing surface width of 0.020 inch, these forces provided sealing pressures from 57,500 psi to 67,500 psi. By using soft nickel plating with a yield stress of about 10,000 psi, it was concluded that the seals would provide a sealing force equal to approximately six times the yield strength of the softer material. Thus the seals appeared to provide ample sealing force, and the specifications for the connectors were prepared, incorporating these dimensions. Figure 90 shows the final seal specifications that were issued, on the basis of this work.

Qualification Tests at Battelle-Columbus

Qualification tests of representative connectors were conducted at Battelle-Columbus as a part of Contract AF 04(611)-9578. A total of twenty-eight 4000-psi stainless steel connectors (20 unions, 4 elbows, and 4 tees) successfully withstood the qualification tests with maximum helium leakage never exceeding 3.9×10^{-7} atm cc/sec per inch of seal circumference. This represented a total of 41 seals successfully tested. On two occasions excessive leakage occurred, once owing to human error and once when an insufficient preload was developed.

A statistical summary was prepared using the maximum leakage measured for each seal. When the data were normalized on the basis of the logarithmic equivalent of the leakage rate, it was found that the data approximated a normal distribution. The mean recorded maximum leakage was 2.6×10^{-8} atm cc/sec of helium per inch of seal circumference.

Qualification Tests at the Rocket Propulsion Laboratory

Concurrently with Contract AF 04(611)-11204, the Rocket Propulsion Laboratory prepared final specifications for the 4000-psi stainless steel connectors, and purchased a number of connector components from Scientific Advances, Inc., (SAI) in Columbus,

Ohio. Qualification tests similar to those conducted at Battelle-Columbus were conducted at the Rocket Propulsion Laboratory. Although these test data were not completely summarized, the results, in substance, duplicated the results obtained at Battelle-Columbus.

Test Installation at the Rocket Propulsion Laboratory

As described previously, twenty 3/4-inch, 4000-psi AFRPL stainless steel unions were installed in a liquid-hydrogen system at the Rocket Propulsion Laboratory. Five of these connectors leaked badly. Three of the connectors and two seals were sent to Battelle-Columbus for examination.

The separate seals were examined first. The disks appeared to have been fully deflected, the tang had apparently been satisfactorily yielded, and a seal seating surface approximately 0.010 inch wide was visible on the four sealing disks. Under a medium-power microscope, the sealing surface of one disk was seen to have a pronounced ridge where the seal had apparently been pressed against the edge of the flange cavity during an improper partial assembly prior to final assembly. The ridge was sufficiently large that the seal could not have sealed properly even in an aligned connector. The other seal showed no obvious cause of leakage. The only visible differences between this seal and seals from past Battelle work were (1) tool marks were visible in the nickel plating, indicating that the surface finish of the machined seals was rougher than Battelle's seals had been, and (2) the nickel on the yielded surfaces had a mat finish, while past Battelle seals showed a very shiny surface where the nickel was yielded.

The absence of structural abnormalities in the separate seals indicated that it was necessary to examine the sealing surfaces at the source of leakage in the three connectors. To find the leaks in these connectors, three corners of the hex nuts of each connector were machined away. This exposed the outside of the seals but left the connectors held together by the three remaining nut corners. An O-ring-sealed plug was made to fit inside the connectors, and the inside of each connector was pressurized with helium. Soap solution was used to locate the sources of leakage.

The three connectors were then cut in half so that each connector half was still held together by 1-1/2 corners of the nuts. The connectors were cut so the leak was contained in one half. This half was then separated so the sealing surfaces at the leak could be examined. The other half was encapsulated, polished, and etched so the cross sections of the assembled connectors could be examined and the hardnesses of the nickel plating could be measured.

An examination of the leakage area in one connector showed that the edge of the flange cavity had been nicked by a sharp object, causing a peened, inward protrusion of the metal. This protrusion scratched the nickel plating on the sealing surface during assembly of the seal. It was believed that this seal could not have sealed satisfactorily even if the connector had been aligned.

The other two connectors showed no obvious cause of leakage. The general appearance of the seals was identical to that of the separate seals. The surfaces of the flange cavity did not exhibit abnormalities, although it appeared that the seals had not pressed as tightly against the flange surface in the general area of leakage as they had

against other areas and against the flange which did not show a leak. Although the disk edges in one connector showed a somewhat different type of deformation, in general it was concluded that the seal structures had deformed normally. The coined sealing surfaces were approximately 0.010 inch wide.

Unfortunately, Battelle's seals that were made to the same dimensions as the leaking seals had been discarded or were assembled in connectors on test. However, it was possible to find seals made of stainless steel and René 41 from earlier research. The shiny appearance of the sealing surfaces on the Battelle seals indicated that the nickel had yielded more than was indicated by the mat sealing surface of the leaking seals. It was suspected that the plating of the leaking seals might be too hard. However, hardness readings showed that the hardness of the plating on the leaking seals was within specifications and compared with the hardness readings taken on a cross-sectioned René 41 seal.

Consideration was then given to the possibility that the seal was not providing sufficient resistance to yielding. This could have been caused by the material in the seals having a low yield strength, or by interaction between the two sides of the seal. Thus, if one disk grossly yielded the seal structure, this might have significantly reduced the resistance to yielding in the other disk-tang area.

Scientific Advances, Inc. had made tensile specimens from the material used for the seal. The company records showed that the yield strength of the material in the 3/4-inch seals was approximately 35,000 psi. This was within the specifications and compared favorably with the yield strength of the Type 310 stainless steel seals of the same dimensions tested at Battelle-Columbus.

However, the difference in appearance of the nickel between the leaking seals and Battelle's past seals had not been explained. Battelle's Laboratory Record books and reports for all of the work on stainless steel seals were reviewed. Two aspects of the past work seemed to be pertinent.

First, it appeared that higher radial sealing pressures had probably been attained during the early research on separable connectors. It was not possible to compare the values directly because so many different seal dimensions had been used, and most of the radial-seal-seating loads were not measured directly. The axial-seal-seating loads were always measured, but these included the force necessary to rotate the disks, and the mechanical advantage of the rotating disks was difficult to estimate. However, the axial-load peaks of early seals with dimensions similar to those of the leaking seals were generally about 30 percent higher than the axial-load peaks of the leaking seals. In addition, the thickness of the disks at the hinge line of the final seals (0.027 inch) was about 30 percent higher than the thickness (0.020 inch) of most of the disks of the early seals. Thus, a greater amount of the axial load required to seat the leaking seals was needed to rotate the disks (this force does not contribute to the radial seal-seating force) than was the case with the seals with thinner disks. In conclusion, it was estimated that the radial seal-seating pressure on the leaking seals was probably significantly lower than for the early seals.

The second aspect was the difference between the appearance of the axial seal-seating-load curve for the early seals and the appearance of that for the seals made to dimensions in the specifications. Most of the early curves showed two distinct humps. (See subsequent Figure 99.) Each hump represented the seating action of a seal disk. Two humps were created because one disk was always stronger than the other disk.

Many of the curves for the specification seals had one full hump and a partial hump. It was believed that the absence of a full second hump may have resulted from the first disk causing the tang to yield sufficiently that the second disk was not supported as much as normal by the tang. The possibility of interaction between the two sides of the tang was increased for the larger seals because the tang was shorter in relation to the tang thickness than was the case for the 3/8-inch seals. This interaction might explain the failure of the seals to function satisfactorily in the misaligned connectors despite the fact that all the seals functioned satisfactorily in the aligned connectors.

As a result of the examination of the connector parts and of Battelle's past work, the following conclusions were reached:

(1) The unretained Bobbin seal was susceptible to damage and improper installation during assembly of the connector.

(2) The leaking connector parts were made within the specifications. Although not apparently a cause of leakage, the machined surface of the seals was noticeably rougher than were earlier Battelle seals.

(3) The radial seal-seating pressure in the 3/4-inch connector was satisfactory for an aligned connector, but higher sealing pressures were attained in many of Battelle's earlier seals.

(4) As the seal tang is made shorter in relation to its thickness, a ratio may be reached for which the disks do not seat sufficiently independently.

The following steps were recommended to overcome the apparent deficiencies of the connector:

(1) A means should be devised to retain the seal in one of the flange cavities during assembly of the connector.

(2) Consideration should be given to changing the rms specification on the seals from 32 to 16.

(3) The radial sealing force of each size of stainless steel seal should be measured, and if necessary, increased.

(4) The length-to-thickness ratio for the tangs of all sizes of stainless steel seals should be checked to insure independent seating action of the sealing disks.

Seal Investigations at the Rocket Propulsion Laboratory

The decision was made to conduct work under Steps 3 and 4 at the Rocket Propulsion Laboratory. Because of the installation problems with the 3/4-inch connectors, it was decided that work would be concentrated on this connector size. However, it was believed that the results of this work would probably apply to 1-inch seals also. Strain-gaged rings were fabricated at Battelle-Columbus from high-strength steel

to replace the retaining lip of the 3/4-inch connector flanges. Plugs were machined to fit inside the rings so the seal tang could be compressed between the plugs and the seal disks would press outwardly against the load rings. These components were calibrated and then forwarded to the Rocket Propulsion Laboratory.

First, the maximum radial sealing loads were measured for seven SAI seals. The first two seals were seated normally, with the disks both being seated in one loading. The next five seals were loaded to seat only one disk at a loading. The results of the load tests with these seals are shown in Table 59. Also shown are the measured maximum axial loads, the original seal disk diameters, and the percent of sealing surface that was matted, or did not seem to be as shiny as desired. Figure 98 shows a plot of the maximum measured radial load as a function of the maximum measured axial load.

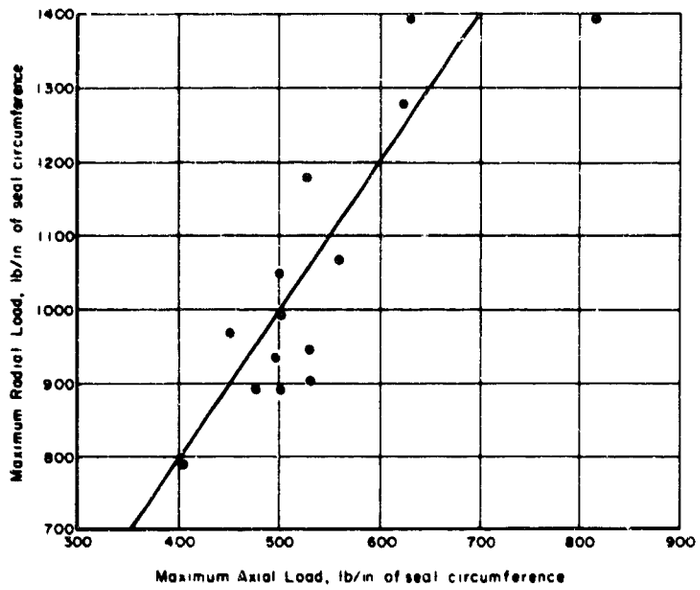

FIGURE 98. COMPARISON OF MAXIMUM RADIAL AND AXIAL SEAL-SEATING LOADS – 3/4-INCH SAI STAINLESS STEEL SEALS

The major conclusion from this work was that the radial sealing load varied much more than was anticipated for seals made by the same manufacturer from one bar of material. Tentative conclusions were: (1) the initial fit of the seal was not a major load-determining factor, (2) dimensional variations within the seal probably were a major load-determining factor, (3) the prevalence of the mat surface indicated the need for increased seal strength, and (4) the rule-of-thumb estimate that the radial sealing force was twice the axial sealing force was an effective approximation.

In a second series of tests it was shown that significant interaction existed between the seal disks. In essence it was shown that the radial load established by the first disk to seat could be reduced as much as 50 percent when the second disk was seated.

In a third series of tests, 3/4-inch seals were machined from Type 304L stainless steel to the dimensions in the specifications. Radial sealing forces from 5 seals varied fairly uniformly from 520 lb/in. to 830 lb/in. of seal circumference. It was thus shown that the introduction of a material-properties variation created a set of

TABLE 59. LOAD TESTS MADE WITH SAI 3/4-INCH STAINLESS STEEL SEALS AT ROCKET PROPULSION LABORATORY

Specimen[a]	Seal Disk Diameter[b], in.	Max Axial Load, lb	Maximum Load per In. of Seal Circumference[c], lb/in.		Percent of Matted Sealing Surface
			Axial	Radial	
1	0.884	1260	452	965	33
	0.887	1740	623	1275	33
2	0.885	1135	407	790	25
	0.887	1480	530	1174	10
3	0.882	1380	495	935	33
	0.887	2280	817	1385	None
4	0.887	1400	502	880	None
	0.887	1485	533	900	33
5	0.885	1330	477	885	50
	0.887	1580	567	1065	25
6	0.886	1410	506	990	25
	0.887	1775	637	1380	33
7	0.885	1400	502	1050	33
	0.881	1480	530	940	75

(a) Disks of Specimens 1 and 2 seated during one loading. Disks of Specimens 3 through 7 seated one at a time.
(b) ID of flange lip = 0.888 in.
(c) Based on ID of flange lip.

readings almost completely below those obtained from the SAI seals. It was also shown, however, that the lowest sealing load was still very close to the original design minimum of 600 lb/in.

In a fourth series of tests, 3/4-inch seals were made from Type 304L stainless steel with different tang lengths. These seals were seated to determine the effect of increased tang length on the radial sealing load and on disk interaction. It was found that a 100 percent increase in tang length resulted in a 50 percent increase in radial sealing load. A greater increase in tang length did not increase the radial sealing load significantly because the seal disks were not strong enough to yield a stronger tang.

On the basis of the work conducted at the Rocket Propulsion Laboratory, it was concluded that the radial sealing load of the 3/4- and 1-inch stainless steel seals should be increased and that the increased load should be accomplished by lengthening the seal tang since this would tend to separate the seating action of the seal disks.

Seal Investigations at Battelle-Columbus

The work on the seal retention and misalignment problems of threaded connectors (see pages 157-164) precipitated a more intensive investigation of the radial sealing loads of the stainless steel threaded seals. This occurred because it was not possible to select a final seal-retention or misalignment-limitation configuration until the seal dimensions had been selected.

As the parameters associated with an increased seal tang length were examined more closely, it became apparent that this approach had several disadvantages. The most important disadvantages were an increase in the size and weight of the connectors. While the increase required for the 3/4- and 1-inch connectors might have been acceptable, the same dimensional increases on the 3/8- and 1/2-inch connectors might have been unacceptable. Related to these problems were secondary problems associated with the change of many of the connector specifications. In addition to the problems associated with an increased tang length, several higher strength materials seemed to be capable of producing the required increase in radial sealing load within the specification seal dimensions. If such a material were used, the higher yield would provide greater springback in the seal and might minimize the problem of disk interaction. Thus, the decision was made to develop an improved seal within the specification dimensions.

The accomplishment of this objective proved to be much more difficult than anticipated. However, considerable work on the problem was accomplished, and it is summarized in the following sections.

Radial Sealing Load Calculations. The improved procedure for calculating radial sealing loads (see pages 166-169) was used to calculate the loads for the 3/4-inch SAI seals. In the original calculation, 30,000 psi had been used as the yield strength of austenitic stainless steel. However, this is a minimum tensile yield strength, and a more extensive search of the literature produced data showing that the compressive yield strength of austenitic stainless steel could be between 40,000 and 50,000 psi for the degree of strain produced in the Bobbin seals. When 50,000 psi was used in the revised calculation procedure, the calculated radial sealing load for the 3/4-inch seals agreed well with the average of the experimental results obtained at the Rocket Propulsion Laboratory for the 3/4-inch SAI seals.

The decision was then made to calculate the radial sealing loads for all the seals in the specification. This calculation was of particular interest because the sealing surfaces of the 3/8-inch SAI seals seemed to be consistently shiny, and it was hoped that the radial sealing load for this seal might be used to estimate the required radial sealing load increases in the 3/4- and 1-inch seals. Table 60 shows the radial sealing loads calculated for the specification seals, using 40,000 and 50,000-psi yield strengths. It can be seen that the calculations for the 3/4-inch seal using a 40,000-psi yield strength agreed well with the average values measured at the Rocket Propulsion Laboratory for 3/4-inch seals made of Type 304L stainless steel.

If the radial sealing load for the 3/8-inch seal was satisfactory, these calculations showed that the 1/8- and 1/4-inch seals were also satisfactory. The calculations also showed that the 1/2-inch seal was slightly understrength, while the 3/4-inch seals were almost 50 percent understrength.

TABLE 60. RADIAL SEALING LOADS CALCULATED FOR SPECIFICATION STAINLESS STEEL SEALS WITH REVISED CALCULATION PROCEDURE

Tubing Size, in.	Radial Sealing Load, lb/in., Using S_y = 40,000 Psi	Radial Sealing Load, lb/in., Using S_y = 50,000 Psi
1/8	948.9	1187.3
1/4	913.9	1142.3
3/8	912.2	1139.5
1/2	805.9	1007.6
3/4	728.8	901.5
1	700.0	875.0

With the need for an increase in radial sealing load further substantiated, the question arose concerning the capability of the connector structures to sustain the loads resulting from stronger seals. The axial load required of the nut would be increased, and the radial load on the lip of the connector flanges would be increased. Work was then undertaken to determine the limits of these factors.

Axial Seal-Seating-Load Calculations. The following formula was used to calculate the axial loads expected for the minimum and maximum torques listed in the specifications:

$$T = 0.2\, dF_1 \quad , \tag{29}$$

where

T = torque, in-lb
d = thread diameter, in.
F_1 = axial force, lb.

Table 61 shows the minimum torques and resulting axial forces, and the total axial seal-seating loads as defined on two bases: (1) experimental values from Table 58, and (2) calculated values based on Table 60, using a ratio of axial load to radial load of 1 to 2.

TABLE 61. AXIAL LOADS FOR SPECIFICATION TORQUES AND AXIAL SEAL-SEATING LOADS FOR STAINLESS STEEL SPECIFICATION SEALS

Tubing Size, in.	Min Torque, in-lb	Min Axial Force, lb	Exp. Seal Seating Force, lb	Calc. Seal Seating Force, S_y = 40,000 Psi, lb	Calc. Seal Seating Force, S_y = 50,000 Psi, lb
1/8	75	666	665	520.0	650.0
1/4	200	1600	950	650.0	808.0
3/8	380	2533	1215	810.0	1000.0
1/2	490	2800	1388	840.0	1110.0
3/4	1240	5510	1595	1010.0	1260.0
1	2300	8764	2030	1200.0	1510.0

From the information in Table 61 it appeared that the available axial loads would permit significant strength increases in 3/8-inch and larger seals. The 1/8-inch seal appeared to be very marginal, and the 1/4-inch seal did not provide much margin if the possible variations in seal loading were considered.

Flange Strength Limitations. An increased diametral requirement is probably the biggest problem to be overcome in designing a lightweight threaded connector with a radial seal. Thus, the lips on the connector flanges were made as thin as possible. On the other hand, the stress calculations for the flange lips were very approximate, and the effect of simplification in the calculations was difficult to estimate. When the specification connectors were designed, a minimum lip thickness of 0.065 inch was selected. If the OD of the seal for a given connector size was such that extra space was available with the use of a standard thread size on the nut, then the lip thickness was increased. Table 62 shows the nominal flange lip thicknesses for the plain flanges of the specification connectors.

TABLE 62. PLAIN FLANGE LIP THICKNESS FOR STAINLESS STEEL SPECIFICATION CONNECTORS

Tubing Size, in.	Plain Flange Lip Thickness, in.
1/8	0.075
1/4	0.065
3/8	0.065
1/2	0.070
3/4	0.079
1	0.065

From Table 62 it can be seen that the 1/4-, 3/8-, and 1-inch plain flanges all had the minimum allowable thickness. Because of its increased diameter, it was concluded that the 1-inch plain flange was the weakest component. Experiments were conducted with the 1-inch plain flange to obtain an experimental approximation of its radial load capacity.

A 1-inch seal was machined from A286 (tensile S_y = 102,000 psi), and the seal was partially seated in a 1-inch plain flange. A diametral expansion of 0.0002 inch was measured with an axial load of 3500 pounds. At 4500 pounds, an additional expansion of 0.001 inch was measured. The test was stopped, the seal tang was reduced 50 percent, and the seal was completely seated with an axial load of 5350 pounds. At this load, the lip diameter had increased 0.002 inch and some flange yielding was indicated. It was concluded that the 1-inch plain flange could sustain an axial seal seating load of 4000 pounds without damage, and an occasional load of approximately 5000 pounds. This conclusion was partially verified later when a 1-inch seal made of 19-9 DL was seated with a maximum axial load of 4000 pounds without yielding of the flange lip.

The ID of the plain flange lip (the OD of the seated seal) is 1.1 inches. If a ratio of axial-to-radial force of 1 to 2 is selected, the tests indicated that the 1-inch plain flange could withstand a radial sealing force of about 2300 lb/in. with an occasional force of about 2900 lb/in. It then appeared that the plain flanges as dimensioned by the specifications would tolerate a significant increase in the radial sealing load.

Load Testing of 3/8-Inch SAI Seals. Because it appeared that the 3/8-inch seal might be found to be satisfactory, load tests were conducted with three 3/8-inch SAI seals. The disks of the first specimen were seated one at a time, while the disks of the second and third specimens were seated during one assembly. For the second type of assembly, one disk was seated in a load ring, and one disk was seated in a flange. Table 63 shows calculated and experimental loads for the 3/8-inch seals. Figure 99 shows the axial load trace obtained from the tensile machine, and associated strain readings obtained from the load ring. An examination of the sealing surfaces showed uniformly shiny, coined sealing surfaces about 0.015 inch wide.

TABLE 63. CALCULATED AND EXPERIMENTAL LOADS FOR 3/8-INCH STAINLESS STEEL SPECIFICATION SEALS

Specimen(a)	Maximum Axial Load, lb	Maximum Load per In. of Seal Circumference, lb/in.		Calculated Radial Load, lb/in., S_y = 50,000 Psi	Radial Load After Seating of Second Disk, lb/in.
		Axial(b)	Radial		
1	1235	705	1410	1139.5	--
	1500	856	1460	--	--
2	1200	685	1150	1139.5	1150
	1285	735	-- (c)	--	--
3	1400	800	1440	1139.5	1230
	1730	990	-- (c)	--	--

(a) Disks of Specimen 1 seated one at a time, disks of Specimens 2 and 3 seated during one loading.
(b) Based on ID of flange lip = 0.564 in.
(c) Seal seated in one load ring and one flange.

Three tentative conclusions were reached from these tests:

(1) The revised calculation was applicable to 3/8-inch seals as well as 3/4-inch seals, and was probably accurate for all sizes of seals for threaded connectors.

(2) A radial sealing load of 1200-1500 lb/in. of seal circumference appeared to be a good minimum value for threaded-connectors

(3) The appearance of two pronounced humps on the axial load curve actually indicates more, rather than less, disk interaction as had been thought.

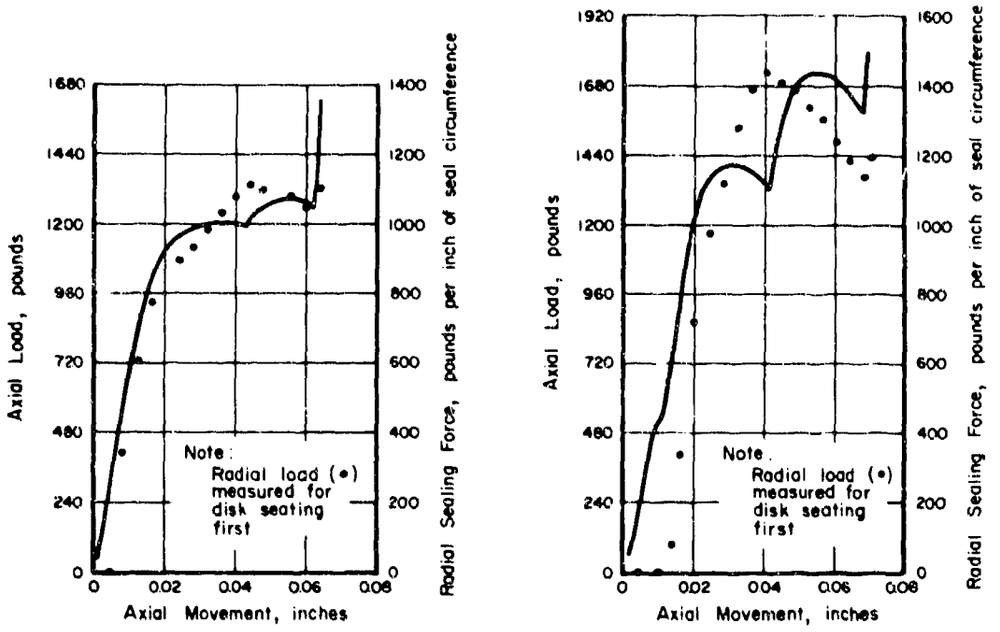

a. Specimen No. 2 - Little Disk Interaction

b. Specimen No. 3 - Significant Disk Interaction Indicated by Reduced Radial Sealing Load

FIGURE 99. AXIAL LOAD TRACE AND RADIAL LOAD INCREMENTS FOR 5/8-INCH STAINLESS STEEL SAI SEALS (SPECIMENS NO. 2 AND 3)

Investigation of Plating Quality. Tests were then conducted to determine the effect of increased radial sealing loads on 3/4- and 1-inch SAI seals. Specimens were forwarded to Battelle-Columbus from the Rocket Propulsion Laboratory. When these appeared to have rougher plating surfaces than expected, additional specimens in most sizes were obtained and examined. In all, approximately 30 SAI seals were examined with a 10-power glass. Typical types of variations included pits, plating nodules, grainy surfaces, edge nicks, scratches, inclusions, and machining marks under the plating.

Although it was believed at first that the quality of the plating should be improved, a discussion with SAI personnel of the production plating of the seals indicated that the plating quality was good as defined by the present state of the art. Although various steps could be taken to improve the plating, these would result in a substantial increase in plating costs. Therefore, it appeared desirable to increase the radial sealing load sufficiently to make the current plating quality acceptable. A similar conclusion was reached at the Rocket Propulsion Laboratory after an examination of the plating. In any case it was clear that the range of radial sealing loads that could occur within the specification for the 3/4- and 1-inch seals would result in a significant percentage of seals with excessive leakage if the nickel plating were of the current quality.

Increased Sealing Loads for Current Plating Quality. The possibility of obtaining reliable sealing for seals with current plating quality was investigated by assembling a number of 3/4- and 1-inch SAI seals with insert rings in the tangs to provide additional radial sealing loads. The disks were able to sustain radial sealing loads of about 1700 lb/in. before their columnar strength was exceeded.

Approximately 20 seals were assembled with varying radial sealing loads. On the basis of detailed examinations of the sealing surfaces before and after seating, it was concluded that an average radial sealing load of 1500 lb/in. would give good sealing with the current plating. Starting at a radial sealing load of about 1200 lb/in., a shiny coined sealing surface was formed that was about 0.015 inch wide. At a load of 1500 lb/in., a similar surface was formed which was about 0.020 inch wide. In both cases, many of the plating variations were coined out. When edge nicks or pits occurred, the coined surface was sufficiently wide to create a seal around the discontinuity.

During a detailed review of this work at the Rocket Propulsion Laboratory, it was mutually agreed that attempts would be made to develop seals with radial sealing loads ranging from 1200 lb/in. to 1700 lb/in. Since the 3/8-inch and smaller seals already provided these loads, attention was to be directed to the 1/2-, 3/4-, and 1-inch seals.

Candidate Materials and Configurations

Over a period of several weeks at the end of Contract AF 04(611)-11204, personnel at the Rocket Propulsion Laboratory and Battelle-Columbus worked closely together in developing and evaluating candidate materials and configurations.

Two basic approaches were visualized for developing the necessary increase in radial seal loading: (1) the use of a stronger material for the entire seal or (2) the use of an insert ring of strong material in the tang of an austenitic stainless steel seal. Called the one-metal and two-metal seal approaches, each had advantages and disadvantages.

The one-metal seal approach offered lower production costs and better production control. However, fewer materials were available for consideration, and the performance of a stronger seal structure against the softer material of the flanges was difficult to envision.

The two-metal seal approach offered higher production costs and poorer production control. On the other hand, several materials appeared to be candidates for the strengthening element, and the performance of the seal disks against the flanges was thought to be more predictable.

Candidate Materials for One-Metal Seals. Candidate material properties for a satisfactory one-metal seal could be closely specified. The compressive yield strength had to be from 50 percent to 100 percent more than for the SAI seals (which was about 50,000 psi). The coefficient of thermal expansion had to be about 9.5×10^{-6} in./in./F to match the austenitic stainless steel flanges. The material had to be compatible with candidate rocket propulsion fluids. It also had to be available in bar stock, cost about $1.00 per pound, and have a machining index of approximately 50.

All relatively common stainless steels were considered. The martensitic and ferritic stainless steels were not acceptable because of their low coefficient of thermal expansion (approximately 5.5×10^{-6} in./in./F). The age-hardenable stainless steels had a low coefficient of thermal expansion and were generally too strong. The nickel-base superalloys were too strong and were not corrosion resistant to N_2H_4 and fluorine. A286 was shown to be too strong (see page 178) and was not compatible with N_2H_4 and fluorine. A cobalt-base superalloy, V-36, appeared to have attractive properties, but it was not generally available and little corrosion data could be found.

The most promising materials for a one-metal seal were: (1) cold-worked Type 304 stainless steel, (2) 19-9DL stainless steel, and (3) a new stainless steel by Armco, called 21-6-9.

Type 304 stainless steel is capable of being cold worked to very high yield strengths. The yield strength of full-hard tubing was found to range from 115,000 to 150,000 psi. Cold-worked bars were available in limited quantities and by special order. Because the general properties of cold-worked Type 304 appeared to be ideal for use in the austenitic stainless steel flanges, the major problems seemed to be associated with the availability of the material in the required yield strength, and the effect of the residual stresses on the machining of the thin seal disks. The further investigation of this material is discussed below.

The second candidate, 19-9DL, was an iron-base superalloy. It had an ideal yield strength (70,000 to 85,000 psi), was readily available, and cost about $1.00 per pound. It had a coefficient of thermal expansion of 10×10^{-6} in./in./F, and its machining index was comparable to austenitic stainless steel. Although an examination of the composition of 19-9DL indicated that it should be more corrosion resistant than A286 (another iron-base superalloy), little data existed for exposure to rocket propulsion fluids. The lack of corrosion data appeared to be the biggest problem with 19-9DL.

The third candidate, 21-6-9, was very similar to austenitic stainless steels. The coefficient of thermal expansion, cost, and machining index were favorable. Although its corrosion resistance to rocket propulsion fluids was not known, its composition indicated that it would be similar to Type 316 stainless steel. The biggest problem with 21-6-9 was the fact that the annealed tensile yield strength was not very high (50,000 to 60,000 psi). While this was some improvement over annealed austenitic stainless steel, it was not as much as desired. Another problem was the fact that there was only one supplier, and 21-6-9 was not readily available in the bar sizes of interest. Although 21-6-9 was able to be cold worked to achieve higher yield strengths, such material was much less available than cold-worked Type 304 stainless steel.

Candidate Materials for Two-Metal Seals. The two-metal seal configuration was envisioned as consisting of an austenitic stainless steel Bobbin seal with some percentage of its tang replaced by a relatively high-strength stainless steel. The percentage to be replaced would depend on the strength of the insert ring, although it was apparent that some of the original tang material had to remain to join the seal disks during machining and to insure proper seating of the seal disks.

Most of the materials discussed for the one-metal seal were also considered for the two-metal seal. Particular attention was given to A286 and Inconel 718. However, because of the corrosion problems with these materials, the final candidate material was hard-drawn and tempered Type 304 stainless steel tubing. Although this material was not readily available in the tubing size and wall thickness desired, there appeared to be several companies that would be willing to supply it in limited quantities for about $1.50 per pound. When used with an annealed Type 304 stainless steel structure, the combination appeared to be ideal. However, as described below, preliminary tests simulating such a configuration produced unanswered questions about the performance of the two-metal seal.

Limited Tests With One-Metal Seals. Limited tests were conducted with one-metal seals to assist in the formulation of recommendations for follow-on effort.

Small quantities of each candidate material were obtained and load tests were conducted with seals machined to the specification dimensions.

A 1-inch bar of 21-6-9 was obtained readily as a sample from Armco (it was not possible to obtain a slightly larger size bar for the 1-inch seals during 6 weeks of requests). The sample had a tensile yield strength of 57,500 psi, which was said to be about average. Four 3/8-inch and three 3/4-inch seals were machined from this bar and load tested. The test results are shown in Table 64, as is a calculated radial sealing load based on an assumed compressive yield strength of 65,000 psi. Although the first two 3/4-inch seals were seated before a 3/4-inch load ring was fabricated, the measured axial loads for all seals and the measured radial sealing loads for Specimen 3 were about as anticipated. It was not possible to explain the similarity of the 3/8-inch, 21-6-9 results shown in Table 64 with those obtained with 3/8-inch seals made of annealed Type 310 stainless steel (see Table 63). An examination of the disk surfaces of the 3/8-inch, 21-6-9 seals showed significant areas of crazing, which indicated a greater surface compressive yielding than had been observed on other seals. It was concluded that the material was promising, but that future tests should determine whether 21-6-9 was weaker in compressive yield than expected.

TABLE 64. LOAD-TEST RESULTS FOR 3/8- AND 3/4-INCH SEALS MACHINED FROM 21-6-9

Tubing Size, in.	Specimen	Maximum Axial Load, lb	Max Load per In. of Seal Circumference, lb/in.		Calculated Radial Load, lb/in., S_y = 65,000 Psi
			Axial	Radial	
3/8	1	1440	822	1420	1485
3/8	2	1230	702	1235	1485
3/8	3	1420	810	1320	1485
3/8	4	1525	870	1600	1485
3/4	1	2400	860	--	1170
3/4	2	2400	860	--	1170
3/4	3	2100	752	1240	1170

A 1-1/4-inch bar of 19-9DL was readily obtained. An accompanying specification listed a tensile yield strength of 84,000 psi. Several sources listed a minimum tensile yield of 70,000 psi, but the specimen that was obtained was apparently typical. One 3/4-inch seal and one 1-inch seal were machined from this bar. Table 65 shows the results obtained from these seals and the calculated radial sealing load based on an assumed compressive yield strength of 95,000 psi. The load results were about as anticipated and the seal deformation appeared to be normal. The 1-inch plain flange did not yield with this assembly, substantiating the earlier tests (see page 178) with an A286 seal. Although the edges of the seal disks did not flatten out but indented slightly into the softer flange material, neither seal was more difficult to remove than the SAI seals. This indicated that flange indentation may not be a problem with a stronger seal. However, it also appeared that a reverse angle may have to be machined on the seal disks if a satisfactorily wide sealing surface is to be obtained. (This procedure worked well for the flanged-connector seals.)

TABLE 65. LOAD-TEST RESULTS FOR 3/4- AND 1-INCH SEALS MACHINED FROM 19-9DL AND ANNEALED AND COLD-DRAWN TYPE 304 STAINLESS STEEL

Tubing Size, in.	Seal Material	Maximum Axial Load, lb	Max Load per In. of Seal Circumference, lb/in.		Calculated Radial Load, lb/in., S_y = 95,000 Psi
			Axial	Radial	
3/4	19-9DL	2900	1040	2120	1715
1	19-9DL	4000	1160	1530	1660
3/4	304	2700	968	2030	1715

A 1-inch bar of annealed and cold-drawn Type 304 stainless steel was found and purchased. Subsequently, an additional 1-inch bar and 1-1/4-inch bar were located but not purchased. These bars had specified tensile yield strengths of 90,000, 89,000, and 84,000 psi, respectively. Through discussions with several steel manufacturers, it was determined that, although annealed and cold-drawn Type 304 bars are usually purchased according to a minimum yield strength, it would be practical to specify a minimum and a maximum yield strength, provided the range was sufficiently broad. On the basis of these discussions, values of 70,000 and 90,000 psi would be acceptable. Bars could be obtained to this specification at any time from a mill if 1000 pounds were ordered. The price would be approximately $0.90 per pound. If smaller quantities were desired, calls to specialty suppliers would have to be made, similar to those made by Battelle-Columbus. While additional effort would be needed to determine accurately the most practical methods for specifying and ordering cold-worked Type 304, it appeared to be practical to obtain the material with the proper yield strength.

There had been concern that a cold-worked bar would have wide stress variations. Table 66 shows hardness readings taken from the Type 304 bar that was purchased. It was concluded that the uniformity was quite good for the purposes of the Bobbin seal.

TABLE 66. ROCKWELL B HARDNESS READINGS TAKEN FROM 90,000-PSI-YIELD, COLD-WORKED TYPE 304 STAINLESS STEEL

Location on 11-Ft Bar	Surface of Bar	Center of Bar	One-Half Radius
One End	106	94	98
Middle	104	91	98
Other End	105	93	98

One 3/4-inch seal was machined from this bar. The machining was judged to be somewhat easier than for annealed Type 304 stainless steel. There was no noticeable effect from residual stresses on the seal dimensions. The results from the load test of this seal are shown in Table 65. Some concern was felt about the ductility of the cold-worked material. However, the accompanying specificiation showed 37 percent elongation, and the deformation of the seal appeared to be normal. The same conditions noted for the edge of the 19-9DL seal disks were also noted for the Type 304 seal disks.

Limited Tests With Two-Metal Seals. A number of load tests were made with SAI seals equipped with insert rings as a means of increasing the radial sealing loads on the plating. On the basis of this work, it appeared relatively easy to select a high-strength material which could be used to replace a portion of the seal tang and obtain the same increased loads. Although detailed consideration was given to A286 and Inconel 718, the only material that was finally acceptable was cold-drawn and tempered tubing made of Type 304 stainless steel. The Superior Tube Company listed a yield-strength range of 115,000 to 150,000 psi for this material. Although this was a wide yield-strength range, tests with the SAI seals had shown that good disk deflection could be obtained even when the tang did not yield. Thus, it was hypothesized that if the weakest tubing did not permit the tang to yield, the behavior of the seal with this material would be the same as it would be with the highest yield tubing. The decision was made to simulate the 115,000-psi-yield tubing by using 99,000-psi-yield A286. Insert rings were designed to provide comparable strength, and one 3/4-inch and one 1-inch SAI seal were modified accordingly.

The load test with the 1-inch seal gave the expected results. Although the tang yielded slightly, a radial load of 1490 lb/in. was measured and the sealing surfaces were comparable with those obtained with previous seals in which the tang did not yield. The 3/4-inch seal, however, was a disappointment. The load curve obtained on the tensile machine did not appear normal, and the radial load was only 1180 lb/in. This occurred despite the fact that the tang yielded less than it did in the 1-inch seal. When a second 3/4-inch seal gave duplicate results, it was concluded that an unknown factor was occurring in the deformation of the 3/4-inch seal.

Recommended Future Activities

Because of the promise of the one-metal seal approach, and because of the apparent deformation problem with the two-metal seal, it was recommended that future activities be concentrated on developing a satisfactory one-metal seal.

At the conclusion of the program, it appeared that the 21-6-9 should be selected for the 1/2-inch seal and that annealed and cold-drawn Type 304 should be selected for the 3/4- and 1-inch seals. However, there were still several areas about these materials and about 19-9DL that needed further understanding. Because the development of these areas might change the evaluations, it was recommended that a program be initiated in which additional material specimens would be purchased, a number of seals of each material and size would be machined and plated, and a number of load tests and selected performance tests would be conducted. Corrosion tests of the 19-9DL and 21-6-9 should also be included.

On the basis of this preliminary work, the best materials and seal designs should be selected for the 1/2- , 3/4- , and 1-inch seals and a comprehensive series of load

tests and performance tests should be conducted to demonstrate the adequacy of the design. Following this effort, the specifications should be revised accordingly.

Stress Relaxation

A previous section of the report has discussed theoretical and experimental efforts to determine the effect of stress relaxation in flanged connectors. The objective of this work was to demonstrate that flanged connectors would perform satisfactorily with a system storage life of 5 years. Similar, though less extensive, work was conducted in relation to threaded connectors.

It was estimated that the high-pressure (4000 psi) stainless steel threaded connectors would be more likely to show the effects of stress relaxation than the low-pressure (1500 psi) aluminum connectors. Further, it was believed that the 3/4-inch connectors would be representative of all the stainless steel threaded connectors. Thus, typical assembly modes were visualized for a number of 3/4-inch connectors, and test conditions were developed to simulate various missile storage applications.

It was expected that stress-relaxation might affect the performance of the threaded connectors in two ways: (1) by reducing the axial force applied by the nut and (2) by reducing the radial force at the sealing surfaces. If the axial force applied by the nut were reduced (by relaxation of the nut or of the connector flanges), combined pressure and structural loads on the connector might result in insufficient residual axial load on the seal, causing excessive leakage. Relaxation in the seal as a result of high compressive loading, or relaxation in the lips of the connector flanges as a result of high tensile and bending stresses, might reduce the radial load at the sealing surfaces sufficiently to cause leakage. Consideration of these failure modes led to the decision to use strain gages to measure nut relaxation, and helium leakage to measure excessive reduction in radial sealing loads.

Test Specimens

Table 67 shows the assembly conditions for the 22 test connectors used for the investigation of the effects of stress relaxation. Each connector was fabricated according to the dimensions in the specifications. Because stress relaxation increases rapidly with stress, it was expected that the amount of initial nut tension would significantly influence the amount of stress relaxation occurring in the nut. The torque levels shown in Table 67, and the different assembly methods were selected to produce the levels of initial nut tension expected in practice.

The nut of each connector is designed as a spring to maintain the proper axial load on the connector despite connector thermal gradients caused by hot or cold fluids. Thus the measurement of strain in the nut was an ideal means of determining the effect of stress relaxation on the axial load produced by the nut. The nut consists of three major sections: (1) the threaded portion, (2) the inward projecting nut ring, and (3) the relatively thin nut hub which connects the ring and the threaded portion. While the ring and the threaded portion contain large hoop strains, the nut hub is subjected for the most part to axial strains, and the strain gages were located on the nut hub.

TABLE 67. ASSEMBLY CONDITIONS FOR 3/4-INCH, STAINLESS STEEL CONNECTORS FOR STRESS-RELAXATION TESTS

Specimen	Assembly Condition	Assembly Method	Nut Load, lb	Helium Leak Rate on Assembly, atm cc/sec per inch of seal circumference
1[a]	Typical preload	Open-end wrench	5075	2.2×10^{-8}
2[a]	Typical preload	Open-end wrench	4830	0.5×10^{-8}
3[a]	Typical preload	Open-end wrench	4400	(c)
4	Min torque, 100 ft-lb	Open-end torque wrench	5100	(c)
5	Min torque, 100 ft-lb	Open-end torque wrench	7450	3.2×10^{-9}
6	Min torque, 100 ft-lb	Open-end torque wrench	3230	4.9×10^{-7}[d]
7[a]	Typical preload	Open-end wrench	4630	1.4×10^{-8}
8[a]	Typical preload	Open-end wrench	4370	0.48×10^{-9}
9[a]	Typical preload	Open-end wrench	7800	2.2×10^{-8}
10	Max torque, 116 ft-lb	Loc Rite torque wrench	7080	0.66×10^{-9}
11	Max torque, 116 ft-lb	Loc Rite torque wrench	8830	(c)
12	Max torque, 116 ft-lb	Open-end torque wrench	9050	(c)
13	Max torque, 116 ft-lb	Open-end torque wrench	10380	2.6×10^{-9}
14	Max torque, 116 ft-lb	Open-end torque wrench	7480	(c)
15	Max torque, 116 ft-lb	Open-end torque wrench	7860	(c)
16	Max torque, 116 ft-lb	Open-end torque wrench	5370	1.2×10^{-8}
17	Max torque, 116 ft-lb	Open-end torque wrench	6420	0.9×10^{-9}
18	Max torque, 116 ft-lb	Open-end torque wrench	7340	0.69×10^{-9}
19	Max torque, 116 ft-lb	Open-end torque wrench	7150	0.48×10^{-9}
20[b]	Max torque, 116 ft-lb	Open-end torque wrench	7370	1.1×10^{-8}
21[b]	Max torque, 116 ft-lb	Open-end torque wrench	7740	(c)
22[b]	Max torque, 116 ft-lb	Open-end torque wrench	9930	4.7×10^{-8}

(a) Nut was tightened to achieve approximate desired strains in nut.
(b) Nut threads were electropolished.
(c) No leakage could be detected.
(d) Connector was left on test even though measured leak rate was excessive on assembly.

One gage was placed on each of three of the six nut flats midway between the ring and the threaded portion. Although it would have been desirable to place the gages on alternating nut flats, this would have prevented proper tightening of the nut with a wrench. Thus two of the gages were placed on adjacent nut flats.

The gages on each nut were calibrated before the connectors were assembled. This was done by loading each nut in a tensile machine and reading each gage at load-level increments. This method was used to circumvent the effects on the measured strains of triaxial stresses in the nut and minor variations in strain-gage locations. Table 68 shows the increment of strain for each gage at the major tensile loads.

Test Conditions

Three types of tests were selected to represent various types of storage systems: (1) static, (2) static with constant, maximum system pressure and end loading, and (3) static with periodic stress-reversal-bending tests. These tests also represented increasing probability of connector leakage.

Each connector for the static relaxation test was equipped with a flange at one end and a welded closure at the other. The flanged end was mounted to a manifold that was connected to a source of 4000-psi helium. When the leakage of the connectors was checked periodically, the manifold was pressurized, and an O-ring sealed vacuum chamber was slipped over each connector. A helium mass spectrometer connected to the vacuum chamber was used to measure the leakage of the connector.

For the static, full-load tests, each connector was mounted to a manifold similar to the static test connectors. In addition, the closed end of each connector was attached to a hydraulic cylinder. For the duration of the test, the manifold and the connector were kept pressurized by 4000-psi helium, and the hydraulic cylinders were kept pressurized to exert a constant, maximum axial structural load on the connectors. For periodic leakage measurement, the hydraulic cylinders were disconnected and a vacuum chamber was slipped over each connector and helium leakage was measured with a mass spectrometer.

Each connector subjected to the dynamic tests was assembled as part of a cantilever beam to fit the stress-reversal-bending equipment used during Contract AF 04(611)-9578. The connectors were maintained in a static condition without load until the periodic checking period. At that time, each connector was subjected to 200,000 cycles of stress-reversal bending and each connector was leak-checked with the helium mass spectrometer.

Leak checks and dynamic tests were conducted at 1, 5, 9, and 24-month intervals. Also at these time intervals, strain-gage readings were made with no load, with internal pressure, and with internal pressure plus axial tension loading.

TABLE 68. INCREMENT OF STRAIN FOR THE NUT STRAIN GAGES AT THE MAJOR TENSILE LOADS, 3/4-INCH STAINLESS STEEL CONNECTORS

Nut	Gage	Nut Tensile Load, lb, Strain, Microin./in. 1000	2000	3000	4000	5000	6000	Strain for 6000-Lb Tensile Load
1	a	180	170	170	180	190	200	1090
	b	165	205	205	205	195	210	1185
	c	210	220	220	225	225	200	1300
2	a	220	180	205	230	230	235	1300
	b	180	175	175	180	190	190	1090
	c	205	180	195	190	205	205	1180
3	a	205	235	235	230	235	240	1380
	b	295	210	195	195	200	215	1310
	c	245	220	215	210	220	235	1345
4	a	195	230	225	235	220	225	1330
	b	240	190	205	215	210	230	1290
	c	260	235	230	240	240	250	1455
5	a	270	235	225	230	225	225	1410
	b	235	240	225	225	220	220	1365
	c	230	205	205	210	215	220	1285
6	a	260	270	245	245	245	245	1510
	b	205	240	240	235	245	240	1405
	c	250	220	220	220	230	220	1360
7	a	160	165	190	210	210	210	1145
	b	230	215	220	225	230	230	1350
	c	290	125	225	220	230	230	1320
8	a	225	210	200	190	195	190	1210
	b	165	165	175	185	190	190	1070
	c	240	200	190	200	200	210	1240
9	a	205	225	230	230	220	225	1335
	b	225	190	205	220	220	230	1290
	c	235	225	230	235	235	245	1405
10	a	180	170	200	200	205	210	1165
	b	300	230	230	220	220	230	1430
	c	250	240	220	215	215	220	1365
11	a	180	190	195	200	205	200	1170
	b	170	180	185	200	210	215	1160
	c	200	200	205	210	220	235	1270
12	a	245	255	230	235	215	220	1400
	b	220	220	210	210	210	220	1290
	c	180	175	190	195	205	210	1155
13	a	180	160	165	180	195	190	1070
	b	180	195	205	210	220	235	1245
	c	225	205	215	215	220	220	1300
14	a	235	260	240	230	230	240	1435
	b	185	165	180	195	200	205	1130
	c	180	150	180	185	195	210	1100
15	a	150	150	155	185	190	190	1020
	b	195	195	200	200	210	205	1205
	c	215	220	225	200	215	210	1285
16	a	195	210	210	210	205	215	1245
	b	240	185	200	200	200	195	1220
	c	240	215	220	225	225	230	1355
17	a	230	230	210	200	215	220	1305
	b	240	210	200	190	190	190	1220
	c	180	215	185	190	200	200	1170
18	a	235	200	195	190	195	195	1210
	b	195	190	200	205	220	215	1225
	c	220	195	200	215	220	220	1270
19	a	225	220	210	205	215	210	1285
	b	205	205	205	200	210	210	1235
	c	245	220	215	220	220	225	1345
20	a	205	185	190	205	205	210	1200
	b	180	215	215	230	230	230	1300
	c	250	225	215	220	215	220	1345
21	a	215	220	210	210	205	210	1270
	b	230	210	215	220	215	225	1315
	c	285	220	220	220	230	230	1405
22	a	155	195	185	190	195	195	1115
	b	195	185	180	205	190	195	1150
	c	195	200	200	220	220	225	1260

Test Results

The tubing of one connector broke during the last stress-reversal-bending "exercise" and it was not possible to leak-check this connector. However, none of the remaining 21 connectors showed an increase in helium leakage during any test above the values measured on initial assembly. In fact, in most cases it was not possible to detect any leakage.

After the strain-gage readings were taken at the 24-month interval, an examination of the readings showed variations which were not explainable by the action of the fitting structure. A discussion of this problem with a Battelle-Columbus specialist led to the conclusion that changes in the resistance of the lead wires during the 2-year period had introduced excessive reading variations. Since the total change in nut tension was the measurement of primary interest, it was decided that the purposes of the test would still be met if strain-gage readings were taken before and after the disassembly of each connector. These strains could then be compared with the strains developed on assembly to determine the relaxation in each nut.

Table 69 shows the tests conducted with each connector, the strains measured by each gage on assembly and on disassembly, and the estimated initial and final axial loads on each nut. Of the 22 nuts involved, six showed an increase in average strain. This resulted when a strain gage that read low on assembly indicated an increasingly higher value during the 2 years, closer to that read with the other two gages. Of the remaining 16 connectors, the average strains for three connectors decreased less than 10 percent, seven decreased less than 20 percent, and four decreased less than 35 percent. Of the remaining two connectors, the average strain for one decreased about 45 percent, and that for the other decreased about 70 percent. In general it was found that the nuts with the highest initial tensile load showed the largest reductions in strain. If the initial tension was above the required minimum of 5690 pounds, the residual tension was within 20 percent of the required minimum. The one exception was the connector that experienced a 70 percent reduction in tension to give a residual tension of 2580 pounds. These results, combined with the fact that no connectors exhibited increased leakage during the 2-year test period, indicated that stress relaxation is not a source of leakage in threaded connectors during 2 years of storage. Since the rate of stress relaxation reduces on a log-log basis with a reduction in stress, it is believed that the successful 2-year-storage tests indicate that the connectors will be satisfactory for a 5-year-storage period.

TABLE 69. MEASURED STRAINS AND AXIAL NUT LOADS FOR 3/4-INCH STAINLESS STEEL CONNECTORS BEFORE AND AFTER 24 MONTHS STRESS RELAXATION TESTS

Connector	Type of Test	Nut Strain, μin./in., 6000-Lb Load	Nut Strains on Assembly, μin./in. a	b	c	Av.	Est. Axial Load, lb	Nut Strains on Disassembly, μin./in. a	b	c	Av.	Est. Axial Load, lb.	Load Change, lb
1	Static, Loaded	1192	1050	1085	890	1008	5075	1045	1025	890	987	4960	-115
2	Static, Loaded	1190	530	1160	1185	958	6830	950	1090	1085	1042	5250	+420
3	Static	1345	635	1145	1175	985	4400	1040	1145	1110	1098	4900	+500
4	Static, Loaded	1358	830	1730	900	1153	5100	825	1360	865	1017	4500	-600
5	Static, Loaded	1353	1410	2255	1380	1682	7450	1280	1580	1245	1368	6060	-1390
6	Static	1425	710	1075	515	767	3230	720	815	660	732	3080	-150
7	Static, Loaded	1272	565	1280	1105	983	4630	1005	1215	1050	1090	5140	+510
8	Static, Loaded	1173	450	1040	1075	855	4370	825	955	1035	938	4790	+420
9	Static	1343	1210	2030	2000	1747	7800	1630	1935	1770	1778	7930	+130
10	Static, Loaded	1320	1505	1490	1685	1560	7080	1340	1485	1500	1442	6550	-530
11	Static, Loaded	1200	1565	2025	1705	1765	8830	1280	1830	1475	1528	7640	-1190
12	Static	1282	1485	2690	1620	1932	9050	1275	1680	1025	1323	6190	-2860
13	Static, Loaded	1205	1590	2640	1830	2020	10380	1210	2310	1625	1715	8820	-1560
14	Static, Loaded	1222	1155	2355	1065	1525	7480	1040	1330	955	1108	5440	-2040
15	Static	1170	1055	2330	1210	1532	7860	875	1050	850	925	4740	-3120
16	Dynamic	1270	940	1400	1075	1138	5370	800	1120	965	955	4520	-850
17	Dynamic	1232	1005	1650	1300	1318	6420	1165	1893	1119	1392	6780	+360
18	Dynamic	1235	1250	2150	1130	1510	7340	745	385	460	530	2580	-4760
19	Dynamic	1288	1650	1590	1360	1533	7150	750	1580	1430	1253	5840	-1310
20	Static, Loaded	1282	1340	2085	1300	1575	7370	960	1845	1050	1285	6020	-1350
21	Static, Loaded	1330	1200	2640	1310	1717	7740	1085	1640	1145	1290	5820	-1920
22	Static	1175	1420	2915	1500	1945	9930	1300	1895	1355	1517	7740	-2190

VI

CONCLUSIONS AND RECOMMENDATIONS

Many conclusions and recommendations have been given in different parts of the report. The major items are repeated here in three categories: (1) aluminum flanged connectors, (2) stainless steel flanged connectors, and (3) threaded-connector support.

Conclusions

Aluminum Flanged Connectors

(1) An effective, computerized procedure has been developed for designing AFRPL flanged connectors for aluminum tubing systems.

(2) Satisfactory qualification tests have been conducted for 100-psi, 200-psi, and 500-psi connectors through 16 inches in diameter, and for 1000-psi and 1500-psi connectors through 3 inches in diameter.

(3) Additional qualification tests are required for selected performance aspects of 1000-psi and 1500-psi connectors through 16 inches in diameter.

(4) Additional test data are required concerning the maximum stress level that can be permitted for all 3-inch connectors in a vibration mode.

Stainless Steel Flanged Connectors

(1) An effective, computerized procedure has been developed for designing AFRPL flanged connectors for stainless steel tubing systems.

(2) Satisfactory qualification tests have been conducted for pressures of 6000 psi for sizes through 3 inches in diameter, and for pressures of 100 psi for sizes through 8 inches in diameter.

(3) Additional qualification tests are required for selected performance aspects for pressures through 1500 psi and for sizes through 16 inches in diameter.

Threaded-Connector Support

(1) Stress relaxation is not expected to cause leakage in AFRPL threaded connectors.

(2) The seal retention and misalignment limitation concepts developed and evaluated during the program are not practical for the purposes of the AFRPL connector.

(3) The radial sealing load should be increased for the seals for the 1/2-, 3/4-, and 1-inch stainless steel connectors. Promising approaches have been determined.

Recommendations

Aluminum Flanged Connectors

(1) It is recommended that specifications be prepared for 100-psi, 200-psi, and 500-psi connectors through 16 inches in diameter, and for 1000-psi and 1500-psi connectors through 3 inches in diameter.

(2) It is recommended that additional qualification tests be conducted to investigate the following performance features of the 1000-psi and 1500-psi connectors through 16 inches in diameter: (a) deformation characteristics of the seal structure and (b) resistance of the connectors to pressure-impulse cycles.

(3) It is recommended that additional vibration tests be conducted with 3-inch connectors to determine an appropriate stress level for a minimum life of 200, 000 cycles.

Stainless Steel Flanged Connectors

(1) It is recommended that specifications be prepared for pressures through 6000 psi for connector sizes through 3 inches in diameter, and for pressures of 100 psi for sizes through 8 inches in diameter.

(2) It is recommended that additional qualification tests be conducted to investigate the following performance characteristics for connectors for pressures through 1500 psi, and for sizes through 16 inches: (a) initial sealing reliability, and (b) resistance to thermal gradients.

(3) It is recommended that dimensions be developed for the remaining connectors listed on page 152.

Threaded Connector Support

(1) It is recommended that a seal retention concept be investigated on the basis of the preseating of the seal in one of the connector flanges prior to assembly of the connector.

(2) It is recommended that the assembly procedures of the AFRPL connector include the requirement that the parts be sufficiently aligned

and free on assembly to permit the seal disks to be placed completely within the flange cavities and the nut made fingertight.

(3) It is recommended that a program be initiated to select the best designs for stronger 1/2-, 3/4-, and 1-inch stainless steel seals, and that the adequacy of these designs be demonstrated by qualification tests.

VII

REFERENCES

(1) MS Standards MS27850 through MS27868 (USAF) and Military Specifications Nos. MIL-P-27417 (USAF) and MIL-P-27418 (USAF), July 14, 1967.

(2) Nadai, A., The Theory of Flow and Fracture of Solids, Second Edition, McGraw-Hill Book Company, Inc. (1950). Vol. I.

(3) Beliaev, N. M., and Sinitskii, A. K., "Stress and Strain in Thick Wall Cylinders in Elastic-Plastic State", Izvestiia Akademii Nauk USSR Otdelenie Teknicheskikh Nauk, No. 2, 3-54 (1938).

(4) Glackin, J. J., and Gowen, E. F., Jr., "Evaluation of Fasteners and Fastener Materials for Space Vehicles", NASA CR-357 (January, 1966).

(5) Price, J. I., and Trask, D. K., "The Relation Between Torque and Tension for High Strength Threaded Fasteners", National Bureau of Standards Report 7308 (August, 1961).

(6) Bronson, K. R., and Faroni, C. C., "Vibration of Thread-Locking Devices", Product Engineering (October 10, 1960).

(7) Glackin, J. J., and Gowen, E. F., Jr., "Evaluation of Fasteners and Fastener Materials for Space Vehicles", Seventh Quarterly Progress Report, Contract NAS8-11125, SPS Laboratories, May, 1965, through July, 1965.

(8) Viglione, J., "Nut Design Factors for Long Life", Machine Design (August 5, 1965).

(9) "Some Problems of Fatigue of Bolts and Bolted Joints in Aircraft Applications", NBS Technical Note 136, PB 161637 (1962).

(10) Yeomans, H., "Programme Loading Fatigue Tests on a Bolted Joint", Technical Note No. Structures 327, Royal Aircraft Establishment, Ministry of Aviation, London, England (1963).

(11) Sproat, R. L., "A Checklist on Fastener Reliability", Missile Design and Development (June, 1960).

(12) Richter, G., "Factors Affecting the Failure of Screws and Bolts in Service", Engineer's Digest (March, 1965).

(13) "Unfired Pressure Vessels", Section VIII, ASME Boiler & Pressure Vessel Code, ASME, New York (1965).

(14) Peterson, R. E., Stress Concentration Design Factors, J. Wiley & Sons, New York (1953), p 3.

(15) "Nuclear Vessels", Section III, ASME Boiler & Pressure Vessel Code, ASME, New York (1968).

(16) Bauer, P., Glickman, M., and Iwatsuki, F., "Analytical Techniques for the Design of Seals for Use in Rocket Propulsion Systems", AFRPL-TR-65-61, 2 Volumes (May, 1965).

(17) Bauer, Paul, "Investigation of Leakage and Sealing Parameters", AFPL-TR-65-153 (August, 1965).

(18) "Zero Leakage Design for Ducts and Tube Connections for Deep Space Travel", 6 Volumes, General Electric Co. Mechanical Technology Laboratory, Contract NAS8-11523 (1967).

(19) Goobich, B., Adam, J. W., Baum, J. V., and Trainer, T. M., "Development of AFRPL Threaded Fittings for Rocket Fluid Systems", Battelle Memorial Institute, RTD-TDR-63-1115, December, 1963 (AD 426290).

(21) Timoshenko, S., and Goodier, J. W., Theory of Elasticity, Second Edition, McGraw-Hill Book Company, Inc. (1951), Chapter 4.

(22) Goobich, B., Thompson, J. R., and Trainer, T., "Development of Aluminum Bobbin Seals for Separable Connectors for Rocket Fluid Systems, Phase I", Battelle Memorial Institute, AFRPL-TR-67-191 (July, 1967) (No foreign nationals without RPL approval).

APPENDIX A

RELAXATION DESIGN OF SEPARABLE TUBE CONNECTORS

(This report has been included with the permission of the National Aeronautics and Space Administration and the Advanced Technology Laboratories of the General Electric Company.)

APPENDIX A

RELAXATION DESIGN OF SEPARABLE TUBE CONNECTORS

by

L. M. Cassidy, E. C. Rodabaugh, D. B. Roach, and T. M. Trainer

INTRODUCTION

The design of separable tube connectors for operating below the temperature which produces significant creep of the metal used in the connector may be based on conventional elastic analysis methods. For example, the ASME Unfired Pressure Vessel Code[1]* gives a widely accepted method for designing bolted-flanged joints, including an approximation of the required bolt load and an elastic analysis of the flanges to insure adequate flange strength for carrying the required bolt load.

Even at temperatures where creep does not occur, the design of a conventional separable tube connector is not simply a strength problem, since the usual criterion of failure is leakage and leakage may occur without necessarily overstressing any part of the connector. In practice, conventional connectors are initially loaded (tightened bolts in a bolted-flanged connector, tightened nut in a threaded connector) so that the elastically stored forces in the connector are sufficient to prevent separation of the connector parts due to the subsequently applied service loads arising from internal pressure or loads on the attached pipe or tubing. Accordingly, not only the stresses but also the strains or displacements are significant in connector design.

At operating temperatures where significant creep occurs, the design method for the connector must take into account the relaxation of the elastically stored forces which occur as a result of the plastic flow of the metal components. In bolted-flanged joints designed in accordance with the ASME Code[1], this relaxation effect is taken into account in an indirect and approximate manner by the use of allowable stresses which are based on creep or stress-to-rupture properties of the material. These allowable stresses, however, do not necessarily reflect the relaxation characteristics of bolted-flanged joints in general, and use of the method may result in excessively conservative design or inadequate performance over the desired service life.

There have been previous discussions and simplified analyses[2,3,4,5,6,7] of relaxation in bolted joints. Unfortunately, a practical solution considering primary creep does not appear to have been developed. The method of analysis presented in this report is intended as a workable approach to the design of separable tube connectors at temperatures where creep or relaxation occurs.

The only known published data on the elevated-temperature testing of separable connectors in order to study leakage is a very comprehensive set of tests[8,9,10] by the British Pipe Flanges Research Committee on bolted-flanged joints. The results of these tests indicate a definite relation between the time to leakage and the temperature. However, the results are not amenable to a theoretical analysis because of the lack of sufficient specimen creep or relaxation data on the materials used in the test.

Material properties are, of course, interrelated with the design procedure. Accurate information of material properties (such as yield strength, modulus of elasticity, and creep or relaxation rates) are needed to apply the design procedure. Accordingly, this report includes a discussion of material properties and tabulation of properties for various materials with desirable high-temperature properties. The section of the report on material properties leads to a selection of an optimum material for use in connector design for aerospace application at 1440 F operating temperature.

SUMMARY

Materials were evaluated for use at 1440 F, with the result that René 41 is the material choice for the connector design. René 41 is equivalent in strength to the other candidate materials at 1440 F, and has a greater amount of data available. In addition, René 41 is readily available and has seen considerable research and service experience. Nevertheless, the lack of a suitable family of creep curves at 1440 F led to the recommendation that creep or relaxation data be generated for René 41.

With the expectation that relaxation data will not be available for most materials, the design method is directed primarily toward the utilization of creep data, with a discussion on the use of relaxation data. The widespread scatter in creep data as well as possible secondary effects, such as those discussed in Appendix C, led to the use of a design factor of safety.

The design procedure utilizes the steady-state or power law of creep with an assumed zero time reduction in stress to account for primary creep. This approach is conservative for short times, the degree of conservatism depending upon the amount of primary creep exhibited by the material at the design temperature. A comparison is shown for predicting relaxation from creep data for various creep theories.

Both bolted-flanged and threaded connectors are included in the relaxation design, and sample calculations are provided to illustrate the design method for each type of connector. The effect of temperature differentials and external loads on the leakage pressure** is considered. Secondary effects such as stress concentrations, creep bending of bolt, dynamic creep, gasket creep, and flange rotations are discussed briefly, but are not included as an integral part of the design procedure.

The design method is suitable for hand calculations, but could be expedited and easily adapted for solution on a high-speed computer. The optimum (minimum weight) design for a given value of leakage pressure can be determined only after calculating a wide range of geometries. A suitable number of calculations enables the static** design to be rated in accordance with various combinations of leakage pressure and time. The detailed gasket design is not considered herein, since Reference (11) is quite comprehensive in this respect.

Various methods of analyses are discussed for the creep design of tubes. The data available indicate that a suitable approach for the tube design is to design for the tangential (hoop) stress on the basis of uniaxial tensile creep data.

RECOMMENDATIONS

On the basis of the subject design study, the following recommendations are made in support of the over-all design effort for separable tube connectors:

(1) Creep and/or relaxation data on René 41 at 1440 F, preferably relaxation data, should be generated.

(2) It is recommended that a design factor of safety of 2.0 be used. However, one or more René 41 connectors should be tested at 1440 F in order to substantiate this factor of safety.

(3) Avoid yielding of the connector components due to stresses incurred during installation.

(4) Even though retightening of the connector compensates for the bolt or nut relaxation, care must be taken not to incur excessive deformations in the component parts which could lead to rupture.

(5) In order to be conservative, the cycle time should be measured from the start of the heating cycle to the end of the cooling cycle.

(6) Consideration should be given to various design configurations. For example, loose-type bolted flanges may offer certain advantages over integral-type flanges which would not be realized in a static design.

NOMENCLATURE**

α	= mean coefficient of thermal expansion, in/in/°F
A	= area of bolt, gasket, tube, or flange, in.
c	= inner radius of flange or tube, in.
C_1	= coefficient in steady-state creep law
C_2	= coefficient in intercept stress law
d	= outer radius of flange or tube, in.
δ	= deflection, in.
e	= moment arm for flange bending, in.
ϵ	= normal strain, in/in.
$\dot{\epsilon}$	= strain rate = $\frac{d\epsilon}{dt}$, in/in/hr
E	= modulus of elasticity, psi
F_B	= bolt flexibility, in/lb
F'_B	= bending flexibility of the "bolt" (threaded connector), in/lb
F_F	= flange flexibility at bolt circle, in/lb
F.S.	= design factor of safety
g	= radius to centerline of gasket, in.
h	= flange thickness, in.
θ	= rotation, radians
K_B	= creep rate of bolts, in/hr
K'_B	= bending creep rate of the "bolt" (threaded connector), in/hr
K_F	= creep rate of flanges, in/hr
L	= influence coefficient from Page 138, Paragraph UA-47, of the ASME Code[1]
L_B, L_F	= effective length of bolt and flange, respectively, in.
m	= exponent in intercept stress law
M	= flange bending moment = Pe, in-lb
ν	= Poisson's ratio
n	= exponent in steady-state creep law

*Numbers in raised parentheses designate References on page 39.

**Leakage pressure refers to the value of uniform internal pressure at or below which tolerable leakage rates occur, and should not be confused with the value of gasket pressure required for (1) initially seating the gasket or (2) residual pressure required on the gasket in order to prevent excessive leakage rates. The determination of these gasket conditions is not covered in this report.

**Static design refers to a conventional type design such as the ASME Boiler Code[1], which is not time dependent.

**The nomenclature of the ASME Code[1] is used consistently in the sample Code calculations on pages A-13 and A-14, and is used elsewhere in the report where necessary for clarity.

p = uniform internal pressure, psi

P = total bolt load, lb

P_i' = design value for residual bolt load = $\frac{P_i}{F.S.}$, lb

r_F = flexibility ratio = F_F/F_B

$r_{F'}$ = flexibility ratio = $F_{F'}/F_B$

r_K = creep ratio = K_F/K_B

$r_{K'}$ = creep ratio = $K_{F'}/K_B$

R = life factor = $\frac{1+r_F}{1+r_K}$ (bolted-flanged connector) or $\frac{1+r_F+r_{F'}}{1+r_K+r_{K'}}$ (threaded connector)

σ = normal stress, psi

t = time, hr

ΔT = temperature differential, °F

V = influence coefficient from Figure UA-51.3, Page 144, Paragraph UA-51 of the ASME Code[1]

w = width of gasket, in.

Subscripts

A = axial load	r = radial direction in tube
B = bolt	R = room temperature
c = creep	t = time
e = elastic	T = tube or design temperature
F = flange	ϕ = circumferential direction in tube
G = gasket	y = yield
M = bending moment	z = axial direction
o = intercept or zero time	

CREEP AND RELAXATION

Creep and relaxation are closely related, even though they are not necessarily interchangeable in a stress-analysis problem. These phenomena play an important role in the behavior of a separable connector operating at elevated temperatures, and are best illustrated by mechanical models.

Creep is the tendency for a material to exhibit time-dependent strains at a constant stress level, typical of metals at elevated temperatures. Figure 1 shows a typical creep curve (neglecting tertiary creep) and the corresponding Maxwell-Kelvin model. Figure 1 is obtained by superposition of the Maxwell and Kelvin models of Figures 2 and 3, representing the steady-state and primary creep, respectively. The enclosed design procedure utilizes an equivalent Maxwell model, shown as the dashed curve in Figure 1. The total strain is made up of an instantaneous strain and a time-dependent (steady-state) strain. The instantaneous or intercept strain ϵ_o includes the elastic strain ϵ_e plus an additional strain $C\sigma_o^m$ which conservatively accounts for the primary creep period.

Relaxation is the reduction or relaxation of stress in time under a constant strain. Elastic strains are replaced by creep strains, causing a progressive reduction in stress. The models in Figures 1-3 can be considered relaxation models by assuming a constant total strain rather than a constant stress.

There has been considerable literature written on how to predict relaxation from creep data, few agreeing on the best creep theory to use. Although there are very few test data available on the same material to enable a comparison of various theories, Finnie and Heller[7] made a comparison of copper at 165 C with an initial stress of 13,500 psi. Figure 4 shows that the steady-state creep law with the intercept stress reduction used herein is conservative for short times and shows good agreement with the experimental results for longer times. Of course, the time scale would be quite reduced for a superalloy at 1440 F.

The most basic form of a separable connector would be flexible bolting in a pair of rigid flanges, in which case the model of Figure 1 would suffice for a relaxation analysis. The tightness of the joint would be dependent on the ability of the bolt to resist creep deformations. However, the flange assembly can also be represented by a Maxwell model in parallel with the bolt assembly. The flange can increase or decrease the rate of bolt relaxation, depending upon the characteristics of the flange geometry. A properly designed flange assembly should be superior to a rigid flange in that the flange elastic recovery as a spring will retard the bolt relaxation.

MATERIALS

At the initiation of the program, it was thought that the connector might be exposed to service temperatures in the range from 70 F to a maximum of 1700 F. The upper temperature limit was subsequently changed to 1440 F. Consequently, material properties are evaluated at both 1700 F and 1440 F, and a material selection made at 1440 F.

Introduction

At the initiation of the materials survey, it was apparent that certain material properties were of major importance in establishing the optimum connector design. Strength over the desired temperature range was an prime criterion. In addition, because of the continued requirement to design space vehicles with minimum weight, density (or strength-to-density ratio) was a major consideration. Also, because service conditions involve cycling from maximum temperature to room temperature, thermal shock, embrittlement, and oxidation were also considered important criteria.

Of the various strength parameters, creep strength and resistance to relaxation were considered of utmost importance. In the installation of a separable connector, the connector is tightened to a given stress. To prevent leakage during service, this stress should remain sufficiently high during service. Relaxation or creep during service will tend to loosen the joint and may give rise to leakage. In addition, good rupture strength and ductility are deemed necessary to insure against complete, catastrophic failure of the connector. Also, because the connector will be installed and tightened at room temperature, consideration must be given to thermal expansion of the connector during heating to the maximum temperature. Variations in thermal expansion of different materials comprising the tubing and the connector could lead to tightening of the connector and undue stress, or to loosening of the connector and leakage.

In addition, consideration was given to the availability, fabricability, machinability, and weldability of the various candidate materials. Of particular importance was the general engineering "know-how" in the handling and use of the various alloys. Finally, since the connector should be capable of being loosened or tightened periodically, consideration was given to bonding or self-welding of the various candidate materials under service conditions.

Material Properties

As indicated above, candidate alloys for separable connectors must have good creep, rupture, and relaxation strengths over the anticipated service-temperature range. Good resistance to thermal shock, oxidation, and embrittlement during cyclic service is also required. These requirements are almost identical to those involved in selection of alloys for turbine-bucket application in aircraft gas turbines. Turbine-bucket materials, however, are not selected on the basis of relaxation resistance, although rupture strength and creep resistance are major requirements. At the present time, turbine-bucket materials are selected on the basis of rupture strength and thermal-shock resistance. Thus, it was evident that the requirements for separable connectors were sufficiently similar to those of turbine buckets that a summary of the various turbine-bucket materials would likely yield those alloys having the most desired combination of properties for the design of high-temperature separable connectors.

A survey of published property data for various nickel- and cobalt-based superalloys was conducted. Emphasis was placed on creep and rupture strength at 1700 F, and on short-time tensile properties over the service-temperature range. A search of the literature revealed that relaxation data were not available for the bulk of the alloys of interest. On the basis of this survey, the following alloys were selected for more thorough examination:

Wrought Alloys

(1) Astroloy
(2) Nimonic 105
(3) Nimonic 115
(4) René 41
(5) Udimet 700
(6) Unitemp 1753
(7) Waspaloy

Cast Alloys

(8) GMR 235
(9) IN-100
(10) Inco 713C
(11) Nicrotung
(12) SM 200
(13) SM 302
(14) SM 322

These alloys have the highest strength at 1700 F. All have been, or, are being considered for use as turbine buckets in gas-turbine engines. Not all of these alloys are readily available, and not all are weldable.

In addition, three more common, lower strength superalloys on which extensive experience in fabrication and usage is available were studied for comparison purposes. These were:

(15) Inconel X
(16) N 155
(17) S 816

Typical compositions for these 17 alloys are given in Table 1.

Alloys for Use at 1700 F

The typical properties of the 17 candidate alloys are given in Table 2. It will be noted in this table that short-time tensile and rupture data were available for the bulk of the alloys. Creep data at 1700 F were quite often lacking. Where creep data were not available at 1700 F, information on the creep strength at lower temperatures was included.

TABLE 1 NOMINAL COMPOSITIONS OF SUPERALLOYS

Alloy	Form: Wrought	Form: Cast	C	Cr	Co	Fe	Ni	Mo	W	Al	B	Ti	Zr	Other
Astroloy	X		0.10	15.0	15.5		Balance	5.0	-	4.2	0.03	4.0	-	-
Nimonic 105	X		0.15	15.0	20.0	-	Balance	5.0	-	4.7	-	1.2	-	-
Nimonic 115	X		-	-	-	-	-	-	-	-	-	-	-	-
Rene' 41	X		0.09	19.0		-	Balance	10.0	-	1.5	0.006	3.0		-
Udimet 700	X	X	0.10	15.0	16.5	-	Balance	5.2	-	4.3	0.030	3.5	-	-
Unitemp 1753	X		0.20	16.0	7.5	9.5	Balance	1.5	0.4	1.9	0.020	3.7	0.05	-
Waspaloy	X		0.08	19.0	13.5	-	Balance	4.3	-	1.3	0.008	3.0	0.08	-
GMR-235		X	0.14	16.0	-	10.0	Balance	5.5	-	3.0	0.05	2.0	-	-
IN 100		X	0.18	10.0	15.0	-	Balance	3.0	-	5.5	0.015	5.0	0.06	-
Inco 713C		X	0.14	12.0	-	-	Balance	4.5	-	6.0	0.012	0.5	0.05	2.0 Cb
Microtung		X	0.10	12.0	10.0	-	Balance	-	3.0	4.0	0.05	4.0	0.05	-
SM-200		X	0.15	9.0	10.0	1.5	Balance	-	12.5	5.0	0.015	2.0	0.4	1.0 Cb
SM-302		X	0.95	21.5	Balance	0.8	-	-	-	10.0	0.005	-	0.2	9.0 Ta
SM-327		X	1.00	21.5	Balance	1.5	-	-	-	9.0	-	0.75	2.25	4.5 Ta
Inconel X	X		0.06	16.0	-	7.0	Balance	-	-	0.80	-	2.5	-	1.0 Cb
N-155	X	X	0.15	21.0	20.0	Balance	20.0	3.0	-	-	-	-	-	1.0 Cb + 2.5 V
S 816	X		0.40	20.0	44.0	Balance	20.0	4.0	4.0	-	-	-	-	4.0 Cb

TABLE 2 PROPERTIES OF SUPERALLOYS AT 1700 F

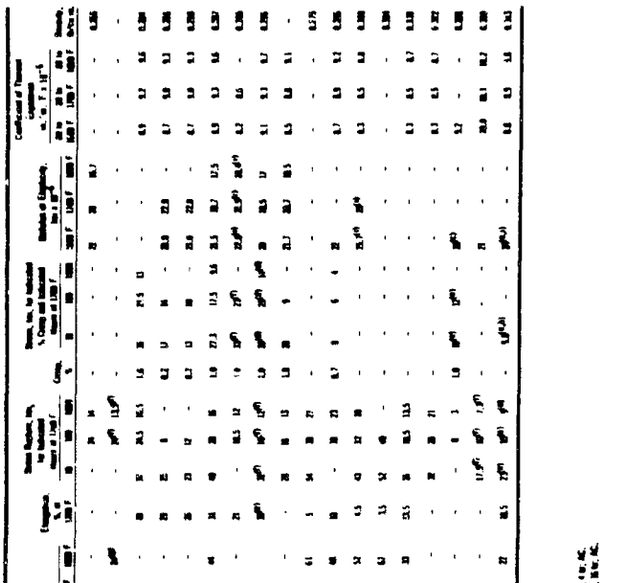

On the basis of yield strength at 1700 F and creep and rupture strengths at 1700 F, it is evident in Table 2 that the cast alloys have significantly higher strength than the wrought alloys. Of the 17 candidate alloys, SM 200, IN 100, Microtung, and Udimet 700 are the highest strength alloys at 1700 F. Of these only Udimet 700 is a wrought material. Of the wrought materials, the order of decreasing strength at 1700 F may be listed as Udimet 700, Nimonic 115, Unitemp 1753, Rene 41, and Waspaloy.

In general, it was found that the cobalt-based alloys were of lower strength than the nickel-based alloys.

It will be noted that the coefficients of thermal expansion of these alloys were quite similar in the temperature range from 1600 to 1800 F. Likewise, the density values for the nickel-base alloys were quite similar. Those alloys containing significant amounts of tungsten, of course, had slightly higher density values than those containing little tungsten. Because the density values were so similar, there was little merit in comparing the alloys on a strength-to-density basis.

Alloys for Use at 1440 F

It was subsequently decided that the maximum operating temperature for the connector should be reduced from 1700 to 1440 F. Consequently, a survey of the properties of the 17 alloys listed in Table 1 was made to ascertain the most promising alloys at this reduced temperature. The properties of the alloys at 1400 and 1500 F are summarized in Table 3. Where possible, values at 1440 F were interpolated.

TABLE 3 PROPERTIES OF SUPERALLOYS AT 1400-1500 F

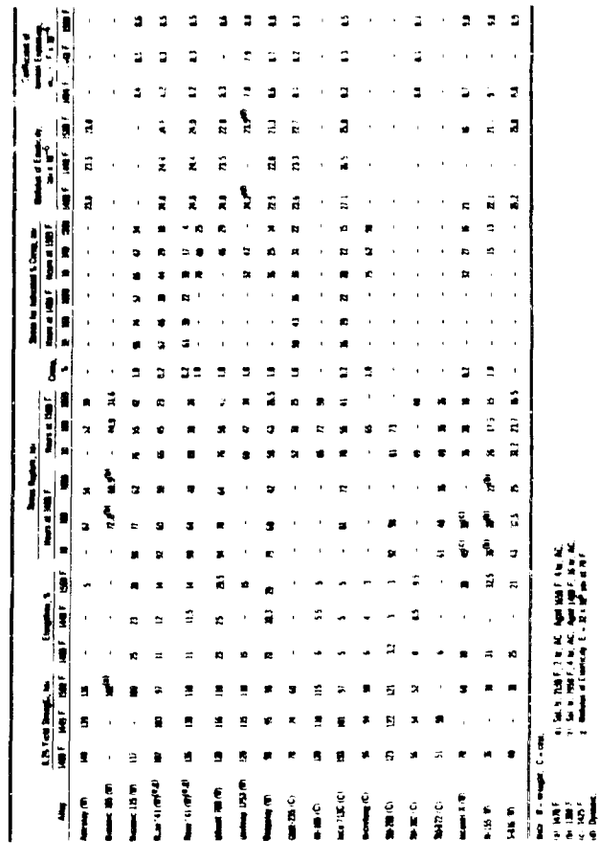

The data given in Table 3 show that the wrought alloys compare more favorably with the cast alloys at this temperature than they did at 1700 F. It will be noted that on the basis of yield strength at 1400 to 1500 F, Rene 41 and Astroloy (Udimet 700) compare favorably with SM 200 and IN 100. On the basis of stress for rupture in 10 hours at 1400 F, SM 200, Udimet 700, Nimonic 115, and Rene 41 have very similar strengths. For longer times at 1400 F and at 1500 F, Rene 41 compares less favorably with these other alloys. It will be noted that at 1500 F and above, Waspaloy has strength properties equal to Rene 41. In the range of 1400 to 1500 F, Rene 41 has appreciably better short-time tensile properties and higher short-time (10-hour) rupture and creep strengths than Waspaloy.

Material Selection

On the basis of the material properties cited in the preceding section, SM 200, Udimet 700, Nimonic 115, IN 100, and Rene 41 appear to have the highest strength at 1440 F. SM 200 is a cast alloy which is used principally as the turbine bucket material in the J57 engine. Extensive experience in its use and handling has not been gained as yet. In addition, it is not normally considered a weldable alloy. Udimet 700 has gained appreciable usage, and many shops are familiar with forging and machining the alloy. It is not readily rolled and is not considered weldable. The Nimonics are British alloys not readily available in the United States, and extensive data and experience are not available on Nimonic 115. IN 100 has gained little commercial acceptance, and little is known of the alloy other than the properties cited.

Extensive experience, on the other hand, has been gained in the use of Rene 41. The alloy is available as forgings, billets, bar, and sheet from several sources. It has excellent strength properties over the temperature range from 70 to 1500 F. In fact, it was for this temperature range that Rene 41 was specifically designed. It was not designed to be used at temperatures above 1500 F.

For these reasons, René 41 was selected as the most promising material for high-temperature separable connectors. Table 1 lists the short-time-tensile and the available creep-rupture properties of René 41. Complete time-deformation curves during creep testing are required in designing connectors for high-temperature use. To obtain specific data for design purposes, a family of complete creep curves at a number of stresses at 1440 F is required. Such curves were not available in the literature. In most creep testing, loads are usually selected to produce rupture in 1000 hours or less. Such loads can result in 0.2 to 0.3 per cent deformation on loading. At lower stress levels where smaller per cent deformation on loading occurs, rupture lives of several thousand hours will result. Such tests are seldom run, and if they are, complete creep data are not reported. Nevertheless, a few complete creep curves for René 41 in the temperature range of interest were uncovered in References (12, 13).

Relaxation data on René 41 were not available in the literature.

René 41 is a precipitation-hardenable nickel-base alloy. The material is usually supplied in the solution-annealed condition. Hardening is accomplished by aging the alloy at 1400 or 1650 F. This causes precipitation of a complex nickel-titanium-aluminum phase (called the gamma-prime phase) and produces excellent strength over the temperature range of interest.

René 41 is readily forged and considerable experience has been accumulated by many forge shops in working the alloy. Like most high-strength nickel-base alloys, René 41 work hardens rapidly during machining and is considered difficult to machine. Nevertheless, it is machined by many shops on a production basis.

René 41 is considered a weldable alloy. Nevertheless, as is the case with all high-strength precipitation-hardenable alloys, welding may be somewhat of a problem. Welding in the solution-annealed condition (the low-strength condition) is recommended. After welding, the part should be reannealed and aged to obtain the properties cited. Welding in the aged condition, particularly under conditions of stress, is not recommended. This is true of all precipitation-hardenable nickel-base alloys. In general, it has been found that the greater the aluminum plus titanium content, the higher is the strength and the more difficult are the welding operations. The use of a significantly more weldable material will consequently entail a very appreciable reduction in strength and a considerable weight penalty.

Two specific heat treatments have been developed for René 41: one to develop maximum short-time strength and one to develop maximum long-time creep and rupture strengths. The former treatment involves solution treating at 1950 F for 4 hours, air cooling, and aging at 1400 F for 16 hours. This treatment yields good short-time tensile properties and acceptable 10-hour rupture and creep strengths. The latter treatment, involving solution treating at 2150 F for 2 hours, air cooling, and aging at 1650 F for 4 hours, produces somewhat reduced short-time tensile properties but significantly improved long-time creep and rupture strength. As indicated previously, René 41 should be welded in the solution-treated condition. Recent welding studies have revealed problems in weld metal cracking for material welded after the high-temperature treatment (2150 F). The use of the lower temperature treatment (1950 F) has reportedly eliminated weld-metal-cracking problems. For this reason, a solution-treatment temperature of 1950 F and an aging treatment of 1400 F are recommended. With such a heat treatment, high short-time tensile properties and good 10-hour rupture and creep properties will be obtained. A sacrifice in long-time creep and rupture strength will result. Long-time strength is not a prime requirement for the present application.

René 41 has excellent oxidation resistance over the specified service-temperature range. It is not known to become embrittled in this temperature range. While comparative data on resistance to thermal shock are not available, it is believed that the alloy has compatable or better resistance to thermal shock than the other candidate materials.

Finally, it is not anticipated that René 41 will show a tendency to bonding or self welding during service. Alloys which contain appreciable amounts of chromium, aluminum, and titanium are exceedingly difficult to bond. Bonding is accomplished only in atmospheres capable of reducing the stable spinel-type oxide on the surface of the alloy and under conditions of high temperature, high stress, and relative metal flow at mating surfaces. Consequently, self-welding of connectors of this alloy is not to be expected. If sticking of the connector is encountered, oxidation of the mating surfaces of the connector should reduce, if not eliminate, the problem. Heating the connector at about 1800 F in an atmosphere containing a low oxygen content should produce a hard, thin oxide layer which is exceedingly difficult to remove. Such an oxide film should prevent self-welding of the connector. If self-bonding persists, the deposition of a very thin layer of titanium or aluminum on the mating surfaces of the connector is recommended. The thin film should be diffused into the connector and oxidized by heating to high temperatures, such as solution treating at 1950 F. This should prevent self-welding.

In summation, René 41 has been selected as the material of construction for high-temperature separable connectors operating from room temperature to 1440 F. Certain other alloys have better creep strength than René 41, however, the combination of properties obtainable in René 41, as well as the availability and experience gained on this alloy, strongly recommends it.

This survey and the recommendations were made with limited knowledge of the tubing material that will be used with the René 41 connector. If the connector is to be welded to the tubing, knowledge of the tubing material is required before the weldability and the compatability of the connector and the tubing can be ascertained. Welding dissimilar materials is often a major problem. While it is not the purpose herein to select a tubing material, consideration was given to various tubing materials capable of being employed with René 41 connectors. René 41 tubing is not currently commercially available. The high-temperature tubing materials capable of being employed in this application and currently commercially available are Inconel X, Hastelloy X, Inconel 718, and Waspaloy. Inconel X, Hastelloy X, and Inconel 718 are of significantly different composition than René 41. In addition, these alloys have significantly lower strength at the design temperature than René 41, and the heat treatments employed to strengthen these alloys are not compatible with that recommended for René 41. Waspaloy, in contrast to Waspaloy, is quite similar in composition to René 41, and has similar physical and mechanical properties. The heat treatment of René 41 is compatible with that of Waspaloy, and welding René 41 connectors to Waspaloy tubing is feasible.

It is therefore suggested that Waspaloy be given full consideration as the tubing material to be used with René 41 connectors. Both the tubing and the connector should be in the solution-treated condition for welding. After welding, the assembly must be completely heat treated. The heat treating sequence recommended is as follows:

(1) Solution treat at 1975 F for 4 hours, air cool

(2) Stabilize at 1550 F for 24 hours, air cool

(3) Age at 1400 F for 12 hours, air cool.

This heat treatment is recommended for Waspaloy. The René 41 connectors, when subjected to this heat treatment, will have properties comparable to those reported herein.

Design Properties of René 41

The minimum or steady-state creep rates are determined from the master creep curve of Reference (14), shown in Figure 5. The data of Figure 5 are replotted in Figure 6 for 1440 and 1500 F. The straight dashed lines in Figure 6 are a conservative fit to the data at the two temperatures. The corresponding constants are:

At 1440 F,

$$C_1 = 4.23 \times 10^{-28},$$

$$n = 4.97.$$

At 1500 F,

$$C_1 = 1.30 \times 10^{-26},$$

$$n = 4.82.$$

A rapid method for determining the constants C_1 and n from creep data, using the creep law $\dot{\epsilon} = C_1\sigma^n$, is as follows:

Determine the strain rates $\dot{\epsilon}_1$ and $\dot{\epsilon}_2$ for the stresses σ_1 and σ_2, respectively. From the steady-state creep law, $\dot{\epsilon}_1/\dot{\epsilon}_2 = (\sigma_1/\sigma_2)^n$, where n is the only unknown, and is easily solved. After calculating n, the constant C_1 can be determined from $\dot{\epsilon}_1 = C_1\sigma_1^n$.

The constants C_2 and m for the intercept stress were obtained from the test data and plotted curves of Reference (13). Since the intercept data of Reference (13) are not very consistent, the following constants are considered only approximate in magnitude. This is one reason for the recommendation that creep data be generated for René 41 at 1440 F.

At 1440 F,

$$C_2 = 1.25 \times 10^{-8},$$

$$m = 1.00.$$

At 1500 F,

$$C_2 = 3.93 \times 10^{-11},$$

$$m = 1.57.$$

The design data for René 41 at 1440 F and 1500 F are plotted in Figure 7 for various stress levels.

Other design properties of René 41 are obtained from Tables 2 and 3.

The yield strength σ_y = 120,000 psi at 70 F,

σ_y = 103,000 psi at 1440 F,

σ_y = 97,000 psi at 1500 F.

The modulus of elasticity E_{70} = 32.0 x 10^6 psi at 70 F,

E_T = 24.4 x 10^6 psi at 1440 F,

E_T = 24.0 x 10^6 psi at 1500 F.

The mean coefficient of thermal expansion α = 8.3 x 10^{-6} in/in/°F at 1440 F,

α = 8.5 x 10^{-6} in/in/°F at 1500 F.

DESIGN PROCEDURE

Basis for Design Procedure

The design procedure considers only the elastic and creep behavior of the bolts and flange assembly. Secondary effects such as flange rotation due to internal pressure, creep of the gasket, creep of the threads, creep bending of the bolt, and dynamic creep are not included in the design procedure, but are discussed in Appendix C. The design factor of safety is intended to account for these secondary effects in addition to the scatter in material properties.

The gasket (seat) design for mechanical fittings is not included in the design procedure, but is discussed in Reference (11), where it was concluded that plastic yielding of seal surfaces is desirable for effective sealing. An initial sealing stress as high as 2.75 times the yield strength of the metal gasket material was considered necessary to achieve the desired degree of yielding in order to keep the leakage rate of helium below the tolerance level (11).

It is assumed that the bolts are flexible compared to the gasket in order that the application of internal pressure results in negligible bolt-load changes. It is not necessary that the gasket be the only load path through the assembly.

The design procedure is intended primarily as a method for calculating relaxation of the connector assembly, and does not include a failure analysis of the component parts. It is assumed that the material possesses sufficient ductility to withstand the progressive deformation incurred if the connector assembly is retightened after each cycle. Various methods of analysis available for predicting the tube strains are discussed in Appendix D. Those methods are intended for the tube design at locations sufficiently removed from discontinuities such as the connector assembly.

The detailed design procedure for bolted-flanged and threaded connectors is described step-by-step for the purpose of obtaining a curve of leakage pressure versus time (or a time to leakage for a specific value of the design pressure). The effects of external loads, temperature differentials, and retightening, and the use of relaxation data are discussed separately from the basic design procedure.

The equations used in the design procedure are derived in Appendix B.

Bolted-Flanged Connectors

The basic design procedure for a bolted-flanged connector consists of nine specific steps in order to arrive at a curve of leakage pressure versus time. Figure 8 shows a typical flange geometry.

(1) Design Conditions

Establish the design temperature, design pressure, nominal connector diameter, tube geometry, life requirements, and temperature differentials.

(2) Material Properties

Determine the yield strength σ_y and the modulus of elasticity E at both room temperature and the design temperature, and the coefficient of thermal expansion α at the design temperature.

From a family of creep curves at the design temperature, determine the constants C_1, C_2, m, and n to fit the following equation:

$$\varepsilon = \varepsilon_o + C_2\sigma_o^{\,m} + C_1\sigma_o^{\,n}\, t \quad , \tag{1}$$

The creep constants should be selected to give the best fit to the experimental data in the range of stress levels expected in the design*.

(3) ASME Code Design

The design procedure can be applied to any arbitrary design. However, it is desirable to use the ASME Boiler and Pressure Vessel Code[1] for the initial static design in order to establish a balanced design. Also, the Code-rated flange can subsequently be rated on a life basis for comparison.

Using the rules of the ASME Code[1], establish either a loose-type or integral-type flange geometry for an appropriate value of internal pressure. This pressure, of course, should be at least as high as the design pressure multiplied by the ratio of the cold-to-hot modulus of elasticity, and multiplied by the design factor of safety. The initial gasket seating load will be dependent on the type seal used and the maximum permissible leakage rate, and need not follow the rules of Reference (1). The allowable Code stress is assumed to equal two-thirds of the room-temperature yield strength in order to avoid yielding of the assembly during the bolt-up operation.

The ASME Code will establish a static design at room temperature. The initial bolt load and bolt stress at room temperature are designated as P_{BR} and σ_{BR}, respectively.

(4) Flexibility Equations

Determine the bolt flexibility F_B (bolt deflection due to a unit bolt load):

$$F_B = \frac{L_B}{A_B E_T} \quad , \tag{2}$$

where

L_B = effective length of the bolt, usually taken as the total length between the nut bearing surfaces plus one nominal bolt diameter,

A_B = total bolt area based on root diameter.

Determine the flange flexibility F_F (total deflection of two flanges at the bolt circle due to a unit bolt load).

For a loose-type flange,

$$F_F = \frac{5.46\, e^2}{E_T h^3 \ln d_F/c_F} \quad , \tag{3}$$

For an integral-type flange,

$$F_F = \frac{1.29\, Ve^2}{L\sqrt{c_F}\,(d_T - c_T)^{5/2}\, E_T} \quad , \tag{4}$$*

(5) Creep Equations

Calculate the rate of creep deflection of the bolts K_B and the rate of creep deflection of the two flanges at the bolt circle, K_F:

$$K_B = \frac{C_1 P_t^{\,n} L_B}{A_B^{\,n}} \quad , \tag{5}$$

and

$$K_F = \frac{\phi \sigma_{Ft}^{\,n} C_1 e c_F}{h} \quad , \tag{6}$$

where

$$\sigma_{Ft} = \left(\frac{h}{2c_F}\right)^{\frac{1}{n}} \left(\frac{P_t e}{2\pi}\right) \left[\frac{\left(2^{1+\frac{1}{n}}\right)\left(1-\frac{1}{n}\right)\left(2+\frac{1}{n}\right)}{\left(d_F^{\,1-\frac{1}{n}} - c_F^{\,1-\frac{1}{n}}\right) h^{2+\frac{1}{n}}}\right]$$

Equation (6) applies only to a loose-type flange. The creep rate of an integral-type flange is assumed equal to that of the loose-type flange, provided the maximum design stresses according to Reference (1) are equal. The procedure for an integral-type flange is to calculate the maximum design stress by Reference (1). Then determine the thickness of a loose-type flange with the same flange inner and outer radii, moment arm, and maximum design stress as the integral-type flange. this results in an equivalent strength loose-type flange. Using the loose-type flange geometry, calculate the creep rate from Equation (6), assuming this to be the creep rate of the integral-type flange.

(6) Flexibility and Creep Ratios

Calculate the life factor R for the purpose of conveniently evaluating a flange geometry on a life basis:

$$R = \frac{1 + r_F}{1 + r_K} \quad , \tag{7}$$

where

r_F = flexibility ratio = F_F/F_B ,

r_K = creep ratio = K_F/K_B .

Equations (5) and (6) should be calculated in terms of the bolt load P_t, in order that the creep ratio r_K be calculable.

(7) Intercept Stress Reduction

Calculate the bolt stress, σ_{BT}. The initial room-temperature bolt stress σ_{BR} is reduced to a new value σ_{BT} at the design temperature due to the change in modulus of elasticity:

$$\sigma_{BT} = \sigma_{BR}\left(\frac{E_T}{E_R}\right) \quad , \tag{8}$$

Calculate a further reduction in bolt stress from σ_{BT} to a value σ_o due to the effects of primary creep:

$$\sigma_o = \sigma_{BT} - \frac{E_T C_2 \sigma_o^{\,m}}{R} \quad , \tag{9}$$

Equation (9) is conveniently solved for σ_o by trial and error. The bolt stress σ_o or corresponding bolt load P_o represents the actual starting point in the life calculations.

(8) Bolt Relaxation

Calculate the time t required for the bolt stress to relax from an initial value σ_o to a new value σ_t:

$$t = \frac{R}{C_1 E_T (n-1)} \left[\frac{1 - \left(\frac{\sigma_t}{\sigma_o}\right)^{n-1}}{\sigma_t^{\,n-1}}\right] \quad , \tag{10}$$

(9) Leakage Pressure

Solve Equation (10) successively in order to obtain a curve of residual bolt stress σ_t or load P_t versus time. Convert these results to an allowable leakage pressure versus time curve by the successive solution of Equation (11):

$$P_t = P_p + P_G \quad , \tag{11}$$

where

$\sigma_t = \dfrac{P_t}{F S_t}$,

P_p = bolt load due to pressure = $\pi p g^2$,

P_G = residual gasket load (or load across flange face) required to prevent excessive leakage (the determination of this load is not included in this report).

---

*Further details on the creep constants and the intercept stress reduction are given in pages [illegible] and B-3.

*The terms V and L in Equation (4) conform to the nomenclature of Reference (1).

In Equation (11), P_t' is established directly from the P_t versus t curve by applying a suitable factor of safety to the load rather than the time scale. The value P_G is dependent on the type of gasket used, and may or may not be a function of the internal pressure p.

Threaded Connectors

The design procedure for threaded connectors commences with Step 1 (design conditions) and Step 2 (material properties) of the bolted-flanged connector design procedure. Six additional steps are then required for the threaded connector in order to obtain a leakage pressure versus time curve.

Reference (15) can be used for the static design of a threaded connector. The nomenclature for the parts of the threaded connector is based on the functional analogy to the parts of the bolted-flanged connector and is not to be taken as a literal description of the parts. A threaded connector model is shown in Figure 9. The nut is considered the "bolt" member of the analysis, and contributes both axial and bending deformations. The flange and union members in Figure 9 are considered the "flange" member of the analysis with axial deformation only.

(1) "Bolt" Flexibility

Calculate the "bolt" flexibility F_B, which represents the axial flexibility of the nut and has the same form as Equation (2):

$$F_B = \frac{L_B}{A_B E_T} \quad , \tag{12}$$

where L_B and A_B are the effective nut length and area, respectively.

Calculate the bending flexibility of the "bolt" F_B' by using the development on pages 194-197 of Reference (15) for inwardly projecting flanges (see Figure 10):

$$F_B' = \alpha^2 \left(\frac{\theta}{M}\right) \quad , \tag{13}$$

where

$$\frac{\theta}{M} = \frac{3(1-\nu^2)}{\pi d_T \beta (d_T - c_T)^3 E_T \left[\frac{(1-\nu^2)}{2\beta d_T}\left(\frac{h}{d_T - c_T}\right)^3 \ln\frac{d_T}{c_F} + 1 + \frac{\Delta h}{2}\right]}$$

and

$$\beta = \sqrt[4]{\frac{3(1-\nu^2)}{d_T^2 (d_T - c_T)^2}} \quad .$$

(2) "Flange" Flexibility

Calculate the axial flexibility of the "flange", F_F:

$$F_F = \frac{L_F}{A_F E_T} \quad . \tag{14}$$

The effective length L_F can be considered equal to L_B in Equation (12). A_F is the cross-sectional area of the "flange".

(3) "Bolt" Creep

Calculate the axial creep rate of the "bolt", K_B:

$$K_B = \frac{C_1 P_t^{\,n} L_B}{A_B^{\,n}} \quad . \tag{15}$$

Calculate the bending creep rate of the "bolt", K_B', in a manner similar to an integral-type flange*, except that the maximum design stress is determined from Reference (15) for an inwardly projecting flange.

The longitudinal hub stress S_H, radial ring stress S_R, and tangential ring stress S_T, respectively, are

$$S_H = \frac{3M}{\pi d_T (d_T - c_T)^2 \left[\frac{(1-\nu^2)}{2\beta d_T}\left(\frac{h}{d_T - c_T}\right)^3 \ln\frac{d_T}{c_F} + 1 + \frac{\Delta h}{2}\right]} \quad ,$$

$$S_R = \frac{3(1 + \frac{\Delta h}{2})M}{\pi d_T h^2 \left[\frac{(1-\nu^2)}{2\beta d_T}\left(\frac{h}{d_T - c_T}\right)^3 \ln\frac{d_T}{c_F} + 1 + \frac{\Delta h}{2}\right]} \quad , \tag{16}$$

$$S_T = \frac{3(1-\nu^2)hM}{2\pi d_T c_F (d_T - c_T)^3 \beta \left[\frac{(1-\nu^2)}{2\beta d_T}\left(\frac{h}{d_T - c_T}\right)^3 \ln\frac{d_T}{c_F} + 1 + \frac{\Delta h}{2}\right]} \quad ,$$

where $\beta = \sqrt[4]{\frac{3(1-\nu^2)}{d_T^2 (d_T - c_T)^2}}$.

*See procedure on page 18 for integral-type flanges.

The maximum stresses from Equations (16) should be combined according to the method of Reference (1). For a threaded connector, Equation (6) herein should be used with a constant of two rather than four because there is one rather than two flange members.

(4) "Flange" Creep

Calculate the axial creep of the "flange", K_F, which has the same form as Equation (15):

$$K_F = \frac{C_1 P_t^{\,n} L_F}{A_F^{\,n}} \quad . \tag{17}$$

(5) Flexibility and Creep Ratios

Calculate the life factor R:

$$R = \frac{1 + r_F + r_F'}{1 + r_K + r_K'} \quad , \tag{18}$$

where

$$r_F = F_F/F_B \quad , \quad r_F' = F_B'/F_B \quad ,$$

$$r_K = K_F/K_B \quad , \quad r_K' = K_B'/K_B \quad .$$

(6) Nut Relaxation

Determine the relaxation of the nut from Equation (10), but using the life factor R from Equation (18). Use Equation (11) to calculate the leakage pressure versus time.

External Loads

Determine the effect of external loads on the leakage pressure by revising Equation (11) to read:

$$P_t' = P_p + P_G + P_A + P_M \quad , \tag{19}$$

where P_A and P_M include the effects of external thrusts and moments, respectively:

$$P_A = \pi p K_A c_T^{\,2} \quad ,$$

$$P_M = \frac{\pi p K_M c_T^{\,2}(d_T^{\,2} + c_T^{\,2})}{2 d_T g} \tag{20}$$

Solve Equation (19) successively in order to obtain a leakage pressure versus time curve.

The constants K_A and K_M are used to define the magnitude of the stress due to tube thrusts (σ_A) and moments (σ_M), respectively, in terms of the axial tube stress (σ_T) due to internal pressure:

$$K_A = \frac{\sigma_A}{\sigma_T} \quad , \quad K_M = \frac{\sigma_M}{\sigma_T} \quad ,$$

where

$$\sigma_T = \frac{p c_T^{\,2}}{(d_T^{\,2} - c_T^{\,2})} \quad .$$

Temperature Differentials

The analysis of temperature differentials is limited herein to the case of components at uniform temperatures, but at a different average temperature from another component of the assembly. In one case, the bolt is assumed to be at a different average temperature than the flange and tube assembly, probably the more critical case. In the other case, the flange and bolt assembly is assumed to be at a different average temperature than the tube. The change in material properties with temperature change is neglected in the thermal calculations. It is also assumed that the temperature differentials are of a short-time nature, occurring almost instantaneously for the purpose of analysis. A more refined analysis would be required for temperature differentials varying considerably with time.

Bolt-Flange Differential

Letting a positive value of ΔT represent the flange at a higher average temperature than the bolt, calculate the change in bolt stress $\Delta\sigma_B$:

$$\Delta\sigma_B = \frac{\alpha(\Delta T) E_T}{1 + r_F} \quad . \tag{21}$$

For a threaded connector, the change in "bolt" (nut) stress is

$$\Delta\sigma_B = \frac{\alpha(\Delta T)\, E_T}{1 + r_F + r_F'} \quad . \tag{22}$$

The change in bolt or nut load in Equations (21) and (22) should be evaluated in a different manner, depending upon the nature of the differential. A positive temperature differential at the start of the cycle would lead to an increase in the bolt load. This increase should be used to guard against overstressing of the bolt (or other connector components), and neglected for short-time differentials in the relaxation analysis. If a negative temperature differential should occur near the end of the operating cycle, the reduction in bolt load should be added to Equation (11) to determine a reduced leakage pressure:

$$P_t' = P_p + P_G + P_T \quad , \tag{23}$$

where $P_T = \delta\sigma_B A_B$ (bolt-load change due to temperature differential).

Flange-Tube Differential

The analysis by Dudley[16] or an extension of the equations presented by Rodabaugh in discussion of Reference (17) can be used to evaluate bolt-load changes due to the tube and flange assembly being at different average temperatures. The method of Rodabaugh[17] is preferred, since it is consistent with the basic equations of the ASME Code[1]. At the start of the operating cycle the tube will possibly be hotter than the remaining assembly, thus causing a reduction in the bolt load. The opposite effect may occur upon cooling down the assembly. An increase in the bolt load should be used to guard against overstressing the connector assembly, whereas a decrease in the bolt load should be used in Equation (23).

Retightening

If the assembly is not retightened between operating cycles, a continuous operating cycle is assumed, consisting of the total time of the individual cycles. This procedure is consistent with the assumption that creep strains are irreversible in nature.

In the event that retightening is contemplated, each cycle is reanalyzed according to the creep design procedure (not repeating static design) as though it were the first cycle. This is a conservative approach because the flange life will probably improve on subsequent cycles to the extent that the primary creep strains are nonrecurring, as evidenced by the British Flange Tests[9].

Relaxation Data

The design procedure is based on the assumption that only creep data are available. Of course, relaxation data are preferred. Relaxation data should be available as a family of curves, starting from various initial stress levels, sufficient to cover the range of initial stress levels expected in the design.

Since the relaxation test is usually run with no elastic follow-up ($R = 1$), the time required for a connector assembly bolt or nut stress to relax from an initial stress σ_o to a final value σ_t is obtained directly from the relaxation test data, multiplied by the life factor R determined from Equation (7) or (18). If the relaxation tests are run with elastic follow-up, the relaxation time is determined by multiplying the test data (time) by the ratio of the life factor R of the connector to that of the test assembly. Interpolation of the test data may be required for specific values of the initial stress σ_o not available in the test data. The use of a direct ratio for various values of the life factor is based on the assumption that the life factor is a constant in the analysis. Baumann[2] justifies this approach, regardless of the creep law observed by the material.

The direct use of relaxation data results in a residual stress versus time curve, similar to that yielded by Equation (10). In generating relaxation data, it would be desirable to run at least one test with sufficient elastic follow-up to simulate the life factor of a connector assembly.

Redesign Considerations

The designer may find that the calculated connector life for a particular design pressure is less than the required design life. If the temperature and material have already been fixed, the only changes that can be made in order to obtain an improved life are geometry changes. Ordinarily, the connector inner diameter, bolt geometry, and gasket geometry will be kept constant during a redesign. Therefore, the logical changes to make if the life factor R in Equation (10) is to be improved are changes in the flange thickness, flange width, and moment arm.

Changes in the moment arm e can have an appreciable effect on the life factor R. Of course, an increase in the moment arm will have to be compensated for by changes in the flange width and/or thickness (or hub geometry for an integral-type flange) in order that the flange stresses be maintained at an acceptable level. It is recommended that improvements in the connector life be made by simultaneous changes in the moment arm for flange bending, the flange width, and the flange thickness. Effects of changes in the length of the bolt L_B (perhaps with the use of a rigid bolt collar) should also be investigated.

If the desired connector life is not attained by the changes described above, the next logical step would be to redesign the bolt geometry and gasket geometry in order to allow for greater percentage reductions in the initial bolt load before leakage occurs.

DISCUSSION OF SAMPLE CALCULATIONS

The sample calculations are presented in order to adequately demonstrate the design procedure, and not to arrive at optimum design connectors. An optimum design can be determined only after calculating a wide range of connector geometries, thus enabling the selection of a minimum-weight design for a given combination of design (leakage) pressure and life.

The loose-type and integral-type flange geometries of Figures 11 and 12, respectively, have nearly the same initial stress σ_o, and the life factor R differs by only 10 per cent. Therefore, the results in Figures 13 and 14 for the loose-type flange very nearly apply for the integral-type flange. The loose-type flange is heavier. This will not always be the case since the loose-type flange can frequently have a much higher flexibility than the equivalent integral-type flange.

The factor of safety used in Figure 13, together with the intercept stress reduction and the bolt load reduction due to change in elastic modulus, leads to a maximum design pressure of 2980 psi in Figure 14, assuming no external loads or temperature differentials. It is shown that a temperature difference between the bolt and flange assembly of -100 F severely affects the leakage pressure and establishes a limiting life of 36 hours. The curves of Figure 14 indicate that, up to approximately 0.5 hour, there is negligible change in the leakage pressure. This would infer that, for accumulated life cycles totaling 0.5 hour or less, retightening after each cycle would not be very beneficial.

René 41 at 1500 F does not exhibit a great deal of primary creep, as shown by the relative insensitivity of the initial stress σ_o to the life factor R in Figure 15. For some materials, the effect of the life factor on the reduced intercept stress would be a strong influence in choosing an optimum design. The life factor R is a convenient measure of the relative merits of various designs with the same initial bolt stress because it is essentially a geometry-dependent constant in the relaxation equation, all other constants in Equation (10) being a function only of the material and temperature.

It is usually considered desirable to preload the bolt or nut as high as possible without yielding any portions of the connector assembly. The high preload is intended to delay the relaxation of stress or load. Various values of the initial bolt stress were used in the relaxation equation (27). The results in Figure 16 indicate that, for design lives over 1-2 hours, there is very little advantage gained by higher prestressing. In fact, the initial prestress σ_o of 45,000 psi would be more desirable for longer lives since it will provide greater safety against yielding. The initial stress of 90,000 psi at 1500 F for René 41 would be difficult to obtain because of the intercept stress reduction, the elastic modulus change, and the limitation imposed on the room-temperature bolt preload to avoid yielding.

Results of the threaded-connector geometry of Figure 17 are shown in Figure 18. The geometry of Figure 17 does not represent a well-balanced design. As a result, the axial nut stress σ_{BR} is limited to 40,000 psi (room-temperature prestress) to avoid overstressing the inwardly projecting flange. The low prestress results in the relatively slow relaxation of the nut load shown in Figure 18.

It is quite possible that the optimum static design will also provide a good design for relaxation, depending upon the material and design temperature. However, for some combinations of material and temperature, the sound static design approach may not suffice because of the importance of the interaction of bolt and flange creep and flexibility ratios. For a static design, the integral-type bolted flange is usually lighter than the loose-type flange. This may not be true for relaxation design. In some cases, loose-type flanges offer advantages in the way of increased flexibility and the ability to better withstand certain types of temperature differentials.

REFERENCES

(1) ASME Boiler and Pressure Vessel Code, Section VIII, "Rules for Construction of Unfired Pressure Vessels", New York (1962).

(2) Baumann, K., "Some Considerations Affecting Future Developments of the Steam Cycle", Engineering, 130, 597-599, 661-664, 723-727 (1930).

(3) Bailey, R. W., "The Utilization of Creep Test Data in Engineering Design", Proceedings of the Institution of Mechanical Engineers, 131, 131-349 (1935).

(4) Bailey, R. W., "Flanged Pipe Joints for High Pressures and Temperatures", Engineering, 144, 364-365, 419-421, 490-492, 538-539, 615-617, 674-676 (1937).

(5) Waters, E. O., "Analysis of Bolted Joints at High Temperature", Transactions of the ASME, 60, 83-86 (1938).

(6) Marin, J., Mechanical Properties of Materials and Design, McGraw-Hill Book Co., Inc., New York (1942).

(7) Finnie, I., and Heller, W. R., Creep of Engineering Materials, McGraw-Hill Book Co., Inc., New York (1959).

(8) Gough, H. J., "First Report of the Pipe Flanges Research Committee", Proceedings of the Institution of Mechanical Engineers, 132, 201-340 (1936).

(9) Tapsell, H. J., "Second Report of the Pipe Flanges Research Committee", Proceedings of the Institution of Mechanical Engineers, 141, 433-471 (1939).

(10) Johnson, A. E., "Pipe Flanges Research Committee - Third Report", Proceedings of the Institution of Mechanical Engineers, 168, 423-463 (1954).

(11) Rathbun, F. O., Jr., "Design Criteria for Zero-Leakage Connectors for Launch Vehicles, Vol 3, Sealing Action at the Seal Interface", General Electric Advanced Technology Laboratories Report No. 63GL43 (March 15, 1963).

(12) Aarnes, M. N., and Tuttle, M. M., "Presentation of Creep Data for Design Purpose", ASD Technical Report 61-216 (June, 1961).

(13) Gluck, J. V., and Freeman, J. W., "Effect of Creep - Exposure on Mechanical Properties of René 41", ASD Technical Report 61-73 (August, 1961).

(14) Sachs, G., and Pray, R. F., "Air Weapons Materials Application Handbook - Metals and Alloys", ARDC Report TR 59-66.

(15) Rodabaugh, E. C., et al., "Development of Mechanical Fittings", Edwards Air Force Base Report No. RTD-TDR-63-1115 (December, 1963).

(16) Dudley, W. M., "Deflection of Heat Exchanger Flanged Joints as Affected by Barreling and Warping", Transactions of the ASME, Series B, 83, 460-466 (November, 1961).

(17) Westrom, D. B., and Bergh, S. E., "Effect of Internal Pressure on Stresses and Strains in Bolted-Flanged Connections", Transactions of the ASME, 73, 121-136 (1951).

(18) Timoshenko, S., "Strength of Materials - Part II", D. Van Nostrand Co., Inc. (1956).

(19) Marin, J., "Stresses and Deformations in Pipe Flanges Subjected to Creep at High Temperatures", Journal of the Franklin Institute, 226, 645-657 (1938).

(20) MacCullough, G. H., "An Experimental and Analytical Investigation of Creep in Bending", Transactions of the ASME, Journal of Applied Mechanics, 55, 55-60 (1933).

(21) Tapsell, H. J., and Johnson, A. E., "An Investigation of the Nature of Creep Under Stresses Produced by Pure Flexure", Journal of the Institute for Metals, 57 (2), 121-140 (1935).

(22) Davis, E. A., "Creep of Metals at High Temperature in Bending", Transactions of the ASME, Journal of Applied Mechanics, 60, A-29-A-31 (March, 1938).

(23) Findley, W. N., and Pocsatek, J. J., "Prediction of Creep - Deflection and Stress Distribution in Beams From Creep in Tension", Transactions of the ASME, 77 (1955).

(24) Hult, J., "Mechanics of a Beam Subject to Primary Creep", Transactions of Chalmers University of Technology, Gothenburg, Sweden (256) (1962).

(25) Voorhees, H. R., Freeman, J. W., and Herzog, J. A., "New Investigations Relating to Stress Concentrations Under Creep Conditions", Transactions of the ASME, Journal of Basic Engineering, 84, 207-213 (June, 1962).

(26) Lazan, B. J., "Dynamic Creep and Rupture Properties of Temperature Resistant Materials Under Tensile Fatigue Stress", ASTM Proceedings, 49, 757-787 (1949).

(27) Vitovec, F. H., and Lazan, B. J., "Fatigue, Creep, and Rupture Properties of Heat Resistant Materials", WADC Technical Report 56-181, ASTIA AD 97240 (August, 1956).

(28) Langenecker, B., "Acoustic Radiation Damage in Materials", Presented at Leak-Tight Separable Fluid Connector Design Conference at Huntsville, Alabama (March 24-25, 1964).

(29) Finnie, I., "Steady-State Creep of a Thick-Walled Cylinder Under Combined Axial Load and Internal Pressure", ASME Paper No. 59-A-57.

(30) Finnie, I., "An Experimental Study of Multiaxial Creep in Tubes", 1963 Joint International Conference on Creep.

(31) Rimrott, F. P. J., Mills, E. J., and Marin, J., "Prediction of Creep Failure Time for Pressure Vessels", Transactions of the ASME, Journal of Applied Mechanics, 27, 303-308 (June, 1960).

(32) Davis, E. A., "Creep Rupture Tests for Design of High-Pressure Steam Equipment", Transactions of the ASME, Journal of Basic Engineering, 82, 453-461 (June, 1960).

(33) Rattinger, I., and Padlog, J., "Design Implications of Creep in Pressurized Cylindrical Shells", Aerospace Engineering, 20, 95-108 (March, 1961).

(34) Coffin, L. F., Jr., Shapler, P. R., and Cherniak, G. S., "Primary Creep in the Design of Internal-Pressure Vessels", Transactions of the ASME, 71, 229-241 (1949).

LMC:ECR:DBR:TMT/all

APPENDIX A

SAMPLE CALCULATIONS

The sample calculations are all performed on René 41 at 1500 F. The following design values apply to René 41 at room temperature and at 1500 F*.

The yield strength:

$$\sigma_y = 120,000 \text{ psi at } 70 \text{ F},$$

$$\sigma_y = 97,000 \text{ psi at } 1500 \text{ F}.$$

The modulus of elasticity:

$$E_R = 32.0 \times 10^6 \text{ psi at } 70 \text{ F},$$

$$E_T = 24.0 \times 10^6 \text{ psi at } 1500 \text{ F}.$$

The mean coefficient of thermal expansion $\alpha = 8.5 \times 10^{-6}$ in/in/°F at 1500 F.

The creep and intercept constants at 1500 F are:

$$C_1 = 1.30 \times 10^{-26}, \qquad C_2 = 3.93 \times 10^{-11},$$

$$n = 4.82, \qquad m = 1.57.$$

The ASME Code calculations are based on an internal pressure of 10,000 psi. This corresponds to a reduced value of the design pressure equal to 10,000 (E_T/E_R) $(1/F.S.)$ = 3750 psi for a factor of safety equal to two. Therefore, the maximum possible value of the design pressure is 3750 psi, and will be further reduced due to the effects of primary creep.

Loose-Type Bolted Flange

ASME Code Design**

The allowable stress for use in Reference (1) equals 2/3 (120,000) = 80,000 psi. The geometry is shown in Figure 11.

The tube thickness can be determined from other considerations, such as discussed in Appendix D, to equal 0.210 in.

For the purpose of the bolt design, assume that a residual gasket stress of 3P (P = 10,000 psi, the ASME Code design pressure) is required to maintain the gasket seal. Also, assume that the gasket plating material has a yield strength of 10,000 psi and that it requires a gasket stress of three times the yield strength (y = 60,000 psi) to seat the metallic gasket. For a gasket width 2b = 0.125 in. (assume full width is effective),

$$H_p = 2b \times 3.14G \times 3P = 45,900 \text{ lb},$$

$$H = 0.785\, G^2 P = 119,000 \text{ lb},$$

$$W_{m1} = H + H_p = 164,900 \text{ lb},$$

$$W_{m2} = 3.14bGy = 45,900 \text{ lb}.$$

The design bolt load W = 164,900 lb.

The required bolt area is

$$A_{m1} = \frac{164,900}{80,000} = 2.06 \text{ in}^2.$$

Use 10-9/16-in.-diameter bolts with a total root area equal to 1.89 in^2. The bolt stress is

$$S_b = \frac{164,900}{1.89} = 87,300 \text{ psi}.$$

For the flange design,

$$h_G = h_T = 0.663 \text{ in.}, \quad h_D = 0.813 \text{ in.},$$

$$H_D = 0.785\, B^2 P = 102,000 \text{ lb},$$

$$H = 0.785\, G^2 P = 119,000 \text{ lb},$$

$$H_G = W - H = 45,900 \text{ lb},$$

$$H_T = H - H_D = 17,000 \text{ lb},$$

$$M_D = H_D h_D = 82,800 \text{ lb},$$

$$M_T = H_T h_T = 11,300 \text{ lb},$$

$$M_G = H_G h_G = 30,500 \text{ lb},$$

$$M_o = M_D + M_T + M_G = 124,600 \text{ in-lb},$$

$$S_T = 80,000 \text{ psi},$$

$$K = A/B = 1.90.$$

From Figure UA-51.1 of Reference (1), Y = 3.3.

Then,

$$t = \sqrt{\frac{Y M_o}{B S_T}} = 1.20 \text{ in}.$$

Flexibility and Creep

From the equations on pages 18-20,

$$F_B = 1.78/E_T, \quad F_F = 1.51/E_T,$$

$$K_B = 0.157 C_1 P_t^{4.82},$$

$$\sigma_{Ft} = 0.215\, P_t,$$

$$K_F = 2.405 \times 10^{-3} C_1 P_t^{4.82},$$

$$r_F = 0.849, \quad r_K = 0.0153,$$

$$R = 1.82.$$

Bolt Relaxation

From Equations (8) and (9),

$$\sigma_{BT} = 87,300 \left(\frac{24 \times 10^6}{32 \times 10^6} \right) = 65,400 \text{ psi},$$

$$\sigma_o = \sigma_{BT} - \frac{E_T C_2 \sigma_o^m}{R} \cdot \qquad (24)$$

Solving Equation (24) by trial and error, $\sigma_o = 52,100$ psi. It is convenient to solve Equation (24) for various values of R in order to construct Figure 15, thus saving considerable calculating time when optimizing the flange geometry. For a rigid flange (R = 1), σ_o would equal 46,000 psi.

From Equation (10), the bolt relaxation equation becomes

$$t = 1.53 \times 10^{18} \left[\frac{\left(\frac{\sigma_t}{\sigma_o} \right)^{n-1}}{\sigma_t^{n-1}} \right] \cdot \qquad (25)$$

*Material properties for René 41 are given on pages 18-19.
**Use the current issue of the ASME Code [1].

With σ_o = 52,100 psi, the successive solution of Equation (25) results in the residual bolt-load curve of Figure 13.

Leakage Pressure

In order to convert residual bolt load to leakage pressure assume a factor of safety F.S. = 2.0 on the residual load, establishing the design curve of Figure 13. For example, if it is assumed that leakage will occur when the gasket pressure reaches a value of 3p, Equation (11) becomes

$$P_t' = \pi pg^2 + 3pA_O. \qquad (26)$$

The solution of Equation (26) for various values of the internal pressure p results in the leakage pressure versus time curve ($K_A = K_M = 0$, $\Delta T = 0$) of Figure 14. For example, at p = 2000, P_t' = 33,000 lb. The time t from Figure 13 for 33,000 lb is 4.9 hours.

Effect of Initial Stress

The relaxation equation for the geometry of Figure 11 is

$$t = 1.55 \times 10^{18} \left[\frac{1 - \left(\frac{\sigma_t}{\sigma_o}\right)^{n-1}}{\sigma_t^{n-1}} \right]. \qquad (27)$$

The effect of varying the bolt stress σ_o in Equation (27) is shown in Figure 16.

Integral-Type Bolted Flange

ASME Code Design*

An integral-type flange was designed in accordance with Reference (1). The gasket geometry, moment arm, outer flange radius, hub geometry, and design bolt load are the same as for the loose-type flange of Figure 11. The integral-type flange geometry is shown in Figure 12:

$$h_T = 0.868 \text{ in.}, \quad h_G = 0.663 \text{ in.}, \quad h_D = 0.863 \text{ in.}$$

From page A-2,

$$W = 164,900 \text{ lb},$$

$$H = 0.785\, G^2 P = 119,000 \text{ lb},$$

$$H_D = 0.785\, B^2 P = 74,500 \text{ lb},$$

$$H_G = W - H = 45,900 \text{ lb},$$

$$H_T = H - H_D = 44,500 \text{ lb},$$

$$M_D = H_D h_D = 64,300 \text{ lb},$$

$$M_T = H_T h_T = 38,600 \text{ lb},$$

$$M_G = H_G h_G = 30,500 \text{ lb},$$

$$M_o = M_D + M_T + M_G = 133,300 \text{ in-lb}.$$

Using an allowable stress of 80,000 psi and a design moment of 133,300 in-lb, the thickness of an integral-type flange is calculated from Reference (1) to be 0.95 in.

Flexibility and Creep

From Equations (2) and (5),

$$F_B = 1.35/E_T,$$

$$K_B = 0.118 C_1 P_t^{4.82}.$$

Since the flange design stress of 80,000 psi is the same as that of the equivalent loose-type flange, the flange creep rate is assumed to equal that of the loose-type flange:

$$X_F = 2.405 \times 10^{-3} C_1 P_t^{4.82}.$$

The flexibility of the integral-type flange from Equation (4) is

$$F_F = 1.43/E_T.$$

Then

$$r_F = 1.06, \quad r_K = 0.0204,$$

$$R = 2.02.$$

Bolt Relaxation

From Figure 15, σ_o = 52,900 psi. The bolt relaxation equation becomes

$$t = 1.69 \times 10^{18} \left[\frac{1 - \left(\frac{\sigma_t}{\sigma_o}\right)^{n-1}}{\sigma_t^{n-1}} \right]. \qquad (28)$$

Equation (28) does not yield results significantly different from Equation (25) for a loose-type flange.

Threaded Connector

Figure 17 shows a threaded-connector geometry, which represents an arbitrary set of dimensions rather than an optimum static design. The design procedure is used to calculate the design life of the geometry of Figure 17, based on Rene' 41 at 1500 F. Figure 9 is a guide for the proper dimensions to use in the analysis.

Bolt Flexibility

$$A_B = \pi(1.05^2 - 0.90^2) = 0.91 \text{ in.}^2,$$

$$L_B = 1.60 - 0.45 = 1.15 \text{ in.}$$

The axial flexibility of the bolt is

$$F_B = \frac{L_B}{A_B E_T} = 1.26/E_T.$$

The bending flexibility of the bolt is

$$F_B' = e^2 \left(\frac{\theta}{M}\right) = 1.14/E_T,$$

where

$$\frac{\theta}{M} = 19.8/E_T,$$

and

$$e = \frac{1.05 + 0.90}{2} - \frac{0.86 + 0.60}{2} = 0.24 \text{ in.}$$

Flange Flexibility

$$L_F = L_B = 1.15 \text{ in.},$$

$$A_F = \pi(0.86^2 - 0.50^2) = 1.54 \text{ in.}^2,$$

$$F_F = \frac{L_F}{A_F E_T} = 0.75/E_T.$$

Bolt Creep

The axial creep of the bolt is

$$K_B = \frac{C_1 P_t^n L_B}{A_B^n} = 1.82\, C_1 P_t^{4.82}.$$

In order to obtain the bending creep rate of the bolt, the stresses for an inwardly projecting flange are calculated from Reference (15). The critical combination of these stresses by the ASME Boiler Code[1] is

$$\frac{S_H + S_T}{2} = 9.18\, M.$$

For a maximum design stress equal to 2/3 σ_y = 80,000 psi, the design moment equals 80,000/9.18, or M = 8710 in-lb. With a moment arm e = 0.24 in., this corresponds to an initial nut design load of 36,300 lb. In this case, the initial load of 36,300 lb is not limited by the axial stress in the nut, but by the stress in the inwardly projecting flange.

The thickness of an equivalent loose-type flange is determined from Reference (1) using the basic geometry of the inwardly projecting flange of Figure 17. The equivalent thickness equals 0.575 in. The creep rate of the equivalent loose-type flange, calculated from Equation (6), is

$$K_B' = \frac{2\sigma_{Ft}^n C_1 e c_F}{h} = 1.26\, C_1 P_t^{4.82},$$

where

$$\sigma_{Ft} = 1.21\, P_t.$$

Flange Creep

$$K_F = \frac{C_1 P_t^n L_F}{A_F^n} = 0.145\, C_1 P_t^{4.82}.$$

Flexibility and Creep Ratios

$$r_F = 0.595, \qquad r_F' = 0.905,$$

$$r_K = 0.0796, \qquad r_K' = 0.693,$$

$$R = \frac{1 + r_F + r_F'}{1 + r_K + r_K'} = 1.41.$$

*Use the nomenclature of the ASME Code[1]

Intercept Stress Reduction

The initial bolt stress is

$$\sigma_{BR} = P/A_B = 36,300/0.91 = 40,000 \text{ psi},$$

$$\sigma_{BT} = 40,000\left(\frac{E_T}{E_R}\right) = 30,000 \text{ psi}.$$

From Equation (9),

$$\sigma_o = 24,700 \text{ psi},$$

or

$$P_o = \sigma_o A_B = 22,500 \text{ lb}.$$

Nut Relaxation

From Equation (10),

$$t = 1.18 \times 10^{18} \left[\frac{1 - \left(\frac{\sigma_t}{\sigma_o}\right)^{n-1}}{\sigma_t^{n-1}}\right]. \tag{29}$$

The relaxation curve is shown in Figure 18.

External Loads

It is assumed that $K_A = K_M = 0.50$ in this example. The leakage criterion used in Equation (26) is used in Equation (19) to calculate a leakage pressure versus time curve. For example (for the connector shown in Figure 11), at a pressure p of 2000 psi, from Equation (26),

$$P_p + P_G = 33,000 \text{ lb}.$$

From Equation (20),

$$P_A = 7440 \text{ lb},$$

$$P_M = 5920 \text{ lb}.$$

Then, from Equation (19),

$$P_t' = 33,000 + 7440 + 5920 = 46,360 \text{ lb}.$$

The design curve of Figure 13 gives t = 0.37 hour. The results are shown in Figure 14 ($K_A = K_M = 0.50$, $\Delta T = 0$).

Bolt-Flange Temperature Differential

It is assumed that at the beginning of the cooling-down cycle, the bolt assembly is hotter than the flange assembly, or

$$\Delta T = -100 \text{ F}.$$

From Equation (21) and the geometry of Figure 11,

$$\Delta\sigma_B = \frac{\alpha(\Delta T)E_T}{1 + \epsilon_F} = 11,000 \text{ psi}.$$

The reduction in bolt load due to the thermal gradient is

$$P_T = (11,000)(1.89) = 20,800 \text{ lb}.$$

From Equation (23),

$$P_t' = P_p + P_G + P_T. \tag{30}$$

From Equations (26) and (30), at a pressure p = 1500 psi,

$$P_t' = \pi(1500)(1.95^2) + 3(1500)(1.53) + 20,800 = 45,580 \text{ lb}.$$

From Figure 13, t = 0.52 hour.

The results of the analysis are shown in Figure 14 ($K_A = K_M = 0$, $\Delta T = -100$ F).

APPENDIX B

DERIVATION OF EQUATIONS

Flange Flexibility

Loose Type

Timoshenko[18] gives the flange rotation θ_F due to a flange moment M as

$$\theta_F = \frac{12M}{2\pi E_T h^3 \ln d_F/c_F}. \tag{31}$$

Since

$$M = Pe,$$

and the flange deflection at the bolt circle is

$$\delta_F = e\theta_F = \frac{1.91Pe^2}{E_T h^3 \ln d_F/c_F} \tag{32}$$

then,

$$F_F = \frac{2\delta_F}{P} = \frac{3.82e^2}{E_T h^3 \ln d_F/c_F}. \tag{33}$$

Integral Type

Waestrom and Bergh[17] present an equation for the flange rotation:

$$\theta_F = \frac{0.645\,VM}{L\sqrt{c_F}\,(d_T - c_T)^{5/2} E_T}. \tag{34}^*$$

Since the total flange moment M = Pe, and the deflection $\delta_F = \theta_F e$,

$$F_F = \frac{2\delta_F}{P} = \frac{1.29\,Ve^2}{L\sqrt{c_F}(d_T - c_T)^{5/2} E_T}. \tag{35}^*$$

Bolt Creep

From the steady-state creep law,

$$\epsilon_B = C_1\sigma_B^n t, \tag{36}$$

or, the bolt deflection is

$$\delta_B = \frac{C_1 P_t^n t L_B}{A_B^n}, \tag{37}$$

where

$$\sigma_B = \frac{P_t}{A_B}.$$

Then,

$$K_B = \frac{\delta_B}{t} = \frac{C_1 P_t^n L_B}{A_B^n} \tag{38}$$

Flange Creep

Marin[19] developed equations for the steady-state creep of a circular ring of rectangular cross section subjected to uniform moments. The flange rotation and maximum stress on the inner surface are

$$\theta_F = \left[\left(\frac{P_t e}{2\pi}\right)\frac{\left(2^{1+\frac{1}{n}}\right)\left(1 - \frac{1}{n}\right)\left(2 + \frac{1}{n}\right)}{\left(d_F^{\,1-\frac{1}{n}} - c_F^{\,1-\frac{1}{n}}\right)h^{2+\frac{1}{n}}}\right]^n C_1 t, \tag{39}$$

$$\sigma_{Ft} = \left(\frac{h}{2c_F}\right)^{\frac{1}{n}}\left(\frac{P_t e}{2\pi}\right)\left[\frac{\left(2^{1+\frac{1}{n}}\right)\left(1 - \frac{1}{n}\right)\left(2 + \frac{1}{n}\right)}{\left(d_F^{\,1-\frac{1}{n}} - c_F^{\,1-\frac{1}{n}}\right)h^{2+\frac{1}{n}}}\right]. \tag{40}$$

Equations (39) and (40) are based on the steady-state creep law $\epsilon = C_1\sigma^n t$ and assume the creep stress distribution in the flange. There exists sufficient test and theoretical data on the creep bending of beams[20, 21, 22, 23, 24] to justify that:

(1) Plane sections remain plane.

(2) The creep deflections can be predicted on the basis of the steady-state creep law.

(3) Individual fibers of the beam creep at a rate equivalent to that predicted by a tensile creep test.

(4) The creep stress distribution is attained shortly after the commencement of the test and does not change for the remainder of the test. This is analytically confirmed by Hult[24]. Because of the like nature of the beam and ring deformations, the above assumptions are also assumed to hold true for the creep deflection of a flange.

From Equations (39) and (40),

$$\theta_F = \frac{2\sigma_{F_t}^n C_1 c_F t}{h}. \tag{41}$$

*The terms V and L in Equations (34) and (35) conform to the nomenclature of Reference (1)

Then,

$$K_T = \frac{2\epsilon\theta_F}{t} = \frac{4\sigma_{T_t}{}^n C_1 \epsilon c_F}{h} . \quad (42)$$

Intercept Stress Reduction

It is assumed that the initial stress σ_{BT} is reduced in zero time to a new value σ_o which has a total intercept strain ϵ_o equal to the initial bolt stress σ_{BT} divided by the modulus of elasticity E_T. From Figure 19,

$$\epsilon_o = \epsilon_o + C_2 \sigma_o{}^m , \quad (43)$$

or

$$\sigma_{BT} = \sigma_o + E_T C_2 \sigma_o{}^m . \quad (44)$$

The constants C_2 and m are determined by a best fit to the intercept data from a family of creep curves at the design temperature.

For a flexible flange, the interaction of the flange and bolt has to be accounted for. The primary creep of the bolt can be represented by

$$\delta_{Bc} = C_2 \sigma_o{}^m L_B . \quad (45)$$

The change in bolt stress is determined by the elastic bolt recovery:

$$\sigma_o = \sigma_{BT} - \frac{\delta_{Bc} E_T}{L_B} . \quad (46)$$

From Figure (20), in order to maintain compatibility of bolt and flange,

$$\delta_{TOTAL} = \delta_{Fe} - \delta_{Fc} = \delta_{Bc} - \delta_{Be} . \quad (47)$$

By definition,

$$r_F = \frac{\delta_{Fc}}{\delta_{Be}}, \quad r_K = \frac{\delta_{Fc}}{\delta_{Bc}}$$

$$R = \frac{1 + r_F}{1 + r_K} ,$$

and Equation (47) becomes

$$\delta_{Be} (r_F + 1) = \delta_{Bc} (r_K + 1), \quad (48)$$

or

$$\frac{\delta_{Be}}{\delta_{Bc}} = \frac{1 + r_K}{1 + r_F} = \frac{1}{R} . \quad (49)$$

Substituting (45) and (46) in (49),

$$\sigma_o = \sigma_{BT} - \frac{E_T C_2 \sigma_o{}^m}{R} . \quad (50)$$

For a rigid flange (R = 1), Equation (50) is identical to Equation (44). The development of Equation (50) for a flexible flange assumes that the creep ratio r_K is the same for primary creep as it is for steady-state creep.

Bolt Relaxation

The analysis of bolt relaxation is similar to that of References (2, 6). The nomenclature is defined as follows:

L_F = original length between nut bearing surfaces

L_B = length of bolt if it is relieved of stress before creep occurs

$\delta' = L_F - L_B$ = initial flange deflection plus bolt extension (or total initial relative movement between nut and bolt)

$K_F t = \delta_{Fc}$ = creep deflection of flanges

$K_B t = \delta_{Bc}$ = creep deflection of bolts

$F_F P = \delta_{Fe}$ = elastic flange deflection

$F_B P = \delta_{Be}$ = elastic bolt deflection.

In order that the flange and bolts maintain contact at any time,

$$L_F - \delta_{Fc} - \delta_{Fe} = L_B + \delta_{Bc} + \delta_{Be} , \quad (51)$$

or

$$\delta' = \delta_{Bc} (1 + r_K) + \delta_{Be} (1 + r_F). \quad (52)$$

Since

$$\delta_{Be} = \frac{\delta_B L_B}{E_T} ,$$

$$\delta' = \delta_{Bc} (1 + r_K) + \frac{\delta_B L_B}{E_T} (1 + r_F),$$

or

$$\sigma_B = \frac{E_T}{L_B} \left[\frac{\delta' - \delta_{Bc} (1 + r_K)}{1 + r_F} \right] . \quad (53)$$

Differentiate (53) with respect to time:

$$\frac{d\sigma_B}{dt} = \frac{-E_T}{L_B} \left(\frac{1 + r_K}{1 + r_F} \right) \frac{d\delta_{Bc}}{dt} . \quad (54)$$

From the steady-state creep law,

$$\dot{\epsilon}_c = C_1 \sigma_B{}^n = \frac{d\epsilon_c}{dt} = \frac{d}{dt} \left(\frac{\delta_{Bc}}{L_B} \right),$$

or

$$\frac{d\delta_{Bc}}{dt} = L_B C_1 \sigma_B{}^n . \quad (55)$$

Substitute (55) in (54):

$$\frac{d\sigma_B}{\sigma_B{}^n} = \frac{-E_T C_1 dt}{R} . \quad (56)$$

Integrate (56), letting $\sigma_B = \sigma_t$:

$$\frac{\sigma_t{}^{-n+1}}{1-n} = \frac{-E_T C_1 t}{R} + C, \quad (57)$$

where C is a constant of integration. At t = 0, $\sigma_t = \sigma_o$. Therefore,

$$C = \frac{\sigma_o{}^{-n+1}}{1-n} .$$

From (57),

$$t = \frac{R}{C_1 E_T (n-1)} \left[\frac{1 - \left(\frac{\sigma_t}{\sigma_o} \right)^{n-1}}{\sigma_t{}^{n-1}} \right] . \quad (58)$$

Equation (58) also applies to the relaxation of the nut in a threaded connector design with R defined by Equation (18).

External Loads

Axial Load

The axial load P_A is assumed to be a tensile force which reduces the gasket pressure. The magnitude of the tube stress σ_A due to the axial load P_A is defined as a constant times the axial tube stress due to internal pressure:

$$P_A = \sigma_A A_T = \sigma_A \pi \left(d_T{}^2 - c_T{}^2 \right), \quad (59)$$

where

$$\sigma_A = K_A \sigma_T = \frac{p K_A c_T{}^2}{\left(d_T{}^2 - c_T{}^2 \right)} . \quad (60)$$

From (59) and (60),

$$P_A = \pi p K_A c_T{}^2 \quad (61)$$

Bending Moment

The required additional bolt load P_M accounts for the tendency of the tube bending moment M_T to reduce the gasket pressure. The magnitude of the tube stress σ_M due to the bending moment M_T is defined as a constant K_M times the axial tube stress due to internal pressure:

$$\sigma_M = K_M \sigma_T = \frac{p K_M c_T{}^2}{\left(d_T{}^2 - c_T{}^2 \right)} . \quad (62)$$

From beam bending theory,

$$\sigma_M = \frac{4 M_T d_T}{\pi \left(d_T{}^4 - c_T{}^4 \right)} . \quad (63)$$

Combining (62) and (63),

$$M_T = \frac{\pi p K_M c_T{}^2 \left(d_T{}^2 + c_T{}^2 \right)}{4 d_T} \quad (64)$$

The bending moment M_T is considered to reduce the gasket pressure by the amount σ_G on one side of the gasket. If the gasket width is assumed small compared to the gasket radius,

$$\sigma_G = \frac{M_T}{\pi g^2 w} = \frac{p K_M c_T{}^2 \left(d_T{}^2 + c_T{}^2 \right)}{4 d_T g^2 w} . \quad (65)$$

If the maximum gasket pressure is assumed to act on the complete gasket surface,

$$P_M = A_G \sigma_G = 2\pi g w \sigma_G = \frac{\pi p K_M c_T{}^2 \left(d_T{}^2 + c_T{}^2 \right)}{2 d_T g} . \quad (66)$$

Bolt-Flange Temperature Differential

The thermal bolt strain $\Delta\epsilon_B = \alpha(\Delta T)$ corresponds to a thermal bolt deflection $\Delta L_B = \alpha(\Delta T)L_B$ which is distributed according to the flexibility of the flange and bolt. From Figure 20,

$$\alpha(\Delta T)L_B = \delta_{Fe} + \delta_{Be} = \delta_{Be}(r_F + 1). \tag{67}$$

The change in bolt stress is

$$\Delta\sigma_B = \left(\frac{\delta_{Be}}{L_B}\right) E_T \quad . \tag{68}$$

From (67) and (68),

$$\Delta\sigma_B = \frac{\alpha(\Delta T)E_T}{1 + r_F} \quad . \tag{69}$$

Following a similar procedure for the threaded connector,

$$\Delta\sigma_B = \frac{\alpha(\Delta T)E_T}{1 + r_F + r_F} \quad . \tag{70}$$

APPENDIX C

SECONDARY EFFECTS

Stress Concentrations

Because of the accelerated rate of creep at higher stress levels, the presence of stress concentrations such as bolt threads might be expected to increase the over-all creep rates of the assembly. However, the results of the British Flange Tests[9] indicate that the creep of the nut assembly was not exceedingly high if the nut material was equivalent to the bolt material. However, when carbon steel nuts were used with alloy steel bolts, the creep of the nut assembly was excessive.

A comprehensive review of stress concentrations under creep conditions was presented in Reference (25). The strength of a specimen with a notch under creep conditions is attributed partly to the ability of the material in the notch area to flow rapidly and redistribute stresses at high temperatures; also because the greater volume of lower stressed material away from the notch restrains the over-all deformations.

Creep Bending of Bolt

The tendency of the bolt in a flanged joint assembly to develop bending moments due to flange rotations and shifting of the nut reaction is well known. Under creep conditions, however, the stress distribution becomes more favorable because of the redistribution of the bending stresses. Bailey[3] developed a solution, based on the steady-state creep law, for the creep stresses due to combined axial and bending loads on a rectangular cross section; the results are shown in Figure 21. The results for a solid circular section should be comparable because of the relative values of the plastic bending factor for the rectangular and solid circular sections.

Dynamic Creep

Superimposed alternating stresses are known to affect the creep rate of metals. However, Lazan[26] showed that the presence of alternating stresses did not appear to affect greatly the creep rate for most materials. Results for Waspaloy at 1500 F from Reference (27) are shown in Figure 22.

Langenecker[28] has recently discussed a problem of possible significance to connectors operating in a high acoustic radiation field. He found that intense ultrasound could have a marked effect on the physical properties of solids.

Gasket Creep*

The gasket will contribute a certain amount of creep and flexibility to the connector assembly. This contribution is neglected in the design procedure in view of the relatively short length of the gasket in most designs. Also, for metallic gaskets, the stresses in the gasket are usually lower than those of the bolt assembly. In fact, the gasket area should be chosen, on the basis of the relative creep strengths of the gasket and bolt material, such that the creep rate of the gasket is negligible. The inclusion of the gasket creep and flexibility properties in the design procedure will unduly complicate the equations, with very little gain in design accuracy for most geometries.

Flange Rotations

Changes in the flange rotation and corresponding bolt-load changes due to the application of internal pressure are neglected in the design procedure. These effects are considered secondary from the standpoint of over-all bolt relaxation, but should be considered in the static design of the connector if found to be significant.

APPENDIX D

TUBE DESIGN

The tube design is considered on page 18 only to the extent that it affects the strength of the connector. The tube, however, is subjected to progressive creep deformations with each operating cycle. The tube thickness should satisfy the minimum requirements for a creep design. Some of the appropriate theories available for the tube creep design are reviewed below.

Finnie and Heller[7] present the equation for the tangential strain rate in a thin-walled tube with closed ends under internal pressure:

$$\dot{\epsilon}_\phi = C_1 \left(\frac{pc_T}{d_T - c_T}\right)^n \left(\frac{3}{4}\right)^{\frac{n+1}{2}} = \dot{\epsilon}\left(\frac{3}{4}\right)^{\frac{n+1}{2}} \quad , \tag{71}$$

where $\dot{\epsilon} = C_1\sigma^n$ = the strain rate which would be produced by the tangential stress

$$\sigma = \frac{pc_T}{d_T - c_T}$$

acting alone in simple tension.

The creep of thin-walled tubes under internal pressure, axial loads, and moments is considered in Reference (7).

Finnie and Heller[7] also analysed the creep of thick-walled tubes subjected to internal pressure. Based on the Mises flow law and the steady-state creep law $\dot{\epsilon} = C_1\sigma^n$, the radial, tangential, and axial stresses, respectively, are

$$\begin{aligned}
\sigma_r &= -p\frac{\left(\frac{d_T}{r}\right)^{2/n} - 1}{\left(\frac{d_T}{c_T}\right)^{2/n} - 1} \quad , \\
\sigma_\phi &= p\frac{\left(\frac{2-n}{n}\right)\left(\frac{d_T}{r}\right)^{2/n} + 1}{\left(\frac{d_T}{c_T}\right)^{2/n} - 1} \quad , \\
\sigma_z &= p\frac{\left(\frac{1-n}{n}\right)\left(\frac{d_T}{r}\right)^{2/n} + 1}{\left(\frac{d_T}{c_T}\right)^{2/n} - 1} \quad ,
\end{aligned} \tag{72}$$

where

r = variable radius, $c_T \leq r \leq d_T$.

Equations (72) reduce to the well-known Lamé formulas for n = 1. The tangential strain rate is

$$\dot{\epsilon}_\phi = C_1\left(\frac{3}{4}\right)^{\frac{n+1}{2}}\left[\frac{p}{\left(\frac{d_T}{c_T}\right)^{2/n} - 1}\left(\frac{2}{n}\right)\right]^n \left(\frac{d_T}{r}\right)^2 \quad . \tag{73}$$

The steady-state creep stresses and strain rates in a thick-walled tube under combined internal pressure and axial load are presented by Finnie[29]. Numerical solutions to the equations are tabulated for various values of the variables. In the case where the additional axial load is either small or large compared to the axial load due to internal pressure, simple approximate solutions are given. Finnie[30] also pointed out the lack of complete agreement between the theoretical and experimental studies on multiaxial creep in tubes, attributing the discrepancies to the effect of hydrostatic stress which is usually assumed negligible in creep strain predictions.

A method for predicting the creep failure time for either thin-walled or thick-walled circular cylinders can be found in Reference (31). True stress and true strain are used and the steady-state creep law is assumed valid until failure. The failure time is based on plastic instability, or the time at which the vessel wall is no longer sufficient to hold the load. Simplified formulas are obtained for both thin-walled and very-thick-walled cylinders.

Creep-rupture tests[32] were run on Type 316 stainless steel tubes at high temperatures and pressures. The results of the tests compare favorably with those of uniaxial tension tests if effective stress and effective strain rate are used. Rattinger and Padlog[33] also present a method of analysis for predicting creep rupture of cylindrical shells using conventional uniaxial creep data.

A method of analysis[34] for predicting the stresses and strains in thick-walled cylinders considers primary as well as secondary creep. The analysis is quite complicated and justifies a computer solution.

Equations (71) and (73) result in quite favorable strain rates for higher values of the exponent n. On this basis, the design procedure of the ASME Boiler Code[1], which compares the maximum design stress to the creep rate or rupture stress of a uniaxial tension test, provides for a safe design.

* This design procedure could be extended to include the effects of gasket creep in an approximate but quite conservative manner.

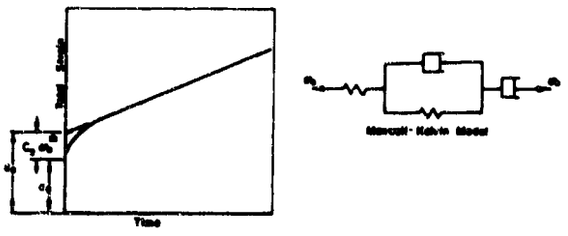

FIGURE 1. TYPICAL CREEP CURVE

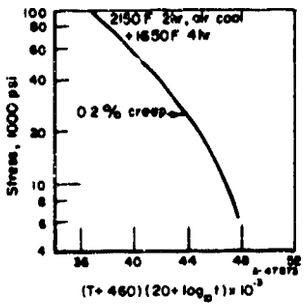

FIGURE 5. MASTER CREEP CURVE FOR RENÉ 41 BAR

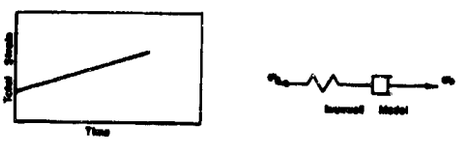

FIGURE 2. STEADY-STATE CREEP

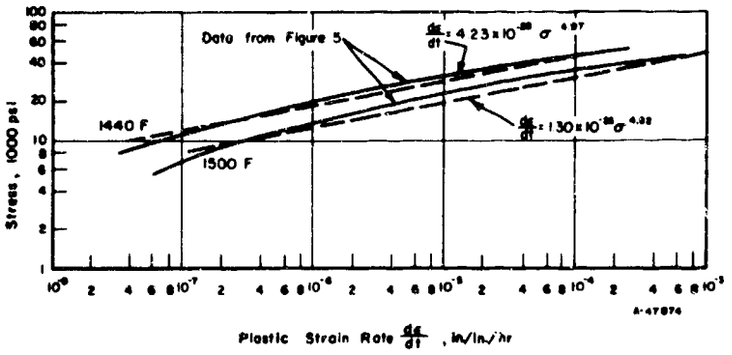

FIGURE 6. CREEP RATE OF RENÉ 41 AT 1440 F AND 1500 F

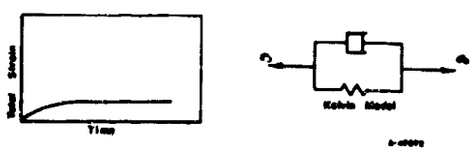

FIGURE 3. PRIMARY CREEP

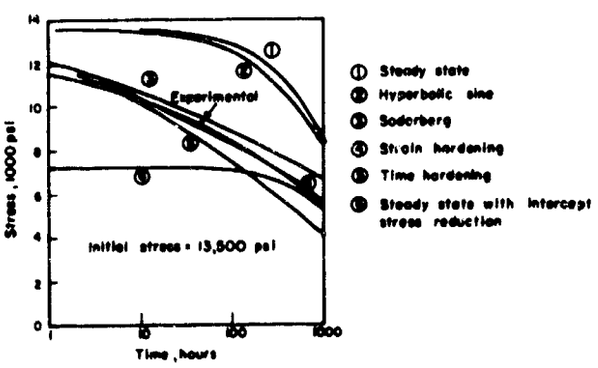

FIGURE 4. CREEP-RELAXATION COMPARISON (COPPER AT 185 C)

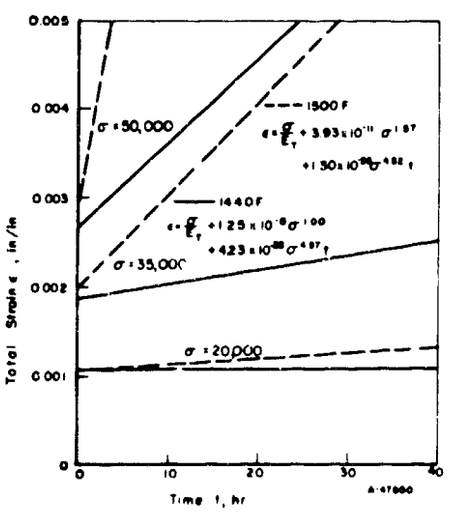

FIGURE 7. DESIGN CREEP PROPERTIES OF RENÉ 41

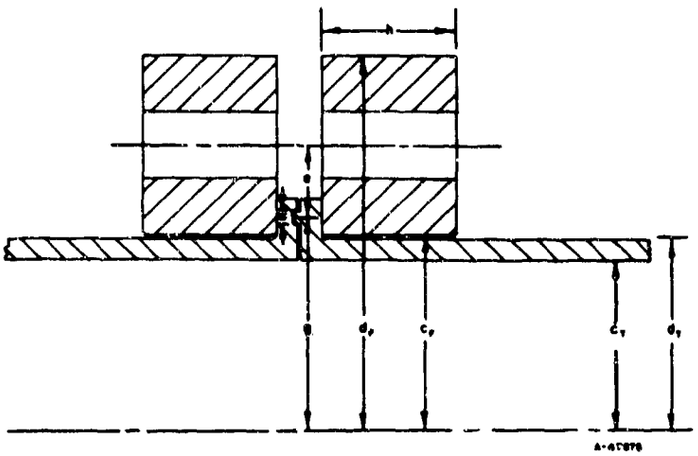

FIGURE 8. TYPICAL FLANGE GEOMETRY

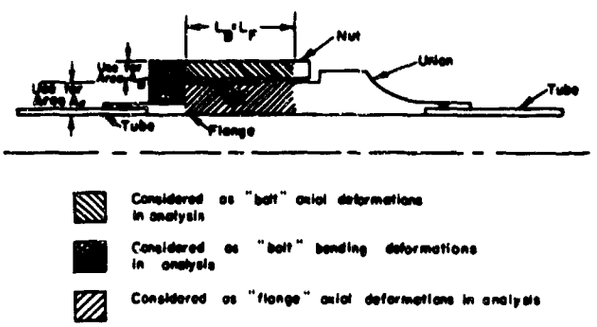

FIGURE 9. THREADED CONNECTOR MODEL

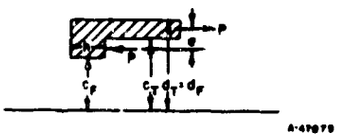

FIGURE 10. INWARDLY PROJECTING FLANGE

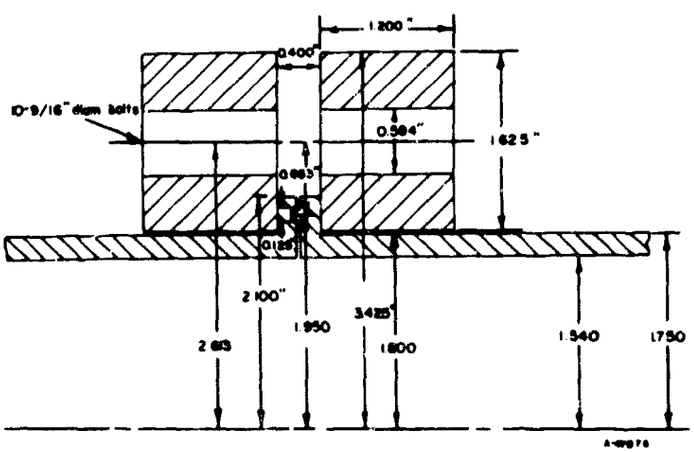

FIGURE 11 LOOSE-TYPE FLANGE GEOMETRY (RENE' 41 - 1500 F)

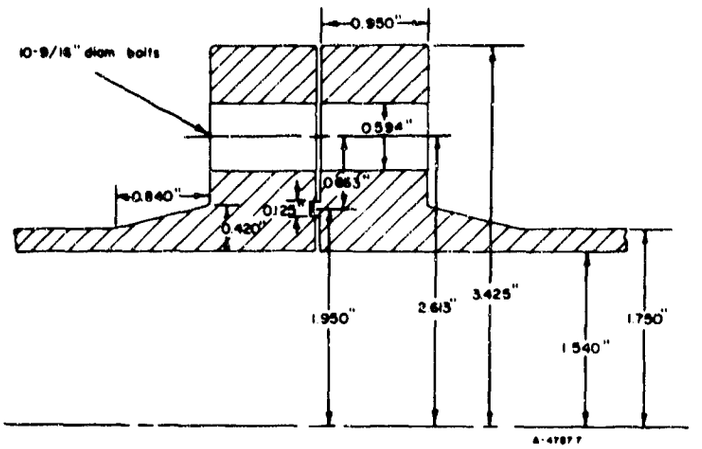

FIGURE 12. INTEGRAL-TYPE FLANGE GEOMETRY (RENÉ 41 - 1500 F)

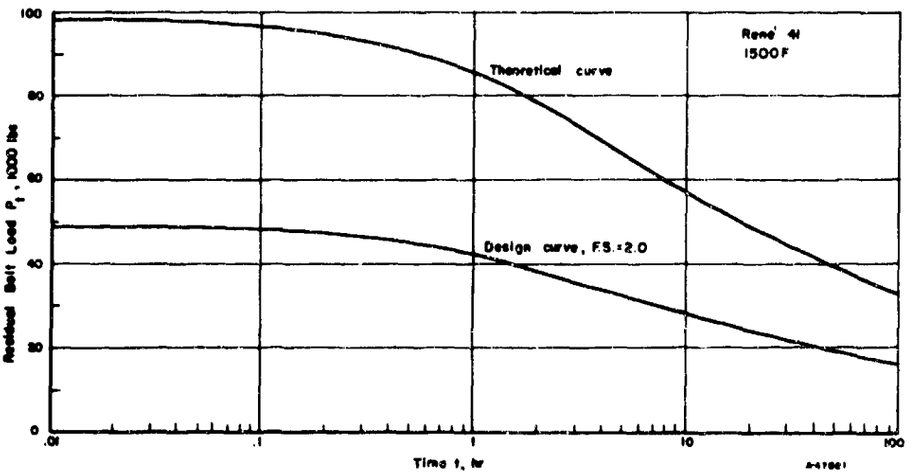

FIGURE 13. RESIDUAL BOLT LOAD VERSUS TIME FOR BOLTED-FLANGED CONNECTOR (SHOWN IN FIGURE 11)

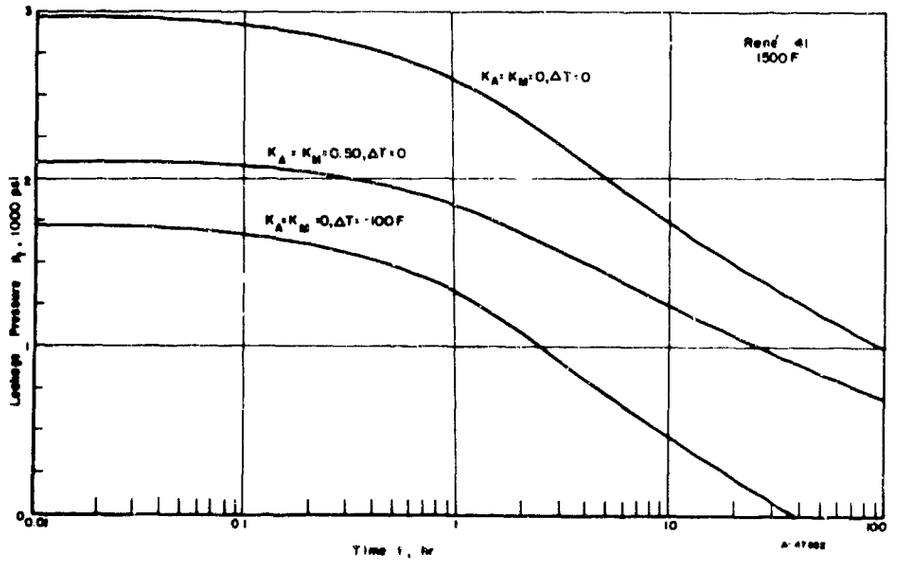

FIGURE 14. LEAKAGE PRESSURE VERSUS TIME FOR BOLTED-FLANGED CONNECTOR (SHOWN IN FIGURE 11)

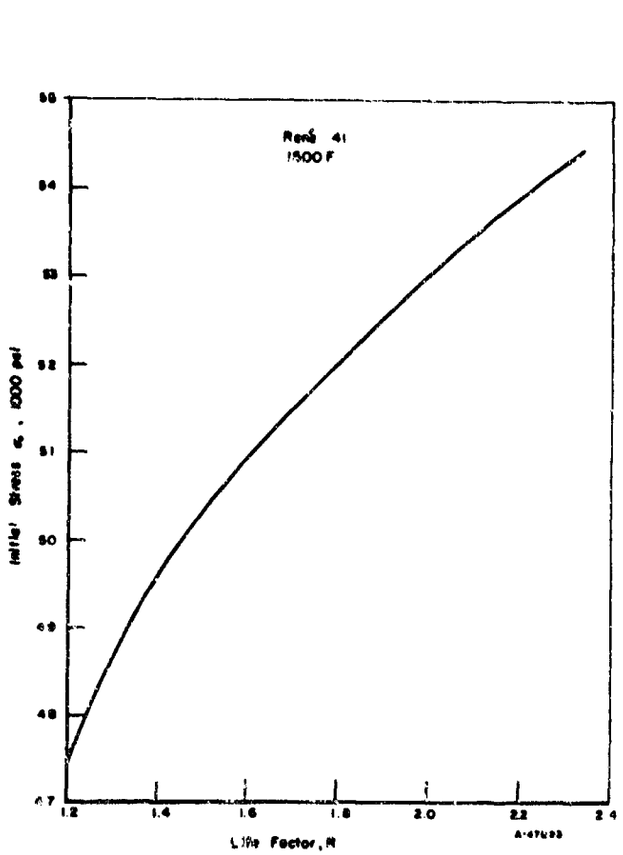

FIGURE 15. EFFECT OF LIFE FACTOR ON INITIAL STRESS (σ_{BT} = 65,000 PSI)

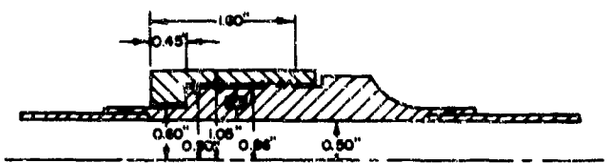

FIGURE 17. THREADED-CONNECTOR GEOMETRY

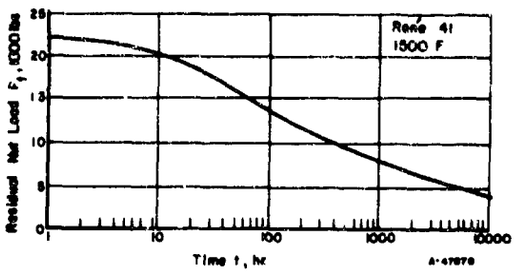

FIGURE 18. RESIDUAL NUT LOAD VERSUS TIME FOR THREADED CONNECTOR (SHOWN IN FIGURE 17)

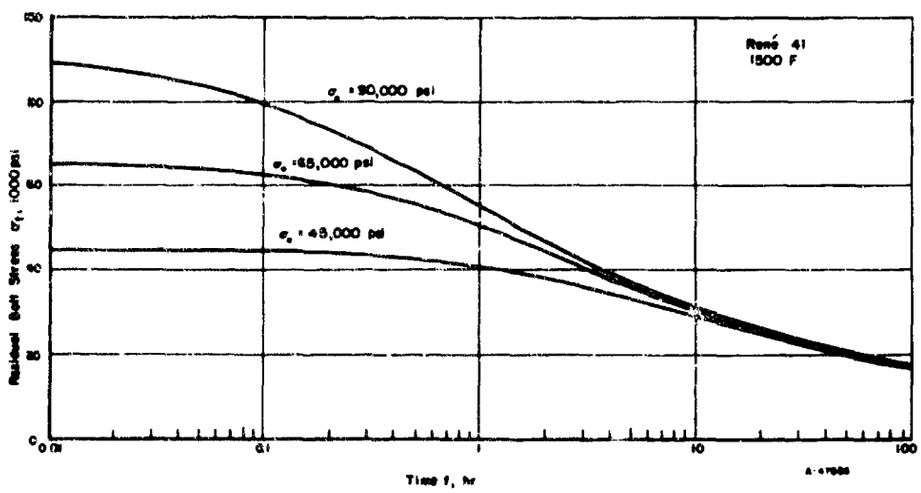

FIGURE 16. EFFECT OF INITIAL BOLT STRESS ON RELAXATION (FLANGE GEOMETRY OF FIGURE 11)

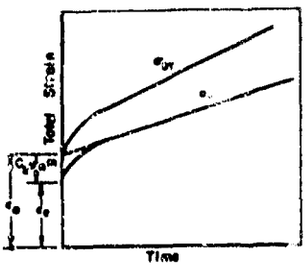

FIGURE 19. INTERCEPT STRESS REDUCTION

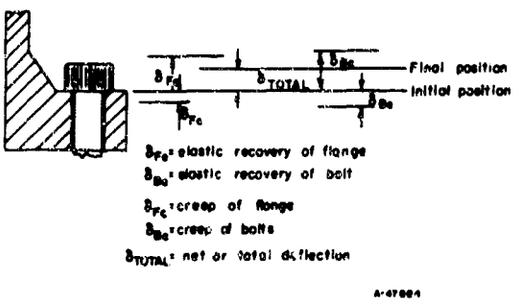

FIGURE 20. CREEP OF FLANGE AND BOLT

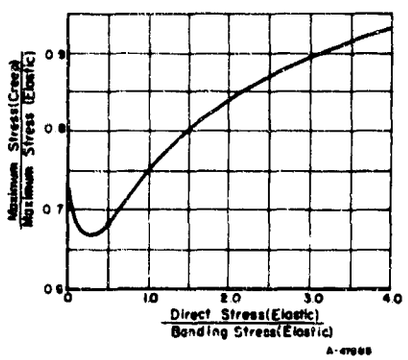

FIGURE 21. CREEP BENDING OF RECTANGULAR SECTION (n = 6)

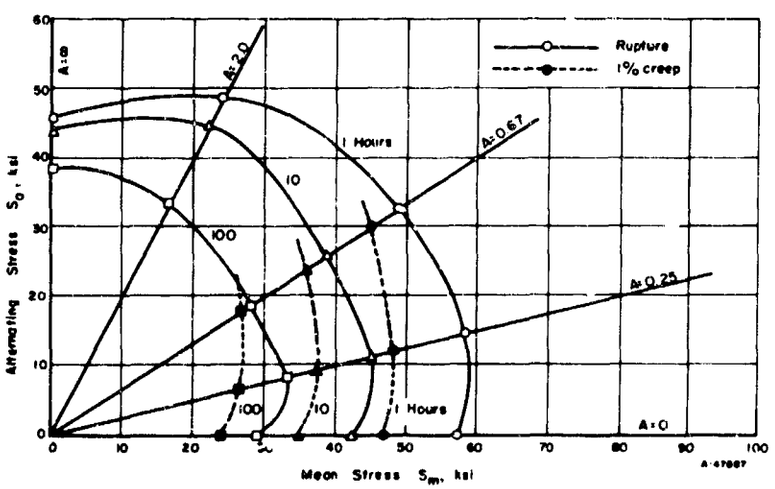

FIGURE 22. COMBINED CREEP AND FRACTURE STRESS RANGE DIAGRAM FOR 6.3% Mo-WASPALLOY AT 1500 F

APPENDIX B

COMPUTER PROGRAM FOR DESIGNING AFRPL FLANGED CONNECTORS

This appendix is intended for those who plan to use the computing programs IRFDP and LRFDP for designing flange connectors of the types shown in Figure 67 of this report. Program IRFDP is used to design connectors containing two integral flanges, and Program LRFDP is used to design connectors containing two loose-ring flanges. By appropriately controlling certain input values of both programs, a design can be obtained for a connector containing one integral flange and one loose-ring flange.

A detailed description is given of the input and output sections of Program IRFDP. Program LRFDP is similar to IRFDP, and the difference is discussed. Also, the integral/loose-ring connector-design approach is described.

Programs IRFDP and LRFDP were written in FORTRAN IV language for the CDC 6400. A list of both the programs is included. It is believed that the programs can easily be converted to run on a different machine with a FORTRAN IV compiler.

Item-by-Item Description of Input Data for IRFDP

The computer input cards that are necessary to perform the design using IRFDP will be described in this section. The numbers refer to the card numbers as read by the program. The following FORMATS were used for the input:

1020 FORMAT (8F10.0)

1021 FORMAT (8F10.4)

1022 FORMAT (8F10.9)

1023 FORMAT (2I10)

Card 1

Read 1020, TBMI

TBMI = Tube bending moment input, lb-in.

Set TBMI = 0.001 if the value of the bending moment is to be selected internally according to Equations (8) and (9) on page 31.

Card 2

Read 1021, TOD, TWI

TOD = Tube outside diameter, in.

TWI = Tube wall thickness input, in.

If TWI $\leq$ 0.001, then the tube wall thickness is internally selected by Equation (6) on page 29. In the final program, Equation (6) also includes tube design for impulse-pressure fatigue.

Card 3

Read 1020, TU, TY, TF, TR, TFRO

TU = Ultimate tensile strength of tube material at maximum operating temperature, psi

TY = Tensile yield strength of tube material at maximum operating temperature, psi

TF = Fatigue strength for R = - 1.0 of tube material at maximum operating temperature, psi

TR = 2 Year-Rupture strength of tube material at maximum operating temperature, psi

TFRO = Fatigue strength for R = 0.0 of tube material at maximum operating temperature, psi.

Card 4

Read 1021, BCDI, HUBII

BCDI = Bolt circle diameter input, in.

If BCDI $\leq$ 0.001, the bolt circle diameter is calculated, also if BCDI $\leq$ 0.001, II = 0 and BNI = 0.0 (See Card 30 and Card 31)

HUBII = Hub reinforcement height, in.

If HUBII < 0.001, the reinforcement height is calculated by the program.

Card 5

Read 1021, G10TWI

G10TWI = Maximum allowable hub reinforcement ratio,

where

$$G10TWI = \frac{(TW + HUBI)}{TW}$$

where

TW = tube wall thickness, in.

HUBI = Selected hub height, in.

Set G10TWI = 3. to 5.

Card 6

Read 1021, FRI, FSFI

FRI = Radius input for fillet at junction of flange and hub reinforcement, in. If FRI = 0.0, the radius is computed by the program. It is recommended that a value no smaller than that computed be used.

FSFI = Factor of safety used in fatigue evaluation. A factor of 2.0 was chosen for all designs.

Card 7 - Card 9

Read, 1020, FUR

Read, 1020, FU, FY, FSU, FCY, FE, FG, FYC, FYR

Read, 1022, FRHO, FMU, FTE, FCR

FUR = Ultimate tensile strength of flange material at room temperature, psi

FU = Ultimate tensile strength of flange material at maximum operating temperature, psi

FY = Tensile yield strength of flange material at maximum operating temperature, psi

FSU = Ultimate shear strength of flange material at maximum operating temperature, psi

FCY = Compressive yield strength of flange material at maximum operating temperature, psi

FE = Young's modulus of elasticity for flange material, psi

FG = Shear modulus for flange material, psi

FYC = Tensile yield strength of flange material at minimum operating temperature, psi

FYR = Tensile yield strength of flange material at room temperature, psi

FRHO = Flange material density, $lb/in.^3$

FMU = Poisson's Ratio for flange material

FTE = Coefficient of thermal expansion for flange material, in./°F

FCR = Flange material creep rate.

Card 10 – Card 13

Read 1021, (R[NN], NN = 1,8)

Read 1021, (R[NN], NN = 9,11)

Read 1020, (FF[NN], NN = 1,8)

Read 1020, (FF[NN], NN = 9,11)

R = Stress Ratio – the algebraic ratio of the minimum stress to the maximum stress in the stress cycle. Eleven standard ratios are read in. They range from -1.0 to 1.0 in steps of 0.2.

FF = Corresponding fatigue strength for flange material at maximum operating temperature for a given number of cycles, psi. The values of FF are obtained from a modified Goodman diagram for the flange material.

Card 14

Read 1021, SODI, SIDI, SELI, TAI, TAOTW, SLEGTI

SODI = Seal outside diameter input, in.

SIDI = Seal inside diameter input, in.

SELI = Seal tang length input, in.

TAI = Seal tang height input, in.

TAOTW = Initial ratio of tang height to tube wall thickness. A value of 0.9 to 1.0 is recommended.

SLEGTI = Seal disk thickness, input, in.

Let SODI $\leq$ 0.001 for the program to calculate seal dimensions.

Card 15

Read 1020, RSLI, SSLI, MSLI

RSLI = Radial sealing load per inch of seal circumference, lb/in.

SSLI = Axial sealing load per inch of seal circumference, lb/in.

MSLI = Minimum axial sealing load per inch of seal circumference, lb/in.

Card 16 - Card 17

Read 1020, SCY, SEE, SCYC, SCYR, SYR

Read 1022, STE

SCY = Compressive yield strength of seal material at maximum operating temperature, psi

SEE = Young's modulus of elasticity for seal material, psi

SCYC = Compressive yield strength of seal material at minimum operating temperature, psi

SCYR = Compressive yield strength of seal material at room temperature, psi

SYR = Tensile yield strength of seal material at room temperature, psi

STE = Coefficient of thermal expansion for seal material, in./°F.

Card 18 - Card 29

Read 1021, (BH[NN], NN = 1, 8)

Read 1021, (BH[NN), NN = 9, 15)

Read 1021, (BWC[NN], NN = 1, 8)

Read 1021, (BWC[NN], NN = 9, 15)

Read 1021, (BS[NN], NN = 1, 8)

Read 1021, (BS[NN], NN = 9, 15)

Read 1021, (BTA[NN], NN = 1, 8)

Read 1021, (BTA[NN], NN = 9, 15)

Read 1021, (NWT[NN], NN = 1, 8)

Read 1021, (NWT[NN], NN = 9, 15)

Read 1021, (DAF[NN], NN = 1, 8)

Read 1021, (DAF[NN], NN = 9, 15)

BH = Hole size for bolts, in.

BWC = Bolt wrench clearance, in.

BS = Nominal bolt size, in.

BTA = Bolt tensile area, $in.^2$

NWT = Weight of a nut, lb.

DAF = Diameter across flats for bolt head, in.

Note: The order of reading the above bolt geometry for 15 different sizes is from the smallest size to the largest size of bolt.

Card 30 – Card 31

Read 1023, II, IMAX

Read 1020, BNI

II = Index for selection of bolt from bolt table input

IMAX = 16

BNI = Number of bolts, input.

Note: See Card 4. If BCDI $\leq$ 0.001, then II = 0 and BNI = 0.0

Card 32 – Card 33

Read 1020, BY, BE, BU, BYC, BYR

Read 1022, BTE, BCR, BRHO

BY = Tensile yield strength of bolt material at maximum operating temperature, psi

BE = Young's modulus of elasticity of bolt material, psi

BU = Ultimate tensile strength of bolt material at maximum operating temperature, psi

BYC = Tensile yield strength of bolt material at minimum operating temperature, psi

BYR = Tensile yield strength of bolt material at room temperature, psi

BTE = Coefficient of thermal expansion of bolt material, in./°F

BCR = Bolt material creep rate

BRHO = Bolt material density, $lb/in.^3$

Card 34

Read 1020, P, PP, PB, PIM, TMAX, TMIN

P = Operating pressure, psi

PP = Proof pressure, psi

PB = Burst pressure, psi

PIM = Impulse pressure, psi

TMAX = Maximum operating temperature, F

TMIN = Minimum operating temperature, F.

Card 35

Read 1020, DTC1, DTC2, DTH1, DTH2

DTC1 = Thermal gradient at minimum temperature from seal or tube to flange, F

DTC2 = Thermal gradient at minimum temperature from flange to bolt, F

DTH1 = Thermal gradient at maximum temperature from seal or tube to flange, F

DTH2 = Thermal gradient at maximum temperature from flange to bolt, F.

Card 36

Read 1021, FS1, FS2, FS3

FS1 = Factor of safety for flange and seal material

FS2 = Factor of safety for bolt material

FS3 is not presently used.

For additional guidance, the actual cards used for designing 3-inch, 1500-psi integral-integral aluminum connectors are reproduced in Figures B-1 and B-2.

Description of Computer Output for IRFDP

The interpretation of the output of Program IRFDP is given below. The value of each variable is printed directly below its symbolic definition. The output sheets obtained for the 3-inch 1500-psi integral-integral aluminum designs are reproduced on pages B-60 through B-62.

The input to the design is first printed out exactly in the same order as read in. This must be reviewed, as it provides a check to insure that the proper data were key punched. As an example, a value of 0.001 is printed under TBMI (for definition of symbols of input item, see pages B-2 through B-8), hence TBMI = 0.001 lb-in. The design output is then printed and consists of several parts. First the tube bending moment (TBM, lb-in.) and corresponding bending stress (TBS, psi) are printed and then the torque per bolt (TRQ, lb-in.) required to assemble the connector is printed.

The second part of the output consists of the calculated component loads for the seven design conditions as described on page 81 of this report. Also, refer to Figures 71 and 72. The definitions of the loads are as follows:

MO = Equivalent flange moment, lb-in

BL = Axial bolt load, lb

SL = Axial seal load, lb

RSL = Radial seal load, lb

MP = Flange moment due to pressure, lb-in.

MC = Flange moment due to creep, lb-in.

Hence MO1 means the equivalent flange moment under Condition 1, and so on. These definitions apply to all the seven design conditions. However, for Condition 2 and Condition 6, the above definitions are expanded and some new terms are defined as follows:

Condition 2

MO2, BL2, SL2, RSL2 are component loads with creep under Condition 2.

MO2P, BL2P, SL2P, RSL2P are component loads under Condition 2 with no creep.

MO2M, BL2M, S12M, RSL2M are component loads under Condition 2 with no creep and a minus bending moment.

Condition 6

MCTG6 = Flange moment due to cold thermal gradient, lb-in.

MHTG6 = Flange moment due to hot thermal gradient, lb-in.

MO6C, BL6C, et al., are component loads under Condition 6 at minimum temperature with creep.

MO6CN, BL6CN, et al., are component loads under Condition 6 at minimum temperature without creep.

MO6H, BL6H, et al., are component loads under Condition 6 at maximum temperature with creep.

MO6HN, BL6HN, et al., are component loads under Condition 6 at maximum temperature without creep.

The stress-concentration factor (KTF) used in the fatigue analysis is printed out. The next section of the output consists of stress values for the seven design conditions. In the following description, A means the value at the inside point of the junction of flange and tube and B implies the values are at the outside point. The other stress values are at the flange inside diameter. Also, the definitions for design conditions are as described in the load values printout.

EXA = Equivalent maximum stress at A, psi

ENA = Equivalent minimum stress at A, psi

EXB = Equivalent maximum stress at B, psi

ENB = Equivalent minimum stress at B, psi

SMAX A = Maximum stress in axial direction at A, psi

SMIN A = Minimum stress in axial direction at A, psi

FFC A = Allowable fatigue stress at A, psi

SMAX B = Maximum axial stress at B, psi

SMIN B = Minimum axial stress at B, psi

FFC B = Allowable fatigue stress at B, psi

SH = Flange axial stress due to bolt load or seal load, psi

SRS = Flange axial stress due to radial seal load, psi

SPR = Axial stress in flange due to pressure, psi

SPA = Axial stress in flange due to axial pressure load, psi

SB = Axial stress in flange due to bending load, psi

SR = Radial stress in flange, psi

ST = Tangential stress in flange, psi

BTS = Bolt tensile stress, psi.

The next section consists of the final dimensions of the design. These dimensions are shown in Figure B-3 and include:

H = Axial length of hub reinforcement, in.

HUBI = Hub reinforcement height, in.

G1 = Hub reinforcement height plus tube wall thickness, in.

FR = Fillet radius, in.

TW = Tube wall thickness, in.

TOD = Tube outside diameter, in.

A = Flange outside diameter, in.

B = Flange inside diameter, in.

XT = Flange thickness, in.

BCD = Bolt circle diameter, in.

SOD = Seal outside diameter, in.

SID = Seal inside diameter, in.

SEL = Seal tang length, in.

TA = Seal tang height, in.

SLEGT = Seal leg thickness, in.

BS(I) = Nominal bolt size, in.

BH(I) = Hole size, in.

BTA(I) = Bolt tensile area, $in.^2$

BWC(I) = Wrench clearance, in.

BN = Number of bolts

WGT = Approximate weight of connector assembly up to and including hub reinforcement length, lb.

Input Description for Program LRFDP

In the following description, the order of card input is 1 to 7, 8, 9a, etc.

Cards 1 to 3, Same as in IRFDP

Card 4, Read 1021, AI, HUBII,

where

AI = Stub flange diameter input, in. If AI = 0.00, then the program computes the diameter.

HUBII, same as in IRFDP.

Card 8a, Read 1021, FCYC, FCYR.

FCYC = Compressive yield strength of flange material at minimum temperature, psi.

FCYR = Compressive yield strength of flange material at room temperature, psi.

Card 9 - Card 33, Same as IRFDP

Card 33a, Read 1021, BCDI

BCDI = Bolt circle diameter input, in. If BCDI $\leq$ 0.000 then II = 0.0 and BNI = 0.0 (see Cards 30-31).

Card 33b - 33d

Read 1020, RU, RY, RSU, RCY, RE, RG, RYC, RYR

Read 1020, RCYC, RCYR

Read 1020, RTE, RCR, RRHO

RU = Ultimate tensile strength of ring material at maximum temperature, psi

RY = Tensile yield strength of ring material at maximum temperature, psi

RSU = Ultimate shear strength of ring material at maximum temperature. psi

RCY = Compressive yield strength of ring material at maximum temperature, psi

RE = Young's modulus of elasticity for Ring material, psi

RG = Shear modulus for Ring material, psi

RYC = Tensile yield strength of ring material at minimum temperature, psi

RYR = Tensile yield strength of ring material at room temperature, psi

RCYC = Compressive yield strength of ring material at minimum temperature, psi

RCYR = Compressive yield strength of ring material at room temperature, psi

RTE = Coefficient of thermal expansion for ring material, in./°F

RCR = Ring material creep rate

RRHO = Density of ring material, lb/in.^{3}

Card 34, Same as in IRFDP.

Card 35, Read 1020, DT1C, DT2C, DT3C, DT1H, DT2H, DT3H

DT1C = Thermal gradient at minimum temperature from seal or tube to flange, F

DT2C = Thermal gradient at minimum temperature from flange to ring, F

DT3C = Thermal gradient at minimum temperature from ring to bolt, F

DT1H = Thermal gradient at maximum temperature from seal or tube to flange, F

DT2H = Thermal gradient at maximum temperature from flange to ring, F

DT3H = Thermal gradient at maximum temperature from ring to bolt, F.

Card 36, Same as in IRFDP.

Description of Output for LRFDP

As in program IRFDP, the input data is first printed out

The design output consists of the same sections as in IRFDP with a few additional print-outs in the "stress for all conditions" section and in the "dimensions" section.

In the stress section after the bolt tensile stress (BTS), the contact stress between the ring and the stub flange (SFB) is printed for all design conditions.

In the dimension section the following interpretations are made:

A = Outside diameter of stub flange, in.

B = Inside diameter of stub flange, in.

XT = Stub flange thickness, in.

ROD = Loose-ring outside diameter, in.

RID = Loose-ring inside diameter, in.

RFR = Ring fillet radius which fits in with the flange fillet radius, in.

The rest of the output interpretation is as described in IRFDP. The dimensions for connectors with loose-ring flanges are shown in Figure B-4.

Designing an Integral Loose-Ring Connector

(1) Design a connector using IRFDP

(2) Design a connector using LRFDP

(3) Select the maximum bolt circle diameter from Steps 1 and 2

(4) If the bolt circle diameter is maximum in Step 1, then run Program LRFDP with the values as the input in Card 33a (LRFDP). Also, the required number of bolts and the bolt index are read in (Card 30-31) as obtained in Step 1.

(5) If bolt circle diameter is maximum in Step 2, then run Program IRFDP with this value as the input in Card 4 (IRFDP). Also, the required number of bolts and the bolt index are read in (Card 30-31) as obtained in Step 2.

(6) By using dimensions in Steps 1 and 4 or Steps 2 and 5, a matching connector is obtained for an integral flange and a loose-ring flange.

```
      PROGRAM IRFDP (INPUT,OUTPUT,TAPE60=INPUT)
      TYPE REAL LT,MSL,K,LCE,LCO,L,MP2,MC2,MO1,NA1,NA2,NA3
      TYPE REAL NB1,NB2,NB3,MO2,MO2P,MO2M,MP3,MO3,MP5,MO5,MO6,MC6,
     1MCTG6,MHTG6,MO6CM,MO6H,MO6HM,MO7,MH,MP6
      TYPE REAL  MSLI
      TYPE REAL NWT
      TYPE REAL KTF
      DIMENSION R(11),FF(11),BH(15),BWC(15),BS(15),BTA(15),NWT(15)
      DIMENSION DAF(15)
C TUBE LOAD-INPUT
 1020 FORMAT (8F10.0)
 1021 FORMAT (8F10.4)
 1022 FORMAT (8F10.9)
 1023 FORMAT (2I10)
  999 READ 1020,TBM1
      IF(EOF,60) 998,997
C TUBE GEOMETRY
  997 READ 1021,TOD,TW1
C TUBE MATERIAL PROPERTIES
      READ 1020,TU,TY,TF,TR,TFR0
C FLANGE GEOMETRY
      READ 1021,BCDI,HUBII
      READ 1021,G1OTWI
      READ 1021,FRI,FSFI
C FLANGE MATERIAL PROPERTIES
      READ 1020,FUR
      READ 1020,FU,FY,FSU,FCY,FE,FG,FYC,FYR
      READ 1022,FRH0,FMU,FTE,FCR
      READ 1021, (R(NN),NN=1,8)
      READ 1021, (R(NN),NN=9,11)
      READ 1020, (FF(NN),NN=1,8)
      READ 1020, (FF(NN),NN=9,11)
C SEAL GEOMETRY
      READ 1021,SODI,SIDI,SELI,TAI,TAOTW,SLEGYI
C SEAL LOADS-INPUT
      READ 1020,RSLI,SSLI,MSLI
C SEAL MATERIAL PROPERTIES
      READ 1020,SCY,SEE,SCYC,SCYR,SYR
      READ 1022,STE
C BOLT GEOMETRY
      READ 1021,(BH(NN),NN=1,8)
      READ 1021,(BH(NN),NN=9,15)
      READ 1021,(BWC(NN),NN=1,8)
      READ 1021,(BWC(NN),NN=9,15)
      READ 1021,(BS(NN),NN=1,8)
      READ 1021,(BS(NN),NN=9,15)
      READ 1021,(BTA(NN),NN=1,8)
      READ 1021,(BTA(NN),NN=9,15)
      READ 1021,(NWT(NN),NN=1,8)
      READ 1021,(NWT(NN),NN=9,15)
      READ 1021,(DAF(NN),NN=1,8)
      READ 1021,(DAF(NN),NN=9,15)
C BOLT INPUT
      READ 1023,I1,IMAX
      READ 1020,BN1
C BOLT MATERIAL PROPERTIES
```

```
      READ 1020,BY,BE,BU,BYC,BYR
      READ 1022,BTE,BCR,BRHO
C SYSTEM PRESSURE AND TEMPERATURE
      READ 1020,P,PP,PB,PIM,TMAX,TMIN
      READ 1020,DTC1,DTC2,DTH1,DTH2
      READ 1021,FS1,FS2,FS3
 9020 FORMAT (8F10.0)
 9021 FORMAT (8F10.4)
 9022 FORMAT (8F10.8)
 9023 FORMAT (2I10)
      PRINT 726
  726 FORMAT(25X,19HINPUT TO THE DESIGN///)
      PRINT 2020
 2020 FORMAT (16H TUBE LOAD-INPUT)
      PRINT 2021
 2021 FORMAT (3X,4HTBM1)
      PRINT 9021,TBM1
      PRINT 2000
 2000 FORMAT (14H TUBE GEOMETRY)
      PRINT 2001
 2001 FORMAT (6X,3HTOD,7X,3HTW1)
      PRINT 9021,TOD,TW1
      PRINT 2002
 2002 FORMAT (25H TUBE MATERIAL PROPERTIES)
      PRINT 2003
 2003 FORMAT (7X,2HTU,8X,2HTY,8X,2HTF,8X,2HTR,8X,4HTFR0)
      PRINT 9020,TU,TY,TF,TR,TFR0
      PRINT 2004
 2004 FORMAT (16H FLANGE GEOMETRY)
      PRINT 2005
 2005 FORMAT(5X,4HBCDI,5X,5HHUBII)
      PRINT 9021,BCDI,HUBII
      PRINT 800
  800 FORMAT(3X,6HG1OTWI)
      PRINT 9021,G1OTWI
      PRINT 2037
 2037 FORMAT(6X,3HFRI,6X,4HFSFI)
      PRINT 9021,FRI,FSFI
      PRINT 2006
 2006 FORMAT (27H FLANGE MATERIAL PROPERTIES)
      PRINT 801
  801 FORMAT(6X,3HFUR)
      PRINT 9020,FUR
      PRINT 2007
 2007 FORMAT (7X,2HFU,8X,2HFY,7X,3HFSU,7X,3HFCY,8X,2HFE,8X,2HFG,7X,
     13HFYC,7X,3HFYR)
      PRINT 9020,FU,FY,FSU,FCY,FE,FG,FYC,FYR
      PRINT 2008
 2008 FORMAT (5X,4HFRHO,5X,3HFMU,7X,3HFTE,7X,3HFCR)
      PRINT 9022,FRHO,FMU,FTE,FCR
      PRINT 2009
 2009 FORMAT (5X,4HR(1),6X,4HR(2),6X,4HR(3),6X,4HR(4),6X,4HR(5),6X,
     14HR(6),6X,4HR(7),6X,4HR(8))
      PRINT 9021,R(1),R(2),R(3),R(4),R(5),R(6),R(7),R(8)
      PRINT 2010
 2010 FORMAT (5X,4HR(9),5X,5HR(10),5X,5HR(11))
```

```
      PRINT 9021,R(9),R(10),R(11)
      PRINT 2011
2011 FORMAT (4X,5HFF(1),5X,5HFF(2),5X,5HFF(3),5X,5HFF(4),5X,5HFF(5),5X,
     15HFF(6),5X,5HFF(7),5X,5HFF(8))
      PRINT 9020,FF(1),FF(2),FF(3),FF(4),FF(5),FF(6),FF(7),FF(8)
      PRINT 2012
2012 FORMAT (4X,5HFF(9),4X,6HFF(10),4X,6HFF(11))
      PRINT 9020,FF(9),FF(10),FF(11)
      PRINT 2013
2013 FORMAT (14H SEAL GEOMETRY)
      PRINT 2014
2014 FORMAT (5X,4HSODI,6X,4HSIDI,6X,4HSELI,6X,3HTAI,5X,5HTAOTW,4X,6HSLE
     1GTI)
      PRINT 9021,SODI,SIDI,SELI,TAI,TAOTW,SLEGTI
      PRINT 2015
2015 FORMAT (18H SEAL LOADS INPUTS)
      PRINT 2016
2016 FORMAT(5X,4HRSLI,4X,4HSSLI,4X,4HMSLI)
      PRINT 9020,RSLI,SSLI,MSLI
      PRINT 2017
2017 FORMAT (25H SEAL MATERIAL PROPERTIES)
      PRINT 2018
2018 FORMAT (7X,3HSCY,7X,3HSEE,6X,4HSCYC,6X,4HSCYR,7X,3HSYR)
      PRINT 9020,SCY,SEE,SCYC,SCYR,SYR
      PRINT 2019
2019 FORMAT (3X,3HSTE)
      PRINT 9022,STE
      PRINT 2022
2022 FORMAT (14H BOLT GEOMETRY)
      PRINT 2023
2023 FORMAT (4X,5HBH(1),5X,5HBH(2),5X,5HBH(3),5X,5HBH(4),5X,5HBH(5),5X,
     15HBH(6),5X,5HBH(7),5X,5HBH(8))
      PRINT 9021,BH(1),BH(2),BH(3),BH(4),BH(5),BH(6),BH(7),BH(8)
      PRINT 2024
2024 FORMAT (4X,5HBH(9),4X,6HBH(10),4X,6HBH(11),4X,6HBH(12),4X,6HBH(13)
     1,4X,6HBH(14),4X,6HBH(15))
      PRINT 9021,BH(9),BH(10),BH(11),BH(12),BH(13),BH(14),BH(15)
      PRINT 2025
2025 FORMAT (4X,6HBWC(1),4X,6HBWC(2),4X,6HBWC(3),4X,6HBWC(4),4X,6HBWC(5
     1),4X,6HBWC(6),4X,6HBWC(7),4X,6HBWC(8))
      PRINT 9021,BWC(1),BWC(2),BWC(3),BWC(4),BWC(5),BWC(6),BWC(7),BWC(8)
      PRINT 2026
2026 FORMAT (4X,6HBWC(9),3X,7HBWC(10),3X,7HBWC(11),3X,7HBWC(12),3X,
     17HBWC(13),3X,7HBWC(14),3X,7HBWC(15))
      PRINT 9021,BWC(9),BWC(10),BWC(11),BWC(12),BWC(13),BWC(14),BWC(15)
      PRINT 2027
2027 FORMAT (5X,5HBS(1),5X,5HBS(2),5X,5HBS(3),5X,5HBS(4),5X,5HBS(5),5X,
     15HBS(6),5X,5HBS(7),5X,5HBS(8))
      PRINT 9021,BS(1),BS(2),BS(3),BS(4),BS(5),BS(6),BS(7),BS(8)
      PRINT 2028
2028 FORMAT (5X,5HBS(9),4X,6HBS(10),4X,6HBS(11),4X,6HBS(12),4X,6HBS(13)
     1,4X,6HBS(14),4X,6HBS(15))
      PRINT 9021,BS(9),BS(10),BS(11),BS(12),BS(13),BS(14),BS(15)
      PRINT 2029
2029 FORMAT (4X,6HBTA(1),4X,6HBTA(2),4X,6HBTA(3),4X,6HBTA(4),4X,6HBTA(5
     1),4X,6HBTA(6),4X,6HBTA(7),4X,6HBTA(8))
```

```
      PRINT 9021,BTA(1),BTA(2),BTA(3),BTA(4),BTA(5),BTA(6),BTA(7),BTA(8)
      PRINT 2030
 2030 FORMAT (4X,6HBTA(9),3X,7HBTA(10),3X,7HBTA(11),3X,7HBTA(12),3X,7HBT
     1A(13),3X,7HBTA(14),3X,7HBTA(15))
      PRINT 9021,BTA(9),BTA(10),BTA(11),BTA(12),BTA(13),BTA(14),BTA(15)
      PRINT 2053
 2053 FORMAT (4X,6HNWT(1),4X,6HNWT(2),4X,6HNWT(3),4X,6HNWT(4),4X,6HNWT(5
     1),4X,6HNWT(6),4X,6HNWT(7),4X,6HNWT(8))
      PRINT 9021,NWT(1),NWT(2),NWT(3),NWT(4),NWT(5),NWT(6),NWT(7),NWT(8)
      PRINT 2054
 2054 FORMAT (4X,6HNWT(9),3X,7HNWT(10),3X,7HNWT(11),3X,7HNWT(12),3X,7HNW
     1T(13),3X,7HNWT(14),3X,7HNWT(15))
      PRINT 9021,NWT(9),NWT(10),NWT(11),NWT(12),NWT(13),NWT(14),NWT(15)
      PRINT 2038
 2038 FORMAT(4X,6HDAF(1),4X,6HDAF(2),4X,6HDAF(3),4X,6HDAF(4),4X,6HDAF(5)
     1,4X,6HDAF(6),4X,6HDAF(7),4X,6HDAF(8))
      PRINT 9021,DAF(1),DAF(2),DAF(3),DAF(4),DAF(5),DAF(6),DAF(7),DAF(8)
      PRINT 2039
 2039 FORMAT(4X,6HDAF(9),3X,7HDAF(10),3X,7HDAF(11),3X,7HDAF(12),3X,7HDAF
     1(13),3X,7HDAF(14),3X,7HDAF(15))
      PRINT 9021,DAF(9),DAF(10),DAF(11),DAF(12),DAF(13),DAF(14),DAF(15)
      PRINT 2050
 2050 FORMAT (11H BOLT INPUT)
      PRINT 2051
 2051 FORMAT (8X,2HII,3X,4HIMAX)
      PRINT 9023,II,IMAX
      PRINT 2052
 2052 FORMAT (6X,3HBNI)
      PRINT 9021,BNI
      PRINT 2031
 2031 FORMAT (25H BOLT MATERIAL PROPERTIES)
      PRINT 2032
 2032 FORMAT (8X,2HBY,8X,2HBE,8X,2HBU,7X,3HBYC,7X,3HBYR)
      PRINT 9020,BY,BE,BU,BYC,BYH
      PRINT 2033
 2033 FORMAT (6X,3HBTE,7X,3HBCR,6X,4HBRHO)
      PRINT 9022,BTE,BCR,BRHO
      PRINT 2034
 2034 FORMAT (32H SYSTEM PRESSURE AND TEMPERATURE)
      PRINT 2035
 2035 FORMAT (9X,1HP,9X,2HPP,8X,2HPB,7X,3HPIM,6X,4HTMAX,6X,4HTMIN)
      PRINT 9020,P,PP,PB,PIM,TMAX,TMIN
      PRINT 2055
 2055 FORMAT (6X,4HDTC1,6X,4HDTC2,6X,4HDTH1,6X,4HDTH2)
      PRINT 9020,DTC1,DTC2,DTH1,DTH2
      PRINT 2036
 2036 FORMAT (7X,3HFS1,7X,3HFS2,7X,3HFS3)
      PRINT 9021,FS1,FS2,FS3
      KOUNT=0
C     TUBE CALCULATIONS TUBE WALL ,TUBE BENDING MOMENT,TUBE BENDING STRESS
      TW2=1.1*PP*TOD/(2.*TY+.8*PP)
      TW3=1.1*PB*TOD/(2.*TU+.8*PB)
      IF(TFRO .EQ. 0.0) GO TO 16
      TW4=1.1*PIM*TOD/(2.*TFRO+.8*PIM)
      GO TO 17
   16 TW4=TW3
```

```
17 CONTINUE
   IF(.001-TW1)1,1,2
 1 TW=TW1
   GO TO 3
 2 TW=MAX1F(TW2,TW3,TW4)
 3 W=3.1416*(TOD**4-(TOD-2.*TW)**4)/(32.*TOD)
   IF(TBM1 .EQ. 0.001)5,4
 4 TBM=TBM1
   GO TO 6
 5 TBM2=W*.6667*TY
   TBM3=W*.8*TR
   TBM4=W*.5*TF
   TBM5=MIN1F(TBM2,TBM3,TBM4)
   TBM6=60.*(TOD*3.)**3
   TBM=MIN1F(TBM5,TBM6)
 6 TBS=TBM/W
   PI=3.1416
   IF(TOD-3.0)26,26,27
26 BLO=.5*TBS*PI*(TOD-TW)*TW*(.5*.5*(TOD/3.))
   GO TO 33
27 BLO=.5*TBS*PI*(TOD-TW)*TW
33 BL1=MAX1F(BLO,SSLI*PI*TOD)
   BNP=4.
   IF(TOD-3.0)60,60,61
60 I=1
   GO TO 62
61 I=2
62 XT=3.*TW
   GO=TW
   IF(.001-HUBII)64,63,63
63 G1=1.25*TW
   GO TO 65
64 G1=TW*HUBII
65 B=TOD-2.*TW
   IF(.001-FRI)700,701,701
700 FR=FRI
   GO TO 702
701 IF(TOD-4.)703,703,704
703 FR=0.125
   GO TO 702
704 IF(TOD-8.)705,705,706
705 FR=0.1875
   GO TO 702
706 IF(TOD-12.)707,707,708
707 FR=0.25
   GO TO 702
708 FR=0.3125
702 CONTINUE
   SLEG=0.1+0.012*TOD
   SID=(TOD-2.*TW)+2.*SLEG*0.15
 14 TA=TAOTW*TW
 15 SOD=SID+2.*TA+2.*SLEG
   D3=SID+2.*TA
   SLEGT1=RSLI*(SOD/D3)/SCYR
   SLEGT2=0.04+(0.001*P**0.5*TOD)/12.0
   SLEGT=MAA1F(SLEGT1,SLEGT2)
```

```
      TARSL=RSLI*(SOD/D3)-SCYR*(SOD*SOD-D3*D3)*SLEGT/(SOD*SOD)
      SEL=2.*RSLI/(SCYR*ALOG(D3/SID))
      SX=SEL/2.
      LT=SEL/TA
   18 IF(4.0-LT)19,19,25
   19 TA=TA+.005
      GO TO 15
   25 IF(.001-SODI)32,32,28
   32 SOD=SODI
      SID=SIDI
      SEL=SELI
      TA=TAI
      SLEGT=SLEGTI
      SX=SEL/2.
C     LOAD CALCULATIONS
   28 MSL=MSLI*PI*SOD
C     PRELIMINARY BOLT CALCULATION
  107 IF(I-IMAX) 108,1009,1009
 1009 PRINT 1010
 1010 FORMAT (3X,36HBOLT REQUIRED NOT AVAILABLE IN TABLE)
      GO TO 999
  108 HUBI=G1-TW
      BCD1=SOD+2.*((SLEGT*6.0*RSLI*FS1/FY)**.5)+BH(I)
      BCD2=SOD+2.*(RSLI*FS1/FSU)+BH(I)
      BCD3=TOD+BWC(I)+2.*HUBI
      BCD4=2.*(.060+TOD*.0075)+SOD+BH(I)
      BCD6=TOD+2.*HUBI+2.*FR+DAF(I)
      BCD5=MAX1F(BCD1,BCD2,BCD3,BCD4,BCD6)
      IF(.001-BCDI)110,113,113
  110 IF(BCD5-BCDI) 112,112,1005
 1005 PRINT 1006
 1006 FORMAT (3X,32HBCD INPUT SMALLER THAN ALLOWABLE)
  112 BCD=BCDI
      BN=BNI
      I=II
      GO TO 114
  113 BCD=BCD5
      BN=BCD*PI/BWC(I)
      NB=BN/2.
      N=2*NB
      BN=N
  114 A=BCD+2.*BH(I)
      H2=(2.*BCD-A-B)/4.
      H3=(A-B-2*TA)/4.
      H4=((A+B)/4.)-(1./3.)*(SOD**2+SOD*B+B**2)/(SOD+B)
      H5=((A-B)/4.)-(TW+HUBI)/2.
      H6=H5
C     FLANGE SIZE CALCULATION
  201 CONTINUE
      H=2.0*(B*G0)**.5
      HG=(BCD-B-G0)/2.
      K=A/B
      T=((K*K)*(1.0+8.55246*ALOG10(K))-1.0)/((1.04720+1.94480*K*K)*(K-1.
     1))
      U=((K*K)*(1.0+8.55246*ALOG10(K))-1.)/(1.36136*(K**2-1.)*(K-1.))
      Y=(1./(K-1.))*(.66845+5.717*((K*K)*ALOG10(K)/(K**2-1.)))
```

```
      Z=(K*K+1.)/(K*K-1.)
      F=.909-.031*(G1/G0-1.)-.1605*(G1/G0-1.)**.5
      V=.55+.15*(G1/G0-1.)-.558*(G1/G0-1.)**.5
      HO=((B+G0)*G0)**.5
      LCE=F/HO
      LCD=(U/V)*HO*G0**2
  202 L=(XT*LCE+1.)/T+(XT**3)/LCD
      GE=0.5*(G1+G0)
      HPO=(B*GE)**.5
      C1=(3.**.5)*(2.-FMU)/(4.*FE*(1.-FMU**2))
      C2=(3./(1.-FMU**2))**.5
      C3=(12.*(1.-FMU**2))**.25
      C4=((12.*(1.-FMU**2))**.25)/(2.*(1.-FMU**2))
      BETA=(3.*(1.-FMU**2)/((((TOD/2.)+GE-G0)**2)*(GE)**2))**.25
      HOP=(B*GE)**.5
      GAMMA=(GE*(FMU+Z)*(1.+C3*XT/HOP))/(1.+(C4*B*GE**3*(FMU+Z)/(HOP*XT*
     1*3)*(2+C3*XT/HOP)))
      DT=FE*GE**3/(12.*(1.-FMU**2))
      DF=FE*XT**3/(12.*(1.-FMU**2))
      XP=((((1.+FMU)/(1.-FMU))*K**2+1.)*B)/((K**2-1.)*(1.+FMU)*2.*DF)
      AT=(PI/4.)*(TOD**2-B**2)
      ZH=PI*((TOD-2.*G0+2.*G1)**4-(TOD-2.*TW)**4)/(32.*(TOD-2.*G0+2.*G1)
     1)
      AH=(((TOD-2.*G0+2.*G1)**2-(TOD-2.*G0)**2)*PI/4.)
C     DEFLECTION RATES
      DSA=-(SX)/(SEE*PI*(B+TA)*TA)
      DSR=-(B+TA)/(2.*PI*SEL*TA*SEE)
      DBA=(.5/BE)*(((SEL+2.*XT)/2.)*(4./(PI*BS(I)**2))+((SEL+BS(I)
     1+2.*XT)/(2.*BTA(I))))/BN
      DFR=(.91*V)/(L*HO*G0**2*FE)
      DFA=-DFR*(H2+H3)**2-(1./(2.*PI*FG*XT))*ALOG(BCD/(B+TA))
     1-(XT)/((PI/4.)*(BCD**2-B**2)*FE)
      RATIO=A/TOD
      IF(RATIO .LE. 1.1)711,712
  711 KTF=0.179*((TOD/FR)**.5)+.914
      GO TO 718
  712 IF(RATIO .LE. 1.2)713,714
  713 KTF=0.202*((TOD/FR)**.5)+.86
      GO TO 718
  714 IF(RATIO .LE. 1.5)715,716
  715 KTF=0.233*((TOD/FR)**.5)+.79
      GO TO 718
  716 KTF=0.282*((TOD/FR)**.5)+.69
  718 CONTINUE
C     LOAD CALCULATIONS CONDITION 1 AND 2
      P1=0.
      P2=P
      TBM1=0.
      TBM2=TBM
      MP2=((L*HO*G0**2*FE)/(.91*V))*(C1*B**2*GAMMA*P2/(XT*(XT**2+C2*GE*G
     1AMMA)))
      FA1=0.
      FA2=P2*(PI/4.)*(B**2)
      FPL1=0.
      FPL2=P2*(PI/4.)*(SOD**2-B**2)
      RSL1=RSLI*PI*SOU
```

```
  111 SL1=BL1
      MO1=-RSL1*XT/2.+BL1*H2+SL1*H3
      MC2=MIN1F((L*G1**2*(B+TW)*FE*FCR),(MO1*FE*FCR/FYR))
C STRESS CALCULATION CONDITION 1
  310 SH=((BL1*H2+SL1*H3)/(L*G1**2*(B+G0)))
  311 SRS=((RSL1*XT/2.))/(L*G1**2*(B+G0)))
      SR=MO1*(1.333*XT*LCE+1.)/(L*XT**2*(B+G0))
      ST=MO1*(Y/(XT**2*B))-Z*SR
      SB=0.
      SPR=0.
      SPA=0.
      SCEA=0.
      SCEB=0.
      FSS=SL1/(TOD*PI*XT)
      SSC=SL1/((B+2.*TA)**2-B**2)*PI/4.)
      BTS=BL1/(BN*BTA(I))
      IF(BTS-BYR/FS2)314,314,414
  414 IF(.001-BNI)314,314,313
  313 I=I+1
      GO TO 107
  314 IF(SR-FYR/FS1)315,315,302
  315 IF(ST-FYR/FS1)316,316,302
  316 IF(FSS-FSU/FS1)317,317,302
  317 IF(SSC-SCYR/FS1)330,330,619
  619 PRINT 620
  620 FORMAT (3X,18H SSC EXCEEDS LIMIT)
  330 XA1=-SH+SB+SPR+SPA+SRS
      XA2=-SCEA+SR
      XA3=ST
      NA1=-SH-SB+SPR+SPA+SRS
      NA2=-SCEA+SR
      NA3=ST
      EXA=.70711*((XA1-XA2)**2+(XA2-XA3)**2+(XA3-XA1)**2)**.5
      ENA=.70711*((NA1-NA2)**2+(NA2-NA3)**2+(NA3-NA1)**2)**.5
      EA =AMAX1(ABS(EXA),ABS(ENA))
      IF(EA-FYR/FS1)352,352,302
  352 XB1=+SH+SB-SPR+SPA-SRS
      XB2=-SCEB+SR
      XB3=ST
      NB1=+SH-SB-SPR+SPA-SRS
      NB2=-SCEB+SR
      NB3=ST
      EXB=.70711*((XB1-XB2)**2+(XB2-XB3)**2+(XB3-XB1)**2)**.5
      ENB=.70711*((NB1-NB2)**2+(NB2-NB3)**2+(NB3-NB1)**2)**.5
      EB=AMAX1(ABS(EXB),ABS(ENB))
      IF(EB-FYR/FS1)362,362,302
  402 IF(MU8II .LT. 0.001)802,302
  802 IF(G10IWI .LT. 0.001)804,803
  803 G10TW=G1/TW
      IF(G10TW .GT. G10TWI)302,804
  804 G1=G1+0.005
      XT=XT-0.030
      GO TO 108
  302 XT=XT+.015
      IF(XT-2.*TOD)202,1003,1003
 1003 PRINT 1004
```

```
 1004 FORMAT (3X,31HFLANGE THICKNESS EXCEEDS 2.*TOD)
      GO TO 999
  850 XT=XT+.015
      KOUNT=KOUNT+1
      IF(KOUNT .LE. 5)860,202
  860 IF(G1 .GT. 1.75*TW)851,202
  851 G1=G1-0.005
      GO TO 108
C     LOAD AND MOMENT CALCULATION FOR CONDITION 2
  362 TL2=FA2+TBS*AT
      Q21=-FA2-FPL2-TBS*AT
      Q22=(P2*PI*B*SX)*XT/2.-FPL2*H4-MP2-MC2-TL2*H5
      Q23=+(P2*B*(B+TA))/(4.*TA*SEE)-(P2*B*((A+B)/2.))/(4.*((A-B)/2.)
     1*FE)
      Q24=-Q21*DBA/(DBA-DSA)+BCR*(XT+SX)/(DBA-DSA)
      Q25=DFA/((DBA-DSA)*(H2+H3))
      Q26=H2*Q21+Q22
      Q27=-DFR*XT/(2.*DSR)
      Q28=1.+Q27*(XT/2.)-Q25*(H2+H3)
      Q29=-(Q23/DSR)*(XT/2.)+Q26+Q24*(H2+H3)
      MO2=MO1-Q29/Q28
      SL2=SL1-Q24-(Q29/Q28)*Q25
      RSL2=RSL1-(Q29/Q28)*Q27-Q23/DSR
      BL2=BL1-Q24-(Q29/Q28)*Q25-Q21
      IF(SL2-MSL)331,332,332
  331 BL1=1.01*BL1
      GO TO 111
  332 Q21P=-FPL2-FA2-TBS*AT
      Q22P=(P2*PI*B*SX)*XT/2.-FPL2*H4-MP2-TL2*H5
      Q23P=+(P2*B*(B+TA))/(4.*TA*SEE)-(P2*B*((A+B)/2.))/(4.*((A-B)/2.)
     1*FE)
      Q24P=-Q21P*DBA/(DBA-DSA)
      Q25P=DFA/((DBA-DSA)*(H2+H3))
      Q26P=H2*Q21P+Q22P
      Q27P=-DFR*XT/(2.*DSR)
      Q28P=1.+Q27P*(XT/2.)-Q25P*(H2+H3)
      Q29P=-(Q23P/DSR)*(XT/2.)+Q26P+Q24P*(H2+H3)
      MO2P=MO1-Q29P/Q28P
      SL2P=SL1-Q24P-(Q29P/Q28P)*Q25P
      RSL2P=RSL1-(Q29P/Q28P)*Q27P-Q23P/DSR
      BL2P=BL1-Q24P-(Q29P/Q28P)*Q25P-Q21P
      Q21M=-FPL2-FA2+TBS*AT
      Q22M=(P2*PI*B*SX)*XT/2.-FPL2*H4-MP2-H5*(FA2-TBS*AT)
      Q23M=+(P2*B*(B+TA))/(4.*TA*SEE)-(P2*B*((A+B)/2.))/(4.*((A-B)/2.)
     1*FE)
      Q24M=-Q21M*DBA/(DBA-DSA)
      Q25M=DFA/((DBA-DSA)*(H2+H3))
      Q26M=H2*Q21M+Q22M
      Q27M=-DFR*XT/(2.*DSR)
      Q28M=1.+Q27M*(XT/2.)-Q25M*(H2+H3)
      Q29M=-(Q23M/DSR)*(XT/2.)+Q26M+Q24M*(H2+H3)
      MO2M=MO1-Q29M/Q28M
      SL2M=SL1-Q24M-(Q29M/Q28M)*Q25M
      RSL2M=RSL1-(Q29M/Q28M)*Q27M-Q23M/DSR
      BL2M=BL1-Q24M-(Q29M/Q28M)*Q25M-Q21M
C     STRESS CALCULATIONS CONDITION 2
```

```
      SH2P=(BL2P*M2+FPL2*M4+TL2*M6+SL2P*M3)/(L*G1**2*(B+G0))
      SH2M=(BL2M*M2+FPL2*M4+(FA2-TBS*AT)*M6+SL2M*M3)/(L*G1**2*(B+G0))
      SRS2P=(RSL2P*XT/2.)/(L*G1**2*(B+G0))
      SRS2M=(RSL2M*XT/2.)/(L*G1**2*(B+G0))
      SPR2=MP2/(L*G1**2*(B+G0))
      SB2=TBM/ZM
      SPA2=FA2/AM
      SCEB2=0
      SCEA2=F2
      SR2P=MO2P*(1.333*XT*LCE+1.)/(L*XT**2*(B+G0))
      SR2M=MO2M*(1.333*XT*LCE+1.)/(L*XT**2*(B+G0))
      ST2P=MO2P*(Y/(XT**2*B))-Z*SR2P
      ST2M=MO2M*(Y/(XT**2*B))-Z*SR2M
      FSS2=BL2P/(TOD*PI*XT)
      SSC2=SL2M/(((B+2.*TA)**2-B**2)*PI/4.)
      BTS2P=BL2P/(BTA(I)*BN)
      IF(BTS2P-BY/FS2)344,344,415
  415 IF(.001-BNI)344,344,313
  344 IF(SR2P-FY/FS1)345,345,302
  345 IF(ST2P-FY/FS1)346,346,302
  346 IF(FSS2-FSU/FS1)347,347,302
  347 IF(SSC2-SCY/FS1)348,348,621
  621 PRINT 622
  622 FORMAT (3X,19H SSC2 EXCEEDS LIMIT)
  348 XA1=-SH2P+SB2+SPR2+SPA2+SRS2P
      XA2=-SCEA2+SR2P
      XA3=ST2P
      NA1=-SH2M-SB2+SPR2+SPA2+SRS2M
      NA2=-SCEA2+SR2M
      NA3=ST2M
      EXA2=.70711*((XA1-XA2)**2+(XA2-XA3)**2+(XA3-XA1)**2)**.5
      ENA2=.70711*((NA1-NA2)**2+(NA2-NA3)**2+(NA3-NA1)**2)**.5
      XA1=XA1-SPA2
      NA1=NA1-SPA2
      IF(ABS(XA1)-ABS(NA1))602,602,601
  602 CMAX2A=NA1
      CMIN2A=XA1
      GO TO 603
  601 CMAX2A=XA1
      CMIN2A=NA1
  603 EA=AMAX1(ABS(EXA2),ABS(ENA2))
      IF(EA-FY/FS1)1352,1352,302
 1352 CALT2A=(CMAX2A-CMIN2A)/2.
      CMN2A=(CMAX2A+CMIN2A)/2.
      FALT2A=CALT2A*FSFI
      SALT2A=FALT2A
      SMN2A=CMN2A
      SCHK2A=ABS(SMN2A+SALT2A)
      IF(SCHK2A .GT. FU)402,805
  805 IF(SCHK2A-FY)806,806,807
  807 IF(ABS(SALT2A)-FY)808,808,809
  808 SMN2A=FY-SALT2A
      GO TO 806
  809 SMN2A=0.
  806 SMAX2A=SMN2A+SALT2A
      SMIN2A=SMN2A-SALT2A
```

```
      RC1=SMIN2A/SMAX2A
      M=0
 1350 M=M+1
      IF(RC1-R(M))1351,7000,1350
 1351 FFC2A=((R(M)-RC1)/(R(M)-R(M-1)))*(FF(M)-FF(M-1))+FF(M-1)
      GO TO 7001
 7000 FFC2A=FF(M)
 7001 CONTINUE
      IF(ABS(SMAX2A)-FFC2A)1363,1363,402
 1363 XB1=SM2P+SB2-SPR2+SPA2-SRS2P
      XB2=-SCEB2+SR2P
      XB3=ST2P
      NB1=SM2M-SB2-SPR2+SPA2-SRS2M
      NB2=-SCEB2+SR2M
      NB3=ST2M
      EXB2=.70711*((XB1-XB2)**2+(XB2-XB3)**2+(XB3-XB1)**2)**.5
      ENB2=.70711*((NB1-NB2)**2+(NB2-NB3)**2+(NB3-NB1)**2)**.5
      EB=AMAX1(ABS(EXB2),ABS(ENB2))
      XB1=XB1-SPA2
      NB1=NB1-SPA2
      IF(EB-FY/FS1)720,720,302
  720 IF(ABS(XB1)-ABS(NB1))605,605,604
  605 CMAX2B=NB1
      CMIN2B=XB1
      GO TO 1362
  604 CMAX2B=XB1
      CMIN2B=NB1
 1362 CALT2B=(CMAX2B-CMIN2B)/2.
      CMN2B=(CMAX2B+CMIN2B)/2.
      FALT2B=CALT2B*FSF1
      SALT2B=FALT2B*KTF
      SMN2B=CMN2B*KTF
      SCHK2B=ABS(SMN2B+SALT2B)
      IF(SCHK2B.GT. FU)402,810
  810 IF(SCHK2B-FY)811,811,812
  812 IF(ABS(SALT2B)-FY)813,813,814
  813 SMN2B=FY-SALT2B
      GO TO 811
  814 SMN2B=0.
  811 SMAX2B=SMN2B+SALT2B
      SMIN2B=SMN2B-SALT2B
      RC2=SMIN2B/SMAX2B
      M=0
 1360 M=M+1
      IF(RC2-R(M))1361,7002,1360
 1361 FFC2B=((R(M)-RC2)/(R(M)-R(M-1)))*(FF(M)-FF(M-1))+FF(M-1))
      GO TO 7003
 7002 FFC2B=FF(M)
 7003 CONTINUE
      IF(ABS(SMAX2B)-FFC2B)380,380,402
C     LOAD CALCULATIONS CONDITION 3
  380 P3=PP
      TBM3=0.
      FA3=P3*(PI/4.)*(B**2)
      FPL3=P3*(PI/4.)*(S00**2-B**2)
      TL3=FA3
```

```
      MP3=((L*H0*G0**2*FE)/(.91*V))*(C1*B**2*GAMMA*P3/(XT*(XT**2+C2*GE*G
     1AMMA)))
      Q31=-FPL3-TL3
      Q32=-FPL3*H4-MP3+(P3*PI*B*SX)*XT/2.-TL3*H5
      Q33=+(P3*B*(B+TA))/(4.*TA*SEE)-(P3*B*((A+B)/2.))/(4.*((A-B)/2.)*
     1SE)
      Q34=-Q31*DBA/(DBA-DSA)
      Q35=DBA/((DBA-DSA)*(H2+H3))
      Q36=H2*Q31+Q32
      Q37=-DBR*XT/(2.*DSR)
      Q38=1.+Q37*XT/2.-Q35*(H2+H3)
      Q39=-(Q33/DSR)*(XT/2.)+Q36+Q34*(H2+H3)
      MO3=MO1-Q39/Q38
      SL3=SL1-Q34-(Q39/Q38)*Q35
      RSL3=RSL1-(Q39/Q38)*Q37-Q33/DSR
      BL3=BL1-Q34-(Q39/Q38)*Q35-Q31
      IF(SL3-MSL)331,390,390
C     STRESS CALCULATIONS CONDITION 3
  390 SH3=(BL3*H2+SL3*H3+FPL3*H4+TL3*H6)/(L*G1**2*(B+G0))
      SRS3=(RSL3*XT/2.)/(L*G1**2*(B+G0))
      SPR3=MP3/(L*G1**2*(B+G0))
      SB3=0.
      SPA3=FA3/AH
      SCEB3=0.
      SCEA3=P3
      SR3=MO3*(1.333*XT*LCE+1.)/(L*XT**2*(B+G0))
      ST3=MO3*(Y/(XT**2*B))-Z*SR3
      FSS3=BL3/(TOD*PI*XT)
      SSC3=SL3/(((B+2.*TA)**2-B**2)*PI/4.)
      BTS3=BL3/(BTA(I)*BN)
      IF(BTS3-BY/FS2)2344,2346,416
  416 IF(.001-BNI)2344,2344,313
 2344 IF(SR3-FY/FS1)2315,2315,302
 2315 IF(ST3-FY/FS1)2316,2316,302
 2316 IF(FSS3-FSU/FS1)2317,2317,302
 2317 IF(SSC3-SCY/FS1)2330,2330,623
  623 PRINT 624
  624 FORMAT(3X,19H SSC3 EXCEEDS LIMIT)
 2330 XA1=-SH3+SB3+SPR3+SPA3+SRS3
      XA2=-SCEA3+SR3
      XA3=ST3
      NA1=-SH3-SB3+SPR3+SPA3+SRS3
      NA2=-SCEA3+SR3
      NA3=ST3
      EXA3=.70711*((XA1-XA2)**2+(XA2-XA3)**2+(XA3-XA1)**2)**.5
      ENA3=.70711*((NA1-NA2)**2+(NA2-NA3)**2+(NA3-NA1)**2)**.5
      EA=AMAX1(ABS(EXA3),ABS(ENA3))
      IF(EA-FY/FS1)2363,302,302
 2363 XB1=SH3+SB3-SPR3+SPA3-SRS3
      XB2=-SCEB3+SR3
      XB3=ST3
      NB1=SH3-SB3-SPR3+SPA3-SRS3
      NB2=-SCEB3+SR3
      NB3=ST3
      EXB3=.70711*((XB1-XB2)**2+(XB2-XB3)**2+(XB3-XB1)**2)**.5
      ENB3=.70711*((NB1-NB2)**2+(NB2-NB3)**2+(NB3-NB1)**2)**.5
```

```
      EB=AMAX1(ABS(EXB3),ABS(ENB3))
      IF(EB-FY/FS1)2373,302,302
C     LOAD CALCULATIONS CONDITION 4
 2373 P4=PB
      FA4=P4*(PI/4.)*(B**2)
      FPL4=P4*(PI/4.)*(SOD**2-B**2)
      TL4=FA4
      BL4=FPL4+FA4
C     STRESS CALCULATION FOR CONDITION 4
      BTS4=BL4/(BTA(I)*BN)
      IF(BTS4-BU/FS2)4344,4344,417
  417 IF(.001-BNI)4344,4344,313
C     LOAD CALCULATION CONDITION 5
 4344 P5=FIM
      FA5=P5*(PI/4.)*(B**2)
      FPL5=P5*(PI/4.)*(SOD**2-B**2)
      TL5=FA5
      MP5=((L*MO*GO**2*FE)/(.91*V))*(C1*B**2*GAMMA*P5/(XT*(XT**2+C2*GE*G
     1AMMA)))
      Q51=-FPL5-TL5
      Q52=-FPL5*H4-MP5+(P5*PI*B*SX)*XT/2.-TL5*H5
      Q53=+(P5*B*(B+TA))/(S.*TA*SEE)-(P5*B*((A+B)/2.))/(4.*((A-B)/2.)*
     1FE)
      Q54=-Q51*DBA/(DBA-DSA)
      Q55=DBA/((DBA-DSA)*(H2+H3))
      Q56=H2*Q51+Q52
      Q57=-DFR*XT/(2.*DSR)
      Q58=1.*Q57*(XT/2.)-Q55*(H2+H3)
      Q59=-(Q53/DSR)*(XT/2.)+Q56+Q54*(H2+H3)
      MO5=MO1-Q59/Q58
      SL5=SL1-Q54-(Q59/Q58)*Q55
      RSL5=RSL1-(Q59/Q58)*Q57-Q53/DSR
      BL5=BL1-Q54-(Q59/Q58)*Q55-Q51
      IF(SL5-MSL)331,5390,5390
 5390 SH5=(BL5*H2+SL5*H3+FPL5*H4+TL5*H6)/(L*G)**2*(B+GO))
      SRS5=(RSL5*XT/2.)/(L*G)**2*(B+GO))
      SPR5=MP5/(L*G)**2*(B+GO))
      SB5=0.
      SPA5=FA5/AH
      SCEB5=0.
      SCEA5=P5
      SR5=MO5*(1.333*XT+LCE+1.)/(L*X)**2*(B+GO))
      ST5=MO5*(Y/(XT**2*B))-Z*SR5
      FSS5=BL5/(TOD*PI*XT)
      SSC5=SL5/(((B+2.*TA)**2-B**2)*PI/4.)
      BTS5=BL5/(BTA(I)*BN)
      IF(BTS5-BYR/FS2)5344,5344,418
  418 IF(.001-BNI)5344,5344,313
 5344 IF(SR5-FYR/FS1)5315,5315,302
 5315 IF(ST5-FYR/FS1)5316,5316,302
 5316 IF(FSS5-FSU/FS1)5317,5317,302
 5317 IF(SSC5-SCYR/FS1)5330,5330,625
  625 PRINT 626
  626 FORMAT (3X,19H SSC5 EXCEEDS LIMIT)
 5330 SM1=SM
      SRS1=SRS
```

```
      SPR1=0.
      SB1=0.
      SPA1=0.
      SCEB1=0.
      SR1=SR
      ST1=ST
      SCEA1=0.
      XA1=-SH5+SB5+SPR5+SPA5+SRS5
      XA2=-SCEA5+SR5
      XA3=ST5
      NA1=-SH1-SB1+SPR1+SPA1+SRS1
      NA2=-SCEA1+SR1
      NA3=ST1
      EXA5=.70711*((XA1-XA2)**2+(XA2-XA3)**2+(XA3-XA1)**2)**.5
      ENA5=.70711*((NA1-NA2)**2+(NA2-NA3)**2+(NA3-NA1)**2)**.5
      IF(ABS(XA1)-ABS(NA1))5602,5602,5601
5602  CMAX5A=NA1
      CMIN5A=XA1
      GO TO 5603
5601  CMAX5A=XA1
      CMIN5A=NA1
5603  EA=AMAX1(ABS(EXA5),ABS(ENA5))
      IF(EA-FYR/FS1)5352,5352,302
5352  CALT5A=(CMAX5A-CMIN5A)/2.
      CMN5A=(CMAX5A+CMIN5A)/2.
      FALT5A=CALT5A
      SALT5A=FALT5A
      SMN5A=CMN5A
      SCHK5A=ABS(SMN5A+SALT5A)
      IF(SCHK5A .GT. FUR)850,815
 815  IF(SCHK5A-FYR)816,816,817
 817  IF(ABS(SALT5A)-FY)818,818,819
 818  SMN5A=FYR-SALT5A
      GO TO 816
 819  SMN5A=0.
 816  SMAX5A=SMN5A+SALT5A
      SMIN5A=SMN5A-SALT5A
      RC1=SMIN5A/SMAX5A
      M=0
5350  M=M+1
      IF(RC1-R(M))5351,7004,5350
5351  FFC5A=((R(M)-RC1)/(R(M)-R(M-1)))*(FF(M)-FF(M-1))+FF(M-1)
      GO TO 7005
7004  FFC5A=FF(M)
7005  CONTINUE
      IF(ABS(SMAX5A)-FFC5A)5363,5363,850
5363  XB1=+SH5+SB5-SPR5+SPA5-SRS5
      XB2=-SCEB5+SR5
      XB3=ST5
      NB1=+SH1-SB1-SPR1+SPA1-SRS1
      NB2=-SCEB1+SR1
      NB3=ST1
      EXB5=.70711*((XB1-XB2)**2+(XB2-XB3)**2+(XB3-XB1)**2)**.5
      ENB5=.70711*((NB1-NB2)**2+(NB2-NB3)**2+(NB3-NB1)**2)**.5
      EB=AMAX1(ABS(EXB5),ABS(ENB5))
      IF(EB-FYR/FS1)721,721,302
```

```
  721 IF(ABS(XB1)-ABS(NB1))5605,5605,5604
 5605 CMAX5B=NB1
      CMIN5B=XB1
      GO TO 5362
 5604 CMAX5B=XB1
      CMIN5B=NB1
 5362 CALT5B=(CMAX5B-CMIN5B)/2.
      CMN5B=(CMAX5B+CMIN5B)/2.
      FALT5B=CALT5B
      SALT5B=FALT5B*KTF
      SMN5B=CMN5B*KTF
      SCHK5B=ABS(SMN5B+SALT5B)
      IF(SCHK5B .GT. FUR)850,820
  820 IF(SCHK5B-FYR)821,821,822
  822 IF(ABS(SALT5B)-FYR)823,823,824
  823 SMN5B=FYR-SALT5B
      GO TO 821
  824 SMN5B=0.
  821 SMAX5B=SMN5B+SALT5B
      SMIN5B=SMN5B-SALT5B
      RC2=SMIN5B/SMAX5B
      M=0
 5360 M=M+1
      IF(RC2-R(M))5361,7006,5360
 5361 FFC5B=((R(M)-RC2)/(R(M)-R(M-1)))*(FF(M)-FF(M-1))+FF(M-1)
      GO TO 7007
 7006 FFC5B=FF(M)
 7007 CONTINUE
      IF(ABS(SMAX5B)-FFC5B)5403,5403,850
C     LOAD CALCULATIONS CONDITION 6 COLD.
 5403 P6=P
      FA6=P6*(PI/4.)*(B**2)
      FPL6=P6*(PI/4.)*(SOD**2-B**2)
      TL6=FA6+.5*TBS*AT
      MP6=(((L*MU*G0**2*FE)/(.91*V))*(C1*B**2*GAMMA*P6/(XT*(XT**2+C2*GE*G
     1AMMA)))
      MC6=MC2
      MCTG6=(PI/3.)*(B**2)*(BETA**2)*((FE*TW**3)/(12.*(1.-FMU**2)))*FTE*
     1(DTC1)*(1.+BETA*XT)
      MHTG6=(PI/3.)*(B**2)*(BETA**2)*((FE*TW**3)/(12.*(1.-FMU**2)))*FTE*
     1(DTH1)*(1.+BETA*XT)
      MHTG6=-MHTG6
      TMIN1=TMIN
      TMIN2=TMIN+DTC1
      TMIN3=TMIN+DTC2+DTC1
      TMAX1=TMAX
      TMAX2=TMAX-DTH1
      TMAX3=TMAX-DTH2-DTH1
      Q61C=-TL6-FPL6
      Q62C=(P6*PI*B*SX)*XT/2.-FPL6*H4-MP6-MC6*MCTG6-TL6*H5
      Q63C=(P6*B*(B+TA))/(4.*TA*SEE)-(P6*B*((A+B)/2.))/(4.*((A-B)/2.)*FE
     1)-FTE*(TMIN2-70.0)*(B+TA)/2.+STE*(TMIN1-70.0)*(B+TA)/2.
      Q64C=(((-Q61C*DBA)/(DBA-DSA))*(BCR*(XT+SX)+BTE*(TMIN3-70.0)*(SX+ T)
     1-STE*SX*(TMIN1-70.0)-FTE*XT*(TMIN2-70.0))/(DBA-DSA)
      Q65C=DFA/((H2+H3)*(DBA-DSA))
      Q66C=H2*Q61C+Q62C
```

```
      Q67C=-DFR*XT/(2.*DSR)
      Q68C=1.+Q67C*(XT/2.)-Q65C*(H2+H3)
      Q69C=-(Q63C/DSR)*(XT/2.)+Q66C+Q64C*(H2+H3)
      MO6=MO1-Q69C/Q68C
      SL6=SL1-Q64C-(Q69C/Q68C)*Q65C
      RSL6=RSL1-(Q69C/Q68C)*Q67C-Q63C/DSR
      BL6=BL1-Q64C-(Q69C/Q68C)*Q65C-Q61C
      IF(SL6-MSL)331,6390,6390
 6390 Q61CN=-TL6-FPL6
      Q62CN=(P6*PI*B*SX)*XT/2.-FPL6*H4-MP6+MCTG6-TL6*H5
      Q63CN=(P6*B*(B+TA))/(4.*TA*SEE)-(P6*B*((A+B)/2.))/(4.*((A-B)/2.)*F
     1E)-FTE*(TMIN2-70.0)*(B+TA)/2.+STE*(TMIN1-70.0)*(B+TA)/2.
      Q64CN=((-Q61CN*DBA)/(DBA-DSA))+(BTE*(TMIN3-70.0)*(SX+XT)-STE*SX*(T
     1MIN1-70.0)-FTE*XT*(TMIN2-70.0))/(DBA-DSA)
      Q65CN=DFA/((H2+H3)*(DBA-DSA))
      Q66CN=H2*Q61CN+Q62CN
      Q67CN=-DFR*XT/(2.*DSR)
      Q68CN=1.+Q67CN*(XT/2.)-Q65CN*(H2+H3)
      Q69CN=-(Q63CN/DSR)*(XT/2.)+Q66CN+Q64CN*(H2+H3)
      MO6CN=MO1-Q69CN/Q68CN
      SL6CN=SL1-Q64CN-(Q69CN/Q68CN)*Q65CN
      RSL6CN=RSL1-(Q69CN/Q68CN)*Q67CN-Q63CN/DSR
      BL6CN=BL1-Q64CN-(Q69CN/Q68CN)*Q65CN-Q61CN
C STRESS CALCULATION CONDITION 6 COLD
      SH6CN=(BL6CN*H2+SL6CN*H3+FPL6*H4+TL6*H6)/(L*G1**2*(B+G0))
      SRS6CN=(RSL6CN*XT/2.)/(L*G1**2*(B+G0))
      SPR6CN=MP6/(L*G1**2*(B+G0))
      SCG6CN=MCTG6/(L*G1**2*(B+G0))
      SB6CN=.5*TBM/ZH
      SPA6CN=FA6/AH
      SCEB6C=0.
      SCEA6C=P6
      SR6CN=MO6CN*(1.333*XT*LCE+1.)/(L*XT*2.*(B+G0))
      ST6CN=MO6CN*(Y/(X1**2*B))-Z*SR6CN
      FSS6CN=BL6CN/(TOD*PI*XT)
      SSC6CN=SL6CN/(((B+2.*TA)**2-B**2)*PI/4.)
      BTS6CN=BL6CN/(BTA(I)*BN)
      IF(BTS6CN-BYC/FS3)6344,6344,419
  419 IF(.001-BNI)6344,6344,313
 6344 IF(SR6CN-FYC/FS1)6315,6315,302
 6315 IF(ST6CN-FYC/FS1)6316,6316,302
 6316 IF(FSS6CN-FSU/FS1)6317,6317,302
 6317 IF(SSC6CN-SCYC/FS1)6330,6330,627
  627 PRINT 628
  628 FORMAT (3A,21H SSC6CN EXCEEDS LIMIT)
 6330 XA1=-SH6CN+SB6CN+SPR6CN+SPA6CN+SRS6CN-SCG6CN
      XA2=-SCEA6C+SR6CN
      XA3=ST6CN
      EXA6CN=.7071*((XA1-XA2)**2+(XA2-XA3)**2+(XA3-XA1)**2)**.5
      EA=EXA6CN
      IF(EA-FYC/FS1)6363,6363,302
 6363 XB1=+SH6CN+SB6CN-SPR6CN+SPA6CN-SRS6CN+SCG6CN
      XB2=-SCEB6C+SR6CN
      XB3=ST6CN
      EXB6CN=.7071*((XB1-XB2)**2+(XB2-XB3)**2+(XB3-XB1)**2)**.5
      EB=EXB6CN
```

```
      IF(SH-FYC/FS1)6371,6371,302
C     LOAD CALCULATIONS CONDITION 6 HOT
 6371 Q61H=-TL6-FPL6
      Q62H=(P6*PI*B*SX)*XT/2.-FPL6*H4-MP6-MC6*MHTG6-TL6*H5
      Q63H=(P6*B*(B+TA))/(4.*TA*SEE)-(P6*B*((A+B)/2.))/(4.*((A-B)/2.)*FE
     1)-FTE*(TMAX2-70.0)*(B+TA)/2.+STE*(TMAX1-70.0)*(B+TA)/2.
      Q64H=((-Q61H*DBA)/(DBA-DSA))+(BCR*(XT+SX)+BTE*(TMAX3-70.0)*(SX+XT)
     1-STE*SX*(TMAX1-70.0)-FTE*XT*(TMAX2-70.0))/(DBA-DSA)
      Q65H=DBA/((H2+H3)*(DBA-DSA))
      Q66H=H2*Q61H+Q62H
      Q67H=-DBR*XT/(2.*DSR)
      Q68H=1.+Q67H*(XT/2.)-Q65H*(H2+H3)
      Q69H=-(Q63H/DSR)*(XT/2.)+Q66H+Q64H*(H2+H3)
      MO6H=MO1-Q69H/Q68H
      SL6H=SL1-Q64H-(Q69H/Q68H)*Q65H
      RSL6H=RSL1-(Q69H/Q68H)*Q67H-Q63H/DSR
      BL6H=BL1-Q64H-(Q69H/Q68H)*Q65H-Q61H
      IF(SL6H-MSL)331,8390,8390
 8390 Q61HN=-TL6-FPL6
      Q62HN=(P6*PI*B*SX)*XT/2.-FPL6*H4-MP6-MHTG6-TL6*H5
      Q63HN=(P6*B*(B+TA))/(4.*TA*SEE)-(P6*B*((A+B)/2.))/(4.*((A-B)/2.)*F
     1E)-FTE*(TMAX2-70.0)*(B+TA)/2.+STE*(TMAX1-70.0)*(B+TA)/2.
      Q64HN=((-Q61HN*DBA)/(DBA-DSA))+(BTE*(TMAX3-70.0)*(SX+XT)-STE*SX*(T
     1MAX1-70.0)-FTE*XT*(TMAX2-70.0))/(DBA-DSA)
      Q65HN=DBA/((H2+H3)*(DBA-DSA))
      Q66HN=H2*Q61HN+Q62HN
      Q67HN=-DBR*XT/(2.*DSR)
      Q68HN=1.+Q67HN*(XT/2.)-Q65CN*(H2+H3)
      Q69HN=-(Q63HN/DSR)*(XT/2.)+Q66HN+Q64HN*(H2+H3)
      MO6HN=MO1-Q69HN/Q68HN
      SL6HN=SL1-Q64HN-(Q69HN/Q68HN)*Q65HN
      RSL6HN=RSL1-(Q69HN/Q68HN)*Q67HN-Q63HN/DSR
      BL6HN=BL1-Q64HN-(Q69HN/Q68HN)*Q65HN-Q61HN
C STRESS CALULATION CONDITION 6 HOT
      SH6HN=(BL6HN*H2+SL6HN*H3+FPL6*H6+TL6*H6)/(L*G1**2*(B+G0))
      SRS6HN=(RSL6HN*XT/2.)/(L*G1**2*(B+G0))
      SHG6CN=MHTG6/(L*G1**2*(B+G0))
      SPR6HN=MP6/(L*G1**2*(B+G0))
      SB6HN=.5*TBM/ZH
      SPA6HN=FA6/AH
      SCEB6H=0.
      SCEA6H=P6
      SR6HN=MO6HN*(1.333*XT*LCE+1.)/(L*XT*2.*(B+G0))
      ST6HN=MO6HN*(Y/(XT**2*B))-Z*SR6HN
      FSS6HN=BL6HN/(100*PI*XT)
      SSC6HN=SL6HN/(((B+2.*TA)**2-B**2)*PI/4.)
      BTS6HN=BL6HN/(BTA(I)*BN)
      IF(BTS6HN-BY/FS3)8344,8344,420
  420 IF(.001-BN1)8344,8344,313
 8344 IF(SR6HN-FY/FS1)8315,8315,302
 8315 IF(ST6HN-FY/FS1)8316,8316,302
 8316 IF(FSS6HN-FSU/FS1)8317,8317,302
 8317 IF(SSC6HN-SCY/FS1)8330,8330,629
  629 PRINT 630
  630 FORMAT (3X,21H SSC6HN EXCEEDS LIMIT)
 8330 XA1=-SH6HN+SB6HN+SPR6HN+SPA6HN+SRS6HN-SHG6CN
```

```
      XA2=-SCEA6H*SR6HN
      XA3=ST6HN
      EXA6HN=.70711*((XA1-XA2)**2+(XA2-XA3)**2+(XA3-XA1)**2)**.5
      EA=EXA6HN
      IF(EA-FY/FS1)8363,302,302
 8363 XB1=+SH6HN+SB6HN-SPR6HN+SPA6HN-SRS6HN+SHG6CN
      XB2=-SCEB6H+SR6HN
      XB3=ST6HN
      EXB6HN=.70711*((XB1-XB2)**2+(XB2-XB3)**2+(XB3-XB1)**2)**.5
      EB=EXB6HN
      IF(EB-FY/FS1)8371,302,302
C     LOAD CALCULATION CONDITION 7
 8371 P7=0.
      FA7=0.
      FPL7=0
      TL7=.5*TBS*AT
      Q71=(DFR/DSR)*(XT/2.)*(XT/2.)
      Q72=(DFA)/(DBA-DSA)
      Q73=TL7*DBA*(H2+H3)/(DBA-DSA)-TL7*H2-TL7*H5
      MO7=MO1-Q73/(1.-Q71-Q72)
      RSL7=RSL1-(MO1-MO7)*DFR*(XT)/2.*DSR
      SL7=SL1-TL7*DBA/(DBA-DSA)-(MO1-MO7)*DFA/((H2+H3)*(DBA-DSA))
      BL7=BL1-SL1+SL7+TL7
      IF(0.001-BN1)871,870,870
  870 BTSCHK=MAX1F(BTS2P,BTS3,BTS6HN)
      IF(BTSCHK .LT. 0.83*BY/FS2)873,871
  873 IF(BTS4 .LT. 0.83*BU/FS2)872,871
  872 BN1=(BN*BTSCHK*FS2)/(0.83*BY)
      BN2=(PI*BCD)/(2.*(BS(I)+XT))+2.
      BN=MAX1F(BN1,BN2)
      NB=BN/2.
      N=2*NB
      BN=N
      BN1=BN
      I1=I
      BCD1=BCD
      GO TO 114
  871 CONTINUE
      T1=PI/4.*TOD**2
      B1=PI/4.*(TOD+2.*FUBI)**2
      WGT=2.*(PI/4.*(A**2-TOD**2-BN*BH(I)**2)*XT)*FRHO+2.*BN*PI/4.*(BS(I
     1)**2)*(SX+XT+2.*BS(I))*BRHO+2.*BN*NWT(I)+2.*H*FRHO*(1./3.*(B1+T1+(
     1B1*T1)**.5)-T1)-2.*PI/4.*(SOD**2-TOD**2)*.025*FRHO-PI/4.*(SOD**2-(
     1B+2.*TA)**2)*SLEG*TAN(PI/9.)*FRHO
      TRQ=(BL1*BS(I))/(BN*5.)
      IF(PI*BCD/BN-2.*(BS(I)+XT))333,333,1000
 1000 PRINT 1001
 1001 FORMAT (30H MAXIMUM SPACING NOT SATISFIED)
  333 CONTINUE
      PRINT 727
  727 FORMAT(1H )
      PRINT 728
  728 FORMAT(25X,14H DESIGN OUTPUT///)
      PRINT 2800
 2800 FORMAT(1X,25HBENDING MOMENT AND STRESS)
      PRINT 2801
```

```
2801 FORMAT(6X,3HTBM,7X,3HTBS)
     PRINT 9020,TBM,TBS
     PRINT 2803
2803 FORMAT (7X,3HTRQ)
     PRINT 9020,TRQ
     PRINT 3001
3001 FORMAT (25H LOADS FOR ALL CONDITIONS)
     PRINT 3002
3002 FORMAT (6X,3HMO1,7X,3HBL1,7X,3HSL1,6X,4HRSL1)
     PRINT 9020,MO1,BL1,SL1,RSL1
     PRINT 3003
3003 FORMAT (6X,3HMO2,7X,3HBL2,7X,3HSL2,6X,4HRSL2,7X,3HMC2,7X,3HMP2)
     PRINT 9020,MO2,BL2,SL2,RSL2,MC2,MP2
     PRINT 3004
3004 FORMAT (5X,4HMO2P,6X,4HBL2P,6X,4HSL2P,5X,5HRSL2P)
     PRINT 9020,MO2P,BL2P,SL2P,RSL2P
     PRINT 3005
3005 FORMAT (5X,4HMO2M,6X,4HBL2M,6X,4HSL2M,6X,5HRSL2M)
     PRINT 9020,MO2M,BL2M,SL2M,RSL2M
     PRINT 3006
3006 FORMAT (6X,3HMO3,7X,3HBL3,7X,3HSL3,6X,4HRSL3,7X,3HMP3)
     PRINT 9020,MO3,BL3,SL3,RSL3,MP3
     PRINT 3007
3007 FORMAT (6X,3HBL4)
     PRINT 9020,BL4
     PRINT 3008
3008 FORMAT (6X,3HMO5,7X,3HBL5,7X,3HSL5,6X,4HRSL5,7X,3HMP5)
     PRINT 9020,MO5,BL5,SL5,RSL5,MP5
     PRINT 3009
3009 FORMAT (6X,3HMO6,7X,3HBL6,7X,3HSL6,6X,4HRSL6,7X,3HMC6,7X,3HMP6)
     PRINT 9020,MO6,BL6,SL6,RSL6,MC6,MP6
     PRINT 3010
3010 FORMAT (5X,5HMCTG6,5X,5HMHTG6)
     PRINT 9020,MCTG6,MHTG6
     PRINT 3011
3011 FORMAT (5X,5HMO6CN,5X,5HBL6CN,5X,5HSL6CN,4X,6HRSL6CN)
     PRINT 9020,MO6CN,BL6CN,SL6CN,RSL6CN
     PRINT 3012
3012 FORMAT (5X,4HMO6H,6X,4HBL6H,6X,4HSL6H,5X,5HRSL6H)
     PRINT 9020,MO6H,BL6H,SL6H,RSL6H
     PRINT 3013
3013 FORMAT (5X,5HMO6HN,5X,5HBL6HN,5X,5HSL6HN,4X,6HRSL6HN)
     PRINT 9020,MO6HN,BL6HN,SL6HN,RSL6HN
     PRINT 3014
3014 FORMAT (6X,3HMO7,7X,3HBL7,7X,3HSL7,6X,4HRSL7)
     PRINT 9020,MO7,BL7,SL7,RSL7
     PRINT 9104
9104 FORMAT(1X,27HSTRESS CONCENTRATION FACTOR)
     PRINT 9105
9105 FORMAT(6X,3HKTF)
     PRINT 9021,KTF
     PRINT 3015
3015 FORMAT (28H STRESSES FOR ALL CONDITIONS)
     PRINT 3016
3016 FORMAT (6X,3HEXA,7X,3HENA,7X,3HEXB,7X,3HENB)
     PRINT 9020,EXA,ENA,EXB,ENB
```

```
      PRINT 3017
 3017 FORMAT (5X,4HEXA2,6X,4HENA2,6X,4HEXB2,6X,4HENB2)
      PRINT 9020,EXA2,ENA2,EXB2,ENB2
      PRINT 3018
 3018 FORMAT(4X,6HSMAX2A,4X,6HSMIN2A,5X,5HFFC2A,4X,6HSMAX2B,4X,6HSMIN2B,
     15X,5HFFC2B)
      PRINT 9020,SMAX2A,SMIN2A,FFC2A,SMAX2B,SMIN2B,FFC2B
      PRINT 722
  722 FORMAT(5X,4HSH2P,5X,5HSRS2P,6X,4HSH2M,5X,5HSRS2M,6X,4HSPR2,7X,3HSB
     12,6X,4HSPA2)
      PRINT 9020,SH2P,SRS2P,SH2M,SRS2M,SPR2,SB2,SPA2
      PRINT 723
  723 FORMAT(5X,4HSR2P,6X,4HSR2M,6X,4HST2P,6X,4HST2M)
      PRINT 9020,SR2P,SR2M,ST2P,ST2M
      PRINT 3019
 3019 FORMAT (5X,4HEXA3,6X,4HENA3,6X,4HEXB3,6X,4HENB3)
      PRINT 9020,EXA3,ENA3,EXB3,ENB3
      PRINT 3020
 3020 FORMAT (5X,4HEXA5,6X,4HENA5,6X,4HEXB5,6X,4HENB5)
      PRINT 9020,EXA5,ENA5,EXB5,ENB5
      PRINT 3021
 3021 FORMAT(4X,6HSMAX5A,4X,6HSMIN5A,5X,5HFFC5A,4X,6HSMAX5B,4X,6HSMIN5B,
     15X,5HFFC5B)
      PRINT 9020,SMAX5A,SMIN5A,FFC5A,SMAX5B,SMIN5B,FFC5B
      PRINT 724
  724 FORMAT(6X,3HSH5,6X,4HSRS5,7X,3HSB5,6X,4HSPA5,7X,3HSR5,7X,3HST5,
     16X,4HSPR5)
      PRINT 9020,SH5,SRS5,SB5,SPA5,SR5,ST5,SPR5
      PRINT 725
  725 FORMAT(6X,3HSH1,6X,4HSRS1,7X,3HSB1,6X,4HSPA1,7X,3HSR1,7X,3HST1,
     16X,4HSPR1)
      PRINT 9020,SH1,SRS1,SB1,SPA1,SR1,ST1,SPR1
      PRINT 3022
 3022 FORMAT (5X,6HEXA6CN,5X,6HEXB6CN,5X,6HEXA6HN,5X,6HEXB6HN)
      PRINT 9020,EXA6CN,EXB6CN,EXA6HN,EXB6HN
      PRINT 3029
 3029 FORMAT (6X,3HBTS,5X,5HBTS2P,6X,4HBTS3,6X,4HBTS4,6X,4HBTS5,4X,
     15HBTS6CN,4X,6HBTS6HN)
      PRINT 9020,BTS,BTS2P,BTS3,BTS4,BTS5,BTS6CN,BTS6HN
      PRINT 3023
 3023 FORMAT (11H DIMENSIONS)
      PRINT 2902
 2802 FORMAT(9X,1HH,6X,4HHUBI,8X,2HG1,8X,2HFR)
      PRINT 9021,H,HUBI,G1,FR
      PRINT 3024
 3024 FORMAT (6X,2HTW,7X,3HTOD)
      PRINT 9021,TW,TOD
      PRINT 3025
 3025 FORMAT (6X,1HA,9X,1HB,8X,2HXT,7X,3HBCD)
      PRINT 9021,A,B,XT,BCD
      PRINT 3026
 3026 FORMAT(6X,3HSOD,7X,3HSID,7X,3HSEL,8X,2HTA,5X,5HSLEGT)
      PRINT 9021,SOD,SID,SEL,TA,SLEGT
      PRINT 3027
 3027 FORMAT (6X,5HBS(I),5X,5HBH(I),4X,6HBTA(I),4X,6HBWC(I),6X,2HBN)
      PRINT 9021,BS(I),BH(I),BTA(I),BWC(I),BN
```

```
      PRINT 3028
3028 FORMAT (6X,3HWGT)
      PRINT 9021,WGT
      PRINT 9103
9103 FORMAT(1H1)
      GO TO 999
 998 CALL EXIT
      END
```

```
      PROGRAM TREDP (INPUT,OUTPUT,TAPE60=INPUT)
      TYPE REAL LT,MSL,K,LCE,LCD,L,MP2,MC2,M01,MA1,MA2,MA3
      TYPE REAL MB1,MB2,MB3,M02,M02P,M02M,MP3,M03,MP5,M05,M06C,MC6,
     1MC1G6,MB1C6,M06CN,M06H,M06HN,M07,MH,MP6
      TYPE REAL KB
      TYPE REAL MR1,MR2,MR2P,MR2M,MR3,MR5,MR6C,MR6CN,MR6H,MR6HN,MR7
      TYPE REAL NWT
      TYPE REAL KTF
      TYPE REAL MSLT
      DIMENSION R(11),FF(11),BH(15),BWC(15),BS(15),BTA(15),NWT(15)
      DIMENSION DAF(15)
      NNN=0
C TUBE LOAD-INPUT
  999 READ 1020,TRM1
      IF(EOF,60) 998,997
C TUBE GEOMETRY
  997 READ 1021,TOD,TW1
 1020 FORMAT (8F10.0)
 1021 FORMAT (8F10.4)
 1022 FORMAT (8F10.9)
 1023 FORMAT (2I10)
C TUBE MATERIAL PROPERTIES
      READ 1020,TU,TY,TF,TR,TFR0
C FLANGE GEOMETRY
      READ 1021,AI,AUBII
      READ 1021,G1OTW1
      READ 1021,FRI,FSFI
C FLANGE MATERIAL PROPERTIES
      READ 1020,FUR
      READ 1020,FU,FY,FSU,FCY,FE,FG,FYC,FYR
      READ 1020,FCYC,FCYR
      READ 1022,FRHO,FMU,FTE,FCR
      READ 1021, (R(NN),NN=1,8)
      READ 1021, (R(NN),NN=9,11)
      READ 1020, (FF(NN),NN=1,8)
      READ 1020, (FF(NN),NN=9,11)
C SEAL GEOMETRY
      READ 1021,SOOI,STOI,SELI,TLI,TAOTW,SLEGTI
C SEAL LOADS-INPUT
      READ 1020,RSLI,SSLI,MSLI
C SEAL MATERIAL PROPERTIES
      READ 1020,SCY,SEF,SCYC,SCYR,SYR
      READ 1022,STF
C BOLT GEOMETRY
      READ 1021,(BH(NN),NN=1,8)
      READ 1021,(BH(NN),NN=9,15)
      READ 1021,(BWC(NN),NN=1,8)
      READ 1021,(BWC(NN),NN=9,15)
      READ 1021,(BS(NN),NN=1,8)
      READ 1021,(BS(NN),NN=9,15)
      READ 1021,(BTA(NN),NN=1,8)
      READ 1021,(BTA(NN),NN=9,15)
      READ 1021,(NWT(NN),NN=1,8)
      READ 1021,(NWT(NN),NN=9,15)
      READ 1021,(DAF(NN),NN=1,8)
      READ 1021,(DAF(NN),NN=9,15)
```

```
C BOLT INPUT
      READ 1023,TI,TMAX
      READ 1020,RNT
C BOLT MATERIAL PROPERTIES
      READ 1020,RY,RE,RU,RYC,RYR
      READ 1022,RTE,RCR,RRHO
C RING GEOMETRY AND PROPERTIES
      READ 1021,RCDT
      READ 1020,RU,RY,RSU,RCY,RE,RG,RYC,RYR
      READ 1020,RCYC,RCYR
      READ 1022,RTE,RCR,RRHO
C SYSTEM PRESSURE AND TEMPERATURE
      READ 1020,P,PP,PR,PIM,TMAX,TMIN
      READ 1020,DT1C,DT2C,DT3C,DT1H,DT2H,DT3H
      READ 1021,FS1,FS2,FS3
      PRINT 726
  726 FORMAT(25X,19HINPUT TO THE DESIGN///)
      PRINT 2020
 2020 FORMAT (16H TUBE LOAD-INPUT)
      PRINT 2021
 2021 FORMAT (3X,4HTRM1)
      PRINT 9021,TRM1
      PRINT 2000
 2000 FORMAT (14H TUBE GEOMETRY)
      PRINT 2001
 2001 FORMAT (6X,3HTOD,7X,3HTW1)
      PRINT 9021,TOD,TW1
      PRINT 2002
 2002 FORMAT (25H TUBE MATERIAL PROPERTIES)
      PRINT 2003
 2003 FORMAT (7X,2HTU,8X,2HTY,8X,2HTF,8X,2HTR,8X,4HTFR0)
      PRINT 9020,TU,TY,TF,TR,TFR0
      PRINT 2004
 2004 FORMAT (16H FLANGE GEOMETRY)
      PRINT 2005
 2005 FORMAT(7X,2HAI,5X,5HHUBII)
      PRINT 9021,AI,HUBII
      PRINT 800
  800 FORMAT(3X,6HG10TW1)
      PRINT 9021,G10TW1
      PRINT 2037
 2037 FORMAT(6X,3HFRI,6X,4HFSFI)
      PRINT 9021,FRI,FSFI
      PRINT 2006
 2006 FORMAT (27H FLANGE MATERIAL PROPERTIES)
      PRINT 801
  801 FORMAT(6X,3HFUR)
      PRINT 9020,FUR
      PRINT 2007
 2007 FORMAT (7X,2HFU,8X,2HFY,7X,3HFSU,7X,3HFCY,8X,2HFE,8X,2HFG,7X,
     13HFYC,7X,3HFYR)
      PRINT 9020,FU,FY,FSU,FCY,FE,FG,FYC,FYR
      PRINT 2040
 2040 FORMAT (6X,4HFCYC,6X,4HFCYR)
      PRINT 9021,FCYC,FCYR
      PRINT 2008
```

```
2008 FORMAT (5X,4HFRHO,5X,3HFMU,7X,3HFTE,7X,3HFCR)
9020 FORMAT (8F10.0)
9021 FORMAT (8F10.4)
9022 FORMAT (8F10.8)
9023 FORMAT (2I10)
     PRINT 9022,FRHO,FMU,FTE,FCR
     PRINT 2009
2009 FORMAT (5X,4HR(1),6X,4HR(2),6X,4HR(3),6X,4HR(4),6X,4HR(5),6X,
    14HR(6),6X,4HR(7),6X,4HR(8))
     PRINT 9021,R(1),R(2),R(3),R(4),R(5),R(6),R(7),R(8)
     PRINT 2010
2010 FORMAT (5X,4HR(9),5X,5HR(10),5X,5HR(11))
     PRINT 9021,R(9),R(10),R(11)
     PRINT 2011
2011 FORMAT (4X,5HFF(1),5X,5HFF(2),5X,5HFF(3),5X,5HFF(4),5X,5HFF(5),5X,
    15HFF(6),5X,5HFF(7),5X,5HFF(8))
     PRINT 9020,FF(1),FF(2),FF(3),FF(4),FF(5),FF(6),FF(7),FF(8)
     PRINT 2012
2012 FORMAT (4X,5HFF(9),4X,6HFF(10),4X,6HFF(11))
     PRINT 9020,FF(9),FF(10),FF(11)
     PRINT 2013
2013 FORMAT (14H SEAL GEOMETRY)
     PRINT 2014
2014 FORMAT (5X,4HSODI,6X,4HSIDI,6X,4HSELI,6X,3HTAI,5X,5HTAOTW,4X,6HSLE
    1GTI)
     PRINT 9021,SODI,SIDI,SELI,TAI,TAOTW,SLEGTI
     PRINT 2015
2015 FORMAT (18H SEAL LOADS INPUTS)
     PRINT 2016
2016 FORMAT(5X,4HRSLI,4X,4HSSLI,4X,4HMSLI)
     PRINT 9020,RSLI,SSLI,MSLI
     PRINT 2017
2017 FORMAT (25H SEAL MATERIAL PROPERTIES)
     PRINT 2018
2018 FORMAT (7X,3HSCY,7X,3HSEE,6X,4HSCYC,6X,4HSCYR,7X,3HSYR)
     PRINT 9020,SCY,SEE,SCYC,SCYR,SYR
     PRINT 2019
2019 FORMAT (3X,3HSTF)
     PRINT 9022,STF
     PRINT 2022
2022 FORMAT (14H BOLT GEOMETRY)
     PRINT 2023
2023 FORMAT (4X,5HBH(1),5X,5HBH(2),5X,5HBH(3),5X,5HBH(4),5X,5HBH(5),5X,
    15HBH(6),5X,5HBH(7),5X,5HBH(8))
     PRINT 9021,BH(1),BH(2),BH(3),BH(4),BH(5),BH(6),BH(7),BH(8)
     PRINT 2024
2024 FORMAT (4X,5HBH(9),4X,6HBH(10),4X,6HBH(11),4X,6HBH(12),4X,6HBH(13)
    1,4X,6HBH(14),4X,6HBH(15))
     PRINT 9021,BH(9),BH(10),BH(11),BH(12),BH(13),BH(14),BH(15)
     PRINT 2025
2025 FORMAT (4X,6HBWC(1),4X,6HBWC(2),4X,6HBWC(3),4X,6HBWC(4),4X,6HBWC(5
    1),4X,6HBWC(6),4X,6HBWC(7),4X,6HBWC(8))
     PRINT 9021,BWC(1),BWC(2),BWC(3),BWC(4),BWC(5),BWC(6),BWC(7),BWC(8)
     PRINT 2026
2026 FORMAT (4X,6HBWC(9),3X,7HBWC(10),3X,7HBWC(11),3X,7HBWC(12),3X,
    17HBWC(13),3X,7HBWC(14),3X,7HBWC(15))
```

```
      PRINT 9021,BWC(9),BWC(10),BWC(11),BWC(12),BWC(13),BWC(14),BWC(15)
      PRINT 2027
 2027 FORMAT (5X,5HBS(1),5X,5HBS(2),5X,5HBS(3),5X,5HBS(4),5X,5HBS(5),5X,
     15HBS(6),5X,5HBS(7),5X,5HBS(8))
      PRINT 9021,BS(1),BS(2),BS(3),BS(4),BS(5),BS(6),BS(7),BS(8)
      PRINT 2028
 2028 FORMAT (5X,5HBS(9),4X,6HBS(10),4X,6HBS(11),4X,6HBS(12),4X,6HBS(13)
     1,4X,6HBS(14),4X,6HBS(15))
      PRINT 9021,BS(9),BS(10),BS(11),BS(12),BS(13),BS(14),BS(15)
      PRINT 2029
 2029 FORMAT (4X,6HBTA(1),4X,6HBTA(2),4X,6HBTA(3),4X,6HBTA(4),4X,6HBTA(5
     1),4X,6HBTA(6),4X,6HBTA(7),4X,6HBTA(8))
      PRINT 9021,BTA(1),BTA(2),BTA(3),BTA(4),BTA(5),BTA(6),BTA(7),BTA(8)
      PRINT 2030
 2030 FORMAT (4X,6HBTA(9),3X,7HBTA(10),3X,7HBTA(11),3X,7HBTA(12),3X,7HBT
     1A(13),3X,7HBTA(14),3X,7HBTA(15))
      PRINT 9021,BTA(9),BTA(10),BTA(11),BTA(12),BTA(13),BTA(14),BTA(15)
      PRINT 2053
 2053 FORMAT (4X,6HNWT(1),4X,6HNWT(2),4X,6HNWT(3),4X,6HNWT(4),4X,6HNWT(5
     1),4X,6HNWT(6),4X,6HNWT(7),4X,6HNWT(8))
      PRINT 9021,NWT(1),NWT(2),NWT(3),NWT(4),NWT(5),NWT(6),NWT(7),NWT(8)
      PRINT 2054
 2054 FORMAT (4X,6HNWT(9),3X,7HNWT(10),3X,7HNWT(11),3X,7HNWT(12),3X,7HNW
     1T(13),3X,7HNWT(14),3X,7HNWT(15))
      PRINT 9021,NWT(9),NWT(10),NWT(11),NWT(12),NWT(13),NWT(14),NWT(15)
      PRINT 2038
 2038 FORMAT(4X,6HDAF(1),4X,6HDAF(2),4X,6HDAF(3),4X,6HDAF(4),4X,6HDAF(5)
     1,4X,6HDAF(6),4X,6HDAF(7),4X,6HDAF(8))
      PRINT 9021,DAF(1),DAF(2),DAF(3),DAF(4),DAF(5),DAF(6),DAF(7),DAF(8)
      PRINT 2039
 2039 FORMAT(4X,6HDAF(9),3X,7HDAF(10),3X,7HDAF(11),3X,7HDAF(12),3X,7HDAF
     1(13),3X,7HDAF(14),3X,7HDAF(15))
      PRINT 9021,DAF(9),DAF(10),DAF(11),DAF(12),DAF(13),DAF(14),DAF(15)
      PRINT 2050
 2050 FORMAT (11H BOLT INPUT)
      PRINT 2051
 2051 FORMAT (8X,2HII,3X,4HIMAX)
      PRINT 9023,II,IMAX
      PRINT 2052
 2052 FORMAT (6X,3HBNI)
      PRINT 9021,BNI
      PRINT 2031
 2031 FORMAT (25H BOLT MATERIAL PROPERTIES)
      PRINT 2032
 2032 FORMAT (8X,2HBY,8X,2HBE,8X,2HBU,7X,3HBYC,7X,3HBYR)
      PRINT 9020,BY,BE,BU,BYC,BYR
      PRINT 2033
 2033 FORMAT (6X,3HBTE,7X,3HBCR,6X,4HBRHO)
      PRINT 9022,BTE,BCR,BRHO
      PRINT 2055
 2055 FORMAT (3X,29H RING GEOMETRY AND PROPERTIES)
      PRINT 2056
 2056 FORMAT (6X,4HRCDI)
      PRINT 9021,RCDI
      PRINT 2057
 2057 FORMAT (7X,2HRU,8X,2HRY,7X,3HRSU,7X,3HRCY,8X,2HRE,8X,2HRG,7X,3HRYC
```

```
     1,7X,3HRYR)
      PRINT 9020,RU,RY,RSU,RCY,RE,RG,RYC,RYR
      PRINT 2058
 2058 FORMAT (5X,4HRCYC,6X,4HRCYR)
      PRINT 9020,RCYC,RCYR
      PRINT 2059
 2059 FORMAT (6X,3HRTE,7X,3HRCR,6X,4HRRHO)
      PRINT 9022,RTE,RCR,RRHO
      PRINT 2034
 2034 FORMAT (32H SYSTEM PRESSURE AND TEMPERATURE)
      PRINT 2035
 2035 FORMAT (9X,1HP,9X,2HPP,8X,2HPB,7X,3HPIM,6X,4HTMAX,6X,4HTMIN)
      PRINT 9020,P,PP,PB,PIM,TMAX,TMIN
      PRINT 2060
 2060 FORMAT (6X,4HDT1C,6X,4HDT2C,6X,4HDT3C,6X,4HDT1H,6X,4HDT2H,6X,4HDT3
     1H)
      PRINT 9020,DT1C,DT2C,DT3C,DT1H,DT2H,DT3H
      PRINT 2036
 2036 FORMAT (7X,3HFS1,7X,3HFS2,7X,3HFS3)
      PRINT 9021,FS1,FS2,FS3
 9110 CONTINUE
      KOUNT=0
C     TUBE CALCULATIONS TUBE WALL ,TUBE BENDING MOMENT,TUBE BENDING STRESS
      TW2=1.1*PP*TOD/(2.*TY+.8*PP)
      TW3=1.1*PB*TOD/(2.*TU+.8*PB)
      IF(TFR0 .EQ. 0.0) GO TO 16
      TW4=1.1*PIM*TOD/(2.*TFR0+.8*PIM)
      GO TO 17
   16 TW4=TW3
   17 CONTINUE
      IF(.001-TW1)1,1,2
    1 TW=TW1
      GO TO 3
    2 TW=MAX1F(TW2,TW3,TW4)
    3 W=3.1416*(TOD**4-(TOD-2.*TW)**4)/(32.*TOD)
      IF(TBM1 .EQ. 0.001)5,4
    4 TBM=TBM1
      GO TO 6
    5 TBM2=W*.6667*TY
      TBM3=W*.8*TR
      TBM4=W*.5*TF
      TBM5=MIN1F(TBM2,TBM3,TBM4)
      TBM6=60.*(TOD+3.)**3
      TBM=MIN1F(TBM5,TBM6)
    6 TBS=TBM/W
      TMD=TOD-TW
      PI=3.1416
      IF(TOD-3.0)26,26,27
   26 BLO=.5*TBS*PI*(TOD-TW)*TW*(.5+.5*(TOD/3.))
      GO TO 33
   27 BLO=.5*TBS*PI*(TOD-TW)*TW
   33 BL1=MAX1F(BLO,SSLI*PI*TOD)
      BNP=4.
      IF(TOD-3.0)60,60,61
   60 I=1
      GO TO 62
```

```
   61 T=7
   62 XT=3.*TW
      ET=2.*TW
      GO=TW
      IF(.001-HUBTI)64,63,63
   63 GI=1.25*TW
      GO TO 65
   64 GI=TW*HUBTI
   65 RETOD=2.*TW
      IF(.001-ERI)700,701,701
  700 ER=ERI
      GO TO 702
  701 IF(TOD-4.)703,703,704
  703 ER=0.125
      GO TO 702
  704 IF(TOD-8.)705,705,706
  705 ER=0.1875
      GO TO 702
  706 IF(TOD-12.)707,707,708
  707 ER=0.25
      GO TO 702
  708 ER=0.3125
  702 CONTINUE
      SLEG=0.1+0.012*TOD
      SID=(TOD-2.*TW)+2.*SLEG*0.15
   14 TA=TAOTW*TW
   15 SOD=SID+2.*TA+2.*SLEG
      D3=SID+2.*TA
      SLEGT1=RSLT*(SOD/D3)/SCYR
      SLEGT2=0.04+(0.001*P**0.5*100)/12.0
      SLEGT=AMAX1F(SLEGT1,SLEGT2)
      TANSL=RSLT*(SOD/D3)-SCYR*(SOD*SOD-D3*D3)*SLEGT/(SOD*SOD)
      SEL=2.*RSLT/(SCYR*ALOG(D3/SID))
      SX=SEL/2.0
      LT=SEL/TA
   18 IF(4.0-LT)19,19,25
   19 TA=TA+0.005
      GO TO 15
   25 IF(.001-SODT)32,32,28
   32 SOD=SODI
      SID=SIDI
      SEL=SELI
      TA=TAI
      SLEGT=SLEGTI
      SX=SEL/2
C     LOAD CALCULATIONS
   28 WSL=WSLI*PI*SOD
C     PRELIMINARY BOLT CALCULATION
      A=0.0
  108 HUBI=GI-TW
      ALFA=ATAN(HUBI/(2.0*(R*GO)**.5))
      D=(ER-ER*SIN(ALFA))*TAN(ALFA)
      BID=TOD+2.*(HUBI-D)
      A1=((5.*RLO)/(PI*FCY)+(RID**2))**.5
      A2=SOD+2.*((SLEGT*6.0*RSLI*FS1/FY)**.5)
      A3 SOD+2.*(RSLT*FS1/FSU)
```

```
      A5=SOD+2.*(0.060+TOD*.0075)
      A4=AMAX1F(A1,A2,A3,A5,A)
      IF(.001-AI)110,110,113
  110 A=AI
      GO TO 107
  113 A=A4
  107 IF(I-IMAX) 116,1009,1009
 1009 PRINT 1010
 1010 FORMAT (3X,36HROOT REQUIRED NOT AVAILABLE IN TABLE)
      GO TO 999
  116 RCO1=A+BH(I)
      RCO2=TOD+2.*HUBI+BWC(I)
      RCO3=MAX1F(RCO1,RCO2)
      IF(.001-RCOT)115,115,114
  115 RCO=RCO1
      BN=BN1
      I=II
      GO TO 117
  114 RCO=RCO3
      RU=RCO*PI/BWC(I)
      NB=BN/2.
      N=2*NB
      BN=N
  117 SMD=B+TA
      C=(2.*A+PID)/3.
      RCO=RCO+2.*BH(I)
      H2=0.5*(C-(A+B)/2.)
      H3=0.5*((A+B)/2.-SMD)
      H4=((A+B)/4.)-(1./3.)*(SOD**2+SOD*B+B**2)/(SOD+B)
      H5=0.5*(RCO-C)
      H6=((A-B)/4.)-(TW+HUBI)/2.
C     FLANGE SIZE CALCULATION
      H=2.0*(R*GO)**.5
      K=A/B
      T=((K*K)*(1.0+R.55246*ALOG10(K))-1.0)/((1.04720+1.94480*K*K)*(K-1.
     1))
      U=((K*K)*(1.0+R.55246*ALOG10(K))-1.)/(1.36136*(K**2-1.)*(K-1.))
      Y=(1./(K-1.))*(.66845+5.717*((K*K)*ALOG10(K)/(K**2-1.)))
      Z=(K*K+1.)/(K*K-1.)
      F=.909-.031*(G1/G0-1.)-.1605*(G1/G0-1.)**.5
      V=.55+.15*(G1/G0-1.)-.558*(G1/G0-1.)**.5
      HO=((H+G1)*G0)**.5
      LCF=F/HO
      LCO=(U/V)*HO*G0**2
  202 L=(XT*LCF+1.)/T+(XT**3)/LCO
      GE=0.5*(G1+G0)
      HOP=(H*GE)**.5
      C1=(3.**.5)*(2.-FMU)/(4.*FF*(1.-FMU**2))
      C2=(3./(1.-FMU**2))**.5
      C3=(12.*(1.-FMU**2))**.25
      C4=((12.*(1.-FMU**2))**.25)/(2.*(1.-FMU**2))
      BETA=(3.*(1.-FMU**2)/((((TOD/2.)+GE-G0)**2)*(GE)**2))**.25
      HOP=(H*GE)**.5
      GAMMA=(GE*(FMU+Z)*(1.+C3*XT/HOP))/(1.+(C4*B*GE**3*(FMU+Z)/(HOP*XT*
     1*3)*(2+C3*XT/HOP)))
      DT=FF*GE**3/(12.*(1.-FMU**2))
```

```
      DF=EE*(T**3)/(12.*(1.-EMU**2))
      XP=((((1.+EMU)/(1.-EMU))*K**2*1.)*B)/((K**2-1.)*(1.+EMU)*2.*DF)
      AI=(PI/4.)*(TOD**2-B**2)
      ZH=PI*((TOD-2.*G0+2.*G1)**4-(TOD-2.*TW)**4)/(32.*(TOD-2.*G0+2.*G1)
     1)
      AH=(((TOD-2.*G0+2.*G1)**2-(TOD-2.*G0)**2)*PI/4.)
C     DEFLECTION RATES
      DSA=-(SX)/(SEE*PI*(B+TA)*TA)
      DSR=-(B+TA)/(2.*PI*SEL*TA*SEE)
  203 DRA=((SX+XT)/(SEE*PI*RS(I)**2/4.))+(RT+RS(I)/2.)/(BE*BTA(I))
      DBA=DSA/BN
      DER=(.91*V)/(L*H0*G0**2*FE)
      DFA=-DER*(H2+H3)**2-(1./(2.*PI*FG*XT))*ALOG(C/SMD)
     1-(XT)/((PI/4.)*(A**2-B**2)*FE)
      DRR=6./(PI*RE*(RT**3)*ALOG(ROD/RID))
      DRA=-DRR*(HS**2)-(1./(2.*PI*RG*RT))*ALOG(RCO/C)
     1-(RT)/((PI/4.)*(RCO**2-RID**2)*RE)
C     RING CALCULATIONS
      KR=ROD/RID
      YR=(1./(KR-1.))*(.66845+5.713*((KR*KR)*ALOG10(KR)/(KR**2-1.)))
      RATIO=A/TOD
      IF(RATIO .LE. 1.1)711,712
  711 KTF=0.179*((TOD/FR)**.5)+.914
      GO TO 718
  712 IF(RATIO .LE. 1.2)713,714
  713 KTF=0.202*((TOD/FR)**.5)+.86
      GO TO 718
  714 IF(RATIO .LE. 1.5)715,716
  715 KTF=0.233*((TOD/FR)**.5)+.79
      GO TO 718
  716 KTF=0.242*((TOD/FR)**.5)+.69
  718 CONTINUE
C     LOAD CALCULATIONS CONDITION 1 AND 2
      P1=0.
      P2=P
      THM1=0.
      THM2=THM
      MP2=((L*H0*G0**2*FE)/(.91*V))*(C1*B**2*GAMMA*P2/(XT*(XT**2+C2*GE*G
     1AMMA)))
      FA1=0.
      FA2=P2*(PI/4.)*(B**2)
      FPL1=0.
      FPL2=P2*(PI/4.)*(SOD**2-B**2)
      RSL1=RSLT*PI*SOD
  111 SL1=RL1
      MO1=-RSL1*XT/2.+RL1*H2+SL1*H3
      MC2=AINIF((L*G1**2*(B+TW)*FE*FCR),(MO1*FE*FCR/FYR))
      MR1=RL1*HS
C STRESS CALCULATION CONDITION 1
  310 SH=((RL1*H2+SL1*H3)/(L*G1**2*(B+G0)))
  311 SRS=((RSL1*XT/2.)/(L*G1**2*(B+G0)))
      SR=MO1*(1.333*XT*CE+1.)/(L*XT**2*(B+G0))
      ST=MO1*(Y/(XT**2*B))-Z*SR
      SH=0.
      SPR=0.
      SPA=0.
```

```
      SCEA=0.
      SCEB=0.
      FSS=BL1/(TOD*PI*XT)
      SSC=SL1/(((B*2.*TA)**2-B**2)*PI/4.)
      BTS=BL1/(3N*BTA(I))
      SFB=4.*BL1/(PI*(A**2-BID**2))
      STR=(MR1*YR)/(RT**2*BID)
      BSS=BL1/(3*PI*BT)
      IF(SFB-FCYR/2.)121,121,122
  122 IF(.001-AT)121,121,120
  120 A=A+.015
      GO TO 116
  121 IF(BTS-BYR/FS2)314,314,903
  903 IF(0-II)314,313,313
  313 I=I+1
      GO TO 107
  314 IF(SR-FYR/FS1)315,315,302
  315 IF(ST-FYR/FS1)316,316,302
  316 IF(FSS-FSU/FS1)317,317,302
  317 IF(SSC-SCYR/FS1)318,318,619
  619 PRINT 620
  620 FORMAT (3X,18H SSC EXCEEDS LIMIT)
  318 IF(STR-BYR/FS1)319,319,303
  319 IF(BSS-BSU/FS1)330,330,303
  402 IF(HIBII .LT. 0.001)802,302
  802 IF(GIOTWT .LT. 0.001)804,803
  803 GIOTW=G1/TW
      IF(GIOTW .GT. GIOTWI)302,804
  804 G1=G1+0.005
      XT=XT-0.030
      GO TO 108
  302 XT=XT+.015
      IF(XT-2.*TOD)202,1003,1003
 1003 PRINT 1004
 1004 FORMAT (3X,31HFLANGE THICKNESS EXCEEDS LIMIT )
      GO TO 999
  303 BT=BT+.015
      IF(BT-2.*TOD)203,1005,1005
 1005 PRINT 1006
 1006 FORMAT (3X,29HRING THICKNESS EXCEEDS 2.*TOD)
      GO TO 999
  850 XT=XT+.015
      KOUNT=KOUNT+1
      IF(KOUNT .LE. 5)860,202
  860 IF(G1 .GT. 1.75*TW)851,202
  851 G1=G1-0.005
      GO TO 108
  330 XA1=-SH+SR+SPR+SPA+SRS
      XA2=-SCEA+SR
      XA3=ST
      NA1=-SH-SR+SPR+SPA+SRS
      NA2=-SCEA+SR
      NA3=ST
      FXA=.7071*((XA1-XA2)**2+(XA2-XA3)**2+(XA3-XA1)**2)**.5
      FNA=.7071*((NA1-NA2)**2+(NA2-NA3)**2+(NA3-NA1)**2)**.5
      FA =AMAX1(ABS(FXA),ABS(FNA))
```

```
      IF(EA-EYP)/ES1)352,352,302
  352 XB1=+SM+SA-SPR+SPA-SRS
      XB2=-SCER+SR
      XB3=ST
      NB1=+SM-SA-SPR+SPA-SRS
      NB2=-SCER+SR
      NB3=ST
      EXB=.7071*((XB1-XB2)**2+(XB2-XB3)**2+(XB3-XB1)**2)**.5
      ENB=.7071*((NB1-NB2)**2+(NB2-NB3)**2+(NB3-NB1)**2)**.5
      EB=AMAX1(ABS(EXB),ABS(ENB))
      IF(EB-EYP/ES1)362,362,302
C     LOAD AND MOMENT CALCULATION CONDITION 2
  362 TL2=FA2+TRS*AT
      R21=-FPL2-TL2
      R22=-FPL2*H4+(P2*PI*B*SX)*(XT/2.)-MP2-MC2-TL2*H6
      R23=-(P2*B*((A+B)/2.))/(4.*((A-B)/2.)*FF)+(P2*B*SMD)/(4.*TA*SEE)
      R24=(BCR*(SX+XT+RT))/(DBA-DRA)
      R25=DFA/((H2+H3)*(DBA-DRA-DSA))
      R26=(DBA-DRA)*(R24-R21)/(DBA-DRA-DSA)
      R27=R26*(H2+H3)+R21*H2-(R23*XT)/(DSR*2.)+R22
      R28=(1.-(R25*(H2+H3))-(DFR*XT**2)/(DSR*4.))
      MO2=MO1-R27/R28
      SL2=SL1-R27*R25/R28-R26
      RSL2=RSL1+(R27*DFR*XT)/(R28*2.*DSR)-R23/DSR
      RL2=RL1-R21-R26-R27*R25/R28
      MR2=RL2*H5
      IF(SL2-MSL)331,332,332
  331 RL1=1.01*RL1
      GO TO 111
  332 R21P=-FPL2-TL2
      R22P=-FPL2*H4+(P2*PI*B*SX)*(XT/2.)-MP2-TL2*H6
      R23P=-(P2*B*((A+B)/2.))/(4.*((A-B)/2.)*FF)+(P2*B*SMD)/(4.*TA*SEE)
      R24P=0.
      R25P=DFA/((H2+H3)*(DBA-DRA-DSA))
      R26P=(DBA-DRA)*(R24P-R21P)/(DBA-DRA-DSA)
      R27P=R26P*(H2+H3)+R21P*H2-(R23P*XT)/(DSR*2.)+R22P
      R28P=(1.-(R25P*(H2+H3))-(DFR*XT**2)/(DSR*4.))
      MO2P=MO1-R27P/R28P
      SL2P=SL1-R27P*R25P/R28P-R26P
      RSL2P=RSL1+(R27P*DFR*XT)/(R28P*2.*DSR)-R23P/DSR
      RL2P=RL1-R21P-R26P-R27P*R25P/R28P
      MR2P=RL2P*H5
      R21M=-FPL2-FA2+TRS*AT
      R22M=-FPL2*H4+(P2*PI*B*SX)*(XT/2.)-MP2-H6*(FA2-TRS*AT)
      R23M=-(P2*B*((A+B)/2.))/(4.*((A-B)/2.)*FF)+(P2*B*SMD)/(4.*TA*SEE)
      R24M=0.
      R25M=DFA/((H2+H3)*(DBA-DRA-DSA))
      R26M=(DBA-DRA)*(R24M-R21M)/(DBA-DRA-DSA)
      R27M=R26M*(H2+H3)+R21M*H2-(R23M*XT)/(DSR*2.)+R22M
      R28M=(1.-(R25M*(H2+H3))-(DFR*XT**2)/(DSR*4.))
      MO2M=MO1-R27M/R28M
      SL2M=SL1-R27M*R25M/R28M-R26M
      RSL2M=RSL1+(R27M*DFR*XT)/(R28M*2.*DSR)-R23M/DSR
      RL2M=RL1-R21M-R26M-R27M*R25M/R28M
      MR2M=RL2M*H5
C     STRESS CALCULATIONS CONDITION 2
```

```
      SH2P=(BL2P*H2+FPL2*H4+TL2*H6+SL2P*H3)/(L*G1**2*(B+G0))
      SH2M=(BL2M*H2+FPL2*H4+(FA2-TRS*AT)*H6+SL2M*H3)/(L*G1**2*(B+G0))
      SRS2P=(RSL2P*XT/2.)/(L*G1**2*(B+G0))
      SRS2M=(RSL2M*XT/2.)/(L*G1**2*(B+G0))
      SPR2=MP2/(L*G1**2*(B+G0))
      SB2=THM//H
      SPA2=FA2/AH
      SCEB2=0
      SCEA2=P2
      SR2P=MO2P*(1.333*XT*LCE+1.)/(L*XT**2*(B+G0))
      SR2M=MO2M*(1.333*XT*LCE+1.)/(L*XT**2*(B+G0))
      ST2P=MO2P*(Y/(XT**2*B))-Z*SR2P
      ST2M=MO2M*(Y/(XT**2*B))-Z*SR2M
      FSS2=BL2P/(TOD*PT*XT)
      SSC2=SL2M/(((B+2.*TA)**2-B**2)*PI/4.)
      HTS2P=BL2P/(BTA(I)*BN)
      SFB2P=4.*BL2P/(PI*(A**2-RID**2))
      SFB2M=4.*BL2M/(PI*(A**2-RID**2))
      STR2P=(MR2P*YR)/(RT**2*RID)
      STR2M=(MR2M*YR)/(RT**2*RID)
      RSS2=BL2P/(A*PT*RT)
      SFB2=AMAX1(SFB2P,SFB2M)
      IF(SFB2-FCY/2.)343,343,123
  123 IF(.001-AT)343,343,120
  343 IF(HTS2P-BY/FS2)344,344,913
  913 IF(0-II)344,313,313
  344 IF(SR2P-FY/FS1)345,345,302
  345 IF(ST2P-FY/FS1)346,346,302
  346 IF(FSS2-FSU/FS1)347,347,302
  347 IF(SSC2-SCY/FS1)348,348,621
  621 PRINT 622
  622 FORMAT (3X,14H SSC2 EXCEEDS LIMIT)
  348 IF(STR2P-BY/FS1)349,349,303
  349 IF(STR2M-BY/FS1)350,350,303
  350 IF(RSS2-PSU/FS1)351,351,303
  351 XA1=-SH2P+SR2+SPR2+SPA2+SRS2P
      XA2=-SCEA2+SR2P
      XA3=ST2P
      NA1=-SH2M-SR2+SPR2+SPA2+SRS2M
      NA2=-SCEA2+SR2M
      NA3=ST2M
      EXA2=.7071*((XA1-XA2)**2+(XA2-XA3)**2+(XA3-XA1)**2)**.5
      ENA2=.7071*((NA1-NA2)**2+(NA2-NA3)**2+(NA3-NA1)**2)**.5
      XA1=XA1-SPA2
      NA1=NA1-SPA2
      IF(ABS(XA1)-ABS(NA1))602,602,601
  602 CMAX2A=NA1
      CMIN2A=XA1
      GO TO 603
  601 CMAX2A=XA1
      CMIN2A=NA1
  603 EA=AMAX1(ABS(EXA2),ABS(ENA2))
      IF(EA-FY/FS1)1352,1352,302
 1352 CALT2A=(CMAX2A-CMIN2A)/2.
      CMN2A=(CMAX2A+CMIN2A)/2.
      FALT2A=CALT2A*FSFI
```

```
      SALT2A=FALT2A
      SMN2A=CMN2A
      SCHK2A=ABS(SMN2A+SALT2A)
      IF(SCHK2A .GT. FU)402,805
  805 IF(SCHK2A-FY)806,806,807
  807 IF(ABS(SALT2A)-FY)808,808,809
  808 SMN2A=FY-SALT2A
      GO TO 806
  809 SMN2A=0.
  806 SMAX2A=SMN2A+SALT2A
      SMIN2A=SMN2A-SALT2A
      RC1=SMIN2A/SMAX2A
      M=0
 1350 M=M+1
      IF(RC1-R(M))1351,7000,1350
 1351 FFC2A=((R(M)-RC1)/(R(M)-R(M-1)))*(FF(M)-FF(M-1))+FF(M-1)
      GO TO 7001
 7000 FFC2A=FF(M)
 7001 CONTINUE
      IF(ABS(SMAX2A)-FFC2A)1363,1363,402
 1363 XB1=SH2P+SB2-SPB2+SPA2-SRS2P
      XB2=-SCEB2+SB2P
      XB3=ST2P
      NB1=SH2M-SB2-SPB2+SPA2-SRS2M
      NB2=-SCEB2+SB2M
      NB3=ST2M
      EXB2=.7071*((XB1-XB2)**2+(XB2-XB3)**2+(XB3-XB1)**2)**.5
      ENB2=.7071*((NB1-NB2)**2+(NB2-NB3)**2+(NB3-NB1)**2)**.5
      EB=AMAX1(ABS(EXB2),ABS(ENB2))
      XB1=XB1-SPA2
      NB1=NB1-SPA2
      IF(EB-FY/FS1)720,720,302
  720 IF(ABS(XB1)-ABS(NB1))605,605,604
  605 CMAX2B=NB1
      CMIN2B=XB1
      GO TO 1362
  604 CMAX2B=XB1
      CMIN2B=NB1
 1362 CALT2B=(CMAX2B-CMIN2B)/2.
      CMN2B=(CMAX2B+CMIN2B)/2.
      FALT2B=CALT2B*FSF1
      SALT2B=FALT2B*KTF
      SMN2B=CMN2B*KTF
      SCHK2B=ABS(SMN2B+SALT2B)
      IF(SCHK2B.GT. FU)402,810
  810 IF(SCHK2B-FY)811,811,812
  812 IF(ABS(SALT2B)-FY)813,813,814
  813 SMN2B=FY-SALT2B
      GO TO 811
  814 SMN2B=0.
  811 SMAX2B=SMN2B+SALT2B
      SMIN2B=SMN2B-SALT2B
      RC2=SMIN2B/SMAX2B
      M=0
 1360 M=M+1
      IF(RC2-R(M))1361,7002,1360
```

```
 1361 FFC2B=((R(M)-RC2)/(R(M)-R(M-1)))*(FF(M)-FF(M-1))+FF(M-1))
      GO TO 7003
 7002 FFC2B=FF(M)
 7003 CONTINUE
      IF(ABS(SMAX2H)-FFC2B)380,380,402
C     LOAD CALCULATIONS CONDITION 3
  380 P3=PP
      TBM3=0.
      FA3=P3*(PI/4.)*(B**2)
      FPL3=P3*(PI/4.)*(SOD**2-B**2)
      TL3=FA3
      MP3=((L*HO*GO**2*FF)/(.91*V))*(C1*B**2*GAMMA*P3/(XT*(XT**2+C2*GE*G
     1AMMA)))
      R31=-FPL3-TL3
      R32=-FPL3*H4+(P3*PI*B*SX)*(XT/2.)-MP3-TL3*H6
      R33=-(P3*B*((A+B)/2.))/(4.*((A-B)/2.)*FF)+(P3*B*SMD)/(4.*TA*SEE)
      R34=0.
      R35=DFA/((H2+H3)*(DBA-DRA-DSA))
      R36=(DBA-DRA)*(R34-R31)/(DBA-DRA-DSA)
      R37=R36*(H2+H3)+R31*H2-(R33*XT)/(DSR*2.)+R32
      R38=(1.-(R35*(H2+H3))-(DFR*XT**2)/(DSR*4.))
      MO3=MO1-R37/R38
      SL3=SL1-R37*R35/R38-R36
      RSL3=RSL1+(R37*DFR*XT)/(R38*2.*DSR)-R33/DSR
      RL3=RL1-R31-R36-R37*R35/R38
      MR3=RL3*H5
      IF(SL3-MSL)331,390,390
C     STRESS CALCULATIONS CONDITION 3
  390 SH3=(RL3*H2+SL3*H3+FPL3*H4+TL3*H6)/(L*G1**2*(B+GO))
      SRS3=(RSL3*XT/2.)/(L*G1**2*(B+GO))
      SPR3=MP3/(L*G1**2*(B+GO))
      SB3=0.
      SPA3=FA3/AH
      SCEB3=0.
      SCEA3=P3
      SR3=MO3*(1.333*XT*LCE+1.)/(L*XT**2*(B+GO))
      ST3=MO3*(Y/(XT**2*B))-Z*SR3
      FSS3=RL3/(TOD*PI*XT)
      SSC3=SL3/(((B+2.*TA)**2-B**2)*PI/4.)
      RTS3=RL3/(RTA(T)*BN)
      SFB3=4.*RL3/(PI*(A**2-RID**2))
      STR3=(MR3*YR)/(RT**2*RID)
      RSS3=RL3/(A*PI*RT)
      IF(SFB3-FCY/2.)2314,2314,124
  124 IF(.001-AI)2314,2314,120
 2314 IF(RTS3-RY/FS2)2344,2344,923
  923 IF(0-II) 2344,313,313
 2344 IF(SR3-FY/FS1)2315,2315,302
 2315 IF(ST3-FY/FS1)2316,2316,302
 2316 IF(FSS3-FSU/FS1)2317,2317,302
 2317 IF(SSC3-SCY/FS1)2330,2330,623
  623 PRINT 624
  624 FORMAT(3X,19H SSC3 EXCEEDS LIMIT)
 2330 IF(STR3-RY/FS1)2331,2331,303
 2331 IF(RSS3-RSU/FS1)2332,2332,303
 2332 XA1=-SH3+SH3+SPR3+SPA3+SRS3
```

```
      XA2=-SCEA3*SR3
      XA3=ST3
      NA1=-SH3-SR3+SPR3+SPA3+SRS3
      NA2=-SCEA3*SR3
      NA3=ST3
      FXA3=.7071*((XA1-XA2)**2+(XA2-XA3)**2+(XA3-XA1)**2)**.5
      ENA3=.7071*((NA1-NA2)**2+(NA2-NA3)**2+(NA3-NA1)**2)**.5
      FA=AMAX1(ABS(FXA3),ABS(ENA3))
      IF(FA-FY/FS1)2363,302,302
 2363 XB1=SH3+SR3-SPR3+SPA3-SRS3
      XB2=-SCEB3*SR3
      XB3=ST3
      NB1=SH3-SR3-SPR3+SPA3-SRS3
      NB2=-SCEB3*SR3
      NB3=ST3
      FXB3=.7071*((XB1-XB2)**2+(XB2-XB3)**2+(XB3-XB1)**2)**.5
      ENB3=.7071*((NB1-NB2)**2+(NB2-NB3)**2+(NB3-NB1)**2)**.5
      FB=AMAX1(ABS(FXB3),ABS(ENB3))
      IF(FB-FY/FS1)2373,302,302
C     LOAD CALCULATIONS CONDITION 4
 2373 P4=PH
      FA4=P4*(PI/4.)*(B**2)
      FPL4=P4*(PI/4.)*(SOD**2-B**2)
      TL4=FA4
      RL4=FPL4+FA4
C     STRESS CALCULATION FOR CONDITION 4
      BTS4=RL4/(BTA(I)*BN)
      IF(BTS4-BU/FS2)4344,4344,933
  933 IF(D-II)4344,313,313
C     LOAD CALCULATION CONDITION 5
 4344 P5=PIM
      FA5=P5*(PI/4.)*(B**2)
      FPL5=P5*(PI/4.)*(SOD**2-B**2)
      TL5=FA5
      MP5=((L*H0*G0**2*FE)/(.91*V))*(C1*B**2*GAMMA*P5/(XT*(XT**2+C2*GE*G
     1AMMA)))
      R51=-FPL5-TL5
      R52=-FPL5*H4+(P5*PI*B*SX)*(XT/2.)-MP5-TL5*H6
      R53=-(P5*B*((A+B)/2.))/(4.*((A-B)/2.)*FE)+(P5*B*SMD)/(4.*TA*SEE)
      R54=0.
      R55=DFA/((H2+H3)*(DBA-DRA-DSA))
      R56=(DBA-DRA)*(R54-R51)/(DBA-DRA-DSA)
      R57=R56*(H2+H3)+R51*H2-(R53*XT)/(DSP*2.)+R52
      R58=(1.-(R55*(H2+H3))-(DFR*XT**2)/(DSR*4.))
      MO5=MO1-R57/R58
      SL5=SL1-R57*R55/R58-R56
      RSL5=RSL1+(R57*DFR*XT)/(R58*4.*DSR)-R53/DSR
      RL5=RL1-R51-R56-R57*R55/R58
      MR5=RL5*H5
      IF(SL5-MSL)331,5390,5390
 5390 SH5=(RL5*H2+SL5*H3+FPL5*H4+TL5*H6)/(L*G1**2*(B+G0))
      SRS5=(RSL5*XT/2.)/(L*G1**2*(B+G0))
      SPR5=MP5/(L*G1**2*(B+G0))
      SR5=0.
      SPA5=FA5/AH
      SCER5=0.
```

```
      SCEA5=P5
      SR5=M05*(1.333*XT*LCF+1.)/(1.*XT**2*(B+GA))
      ST5=M05*(Y/(XT**2*B))-Z*SR5
      FSS5=ML5/(TOD*PI*XT)
      SSC5=SL5/(((B+2.*TA)**2-B**2)*PI/4.)
      RTS5=ML5/(GTA(T)*BN)
      SFB5=4.*ML5/(PI*(A**2-RID**2))
      STR5=(MR5*YR)/(RT**2*RID)
      RSS5=ML5/(PI*A*RT)
      IF(SFB5-FCYR/2.)5314,5314,125
  125 IF(.001-AT)5314,5314,120
 5314 IF(RTS5-RYR/FS2)5344,5344,943
  943 IF(0-II)5344,313,313
 5344 IF(SR5-FYR/FS1)5315,5315,302
 5315 IF(ST5-FYR/FS1)5316,5316,302
 5316 IF(FSS5-FSU/FS1)5317,5317,302
 5317 IF(SSC5-SCYR/FS1)5330,5330,625
  625 PRINT 626
  626 FORMAT (3X,19H SSC5 EXCEEDS LIMIT)
 5330 IF(STR5-RYR/FS1)5331,5331,303
 5331 IF(RSS5-RSU/FS1)5332,5332,303
 5332 SH1=SH
      SRS1=SRS
      SPR1=0.
      SH1=0.
      SPA1=0.
      SCEH1=0.
      SR1=SR
      ST1=ST
      SCEA1=0.
      XA1=-SH5+SB5+SPR5+SPA5+SRS5
      XA2=-SCEA5+SR5
      XA3=ST5
      NA1=-SH1-SH1+SPR1+SPA1+SRS1
      NA2=-SCEA1+SR1
      NA3=ST1
      EXA5=.70711*((XA1-XA2)**2+(XA2-XA3)**2+(XA3-XA1)**2)**.5
      ENA5=.70711*((NA1-NA2)**2+(NA2-NA3)**2+(NA3-NA1)**2)**.5
      IF(ABS(XA1)-ABS(NA1))5602,5602,5601
 5602 CMAX5A=NA1
      CMIN5A=XA1
      GO TO 5603
 5601 CMAX5A=XA1
      CMIN5A=NA1
 5603 EA=AMAX1(ABS(EXA5),ABS(ENA5))
      IF(EA-FYR/FS1)5352,5352,302
 5352 CALT5A=(CMAX5A-CMIN5A)/2.
      CMN5A=(CMAX5A+CMIN5A)/2.
      EALT5A=CALT5A
      SALT5A=EALT5A
      SMN5A=CMN5A
      SCHK5A=ABS(SMN5A+SALT5A)
      IF(SCHK5A .GT. FUR)850,815
  815 IF(SCHK5A-FYR)816,816,817
  817 IF(ABS(SALT5A)-FY)818,818,819
  818 SMN5A=FYR-SALT5A
```

```
      GO TO 816
  819 SMNSA=0.
  816 SMAXSA=SMNSA+SALTSA
      SMINSA=SMNSA-SALTSA
      RC1=SMINSA/SMAXSA
      M=0
 5350 M=M+1
      IF(RC1-R(M))5351,7004,5350
 5351 FFCSA=((R(M)-RC1)/(R(M)-R(M-1)))*(FF(M)-FF(M-1))+FF(M-1)
      GO TO 7005
 7004 FFCSA=FF(M)
 7005 CONTINUE
      IF(ABS(SMAXSA)-FFCSA)5363,5363,850
 5363 XB1=+SH5+SR5-SPR5+SPA5-SRS5
      XB2=-SCFR5+SR5
      XB3=ST5
      NB1=+SH1-SR1-SPR1+SPA1-SRS1
      NB2=-SCFR1+SR1
      NB3=ST1
      EXB5=.7071*((XB1-XB2)**2+(XB2-XB3)**2+(XB3-XB1)**2)**.5
      ENB5=.7071*((NB1-NB2)**2+(NB2-NB3)**2+(NB3-NB1)**2)**.5
      ER=AMAX1(ABS(EXB5),ABS(ENB5))
      IF(ER-FYR/FS1)721,721,302
  721 IF(ABS(XB1)-ABS(NB1))5605,5605,5604
 5605 CMAXSR=NB1
      CMINSR=XB1
      GO TO 5362
 5604 CMAXSR=XB1
      CMINSR=NB1
 5362 CALTSR=(CMAXSR-CMINSR)/2.
      CMNSR=(CMAXSR+CMINSR)/2.
      FALTSR=CALTSR
      SALTSR=FALTSR*KTF
      SMNSR=CMNSR*KTF
      SCHKSR=ABS(SMNSR+SALTSR)
      IF(SCHKSR .GT. FUR)850,820
  820 IF(SCHKSR-FYR)821,821,822
  822 IF(ABS(SALTSR)-FYR)823,823,824
  823 SMNSR=FYR-SALTSR
      GO TO 821
  824 SMNSR=0.
  821 SMAXSR=SMNSR+SALTSR
      SMINSR=SMNSR-SALTSR
      RC2=SMINSR/SMAXSR
      M=0
 5360 M=M+1
      IF(RC2-R(M))5361,7006,5360
 5361 FFCSR=((R(M)-RC2)/(R(M)-R(M-1)))*(FF(M)-FF(M-1))+FF(M-1)
      GO TO 7007
 7006 FFCSR=FF(M)
 7007 CONTINUE
      IF(ABS(SMAXSR)-FFCSR)5403,5403,850
C     LOAD CALCULATIONS CONDITION 6 COLD.
 5403 P6=P
      FA6=P6*(PI/4.)*(R**2)
      FPL6=P6*(PI/4.)*(SOD**2-R**2)
```

```
      TL6=FA6+.5*THS*AT
      MP6=((L*H0*G0**2*FE)/(.91*V))*(C1*B**2*GAMMA*P6/(XT*(XT**2+C2*GE*G
     1AMMA)))
      MC6=MC2
      DTC1=DT1C
      DTC2=DT2C
      DTC3=DT3C
      DTH1=DT1H
      DTH2=DT2H
      DTH3=DT3H
      TMIN1=TMIN
      TMIN2=TMIN+DTC1
      TMIN3=TMIN+DTC2+DTC1
      TMIN4=TMIN+DTC3+DTC2+DTC1
      TMAX1=TMAX
      TMAX2=TMAX+DTH1
      TMAX3=TMAX+DTH2+DTH1
      TMAX4=TMAX+DTH3+DTH2+DTH1
      MCTG6=(PI/3.)*(B**2)*(BETA**2)*((FE*TW**3)/(12.*(1.-EMU**2)))*FTE*
     1(DTC1)*(1.+BETA*XT)
      IF(DTC1 .EQ. 0.0)7008,7009
 7009 MHTG6=MCTG6*DTH1/DTC1
      GO TO 7010
 7008 MHTG6=MCTG6
 7010 CONTINUE
      R61C=-FPL6-TL6
      R62C=-FPL6*H4+(P6*PI*B*SX)*(XT/2.)-MP6-MC6+MCTG6-TL6*H6
      R63C=(P6*B*SMD)/(4.*TA*SEE)-(P6*B*((A+B)/2.))/(4.*((A-B)/2.)*FE)
     1-FTE*(TMIN2-70.0)*SMD/2.+STE*(TMIN1-70.0)*SMD/2.
      R64C=(HCR*(SX+XT+RT)+RTE*(TMIN4-70.0)*(SX+XT+RT)-STE*(TMIN1-70.0)*
     1SX-FTE*XT*(TMIN2-70.0)-RTE*RT*(TMIN3-70.0))/(DBA-DRA)
      R65C=DFA/((H2+H3)*(DBA-DRA-DSA))
      R66C=(DBA-DRA)*(R64C-R61C)/(DBA-DRA-DSA)
      R67C=R66C*(H2+H3)+R61C*H2-(R63C*XT)/(DSR*2.)+R62C
      R68C=(1.-(R65C*(H2+H3))-(DFR*XT**2)/(DSR*4.))
      M06C=M01-R67C/R68C
      SL6C=SL1-R67C*R65C/R68C-R66C
      RSL6C=RSL1+(R67C*DFR*XT)/(R68C*2.*DSR)-R63C/DSR
      RL6C=RL1-R61C-R66C-R67C*R65C/R68C
      MR6C=RL6C*H5
      IF(SL6C-MSL)331,6390,6390
 6390 R61CN=-FPL6-TL6
      R62CN=-FPL6*H4+(P6*PI*B*SX)*(XT/2.)-MP6+MCTG6-TL6*H6
      R63CN=(P6*B*SMD)/(4.*TA*SEE)-(P6*B*((A+B)/2.))/(4.*((A-B)/2.)*FE)
     1-FTE*(TMIN2-70.0)*SMD/2.+STE*(TMIN1-70.0)*SMD/2.
      R64CN=(RTE*(TMIN4-70.0)*(SX+XT+RT)-STE*(TMIN1-70.0)*
     1SX-FTE*XT*(TMIN2-70.0)-RTE*RT*(TMIN3-70.0))/(DBA-DRA)
      R65CN=DFA/((H2+H3)*(DBA-DRA-DSA))
      R66CN=(DBA-DRA)*(R64CN-R61CN)/(DBA-DRA-DSA)
      R67CN=R66CN*(H2+H3)+R61CN*H2-(R63CN*XT)/(DSR*2.)+R62CN
      R68CN=(1.-(R65CN*(H2+H3))-(DFR*XT**2)/(DSR*4.))
      M06CN=M01-R67CN/R68CN
      SL6CN=SL1-R67CN*R65CN/R68CN-R66CN
      RSL6CN=RSL1+(R67CN*DFR*XT)/(R68CN*2.*DSR)-R63CN/DSR
      RL6CN=RL1-R61CN-R66CN-R67CN*R65CN/R68CN
      MR6CN=RL6C*H5
```

```
C STRESS CALCULATION CONDITION 6 COLD
      SH6CN=(BL6CN*H2+SL6CN*H3+FPL6*H4+TL6*H6)/(L*G1**2*(B+G0))
      SRS6CN=(RSL6CN*XT/2.)/(L*G1**2*(B+G0))
      SPR6CN=MP6/(L*G1**2*(B+G0))
      SCG6CN=MCTG6/(L*G1**2*(B+G0))
      SH6CN=.5*THM/H
      SPA6CN=FA6/AP
      SCEB6C=0.
      SCEA6C=P6
      SR6CN=M06CN*(1.333*XT*LCE+1.)/(L*XT*2.*(B+G0))
      ST6CN=M06CN*(Y/(XT**2*B))-Z*SR6CN
      FSS6CN=BL6CN/(T00*PI*XT)
      SSC6CN=SL6CN/(((B+2.*TA)**2-B**2)*PI/4.)
      RTS6CN=BL6CN/(RTA(I)*BN)
      STR6CN=(MR6CN*YR)/(RT**2*RID)
      RSS6CN=BL6CN/(A*PI*RT)
      SFB6CN=4.*BL6CN/(PI*(A**2-RID**2))
      IF(SFB6CN-FCYC/2.)6314,6314,126
  126 IF(.001-AI)6314,6314,120
 6314 IF(RTS6CN-RYC/FS3)6344,6344,953
  953 IF(0-II)6344,313,313
 6344 IF(SR6CN-FYC/FS1)6315,6315,302
 6315 IF(ST6CN-FYC/FS1)6316,6316,302
 6316 IF(FSS6CN-FSU/FS1)6317,6317,302
 6317 IF(SSC6CN-SCYC/FS1)6330,6330,627
  627 PRINT 628
  628 FORMAT (3X,21H SSC6CN EXCEEDS LIMIT)
 6330 IF(STR6CN-RYC/FS1)6331,6331,303
 6331 IF(RSS6CN-RSU/FS1)6332,6332,303
 6332 XA1=-SH6CN+SR6CN+SPR6CN+SPA6CN+SRS6CN-SCG6CN
      XA2=-SCEA6C+SR6CN
      XA3=ST6CN
      EXA6CN=.70711*((XA1-XA2)**2+(XA2-XA3)**2+(XA3-XA1)**2)**.5
      EA=EXA6CN
      IF(EA-FYC/FS1)6363,6363,302
 6363 XB1=+SH6CN+SR6CN-SPR6CN+SPA6CN-SRS6CN+SCG6CN
      XB2=-SCEB6C+SR6CN
      XB3=ST6CN
      EXB6CN=.70711*((XB1-XB2)**2+(XB2-XB3)**2+(XB3-XB1)**2)**.5
      EB=EXB6CN
      IF(EB-FYC/FS1)6371,6371,302
C     LOAD CALCULATIONS CONDITION 6 HOT
 6371 R61H=-FPL6-TL6
      R62H=-FPL6*H4+(P6*PI*H*SX)*(XT/2.)-MP6-MC6+MHTG6-TL6*H6
      R63H=(P6*B*SMD)/(4.*TA*SEE)-(P6*B*((A+B)/2.))/(4.*((A-B)/2.)*FE)
     1-FTE*(TMAX2-70.0)*SMD/2.+STE*(TMAX1-70.0)*SMD/2.
      R64H=(HCR*(SX+XT+RT)+RTE*(TMAX4-70.0)*(SX+XT+RT)-STE*(TMAX1-70.0)*
     1SX-FTE*XT*(TMAX2-70.0)-RTF*RT*(TMAX3-70.0))/(DBA-DRA)
      R65H=DFA/((H2+H3)*(DBA-DRA-DSA))
      R66H=(DBA-DRA)*(R64H-R61H)/(DBA-DRA-DSA)
      R67H=R66H*(H2+H3)+R61H*H2-(R63H*XT)/(DSR*2.)+R62H
      R68H=(1.-(R65H*(H2+H3))-(DFR*XT**2)/(DSR*4.))
      M06H=M01-R67H/R68H
      SL6H=SL1-R67H*R65H/R68H-R66H
      RSL6H=RSL1+(R67H*DFR*XT)/(R68H*2.*DSR)-R63H/DSR
      BL6H=BL1-R61H-R66H-R67H*R65H/R68H
```

```
      MR6H=BL6H*H5
      IF(SL6H-MSL)331,8390,8390
 8390 R61HN=-FPL6-TL6
      R62HN=-FPL6*H4+(P6*PI*B*SX)*(XT/2.)-MP6+MHTG6-TL6*H6
      R63HN=(P6*B*SMD)/(4.*TA*SEE)-(P6*B*((A+B)/2.))/(4.*((A-B)/2.)*FE)
     1-FTE*(TMAX2-70.0)*SMD/2.+STF*(TMAX1-70.0)*SMD/2.
      R64HN=(BTE*(TMAX4-70.0)*(SX+XT+RT1-STE*(TMAX1-70.0)*
     1SX-FTE*XT*(TMAX2-70.0)-RTE*RT*(TMAX3-70.0))/(DBA-DRA)
      R65HN=DFA/((H2+H3)*(DBA-DRA-DSA))
      R66HN=(DBA-DRA)*(R64HN-R61HN)/(DBA-DRA-DSA)
      R67HN=R66HN*(H2+H3)+R61HN*H2-(R63HN*XT)/(DSR*2.)+R62HN
      R68HN=(1.-(R65HN*(H2+H3))-(DFR*XT**2)/(DSR*4.))
      MO6HN=MO1-R67HN/R68HN
      SL6HN=SL1-R67HN*R65HN/R68HN-R66HN
      RSL6HN=RSL1+(R67HN*DFR*XT)/(R68HN*2.*DSR)-R63HN/DSR
      BL6HN=BL1-R61HN-R65HN-R67HN*R65HN/R68HN
      MR6HN=BL6HN*H5
C STRESS CALULATION CONDITION 6 HOT
      SH6HN=(BL6HN*H2+SL6HN*H3+FPL6*H6+TL6*H6)/(L*G1**2*(B+G0))
      SRS6HN=(RSL6HN*XT/2.)/(L*G1**2*(B+G0))
      SHG6CN=MHTG6/(L*G1**2*(B+G0))
      SPR6HN=MP6/(L*G1**2*(B+G0))
      SH6HN=.5*TRM/ZH
      SPA6HN=FA6/AH
      SCEH6H=0.
      SCEA6H=P6
      SR6HN=MO6HN*(1.333*XT*LCE+1.)/(L*XT*2.*(B+G0))
      ST6HN=MO6HN*(Y/(XT**2*B))-Z*SR6HN
      FSS6HN=BL6HN/(TOD*PI*XT)
      SSC6HN=SL6HN/(((B+2.*TA)**2-B**2)*PI/4.)
      RTS6HN=BL6HN/(BTA(I)*HN)
      STR6HN=(MR6HN*YR)/(RT**2*RID)
      RSS6HN=BL6HN/(A*PI*RT)
      SFB6HN=4.*BL6HN/(PI*(A**2-RID**2))
      IF(SFB6HN-FCY/2.)8314,8314,127
  127 IF(.001-AT)8314,8314,120
 8314 IF(RTS6HN-RY/FS3)8344,8344,963
  963 IF(0-II)8344,313,313
 8344 IF(SR6HN-FY/FS1)8315,8315,302
 8315 IF(ST6HN-FY/FS1)8316,8316,302
 8316 IF(FSS6HN-FSU/FS1)8317,8317,302
 8317 IF(SSC6HN-SCY/FS1)8330,8330,629
  629 PRINT 630
  630 FORMAT (3X,21H SSC6HN EXCEEDS LIMIT)
 8330 IF(STR6HN-RY/FS1)8331,8331,303
 8331 IF(RSS6HN-RSU/FS1)8332,8332,303
 8332 XA1=-SH6HN+SR6HN+SPR6HN+SPA6HN+SRS6HN-SHG6CN
      XA2=-SCEA6H+SR6HN
      XA3=ST6HN
      EXA6HN=.70711*((XA1-XA2)**2+(XA2-XA3)**2+(XA3-XA1)**2)**.5
      EA=EXA6HN
      IF(EA-FY/FS1)8363,302,302
 8363 XB1=+SH6HN+SR6HN-SPR6HN+SPA6HN-SRS6HN+SHG6CN
      XB2=-SCEB6H+SR6HN
      XB3=ST6HN
      EXB6HN=.70711*((XB1-XB2)**2+(XB2-XB3)**2+(XB3-XB1)**2)**.5
```

```
      FH=EXH6HN
      IF(ER-FY/FS1)8371,302,302
C     LOAD CALCULATION CONDITION 7
 8371 R7=0.
      FA7=0.
      FPL7=0
      TL7=.5*THS*AT
      R71=-TL7
      R72=-TL7*H6
      R73=0.
      R74=0.
      R75=DFA/((H2+H3)*(DBA-DRA-DSA))
      R76=(DBA-DRA)*(R74-R71)/(DBA-DRA-DSA)
      R77=R76*(H2+H3)+R71*H2-(R73*XT)/(DSR*2.)+R72
      R78=(1.-(R75*(H2+H3))-(DFR*XT**2)/(DSR*4.))
      M07=M01-R77/R78
      SL7=SL1-R77*R75/R78
      RSL7=RSL1+(R77*DFR*XT)/(R78*2.*DSR)-R73/DSR
      RL7=RL1-R71-R76-R77*R75/R78
      MR7=RL7*H5
      IF(0.001-HNT)8371,8370,870
 8370 BTSCHK=MAXIF(BTS2P,BTS3,BTS6HN)
      IF(BTSCHK .LT. 0.83*BY/FS2)8373,8371
 8373 IF(BTS4 .LT. 0.83*BU/FS2)8372,8371
 8372 BN1=(BN*BTSCHK*FS2)/(0.83*BY)
      BN2=(PI*BCD)/(2.*(BS(I)+XT))+2.
      BN=MAXIF(BN1,BN2)
      NB=BN/2.
      N=2*NB
      BN=N
      BNI=BN
      II=I
      BCDI=BCD
      GO TO 117
  971 CONTINUE
      T1=PI/4.*TOD**2
      R1=PI/4.*(TOD+2.*HUBI)**2
      WGT=2.*PI/4.*((A**2-TOD**2)*XT*FRHO+(ROD**2-RID**2-BN*BH(I)**2)*RT
     1*RRHO+BN*BS(I)**2*(SX+XT+RT+2.*BS(I))*BRHO)+2.*BN*NWT(I)+2.*H*FRHO
     1*(1./3.*(R1+T1+(R1*T1)**.5)-T1)-2.*PI/4.*(SOD**2-TOD**2)*.025*FRHO
     1-PI/4.*(SOD**2-(R+2.*TA)**2)*SLEG*TAN(PT/9.)*FRHO
      TRQ=(RL1*BS(I))/(BN*5.)
      IF(PI*BCD/BN-2.*(BS(I)+XT))333,333,1000
 1000 PRINT 1001
 1001 FORMAT (30H MAXIMUM SPACING NOT SATISFIED)
  333 CONTINUE
      IF((BCD-RID)/2.-BH(I))118,119,119
  118 PRINT 35
   35 FORMAT (3X,41HDIFFERENCE IN BCD AND RID LESS THEN BH(I))
  119 CONTINUE
      PRINT 727
  727 FORMAT(1H )
      PRINT 728
  728 FORMAT(25X,14H DESIGN OUTPUT///)
      PRINT 2800
 2800 FORMAT(1X,25HBENDING MOMENT AND STRESS)
```

```
      PRINT 2801
 2801 FORMAT(6X,3HTRM,7X,3HTRS)
      PRINT 9020,TRM,TRS
      PRINT 2803
 2803 FORMAT (7X,3HTRO)
      PRINT 9020,TRO
      PRINT 3001
 3001 FORMAT (25H LOADS FOR ALL CONDITIONS)
      PRINT 3002
 3002 FORMAT (6X,3HM01,7X,3HBL1,7X,3HSL1,6X,4HRSL1)
      PRINT 9020,M01,BL1,SL1,RSL1
      PRINT 3003
 3003 FORMAT (6X,3HM02,7X,3HBL2,7X,3HSL2,6X,4HRSL2,7X,3HMC2,7X,3HMP2)
      PRINT 9020,M02,BL2,SL2,RSL2,MC2,MP2
      PRINT 3004
 3004 FORMAT (5X,4HM02P,6X,4HBL2P,6X,4HSL2P,5X,5HRSL2P)
      PRINT 9020,M02P,BL2P,SL2P,RSL2P
      PRINT 3005
 3005 FORMAT (5X,4HM02M,6X,4HBL2M,6X,4HSL2M,6X,5HRSL2M)
      PRINT 9020,M02M,BL2M,SL2M,RSL2M
      PRINT 3006
 3006 FORMAT (6X,3HM03,7X,3HBL3,7X,3HSL3,6X,4HRSL3,7X,3HMP3)
      PRINT 9020,M03,BL3,SL3,RSL3,MP3
      PRINT 3007
 3007 FORMAT (6X,3HBL4)
      PRINT 9020,BL4
      PRINT 3008
 3008 FORMAT (6X,3HM05,7X,3HBL5,7X,3HSL5,6X,4HRSL5,7X,3HMP5)
      PRINT 9020,M05,BL5,SL5,RSL5,MP5
      PRINT 3009
 3009 FORMAT (5X,4HM06C,6X,4HBL6C,6X,4HSL6C,5X,5HRSL6C,6X,3HMC6,7X,3HMP6
     1)
      PRINT 9020,M06C,BL6C,SL6C,RSL6C,MC6,MP6
      PRINT 3010
 3010 FORMAT (5X,5HMCTG6,5X,5HMHTG6)
      PRINT 9020,MCTG6,MHTG6
      PRINT 3011
 3011 FORMAT (5X,5HM06CN,5X,5HBL6CN,5X,5HSL6CN,4X,6HRSL6CN)
      PRINT 9020,M06CN,BL6CN,SL6CN,RSL6CN
      PRINT 3012
 3012 FORMAT (5X,4HM06H,6X,4HBL6H,6X,4HSL6H,5X,5HRSL6H)
      PRINT 9020,M06H,BL6H,SL6H,RSL6H
      PRINT 3013
 3013 FORMAT (5X,5HM06HN,5X,5HBL6HN,5X,5HSL6HN,4X,6HRSL6HN)
      PRINT 9020,M06HN,BL6HN,SL6HN,RSL6HN
      PRINT 3014
 3014 FORMAT (6X,3HM07,7X,3HBL7,7X,3HSL7,6X,4HRSL7)
      PRINT 9020,M07,BL7,SL7,RSL7
      PRINT 9104
 9104 FORMAT(1X,27HSTRESS CONCENTRATION FACTOR)
      PRINT 9105
 9105 FORMAT(6X,3HKTF)
      PRINT 9021,KTF
      PRINT 3015
 3015 FORMAT (28H STRESSES FOR ALL CONDITIONS)
      PRINT 3016
```

```
3016 FORMAT (6X,3HEXA,7X,3HENA,7X,3HEXB,7X,3HENB)
     PRINT 9020,EXA,ENA,EXB,ENB
     PRINT 3017
3017 FORMAT (5X,4HEXA2,6X,4HENA2,6X,4HEXB2,6X,4HENB2)
     PRINT 9020,EXA2,ENA2,EXB2,ENB2
     PRINT 3018
3018 FORMAT(4X,6HSMAX2A,4X,6HSMIN2A,5X,5HFFC2A,4X,6HSMAX2B,4X,6HSMIN2B,
    15X,5HFFC2B)
     PRINT 9020,SMAX2A,SMIN2A,FFC2A,SMAX2B,SMIN2B,FFC2B
     PRINT 722
 722 FORMAT(5X,4HSH2P,5X,5HSRS2P,6X,4HSH2M,5X,5HSRS2M,6X,4HSPR2,7X,3HSB
    12,6X,4HSPA2)
     PRINT 9020,SH2P,SRS2P,SH2M,SRS2M,SPR2,SB2,SPA2
     PRINT 723
 723 FORMAT(5X,4HSR2P,6X,4HSR2M,6X,4HST2P,6X,4HST2M)
     PRINT 9020,SR2P,SR2M,ST2P,ST2M
     PRINT 3019
3019 FORMAT (5X,4HEXA3,6X,4HENA3,6X,4HEXB3,6X,4HENB3)
     PRINT 9020,EXA3,ENA3,EXB3,ENB3
     PRINT 3020
3020 FORMAT (5X,4HEXA5,6X,4HENA5,6X,4HEXB5,6X,4HENB5)
     PRINT 9020,EXA5,ENA5,EXB5,ENB5
     PRINT 3021
3021 FORMAT(4X,6HSMAX5A,4X,6HSMIN5A,5X,5HFFC5A,4X,6HSMAX5B,4X,6HSMIN5B,
    15X,5HFFC5B)
     PRINT 9020,SMAX5A,SMIN5A,FFC5A,SMAX5B,SMIN5B,FFC5B
     PRINT 724
 724 FORMAT(5X,3HSH5,6X,4HSRS5,7X,3HSB5,6X,4HSPA5,7X,3HSR5,7X,3HST5,
    16X,4HSPR5)
     PRINT 9020,SH5,SRS5,SB5,SPA5,SR5,ST5,SPR5
     PRINT 725
 725 FORMAT(6X,3HSH1,6X,4HSRS1,7X,3HSB1,6X,4HSPA1,7X,3HSR1,7X,3HST1,
    16X,4HSPR1)
     PRINT 9020,SH1,SRS1,SB1,SPA1,SR1,ST1,SPR1
     PRINT 3022
3022 FORMAT (5X,6HEXA6CN,5X,6HEXB6CN,5X,6HEXA6HN,5X,6HEXB6HN)
     PRINT 9020,EXA6CN,EXB6CN,EXA6HN,EXB6HN
     PRINT 3029
3029 FORMAT (6X,3HBTS,5X,5HBTS2P,6X,4HBTS3,6X,4HBTS4,5X,4HBTS5,4X,
    16HBTS6CN,4X,6HBTS6HN)
     PRINT 9020,BTS,BTS2P,BTS3,BTS4,BTS5,BTS6CN,BTS6HN
     PRINT 3031
3031 FORMAT (7X,3HSFB,5X,5HSFB2P,5X,5HSFB2M,6X,4HSFB3,6X,4HSFB5,4X,6HSF
    1B6CN,4X,6HSFB6HN)
     PRINT 9020,SFB,SFB2P,SFB2M,SFB3,SFB5,SFB6CN,SFB6HN
     PRINT 3023
3023 FORMAT (1)H DIMENSIONS)
     PRINT 2802
2802 FORMAT(9X,1HH,6X,4HHUB1,8X,2HG1,8X,2HFR)
     PRINT 9021,H,HUB1,G1,FR
     PRINT 3024
3024 FORMAT (6X,2HTW,7X,3HTOD)
     PRINT 9021,TW,TOD
     PRINT 3025
3025 FORMAT (6X,1HA,9X,1HB,8X,2HXT,7X,3HBCD)
     PRINT 9021,A,B,XT,BCD
```

```
      PRINT 3030
3030  FORMAT (6X,3HROD,7X,3HRID,7X,2HRT)
      PRINT 9021,ROD,RID,RT
      PRINT 3026
3026  FORMAT(6X,3HSOD,7X,3HSID,7X,3HSEL,8X,2HTA,5X,5HSLEGT)
      PRINT 9021,SOD,SID,SFL,TA,SLEGT
      PRINT 3027
3027  FORMAT (6X,5HBS(I),5X,5HBH(I),4X,6HBTA(I),4X,6HBWC(I),6X,2HBN)
      PRINT 9021,BS(I),BH(I),BTA(I),BWC(I),BN
      PRINT 3028
3028  FORMAT (6X,3HWGT)
      PRINT 9021,WGT
      PRINT 9103
9103  FORMAT(1H1)
      GO TO 999
 998  CALL EXIT
      END
```

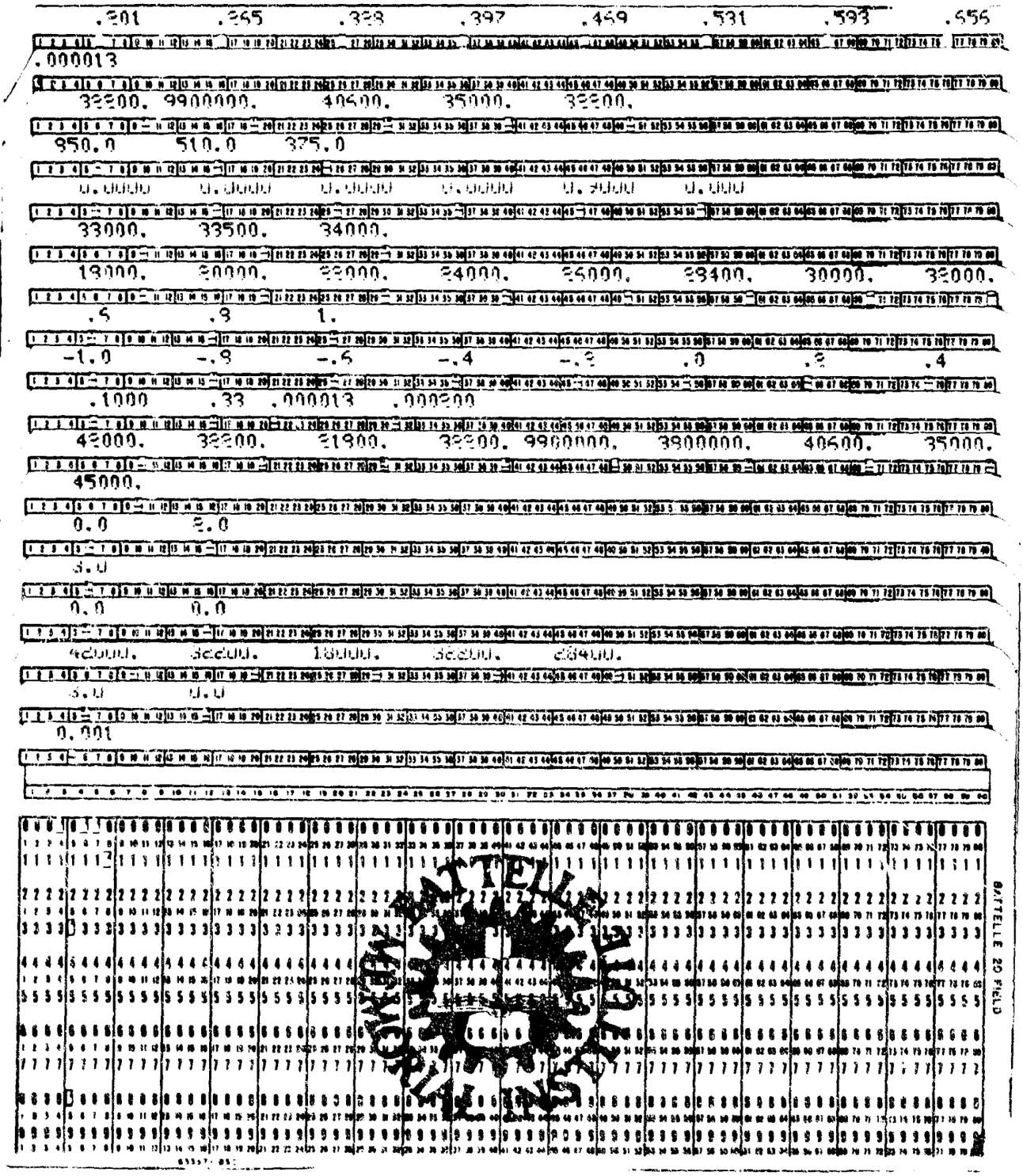

FIGURE B-1. PUNCHED INPUT CARDS 1 TO 18 FOR 3-INCH 1500-PSI ALUMINUM INTEGRAL, INTEGRAL CONNECTOR

(Read from Bottom of Page to Top)

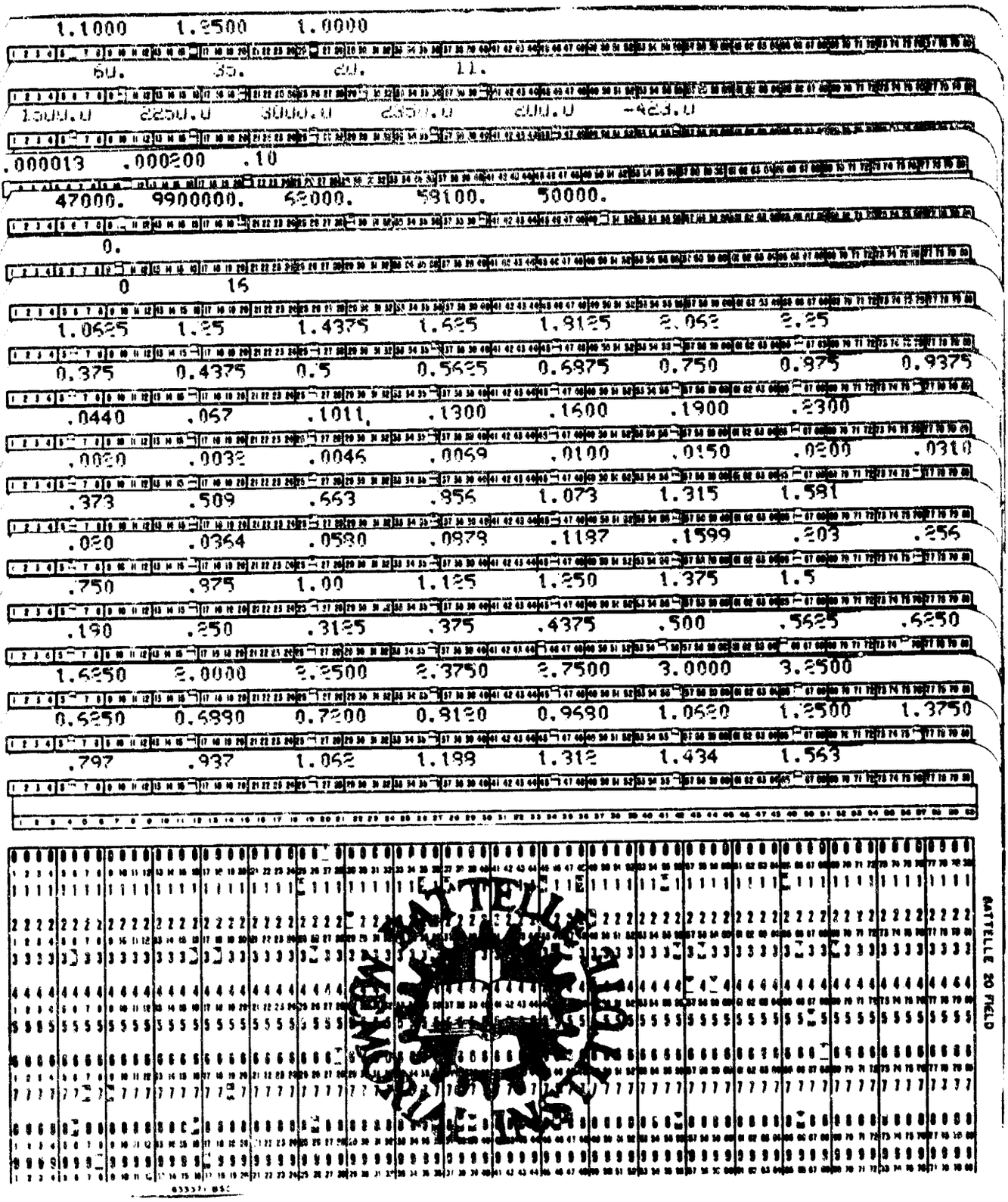

FIGURE B-2. PUNCHED INPUT CARDS 19 TO 36 FOR 3-INCH 1500-PSI ALUMINUM INTEGRAL-INTEGRAL CONNECTOR

(Read from Bottom of Page to Top)

INPUT TO THE DESIGN

TUBE LOAD-INPUT

TBMI
.0010

TUBE GEOMETRY

TCO	TWI
3.0000	0.0000

TUBE MATERIAL PROPERTIES

TU	TY	TF	TM	TFRO
42000	32200	18000	32200	28400

FLANGE GEOMETRY

RCOI	HUBII
0.0000	0.0000

GIOTWI
3.0000

FRI	FSFI
0.0000	2.0000

FLANGE MATERIAL PROPERTIES

FUR
45000

FU	FY	FSU	FCY	FE	FG	FYC	FYR
42000	32200	21800	32200	9900000	3800000	40600	35000

FRMO	FMU	FTE	FCR
.10000000	.33000000	.00001300	.00020000

R(1)	R(2)	R(3)	R(4)	R(5)	R(6)	R(7)	R(8)
-1.0000	-.8000	-.6000	-.4000	-.2000	0.0000	.2000	.4000

R(9)	R(10)	R(11)
.6000	.8000	1.0000

FF(1)	FF(2)	FF(3)	FF(4)	FF(5)	FF(6)	FF(7)	FF(8)
18000	20000	22000	24000	26000	28400	30000	32000

FF(9)	FF(10)	FF(11)
33000	33500	34000

SEAL GEOMETRY

SODI	SIDI	SELI	TAI	TAOTW	SLEGTI
0.0000	0.0000	0.0000	0.0000	.9000	0.0000

SEAL LOADS INPUTS

RSLI	SSLI	HSLI
850	510	375

SEAL MATERIAL PROPERTIES

SCY	SEE	SCYC	SCYR	SYR
32200	9900000	40600	35000	32200

STF
.00001300

BOLT GEOMETRY

BH(1)	BH(2)	BH(3)	BH(4)	BH(5)	BH(6)	BH(7)	BH(8)
.2010	.2650	.3280	.3970	.4690	.5310	.5930	.6560

BH(9)	BH(10)	BH(11)	BH(12)	BH(13)	BH(14)	BH(15)
.7970	.9370	1.0620	1.1880	1.3120	1.4340	1.5630

BWC(1)	BWC(2)	BWC(3)	BWC(4)	BWC(5)	BWC(6)	BWC(7)	BWC(8)
.6250	.6880	.7200	.8120	.9680	1.0620	1.2500	1.3750

BWC(9)	BWC(10)	BWC(11)	BWC(12)	BWC(13)	BWC(14)	BWC(15)
1.6250	2.0000	2.2500	2.3750	2.7500	3.0000	3.2500

BS(1)	BS(2)	BS(3)	BS(4)	BS(5)	BS(6)	BS(7)	BS(8)
.1900	.2500	.3125	.3750	.4375	.5000	.5625	.6250
BS(9)	BS(10)	BS(11)	BS(12)	BS(13)	BS(14)	BS(15)	
.7500	.8750	1.0000	1.1250	1.2500	1.3750	1.5000	
BTA(1)	BTA(2)	BTA(3)	BTA(4)	BTA(5)	BTA(6)	BTA(7)	BTA(8)
.0200	.0304	.0580	.0878	.1187	.1599	.2030	.2560
BTA(9)	BTA(10)	BTA(11)	BTA(12)	BTA(13)	BTA(14)	BTA(15)	
.3730	.5090	.6630	.8560	1.0730	1.3150	1.5810	
NWT(1)	NWT(2)	NWT(3)	NWT(4)	NWT(5)	NWT(6)	NWT(7)	NWT(8)
.0020	.0032	.0046	.0069	.0100	.0150	.0200	.0310
NWT(9)	NWT(10)	NWT(11)	NWT(12)	NWT(13)	NWT(14)	NWT(15)	
.0440	.0670	.1011	.1300	.1600	.1900	.2300	
DAF(1)	DAF(2)	DAF(3)	DAF(4)	DAF(5)	DAF(6)	DAF(7)	DAF(8)
.3750	.4375	.5000	.5625	.6875	.7500	.8750	.9375
DAF(9)	DAF(10)	DAF(11)	DAF(12)	DAF(13)	DAF(14)	DAF(15)	
1.0625	1.2500	1.4375	1.6250	1.8125	2.0620	2.2500	

BOLT INPUT

II	IMAX
0	16

BN1
0.0000

BOLT MATERIAL PROPERTIES

BY	BE	BU	BYC	BYR
47000	9900000	62000	58100	50000

BTE	BCR	BRHO
.00001300	.00020000	.10000000

SYSTEM PRESSURE AND TEMPERATURE

P	PP	PB	PIM	TMAX	TMIN
1500	2250	3000	2350	200	-423

DTC1	DTC2	DTH1	DTH2
60	35	20	11

FS1	FS2	FS3
1.1000	1.2500	1.0000

DESIGN OUTPUT

BENDING MOMENT AND STRESS

TBM	TRS
7360	9000

TRQ
102

LOADS FOR ALL CONDITIONS

M01	BL1	SL1	RSL1		
14581	25065	26064	8856		
M02	BL2	SL2	RSL2	MC2	MP2
14619	28119	4446	11709	825	3444
M02P	BL2P	SL2P	RSL2P		
14776	29520	5847	11734		
M02M	BL2M	SL2M	RSL2M		
14990	25814	23573	11767		
M03	BL3	SL3	RSL3	MP3	
15034	28469	9031	13198	5166	

BL4
25914

MO5	BL5	SL5	RSL5	MP5		
15054	28573	8273	13391	5396		
MO6	BL6	SL6	RSL6	MC6	MP6	
13233	24145	5830	9777	825	3444	
MCTG6	MHTG6					
133	-44					
MO6CN	BL6CN	SL6CN	RSL6CN			
13389	25546	7231	9802			
MO6H	BL6H	SL6H	RSL6H			
15129	28172	9857	12360			
MO6HN	BL6HN	SL6HN	RSL6HN			
15286	29573	11258	12385			
MO7	BL7	SL7	RSL7			
14528	26995	21637	8856			

STRESS CONCENTRATION FACTOR

KTF
2.0715

STRESSES FOR ALL CONDITIONS

EXA	ENA	EXB	ENB			
24053	24053	6984	6984			
EXA2	ENA2	EXB2	ENB2			
14100	19420	6657	4334			
SMAX2A	SMIN2A	FFC2A	SMAX2B	SMIN2B	FFC2B	
-15011	-4014	31326	30207	9202	30954	
SH2P	SRS2P	SH2M	SRS2M	SPR2	SB2	SPA2
18017	5157	18246	5172	3454	2642	2236
SR2P	SR2M	ST2P	ST2M			
6711	6808	11643	11811			
EXA3	ENA3	EXB3	ENB3			
13386	13386	4454	4454			
EXA5	ENA5	EXB5	ENB5			
12968	24053	4419	6984			
SMAX5A	SMIN5A	FFC5A	SMAX5B	SMIN5B	FFC5B	
-14625	-3112	31872	30295	20961	33270	
SH5	SRS5	SB5	SPA5	SR5	ST5	SPR5
17913	5886	0	3504	6837	11862	5412
SH1	SRS1	SB1	SPA1	SR1	ST1	SPR1
18517	3893	0	0	6622	11489	0
EXA6CN	EXB6CN	EXA6HN	EXB6HN			
10444	12504	22630	14293			
BTS	BTS2P	BTS3	BTS4	BTS5	BTS6CN	BTS6HN
28091	31810	30675	27925	30790	27529	31868

DIMENSIONS

H	HUBI	G1	FR			
1.2026	.2680	.4002	.1250			
TW	TOD					
.1322	3.0000					
A	B	XT	BCD			
4.9421	2.7357	.8705	4.2861			
SOD	SID	SEL	TA	SLEGT		
3.3164	2.7795	.5273	.1339	.0497		
RS(I)	RM(I)	BTA(I)	BWC(I)	BN		
.3125	.3260	.0580	.7200	16.0000		
WGT						
2.7733						

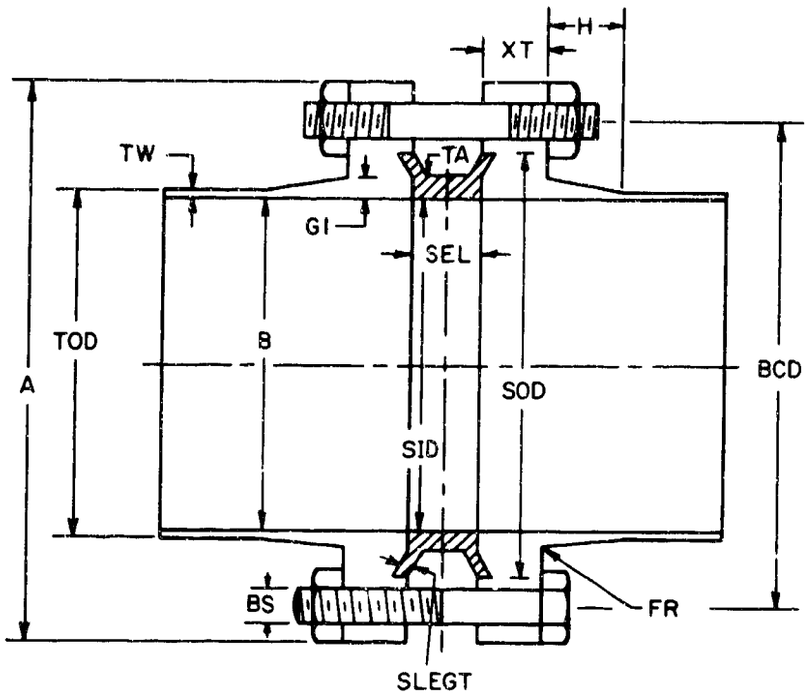

FIGURE B-3. DIMENSIONS FOR CONNECTORS WITH INTEGRAL FLANGES

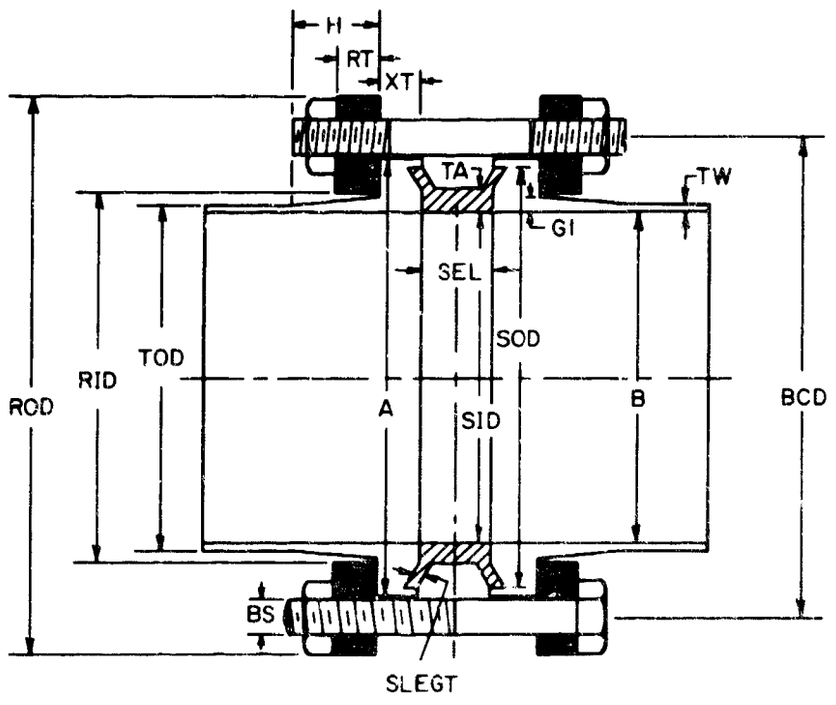

FIGURE B-4. DIMENSIONS FOR CONNECTORS WITH LOOSE-RING FLANGES

APPENDIX C

NOMINAL DIMENSIONS AND ASSEMBLY INSTRUCTIONS FOR AFRPL FLANGED CONNECTORS FOR CRYOGENIC SERVICE

This appendix contains nominal dimensions and assembly instructions for aluminum and stainless steel AFRPL flanged connectors for cryogenic service. The maximum operating pressures are 100, 200, 500, 1000, and 1500 psi. The line sizes include pipe and tubing from 1 inch through 16 inches in diameter. Standard wall thicknesses have been selected for the pipe sizes. The tubing wall thicknesses have been based on stress calculations because of the lack of industry standards. The dimensions are applicable to the assemblies shown in Figure 1: (1) integral/integral flange assembly, (2) loose-ring/loose-ring flange assembly, and (3) integral/loose-ring flange assembly. Stud dimensions are given in addition to bolt dimensions because the stud form facilitates the use of special fastener materials.

As discussed in the report body, it is recommended that military standards be prepared: (1) for all connectors for tubing from 1 inch through 3 inches in diameter, (2) for aluminum connectors for pressures of 100, 200, and 500 psi for tubing through 16 inches in diameter, and (3) for stainless steel connectors for 100 psi for tubing through 8 inches in diameter. While the other connectors are probably satisfactory, further testing is recommended for selected connectors prior to the preparation of military standards. Some of this testing and the preparation of additional connector dimensions will be accomplished as a part of further work under Contract AF 04(611)-11204. A supplementary report will summarize this information.

It was mutually realized that considerable work would be required by the Air Force to complete the preparation of the recommended military standards. However, because of the number of decisions that had to be made by the Air Force concerning the scope and form of the military standards and specifications, it was decided to limit the data presented in this report. General recommendations concerning various aspects of possible standards and specifications are contained in the report body. The nominal dimensions and assembly instructions for cryogenic connectors are contained in Tables C-1 through C-16 of this appendix. Additional information is given below.

Materials

Connectors have been designed for use with aluminum and stainless steel tubing materials. The material for the connector flanges has been made the same as the tubing to minimize welding and corrosion problems. Different materials have been selected for other parts of the connectors to achieve improved performance. The materials for each type of connector are discussed briefly.

Aluminum Connectors

Aluminum alloy AMS 4117 (6061-T6) was selected for the integral flanges and the loose-ring flanges.

Overaged 6061-T6 aluminum was selected for the seal material on the basis of the work described in Technical Documentary Report No. AFRPL-TR-67-191. In an appendix to that report it was recommended that MIL-F-27417 be revised to include the necessary information for aluminum threaded connectors. Thus the military standards for flanged connectors could bear the same material designation, i.e.: aluminum alloy, AMS 4117, overaged per MIL-F-27417, paragraph 3.2.1.1.2.

The material selected for the aluminum bolts and nuts was aluminum alloy AMS 4119 (2024-T351).

Stainless Steel Connectors

Corrosion-resistant steel AMS 5646 was selected for the stainless steel integral flanges and loose-ring flanges.

The material selected for the stainless steel seals was the same as for the threaded connectors, i.e.: corrosion-resistant steel, AMS 5639, AMS 5650, or AMS 5651. The nickel plating required for the stainless steel seals for flanged connectors should be covered by MIL-P-27418.

The material selected for the bolts and nuts was A286. The specification given in MS 27852 for the A286 threaded-connector nuts was AMS 5735. In bolt form this material is cold-worked to a high yield strength and these are the types of bolts that were purchased and used in the test program. It is not known whether a standard specification exists for this condition.

Nut Form

For the test program, self-locking, hexagonal, ring-base, corrosion-resistant-steel A286 nuts were used. They were machined as per MS 21043. The 2024-T351 aluminum nuts were plain hexagonal type and machined as per AN 315-UNF-3B.

It is recommended that Specification AN 315 with UNF-3B threads be used for aluminum 2024-T351 nuts. The corrosion-resistant-steel nuts with UNF-3B threads can be made according to MS 21043. MS 21043 will have to be extended to include larger size nuts. As an alternative, the steel nuts can also be made according to AN 315.

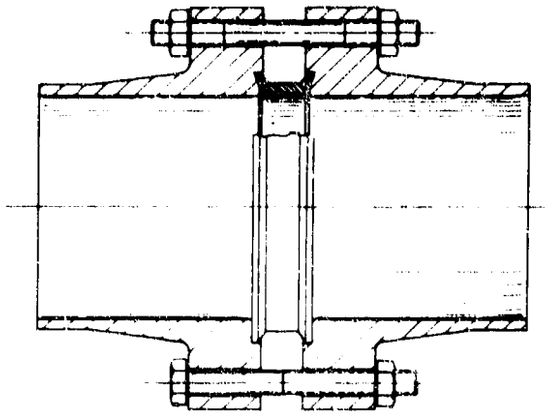

a. Integral / Integral Flange Assembly

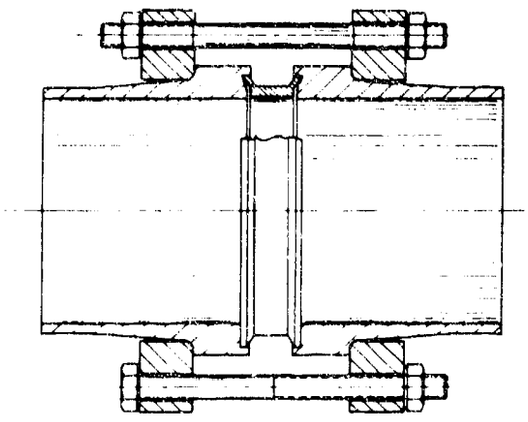

b. Loose-Ring / Loose-Ring Flange Assembly

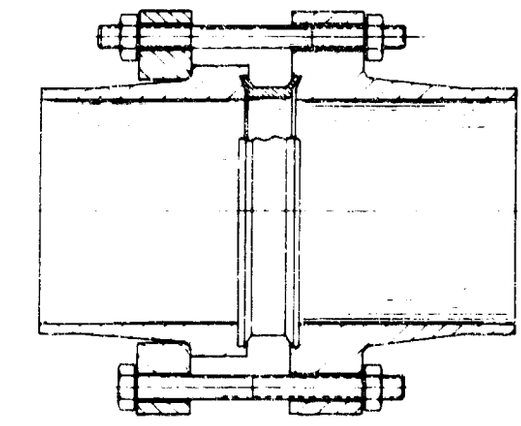

c. Integral / Loose-Ring Flange Assembly

FIGURE C-1. TYPICAL AFRPL FLANGED-CONNECTOR ASSEMBLIES

Bolts and studs both are shown; seals are shown unseated.

TABLE C-1. FLANGE, INTEGRAL, ALUMINUM, CRYOGENIC FLUID CONNECTOR

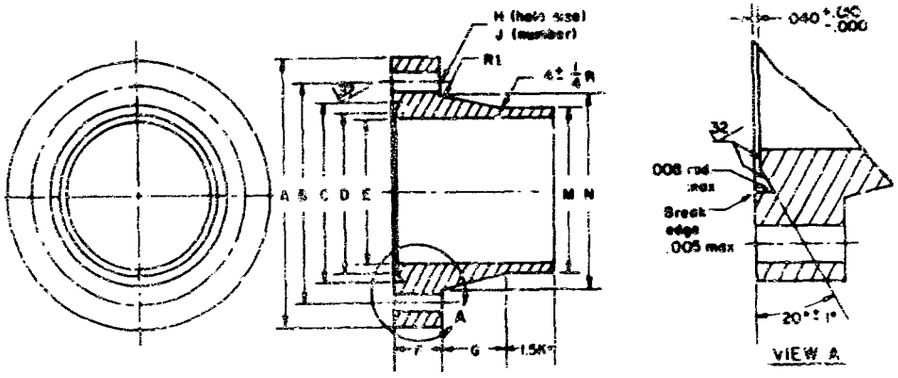

PRESSURE	PIPE TUBE OD	A	B	C	D	E	F	G	H	J	M	N	R1	K
100.0	1.000	2.151	1.749	1.384	1.070	.944	.264	.325	.201	8.000	1.000	1.124	.125	.500
100.0	1.250	2.411	2.009	1.641	1.341	1.194	.279	.366	.201	10.000	1.250	1.374	.125	.517
100.0	1.500	2.608	2.286	1.918	1.612	1.444	.294	.402	.201	10.000	1.500	1.634	.125	.533
100.0	2.000	3.233	2.831	2.462	2.144	1.944	.324	.467	.201	12.000	2.000	2.154	.125	.567
100.0	2.375	3.714	3.312	2.790	2.463	2.245	.450	.764	.281	14.000	2.375	2.687	.125	.592
100.0	2.500	3.778	3.376	3.005	2.675	2.444	.354	.523	.201	14.000	2.500	2.664	.125	.600
100.0	3.000	4.312	3.910	3.539	3.197	2.944	.369	.574	.201	14.000	3.000	3.194	.125	.633
100.0	3.500	5.169	4.639	3.962	3.608	3.334	.549	1.052	.265	12.000	3.500	3.931	.125	.667
100.0	4.000	5.568	5.038	4.595	4.229	3.930	.435	.742	.265	16.000	4.000	4.247	.125	.700
100.0	4.500	6.294	5.764	5.830	4.652	4.334	.624	1.200	.265	18.000	4.500	4.941	.188	.733
100.0	5.000	6.651	6.121	5.663	5.273	4.930	.510	.831	.265	18.000	5.000	5.227	.188	.767
100.0	5.563	7.470	6.940	6.107	5.703	5.345	.732	1.527	.265	28.000	5.563	6.127	.188	.804
100.0	6.000	7.725	7.194	6.721	6.307	5.935	.570	.911	.265	20.000	6.000	6.247	.188	.833
100.0	6.625	8.622	8.092	7.220	6.799	6.407	.777	1.671	.265	32.000	6.625	7.279	.188	.875
100.0	8.000	9.869	9.339	8.836	8.374	7.930	.615	1.054	.265	22.000	8.000	8.317	.188	.967
100.0	8.625	10.827	10.297	9.243	8.866	8.407	.882	1.915	.265	44.000	8.625	9.359	.250	1.008
100.0	10.000	12.120	11.590	10.885	10.375	9.870	.795	1.602	.265	40.000	10.000	10.652	.250	1.100
100.0	10.750	13.134	12.604	11.532	11.004	10.482	1.002	2.370	.265	56.000	10.750	11.687	.250	1.150
100.0	12.000	14.220	13.590	12.980	12.422	11.870	.855	1.757	.265	50.000	12.000	12.852	.250	1.233
100.0	12.750	15.643	14.687	13.361	12.985	12.420	1.170	2.863	.328	56.000	12.750	13.862	.313	1.283
100.0	14.000	16.245	15.715	15.085	14.479	13.870	.906	1.859	.265	62.000	14.000	14.652	.313	1.367
100.0	16.000	18.334	17.804	17.181	16.527	15.870	1.650	2.601	.265	72.000	16.000	16.992	.313	1.500
200.0	1.000	2.141	1.739	1.364	1.070	.944	.264	.325	.201	8.000	1.000	1.114	.125	.500
200.0	1.250	2.412	2.010	1.641	1.341	1.194	.294	.366	.201	10.000	1.250	1.374	.125	.517
200.0	1.500	2.689	2.287	1.918	1.612	1.444	.309	.402	.201	10.000	1.500	1.634	.125	.533
200.0	2.000	3.234	2.832	2.462	2.144	1.944	.339	.467	.201	12.000	2.000	2.154	.125	.567
200.0	2.375	3.714	3.312	2.790	2.463	2.245	.450	.764	.201	14.000	2.375	2.687	.125	.592
200.0	2.500	3.779	3.377	3.005	2.675	2.444	.359	.523	.201	14.000	2.500	2.674	.125	.600
200.0	3.000	4.311	3.912	3.539	3.197	2.944	.414	.574	.201	14.000	3.000	3.164	.125	.633
200.0	3.500	5.149	4.619	3.962	3.608	3.334	.564	1.052	.265	14.000	3.500	3.931	.125	.667
200.0	4.000	5.568	5.038	4.595	4.229	3.930	.480	.742	.265	14.000	4.000	4.257	.125	.700
200.0	4.500	6.284	5.754	5.030	4.652	4.334	.654	1.200	.265	18.000	4.500	4.941	.188	.733
200.0	5.000	6.651	6.121	5.663	5.273	4.930	.585	.831	.265	16.000	5.000	5.217	.188	.767
200.0	5.563	7.460	6.930	6.107	5.703	5.345	.762	1.527	.265	28.000	5.563	6.127	.188	.804
200.0	6.000	7.723	7.193	6.720	6.306	5.927	.649	.928	.265	20.000	6.000	6.248	.188	.833
200.0	6.625	8.622	8.092	7.228	6.799	6.407	.822	1.671	.265	36.000	6.625	7.279	.188	.875
200.0	8.000	9.836	9.306	8.803	8.341	7.903	.715	1.237	.265	32.000	8.000	8.484	.188	.967
200.0	8.625	10.997	10.447	9.343	8.866	8.407	.957	1.915	.265	46.000	8.625	9.509	.250	1.008
200.0	10.000	11.949	11.419	10.886	10.376	9.879	.872	1.547	.265	46.000	10.000	10.470	.250	1.100
200.0	10.750	13.423	12.767	11.532	11.004	10.482	1.092	2.370	.328	48.000	10.750	11.767	.250	1.150
200.0	12.000	14.204	13.674	12.969	12.411	11.855	1.013	1.856	.265	62.000	12.000	12.736	.250	1.233
200.0	12.750	15.693	15.037	13.561	12.985	12.420	1.305	2.863	.328	64.000	12.750	13.912	.313	1.283
200.0	14.000	16.623	15.967	15.041	14.435	13.830	1.169	2.165	.328	54.000	14.000	14.842	.313	1.367
200.0	16.000	18.759	18.103	17.114	16.460	15.806	1.296	2.475	.328	70.000	16.000	16.978	.313	1.500

500.0	1.000	2.141	1.739	1.364	1.070	.944	.294	.325	.201	8.000	1.000	1.114	.125	.500
500.0	1.250	2.414	2.012	1.641	1.341	1.194	.309	.366	.201	8.000	1.250	1.374	.125	.517
500.0	1.500	2.691	2.269	1.918	1.612	1.444	.339	.402	.201	10.000	1.500	1.634	.125	.533
500.0	2.000	3.237	2.835	2.441	2.143	1.940	.390	.483	.201	12.000	2.000	2.155	.125	.567
500.0	2.375	3.925	3.395	2.790	2.463	2.245	.495	.764	.265	10.000	2.375	2.707	.125	.592
500.0	2.500	3.751	3.354	2.983	2.653	2.425	.443	.604	.201	16.000	2.500	2.719	.125	.600
500.0	3.000	4.477	3.947	3.506	3.184	2.910	.510	.725	.265	12.000	3.000	3.253	.125	.633
500.0	3.500	5.149	4.619	3.962	3.608	3.334	.639	1.052	.265	18.000	3.500	3.931	.125	.667
500.0	4.000	5.578	5.048	4.540	4.174	3.880	.645	.966	.265	18.000	4.000	4.380	.125	.700
500.0	4.500	6.256	5.734	5.030	4.652	4.334	.774	1.200	.265	24.000	4.500	4.921	.188	.733
500.0	5.000	6.750	6.220	5.575	5.185	4.850	.811	1.208	.265	28.000	5.000	5.408	.188	.767
500.0	5.563	7.704	7.052	6.107	5.703	5.345	.927	1.527	.328	22.000	5.563	6.177	.188	.804
500.0	6.000	7.838	7.308	6.610	6.196	5.820	.946	1.449	.265	32.000	6.000	6.495	.188	.833
500.0	6.625	8.770	8.114	7.228	6.799	6.407	1.077	1.671	.328	30.000	6.625	7.239	.188	.875
500.0	8.000	10.231	9.575	8.659	8.197	7.759	1.261	1.932	.328	40.000	8.000	8.700	.188	.967
500.0	8.625	11.065	10.409	9.265	8.788	8.329	1.404	2.221	.328	44.000	8.625	9.405	.250	1.000
500.0	10.000	12.772	11.918	10.708	10.198	9.699	1.591	2.415	.397	40.000	10.000	10.855	.250	1.100
500.0	10.750	13.549	12.755	11.466	10.938	10.420	1.710	2.622	.397	46.000	10.750	11.692	.250	1.150
500.0	12.000	14.817	14.103	12.747	12.189	11.639	1.921	2.898	.397	54.000	12.000	13.040	.250	1.233
500.0	12.750	15.584	14.790	13.253	12.677	11.938	2.148	4.403	.397	56.000	12.750	13.653	.31	1.283
500.0	14.000	17.466	16.528	14.786	14.180	13.579	2.252	3.381	.469	52.000	14.000	15.215	.313	1.367
500.0	16.000	19.417	18.775	16.815	16.161	15.519	2.597	3.864	.531	52.000	16.000	17.400	.313	1.500
1000.0	1.000	2.152	1.750	1.364	1.070	.991	.329	.335	.201	6.000	1.000	1.125	.125	.500
1000.0	1.250	2.436	2.034	1.629	1.329	1.176	.367	.418	.201	8.000	1.250	1.409	.125	.517
1000.0	1.500	2.709	2.307	1.884	1.578	1.411	.434	.502	.201	10.000	1.500	1.602	.125	.533
1000.0	2.000	3.458	2.928	2.395	2.077	1.881	.553	.669	.265	10.000	2.000	2.240	.125	.567
1000.0	2.375	4.037	3.507	2.701	2.374	2.157	.672	.970	.265	14.000	2.375	2.819	.125	.592
1000.0	2.500	4.025	3.495	2.906	2.576	2.351	.643	.836	.265	14.000	2.500	2.807	.125	.600
1000.0	3.000	4.583	4.053	3.407	3.065	2.822	.763	1.004	.265	18.000	3.000	3.365	.125	.633
1000.0	3.500	5.396	4.740	3.885	3.531	3.260	.915	1.251	.328	16.000	3.500	3.990	.125	.667
1000.0	4.000	5.895	5.229	4.419	4.053	3.762	.957	1.339	.328	20.000	4.000	4.479	.125	.700
1000.0	4.500	7.020	6.226	4.809	4.431	4.026	1.116	1.954	.397	18.000	4.500	5.288	.188	.733
1000.0	5.000	7.135	6.679	5.420	5.030	4.703	1.151	1.673	.328	28.000	5.000	5.604	.188	.767
1000.0	5.563	7.993	7.199	5.897	5.493	5.047	1.299	2.282	.397	24.000	5.563	6.262	.188	.804
1000.0	6.000	8.451	7.657	6.422	6.008	5.643	1.375	2.007	.397	26.000	6.000	6.719	.188	.833
1000.0	6.625	9.106	8.312	6.984	6.555	6.065	1.500	2.606	.397	32.000	6.625	7.375	.188	.875
1000.0	8.000	10.959	10.021	8.415	7.953	7.524	1.794	2.676	.469	30.000	8.000	8.959	.188	.967
1000.0	8.625	11.511	10.573	9.031	8.554	7.981	1.991	3.206	.469	34.000	8.625	9.386	.250	1.000
1000.0	10.000	13.261	12.199	10.449	9.939	9.405	2.167	3.345	.531	32.000	10.000	10.949	.250	1.100
1000.0	10.750	13.904	12.842	11.206	10.678	10.020	2.460	3.825	.531	36.000	10.750	11.592	.250	1.150
1000.0	12.000	15.260	14.198	12.492	11.934	11.286	2.706	4.014	.531	42.000	12.000	12.960	.250	1.233
1000.0	12.750	16.030	14.968	13.253	12.677	11.938	2.898	4.403	.531	44.000	12.750	13.593	.313	1.283
1000.0	14.000	17.624	16.438	14.535	13.929	13.167	3.124	4.683	.593	40.000	14.000	14.938	.313	1.367
1000.0	16.000	19.492	18.580	16.578	15.924	15.048	3.708	5.352	.656	42.000	16.000	17.018	.313	1.500
1500.0	1.000	2.199	1.797	1.371	1.037	.912	.372	.401	.201	8.000	1.000	1.172	.125	.500
1500.0	1.250	2.686	2.156	1.585	1.285	1.140	.435	.501	.263	6.000	1.250	1.468	.125	.517
1500.0	1.500	2.991	2.461	1.840	1.534	1.360	.498	.601	.265	8.000	1.500	1.773	.125	.533
1500.0	2.000	3.572	3.042	2.340	2.022	1.824	.609	.802	.265	12.000	2.000	2.384	.125	.567
1500.0	2.375	4.225	3.569	2.701	2.374	2.157	.732	.970	.328	10.000	2.375	2.819	.125	.592
1500.0	2.500	4.251	3.695	2.829	2.499	2.280	.765	1.002	.328	12.000	2.500	2.965	.125	.600
1500.0	3.000	4.942	4.286	3.318	2.976	2.736	.876	1.203	.328	16.000	3.000	3.536	.125	.633
1500.0	3.500	5.934	5.140	3.785	3.431	3.068	1.036	1.628	.397	16.000	3.500	4.328	.125	.667
1500.0	4.000	6.315	5.521	4.307	3.941	3.648	1.159	1.603	.397	18.000	4.000	4.708	.125	.700
1500.0	4.500	7.050	6.256	4.809	4.431	4.026	1.251	1.954	.397	22.000	4.500	5.318	.188	.733
1500.0	5.000	7.602	6.808	5.326	4.936	4.559	1.351	2.004	.397	26.000	5.000	5.878	.188	.767
1500.0	5.563	8.422	7.484	5.897	5.493	5.047	1.539	2.282	.469	22.000	5.563	6.422	.188	.804
1500.0	6.000	8.793	7.855	6.345	5.931	5.471	1.588	2.405	.469	24.000	6.000	6.792	.188	.833
1500.0	6.625	9.408	8.346	6.953	6.524	5.761	1.941	3.155	.531	22.000	6.625	7.221	.188	.875
1500.0	8.000	10.973	9.911	8.382	7.920	7.295	2.212	3.207	.531	28.000	8.000	8.786	.188	.967
1500.0	8.625	11.467	10.405	8.995	8.518	7.625	2.505	3.505	.531	30.000	8.625	9.155	.250	1.000
1500.0	10.000	13.281	12.095	10.420	9.910	9.119	2.792	4.009	.593	30.000	10.000	10.720	.250	1.100
1500.0	10.750	14.076	12.764	11.160	10.632	9.564	3.249	4.763	.656	28.000	10.750	11.326	.250	1.150
1500.0	12.000	16.013	14.419	12.457	11.899	10.943	3.506	4.810	.797	26.000	12.000	12.794	.250	1.233
1500.0	12.750	16.565	14.971	13.196	12.620	11.376	3.831	5.591	.797	28.000	12.750	13.283	.313	1.283
1500.0	14.000	18.642	16.768	14.495	13.889	12.767	4.190	5.612	.937	26.000	14.000	14.768	.313	1.367
1500.0	16.000	21.196	19.072	16.533	15.879	14.590	4.958	6.414	1.062	26.000	16.000	16.822	.313	1.500

TABLE C-2. FLANGE, LOOSE RING, ALUMINUM, CRYOGENIC FLUID CONNECTOR

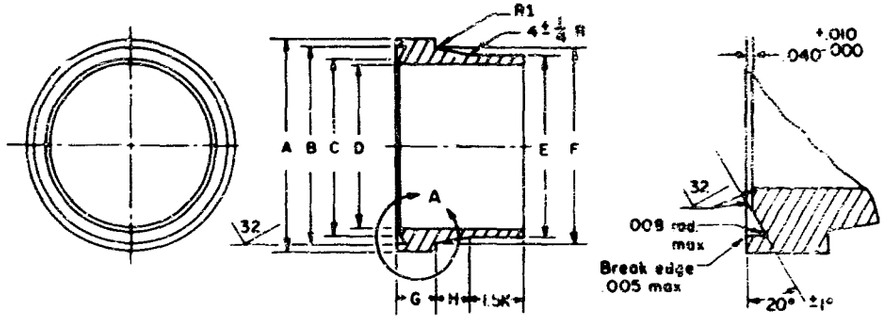

View A

PRESSURE	PIPE/ TUBE OD	A	B	C	D	E	F	G	H	R1	K
100.0	1.000	1.531	1.364	1.070	.944	1.000	1.104	.174	.325	.125	.500
100.0	1.250	1.808	1.641	1.341	1.194	1.250	1.364	.189	.366	.125	.517
100.0	1.500	2.085	1.918	1.612	1.444	1.500	1.634	.204	.402	.125	.533
100.0	2.000	2.630	2.462	2.144	1.944	2.000	2.154	.219	.467	.125	.567
100.0	2.375	2.959	2.790	2.463	2.245	2.375	2.577	.300	.764	.125	.592
100.0	2.500	3.175	3.005	2.675	2.444	2.500	2.674	.234	.523	.125	.600
100.0	3.000	3.709	3.539	3.197	2.944	3.000	3.184	.249	.574	.125	.633
100.0	3.500	4.133	3.962	3.608	3.336	3.500	3.751	.384	1.052	.125	.667
100.0	4.000	4.773	4.595	4.229	3.930	4.000	4.227	.315	.742	.125	.700
100.0	4.500	5.215	5.030	4.652	4.334	4.500	4.781	.429	1.200	.188	.733
100.0	5.000	5.856	5.663	5.273	4.930	5.000	5.247	.345	.831	.188	.767
100.0	5.563	6.308	6.107	5.783	5.345	5.563	5.877	.537	1.527	.188	.804
100.0	6.000	6.929	6.721	6.307	5.930	6.000	6.267	.375	.911	.188	.833
100.0	6.625	7.445	7.228	6.799	6.407	6.625	6.969	.582	1.671	.188	.875
100.0	8.000	9.074	8.836	8.374	7.930	8.000	8.357	.450	1.054	.188	.967
100.0	8.625	9.591	9.343	8.866	8.407	8.625	9.019	.657	1.915	.250	1.008
100.0	10.000	11.153	10.885	10.375	9.870	10.000	10.432	.600	1.602	.250	1.100
100.0	10.750	11.811	11.532	11.004	10.482	10.750	11.197	.792	2.370	.250	1.150
100.0	12.000	13.278	12.980	12.422	11.870	12.000	12.532	.675	1.757	.250	1.233
100.0	12.750	13.870	13.561	12.985	12.420	12.750	13.222	.930	2.863	.313	1.283
100.0	14.000	15.413	15.085	14.479	13.870	14.000	14.562	.735	1.899	.313	1.367
100.0	16.000	17.539	17.181	16.527	15.870	16.000	16.592	.810	2.031	.313	1.500
200.0	1.000	1.531	1.364	1.070	.944	1.000	1.114	.189	.325	.125	.500
200.0	1.250	1.809	1.641	1.341	1.194	1.250	1.374	.204	.366	.125	.517
200.0	1.500	2.086	1.918	1.612	1.444	1.500	1.634	.204	.402	.125	.533
200.0	2.000	2.631	2.462	2.144	1.944	2.000	2.154	.234	.467	.125	.567
200.0	2.375	2.960	2.790	2.463	2.245	2.375	2.577	.315	.764	.125	.592
200.0	2.500	3.176	3.005	2.675	2.444	2.500	2.674	.249	.523	.125	.600
200.0	3.000	3.711	3.539	3.197	2.944	3.000	3.194	.279	.574	.125	.633
200.0	3.500	4.135	3.962	3.608	3.336	3.500	3.751	.414	1.052	.125	.667
200.0	4.000	4.773	4.595	4.229	3.930	4.000	4.237	.330	.742	.125	.700
200.0	4.500	5.215	5.030	4.652	4.334	4.500	4.781	.459	1.200	.188	.733
200.0	5.000	5.856	5.663	5.273	4.930	5.000	5.237	.375	.831	.188	.767
200.0	5.563	6.308	6.107	5.783	5.345	5.563	5.877	.567	1.527	.188	.804
200.0	6.000	6.928	6.720	6.306	5.927	6.000	6.268	.424	.928	.188	.833
200.0	6.625	7.445	7.228	6.799	6.407	6.625	6.979	.612	1.671	.188	.875
200.0	8.000	9.041	8.803	8.341	7.903	8.000	8.424	.550	1.237	.188	.967
200.0	8.625	9.591	9.343	8.866	8.407	8.625	9.019	.717	1.915	.250	1.008
200.0	10.000	11.154	10.886	10.376	9.879	10.000	10.480	.677	1.547	.250	1.100
200.0	10.750	11.811	11.532	11.004	10.482	10.750	11.207	.852	2.370	.250	1.150
200.0	12.000	13.267	12.969	12.411	11.855	12.000	12.556	.788	1.854	.250	1.233
200.0	12.750	13.870	13.561	12.985	12.420	12.750	13.242	1.020	2.863	.313	1.283
200.0	14.000	15.369	15.041	14.435	13.830	14.000	14.512	.944	2.145	.313	1.367
200.0	16.000	17.472	17.114	16.460	15.805	16.000	16.588	1.086	2.475	.313	1.500

500.0	1.000	1.533	1.364	1.070	.944	1.000	1.114	.204	.325	.125	.300
500.0	1.250	1.811	1.641	1.341	1.134	1.250	1.374	.219	.366	.125	.317
500.0	1.500	2.068	1.918	1.612	1.444	1.500	1.634	.234	.402	.125	.333
500.0	2.000	2.534	2.441	2.143	1.960	2.000	2.155	.270	.483	.125	.367
500.0	2.375	2.934	2.760	2.463	2.265	2.375	2.587	.305	.764	.125	.392
500.0	2.500	3.058	2.883	2.563	2.425	2.500	2.699	.323	.804	.125	.400
500.0	3.000	3.562	3.506	3.164	2.910	3.000	3.233	.360	.725	.125	.433
500.0	3.500	4.140	3.962	3.608	3.334	3.500	3.771	.459	1.052	.125	.467
500.0	4.000	4.720	4.350	4.174	3.880	4.000	4.280	.463	.966	.125	.700
500.0	4.500	5.215	5.010	4.652	4.334	4.500	4.791	.434	1.400	.250	.733
500.0	5.000	5.768	5.575	5.185	4.850	5.000	5.308	.556	1.208	.188	.767
500.0	5.563	6.388	6.107	5.703	5.345	5.563	5.867	.642	1.527	.188	.804
500.0	6.000	6.814	6.910	6.196	5.820	6.000	6.343	.691	1.449	.188	.833
500.0	6.625	7.445	7.228	6.799	6.407	6.625	6.999	.777	1.671	.188	.875
500.0	8.000	8.497	8.069	8.197	7.759	8.000	8.420	.946	1.932	.188	.967
500.0	8.625	9.513	9.265	8.788	8.329	8.625	9.049	1.059	2.221	.250	1.008
500.0	10.000	10.975	10.780	10.198	9.699	10.000	10.465	1.186	2.415	.250	1.100
500.0	10.750	11.745	11.446	10.938	10.420	10.750	11.232	1.320	2.622	.250	1.150
500.0	12.000	13.065	12.747	12.189	11.639	12.000	12.529	1.501	2.898	.250	1.233
500.0	12.750	13.852	13.562	12.677	11.938	12.750	12.993	1.703	4.403	.313	1.283
500.0	14.000	15.116	14.786	14.180	13.579	14.000	14.555	1.787	3.381	.313	1.367
500.0	16.000	17.173	16.815	16.141	15.519	16.000	16.600	2.117	3.864	.313	1.500
1000.0	1.000	1.534	1.364	1.070	.941	1.000	1.005	.224	.335	.125	.300
1000.0	1.250	1.801	1.629	1.329	1.176	1.250	1.359	.282	.418	.125	.317
1000.0	1.500	2.057	1.884	1.578	1.411	1.500	1.632	.299	.502	.125	.333
1000.0	2.000	2.571	2.395	2.077	1.881	2.000	2.170	.358	.669	.125	.367
1000.0	2.375	2.978	2.771	2.474	2.257	2.375	2.589	.462	.970	.125	.392
1000.0	2.500	3.084	2.904	2.576	2.351	2.500	2.697	.448	.836	.125	.400
1000.0	3.000	3.588	3.407	3.065	2.822	3.000	3.215	.538	1.004	.125	.433
1000.0	3.500	4.068	3.885	3.531	3.260	3.500	3.750	.665	1.251	.125	.467
1000.0	4.000	4.684	4.419	4.053	3.762	4.000	4.269	.717	1.338	.125	.700
1000.0	4.500	5.192	4.909	4.631	4.026	4.500	4.800	.906	1.956	.188	.733
1000.0	5.000	5.643	5.420	5.030	4.703	5.000	5.274	.896	1.673	.188	.767
1000.0	5.563	6.278	5.997	5.493	5.047	5.563	5.862	1.134	2.282	.188	.804
1000.0	6.000	6.780	6.422	6.000	5.643	6.000	6.339	1.156	2.007	.188	.833
1000.0	6.625	7.396	6.984	6.535	6.055	6.625	6.935	1.335	2.606	.188	.875
1000.0	8.000	8.833	8.415	7.953	7.524	8.000	8.329	1.569	2.676	.188	.967
1000.0	8.625	9.383	9.031	8.554	7.981	8.625	8.836	1.656	3.206	.250	1.008
1000.0	10.000	10.822	10.449	9.939	9.405	10.000	10.229	2.017	3.345	.250	1.100
1000.0	10.750	11.575	11.204	10.678	10.020	10.756	10.942	2.205	3.825	.250	1.150
1000.0	12.000	12.990	12.492	11.934	11.286	12.000	12.248	2.496	4.014	.250	1.233
1000.0	12.750	13.667	13.253	12.677	11.938	12.750	12.953	2.598	4.603	.313	1.283
1000.0	14.000	14.998	14.535	13.929	13.167	14.000	14.218	2.929	4.603	.313	1.367
1000.0	16.000	17.116	16.574	15.924	15.048	16.000	16.238	3.318	5.352	.313	1.500
1500.0	1.000	1.502	1.331	1.037	.912	1.000	1.092	.267	.401	.125	.300
1500.0	1.250	1.759	1.585	1.285	1.140	1.250	1.340	.315	.501	.125	.317
1500.0	1.500	2.015	1.840	1.534	1.368	1.500	1.663	.368	.601	.125	.333
1500.0	2.000	2.528	2.340	2.022	1.824	2.000	2.184	.459	.802	.125	.367
1500.0	2.375	2.881	2.701	2.374	2.157	2.375	2.579	.537	.970	.125	.392
1500.0	2.500	3.010	2.829	2.499	2.280	2.500	2.705	.570	1.002	.125	.400
1500.0	3.000	3.567	3.318	2.976	2.736	3.000	3.216	.696	1.203	.125	.433
1500.0	3.500	4.317	3.785	3.431	3.066	3.500	3.908	.908	1.628	.125	.467
1500.0	4.000	4.737	4.307	3.941	3.644	4.000	4.318	1.024	1.803	.125	.700
1500.0	4.500	5.232	4.809	4.431	4.026	4.500	4.798	1.101	1.954	.188	.733
1500.0	5.000	5.742	5.326	4.936	4.559	5.000	5.310	1.240	2.904	.188	.767
1500.0	5.563	6.366	5.897	5.493	5.047	5.563	5.852	1.389	2.282	.188	.804
1500.0	6.000	6.823	6.345	5.931	5.471	6.000	6.282	1.483	2.605	.188	.833
1500.0	6.625	7.441	6.953	6.524	5.751	6.625	6.841	1.671	3.155	.188	.875
1500.0	8.000	8.959	8.582	7.920	7.295	8.000	8.276	2.047	3.207	.188	.967
1500.0	8.625	9.587	8.995	8.518	7.625	8.625	8.875	2.145	3.905	.250	1.008
1500.0	10.000	11.063	10.420	9.910	9.119	10.000	10.240	2.662	4.009	.250	1.100
1500.0	10.750	11.934	11.160	10.632	9.504	10.750	11.048	2.889	4.763	.250	1.150
1500.0	12.000	13.235	12.457	11.899	10.943	12.000	12.264	3.256	4.810	.250	1.233
1500.0	12.750	14.134	13.196	12.620	11.376	12.750	13.093	3.486	5.591	.313	1.283
1500.0	14.000	15.438	14.495	13.889	12.767	14.000	14.308	3.785	5.612	.313	1.367
1500.0	16.000	17.641	16.533	15.879	14.590	16.000	16.352	4.670	6.414	.313	1.500

TABLE C-3. RING, LOOSE, ALUMINUM, CRYOGENIC FLUID CONNECTOR

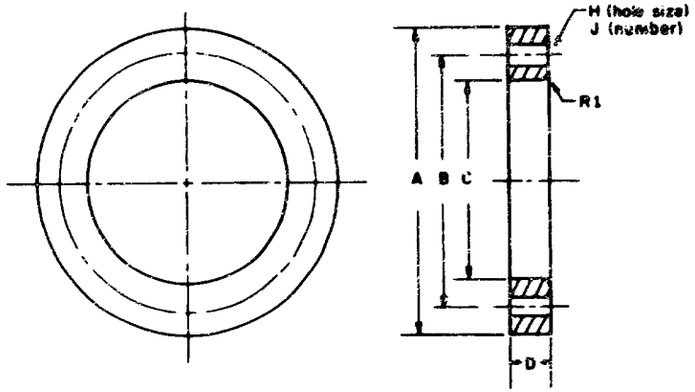

PRESSURE	PIPE/ TUBE OD	A	B	C	D	H	J	R1
100.0	1.000	2.151	1.749	1.078	.191	.201	8.000	.125
100.0	1.250	2.411	2.009	1.331	.206	.201	10.000	.125
100.0	1.500	2.686	2.286	1.599	.206	.201	10.000	.125
100.0	2.000	3.233	2.831	2.119	.236	.201	12.000	.125
100.0	2.375	3.724	3.322	2.549	.325	.201	14.000	.125
100.0	2.500	3.778	3.376	2.639	.266	.201	14.000	.125
100.0	3.000	4.313	3.910	3.158	.281	.201	14.000	.125
100.0	3.500	5.169	4.639	3.725	.421	.265	12.000	.125
100.0	4.000	5.568	5.038	4.195	.340	.265	16.000	.125
100.0	4.500	6.294	5.764	4.743	.496	.265	18.000	.188
100.0	5.000	6.651	6.121	5.200	.370	.265	18.000	.188
100.0	5.563	7.470	6.940	5.843	.688	.265	26.000	.188
100.0	6.000	7.724	7.194	6.220	.415	.265	20.000	.188
100.0	6.625	8.622	8.092	6.935	.668	.265	32.000	.188
100.0	8.000	9.869	9.339	8.385	.475	.265	22.000	.188
100.0	8.625	10.827	10.297	8.973	.773	.265	44.000	.250
100.0	10.000	12.120	11.590	10.374	.655	.265	40.000	.250
100.0	10.750	13.134	12.604	11.145	.928	.265	56.000	.250
100.0	12.000	14.120	13.590	12.468	.685	.265	50.000	.250
100.0	12.750	15.643	14.987	13.175	1.140	.328	56.000	.313
100.0	14.000	16.265	15.715	14.483	.760	.265	62.000	.313
100.0	16.000	18.334	17.804	16.515	.805	.265	72.000	.313
200.0	1.000	2.141	1.739	1.078	.191	.201	8.000	.125
200.0	1.250	2.412	2.010	1.339	.206	.201	10.000	.125
200.0	1.500	2.686	2.287	1.599	.221	.201	10.000	.125
200.0	2.000	3.234	2.832	2.119	.251	.201	12.000	.125
200.0	2.375	3.714	3.312	2.549	.340	.201	14.000	.125
200.0	2.500	3.779	3.377	2.639	.281	.201	14.000	.125
200.0	3.000	4.314	3.912	3.159	.296	.201	14.000	.125
200.0	3.500	5.149	4.619	3.725	.451	.265	14.000	.125
200.0	4.000	5.568	5.038	4.204	.355	.265	14.000	.125
200.0	4.500	6.284	5.754	4.743	.511	.265	18.000	.188
200.0	5.000	6.651	6.121	5.191	.400	.265	16.000	.188
200.0	5.563	7.460	6.930	5.843	.638	.265	28.000	.188
200.0	6.000	7.723	7.193	6.222	.448	.265	20.000	.188
200.0	6.625	8.622	8.092	6.944	.698	.265	36.000	.188
200.0	8.000	9.836	9.306	8.371	.562	.265	32.000	.188
200.0	8.625	10.997	10.467	8.973	.843	.265	46.000	.250
200.0	10.000	11.949	11.419	10.415	.661	.265	46.000	.250
200.0	10.750	13.423	12.767	11.163	1.018	.328	48.000	.250
200.0	12.000	14.204	13.674	12.492	.820	.265	62.000	.250
200.0	12.750	15.693	15.037	13.193	1.230	.328	64.000	.313
200.0	14.000	16.623	15.967	14.447	.965	.328	54.000	.31
200.0	16.000	18.759	18.103	16.523	1.094	.328	70.000	.313

500.0	1.000	2.141	1.739	1.078	.206	.201	8.000	.125
500.0	1.250	2.414	2.012	1.339	.221	.201	8.000	.125
500.0	1.500	2.691	2.289	1.599	.236	.201	10.000	.125
500.0	2.000	3.237	2.835	2.121	.265	.201	12.000	.125
500.0	2.375	3.925	3.395	2.558	.370	.265	10.000	.125
500.0	2.500	3.761	3.359	2.664	.315	.201	16.000	.125
500.0	3.000	4.477	3.947	3.189	.380	.265	12.000	.125
500.0	3.500	5.149	4.619	3.743	.496	.265	18.000	.125
500.0	4.000	5.578	5.048	4.249	.465	.265	16.000	.125
500.0	4.500	6.264	5.734	4.751	.556	.265	24.000	.188
500.0	5.000	6.750	6.220	5.266	.585	.265	28.000	.188
500.0	5.563	7.708	7.052	5.852	.728	.328	22.000	.188
500.0	6.000	7.838	7.308	6.306	.690	.265	32.000	.188
500.0	6.625	8.770	8.114	6.962	.788	.328	30.000	.188
500.0	8.000	10.231	9.575	8.384	.916	.328	40.000	.188
500.0	8.625	11.065	10.409	9.006	1.061	.328	44.000	.250
500.0	10.000	12.712	11.918	10.422	1.156	.397	40.000	.250
500.0	10.750	13.549	12.755	11.191	1.245	.397	46.000	.250
500.0	12.000	14.897	14.103	12.479	1.381	.397	54.000	.250
500.0	12.750	15.584	14.790	12.976	1.532	.397	56.000	.313
500.0	14.000	17.466	16.528	14.509	1.636	.469	52.000	.313
500.0	16.000	19.837	18.775	16.556	1.861	.531	52.000	.313
1000.0	1.000	2.152	1.750	1.057	.224	.201	6.000	.125
1000.0	1.250	2.436	2.034	1.330	.254	.201	8.000	.125
1000.0	1.500	2.709	2.307	1.604	.299	.201	10.000	.125
1000.0	2.000	3.458	2.928	2.142	.359	.265	10.000	.125
1000.0	2.375	4.037	3.507	2.565	.503	.265	14.000	.125
1000.0	2.500	4.025	3.495	2.671	.449	.265	14.000	.125
1000.0	3.000	4.583	4.053	3.191	.523	.265	18.000	.125
1000.0	3.500	5.185	4.529	3.728	.570	.328	16.000	.125
1000.0	4.000	5.885	5.229	4.247	.673	.328	20.000	.125
1000.0	4.500	7.020	6.226	4.781	.989	.397	18.000	.188
1000.0	5.000	7.135	6.479	5.246	.867	.328	28.000	.188
1000.0	5.563	7.993	7.199	5.839	.981	.397	24.000	.188
1000.0	6.000	8.451	7.657	6.329	1.017	.397	26.000	.188
1000.0	6.625	9.106	8.312	6.914	1.100	.397	32.000	.188
1000.0	8.000	10.959	10.021	8.307	1.286	.469	30.000	.188
1000.0	8.625	11.511	10.573	8.820	1.334	.469	34.000	.250
1000.0	10.000	13.261	12.199	10.212	1.495	.531	32.000	.250
1000.0	10.750	13.904	12.842	10.930	1.555	.531	36.000	.250
1000.0	12.000	15.260	14.198	12.233	1.689	.531	42.000	.250
1000.0	12.750	16.030	14.968	12.939	1.772	.531	44.000	.313
1000.0	14.000	17.624	16.438	14.284	1.928	.593	40.000	.313
1000.0	16.000	19.892	18.580	16.224	2.152	.696	42.000	.313
1500.0	1.000	2.199	1.797	1.067	.268	.201	8.000	.125
1500.0	1.250	2.686	2.156	1.326	.320	.265	6.000	.125
1500.0	1.500	2.991	2.461	1.617	.372	.265	8.000	.125
1500.0	2.000	3.572	3.042	2.141	.461	.265	12.000	.125
1500.0	2.375	4.225	3.569	2.556	.548	.328	10.000	.125
1500.0	2.500	4.351	3.695	2.682	.565	.328	12.000	.125
1500.0	3.000	4.942	4.286	3.196	.654	.328	16.000	.125
1500.0	3.500	5.934	5.140	3.881	.837	.397	16.000	.125
1500.0	4.000	6.315	5.521	4.296	.847	.397	18.000	.125
1500.0	4.500	7.050	6.256	4.772	.984	.397	22.000	.188
1500.0	5.000	7.602	6.808	5.283	1.041	.397	26.000	.188
1500.0	5.563	8.422	7.484	5.830	1.116	.469	22.000	.188
1500.0	6.000	8.793	7.855	6.261	1.144	.469	24.000	.188
1500.0	6.625	9.408	8.346	6.829	1.134	.531	22.000	.188
1500.0	8.000	10.973	9.911	8.261	1.335	.531	28.000	.188
1500.0	8.625	11.467	10.405	8.860	1.360	.531	30.000	.250
1500.0	10.000	13.281	12.095	10.226	1.601	.593	30.000	.250
1500.0	10.750	14.076	12.764	11.031	1.591	.656	28.000	.250
1500.0	12.000	15.013	14.419	12.251	1.852	.797	26.000	.250
1500.0	12.750	16.565	14.971	13.075	1.794	.797	28.000	.313
1500.0	14.000	18.542	16.768	14.292	2.133	.937	26.000	.313
1500.0	16.000	21.196	19.072	16.336	2.385	1.062	26.000	.313

TABLE C-4. SEAL, ALUMINUM, CRYOGENIC FLUID CONNECTOR

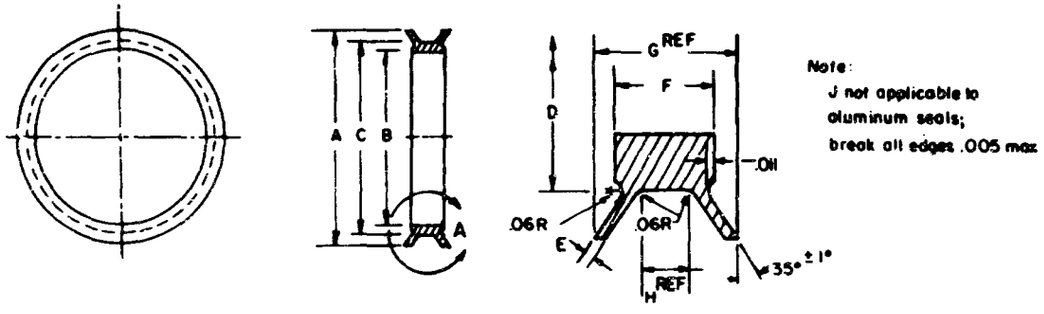

Note:
J not applicable to aluminum seals;
break all edges .005 max

VIEW A

PRESSURE	PIPE/ TUBE OD	A	B	C	D	E	F	G	H	J
100.0	1.000	1.362	.978	1.138	1.070	.041	.320	.477	.220	1.362
100.0	1.250	1.639	1.228	1.409	1.341	.041	.354	.516	.254	1.639
100.0	1.500	1.916	1.479	1.680	1.612	.041	.382	.548	.282	1.916
100.0	2.000	2.460	1.981	2.212	2.144	.042	.442	.615	.340	2.460
100.0	2.375	2.788	2.284	2.531	2.463	.042	.473	.653	.370	2.788
100.0	2.500	3.003	2.483	2.743	2.675	.042	.487	.669	.384	3.003
100.0	3.000	3.537	2.985	3.265	3.197	.042	.541	.731	.437	3.537
100.0	3.500	3.960	3.377	3.676	3.608	.043	.572	.771	.467	3.960
100.0	4.000	4.593	3.974	4.297	4.229	.043	.622	.829	.516	4.593
100.0	4.500	5.028	4.380	4.720	4.652	.044	.651	.866	.544	5.028
100.0	5.000	5.661	4.978	5.341	5.273	.044	.690	.914	.582	5.661
100.0	5.563	6.105	5.395	5.771	5.703	.045	.721	.954	.612	6.105
100.0	6.000	6.719	5.982	6.375	6.307	.045	.763	1.004	.653	6.719
100.0	6.625	7.226	6.461	6.867	6.799	.046	.797	1.048	.685	7.226
100.0	8.000	8.834	7.989	8.442	8.374	.047	.881	1.155	.767	8.834
100.0	8.625	9.341	8.468	8.934	8.866	.047	.906	1.191	.791	9.341
100.0	10.000	10.883	9.936	10.443	10.375	.048	.976	1.284	.858	10.883
100.0	10.750	11.530	10.551	11.072	11.004	.049	1.007	1.328	.888	11.530
100.0	12.000	12.978	11.943	12.490	12.422	.050	1.085	1.426	.963	12.978
100.0	12.750	13.559	12.496	13.053	12.985	.051	1.114	1.468	.990	13.559
100.0	14.000	15.083	13.950	14.567	14.479	.052	1.159	1.534	1.033	15.083
100.0	16.000	17.179	15.958	16.595	16.527	.053	1.241	1.650	1.111	17.179
200.0	1.000	1.362	.978	1.138	1.070	.041	.320	.477	.219	1.362
200.0	1.250	1.639	1.228	1.409	1.341	.041	.354	.516	.253	1.639
200.0	1.500	1.916	1.479	1.680	1.612	.042	.382	.548	.280	1.916
200.0	2.000	2.460	1.981	2.212	2.144	.042	.442	.615	.338	2.460
200.0	2.375	2.788	2.284	2.531	2.463	.043	.473	.653	.368	2.788
200.0	2.500	3.003	2.483	2.743	2.675	.043	.487	.669	.382	3.003
200.0	3.000	3.537	2.985	3.265	3.197	.044	.541	.731	.435	3.537
200.0	3.500	3.960	3.377	3.676	3.608	.044	.572	.771	.464	3.960
200.0	4.000	4.593	3.974	4.297	4.229	.045	.622	.829	.512	4.593
200.0	4.500	5.028	4.380	4.720	4.652	.045	.651	.866	.540	5.028
200.0	5.000	5.661	4.978	5.341	5.273	.046	.690	.914	.578	5.661
200.0	5.563	6.105	5.395	5.771	5.703	.047	.721	.954	.607	6.105
200.0	6.000	6.718	5.979	6.374	6.306	.047	.759	.999	.644	6.718
200.0	6.625	7.226	6.461	6.867	6.799	.048	.797	1.048	.680	7.226
200.0	8.000	8.801	7.962	8.409	8.341	.049	.889	1.163	.768	8.801
200.0	8.625	9.341	8.468	8.934	8.866	.050	.906	1.191	.784	9.341
200.0	10.000	10.884	9.945	10.444	10.376	.052	.992	1.300	.866	10.884
200.0	10.750	11.530	10.551	11.072	11.004	.053	1.007	1.328	.879	11.530
200.0	12.000	12.967	11.928	12.479	12.411	.054	1.076	1.418	.944	12.967
200.0	12.750	13.559	12.496	13.053	12.985	.055	1.114	1.468	.979	13.559
200.0	14.000	15.039	13.911	14.503	14.435	.056	1.164	1.540	1.026	15.039
200.0	16.000	17.112	15.894	16.528	16.460	.059	1.241	1.650	1.097	17.112

500.0	1.000	1.362	.975	1.138	1.070	.042	.320	.477	.217	1.362
500.0	1.250	1.639	1.226	1.409	1.341	.042	.334	.516	.251	1.639
500.0	1.500	1.916	1.479	1.680	1.612	.043	.382	.548	.278	1.916
500.0	2.000	2.459	1.977	2.211	2.143	.044	.434	.608	.327	2.459
500.0	2.375	2.788	2.284	2.531	2.463	.044	.473	.653	.364	2.788
500.0	2.500	2.901	2.464	2.721	2.653	.045	.488	.670	.379	2.981
500.0	3.000	3.504	2.951	3.232	3.164	.046	.534	.724	.422	3.504
500.0	3.500	3.960	3.377	3.676	3.604	.047	.572	.771	.458	3.960
500.0	4.000	4.538	3.924	4.242	4.174	.047	.623	.830	.507	4.538
500.0	4.500	5.028	4.380	4.720	4.652	.048	.651	.866	.533	5.028
500.0	5.000	5.573	4.898	5.253	5.185	.049	.693	.918	.573	5.573
500.0	5.563	6.105	5.395	5.771	5.703	.050	.721	.954	.598	6.105
500.0	6.000	6.608	5.871	6.244	6.176	.051	.751	.992	.626	6.608
500.0	6.625	7.226	6.461	6.867	6.799	.052	.797	1.048	.669	7.226
500.0	7.000	7.657	6.818	7.245	7.177	.053	.825	1.084	.695	7.657
500.0	7.625	8.263	7.390	8.856	8.788	.054	.872	1.143	.740	8.263
500.0	8.000	8.706	7.785	8.246	8.178	.055	.899	1.183	.761	8.706
500.0	8.750	9.564	8.489	9.009	8.938	.056	.971	1.280	.820	9.564
500.0	9.000	9.745	8.712	9.257	9.189	.057	1.004	1.320	.843	9.745
500.0	9.750	10.551	9.414	9.965	9.897	.058	1.023	1.377	.887	10.551
500.0	10.000	10.784	9.659	10.246	10.178	.059	1.131	1.526	.989	10.784
500.0	10.000	10.813	9.686	10.229	10.161	.060	1.241	1.650	1.070	10.813
1000.0	1.000	1.362	.974	1.138	1.070	.043	.313	.470	.209	1.362
1000.0	1.250	1.627	1.210	1.397	1.329	.043	.338	.499	.232	1.627
1000.0	1.500	1.882	1.446	1.646	1.578	.044	.374	.540	.267	1.882
1000.0	2.000	2.393	1.918	2.145	2.077	.045	.434	.608	.324	2.393
1000.0	2.375	2.699	2.196	2.442	2.374	.046	.457	.637	.344	2.699
1000.0	2.500	2.904	2.390	2.644	2.576	.047	.481	.663	.367	2.904
1000.0	3.000	3.485	2.862	3.133	3.065	.048	.538	.728	.421	3.485
1000.0	3.500	3.883	3.303	3.599	3.531	.049	.566	.765	.446	3.883
1000.0	4.000	4.417	3.806	4.121	4.053	.051	.612	.820	.489	4.417
1000.0	4.500	4.867	4.272	4.499	4.431	.052	.688	.703	.361	4.867
1000.0	5.000	5.418	4.751	5.098	5.030	.053	.688	.912	.558	5.418
1000.0	5.563	5.895	5.097	5.561	5.493	.055	.557	.791	.424	5.895
1000.0	6.000	6.420	5.695	6.076	6.008	.056	.749	.996	.613	6.420
1000.0	6.625	6.982	6.119	6.623	6.555	.057	.614	.865	.473	6.982
1000.0	7.000	7.413	7.583	8.021	7.953	.061	.864	1.139	.715	8.413
1000.0	8.625	9.029	8.042	8.622	8.554	.063	.698	.983	.545	9.029
1000.0	10.000	10.447	9.471	10.087	9.939	.066	.883	1.191	.721	10.447
1000.0	10.750	11.204	10.089	10.746	10.678	.068	.770	1.091	.603	11.204
1000.0	12.000	12.490	11.358	12.002	11.934	.072	.883	1.224	.708	12.490
1000.0	12.756	13.251	12.814	12.765	12.677	.074	.823	1.177	.643	13.251
1000.0	14.000	14.533	13.247	13.997	13.929	.077	.882	1.258	.695	14.533
1000.0	16.000	16.576	15.136	15.992	15.924	.082	.882	1.291	.682	16.576
1500.0	1.000	1.329	.945	1.105	1.037	.043	.312	.469	.206	1.329
1500.0	1.250	1.563	1.174	1.353	1.285	.044	.342	.503	.235	1.563
1500.0	1.500	1.838	1.403	1.602	1.534	.045	.366	.532	.257	1.838
1500.0	2.000	2.338	1.861	2.090	2.022	.046	.419	.593	.306	2.338
1500.0	2.375	2.699	2.196	2.442	2.374	.048	.457	.637	.341	2.699
1500.0	2.500	2.827	2.319	2.567	2.499	.048	.478	.660	.360	2.827
1500.0	3.000	3.316	2.776	3.044	2.976	.050	.527	.718	.406	3.316
1500.0	3.500	3.783	3.111	3.499	3.431	.051	.412	.611	.287	3.783
1500.0	4.000	4.305	3.692	4.009	3.941	.053	.589	.797	.460	4.305
1500.0	4.500	4.807	4.072	4.499	4.431	.055	.488	.703	.354	4.807
1500.0	5.000	5.324	4.607	5.004	4.936	.056	.588	.812	.451	5.324
1500.0	5.563	5.895	5.097	5.561	5.493	.058	.557	.791	.416	5.895
1500.0	6.000	6.343	5.523	5.999	5.931	.059	.588	.829	.443	6.343
1500.0	6.625	6.951	6.115	6.592	6.524	.061	.387	.638	.237	6.951
1500.0	8.000	8.380	7.354	7.988	7.920	.066	.587	.862	.426	8.380
1500.0	8.625	8.993	7.886	8.586	8.518	.068	.439	.724	.273	8.993
1500.0	10.000	10.418	9.185	9.978	9.910	.072	.587	.895	.418	10.418
1500.0	10.750	11.158	9.833	10.700	10.632	.075	.462	.783	.280	11.158
1500.0	12.000	12.455	11.016	11.967	11.899	.079	.586	.928	.394	12.455
1500.0	12.756	13.194	11.652	12.658	12.620	.081	.474	.828	.276	13.194
1500.0	14.000	14.493	12.847	13.957	13.889	.085	.586	.961	.378	14.493
1500.0	16.000	16.531	14.678	15.947	15.879	.092	.586	.995	.362	16.531

TABLE C-5. BOLT, ALUMINUM, INTEGRAL/INTEGRAL, CRYOGENIC FLUID CONNECTOR

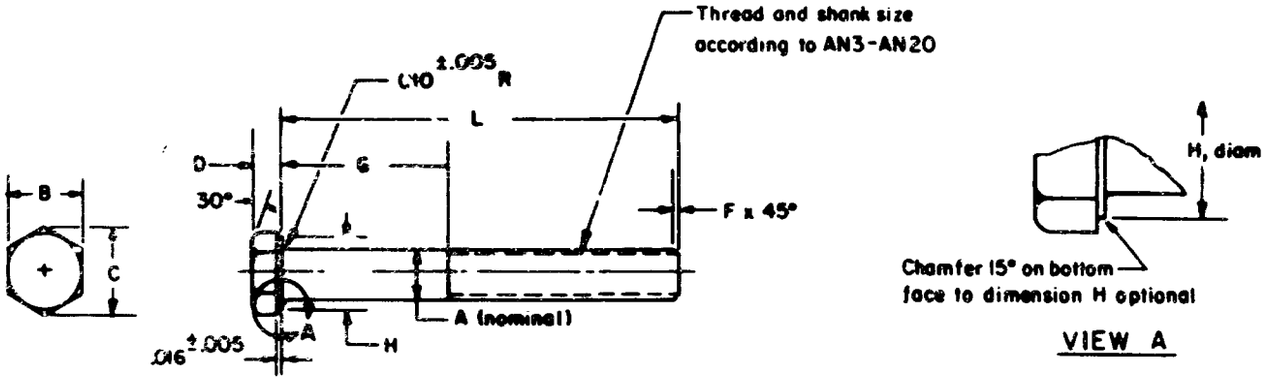

PRESSURE	PIPE/ TUBE OD	A	B	C	D	F	H	G	L	J
100.0	1.000	.190	.375	.433	.141	.063	.375	.424	1.133	8.000
100.0	1.250	.190	.375	.433	.141	.063	.375	.456	1.197	10.000
100.0	1.500	.190	.375	.433	.141	.063	.375	.485	1.255	10.000
100.0	2.000	.190	.375	.433	.141	.063	.375	.545	1.375	12.000
100.0	2.375	.190	.375	.433	.141	.063	.375	.671	1.628	14.000
100.0	2.500	.190	.375	.433	.141	.063	.375	.598	1.480	14.000
100.0	3.000	.190	.375	.433	.141	.063	.375	.639	1.564	14.000
100.0	3.500	.250	.438	.505	.172	.063	.438	.835	2.045	12.000
100.0	4.000	.250	.438	.505	.172	.063	.438	.746	1.867	16.000
100.0	4.500	.250	.438	.505	.172	.063	.438	.949	2.274	18.000
100.0	5.000	.250	.438	.505	.172	.063	.438	.855	2.085	18.000
100.0	5.563	.250	.438	.505	.172	.063	.438	1.092	2.560	26.000
100.0	6.000	.250	.438	.505	.172	.063	.438	.952	2.278	20.000
100.0	6.625	.250	.438	.505	.172	.063	.438	1.175	2.726	32.000
100.0	8.000	.250	.438	.505	.172	.063	.438	1.055	2.486	22.000
100.0	8.625	.250	.438	.505	.172	.063	.438	1.335	3.045	44.000
100.0	10.000	.250	.438	.505	.172	.063	.438	1.283	2.941	40.000
100.0	10.750	.250	.438	.505	.172	.063	.438	1.506	3.386	56.000
100.0	12.000	.250	.438	.505	.172	.063	.438	1.397	3.170	50.000
100.0	12.750	.313	.500	.577	.204	.063	.500	1.727	3.923	56.000
100.0	14.000	.250	.438	.505	.172	.063	.438	1.540	3.454	62.000
100.0	16.000	.250	.438	.505	.172	.063	.438	1.670	3.716	72.000
200.0	1.000	.190	.375	.433	.141	.063	.375	.424	1.133	8.000
200.0	1.250	.190	.375	.433	.141	.063	.375	.471	1.227	10.000
200.0	1.500	.190	.375	.433	.141	.063	.375	.500	1.285	10.000
200.0	2.000	.190	.375	.433	.141	.063	.375	.560	1.405	12.000
200.0	2.375	.190	.375	.433	.141	.063	.375	.686	1.658	14.000
200.0	2.500	.190	.375	.433	.141	.063	.375	.613	1.510	14.000
200.0	3.000	.190	.375	.433	.141	.063	.375	.684	1.654	14.000
200.0	3.500	.250	.438	.505	.172	.063	.438	.850	2.075	14.000
200.0	4.000	.250	.438	.505	.172	.063	.438	.791	1.957	14.000
200.0	4.500	.250	.438	.505	.172	.063	.438	.979	2.334	18.000
200.0	5.000	.250	.438	.505	.172	.063	.438	.930	2.235	16.000
200.0	5.563	.250	.438	.505	.172	.063	.438	1.122	2.620	28.000
200.0	6.000	.250	.438	.505	.172	.063	.438	1.028	2.431	20.000
200.0	6.625	.250	.438	.505	.172	.063	.438	1.220	2.816	36.000
200.0	8.000	.250	.438	.505	.172	.063	.438	1.160	2.694	32.000
200.0	8.625	.250	.438	.505	.172	.063	.438	1.410	3.195	46.000
200.0	10.000	.250	.438	.505	.172	.063	.438	1.368	3.110	46.000
200.0	10.750	.313	.500	.577	.204	.063	.500	1.596	3.660	48.000
200.0	12.000	.250	.438	.505	.172	.063	.438	1.551	3.477	62.000
200.0	12.750	.313	.500	.577	.204	.063	.500	1.862	4.193	64.000
200.0	14.000	.313	.500	.577	.204	.063	.500	1.751	3.972	54.000
200.0	16.000	.313	.500	.577	.204	.063	.500	1.916	4.301	70.000

900.0	1.000	.190	.375	.433	.141	.063	.375	.484	1.103	8.000
900.0	1.250	.190	.375	.433	.141	.063	.375	.486	1.207	8.000
900.0	1.500	.190	.375	.433	.141	.063	.375	.530	1.348	10.000
900.0	2.000	.190	.375	.433	.141	.063	.375	.667	1.499	12.000
900.0	2.375	.250	.438	.505	.172	.063	.438	.731	1.838	10.000
900.0	2.500	.190	.375	.433	.141	.063	.375	.687	1.689	14.000
900.0	3.000	.250	.438	.505	.172	.063	.438	.777	1.929	12.000
900.0	3.500	.250	.438	.505	.172	.063	.438	.929	2.225	18.000
900.0	4.000	.250	.438	.505	.172	.063	.438	.957	2.289	16.000
900.0	4.500	.250	.438	.505	.172	.063	.438	1.099	2.574	24.000
900.0	5.000	.250	.438	.505	.172	.063	.438	1.157	2.698	28.000
900.0	5.563	.313	.500	.577	.204	.063	.500	1.287	3.043	22.000
900.0	6.000	.250	.438	.505	.172	.063	.438	1.321	3.017	32.000
900.0	6.625	.313	.500	.577	.204	.063	.500	1.475	3.419	30.000
900.0	8.000	.313	.500	.577	.204	.063	.500	1.698	3.865	40.000
900.0	8.625	.313	.500	.577	.204	.063	.500	1.853	4.175	44.000
900.0	10.000	.375	.563	.650	.235	.063	.563	2.077	4.716	40.000
900.0	10.750	.375	.563	.650	.235	.063	.563	2.215	4.992	46.000
900.0	12.000	.375	.563	.650	.235	.063	.563	2.455	5.473	54.000
900.0	12.750	.375	.563	.650	.235	.063	.563	2.559	5.681	50.000
900.0	14.000	.438	.688	.794	.266	.063	.688	2.827	6.310	52.000
900.0	16.000	.500	.750	.866	.297	.063	.750	3.217	7.184	52.000
1000.0	1.000	.190	.375	.433	.141	.063	.375	.485	1.256	8.000
1000.0	1.250	.190	.375	.433	.141	.063	.375	.536	1.356	8.000
1000.0	1.500	.190	.375	.433	.141	.063	.375	.621	1.527	10.000
1000.0	2.000	.250	.438	.505	.172	.063	.438	.771	1.916	10.000
1000.0	2.375	.250	.438	.505	.172	.063	.438	.901	2.176	14.000
1000.0	2.500	.250	.438	.505	.172	.063	.438	.884	2.142	14.000
1000.0	3.000	.250	.438	.505	.172	.063	.438	1.032	2.438	18.000
1000.0	3.500	.313	.500	.577	.204	.063	.500	1.198	2.865	16.000
1000.0	4.000	.313	.500	.577	.204	.063	.500	1.263	2.995	20.000
1000.0	4.500	.375	.563	.650	.235	.063	.563	1.360	3.282	18.000
1000.0	5.000	.313	.500	.577	.204	.063	.500	1.495	3.459	28.000
1000.0	5.563	.375	.563	.650	.235	.063	.563	1.578	3.718	24.000
1000.0	6.000	.375	.563	.650	.235	.063	.563	1.750	4.063	26.000
1000.0	6.625	.375	.563	.650	.235	.063	.563	1.807	4.176	32.000
1000.0	8.000	.438	.688	.794	.266	.063	.688	2.226	5.108	30.000
1000.0	8.625	.438	.688	.794	.266	.063	.688	2.290	5.236	34.000
1000.0	10.000	.500	.750	.866	.297	.063	.750	2.609	5.968	32.000
1000.0	10.750	.500	.750	.866	.297	.063	.750	2.845	6.440	36.000
1000.0	12.000	.500	.750	.866	.297	.063	.750	3.147	7.065	42.000
1000.0	12.750	.500	.750	.866	.297	.063	.750	3.309	7.369	44.000
1000.0	14.000	.563	.875	1.010	.328	.063	.875	3.506	7.975	40.000
1000.0	16.000	.625	.938	1.082	.360	.063	.938	4.169	9.235	42.000
1500.0	1.000	.190	.375	.433	.141	.063	.375	.520	1.341	8.000
1500.0	1.250	.250	.438	.505	.172	.063	.438	.606	1.508	6.000
1500.0	1.500	.250	.438	.505	.172	.063	.438	.681	1.738	8.000
1500.0	2.000	.250	.438	.505	.172	.063	.438	.819	2.013	12.000
1500.0	2.375	.313	.500	.577	.204	.063	.500	.961	2.390	16.000
1500.0	2.500	.313	.500	.577	.204	.063	.500	1.004	2.477	12.000
1500.0	3.000	.313	.500	.577	.204	.063	.500	1.140	2.749	16.000
1500.0	3.500	.375	.563	.650	.235	.063	.563	1.244	3.051	18.000
1500.0	4.000	.375	.563	.650	.235	.063	.563	1.453	3.469	18.000
1500.0	4.500	.375	.563	.650	.235	.063	.563	1.495	3.552	22.000
1500.0	5.000	.375	.563	.650	.235	.063	.563	1.645	3.852	26.000
1500.0	5.563	.438	.688	.794	.266	.063	.688	1.818	4.291	22.000
1500.0	6.000	.438	.688	.794	.266	.063	.688	1.882	4.420	24.000
1500.0	6.625	.500	.750	.866	.297	.063	.750	2.134	5.019	22.000
1500.0	8.000	.500	.750	.866	.297	.063	.750	2.506	5.762	20.000
1500.0	8.625	.500	.750	.866	.297	.063	.750	2.724	6.199	30.000
1500.0	10.000	.563	.875	1.010	.328	.063	.875	3.085	7.013	30.000
1500.0	10.750	.625	.938	1.082	.360	.063	.938	3.480	7.898	28.000
1500.0	12.000	.750	1.063	1.228	.422	.063	1.063	3.799	8.723	26.000
1500.0	12.750	.750	1.063	1.228	.422	.063	1.063	4.068	9.261	28.000
1500.0	14.000	.875	1.250	1.445	.485	.063	1.250	4.483	10.279	24.000
1500.0	16.000	1.000	1.438	1.660	.547	.063	1.438	5.242	11.905	26.000

TABLE C-6. BOLT, ALUMINUM, LOOSE-RING/LOOSE-RING, CRYOGENIC FLUID CONNECTOR

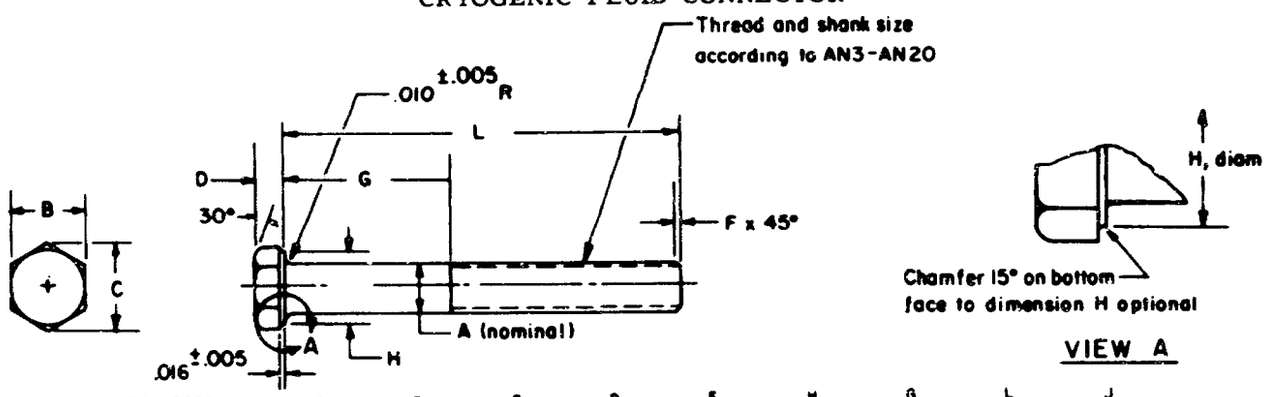

PRESSURE	PIPE/TUBE OD	A	B	C	D	F	H	G	L	J
100.0	1.000	.190	.375	.433	.141	.063	.375	.545	1.335	8.000
100.0	1.250	.190	.375	.433	.141	.063	.375	.572	1.429	10.000
100.0	1.500	.190	.375	.433	.141	.063	.375	.601	1.487	10.000
100.0	2.000	.190	.375	.433	.141	.063	.375	.676	1.637	12.000
100.0	2.375	.190	.375	.433	.141	.063	.375	.861	2.008	14.000
100.0	2.500	.190	.375	.433	.141	.063	.375	.744	1.772	14.000
100.0	3.000	.190	.375	.433	.141	.063	.375	.800	1.886	14.000
100.0	3.500	.250	.438	.505	.172	.063	.438	1.091	2.557	12.000
100.0	4.000	.250	.438	.505	.172	.063	.438	.966	2.307	16.000
100.0	4.500	.250	.438	.505	.172	.063	.438	1.250	2.878	18.000
100.0	5.000	.250	.438	.505	.172	.063	.438	1.060	2.495	18.000
100.0	5.563	.250	.438	.505	.172	.063	.438	1.505	3.386	26.000
100.0	6.000	.250	.438	.505	.172	.063	.438	1.172	2.718	20.000
100.0	6.625	.250	.438	.505	.172	.063	.438	1.648	3.672	32.000
100.0	8.000	.250	.438	.505	.172	.063	.438	1.365	3.106	22.000
100.0	8.625	.250	.438	.505	.172	.063	.438	1.883	4.141	44.000
100.0	10.000	.250	.438	.505	.172	.063	.438	1.743	3.861	40.000
100.0	10.750	.250	.438	.505	.172	.063	.438	2.224	4.822	56.000
100.0	12.000	.250	.438	.505	.172	.063	.438	1.982	4.180	50.000
100.0	12.750	.313	.500	.577	.204	.063	.500	2.627	5.723	56.000
100.0	14.000	.250	.438	.505	.172	.063	.438	2.075	4.524	62.000
100.0	16.000	.250	.438	.505	.172	.063	.438	2.235	4.846	72.000
200.0	1.000	.190	.375	.433	.141	.063	.375	.540	1.365	8.000
200.0	1.250	.190	.375	.433	.141	.063	.375	.587	1.459	10.000
200.0	1.500	.190	.375	.433	.141	.063	.375	.616	1.517	10.000
200.0	2.000	.190	.375	.433	.141	.063	.375	.706	1.697	12.000
200.0	2.375	.190	.375	.433	.141	.063	.375	.891	2.068	14.000
200.0	2.500	.190	.375	.433	.141	.063	.375	.774	1.832	14.000
200.0	3.000	.190	.375	.433	.141	.063	.375	.845	1.976	14.000
200.0	3.500	.250	.438	.505	.172	.063	.438	1.151	2.677	14.000
200.0	4.000	.250	.438	.505	.172	.063	.438	.996	2.367	14.000
200.0	4.500	.250	.438	.505	.172	.063	.438	1.295	2.966	18.000
200.0	5.000	.250	.438	.505	.172	.063	.438	1.120	2.615	16.000
200.0	5.563	.250	.438	.505	.172	.063	.438	1.565	3.506	20.000
200.0	6.000	.250	.438	.505	.172	.063	.438	1.251	2.877	20.000
200.0	6.625	.250	.438	.505	.172	.063	.438	1.708	3.792	36.000
200.0	8.000	.250	.438	.505	.172	.063	.438	1.557	3.488	32.000
200.0	8.625	.250	.438	.505	.172	.063	.438	2.033	4.441	46.000
200.0	10.000	.250	.438	.505	.172	.063	.438	1.834	4.043	46.000
200.0	10.750	.313	.500	.577	.204	.063	.500	2.374	5.216	48.000
200.0	12.000	.250	.438	.505	.172	.063	.438	2.146	4.659	62.000
200.0	12.750	.313	.500	.577	.204	.063	.500	2.807	6.083	64.000
200.0	14.000	.313	.500	.577	.204	.063	.500	2.491	5.451	54.000
200.0	16.000	.313	.500	.577	.204	.063	.500	2.800	6.069	70.000

500.0	1.000	.190	.375	.433	.141	.063	.375	.570	1.425	8.000
500.0	1.250	.190	.375	.433	.141	.063	.375	.617	1.519	8.000
500.0	1.500	.190	.375	.433	.141	.063	.375	.661	1.607	10.000
500.0	2.000	.190	.375	.433	.141	.063	.375	.772	1.830	12.000
500.0	2.375	.250	.438	.505	.172	.063	.438	.951	2.278	10.000
500.0	2.500	.190	.375	.433	.141	.063	.375	.882	2.049	16.000
500.0	3.000	.250	.438	.505	.172	.063	.438	.987	2.350	12.000
500.0	3.500	.250	.438	.505	.172	.063	.438	1.241	2.857	18.000
500.0	4.000	.250	.438	.505	.172	.063	.438	1.242	2.859	16.000
500.0	4.500	.250	.438	.505	.172	.063	.438	1.445	3.266	24.000
500.0	5.000	.250	.438	.505	.172	.063	.438	1.488	3.350	28.000
500.0	5.563	.313	.500	.577	.204	.063	.500	1.730	3.929	22.000
500.0	6.000	.250	.438	.505	.172	.063	.438	1.756	3.988	32.000
500.0	6.625	.313	.500	.577	.204	.063	.500	1.983	4.395	30.000
500.0	8.000	.313	.500	.577	.204	.063	.500	2.299	5.066	40.000
500.0	8.625	.313	.500	.577	.204	.063	.500	2.569	5.607	44.000
500.0	10.000	.375	.563	.650	.235	.063	.563	2.828	6.218	40.000
500.0	10.750	.375	.563	.650	.235	.063	.563	3.070	6.702	46.000
500.0	12.000	.375	.563	.650	.235	.063	.563	3.416	7.395	54.000
500.0	12.750	.375	.563	.650	.235	.063	.563	3.688	7.935	56.000
500.0	14.000	.438	.688	.794	.266	.063	.688	3.998	8.652	52.000
500.0	16.000	.500	.750	.866	.297	.063	.750	4.598	9.947	52.000
1000.0	1.000	.190	.375	.433	.141	.063	.375	.605	1.495	6.000
1000.0	1.250	.190	.375	.433	.141	.063	.375	.685	1.655	8.000
1000.0	1.500	.190	.375	.433	.141	.063	.375	.785	1.856	10.000
1000.0	2.000	.250	.438	.505	.172	.063	.438	.935	2.244	10.000
1000.0	2.375	.250	.438	.505	.172	.063	.438	1.194	2.762	14.000
1000.0	2.500	.250	.438	.505	.172	.063	.438	1.137	2.650	14.000
1000.0	3.000	.250	.438	.505	.172	.063	.438	1.330	3.035	18.000
1000.0	3.500	.313	.500	.577	.204	.063	.500	1.498	3.465	16.000
1000.0	4.000	.313	.500	.577	.204	.063	.500	1.696	3.861	20.000
1000.0	4.500	.375	.563	.650	.235	.063	.563	2.059	4.688	18.000
1000.0	5.000	.313	.500	.577	.204	.063	.500	2.107	4.684	28.000
1000.0	5.563	.375	.563	.650	.235	.063	.563	2.394	5.350	24.000
1000.0	6.000	.375	.563	.650	.235	.063	.563	2.542	5.647	26.000
1000.0	6.625	.375	.563	.650	.235	.063	.563	2.742	6.096	32.000
1000.0	8.000	.438	.688	.794	.266	.063	.688	3.287	7.238	30.000
1000.0	8.625	.438	.688	.794	.266	.063	.688	3.339	7.334	34.000
1000.0	10.000	.500	.750	.866	.297	.063	.750	3.954	8.658	32.000
1000.0	10.750	.500	.750	.866	.297	.063	.750	4.145	9.040	36.000
1000.0	12.000	.500	.750	.866	.297	.063	.750	4.626	10.002	42.000
1000.0	12.750	.500	.750	.866	.297	.063	.750	4.781	10.313	44.000
1000.0	14.000	.563	.875	1.010	.328	.063	.875	5.299	11.441	40.000
1000.0	16.000	.625	.938	1.082	.360	.063	.938	5.911	12.759	42.000
1500.0	1.000	.190	.375	.433	.141	.063	.375	.691	1.667	8.000
1500.0	1.250	.250	.438	.505	.172	.063	.438	.806	1.988	6.000
1500.0	1.500	.250	.438	.505	.172	.063	.438	.904	2.182	8.000
1500.0	2.000	.250	.438	.505	.172	.063	.438	1.130	2.635	12.000
1500.0	2.375	.313	.500	.577	.204	.063	.500	1.314	3.096	10.000
1500.0	2.500	.313	.500	.577	.204	.063	.500	1.374	3.218	12.000
1500.0	3.000	.313	.500	.577	.204	.063	.500	1.614	3.698	16.000
1500.0	3.500	.375	.563	.650	.235	.063	.563	1.991	4.545	16.000
1500.0	4.000	.375	.563	.650	.235	.063	.563	2.166	4.894	18.000
1500.0	4.500	.375	.563	.650	.235	.063	.563	2.329	5.220	22.000
1500.0	5.000	.375	.563	.650	.235	.063	.563	2.581	5.724	26.000
1500.0	5.563	.438	.688	.794	.266	.063	.688	2.784	6.223	22.000
1500.0	6.000	.438	.688	.794	.266	.063	.688	2.920	6.497	24.000
1500.0	6.625	.500	.750	.866	.297	.063	.750	2.998	6.747	22.000
1500.0	8.000	.500	.750	.866	.297	.063	.750	3.676	8.101	28.000
1500.0	8.625	.500	.750	.866	.297	.063	.750	3.724	8.199	30.000
1500.0	10.000	.563	.875	1.010	.328	.063	.875	4.530	9.916	30.000
1500.0	10.750	.625	.938	1.082	.360	.063	.938	4.711	10.360	28.000
1500.0	12.000	.750	1.063	1.228	.422	.063	1.063	5.501	12.128	26.000
1500.0	12.750	.750	1.063	1.228	.422	.063	1.063	5.517	12.159	28.000
1500.0	14.000	.875	1.250	1.445	.485	.063	1.250	6.212	13.736	26.000
1500.0	16.000	1.000	1.438	1.660	.547	.063	1.438	7.147	15.794	26.000

TABLE C-7. STUD, ALUMINUM, INTEGRAL/INTEGRAL AND LOOSE-RING/ LOOSE-RING CRYOGENIC FLUID CONNECTOR

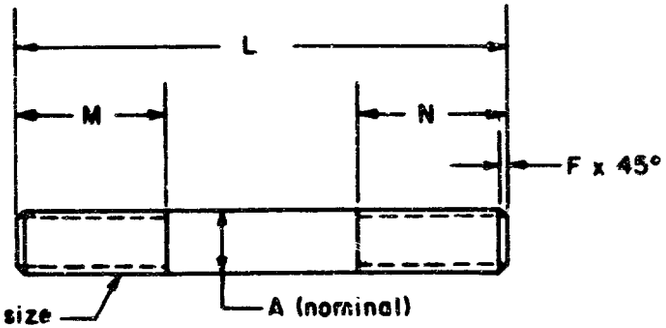

Note: J = Number of studs

PRESSURE	PIPE/TUBE OD	Integral/Integral Flanges A	L	F	M	N	J	Loose-Ring/Loose-Ring Flanges A	L	F	M	N	J
100.0	1.000	.190	1.418	.063	.402	.402	8.000	.190	1.620	.063	.452	.452	8.000
100.0	1.250	.190	1.482	.063	.418	.418	10.000	.190	1.714	.063	.476	.476	10.000
100.0	1.500	.190	1.540	.063	.433	.433	10.000	.190	1.772	.063	.491	.491	10.000
100.0	2.000	.190	1.660	.063	.462	.462	12.000	.190	1.922	.063	.528	.528	12.000
100.0	2.375	.190	1.913	.063	.526	.526	14.000	.190	2.293	.063	.621	.621	14.000
100.0	2.500	.190	1.765	.063	.489	.489	14.000	.190	2.057	.063	.562	.562	14.000
100.0	3.000	.190	1.849	.063	.510	.510	14.000	.190	2.171	.063	.590	.590	14.000
100.0	3.500	.250	2.420	.063	.667	.667	12.000	.250	2.932	.063	.795	.795	12.000
100.0	4.000	.250	2.242	.063	.623	.623	16.000	.250	2.682	.063	.733	.733	16.000
100.0	4.500	.250	2.649	.063	.725	.725	18.000	.250	3.251	.063	.875	.875	18.000
100.0	5.000	.250	2.460	.063	.678	.678	18.000	.250	2.870	.063	.780	.780	18.000
100.0	5.563	.250	2.935	.063	.796	.796	26.000	.250	3.761	.063	1.003	1.003	26.000
100.0	6.000	.250	2.653	.063	.726	.726	20.000	.250	3.093	.063	.836	.836	20.000
100.0	6.625	.250	3.101	.063	.838	.838	32.000	.250	4.047	.063	1.074	1.074	32.000
100.0	8.000	.250	2.861	.063	.778	.778	22.000	.250	3.481	.063	.933	.933	22.000
100.0	8.625	.250	3.420	.063	.918	.918	44.000	.250	4.516	.063	1.192	1.192	44.000
100.0	10.000	.250	3.316	.063	.891	.891	40.000	.250	4.236	.063	1.121	1.121	40.000
100.0	10.750	.250	3.761	.063	1.003	1.003	56.000	.250	5.197	.063	1.362	1.362	56.000
100.0	12.000	.250	3.545	.063	.949	.949	50.000	.250	4.555	.063	1.201	1.291	50.000
100.0	12.750	.313	4.391	.063	1.176	1.176	56.000	.313	6.191	.063	1.626	1.626	56.000
100.0	14.000	.250	3.829	.063	1.020	1.020	62.000	.250	4.899	.063	1.287	1.287	62.000
100.0	16.000	.250	4.091	.063	1.085	1.085	72.000	.250	5.221	.063	1.368	1.368	72.000
200.0	1.000	.190	1.418	.063	.402	.402	8.000	.190	1.650	.063	.460	.460	8.000
200.0	1.250	.190	1.512	.063	.426	.426	10.000	.190	1.744	.063	.484	.484	10.000
200.0	1.500	.190	1.570	.063	.440	.440	10.000	.190	1.802	.063	.498	.498	10.000
200.0	2.000	.190	1.690	.063	.470	.470	12.000	.190	1.982	.063	.543	.543	12.000
200.0	2.375	.190	1.943	.063	.533	.533	14.000	.190	2.353	.063	.636	.636	14.000
200.0	2.500	.190	1.795	.063	.496	.496	14.000	.190	2.117	.063	.577	.577	14.000
200.0	3.000	.190	1.939	.063	.532	.532	14.000	.190	2.261	.063	.613	.613	14.000
200.0	3.500	.250	2.450	.063	.675	.675	14.000	.250	3.052	.063	.825	.825	14.000
200.0	4.000	.250	2.332	.063	.645	.645	14.000	.250	2.742	.063	.748	.748	14.000
200.0	4.500	.250	2.709	.063	.740	.740	18.000	.250	3.341	.063	.898	.898	18.000
200.0	5.000	.250	2.610	.063	.715	.715	16.000	.250	2.990	.063	.810	.810	16.000
200.0	5.563	.250	2.995	.063	.811	.811	28.000	.250	3.881	.063	1.033	1.033	28.000
200.0	6.000	.250	2.806	.063	.764	.764	20.000	.250	3.252	.063	.875	.875	20.000
200.0	6.625	.250	3.191	.063	.860	.860	36.000	.250	4.167	.063	1.104	1.104	36.000
200.0	8.000	.250	3.069	.063	.830	.830	32.000	.250	3.863	.063	1.028	1.028	32.000
200.0	8.625	.250	3.570	.063	.955	.955	46.000	.250	4.816	.063	1.267	1.267	46.000
200.0	10.000	.250	3.485	.063	.934	.934	46.000	.250	4.418	.063	1.167	1.167	46.000
200.0	10.750	.313	4.129	.063	1.110	1.110	48.000	.313	5.685	.063	1.499	1.499	48.000
200.0	12.000	.250	3.852	.063	1.025	1.025	62.000	.250	5.043	.063	1.323	1.323	62.000
200.0	12.750	.313	4.661	.063	1.243	1.243	64.000	.313	6.551	.063	1.716	1.716	64.000
200.0	14.000	.313	4.440	.063	1.188	1.188	54.000	.313	5.919	.063	1.558	1.558	54.000
200.0	16.000	.313	4.770	.063	1.271	1.271	70.000	.313	6.537	.063	1.712	1.712	70.000

500.0	1.000	.190	1.478	.063	.417	.417	8.000
500.0	1.250	.190	1.542	.063	.433	.433	8.000
500.0	1.500	.190	1.630	.063	.455	.455	10.000
500.0	2.000	.190	1.784	.063	.494	.494	12.000
500.0	2.375	.250	2.213	.063	.616	.616	10.000
500.0	2.500	.190	1.944	.063	.533	.533	16.000
500.0	3.000	.250	2.304	.063	.639	.639	12.000
500.0	3.500	.250	2.600	.063	.712	.712	18.000
500.0	4.000	.250	2.664	.063	.728	.728	18.000
500.0	4.500	.250	2.949	.063	.800	.800	24.000
500.0	5.000	.250	3.065	.063	.829	.829	28.000
500.0	5.563	.313	3.512	.063	.956	.956	22.000
500.0	6.000	.250	3.392	.063	.911	.911	32.000
500.0	6.625	.313	3.886	.063	1.050	1.050	30.000
500.0	8.000	.438	4.934	.063	1.162	1.162	40.000
500.0	8.625	.313	4.643	.063	1.239	1.239	44.000
500.0	10.000	.375	5.279	.063	1.413	1.413	40.000
500.0	10.750	.375	5.554	.063	1.482	1.482	46.000
500.0	12.000	.375	6.038	.063	1.603	1.603	54.000
500.0	12.750	.375	6.244	.063	1.655	1.655	56.000
500.0	14.000	.438	6.966	.063	1.851	1.851	52.000
500.0	16.000	.500	7.934	.063	2.109	2.109	52.000
1000.0	1.000	.190	1.541	.063	.433	.433	6.000
1000.0	1.250	.190	1.641	.063	.454	.454	8.000
1000.0	1.500	.190	1.812	.063	.501	.501	10.000
1000.0	2.000	.250	2.291	.063	.635	.635	10.000
1000.0	2.375	.250	2.551	.063	.730	.730	14.000
1000.0	2.500	.250	2.517	.063	.692	.692	14.000
1000.0	3.000	.250	2.813	.063	.766	.766	18.000
1000.0	3.500	.313	3.333	.063	.911	.911	16.000
1000.0	4.000	.313	3.488	.063	.944	.944	20.000
1000.0	4.500	.375	3.945	.063	1.055	1.055	18.000
1000.0	5.000	.313	3.927	.063	1.060	1.060	26.000
1000.0	5.563	.375	4.280	.063	1.164	1.164	24.000
1000.0	6.000	.375	4.625	.063	1.250	1.250	26.000
1000.0	6.625	.375	4.739	.063	1.274	1.274	32.000
1000.0	8.000	.438	5.765	.063	1.551	1.551	30.000
1000.0	8.625	.438	5.942	.063	1.582	1.582	34.000
1000.0	10.000	.500	6.718	.063	1.805	1.805	32.000
1000.0	10.750	.500	7.190	.063	1.922	1.922	36.000
1000.0	12.000	.500	7.795	.063	2.074	2.074	42.000
1000.0	12.750	.500	8.114	.063	2.155	2.155	44.000
1000.0	14.000	.563	8.819	.063	2.345	2.345	40.000
1000.0	16.000	.625	10.173	.063	2.699	2.699	42.000
1500.0	1.000	.190	1.620	.063	.454	.454	8.000
1500.0	1.250	.250	1.963	.063	.553	.553	6.000
1500.0	1.500	.250	2.113	.063	.591	.591	8.000
1500.0	2.000	.250	2.388	.063	.659	.659	12.000
1500.0	2.375	.313	2.859	.063	.793	.793	10.000
1500.0	2.500	.313	2.946	.063	.815	.815	12.000
1500.0	3.000	.313	3.218	.063	.883	.883	16.000
1500.0	3.500	.375	3.613	.063	.997	.997	16.000
1500.0	4.000	.375	4.032	.063	1.102	1.102	18.000
1500.0	4.500	.375	4.115	.063	1.122	1.122	22.000
1500.0	5.000	.375	4.415	.063	1.197	1.197	26.000
1500.0	5.563	.438	4.948	.063	1.346	1.346	22.000
1500.0	6.000	.438	5.076	.063	1.378	1.378	24.000
1500.0	6.625	.500	5.769	.063	1.567	1.567	22.000
1500.0	8.000	.500	6.512	.063	1.753	1.753	28.000
1500.0	8.625	.500	6.949	.063	1.862	1.862	30.000
1500.0	10.000	.563	7.857	.063	2.105	2.105	30.000
1500.0	10.750	.625	8.835	.063	2.365	2.365	28.000
1500.0	12.000	.750	9.848	.063	2.650	2.650	26.000
1500.0	12.750	.750	10.386	.063	2.784	2.784	28.000
1500.0	14.000	.875	11.591	.063	3.117	3.117	26.000
1500.0	16.000	1.000	13.685	.063	3.621	3.621	26.000
.190	1.710	.063	.475	.475	8.000		
.190	1.804	.063	.499	.499	8.000		
.190	1.892	.063	.521	.521	10.000		
.190	2.115	.063	.576	.576	12.000		
.250	2.653	.063	.726	.726	10.000		
.190	2.334	.063	.631	.631	16.000		
.250	2.725	.063	.744	.744	12.000		
.250	3.232	.063	.870	.870	18.000		
.250	3.234	.063	.871	.871	18.000		
.250	3.641	.063	.973	.973	24.000		
.250	3.725	.063	.994	.994	28.000		
.313	4.398	.063	1.178	1.178	22.000		
.250	4.262	.063	1.128	1.128	32.000		
.313	4.664	.063	1.294	1.294	30.000		
.313	5.535	.063	1.462	1.462	40.000		
.313	6.075	.063	1.597	1.597	44.000		
.375	6.780	.063	1.769	1.769	40.000		
.375	7.264	.063	1.910	1.910	46.000		
.375	7.958	.063	2.083	2.083	54.000		
.375	8.498	.063	2.218	2.218	56.000		
.438	9.308	.063	2.438	2.438	52.000		
.500	10.697	.063	2.799	2.799	52.000		
.190	1.780	.063	.493	.493	6.000		
.190	1.940	.063	.532	.532	8.000		
.190	2.141	.063	.583	.583	10.000		
.250	2.619	.063	.717	.717	10.000		
.250	3.137	.063	.847	.847	14.000		
.250	3.025	.063	.819	.819	16.000		
.250	3.419	.063	.915	.915	18.000		
.313	3.933	.063	1.061	1.061	16.000		
.313	4.330	.063	1.161	1.161	20.000		
.375	5.243	.063	1.404	1.404	18.000		
.313	5.152	.063	1.366	1.366	28.000		
.375	5.912	.063	1.572	1.572	24.000		
.375	6.209	.063	1.646	1.646	26.000		
.375	6.609	.063	1.746	1.746	32.000		
.438	7.687	.063	2.081	2.081	30.000		
.438	7.990	.063	2.167	2.167	34.000		
.500	9.408	.063	2.477	2.477	32.000		
.500	9.790	.063	2.572	2.572	36.000		
.500	10.752	.063	2.813	2.813	42.000		
.500	11.063	.063	2.891	2.891	44.000		
.563	12.285	.063	3.212	3.212	40.000		
.625	13.697	.063	3.588	3.588	42.000		
.190	1.952	.063	.536	.536	8.000		
.250	2.363	.063	.653	.653	6.000		
.250	2.557	.063	.702	.702	8.000		
.250	3.010	.063	.815	.815	12.000		
.313	3.565	.063	.969	.969	10.000		
.313	3.686	.063	1.000	1.000	12.000		
.313	4.166	.063	1.120	1.120	16.000		
.375	5.107	.063	1.371	1.371	16.000		
.375	5.456	.063	1.458	1.458	18.000		
.375	5.783	.063	1.539	1.539	22.000		
.375	6.206	.063	1.665	1.665	26.000		
.438	6.880	.063	1.829	1.829	22.000		
.438	7.153	.063	1.898	1.898	24.000		
.500	7.497	.063	1.999	1.999	22.000		
.500	8.851	.063	2.338	2.338	28.000		
.500	8.949	.063	2.362	2.362	30.000		
.563	10.759	.063	2.830	2.830	30.000		
.625	11.297	.063	2.981	2.981	28.000		
.750	13.253	.063	3.501	3.501	26.000		
.750	13.284	.063	3.508	3.508	28.000		
.875	15.048	.063	3.981	3.981	26.000		
1.000	17.294	.063	4.574	4.574	26.000		

TABLE C-8. FLANGE, INTEGRAL, CRES, CRYOGENIC FLUID CONNECTOR

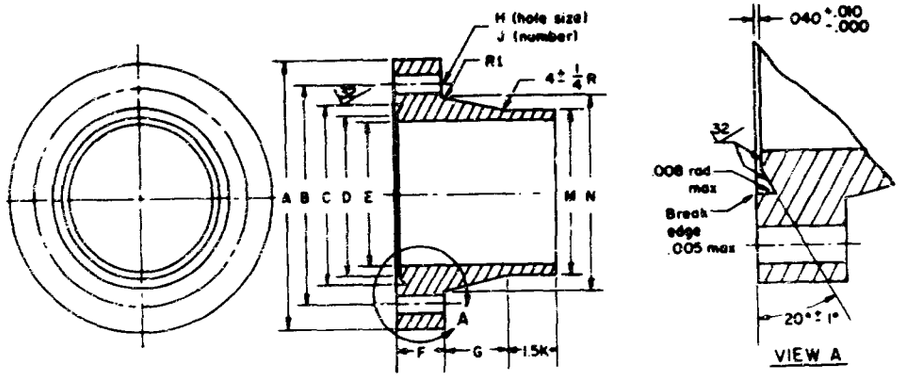

PRESSURE	PIPE/TUBE OD	A	B	C	D	E	F	G	H	J	M	N	R1	K
100.0	1.000	2.173	1.771	1.364	1.070	.944	.324	.325	.201	6.000	1.000	1.034	.125	.500
100.0	1.250	2.450	2.048	1.641	1.341	1.194	.339	.366	.201	8.000	1.250	1.294	.125	.517
100.0	1.500	2.728	2.326	1.918	1.612	1.444	.354	.402	.201	8.000	1.500	1.544	.125	.533
100.0	2.000	3.272	2.878	2.462	2.144	1.944	.384	.467	.201	8.000	2.000	2.054	.125	.567
100.0	2.375	3.681	3.199	2.790	2.463	2.245	.540	.764	.201	10.000	2.375	2.517	.125	.592
100.0	2.500	3.807	3.465	2.995	2.665	2.444	.414	.523	.201	10.300	2.500	2.564	.125	.600
100.0	3.000	4.352	3.950	3.539	3.197	2.944	.444	.574	.201	10.000	3.000	3.064	.125	.633
100.0	3.500	4.968	4.438	3.962	3.608	3.334	.699	1.052	.265	10.000	3.500	3.691	.125	.667
100.0	4.000	5.602	5.072	4.595	4.229	3.930	.555	.742	.265	10.000	4.000	4.097	.125	.700
100.0	4.500	6.038	5.508	5.030	4.652	4.334	.789	1.200	.265	14.000	4.500	4.681	.188	.733
100.0	5.000	6.662	6.132	5.653	5.263	4.930	.615	.831	.265	12.000	5.000	5.087	.188	.767
100.0	5.563	7.160	6.630	6.097	5.693	5.345	.972	1.527	.265	20.000	5.563	5.817	.188	.804
100.0	6.000	7.737	7.202	6.721	6.307	5.930	.660	.911	.265	14.000	6.000	6.097	.188	.833
100.0	6.625	8.262	7.712	7.228	6.799	6.407	1.002	1.671	.265	26.000	6.625	6.899	.188	.875
100.0	8.000	9.869	9.339	8.836	8.374	7.930	.765	1.054	.265	16.000	8.000	8.107	.188	.967
100.0	8.625	10.386	9.856	9.343	8.866	8.407	1.167	1.915	.265	34.000	8.625	8.909	.250	1.008
100.0	10.000	11.938	11.408	10.895	10.365	9.870	1.080	1.602	.265	30.000	10.000	10.182	.250	1.100
100.0	10.750	12.596	12.066	11.522	10.996	10.482	1.362	2.370	.265	46.000	10.750	11.037	.250	1.150
100.0	12.000	14.073	13.543	12.980	12.422	11.870	1.185	1.757	.265	36.000	12.000	12.202	.250	1.233
100.0	12.750	14.665	14.135	13.561	12.985	12.420	1.575	2.863	.265	60.000	12.750	13.002	.313	1.283
100.0	14.000	16.198	15.668	15.075	14.469	13.870	1.320	1.899	.265	44.000	14.000	14.192	.313	1.367
100.0	16.000	18.324	17.794	17.171	16.517	15.870	1.455	2.031	.265	52.000	16.000	16.202	.313	1.500
200.0	1.000	2.174	1.772	1.364	1.070	.944	.324	.325	.201	6.000	1.000	1.034	.125	.500
200.0	1.250	2.451	2.049	1.641	1.341	1.194	.339	.366	.201	8.000	1.250	1.294	.125	.517
200.0	1.500	2.729	2.327	1.918	1.612	1.444	.369	.402	.201	8.000	1.500	1.544	.125	.533
200.0	2.000	3.274	2.872	2.462	2.144	1.944	.399	.467	.201	8.000	2.000	2.054	.125	.567
200.0	2.375	3.683	3.201	2.790	2.463	2.245	.555	.764	.201	12.000	2.375	2.507	.125	.592
200.0	2.500	3.809	3.467	2.995	2.665	2.444	.429	.523	.201	10.000	2.500	2.564	.125	.600
200.0	3.000	4.355	3.953	3.539	3.197	2.944	.474	.574	.201	10.000	3.000	3.064	.125	.633
200.0	3.500	4.971	4.441	3.962	3.608	3.334	.714	1.052	.265	10.000	3.500	3.691	.125	.667
200.0	4.000	5.606	5.076	4.595	4.229	3.930	.565	.742	.265	10.000	4.000	4.097	.125	.700
200.0	4.500	6.041	5.511	5.030	4.652	4.334	.819	1.200	.265	14.000	4.500	4.681	.188	.733
200.0	5.000	6.666	6.136	5.653	5.263	4.930	.645	.831	.265	12.000	5.000	5.087	.188	.767
200.0	5.563	7.150	6.620	6.097	5.693	5.345	.987	1.527	.265	22.000	5.563	5.807	.188	.804
200.0	6.000	7.737	7.207	6.721	6.307	5.930	.705	.911	.265	14.000	6.000	6.097	.188	.833
200.0	6.625	8.246	7.716	7.228	6.799	6.407	1.047	1.671	.265	28.000	6.625	6.899	.188	.875
200.0	8.000	9.847	9.317	8.814	8.352	7.912	.896	1.178	.265	22.000	8.000	8.162	.188	.967
200.0	8.625	10.386	9.856	9.343	8.866	8.407	1.212	1.915	.265	38.000	8.625	8.909	.250	1.008
200.0	10.000	11.960	11.430	10.897	10.387	9.890	1.169	1.472	.265	32.000	10.000	10.147	.250	1.100
200.0	10.750	12.596	12.066	11.522	10.996	10.482	1.437	2.370	.265	52.000	10.750	11.027	.250	1.150
200.0	12.000	14.073	13.543	12.980	12.422	11.869	1.307	1.767	.265	44.000	12.000	12.193	.250	1.233
200.0	12.750	14.665	14.135	13.561	12.985	12.420	1.650	2.863	.265	64.000	12.750	13.002	.313	1.283
200.0	14.000	16.176	15.646	15.053	14.447	13.847	1.520	2.061	.265	58.000	14.000	14.218	.313	1.367
200.0	16.000	18.279	17.749	17.126	16.472	15.825	1.718	2.355	.265	74.000	16.000	16.264	.313	1.500

500.0	1.000	2.175	1.773	1.364	1.070	.944	.354	.325	.201	6.000	1.000	1.034	.125	.500
500.0	1.250	2.453	2.051	1.641	1.341	1.194	.369	.366	.201	6.000	1.250	1.294	.125	.517
500.0	1.500	2.731	2.329	1.916	1.612	1.444	.384	.402	.201	8.000	1.500	1.544	.125	.533
500.0	2.000	3.278	2.876	2.462	2.144	1.946	.442	.460	.201	6.000	2.000	2.054	.125	.567
500.0	2.375	3.607	3.205	2.790	2.463	2.245	.505	.764	.201	12.000	2.375	2.507	.125	.592
500.0	2.500	3.802	3.400	2.984	2.654	2.432	.492	.575	.201	10.000	2.500	2.577	.125	.600
500.0	3.000	4.327	3.925	3.507	3.165	2.918	.573	.690	.201	14.000	3.000	3.090	.125	.633
500.0	3.500	4.977	4.447	3.962	3.600	3.334	.759	1.052	.265	14.000	3.500	3.691	.125	.667
500.0	4.000	5.568	5.030	4.552	4.186	3.891	.733	.921	.265	12.000	4.000	4.137	.125	.700
500.0	4.500	6.049	5.519	5.030	4.652	4.334	.804	1.200	.265	18.000	4.500	4.681	.188	.733
500.0	5.000	6.600	6.078	5.586	5.196	4.864	.879	1.151	.265	20.000	5.000	5.154	.188	.767
500.0	5.563	7.150	6.620	6.097	5.693	5.345	1.047	1.527	.265	20.000	5.563	5.807	.188	.804
500.0	6.000	7.647	7.117	6.621	6.207	5.837	1.010	1.301	.265	26.000	6.000	6.211	.188	.833
500.0	6.625	8.256	7.726	7.228	6.799	6.407	1.137	1.671	.265	34.000	6.625	6.899	.188	.875
500.0	8.000	9.715	9.185	8.681	8.219	7.782	1.242	1.841	.265	40.000	8.000	8.384	.188	.967
500.0	8.625	10.298	9.760	9.255	8.778	8.329	1.374	2.221	.265	44.000	8.625	8.819	.250	1.000
500.0	10.000	11.963	11.327	10.731	10.221	9.728	1.540	2.302	.320	40.000	10.000	10.258	.250	1.100
500.0	10.750	12.729	12.073	11.466	10.938	10.420	1.650	2.622	.320	44.000	10.750	10.982	.250	1.150
500.0	12.000	14.553	13.497	12.781	12.223	11.673	1.795	2.762	.320	52.000	12.000	12.272	.250	1.233
500.0	12.750	14.734	14.070	13.273	12.677	11.938	1.863	3.403	.320	56.000	12.750	12.953	.313	1.283
500.0	14.000	16.132	15.476	14.820	14.214	13.619	2.087	3.222	.320	66.000	14.000	14.245	.313	1.367
500.0	16.000	18.202	17.546	16.860	16.206	15.564	2.363	3.603	.320	76.000	16.000	16.249	.313	1.500
1000.0	1.000	2.406	2.004	1.464	1.150	.944	.366	.319	.201	6.000	1.000	1.043	.125	.500
1000.0	1.250	2.667	2.265	1.715	1.410	1.183	.401	.399	.201	8.000	1.250	1.307	.125	.517
1000.0	1.500	2.930	2.528	1.975	1.669	1.419	.436	.479	.201	10.000	1.500	1.570	.125	.533
1000.0	2.000	3.457	3.055	2.506	2.188	1.892	.507	.639	.201	14.000	2.000	2.107	.125	.567
1000.0	2.375	3.848	3.445	2.790	2.573	2.245	.555	.764	.201	16.000	2.375	2.517	.125	.592
1000.0	2.500	4.167	3.637	3.025	2.698	2.365	.507	.799	.265	12.000	2.500	2.654	.125	.600
1000.0	3.000	4.647	4.157	3.549	3.207	2.838	.663	.958	.265	14.000	3.000	3.210	.125	.633
1000.0	3.500	5.152	4.622	4.017	3.661	3.260	.763	1.251	.265	20.000	3.500	3.770	.125	.667
1000.0	4.000	5.717	5.187	4.581	4.215	3.784	.804	1.270	.265	22.000	4.000	4.274	.125	.700
1000.0	4.500	5.945	5.455	4.849	4.471	4.026	.876	1.954	.265	24.000	4.500	4.618	.188	.733
1000.0	5.000	6.738	6.208	5.603	5.213	4.730	.947	1.557	.265	28.000	5.000	5.227	.188	.767
1000.0	5.563	7.286	6.530	5.957	5.553	5.047	1.029	2.202	.328	24.000	5.563	5.692	.188	.804
1000.0	6.000	7.958	7.302	6.625	6.211	5.676	1.115	1.917	.328	28.000	6.000	6.211	.188	.833
1000.0	6.625	8.391	7.735	7.054	6.625	6.065	1.140	2.506	.328	30.000	6.625	6.765	.188	.875
1000.0	8.000	10.008	9.352	8.660	8.198	7.569	1.427	2.555	.328	40.000	8.000	8.160	.188	.967
1000.0	8.625	10.454	9.798	9.101	8.624	7.981	1.386	3.286	.328	42.000	8.625	8.786	.250	1.000
1000.0	10.000	12.038	11.382	10.674	10.164	9.461	1.694	3.196	.328	48.000	10.000	10.135	.250	1.100
1000.0	10.750	12.645	11.989	11.276	10.748	10.020	1.635	3.825	.328	52.000	10.750	10.932	.250	1.150
1000.0	12.000	14.274	13.480	12.688	12.130	11.353	2.036	3.833	.397	52.000	12.000	12.152	.250	1.233
1000.0	12.750	14.934	14.160	13.313	12.737	11.938	1.998	4.403	.397	54.000	12.750	12.953	.313	1.283
1000.0	14.000	16.293	15.499	14.693	14.057	13.245	2.257	4.472	.397	58.000	14.000	14.189	.313	1.367
1000.0	16.000	18.527	17.589	16.697	16.043	15.137	2.569	5.111	.469	56.000	16.000	16.216	.313	1.500
1500.0	1.000	2.374	1.972	1.412	1.118	.920	.420	.384	.201	8.000	1.000	1.080	.125	.500
1500.0	1.250	2.635	2.233	1.676	1.376	1.156	.480	.480	.201	10.000	1.250	1.325	.125	.517
1500.0	1.500	2.896	2.494	1.941	1.635	1.360	.525	.576	.265	12.000	1.500	1.624	.125	.533
1500.0	2.000	3.594	3.064	2.451	2.133	1.846	.645	.763	.265	10.000	2.000	2.150	.125	.567
1500.0	2.375	3.942	3.412	2.801	2.474	2.157	.702	.970	.265	14.000	2.375	2.509	.125	.592
1500.0	2.500	4.101	3.571	2.961	2.631	2.306	.720	.969	.265	16.000	2.500	2.720	.125	.600
1500.0	3.000	4.609	4.077	3.471	3.129	2.760	.795	1.152	.265	18.000	3.000	3.276	.125	.633
1500.0	3.500	4.943	4.413	3.805	3.451	3.068	.873	1.629	.265	20.000	3.500	3.648	.125	.667
1500.0	4.000	5.796	5.140	4.470	4.104	3.680	1.003	1.536	.328	20.000	4.000	4.240	.125	.700
1500.0	4.500	6.177	5.521	4.849	4.471	4.026	1.116	1.654	.328	24.000	4.500	4.618	.188	.733
1500.0	5.000	6.803	6.147	5.470	5.080	4.600	1.216	1.719	.328	26.000	5.000	5.150	.188	.767
1500.0	5.563	7.246	6.640	5.957	5.553	5.047	1.269	2.282	.328	28.000	5.563	5.692	.188	.804
1500.0	6.000	7.803	7.147	6.460	6.046	5.510	1.366	2.303	.328	36.000	6.000	6.128	.188	.833
1500.0	6.625	8.610	7.816	7.054	6.625	6.065	1.515	2.606	.397	28.000	6.625	6.765	.188	.875
1500.0	8.000	10.008	9.214	8.439	7.977	7.359	1.676	3.071	.397	30.000	8.000	8.180	.188	.967
1500.0	8.625	10.731	9.930	8.995	8.518	7.625	1.806	3.905	.397	30.000	8.625	8.875	.250	1.000
1500.0	10.000	12.057	11.263	10.428	9.918	9.199	2.011	3.839	.397	42.000	10.000	10.288	.250	1.100
1500.0	10.750	12.903	12.109	11.160	10.632	9.564	2.066	4.763	.397	46.000	10.750	11.046	.250	1.150
1500.0	12.000	14.552	13.490	12.467	11.909	11.039	2.522	4.607	.531	38.000	12.000	12.248	.250	1.233
1500.0	12.750	15.344	14.406	13.196	12.620	11.376	2.559	5.591	.469	46.000	12.750	13.093	.313	1.283
1500.0	14.000	16.717	15.655	14.506	13.900	12.879	2.942	5.374	.531	46.000	14.000	14.280	.313	1.367
1500.0	16.000	18.757	17.695	16.545	15.891	14.718	3.242	6.142	.531	52.000	16.000	16.320	.313	1.500

TABLE C-9. FLANGE, LOOSE-RING, CRES, CRYOGENIC FLUID CONNECTOR

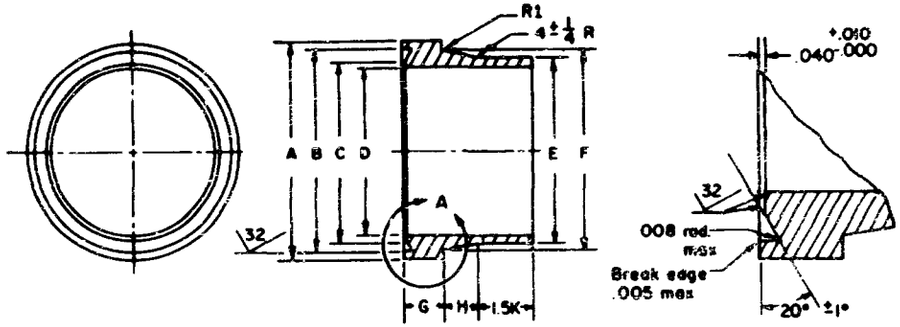

PRESSURE	PIPE/ TUBE OD	A	B	C	D	E	F	G	H	R1	K
100.0	1.000	1.570	1.364	1.070	.944	1.000	1.044	.189	.325	.125	.500
100.0	1.250	1.847	1.641	1.341	1.194	1.250	1.304	.189	.366	.125	.517
100.0	1.500	2.125	1.918	1.612	1.444	1.500	1.564	.204	.402	.125	.533
100.0	2.000	2.669	2.462	2.144	1.944	2.000	2.084	.219	.467	.125	.567
100.0	2.375	3.098	2.790	2.463	2.245	2.375	2.487	.345	.764	.125	.592
100.0	2.500	3.204	2.995	2.665	2.444	2.500	2.594	.234	.523	.125	.600
100.0	3.000	3.749	3.539	3.197	2.944	3.000	3.104	.264	.574	.125	.633
100.0	3.500	4.173	3.962	3.608	3.334	3.500	3.661	.444	1.052	.125	.667
100.0	4.000	4.807	4.595	4.229	3.930	4.000	4.147	.315	.742	.125	.700
100.0	4.500	5.243	5.030	4.652	4.334	4.500	4.661	.480	1.200	.188	.733
100.0	5.000	5.867	5.653	5.263	4.930	5.000	5.147	.345	.831	.188	.767
100.0	5.563	6.312	6.097	5.693	5.345	5.563	5.837	.612	1.527	.188	.804
100.0	6.000	6.937	6.721	6.307	5.930	6.000	6.167	.375	.911	.188	.833
100.0	6.625	7.445	7.228	6.799	6.407	6.625	6.859	.672	1.671	.188	.875
100.0	8.000	9.074	8.836	8.374	7.930	8.000	8.197	.450	1.054	.188	.967
100.0	8.625	9.591	9.343	8.866	8.407	8.625	8.869	.762	1.915	.250	1.008
100.0	10.000	11.143	10.875	10.365	9.870	10.000	10.252	.645	1.682	.250	1.100
100.0	10.750	11.801	11.522	10.994	10.482	10.750	10.997	.897	2.370	.250	1.150
100.0	12.000	13.278	12.980	12.422	11.870	12.000	12.282	.735	1.757	.250	1.233
100.0	12.750	13.870	13.561	12.985	12.420	12.750	12.982	1.020	2.863	.313	1.283
100.0	14.000	15.403	15.075	14.469	13.870	14.000	14.292	.810	1.899	.313	1.367
100.0	16.000	17.529	17.171	16.517	15.870	16.000	16.292	.885	2.031	.313	1.500
200.0	1.000	1.571	1.364	1.070	.944	1.000	1.044	.189	.325	.125	.500
200.0	1.250	1.848	1.641	1.341	1.194	1.250	1.304	.204	.366	.125	.517
200.0	1.500	2.126	1.918	1.612	1.444	1.500	1.564	.219	.402	.125	.533
200.0	2.000	2.671	2.462	2.144	1.944	2.000	2.074	.234	.467	.125	.567
200.0	2.375	3.000	2.790	2.463	2.245	2.375	2.487	.360	.764	.125	.592
200.0	2.500	3.206	2.995	2.665	2.444	2.500	2.584	.249	.523	.125	.600
200.0	3.000	3.752	3.539	3.197	2.944	3.000	3.104	.279	.574	.125	.633
200.0	3.500	4.176	3.962	3.608	3.334	3.500	3.651	.459	1.052	.125	.667
200.0	4.000	4.811	4.595	4.229	3.930	4.000	4.147	.345	.742	.125	.700
200.0	4.500	5.246	5.030	4.652	4.334	4.500	4.661	.519	1.200	.188	.733
200.0	5.000	5.871	5.653	5.263	4.930	5.000	5.137	.375	.831	.188	.767
200.0	5.563	6.316	6.097	5.693	5.345	5.563	5.807	.642	1.527	.188	.804
200.0	6.000	6.942	6.721	6.307	5.930	6.000	6.157	.420	.911	.188	.833
200.0	6.625	7.451	7.228	6.799	6.407	6.625	6.869	.702	1.671	.188	.875
200.0	8.000	9.052	8.814	8.352	7.912	8.000	8.202	.536	1.178	.188	.967
200.0	8.625	9.591	9.343	8.866	8.407	8.625	8.869	.807	1.915	.250	1.008
200.0	10.000	11.165	10.897	10.387	9.890	10.000	10.227	.689	1.472	.250	1.100
200.0	10.750	11.801	11.522	10.994	10.482	10.750	11.007	.957	2.370	.250	1.150
200.0	12.000	13.278	12.980	12.422	11.869	12.000	12.273	.827	1.767	.250	1.233
200.0	12.750	13.870	13.561	12.985	12.420	12.750	13.002	1.080	2.863	.313	1.283
200.0	14.000	15.381	15.053	14.447	13.847	14.000	14.278	.965	2.061	.313	1.367
200.0	16.000	17.484	17.126	16.472	15.825	16.000	16.314	1.118	2.355	.313	1.500

500.0	1.000	1.572	1.364	1.070	.944	1.000	1.044	.204	.325	.125	.500
500.0	1.250	1.850	1.641	1.341	1.194	1.250	1.304	.219	.366	.125	.517
500.0	1.500	2.128	1.918	1.612	1.444	1.500	1.554	.234	.402	.125	.533
500.0	2.000	2.675	2.462	2.144	1.946	2.000	2.074	.262	.460	.125	.567
500.0	2.375	3.004	2.790	2.463	2.245	2.375	2.487	.390	.764	.125	.592
500.0	2.500	3.199	2.984	2.654	2.432	2.500	2.587	.312	.575	.125	.600
500.0	3.000	3.724	3.507	3.165	2.918	3.000	3.110	.363	.690	.125	.633
500.0	3.500	4.182	3.962	3.608	3.334	3.500	3.651	.504	1.092	.125	.667
500.0	4.000	4.773	4.552	4.186	3.891	4.000	4.147	.463	.921	.125	.700
500.0	4.500	5.254	5.030	4.652	4.334	4.500	4.661	.579	1.200	.188	.733
500.0	5.000	5.813	5.586	5.196	4.864	5.000	5.184	.579	1.151	.188	.767
500.0	5.563	6.325	6.097	5.693	5.345	5.563	5.787	.717	1.527	.188	.804
500.0	6.000	6.852	6.621	6.207	5.837	6.000	6.201	.680	1.381	.188	.833
500.0	6.625	7.461	7.228	6.799	6.407	6.625	6.849	.792	1.671	.188	.875
500.0	8.000	8.920	8.681	8.219	7.782	8.000	8.254	.882	1.841	.188	.967
500.0	8.625	9.503	9.255	8.778	8.329	8.625	8.799	.969	2.221	.250	1.008
500.0	10.000	10.999	10.731	10.221	9.728	10.000	10.228	1.083	2.302	.250	1.100
500.0	10.750	11.745	11.466	10.938	10.420	10.750	10.942	1.170	2.622	.250	1.150
500.0	12.000	13.079	12.781	12.223	11.673	12.000	12.222	1.300	2.762	.250	1.233
500.0	12.750	13.562	13.253	12.677	11.938	12.750	12.953	1.218	4.403	.313	1.283
500.0	14.000	15.148	14.820	14.214	13.619	14.000	14.205	1.547	3.222	.313	1.367
500.0	16.000	17.218	16.860	16.206	15.564	16.000	16.209	1.778	3.683	.313	1.500
1000.0	1.000	1.803	1.444	1.150	.944	1.000	1.054	.204	.325	.125	.500
1000.0	1.250	2.064	1.710	1.410	1.183	1.250	1.317	.221	.399	.125	.517
1000.0	1.500	2.327	1.975	1.669	1.419	1.500	1.580	.256	.479	.125	.533
1000.0	2.000	2.854	2.506	2.188	1.892	2.000	2.127	.312	.639	.125	.567
1000.0	2.375	3.245	2.900	2.573	2.245	2.375	2.527	.360	.764	.125	.592
1000.0	2.500	3.372	3.028	2.698	2.365	2.500	2.664	.367	.799	.125	.600
1000.0	3.000	3.892	3.549	3.207	2.838	3.000	3.190	.438	.958	.125	.633
1000.0	3.500	4.357	4.015	3.661	3.260	3.500	3.730	.540	1.251	.125	.667
1000.0	4.000	4.922	4.581	4.215	3.784	4.000	4.254	.564	1.278	.125	.700
1000.0	4.500	5.190	4.849	4.471	4.026	4.500	4.618	.711	1.934	.188	.733
1000.0	5.000	5.943	5.603	5.213	4.730	5.000	5.207	.644	1.597	.188	.767
1000.0	5.563	6.302	5.957	5.553	5.047	5.563	5.692	.774	2.282	.188	.804
1000.0	6.000	6.974	6.625	6.211	5.676	6.000	6.191	.710	1.917	.188	.833
1000.0	6.625	7.407	7.054	6.625	6.065	6.625	6.765	.840	2.606	.188	.875
1000.0	8.000	9.024	8.660	8.198	7.569	8.000	8.148	.917	2.555	.188	.967
1000.0	8.625	9.470	9.101	8.624	7.981	8.625	8.786	.966	3.206	.250	1.008
1000.0	10.000	11.054	10.674	10.164	9.461	10.000	10.135	1.109	3.184	.250	1.100
1000.0	10.750	11.661	11.276	10.748	10.020	10.750	10.932	1.125	3.825	.250	1.150
1000.0	12.000	13.083	12.688	12.130	11.353	12.000	12.162	1.301	3.833	.250	1.233
1000.0	12.750	13.713	13.313	12.737	11.938	12.756	12.953	1.323	4.403	.313	1.283
1000.0	14.000	15.102	14.693	14.087	13.265	14.000	14.189	1.477	4.472	.313	1.367
1000.0	16.000	17.120	16.697	16.043	15.137	16.000	16.216	1.729	5.111	.313	1.500
1500.0	1.000	1.771	1.412	1.118	.920	1.000	1.068	.255	.384	.125	.500
1500.0	1.250	2.032	1.676	1.376	1.150	1.250	1.335	.285	.480	.125	.517
1500.0	1.500	2.293	1.941	1.635	1.380	1.500	1.610	.315	.576	.125	.533
1500.0	2.000	2.799	2.451	2.133	1.849	2.000	2.140	.390	.768	.125	.567
1500.0	2.375	3.147	2.801	2.474	2.157	2.375	2.569	.462	.970	.125	.592
1500.0	2.500	3.308	2.961	2.631	2.300	2.500	2.680	.480	.960	.125	.600
1500.0	3.000	3.814	3.471	3.129	2.760	3.000	3.210	.535	1.152	.125	.633
1500.0	3.500	4.148	3.805	3.451	3.068	3.500	3.648	.648	1.628	.125	.667
1500.0	4.000	4.812	4.470	4.104	3.680	4.000	4.190	.661	1.536	.125	.700
1500.0	4.500	5.193	4.849	4.471	4.026	4.500	4.618	.711	1.954	.188	.733
1500.0	5.000	5.813	5.470	5.080	4.600	5.000	5.100	.811	1.919	.188	.767
1500.0	5.563	6.312	5.957	5.553	5.047	5.563	5.692	.836	2.282	.188	.804
1500.0	6.000	6.819	6.460	6.046	5.519	6.000	6.120	.901	2.303	.188	.833
1500.0	6.625	7.419	7.054	6.625	6.065	6.625	6.765	.975	2.606	.188	.875
1500.0	8.000	8.917	8.434	7.977	7.359	8.000	8.150	1.156	3.071	.188	.967
1500.0	8.625	9.409	8.995	8.518	7.625	8.625	8.875	1.500	3.905	.250	1.008
1500.0	10.000	10.965	10.428	9.918	9.199	10.000	10.200	1.381	3.839	.250	1.100
1500.0	10.750	11.883	11.160	10.632	9.564	10.750	11.046	1.779	4.763	.250	1.150
1500.0	12.000	12.941	12.467	11.909	11.039	12.000	12.240	1.697	4.607	.250	1.233
1500.0	12.750	13.797	13.196	12.620	11.376	12.750	13.093	2.081	5.591	.313	1.283
1500.0	14.000	15.057	14.506	13.900	12.879	14.000	14.260	2.092	5.574	.313	1.367
1500.0	16.000	17.202	16.545	15.891	14.718	16.000	16.320	2.402	6.142	.313	1.500

TABLE C-10. RING, LOOSE, CRES, CRYOGENIC FLUID CONNECTOR

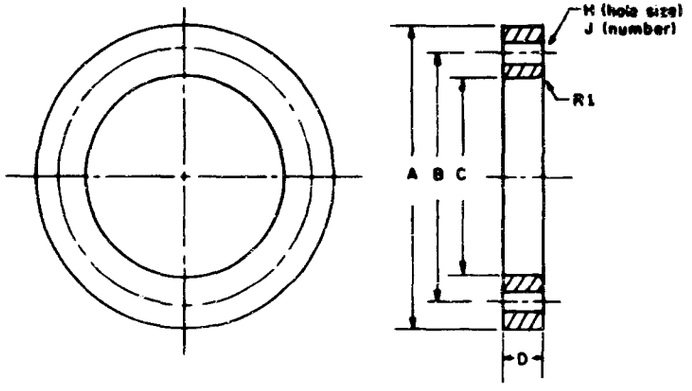

PRESSURE	PIPE/ TUBE OD	A	B	C	D	H	J	R1
100.0	1.000	2.173	1.771	1.028	.146	.201	6.000	.125
100.0	1.250	2.450	2.048	1.287	.161	.201	8.000	.125
100.0	1.500	2.728	2.326	1.546	.176	.201	8.000	.125
100.0	2.000	3.272	2.870	2.064	.191	.201	8.000	.125
100.0	2.375	3.601	3.199	2.470	.258	.201	10.000	.125
100.0	2.500	3.887	3.405	2.574	.221	.201	10.000	.125
100.0	3.000	4.352	3.950	3.083	.236	.201	10.000	.125
100.0	3.500	4.968	4.438	3.644	.331	.265	10.000	.125
100.0	4.000	5.602	5.072	4.125	.280	.265	10.000	.125
100.0	4.500	6.038	5.508	4.638	.376	.265	14.000	.188
100.0	5.000	6.662	6.132	5.117	.310	.265	12.000	.188
100.0	5.563	7.160	6.636	5.807	.458	.265	20.000	.188
100.0	6.000	7.732	7.202	6.136	.340	.265	14.000	.188
100.0	6.625	8.242	7.712	6.835	.488	.265	26.000	.188
100.0	8.000	9.869	9.339	8.166	.480	.265	16.000	.188
100.0	8.625	10.386	9.856	8.840	.548	.265	34.000	.250
100.0	10.000	11.938	11.408	10.216	.520	.265	30.000	.250
100.0	10.750	12.596	12.066	10.972	.643	.265	46.000	.250
100.0	12.000	14.073	13.543	12.246	.565	.265	36.000	.250
100.0	12.750	14.665	14.135	12.958	.720	.265	60.000	.313
100.0	14.000	16.198	15.668	14.248	.625	.265	44.000	.313
100.0	16.000	18.324	17.794	16.251	.670	.265	52.000	.313
200.0	1.000	2.174	1.772	1.028	.161	.201	6.000	.125
200.0	1.250	2.451	2.049	1.287	.176	.201	8.000	.125
200.0	1.500	2.729	2.327	1.546	.176	.201	8.000	.125
200.0	2.000	3.274	2.872	2.056	.206	.201	8.000	.125
200.0	2.375	3.603	3.201	2.470	.265	.201	12.000	.125
200.0	2.500	3.889	3.487	2.566	.221	.201	10.000	.125
200.0	3.000	4.355	3.953	3.083	.251	.201	10.000	.125
200.0	3.500	4.971	4.441	3.635	.346	.265	10.000	.125
200.0	4.000	5.606	5.076	4.125	.295	.265	10.000	.125
200.0	4.500	6.041	5.511	4.638	.376	.265	14.000	.188
200.0	5.000	6.664	6.136	5.189	.325	.265	12.000	.188
200.0	5.563	7.159	6.629	5.780	.473	.265	22.000	.188
200.0	6.000	7.737	7.207	6.128	.370	.265	14.000	.188
200.0	6.625	8.246	7.716	6.844	.503	.265	28.000	.188
200.0	8.000	9.867	9.317	8.173	.448	.265	22.000	.188
200.0	8.625	10.386	9.856	8.840	.593	.265	36.000	.250
200.0	10.000	11.960	11.430	10.192	.545	.265	32.000	.250
200.0	10.750	12.596	12.066	10.981	.673	.265	52.000	.250
200.0	12.000	14.073	13.543	12.237	.626	.265	44.000	.250
200.0	12.750	14.665	14.135	12.976	.745	.265	64.000	.313
200.0	14.000	16.176	15.646	14.239	.708	.265	58.000	.313
200.0	16.000	18.279	17.749	16.275	.805	.265	74.000	.313

500.0	1.000	2.175	1.773	1.028	.161	.201	6.000	.125
500.0	1.250	2.453	2.051	1.287	.176	.201	6.000	.125
500.0	1.500	2.731	2.329	1.538	.191	.201	8.000	.125
500.0	2.000	3.278	2.876	2.055	.219	.201	8.000	.125
500.0	2.375	3.607	3.205	2.470	.280	.201	12.000	.125
500.0	2.500	3.802	3.400	2.570	.263	.201	10.000	.125
500.0	3.000	4.327	3.925	3.092	.292	.201	14.000	.125
500.0	3.500	4.977	4.447	3.635	.376	.265	14.000	.125
500.0	4.000	5.568	5.038	4.129	.364	.265	12.000	.125
500.0	4.500	6.049	5.519	4.638	.421	.265	18.000	.188
500.0	5.000	6.608	6.078	5.139	.436	.265	20.000	.188
500.0	5.563	7.150	6.620	5.762	.518	.265	28.000	.188
500.0	6.000	7.647	7.117	6.176	.493	.265	26.000	.188
500.0	6.625	8.256	7.726	6.826	.563	.265	34.000	.188
500.0	8.000	9.715	9.185	8.230	.638	.265	40.000	.188
500.0	8.625	10.298	9.766	8.780	.671	.265	44.000	.250
500.0	10.000	11.983	11.327	10.205	.752	.328	40.000	.250
500.0	10.750	12.729	12.073	10.925	.795	.328	44.000	.250
500.0	12.000	14.063	13.407	12.202	.852	.328	52.000	.250
500.0	12.750	14.734	14.078	12.939	.977	.328	56.000	.313
500.0	14.000	16.132	15.476	14.186	.966	.328	68.000	.313
500.0	16.000	18.202	17.546	16.192	1.081	.328	76.000	.313
1000.0	1.000	2.486	2.004	1.035	.206	.201	6.000	.125
1000.0	1.250	2.667	2.265	1.288	.232	.201	8.000	.125
1000.0	1.500	2.930	2.528	1.569	.246	.201	10.000	.125
1000.0	2.000	3.457	3.055	2.105	.303	.201	14.000	.125
1000.0	2.375	3.848	3.446	2.505	.340	.201	16.000	.125
1000.0	2.500	4.167	3.637	2.641	.345	.265	12.000	.125
1000.0	3.000	4.687	4.157	3.168	.402	.265	14.000	.125
1000.0	3.500	5.152	4.622	3.709	.465	.265	20.000	.125
1000.0	4.000	5.717	5.187	4.232	.501	.265	22.000	.125
1000.0	4.500	5.985	5.455	4.607	.534	.265	24.000	.188
1000.0	5.000	6.738	6.208	5.185	.570	.265	28.000	.188
1000.0	5.563	7.286	6.630	5.682	.606	.328	26.000	.188
1000.0	6.000	7.958	7.382	6.173	.639	.328	28.000	.188
1000.0	6.625	8.391	7.735	6.795	.665	.328	30.000	.188
1000.0	8.000	10.008	9.352	8.137	.776	.328	40.000	.188
1000.0	8.625	10.484	9.798	8.774	.809	.328	42.000	.250
1000.0	10.000	12.038	11.382	10.124	.914	.328	48.000	.250
1000.0	10.750	12.845	11.989	10.921	.955	.328	52.000	.250
1000.0	12.000	14.274	13.480	12.151	1.052	.397	52.000	.250
1000.0	12.750	14.934	14.140	12.939	1.112	.397	54.000	.313
1000.0	14.000	16.203	15.499	14.176	1.190	.397	58.000	.313
1000.0	16.000	18.527	17.589	16.203	1.328	.469	56.000	.313
1500.0	1.000	2.374	1.972	1.042	.230	.201	8.000	.125
1500.0	1.250	2.635	2.233	1.315	.265	.201	10.000	.125
1500.0	1.500	2.896	2.494	1.588	.285	.201	12.000	.125
1500.0	2.000	3.394	3.004	2.119	.355	.265	10.000	.125
1500.0	2.375	3.742	3.412	2.529	.398	.265	14.000	.125
1500.0	2.500	4.101	3.571	2.659	.410	.265	16.000	.125
1500.0	3.000	4.669	4.079	3.189	.465	.265	18.000	.125
1500.0	3.500	4.963	4.413	3.600	.507	.265	20.000	.125
1500.0	4.000	5.496	5.140	4.176	.560	.328	20.000	.125
1500.0	4.500	6.177	5.821	4.607	.594	.328	24.000	.188
1500.0	5.000	6.803	6.147	5.091	.640	.328	26.000	.188
1500.0	5.563	7.296	6.640	5.682	.681	.328	28.000	.188
1500.0	6.000	7.803	7.147	6.111	.721	.328	30.000	.188
1500.0	6.625	8.810	7.816	6.755	.785	.397	28.000	.188
1500.0	8.000	10.008	9.214	8.151	.896	.397	34.000	.188
1500.0	8.625	10.732	9.938	8.880	1.015	.397	38.000	.250
1500.0	10.000	12.357	11.263	10.188	1.086	.397	42.000	.250
1500.0	10.750	12.963	12.109	11.031	1.186	.397	46.000	.250
1500.0	12.000	14.552	13.490	12.228	1.261	.531	38.000	.250
1500.0	12.750	15.344	14.400	13.075	1.387	.469	46.000	.313
1500.0	14.000	16.711	15.655	14.265	1.466	.531	46.000	.313
1500.0	16.000	18.757	17.695	16.305	1.582	.531	52.000	.313

TABLE C-11. SEAL, CRES, NICKEL PLATED, CRYOGENIC FLUID CONNECTOR

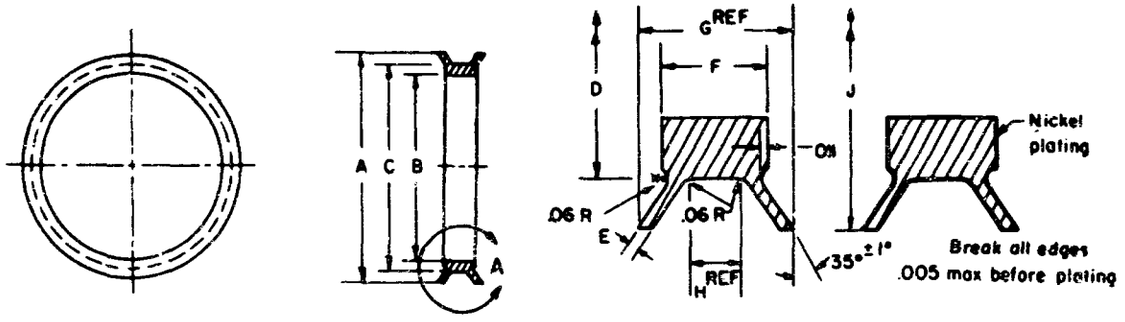

						VIEW A Before Plating		VIEW A After Plating		
PRESSURE	PIPE/ TUBE OD	A	B	C	D	E	F	G	H	J
100.0	1.000	1.356	.978	1.138	1.070	.041	.316	.473	.216	1.362
100.0	1.250	1.633	1.228	1.409	1.341	.041	.350	.511	.250	1.639
100.0	1.500	1.910	1.479	1.680	1.612	.041	.378	.543	.277	1.916
100.0	2.000	2.454	1.981	2.212	2.144	.042	.436	.610	.335	2.460
100.0	2.375	2.782	2.284	2.531	2.463	.042	.467	.647	.365	2.788
100.0	2.500	2.907	2.483	2.733	2.665	.042	.500	.682	.397	2.993
100.0	3.000	3.531	2.985	3.265	3.197	.042	.535	.725	.431	3.537
100.0	3.500	3.954	3.377	3.676	3.608	.043	.565	.764	.468	3.960
100.0	4.000	4.587	3.974	4.297	4.229	.043	.614	.822	.509	4.593
100.0	4.500	5.022	4.386	4.720	4.652	.044	.643	.859	.536	5.028
100.0	5.000	5.645	4.978	5.331	5.263	.044	.701	.925	.593	5.651
100.0	5.563	6.089	5.395	5.761	5.693	.045	.731	.964	.622	6.095
100.0	6.000	6.713	5.982	6.375	6.307	.045	.754	.995	.644	6.719
100.0	6.625	7.220	6.461	6.867	6.799	.046	.787	1.039	.676	7.226
100.0	8.000	8.828	7.989	8.442	8.374	.047	.870	1.145	.756	8.834
100.0	8.625	9.335	8.468	8.934	8.866	.047	.896	1.181	.780	9.341
100.0	10.000	10.867	9.936	10.433	10.365	.048	.983	1.292	.865	10.873
100.0	10.750	11.514	10.551	11.082	10.994	.049	1.014	1.335	.895	11.520
100.0	12.000	12.972	11.943	12.490	12.422	.050	1.072	1.414	.950	12.978
100.0	12.750	13.553	12.496	13.053	12.985	.051	1.101	1.455	.977	13.559
100.0	14.000	15.047	13.950	14.537	14.469	.052	1.165	1.540	1.038	15.073
100.0	16.000	17.163	15.958	16.585	16.517	.053	1.245	1.654	1.115	17.169
200.0	1.000	1.356	.978	1.138	1.070	.041	.316	.473	.215	1.362
200.0	1.250	1.633	1.228	1.409	1.341	.041	.350	.511	.249	1.639
200.0	1.500	1.910	1.479	1.680	1.612	.042	.378	.543	.276	1.916
200.0	2.000	2.454	1.981	2.212	2.144	.042	.436	.610	.333	2.460
200.0	2.375	2.782	2.284	2.531	2.463	.043	.467	.647	.363	2.788
200.0	2.500	2.907	2.483	2.733	2.665	.043	.500	.682	.395	2.993
200.0	3.000	3.531	2.985	3.265	3.197	.044	.535	.725	.428	3.537
200.0	3.500	3.954	3.377	3.676	3.608	.044	.565	.764	.457	3.960
200.0	4.000	4.587	3.974	4.297	4.229	.045	.614	.822	.505	4.593
200.0	4.500	5.022	4.380	4.720	4.652	.045	.643	.859	.533	5.028
200.0	5.000	5.645	4.978	5.331	5.263	.046	.701	.925	.589	5.651
200.0	5.563	6.089	5.395	5.761	5.693	.047	.731	.964	.617	6.095
200.0	6.000	6.713	5.982	6.375	6.307	.047	.754	.995	.639	6.719
200.0	6.625	7.220	6.461	6.867	6.799	.048	.787	1.039	.670	7.226
200.0	8.000	8.806	7.971	8.420	8.352	.049	.876	1.151	.755	8.812
200.0	8.625	9.335	8.468	8.934	8.866	.050	.896	1.181	.773	9.341
200.0	10.000	10.889	9.956	10.455	10.387	.052	.982	1.290	.856	10.895
200.0	10.750	11.514	10.551	11.062	10.994	.053	1.014	1.335	.886	11.520
200.0	12.000	12.972	11.942	12.490	12.422	.054	1.069	1.411	.937	12.978
200.0	12.750	13.553	12.496	13.053	12.985	.055	1.101	1.455	.966	13.559
200.0	14.000	15.045	13.927	14.515	14.447	.056	1.161	1.536	1.023	15.051
200.0	16.000	17.118	15.912	16.540	16.472	.059	1.241	1.649	1.097	17.124

500.0	1.000	1.356	.978	1.138	1.070	.042	.316	.473	.214	1.362
500.0	1.250	1.633	1.228	1.409	1.341	.042	.350	.511	.247	1.639
500.0	1.500	1.916	1.479	1.680	1.612	.043	.378	.543	.273	1.916
500.0	2.000	2.454	1.983	2.212	2.144	.044	.439	.613	.332	2.460
500.0	2.375	2.782	2.284	2.531	2.463	.044	.467	.647	.359	2.788
500.0	2.500	2.976	2.471	2.722	2.654	.045	.496	.678	.387	2.982
500.0	3.000	3.499	2.959	3.233	3.165	.046	.543	.733	.432	3.505
500.0	3.500	3.954	3.377	3.676	3.608	.047	.565	.764	.451	3.960
500.0	4.000	4.544	3.935	4.254	4.186	.047	.618	.825	.502	4.550
500.0	4.500	5.022	4.380	4.720	4.652	.048	.643	.859	.525	5.028
500.0	5.000	5.578	4.912	5.264	5.196	.049	.693	.917	.572	5.584
500.0	5.563	6.089	5.395	5.761	5.693	.050	.731	.964	.608	6.095
500.0	6.000	6.613	5.888	6.275	6.207	.051	.754	.995	.629	6.619
500.0	6.625	7.220	6.461	6.867	6.799	.052	.787	1.039	.659	7.226
500.0	8.000	8.673	7.841	8.287	8.219	.055	.868	1.142	.734	8.679
500.0	8.625	9.247	8.390	8.846	8.778	.056	.906	1.191	.769	9.253
500.0	10.000	10.723	9.794	10.289	10.221	.059	.973	1.281	.830	10.729
500.0	10.750	11.458	10.489	11.006	10.938	.060	.996	1.318	.851	11.464
500.0	12.000	12.773	11.746	12.291	12.223	.062	1.060	1.402	.908	12.779
500.0	12.750	13.245	12.614	12.745	12.677	.064	.813	1.167	.657	13.251
500.0	14.000	14.812	13.699	14.282	14.214	.066	1.152	1.527	.990	14.818
500.0	16.000	16.852	15.652	16.274	16.206	.070	1.232	1.640	1.061	16.858
1000.0	1.000	1.436	.978	1.218	1.150	.059	.455	.612	.310	1.442
1000.0	1.250	1.702	1.217	1.478	1.410	.058	.515	.676	.374	1.708
1000.0	1.500	1.967	1.455	1.737	1.669	.057	.563	.728	.424	1.973
1000.0	2.000	2.498	1.929	2.256	2.188	.055	.639	.812	.503	2.504
1000.0	2.375	2.892	2.284	2.641	2.573	.055	.688	.868	.554	2.898
1000.0	2.500	3.020	2.434	2.766	2.698	.055	.714	.896	.581	3.026
1000.0	3.000	3.541	2.879	3.275	3.207	.054	.777	.967	.644	3.547
1000.0	3.500	4.007	3.303	3.729	3.661	.054	.824	1.023	.693	4.013
1000.0	4.000	4.573	3.829	4.283	4.215	.053	.892	1.099	.762	4.579
1000.0	4.500	4.841	4.072	4.539	4.471	.053	.922	1.137	.791	4.847
1000.0	5.000	5.595	4.778	5.281	5.213	.053	1.000	1.224	.870	5.601
1000.0	5.563	5.949	5.097	5.621	5.553	.055	1.021	1.255	.888	5.955
1000.0	6.000	6.617	5.728	6.279	6.211	.056	1.088	1.329	.952	6.623
1000.0	6.625	7.046	6.119	6.693	6.625	.057	1.113	1.367	.975	7.052
1000.0	8.000	8.652	7.627	8.266	8.198	.061	1.244	1.519	1.095	8.658
1000.0	8.625	9.093	8.042	8.692	8.624	.063	1.287	1.572	1.134	9.099
1000.0	10.000	10.666	9.527	[illegible]	10.164	.066	1.400	1.708	1.238	10.672
1000.0	10.750	11.268	10.089	10.816	10.748	.068	1.437	1.750	1.270	11.274
1000.0	12.000	12.680	11.426	12.198	12.130	.072	1.529	1.871	1.354	12.686
1000.0	12.750	13.305	12.014	12.805	12.737	.074	1.569	1.923	1.389	13.311
1000.0	14.000	14.685	13.325	14.155	14.087	.077	1.656	2.031	1.468	14.691
1000.0	16.000	16.689	15.225	16.111	16.043	.082	1.767	2.176	1.566	16.695
1500.0	1.000	1.404	.954	1.186	1.118	.059	.459	.616	.314	1.410
1500.0	1.250	1.668	1.184	1.444	1.376	.058	.504	.665	.362	1.674
1500.0	1.500	1.933	1.415	1.703	1.635	.057	.540	.705	.401	1.939
1500.0	2.000	2.443	1.877	2.201	2.133	.056	.628	.801	.492	2.449
1500.0	2.375	2.793	2.196	2.542	2.474	.055	.683	.863	.549	2.799
1500.0	2.500	2.953	2.339	2.699	2.631	.055	.698	.880	.564	2.959
1500.0	3.000	3.463	2.801	3.197	3.129	.054	.756	.946	.623	3.469
1500.0	3.500	3.797	3.111	3.519	3.451	.054	.810	1.009	.678	3.803
1500.0	4.000	4.462	3.724	4.172	4.104	.054	.880	1.087	.749	4.468
1500.0	4.500	4.841	4.072	4.539	4.471	.055	.922	1.137	.789	4.847
1500.0	5.000	5.462	4.648	5.148	5.080	.056	.978	1.202	.841	5.468
1500.0	5.563	5.949	5.097	5.621	5.553	.058	1.021	1.255	.880	5.955
1500.0	6.000	6.452	5.571	6.114	6.046	.059	1.076	1.317	.931	6.458
1500.0	6.625	7.046	6.119	6.693	6.625	.061	1.115	1.367	.965	7.052
1500.0	8.000	8.431	7.418	8.045	7.977	.066	1.233	1.507	1.072	8.437
1500.0	8.625	8.987	7.686	8.586	8.518	.068	.903	1.188	.737	8.993
1500.0	10.000	10.420	9.265	9.986	9.918	.072	1.335	1.643	1.158	10.426
1500.0	10.750	11.152	9.633	10.700	10.632	.075	.952	1.272	.769	11.158
1500.0	12.000	12.459	11.112	11.977	11.909	.079	1.334	1.676	1.142	12.465
1500.0	12.750	13.188	11.452	12.688	12.620	.081	.975	1.330	.777	13.194
1500.0	14.000	14.498	12.959	13.968	13.900	.085	1.333	1.709	1.125	14.504
1500.0	16.000	16.537	14.806	15.959	15.891	.092	1.333	1.742	1.109	16.543

TABLE C-12. BOLT, CRES, INTEGRAL/INTEGRAL, CRYOGENIC FLUID CONNECTOR

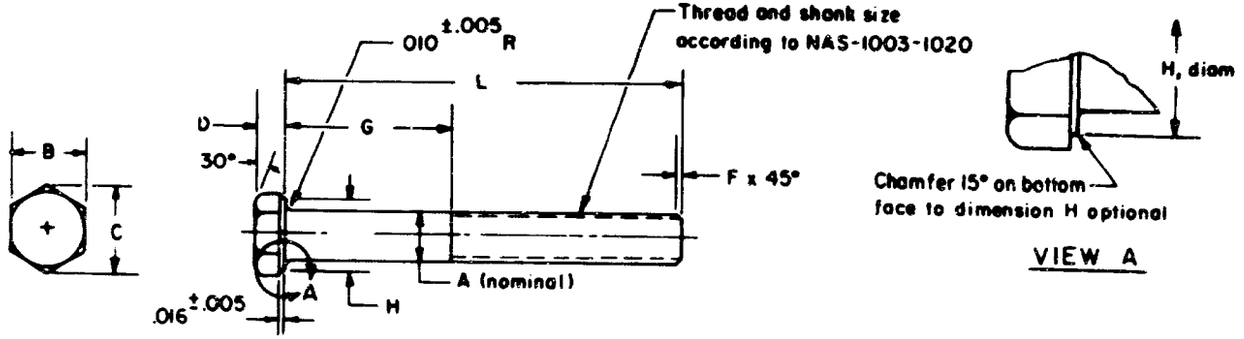

PRESSURE	PIPE/TUBE OD	A	H	C	D	F	H	G	L	J
100.0	1.000	.190	.375	.433	.141	.063	.375	.482	1.249	6.000
100.0	1.250	.190	.375	.433	.141	.063	.375	.514	1.313	8.000
100.0	1.500	.190	.375	.433	.141	.063	.375	.543	1.371	8.000
100.0	2.000	.190	.375	.433	.141	.063	.375	.602	1.489	8.000
100.0	2.375	.190	.375	.433	.141	.063	.375	.774	1.832	10.000
100.0	2.500	.190	.375	.433	.141	.063	.375	.664	1.613	10.000
100.0	3.000	.190	.375	.433	.141	.063	.375	.711	1.708	10.000
100.0	3.500	.250	.438	.505	.172	.063	.438	.981	2.338	10.000
100.0	4.000	.250	.438	.505	.172	.063	.438	.862	2.099	10.000
100.0	4.500	.250	.438	.505	.172	.063	.438	1.111	2.596	14.000
100.0	5.000	.250	.438	.505	.172	.063	.438	.965	2.306	12.000
100.0	5.563	.250	.438	.505	.172	.063	.438	1.337	3.050	20.000
100.0	6.000	.250	.438	.505	.172	.063	.438	1.037	2.449	14.000
100.0	6.625	.250	.438	.505	.172	.063	.438	1.396	3.166	26.000
100.0	8.000	.250	.438	.505	.172	.063	.438	1.200	2.775	16.000
100.0	8.625	.250	.438	.505	.172	.063	.438	1.615	3.695	34.000
100.0	10.000	.250	.438	.505	.172	.063	.438	1.572	3.518	30.000
100.0	10.750	.250	.438	.505	.172	.063	.438	1.869	4.113	46.000
100.0	12.000	.250	.438	.505	.172	.063	.438	1.721	3.817	36.000
100.0	12.750	.250	.438	.505	.172	.063	.438	2.125	4.626	60.000
100.0	14.000	.250	.438	.505	.172	.063	.438	1.902	4.180	44.000
100.0	16.000	.250	.438	.505	.172	.063	.438	2.078	4.530	52.000
200.0	1.000	.190	.375	.433	.141	.063	.375	.482	1.249	6.000
200.0	1.250	.190	.375	.433	.141	.063	.375	.514	1.313	8.000
200.0	1.500	.190	.375	.433	.141	.063	.375	.558	1.401	8.000
200.0	2.000	.190	.375	.433	.141	.063	.375	.617	1.519	8.000
200.0	2.375	.190	.375	.433	.141	.063	.375	.789	1.862	12.000
200.0	2.500	.190	.375	.433	.141	.063	.375	.679	1.643	10.000
200.0	3.000	.190	.375	.433	.141	.063	.375	.741	1.768	10.000
200.0	3.500	.250	.438	.505	.172	.063	.438	.996	2.368	10.000
200.0	4.000	.250	.438	.505	.172	.063	.438	.892	2.159	10.000
200.0	4.500	.250	.438	.505	.172	.063	.438	1.141	2.656	14.000
200.0	5.000	.250	.438	.505	.172	.063	.438	.995	2.366	12.000
200.0	5.563	.250	.438	.505	.172	.063	.438	1.352	3.080	22.000
200.0	6.000	.250	.438	.505	.172	.063	.438	1.082	2.539	14.000
200.0	6.625	.250	.438	.505	.172	.063	.438	1.441	3.256	28.000
200.0	8.000	.250	.438	.505	.172	.063	.438	1.335	3.044	22.000
200.0	8.625	.250	.438	.505	.172	.063	.438	1.660	3.695	38.000
200.0	10.000	.250	.438	.505	.172	.063	.438	1.600	3.576	32.000
200.0	10.750	.250	.438	.505	.172	.063	.438	1.944	4.263	52.000
200.0	12.000	.250	.438	.505	.172	.063	.438	1.842	4.059	44.000
200.0	12.750	.250	.438	.505	.172	.063	.438	2.280	4.776	64.000
200.0	14.000	.250	.438	.505	.172	.063	.438	2.100	4.576	58.000
200.0	16.000	.250	.438	.505	.172	.063	.438	2.338	5.051	74.000

500.0	1.000	.190	.375	.433	.141	.063	.375	.512	1.309	6.000
500.0	1.250	.190	.375	.433	.141	.063	.375	.564	1.373	6.000
500.0	1.500	.190	.375	.433	.141	.063	.375	.573	1.431	8.000
500.0	2.000	.190	.375	.433	.141	.063	.375	.681	1.608	8.000
500.0	2.375	.190	.375	.433	.141	.063	.375	.819	1.922	12.000
500.0	2.500	.190	.375	.433	.141	.063	.375	.740	1.765	10.000
500.0	3.000	.190	.375	.433	.141	.063	.375	.844	1.973	14.000
500.0	3.500	.250	.438	.505	.172	.063	.438	1.041	2.458	14.000
500.0	4.000	.250	.438	.505	.172	.063	.438	1.042	2.459	12.000
500.0	4.500	.250	.438	.505	.172	.063	.438	1.186	2.746	18.000
500.0	5.000	.250	.438	.505	.172	.063	.438	1.225	2.826	20.000
500.0	5.563	.250	.438	.505	.172	.063	.438	1.412	3.200	28.000
500.0	6.000	.250	.438	.505	.172	.063	.438	1.387	3.149	26.000
500.0	6.625	.250	.438	.505	.172	.063	.438	1.531	3.436	34.000
500.0	8.000	.250	.438	.505	.172	.063	.438	1.676	3.726	40.000
500.0	8.625	.250	.438	.505	.172	.063	.438	1.827	4.029	44.000
500.0	10.000	.313	.500	.577	.204	.063	.500	2.035	4.539	40.000
500.0	10.750	.313	.500	.577	.204	.063	.500	2.149	4.766	44.000
500.0	12.000	.313	.500	.577	.204	.063	.500	2.325	5.119	52.000
500.0	12.750	.313	.500	.577	.204	.063	.500	2.269	5.008	56.000
500.0	14.000	.313	.500	.577	.204	.063	.500	2.663	5.794	66.000
500.0	16.000	.313	.500	.577	.204	.063	.500	2.979	6.427	76.000
1000.0	1.000	.190	.375	.433	.141	.063	.375	.595	1.476	6.000
1000.0	1.250	.190	.375	.433	.141	.063	.375	.659	1.603	8.000
1000.0	1.500	.190	.375	.433	.141	.063	.375	.718	1.721	10.000
1000.0	2.000	.190	.375	.433	.141	.063	.375	.826	1.937	14.000
1000.0	2.375	.190	.375	.433	.141	.063	.375	.899	2.083	16.000
1000.0	2.500	.250	.438	.505	.172	.063	.438	.964	2.304	12.000
1000.0	3.000	.250	.438	.505	.172	.063	.438	1.051	2.477	14.000
1000.0	3.500	.250	.438	.505	.172	.063	.438	1.177	2.729	20.000
1000.0	4.000	.250	.438	.505	.172	.063	.438	1.250	2.874	22.000
1000.0	4.500	.250	.438	.505	.172	.063	.438	1.337	3.049	24.000
1000.0	5.000	.250	.438	.505	.172	.063	.438	1.444	3.264	28.000
1000.0	5.563	.313	.500	.577	.204	.063	.500	1.540	3.548	24.000
1000.0	6.000	.313	.500	.577	.204	.063	.500	1.660	3.788	28.000
1000.0	6.625	.313	.500	.577	.204	.063	.500	1.698	3.864	30.000
1000.0	8.000	.313	.500	.577	.204	.063	.500	2.049	4.567	40.000
1000.0	8.625	.313	.500	.577	.204	.063	.500	2.030	4.528	42.000
1000.0	10.000	.313	.500	.577	.204	.063	.500	2.394	5.257	48.000
1000.0	10.750	.313	.500	.577	.204	.063	.500	2.354	5.176	52.000
1000.0	12.000	.375	.563	.650	.235	.063	.563	2.800	6.163	52.000
1000.0	12.750	.375	.563	.650	.235	.063	.563	2.782	6.127	54.000
1000.0	14.000	.375	.563	.650	.235	.063	.563	3.085	6.733	58.000
1000.0	16.000	.438	.688	.794	.266	.063	.688	3.453	7.561	56.000
1500.0	1.000	.190	.375	.433	.141	.063	.375	.650	1.584	8.000
1500.0	1.250	.190	.375	.433	.141	.063	.375	.732	1.749	10.000
1500.0	1.500	.190	.375	.433	.141	.063	.375	.795	1.875	12.000
1500.0	2.000	.250	.438	.505	.172	.063	.438	.959	2.293	10.000
1500.0	2.375	.250	.438	.505	.172	.063	.438	1.043	2.462	14.000
1500.0	2.500	.250	.438	.505	.172	.063	.438	1.069	2.514	16.000
1500.0	3.000	.250	.438	.505	.172	.063	.438	1.173	2.722	18.000
1500.0	3.500	.250	.438	.505	.172	.063	.438	1.278	2.931	20.000
1500.0	4.000	.313	.500	.577	.204	.063	.500	1.445	3.360	20.000
1500.0	4.500	.313	.500	.577	.204	.063	.500	1.577	3.623	24.000
1500.0	5.000	.313	.500	.577	.204	.063	.500	1.705	3.878	26.000
1500.0	5.563	.313	.500	.577	.204	.063	.500	1.780	4.028	28.000
1500.0	6.000	.313	.500	.577	.204	.063	.500	1.904	4.277	30.000
1500.0	6.625	.375	.563	.650	.235	.063	.563	2.073	4.708	28.000
1500.0	8.000	.375	.563	.650	.235	.063	.563	2.313	5.188	34.000
1500.0	8.625	.375	.563	.650	.235	.063	.563	2.252	5.066	38.000
1500.0	10.000	.375	.563	.650	.235	.063	.563	2.679	5.920	42.000
1500.0	10.750	.375	.563	.650	.235	.063	.563	2.540	5.642	46.000
1500.0	12.000	.500	.750	.866	.297	.063	.750	3.189	7.127	38.000
1500.0	12.750	.438	.688	.794	.266	.063	.688	3.044	6.743	46.000
1500.0	14.000	.500	.750	.866	.297	.063	.750	3.609	7.968	46.000
1500.0	16.000	.500	.750	.866	.297	.063	.750	3.909	8.568	52.000

TABLE C-13. BOLT, CRES, LOOSE-RING/LOOSE-RING, CRYOGENIC FLUID CONNECTOR

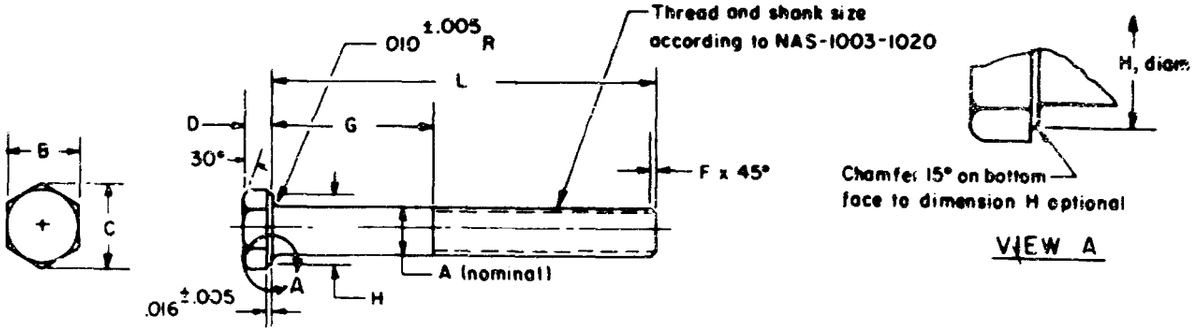

PRESSURE	PIPE/ TUBE OD	A	B	C	D	F	H	G	L	J
100.0	1.000	.190	.375	.433	.141	.063	.375	.493	1.271	6.000
100.0	1.250	.190	.375	.433	.141	.063	.375	.525	1.335	8.000
100.0	1.500	.190	.375	.433	.141	.063	.375	.569	1.423	8.000
100.0	2.000	.190	.375	.433	.141	.063	.375	.628	1.541	8.000
100.0	2.375	.190	.375	.433	.141	.063	.375	.829	1.942	10.000
100.0	2.500	.190	.375	.433	.141	.063	.375	.705	1.695	10.000
100.0	3.000	.190	.375	.433	.141	.063	.375	.767	1.820	10.000
100.0	3.500	.250	.438	.505	.172	.063	.438	1.057	2.490	10.000
100.0	4.000	.250	.438	.505	.172	.063	.438	.902	2.179	10.000
100.0	4.500	.250	.438	.505	.172	.063	.438	1.187	2.748	14.000
100.0	5.000	.250	.438	.505	.172	.063	.438	1.005	2.386	12.000
100.0	5.563	.250	.438	.505	.172	.063	.438	1.435	3.246	20.000
100.0	6.000	.250	.438	.505	.172	.063	.438	1.092	2.559	14.000
100.0	6.625	.250	.438	.505	.172	.063	.438	1.554	3.482	26.000
100.0	8.000	.250	.438	.505	.172	.063	.438	1.285	2.945	16.000
100.0	8.625	.250	.438	.505	.172	.063	.438	1.758	3.891	34.000
100.0	10.000	.250	.438	.505	.172	.063	.438	1.657	3.688	38.000
100.0	10.750	.250	.438	.505	.172	.063	.438	2.047	4.469	46.000
100.0	12.000	.250	.438	.505	.172	.063	.438	1.836	4.047	36.000
100.0	12.750	.250	.438	.505	.172	.063	.438	2.290	4.956	60.000
100.0	14.000	.250	.438	.505	.172	.063	.438	2.017	4.410	44.000
100.0	16.000	.250	.438	.505	.172	.063	.438	2.178	4.730	52.000
200.0	1.000	.190	.375	.433	.141	.063	.375	.508	1.301	6.000
200.0	1.250	.190	.375	.433	.141	.063	.375	.555	1.395	8.000
200.0	1.500	.190	.375	.433	.141	.063	.375	.584	1.453	8.000
200.0	2.000	.190	.375	.433	.141	.063	.375	.658	1.601	8.000
200.0	2.375	.190	.375	.433	.141	.063	.375	.559	2.002	12.000
200.0	2.500	.190	.375	.433	.141	.063	.375	.720	1.725	10.000
200.0	3.000	.190	.375	.433	.141	.063	.375	.797	1.980	10.000
200.0	3.500	.250	.438	.505	.172	.063	.438	1.087	2.550	10.000
200.0	4.000	.250	.438	.505	.172	.063	.438	.947	2.269	10.000
200.0	4.500	.250	.438	.505	.172	.063	.438	1.217	2.808	14.000
200.0	5.000	.250	.438	.505	.172	.063	.438	1.050	2.476	12.000
200.0	5.563	.250	.438	.505	.172	.063	.438	1.480	3.336	22.000
200.0	6.000	.250	.438	.505	.172	.063	.438	1.167	2.709	14.000
200.0	6.625	.250	.438	.505	.172	.063	.438	1.599	3.572	28.000
200.0	8.000	.250	.438	.505	.172	.063	.438	1.422	3.219	22.000
200.0	9.625	.250	.438	.505	.172	.063	.438	1.848	4.071	38.000
200.0	10.000	.250	.438	.505	.172	.063	.438	1.725	3.825	32.000
200.0	10.750	.250	.438	.505	.172	.063	.438	2.137	4.649	52.000
200.0	12.000	.250	.438	.505	.172	.063	.438	1.988	4.352	44.000
200.0	12.750	.250	.438	.505	.172	.063	.438	2.395	5.166	64.000
200.0	14.000	.250	.438	.505	.172	.063	.438	2.254	4.883	58.000
200.0	16.000	.250	.438	.505	.172	.063	.438	2.544	5.462	74.000

500.0	1.000	.190	.375	.433	.141	.063	.375	.523	1.331	6.000
500.0	1.250	.190	.375	.433	.141	.063	.375	.570	1.425	6.000
500.0	1.500	.190	.375	.433	.141	.063	.375	.614	1.513	8.000
500.0	2.000	.190	.375	.433	.141	.063	.375	.701	1.686	8.000
500.0	2.375	.190	.375	.433	.141	.063	.375	.904	2.092	12.000
500.0	2.500	.190	.375	.433	.141	.063	.375	.823	1.931	10.000
500.0	3.000	.190	.375	.433	.141	.063	.375	.926	2.136	14.000
500.0	3.500	.250	.438	.505	.172	.063	.438	1.162	2.700	14.000
500.0	4.000	.250	.438	.505	.172	.063	.438	1.136	2.647	12.000
500.0	4.500	.250	.438	.505	.172	.063	.438	1.322	3.018	18.000
500.0	5.000	.250	.438	.505	.172	.063	.438	1.362	3.098	20.000
500.0	5.563	.250	.438	.505	.172	.063	.438	1.400	3.576	28.000
500.0	6.000	.250	.438	.505	.172	.063	.438	1.550	3.476	26.000
500.0	6.625	.250	.438	.505	.172	.063	.438	1.749	3.872	34.000
500.0	8.000	.250	.438	.505	.172	.063	.438	1.953	4.282	48.000
500.0	8.625	.250	.438	.505	.172	.063	.438	2.093	4.561	44.000
500.0	10.000	.313	.500	.577	.204	.063	.500	2.322	5.114	40.000
500.0	10.750	.313	.500	.577	.204	.063	.500	2.464	5.396	44.000
500.0	12.000	.313	.500	.577	.204	.063	.500	2.682	5.833	52.000
500.0	12.750	.313	.500	.577	.204	.063	.500	2.801	5.672	56.000
500.0	14.000	.313	.500	.577	.204	.063	.500	3.089	6.646	66.000
500.0	16.000	.313	.500	.577	.204	.063	.500	3.475	7.419	76.000
1000.0	1.000	.190	.375	.433	.141	.063	.375	.637	1.568	6.000
1000.0	1.250	.190	.375	.433	.141	.063	.375	.711	1.707	8.000
1000.0	1.500	.190	.375	.433	.141	.063	.375	.784	1.852	10.000
1000.0	2.000	.190	.375	.433	.141	.063	.375	.934	2.153	14.000
1000.0	2.375	.190	.375	.433	.141	.063	.375	1.044	2.373	16.000
1000.0	2.500	.250	.438	.505	.172	.063	.438	1.069	2.513	12.000
1000.0	3.000	.250	.438	.505	.172	.063	.438	1.228	2.831	14.000
1000.0	3.500	.250	.438	.505	.172	.063	.438	1.417	3.209	20.000
1000.0	4.000	.250	.438	.505	.172	.063	.438	1.510	3.396	22.000
1000.0	4.500	.250	.438	.505	.172	.063	.438	1.706	3.787	24.000
1000.0	5.000	.250	.438	.505	.172	.063	.438	1.714	3.803	28.000
1000.0	5.563	.313	.500	.577	.204	.063	.500	1.891	4.250	24.000
1000.0	6.000	.313	.500	.577	.204	.063	.500	1.893	4.255	28.000
1000.0	6.625	.313	.500	.577	.204	.063	.500	2.363	4.594	30.000
1000.0	8.000	.313	.500	.577	.204	.063	.500	2.316	5.100	40.000
1000.0	8.625	.313	.500	.577	.204	.063	.500	2.419	5.306	42.000
1000.0	10.000	.313	.500	.577	.204	.063	.500	2.723	5.915	48.000
1000.0	10.750	.313	.500	.577	.204	.063	.500	2.799	6.068	52.000
1000.0	12.000	.375	.563	.650	.235	.063	.563	3.117	6.797	52.000
1000.0	12.750	.375	.563	.650	.235	.063	.563	3.219	7.001	54.000
1000.0	14.000	.375	.563	.650	.235	.063	.563	3.495	7.553	58.000
1000.0	16.000	.438	.688	.794	.266	.063	.688	3.940	8.537	56.000
1500.0	1.000	.190	.375	.433	.141	.063	.375	.715	1.715	8.000
1500.0	1.250	.190	.375	.433	.141	.063	.375	.802	1.889	10.000
1500.0	1.500	.190	.375	.433	.141	.063	.375	.870	2.025	12.000
1500.0	2.000	.250	.438	.505	.172	.063	.438	1.059	2.494	10.000
1500.0	2.375	.250	.438	.505	.172	.063	.438	1.201	2.778	14.000
1500.0	2.500	.250	.438	.505	.172	.063	.438	1.240	2.854	16.000
1500.0	3.000	.250	.438	.505	.172	.063	.438	1.399	3.172	18.000
1500.0	3.500	.250	.438	.505	.172	.063	.438	1.560	3.495	20.000
1500.0	4.000	.313	.500	.577	.204	.063	.500	1.661	3.790	20.000
1500.0	4.500	.313	.500	.577	.204	.063	.500	1.786	4.001	24.000
1500.0	5.000	.313	.500	.577	.204	.063	.500	1.940	4.369	26.000
1500.0	5.563	.313	.500	.577	.204	.063	.500	2.020	4.520	28.000
1500.0	6.000	.313	.500	.577	.204	.063	.500	2.160	4.788	30.000
1500.0	6.625	.375	.563	.650	.235	.063	.563	2.318	5.198	28.000
1500.0	8.000	.375	.563	.650	.235	.063	.563	2.668	5.899	34.000
1500.0	8.625	.375	.563	.650	.235	.063	.563	2.987	6.496	36.000
1500.0	10.000	.375	.563	.650	.235	.063	.563	3.135	6.832	42.000
1500.0	10.750	.375	.563	.650	.235	.063	.563	3.491	7.444	46.000
1500.0	12.000	.500	.750	.866	.297	.063	.750	3.625	8.000	38.000
1500.0	12.750	.438	.688	.794	.266	.063	.688	3.938	8.531	46.000
1500.0	14.000	.500	.750	.866	.297	.063	.750	4.175	9.100	46.000
1500.0	16.000	.500	.750	.866	.297	.063	.750	4.650	10.051	52.000

TABLE C-14. STUD, CRES, INTEGRAL/INTEGRAL AND LOOSE-RING/ LOOSE-RING CRYOGENIC FLUID CONNECTOR

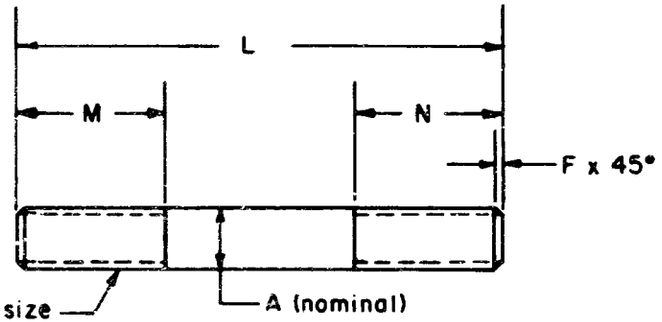

Note: J = Number of studs

PRESSURE	PIPE/TUBE OD	A	L	F	M	N	J	A	L	F	M	N	J
100.0	1.000	.190	1.534	.063	.431	.431	6.000	.190	1.556	.063	.436	.436	6.000
100.0	1.250	.190	1.598	.063	.447	.447	8.000	.190	1.620	.063	.453	.453	8.000
100.0	1.500	.190	1.656	.063	.461	.461	8.000	.190	1.708	.063	.474	.474	8.000
100.0	2.000	.190	1.774	.063	.491	.491	8.000	.190	1.826	.063	.504	.504	8.000
100.0	2.375	.190	2.117	.063	.577	.577	10.000	.190	2.227	.063	.604	.604	10.000
100.0	2.500	.190	1.898	.063	.522	.522	10.000	.190	1.980	.063	.542	.542	10.000
100.0	3.000	.190	1.993	.063	.546	.546	10.000	.190	2.105	.063	.574	.574	10.000
100.0	3.500	.250	2.713	.063	.741	.741	10.000	.250	2.865	.063	.779	.779	10.000
100.0	4.000	.250	2.474	.063	.681	.681	10.000	.250	2.554	.063	.701	.701	10.000
100.0	4.500	.250	2.971	.063	.805	.805	14.000	.250	3.123	.063	.843	.843	14.000
100.0	5.000	.250	2.681	.063	.733	.733	12.000	.250	2.761	.063	.753	.753	12.000
100.0	5.563	.250	3.425	.063	.919	.919	20.000	.250	3.621	.063	.968	.968	20.000
100.0	6.000	.250	2.824	.063	.769	.769	14.000	.250	2.934	.063	.796	.796	14.000
100.0	6.625	.250	3.541	.063	.948	.948	26.000	.250	3.857	.063	1.027	1.027	26.000
100.0	8.000	.250	3.150	.063	.850	.850	16.000	.250	3.320	.063	.893	.893	16.000
100.0	8.625	.250	3.980	.063	1.057	1.057	34.000	.250	4.266	.063	1.129	1.129	34.000
100.0	10.000	.250	3.893	.063	1.036	1.036	30.000	.250	4.063	.063	1.078	1.078	30.000
100.0	10.750	.250	4.488	.063	1.185	1.185	46.000	.250	4.844	.063	1.274	1.274	46.000
100.0	12.000	.250	4.192	.063	1.110	1.110	36.000	.250	4.422	.063	1.168	1.168	36.000
100.0	12.750	.250	5.001	.063	1.313	1.313	60.000	.250	5.331	.063	1.395	1.395	60.000
100.0	14.000	.250	4.555	.063	1.201	1.201	44.000	.250	4.785	.063	1.259	1.259	44.000
100.0	16.000	.250	4.905	.063	1.289	1.289	52.000	.250	5.105	.063	1.339	1.339	52.000
200.0	1.000	.190	1.534	.063	.431	.431	6.000	.190	1.586	.063	.444	.444	6.000
200.0	1.250	.190	1.598	.063	.447	.447	8.000	.190	1.680	.063	.468	.468	8.000
200.0	1.500	.190	1.686	.063	.469	.469	8.000	.190	1.738	.063	.482	.482	8.000
200.0	2.000	.190	1.804	.063	.499	.499	8.000	.190	1.886	.063	.519	.519	8.000
200.0	2.375	.190	2.147	.063	.584	.584	12.000	.190	2.287	.063	.619	.619	12.000
200.0	2.500	.190	1.928	.063	.529	.529	10.000	.190	2.010	.063	.550	.550	10.000
200.0	3.000	.190	2.053	.063	.561	.561	10.000	.190	2.165	.063	.589	.589	10.000
200.0	3.500	.250	2.743	.063	.748	.748	10.000	.250	2.925	.063	.794	.794	10.000
200.0	4.000	.250	2.534	.063	.696	.696	10.000	.250	2.644	.063	.724	.724	10.000
200.0	4.500	.250	3.031	.063	.820	.820	14.000	.250	3.183	.063	.858	.858	14.000
200.0	5.000	.250	2.741	.063	.748	.748	12.000	.250	2.851	.063	.775	.775	12.000
200.0	5.563	.250	3.455	.063	.926	.926	22.000	.250	3.711	.063	.990	.990	22.000
200.0	6.000	.250	2.914	.063	.791	.791	14.000	.250	3.084	.063	.834	.834	14.000
200.0	6.625	.250	3.631	.063	.970	.970	28.000	.250	3.947	.063	1.049	1.049	28.000
200.0	8.000	.250	3.419	.063	.917	.917	22.000	.250	3.594	.063	.961	.961	22.000
200.0	8.625	.250	4.070	.063	1.080	1.080	38.000	.250	4.446	.063	1.174	1.174	38.000
200.0	10.000	.250	3.951	.063	1.050	1.050	32.000	.250	4.200	.063	1.113	1.113	32.000
200.0	10.750	.250	4.638	.063	1.222	1.222	52.000	.250	5.024	.063	1.319	1.319	52.000
200.0	12.000	.250	4.434	.063	1.171	1.171	44.000	.250	4.727	.063	1.244	1.244	44.000
200.0	12.750	.250	5.151	.063	1.350	1.350	64.000	.250	5.541	.063	1.448	1.448	64.000
200.0	14.000	.250	4.951	.063	1.300	1.300	58.000	.250	5.258	.063	1.377	1.377	58.000
200.0	16.000	.250	5.426	.063	1.419	1.419	74.000	.250	5.837	.063	1.522	1.522	74.000

500.0	1.000	.190	1.594	.063	.446	.446	6.000
500.0	1.250	.190	1.658	.063	.462	.462	6.000
500.0	1.500	.190	1.716	.063	.476	.476	8.000
500.0	2.000	.190	1.893	.063	.521	.521	8.000
500.0	2.375	.190	2.207	.063	.599	.599	12.000
500.0	2.500	.190	2.050	.063	.560	.560	10.000
500.0	3.000	.190	2.259	.063	.612	.612	14.000
500.0	3.500	.250	2.833	.063	.771	.771	14.000
500.0	4.000	.250	2.834	.063	.771	.771	12.000
500.0	4.500	.250	3.121	.063	.843	.843	18.000
500.0	5.000	.250	3.201	.063	.863	.863	20.000
500.0	5.563	.250	3.575	.063	.956	.956	26.000
500.0	6.000	.250	3.524	.063	.944	.944	26.000
500.0	6.625	.250	3.811	.063	1.015	1.015	34.000
500.0	8.000	.250	4.161	.063	1.088	1.088	40.000
500.0	8.625	.250	4.404	.063	1.164	1.164	44.000
500.0	10.000	.313	5.008	.063	1.330	1.330	40.000
500.0	10.750	.313	5.235	.063	1.387	1.387	44.000	
500.0	12.000	.313	5.588	.063	1.475	1.475	52.000
500.0	12.750	.313	5.476	.063	1.447	1.447	56.000
500.0	14.000	.313	6.263	.063	1.644	1.644	66.000
500.0	16.000	.313	6.696	.063	1.802	1.802	76.000
1000.0	1.000	.190	.761	.063	.488	.488	6.000
1000.0	1.250	.190	1.888	.063	.519	.519	8.000
1000.0	1.500	.190	2.006	.063	.549	.549	10.000
1000.0	2.000	.190	2.222	.063	.603	.603	14.000
1000.0	2.375	.190	2.368	.063	.640	.640	16.000
1000.0	2.500	.250	2.679	.063	.732	.732	12.000
1000.0	3.000	.250	2.852	.063	.776	.776	14.000
1000.0	3.500	.250	3.104	.063	.839	.839	20.000
1000.0	4.000	.250	3.249	.063	.875	.875	22.000
1000.0	4.500	.250	3.424	.063	.918	.918	24.000
1000.0	5.000	.250	3.639	.063	.972	.972	28.000
1000.0	5.563	.313	4.017	.063	1.082	1.082	24.000
1000.0	6.000	.313	4.257	.063	1.142	1.142	28.000
1000.0	6.625	.313	4.333	.063	1.161	1.161	30.000
1000.0	8.000	.313	5.036	.063	1.337	1.337	40.000
1000.0	8.625	.313	4.997	.063	1.327	1.327	42.000
1000.0	10.000	.313	5.725	.063	1.509	1.509	48.000
1000.0	10.750	.313	5.645	.063	1.489	1.489	52.000
1000.0	12.000	.375	6.725	.063	1.775	1.775	52.000
1000.0	12.750	.375	6.690	.063	1.766	1.766	54.000
1000.0	14.000	.375	7.296	.063	1.918	1.918	58.000
1000.0	16.000	.438	8.218	.063	2.164	2.164	56.000
1500.0	1.000	.190	1.869	.063	.515	.515	8.000
1500.0	1.250	.190	2.034	.063	.556	.556	10.000
1500.0	1.500	.190	2.160	.063	.588	.588	12.000
1500.0	2.000	.250	2.668	.063	.730	.730	10.000
1500.0	2.375	.250	2.837	.063	.772	.772	14.000
1500.0	2.500	.250	2.849	.063	.785	.785	16.000
1500.0	3.000	.250	3.097	.063	.837	.837	18.000
1500.0	3.500	.250	3.306	.063	.889	.889	20.000
1500.0	4.000	.313	3.828	.063	1.035	1.035	20.000
1500.0	4.500	.313	4.091	.063	1.101	1.101	24.000
1500.0	5.000	.313	4.347	.063	1.165	1.165	26.000
1500.0	5.563	.313	4.497	.063	1.202	1.202	28.000
1500.0	6.000	.313	4.745	.063	1.264	1.264	30.000
1500.0	6.625	.375	5.270	.063	1.411	1.411	28.000
1500.0	8.000	.375	5.750	.063	1.531	1.531	34.000
1500.0	8.625	.375	5.628	.063	1.501	1.501	38.000
1500.0	10.000	.375	6.483	.063	1.714	1.714	42.000
1500.0	10.750	.375	6.205	.063	1.645	1.645	46.000
1500.0	12.000	.500	7.877	.063	2.094	2.094	38.000
1500.0	12.750	.438	7.400	.063	1.959	1.959	46.000
1500.0	14.000	.500	8.718	.063	2.304	2.304	46.000
1500.0	16.000	.500	9.318	.063	2.454	2.454	52.000

.190	1.016	.063	.451	.451	6.000
.190	1.710	.063	.475	.475	6.000
.190	1.798	.063	.497	.497	8.000
.190	1.971	.063	.540	.540	8.000
.190	2.377	.063	.642	.642	12.000
.190	2.216	.063	.601	.601	10.000
.190	2.421	.063	.653	.653	14.000
.250	3.075	.063	.831	.831	14.000
.250	3.022	.063	.818	.818	12.000
.250	3.393	.063	.911	.911	18.000
.250	3.473	.063	.931	.931	20.000
.250	3.951	.063	1.050	1.050	28.000
.250	3.851	.063	1.025	1.025	26.000
.250	4.247	.063	1.124	1.124	34.000
.250	4.657	.063	1.227	1.227	40.000
.250	4.936	.063	1.297	1.297	44.000
.313	5.582	.063	1.474	1.474	40.000
.313	5.865	.063	1.544	1.544	44.000
.313	6.301	.063	1.653	1.653	52.000
.313	6.140	.063	1.613	1.613	56.000
.313	7.115	.063	1.857	1.857	66.000
.313	7.887	.063	2.050	2.050	76.000
.190	1.845	.063	.509	.509	6.000
.190	1.992	.063	.546	.546	8.000
.190	2.137	.063	.582	.582	10.000
.190	2.438	.063	.657	.657	14.000
.190	2.650	.063	.712	.712	16.000
.250	2.888	.063	.785	.785	12.000
.250	3.206	.063	.864	.864	14.000
.250	3.584	.063	.959	.959	20.000
.250	3.771	.063	1.005	1.005	22.000
.250	4.162	.063	1.103	1.103	24.000
.250	4.178	.063	1.107	1.107	26.000
.313	4.719	.063	1.258	1.258	24.000
.313	4.724	.063	1.259	1.259	28.000
.313	5.053	.063	1.344	1.344	30.000
.313	5.569	.063	1.470	1.470	40.000
.313	5.775	.063	1.522	1.522	42.000
.313	6.384	.063	1.674	1.674	48.000
.313	6.535	.063	1.712	1.712	52.000
.375	7.399	.063	1.934	1.934	52.000
.375	7.364	.063	1.985	1.985	54.000
.375	8.116	.063	2.123	2.123	58.000
.438	9.193	.063	2.408	2.408	56.000
.190	2.000	.063	.547	.547	8.000
.190	2.174	.063	.591	.591	10.000
.190	2.310	.063	.625	.625	12.000
.250	2.869	.063	.780	.780	10.000
.250	3.153	.063	.851	.851	14.000
.250	3.229	.063	.870	.870	16.000
.250	3.547	.063	.949	.949	18.000
.250	3.870	.063	1.030	1.030	20.000
.313	4.259	.063	1.143	1.143	20.000
.313	4.469	.063	1.195	1.195	24.000
.313	4.618	.063	1.233	1.233	26.000
.313	4.989	.063	1.325	1.325	28.000
.313	5.257	.063	1.392	1.392	30.000
.375	5.760	.063	1.534	1.534	28.000
.375	6.402	.063	1.709	1.709	34.000
.375	7.058	.063	1.858	1.858	38.000
.375	7.394	.063	1.942	1.942	42.000
.375	8.007	.063	2.095	2.095	46.000
.500	8.730	.063	2.312	2.312	38.000
.438	9.188	.063	2.408	2.408	46.000
.500	9.650	.063	2.588	2.588	46.000
.500	10.801	.063	2.825	2.825	52.000

TABLE C-15. INSTALLATION OF AFRPL FLANGED CONNECTORS FOR CRYOGENIC SERVICE

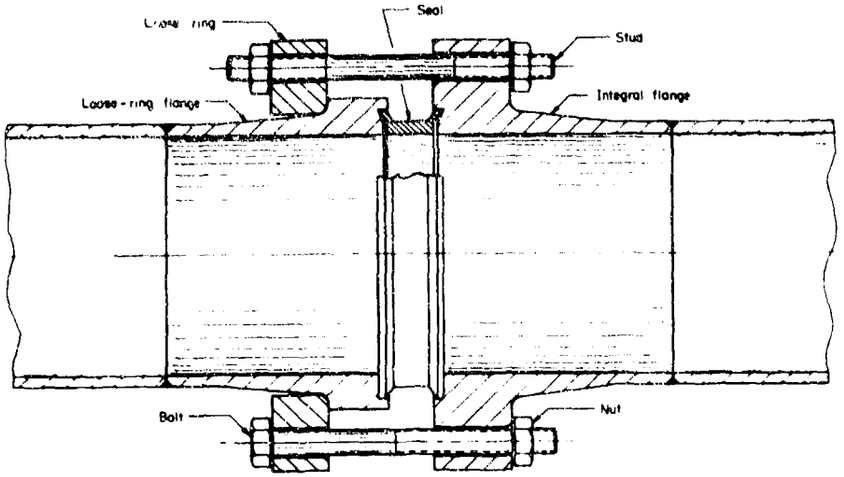

Pressure	Pipe/Tube OD	Wrench Torque for Aluminum Connectors-Per Bolt - Lb-In. Minimum	Wrench Torque for Aluminum Connectors-Per Bolt - Lb-In. Maximum	Wrench Torque for Stainless Steel Connectors-Per Bolt - Lb-In. Minimum	Wrench Torque for Stainless Steel Connectors-Per Bolt - Lb-In. Maximum
100	1.0	12.4	13.0	21.5	23.6
	1.25	12.4	13.0	20.0	22.0
	1.5	14.7	15.4	23.8	26.2
	2.0	16.4	17.2	32.0	35.2
	2.375	22.9	24.0	46.2	50.6
	2.5	17.7	18.6	32.0	35.2
	3.0	21.4	22.5	38.8	42.6
	3.5	60.7	65.0	108.1	118.0
	4.0	36.4	38.5	78.2	85.6
	4.5	53.6	56.0	101.3	111.0
	5.0	41.6	43.7	83.1	91.0
	5.563	54.3	57.2	105.7	116.0
	6.00	46.3	48.5	87.2	95.6
	6.625	53.6	56.5	98.9	108.6
	8.0	59.6	62.8	106.9	117.5
	8.625	53.4	56.0	102.0	112.0
	10.00	54.7	57.2	102.0	112.0
	10.75	60.5	63.0	101.5	111.5
	12.0	54.6	57.0	105.0	115.5
	12.75	104.9	110.0	98.7	118.5
	14.0	54.0	56.6	103.0	113.0
	16.0	55.3	58.4	103.9	114.0
200	1.0	13.0	14.0	22.2	24.4
	1.25	13.0	14.0	20.6	23.9
	1.5	15.8	17.0	25.2	27.7
	2.0	17.7	19.0	34.0	37.4
	2.375	24.3	25.5	40.4	44.5
	2.5	19.6	21.0	34.6	38.0
	3.0	23.9	25.0	42.4	46.7
	3.5	55.8	59.0	113.6	124.0
	4.0	47.3	50.0	86.4	95.0
	4.5	58.6	62.0	108.6	118.0
	5.0	54.9	58.0	93.6	103.0
	5.563	55.2	58.6	103.0	113.0
	6.00	56.0	59.0	101.2	111.5
	6.625	53.2	56.0	99.3	109.0
	8.0	55.3	58.6	101.7	111.0
	8.625	58.1	62.0	100.8	110.0
	10.00	55.8	59.0	102.5	112.0
	10.75	102.0	108.0	100.0	110.0
	12.0	57.1	60.0	102.8	112.5
	12.75	105.6	110.0	104.3	115.0
	14.0	106.6	111.0	102.5	112.0
	16.0	105.0	110.0	101.5	111.5

TABLE C-15. (Continued)

Pressure	Pipe/Tube OD	Wrench Torque for Aluminum Connectors-Per Bolt - Lb-In.		Wrench Torque for Stainless Steel Connectors-Per Bolt - Lb-In.	
		Minimum	Maximum	Minimum	Maximum
500	1.0	14.8	16.0	25.8	28.4
	1.25	18.9	20.6	32.2	35.4
	1.5	18.5	20.0	29.0	31.8
	2.0	22.3	23.6	40.6	44.6
	2.375	53.0	55.6	45.6	50.0
	2.5	23.0	25.0	44.9	49.4
	3.0	53.6	56.2	42.9	47.2
	3.5	52.9	55.5	94.2	104.0
	4.0	56.4	59.2	108.2	119.0
	4.5	55.3	58.0	100.0	110.0
	5.0	53.2	55.7	95.2	104.0
	5.563	111.0	117.0	95.8	105.0
	6.0	63.5	67.0	101.0	111.0
	6.625	104.4	109.0	99.8	110.0
	8.0	106.0	111.0	109.2	120.5
	8.625	115.5	121.0	109.8	121.0
	10.0	191.0	200.0	192.1	210.0
	10.75	190.0	200.0	194.8	214.0
	12.0	197.7	207.0	196.8	216.0
	12.75	226.6	238.0	204.5	224.0
	14.0	316.5	332.0	197.4	217.0
	16.0	462.6	485.0	213.6	232.0
1000	1.0	23.9	25.0	39.8	43.6
	1.25	24.5	26.0	38.5	42.4
	1.5	25.4	27.0	38.8	42.7
	2.0	51.8	54.5	40.8	45.0
	2.375	54.7	57.5	45.5	50.0
	2.5	52.6	55.4	91.0	100.0
	3.0	55.4	58.4	101.3	111.0
	3.5	105.8	111.0	98.0	108.0
	4.0	102.2	107.0	102.8	113.0
	4.5	205.5	215.0	108.2	119.0
	5.0	107.5	112.5	109.4	120.1
	5.563	202.5	212.0	182.8	200.0
	6.0	194.2	204.0	181.2	199.0
	6.625	194.5	204.0	186.7	205.0
	8.0	306.7	322.0	194.4	213.0
	8.625	322.5	338.0	199.7	220.0
	10.0	484.0	510.0	225.9	247.0
	10.75	502.0	520.0	228.7	251.0
	12.0	511.0	530.0	348.6	383.0
	12.75	550.0	580.0	360.3	396.0
	14.0	800.0	840.0	390.9	429.0
	16.0	1097.0	1140.0	608.4	668.0
1500	1.0	21.8	23.0	37.2	40.9
	1.25	53.5	56.5	40.0	44.0
	1.5	52.6	55.0	42.0	46.2
	2.0	55.4	58.0	104.5	114.5
	2.375	111.0	117.0	97.0	106.8
	2.5	100.5	105.0	91.0	100.0
	3.0	102.0	107.0	106.2	117.0
	3.5	193.0	203.0	112.6	123.0
	4.0	182.0	191.0	186.8	205.0
	4.5	199.0	210.0	177.0	190.0
	5.0	188.0	197.0	192.6	210.0
	5.563	311.0	327.0	203.0	223.0
	6.0	318.0	332.0	214.7	236.0
	6.625	501.0	525.0	333.4	368.0
	8.0	510.0	535.0	359.0	395.0
	8.625	575.0	610.0	378.8	416.0
	10.0	830.0	870.0	413.5	454.0
	10.75	1180.0	1240.0	443.8	487.0
	12.0	1860.0	1960.0	883.4	970.0
	12.75	1997.0	2080.0	706.0	770.0
	14.0	2962.0	3000.0	959.4	1051.0
	16.0	4430.0	4500.0	1071.0	1180.0

TABLE C-16. INSTALLATION OF AFRPL CRYOGENIC FLANGED CONNECTORS

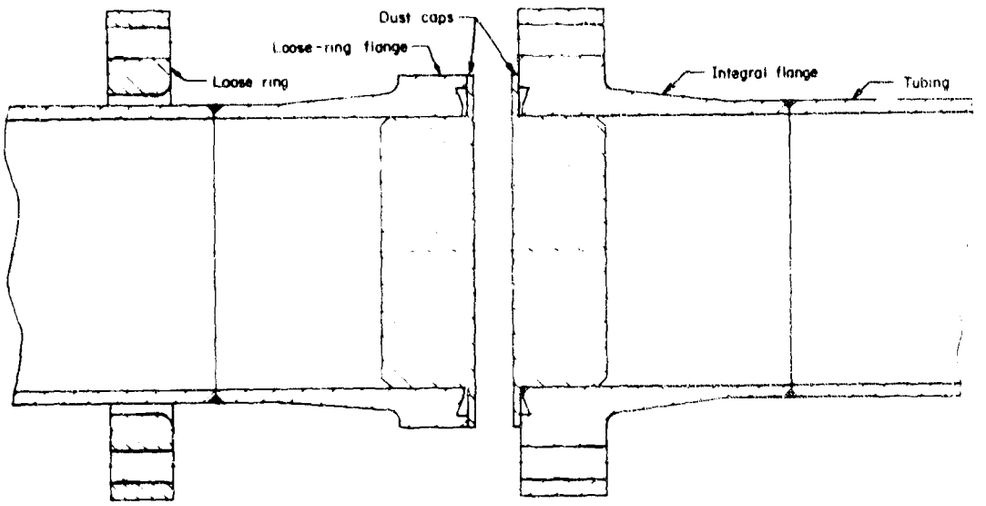

Step 1

A connector may consist of two integral flanges, two loose-ring flanges, or one flange of each type, as shown. Weld the integral flange directly to the tubing. For a loose-ring flange first place the loose ring on the tubing. Be sure the radius of the loose ring faces the flange. Weld the loose-ring flange to the tubing.

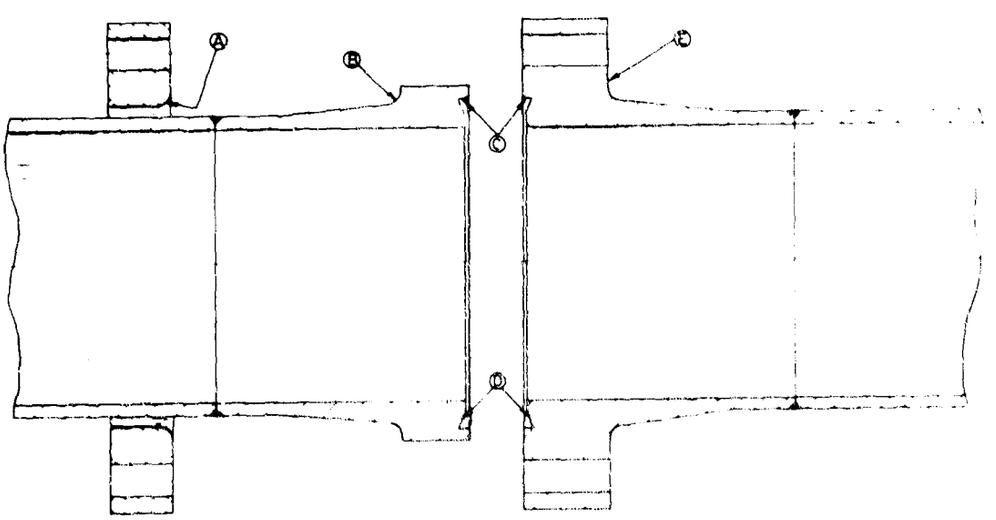

Step 2

Remove the dust caps. Inspect Surfaces A, B, C, D, and E for dirt, contamination, or surface irregularities. If necessary, rinse the surfaces with methylethylketone and dry parts with a filtered air stream or wipe parts with clean paper tissue moistened with methylethylketone. Replace the dust caps.

TABLE C-16. (Continued)

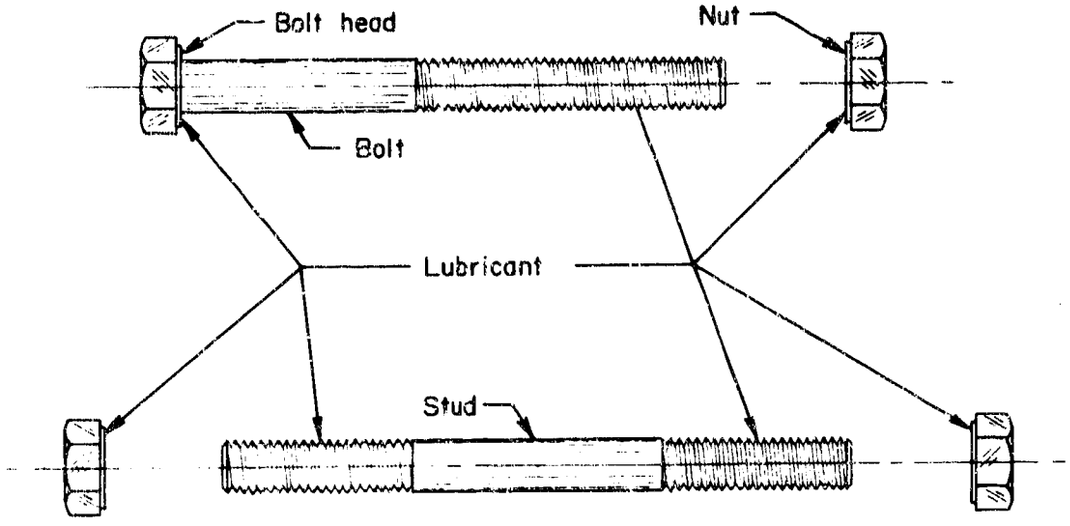

Step 3

Coat the threads of the studs and bolts and the bearing surfaces of the nuts and bolt heads with lubricant. Apply the lubricant sparingly. Work the nuts on the male threads by hand. Remove the nuts and inspect the thread surfaces for an even coating of lubricant.

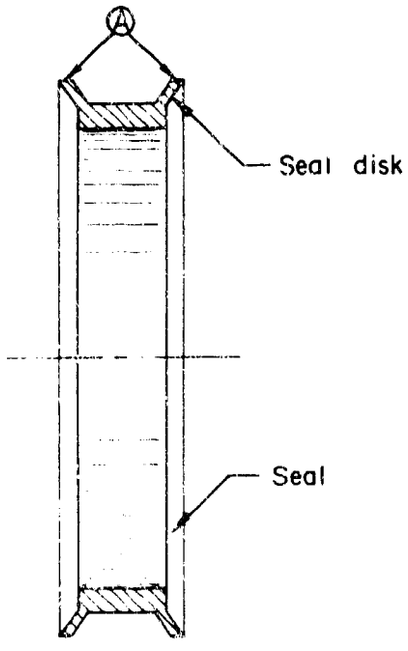

Step 4

Remove the seal from the protective wrapping. Inspect Surfaces A of the seal disks with a 5-power lens. Discard the seal if the surfaces are scratched or irregular. Clean the surfaces with methylethylketone if dirty.

TABLE C-16. (Continued)

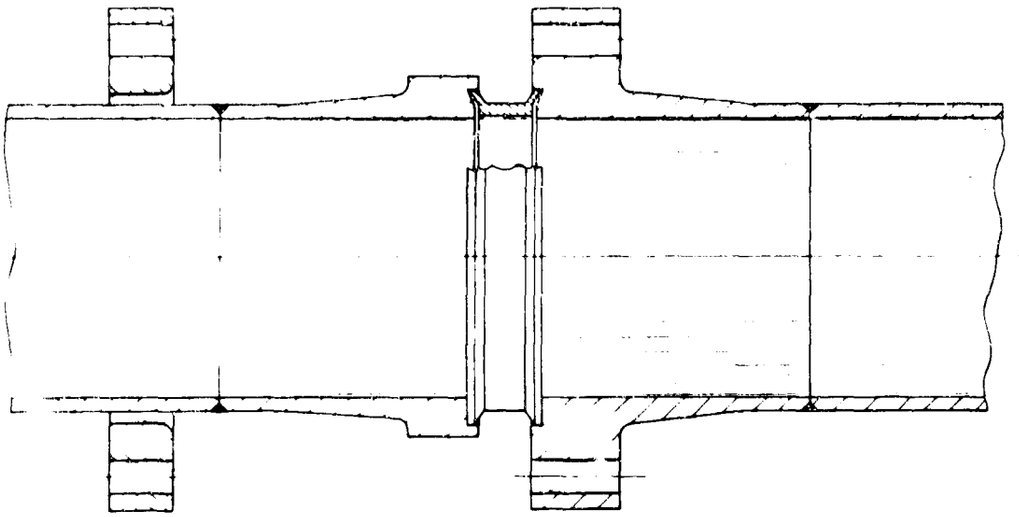

Step 5

Remove the dust caps from the flanges and locate the seal in the flange cavities. Care must be exercized to avoid nicking the edges of the seal. Handling with clean hands is permissible, but the sealing surfaces must not be contaminated with dirt or lubricant.

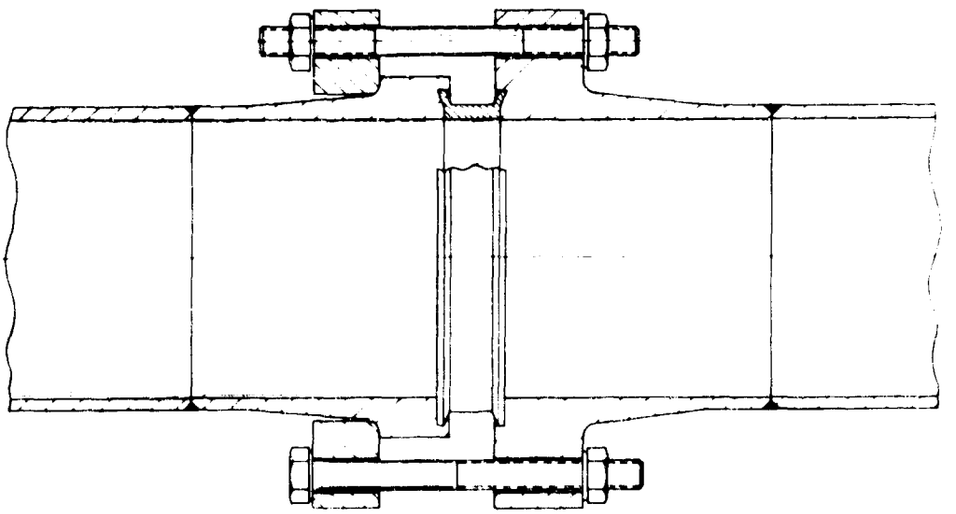

Step 6

Tighten the nuts of the studs or bolts fingertight while maintaining an axial force on the flange to keep the seal in place. Tighten the nuts with a calibrated torque wrench to the recommended torque. The nuts should be tightened in sequence with a maximum of 1/2 turn per nut. Several tightening cycles are required to seat the seal and preload the connector.

Unclassified

Security Classification

DOCUMENT CONTROL DATA - R & D

(Security classification of title, body of abstract and indexing annotation must be entered when the overall report is classified)

1. ORIGINATING ACTIVITY *(Corporate author)*

Battelle Memorial Institute
Columbus Laboratories
505 King Avenue, Columbus, Ohio 43201

2a. REPORT SECURITY CLASSIFICATION
Unclassified

2b. GROUP

3. REPORT TITLE

Development of AFRPL Flanged Connectors for Rocket Fluid Systems

4. DESCRIPTIVE NOTES *(Type of report and inclusive dates)*
Final Report

5. AUTHOR(S) *(First name, middle initial, last name)*

Trainer, Thomas M.
Baum, Joseph V.
Thompson, John R.
Ghadiali, Nuruddin D.

6. REPORT DATE	7a. TOTAL NO. OF PAGES	7b. NO. OF REFS
July 1969	311	22

8a. CONTRACT OR GRANT NO.	9a. ORIGINATOR'S REPORT NUMBER(S)
AF 04(611)-11204	AFRPL-TR-69-97
b. PROJECT NO. 3058	
c.	9b. OTHER REPORT NO(S) *(Any other numbers that may be assigned this report)*
d.	

10. DISTRIBUTION STATEMENT

Qualified requestors may obtain copies of this report from DDC. This document is subject to special export controls and each transmittal to foreign nationals may be made only with prior approval of AFRPL (RPOR/STINFO), Edwards, California 93523.

11. SUPPLEMENTARY NOTES	12. SPONSORING MILITARY ACTIVITY
	Air Force Rocket Propulsion Laboratory AFRPL (RPRPD) Edwards, California 93523

13. ABSTRACT

A 3-year program was conducted to develop a family of flight-weight flanged tube connectors which utilize the "Bobbin" seal concept for both 6061-T6 aluminum and Type 347 stainless steel tubing systems. In addition, engineering support was furnished during the evaluation of AFRPL stainless steel threaded connectors by selected organizations. The activities in relation to the first objective consisted of: (1) the selection of bolted, flanged connectors as the best means of joining tubing from 1 to 16 inches in diameter, (2) the development of stainless steel and aluminum Bobbin seals for typical flanged connector sizes, (3) the preparation of a detailed computer program for the optimum design of flanged connectors incorporating Bobbin seals, (4) the design, fabrication, and qualification testing of representative flanged connectors, and (5) the preparation of designs for a family of stainless steel and aluminum flanged connectors. The activities directed toward the second objective consisted of: (1) the investigation of seal-removal tools, (2) the design and evaluation of connector modifications to achieve seal retention and misalignment limitation, (3) the investigation of increased radial seal loading techniques, and (4) the investigation of stress relaxation in threaded connectors. In addition to a summary of the technical activities, the report contains the computer design program for flanged connectors, and designs for aluminum and stainless steel flanged connectors for pressures up to 1500 psi and for tube sizes through 16 inches. It is recommended that MS standards and specifications be prepared for cryogenic stainless steel and aluminum flanged connectors for tubing through 3 in. in diameter. Additional developmental work is recommended in regard to larger flanged connectors, and in regard to certain aspects of the stainless steel threaded connectors.

DD FORM 1 NOV 68 1473

Unclassified

Security Classification

14. KEY WORDS	LINK A		LINK B		LINK C	
	ROLE	WT	ROLE	WT	ROLE	WT
Flanged Connectors						
Threaded Connectors						
Metal Seals						
Bobbin Seals						
Thermal Gradients						
Fatigue Testing						
AFRPL Connectors						
Nickel Plating						
Stress Relaxation						
Helium Leakage						
Cryogenic Testing						